GCOS – 184
GOOS – 206
WCRP – 6/2014

Report of the

Tropical Pacific Observing System 2020 Workshop

(TPOS 2020)

VOLUME II – White Papers

27-30th January 2014,
Scripps Institution of Oceanography, San Diego, United States

Sponsored by:

The Ocean Observations Panel for Climate (OOPC) is sponsored by the Global Ocean Observing System, the Global Climate Observing System and the World Climate Research Programmeme. OOPC provides advice on observations to the WMO-IOC Joint Technical Commission for Oceanography and Marine Meteorology.

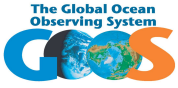

Contents

White Paper #2 - Some societal impacts of ENSO

Harrison, D.E.[1], Bond, N.[2], Goddard, L.[3], Martinez, R.[4], and Yamagata, T.[5]

[1] NOAA Pacific Marine Environmental Laboratory, United States
[2] University of Washington, United States
[3] International Research Institute for Climate and Society, United States
[4] International Research Center on El Niño, Ecuador
[5] University of Tokyo, Japan

1. Introduction

We monitor oceanic and atmospheric conditions and air-sea interactions over the Tropical Pacific for many reasons. One of these is for forecasts of Tropical Pacific conditions, because the state of the El Niño - Southern Oscillation phenomenon affects so many nations around the basin and around the world. This brief document for the Tropical Pacific Observing System 2020 (TPOS 2020) workshop will describe some examples of the impacts of the El Niño - Southern Oscillation on seasonal weather anomalies in temperature and precipitation, marine ecosystems, tropical cyclones, changes in atmospheric CO_2 concentration and recent conditions in Latin America. We make no attempt to be comprehensive; the literature is full of other examples of phenomena connected to ENSO with a societal impact. For those interested in further examples, we call the reader's attention to a paper authored mostly by members of the International Research Institute for Climate and Society (Zebiak et al., 2014) for an excellent overview and material additional to that presented here.

ENSO is a coupled air-sea phenomenon with global reach, but maximum anomalies in the Tropical Pacific, that typically spans from boreal summer through the following boreal spring, peaking in boreal winter. Thus it is convenient to categorize years as being "El Niño" years, "ENSO-neutral" years, or "La Niña" years. A notation introduced early in the modern study of ENSO was to characterize the years in which major anomalies first appeared as "Yr (0)" and the previous and succeeding years as "Yr (-1)" and "Yr (+1)" (Rasmussen and Carpenter, 1982), but for many impacts it is sufficient to identify the Yr (0), and it is understood that anomalies extend from mid-Yr (0) into Yr (1). Yr (0) traditionally has been identified as the year in which some measure of the ENSO-state of the climate system exceeds and remains beyond some threshold value for some period of time. Traditional measures of ENSO have included the Troup Southern Oscillation Index (SOI), a normalized measure of the sea level pressure (SLP) difference between Tahiti and Darwin, and several area-averages of sea surface temperature anomaly (SSTA) near the equator (NIÑO 1, 2, 3, 3.4, 4). With appropriate smoothing, Darwin SLP alone has been used to study the longer time history of ENSO. There also are asymmetries between El Niño and La Niña (Deser and Wallace, 1990), which are evident in the ENSO measures and in the associated impacts (Larkin and Harrison, 2002; Harrison and Larkin, 2002), which means that attempting to characterize ENSO impacts by simple correlation with an ENSO measure time series can lead to results that are not fully typical of either ENSO state.

Deser and Wallace (1987) noted that the different ENSO measures did not always agree on whether a particular year was an "El Niño" year. As ENSO impacts have been more thoroughly investigated, the effects of the criterion selected for year identification on impact associations

has become clear: different regions of the planet have ENSO associations that sometimes can be optimized by selecting particular ENSO measures. The idea that there are at least two different types of El Niño events with different associated impacts has recently also been advocated (e.g., Larkin and Harrison, 2005; Ashok and Yamagata, 2009; Chiodi and Harrison, 2013). We shall offer an example below of how the use of a particular ENSO measure can optimize the connection to a seasonal weather impact. In many cases, a useful 'big picture' view of ENSO societal impacts can be obtained via simple compositing of the anomalies based on El Niño or La Niña Yr (0)s. However, the big picture glosses over many important aspects of event-to-event variability, and is vulnerable to the effects of a few years with major surface anomalies.

ENSO, while an event with a typical duration of substantial anomalies lasting about one year, and with events occurring sporadically with an average time of several years (e.g., Harrison and Larkin, 1998; Larkin and Harrison, 2001; Larkin and Harrison, 2002), also exhibits very substantial multi-decadal variability (e.g., Harrison and Chiodi, 2014). This makes inferences about trends in ENSO statistics challenging (Harrison and Larkin, 1997). Because a considerable percentage of the Tropical Pacific ocean surface is anomalously warm or cool during a major ENSO event, the ENSO statistics of a particular decade can have a significant effect on global surface temperature especially if the North Pacific has a widespread anomaly of the same sign (Ashok and Yamagata, 2009). Recently there has been much interest in the extent to which there has been little global surface warming over the past 15 years, and it has been suggested that the recent frequency of La Niña events may be a significant factor (Kosaka and Xie, 2013). Whether the statistics of ENSO events will change as the planet warms is an area of much current interest.

The financial costs to society of ENSO events have been estimated to be as much as $25 billion for the extreme 1997-1998 El Niño. Lazo et al. (2011) have estimated that for the US, as well as Australia, the economic consequences of ENSO events can be on the order of 1% of national GDP, which is very substantial indeed. Goddard and Dilley (2005) have, however, emphasized that a thoughtful consideration of the 'cost' of ENSO events involves consideration of many factors, not least placing the frequency of weather 'disasters' in comparison with the typical frequency and severity of occurrences during ENSO-neutral years. Also important is the consideration of the vulnerability of the regions most strongly affected. Therefore, skillful forecasts of ENSO events, with sufficient lead time, offer the possibility of greatly reducing impacts in some regions.

We now offer several examples of ENSO connections to climate variability that affects societies.

2. Seasonal Weather Anomalies

A big picture overview of seasonal weather impacts associated with ENSO events was offered by Ropelewski and Halpert (1987 and 1989), and Halpert and Ropelewski (1992), and is summarized in Figure 2.1 and 2.2. The areas affected are indicated schematically and the magnitude of the seasonal anomalies is not indicated, but it tells the now-familiar story of ENSO seasonal weather impacts. Regions are affected across the globe, but most strongly in and adjacent to the Tropical Pacific and over the Americas. Effects are felt in December - February (DJF) as well as in June - August (JJA).

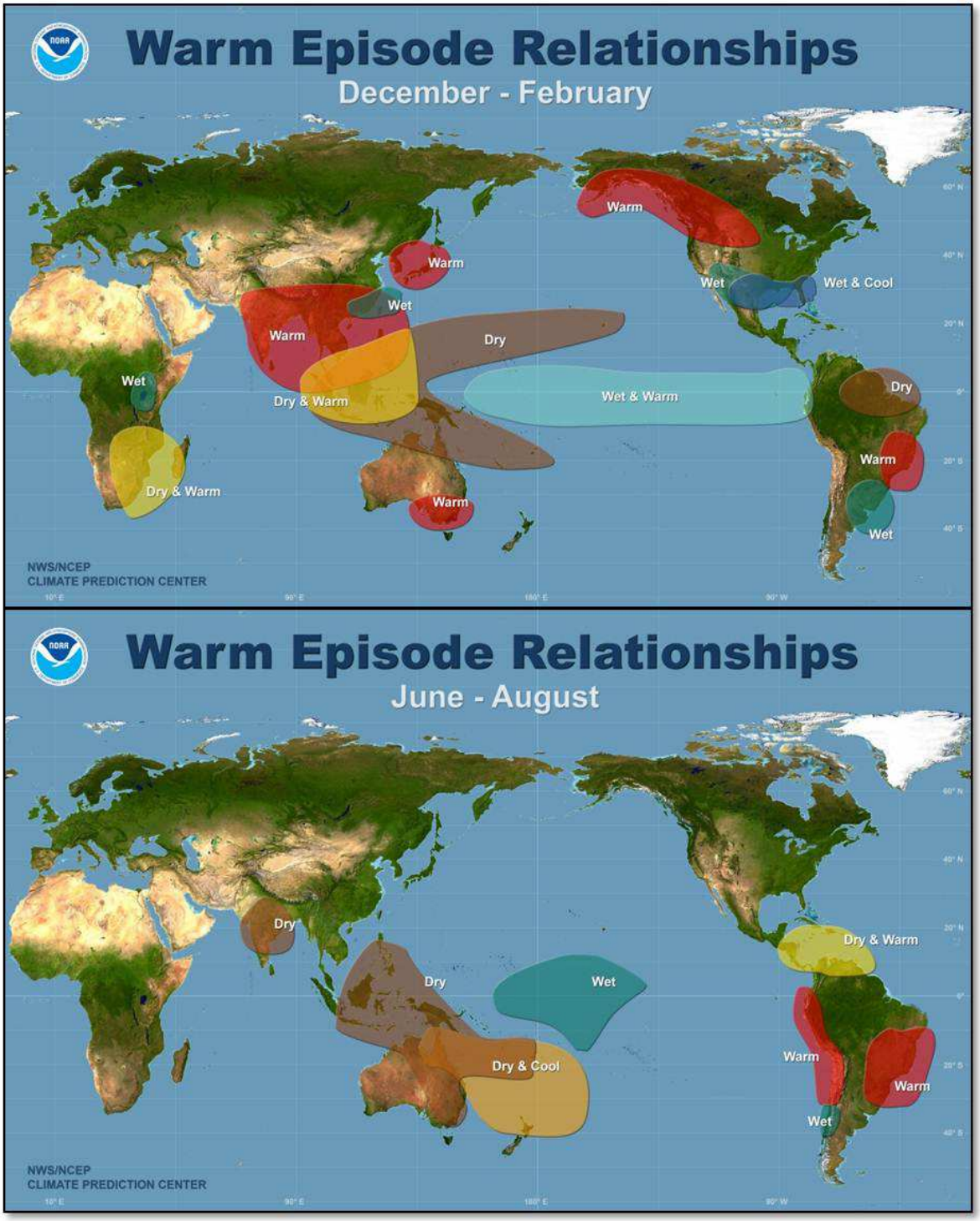

High Resolution Images can be found at:
http://www.cpc.ncep.noaa.gov/products/precip/CWlink/ENSO/ENSO-Global-Impacts/

Figure 2.1 - Large scale seasonal weather anomalies associated with the warm phase of ENSO (El Niño).

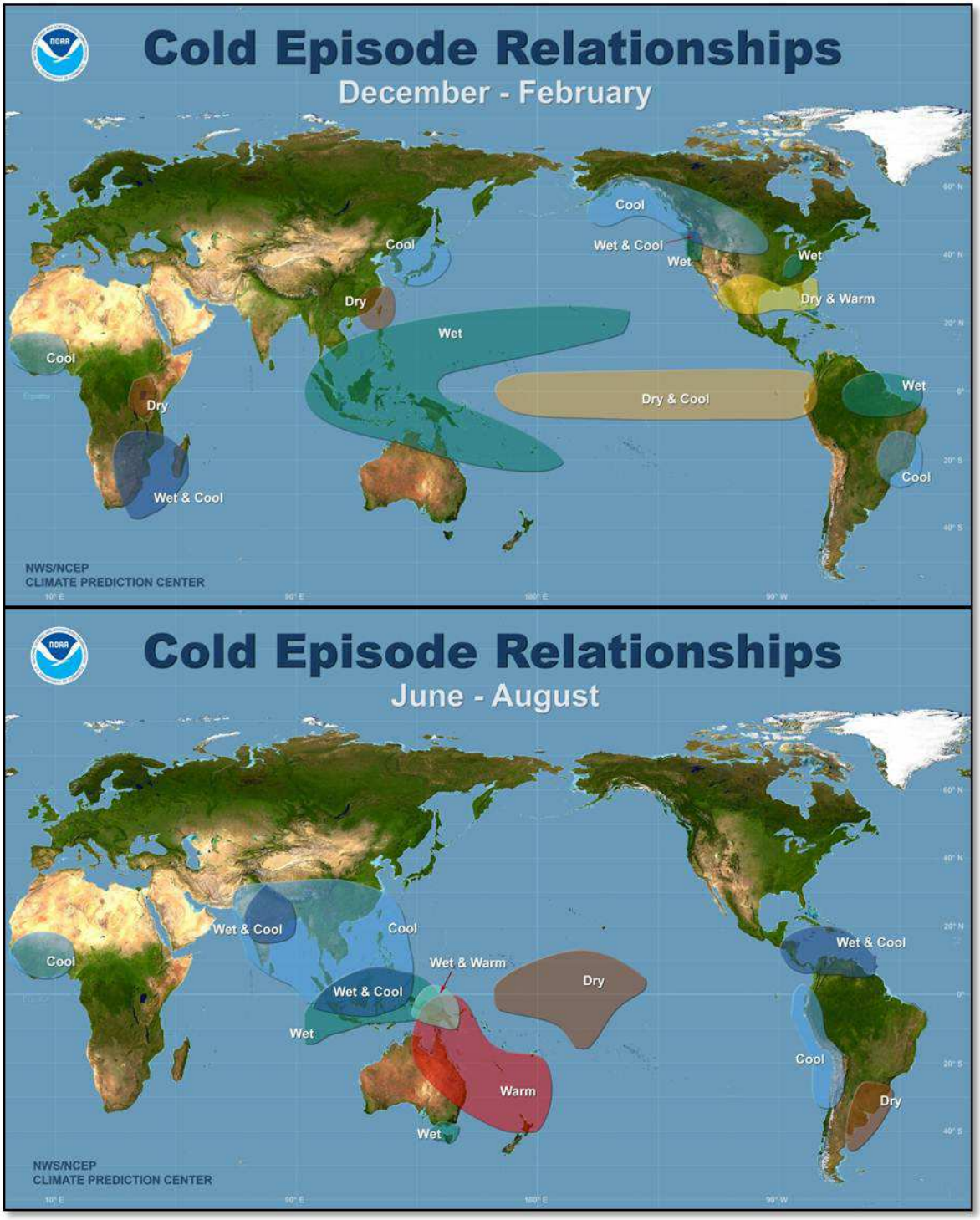

High Resolution Images can be found at:
http://www.cpc.ncep.noaa.gov/products/precip/CWlink/ENSO/ENSO-Global-Impacts/

Figure 2.2 - Large scale seasonal weather anomalies associated with the cold phase of ENSO (La Niña).

However, these figures do not convey the interesting complexity of ENSO-seasonal weather associations. Using the now wide-spread NIÑO3.4 SSTA measure of ENSO, particularly with a low threshold of 3-month-running-average value in excess of 0.5C (-0.5C) to identify El Niño (La Niña) years, leads to many years being designated El Niño or La Niña, and many of the seasonal anomalies during these years are not a sign for one of those events as suggested by Figures 2.1 and 2.2. Under these measures of ENSO, there is very strong event-to-event variation in seasonal weather anomaly. Larkin and Harrison (2005) noted that winter seasonal weather anomalies over the US were substantially affected by how El Niño events were defined, and suggested that it was useful to treat events with anomalies primarily in the central Pacific (which they called Dateline events) as distinct from events that spanned the eastern and central Pacific (which they called Conventional events). There has been considerable research done on how best to characterize ENSO events when the focus is on seasonal weather anomalies. Another perspective has introduced the concept of El Niño Modoki for the Central Pacific El Niño events (e.g., Ashok et al, 2007). A third perspective has used the characteristics of outgoing long wave radiation (OLR) to identify events (Chiodi and Harrison, 2010 and 2013).

The OLR perspective turns out to have considerable skill in identifying El Niño events with much less event-to-event seasonal weather anomalies. Figure 2.3 shows time series of NIÑO3.4 SSTA and of the OLR index proposed by Chiodi and Harrison (2013). The years identified as distinctive by the OLR index are a subset of the years typically identified as El Niño events by a common NIÑO3.4 criterion, so we shall speak of “OLR El Niño” and “Non-OLR El Niño” years.

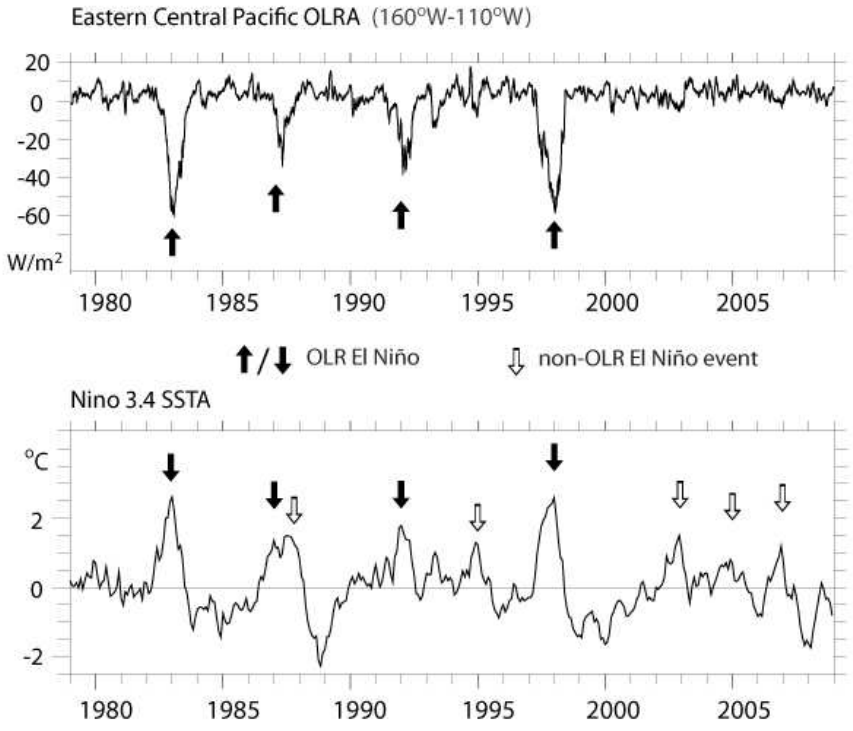

Figure 2.3 - An OLR index for El Niño events vs. NIÑO3.4 SSTA.

OLR El Niño years are characterized by the presence of deep atmospheric convection east of the normal region of deep convection; they accord to the Tropical Pacific waveguide wet anomaly in the Ropelewski and Halpert “Warm Episode” figures. Clearly there are only about half as many OLR El Niño years as Non-OLR El Niño years. The unique waveguide-convection feature of the OLR El Niño years has typically (3 out of 4 events) been apparent by the end of boreal fall of Yr 0, thereby distinguishing the OLR El Niño years from the other years before the arrival of the strongly affected boreal winter (DJF Yr 0/+1) season.

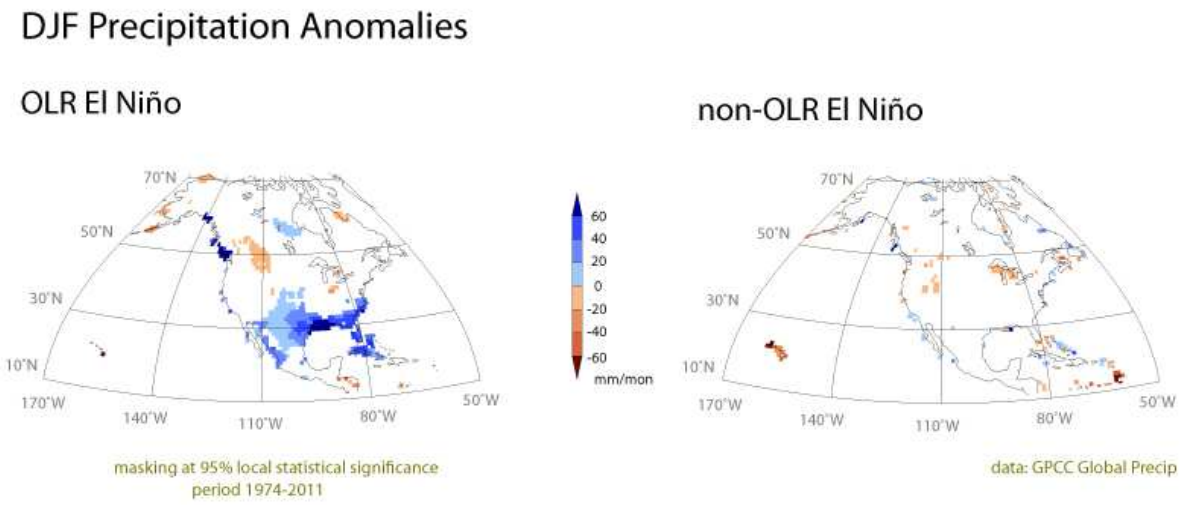

Figure 2.4 - El Niño 95% statistically significant DJF precipitation anomalies, OLR events vs. non-OLR events.

Figure 2.4 shows the DJF average OLR El Niño average and Non-OLR El Niño average surface precipitation anomalies over North and Central America. A striking result is that there are very few areas with any statistically significant (at 95%) precipitation anomalies for the Non-OLR El Niño average; the event-to-event variability in these events is large and of inconsistent signs. By contrast there are substantial areas of significant precipitation anomaly for the OLR El Niño average. Space constrains us from showing the individual year anomalies for all these years, but the OLR El Niño events show many common features in each event. Figure 2.5 presents DJF surface temperature anomaly averages, with the same overall result; the Non-OLR El Niño events do not exhibit much highly statistically significant average anomaly, whereas the OLR El Niño events have considerable regions of significance. As for precipitation, event-to-event variability is large in Non-OLR events and much smaller in OLR events.

The OLR El Niño results of Figures 2.4 and 2.5 show many differences in detail from the Ropelewski and Halpert type figures (2.1), but overall are quite similar. Some of the difference surely arises from the very broad-brush approach taken in Figs 2.1, but OLR observations are only available from 1974 so the set of events is also different. It remains to be determined if the success of the OLR El Niño approach, for seasonal weather anomalies, will persist in coming decades, given the large amount of multi-decadal variability of ENSO.

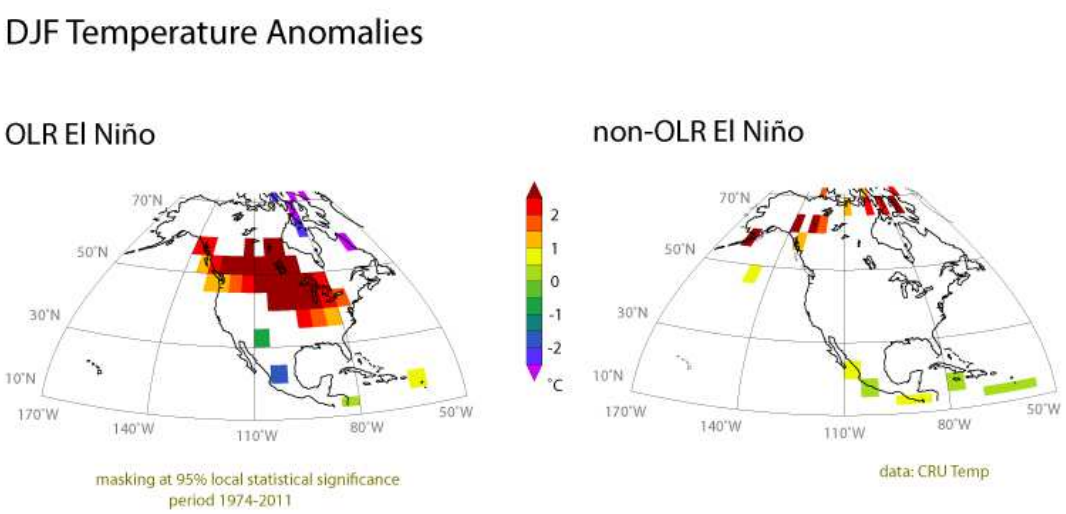

Figure 2.5 - El Niño 95% statistically significant DJF surface temp anomalies, OLR events vs. non-OLR events.

For ease of viewing, only results over North and Central America have been presented, but there is considerable power to the OLR approach for seasonal weather over most of the globe. Similar advantage in identifying La Niña years using an OLR index is also possible, but is not described here in the interests of space.

The take-home message concerning the relationships between El Niño and La Niña, and regional seasonal weather should be that there remains much to be explored about how to optimize characterization of these relationships. The tighter the relationships, the more skillful the seasonal weather predictions that can be offered to society. Each region of the globe that experiences substantial anomalies during ENSO events would be well advised to explore the most effective way of identifying those aspects of ENSO that are most determinative of their regional weather anomalies. The OLR perspective simply offers one new approach that might be useful for many regions.

3. Tropical Cyclones

For affected regions, tropical cyclones are among the most damaging of weather events. A big picture view of the areas of the globe can be gained from Figure 3.1, which is a satellite era summary of all tropical cyclone tracks. Many millions of humans are affected every year, and more developed regions can suffer losses in excess of a billion US Dollars from a single event.

ENSO influences tropical cyclone activity in the Atlantic and Pacific, and to a somewhat lesser extent, the Indian Ocean. Therefore, information on the present and future states of the Tropical Pacific atmosphere-ocean system has societal benefits in terms of seasonal forecasts of tropical cyclones and their impacts. There exists a large body of work on ENSO and tropical cyclones; here we include only a brief review with a few citations for those interested in pursuing the subject further.

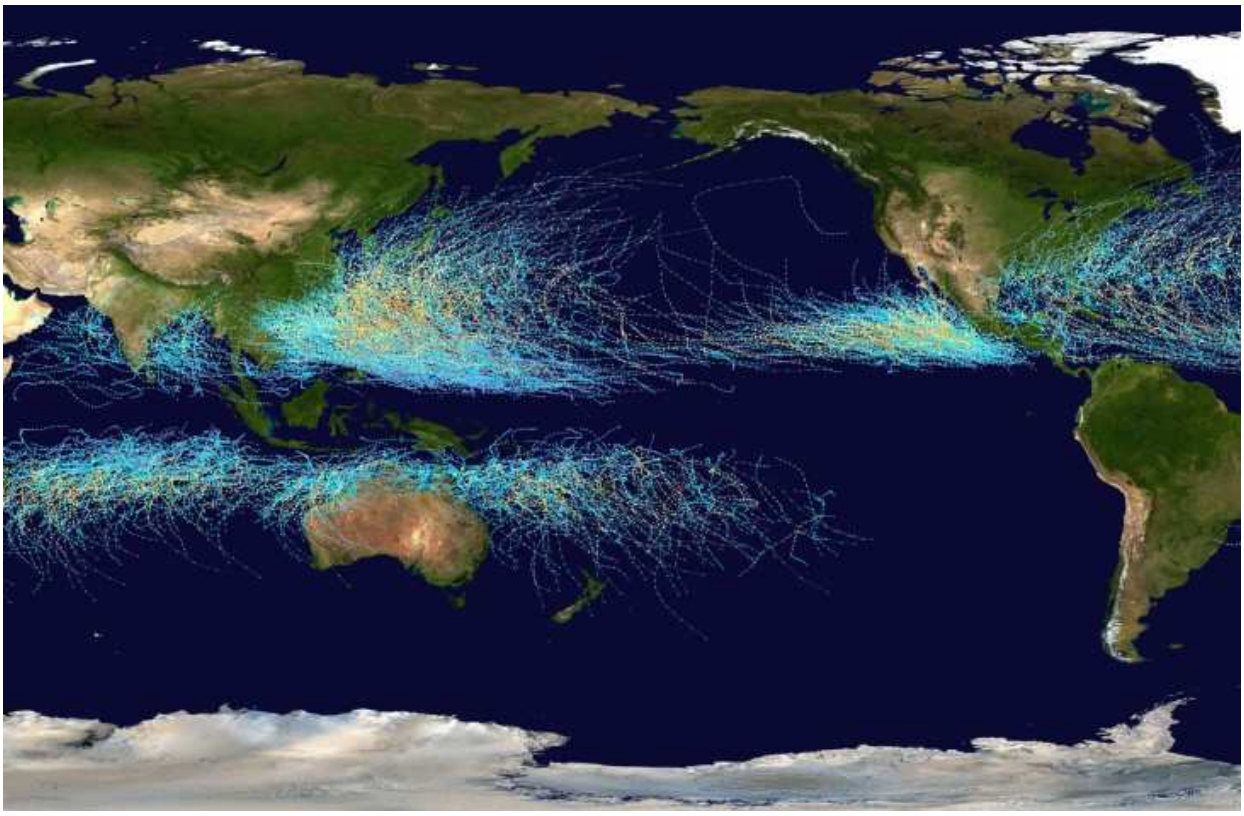

Figure 3.1 - Global tropical cyclone track summary (Source: http://www.wallpapersas.com/wallpaper/global-tropical-cyclone-tracks.html).

ENSO modulates the kinematic and thermodynamic properties of the environment related to the genesis, intensification and tracks of tropical cyclones, as reviewed by Landsea (2000), and Chu (2004). Its effects may be considered more direct in the Pacific and less direct in the Atlantic, with the latter response attributable to teleconnection patterns akin to those associated with ENSO-related seasonal weather anomalies outside of the Tropical Pacific. One of the systematic consequences of El Niño, for example, is an increase in the westerly wind in the upper troposphere across the Atlantic. This implies increased vertical wind shear, which suppresses the formation and intensification of tropical storms (Gray, 1984). It has also been shown that El Niño also tends to be accompanied by a more stable thermodynamic environment (Tang and Landsea, 2004). Hurricane seasons during El Niño also generally have fewer storms that form in the deep tropics from African easterly waves. This type of storm is more likely to enter the Caribbean Sea and make landfall in the US versus curving poleward over the open Atlantic Ocean. More or less opposite effects, in a general sense, have been found for La Niña, as illustrated in the tendency for the larger monetary damages during La Niña than El Niño (Figure 3.2, from Pielke and Landsea, 1999).

The Pacific Ocean includes three separate regions that feature tropical cyclones (Chu, 2004, among others). In the eastern North Pacific, tropical cyclone activity is enhanced during El Niño (opposite to that in the North Atlantic) and suppressed during La Niña. These variations in activity are less due to the frequency of individual storms (hurricanes) but rather more to ENSO's impact on their intensities. ENSO also tends to have effects on their tracks, with more

hurricanes propagating into the central Pacific, including near the Hawaiian Islands, during El Niño.

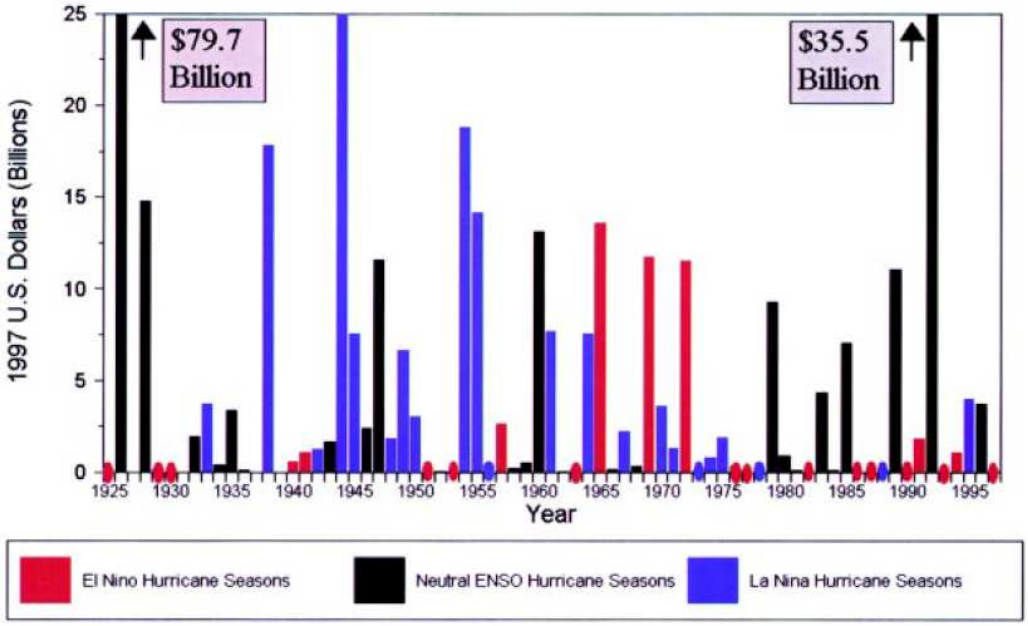

Figure 3.2 - Hurricane damage in normalized dollars for 1925-1997. Years with damages less than $500 million are indicated with ellipses on the x-axis (adapted from Pielke and Landsea 1999).

The western North Pacific both experiences a high frequency of tropical cyclones (typhoons) and is strongly influenced by ENSO, and so not surprisingly, the relationships here have received a fair amount of attention (Chan, 1985). The favored region of genesis for typhoons is shifted to the southeast during El Niño and this often results in longer tracks over warm water and hence greater intensities. They also tend to recurve sooner, and hence make landfall in the northern locations of Japan, South Korea and northern half of China. During La Niña, the landfall of typhoons is favored in the Philippines, Vietnam and southern China. The southwestern Pacific experiences a similar response with respect to ENSO. As shown in Figure 3.3 (adapted from Camargo et al., 2007), ENSO tends to shift the genesis region for tropical cyclones similarly for north and south of the equator in the western Pacific. But while there are fewer storms that develop in the vicinity of Australia during El Niño, the overall tropical cyclone activity here is actually greater when the SLP at Darwin was lower in the preceding season (Nicholls, 1979), i.e., when the SOI is negative.

The relationships between ENSO and Indian Ocean tropical cyclones are of a similar nature to those for the western Pacific. In particular, ENSO appears to have little systematic effect on the frequency of storms, but does influence genesis locations and tracks in the southwestern part of the basin, with implications for the risk of storms making landfall in Madagascar and southeast Africa.

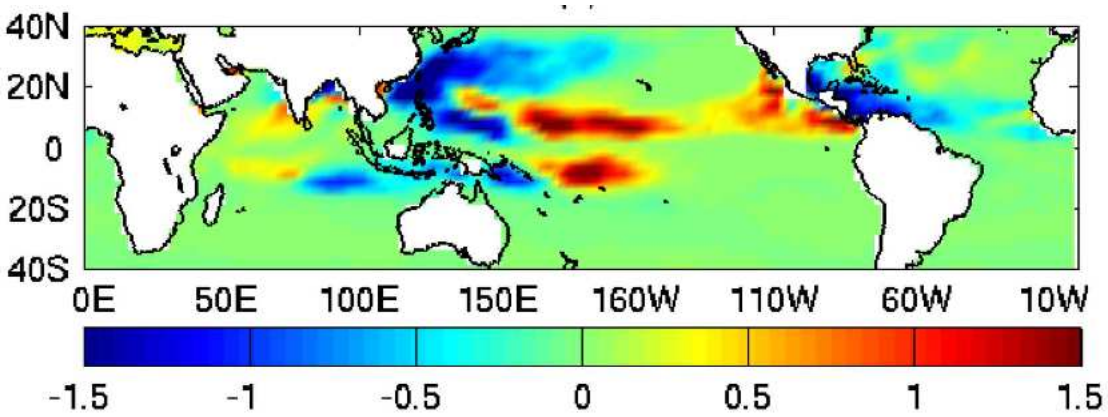

Figure 3.3 - Difference between El Niña and La Niña in terms of genesis potential (based on a combination of vorticity, vertical wind shear, potential intensity, and humidity) during August-October (adapted from Camargo et al., 2007).

Finally, we note that the linkages between ENSO and tropical cyclones are not fully understood. Future research should ultimately improve not just seasonal predictions, but could also address a number of open questions. For example, considerable recent attention has focused on the diversity in the nature of individual ENSO events. Some research has been carried out on how different kinds of events impact tropical cyclones (Kim et al., 2011), but there is more to be done. Many tropical cyclones undergo a transition to extra-tropical storms, especially late in the season, and these storms can be intense. The transitions are presumably modulated by perturbations in SST and mean atmospheric circulation patterns associated with ENSO, but these modulations have not been elucidated. From a climate perspective, tropical cyclones have been recognized for their role in transporting heat poleward (Emanuel, 2001), and it stands to reason that this process is influenced by upper ocean temperature patterns accompanying ENSO. How will global climate change impact the characteristics of ENSO related to tropical cyclones? These are issues of scientific interest and practical importance.

4. Ecosystem Impacts

Fluctuations in the atmosphere-ocean climate system associated with ENSO are known to impact a variety of marine ecosystems. The objective of this section is to point out the nature of some of these connections, drawing upon examples from the Pacific Ocean. Because the effects of ENSO can be large, its ramifications on ecosystems and fisheries are important from a host of perspectives (economic, conservation, cultural, etc.).

The eastern equatorial Pacific features the upwelling of nutrients from depth into the euphotic zone, and hence relatively high rates of primary production. As might be expected, ENSO modulates this process (Pennington et al., 2006), with implications for the entire marine food web (Barber and Chavez, 1983). Figure 4.1 from Harrison and Chiodi (2014) offers snapshots of satellite-based estimates of near-surface chlorophyll-a across the Tropical Pacific; one near the end of the major 1997 El Niño and the other in the middle of the intense 1998 La Niña. The suppression of upwelling in the first case results in a dramatic reduction of chlorophyll-a compared with the levels in the La Niña conditions.

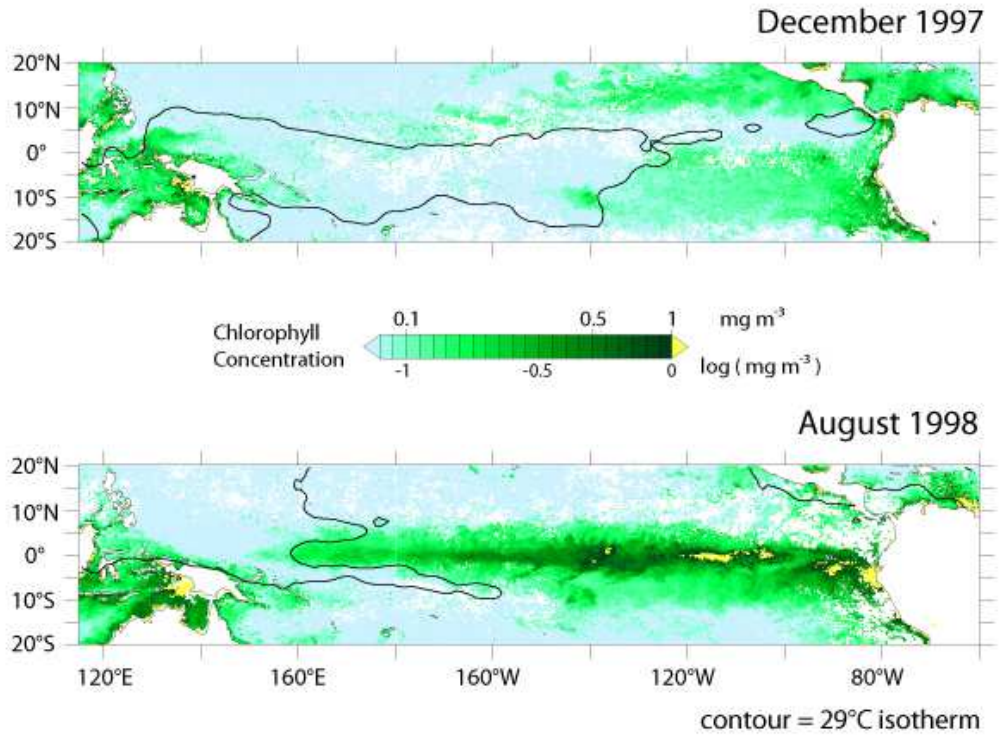

Figure 4.1 - Monthly average near-surface chlorophyll during peak El Niño conditions (December 1997) and strong La Niña conditions (August 1998).

ENSO's impacts on the ecosystem are not solely through bottom-up processes. For example, anomalies in upper ocean temperatures in the western Tropical Pacific with El Niño and La Niña result in systematic shifts in the range of longitudes favored by skipjack tuna (*Katsuwonus pelamis*) as shown in Figure 4.2 (from Lehodey et al., 1997). This species typically ranks as second or third worldwide in terms of catch by weight, and so being able to anticipate variations in its distribution is of great practical importance, particularly since it is targeted by fisheries from a number of countries and subject to international management. In addition, the inter-dependency among the various species comprising the ecosystem can produce indirect effects. Breeding success for two species of western Pacific pelagic terns is systematically related to ENSO (Figure 4.3; Devney et al., 2009); this relationship has been attributed in part to the accessibility of their prey (forage fish) which tend to be more concentrated near the surface in the presence of sub-surface predators such as tuna (Jaquemet et al., 2004).

A variety of regions outside of the Tropical Pacific also have been shown to have a strong biological response to ENSO. A prime example is the California Current System (CCS), for which a large body of research has already been carried out (Chelton et al., 1982, McGowan et al., 1998, Chavez et al., 2002, among others). The physical connection between this region and the Tropical Pacific is through both coastally-trapped waves in the upper ocean, and the local response to anomalous winds accompanying large-scale atmospheric teleconnection patterns, primarily involving changes in the strength and location of the Aleutian Low. The typical result of El Niño is a depression of the thermocline and warmer SST, and a decline in lower-trophic level productivity, especially in the southern portion of the CCS.

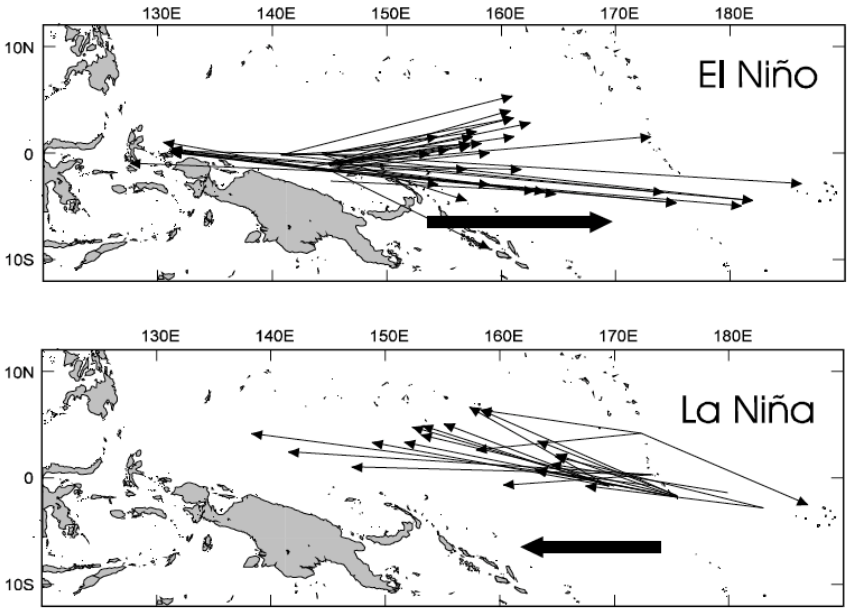

Figure 4.2 - Displacement of tagged skipjack tuna with ENSO events from a programme carried out by the Secretariat of the Pacific Community (SPC) organization (adapted from Lehodey et al. 1997).

An important consequence of ENSO for the CCS is a change in zooplankton community structure. Hooff and Peterson (2006) have shown that sub-tropical (sub-arctic) species of copepods are favored off the coast of Oregon during El Niño (La Niña and neutral intervals), as shown in Figure 4.4.

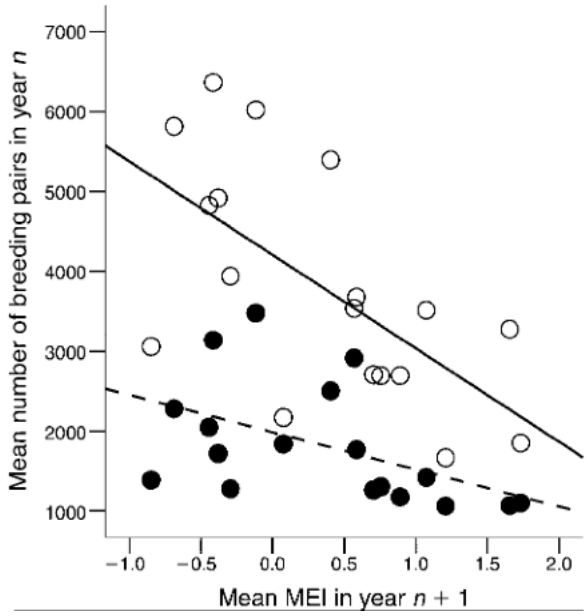

Figure 4.3 Number of breeding pairs of sooty terns (open circles) and common noddy (solid circles) on Michaelmas Cay of the Great Barrier Reef of Australia versus the Multivariate El Niño index (MEI) for the period of 1984-2001 (adapted from Devney et al. 2009).

This is an important effect because the copepod species frequent in this region that are characteristic of cooler waters tend to have relatively high lipid contents, and represent superior prey for juvenile salmon and other species ranging from forage fish to seabirds. It bears noting that ENSO's reach also extends well south of the tropics along the west coast of South America (Jordan) and as far as 60 N in the Gulf of Alaska (Bailey et al., 1995).

We close this sub-section with a few general points regarding linkages between ENSO and marine ecosystems, with relevance to other ENSO applications. Perhaps to an extent it is obvious, but it is worth emphasizing that the diversity in the strength and nature (e.g., longitude of peak anomalies) of ENSO events, and hence their remote effects/teleconnections, imply corresponding differences in the biological response (DiLorenzo et al., 2013 and references therein). The variability in the biological response means there is a potential for false attribution. That being said, accounting for the variability in the physical environment, including but not limited to phenomenon such as ENSO, should be incorporated in fisheries management.

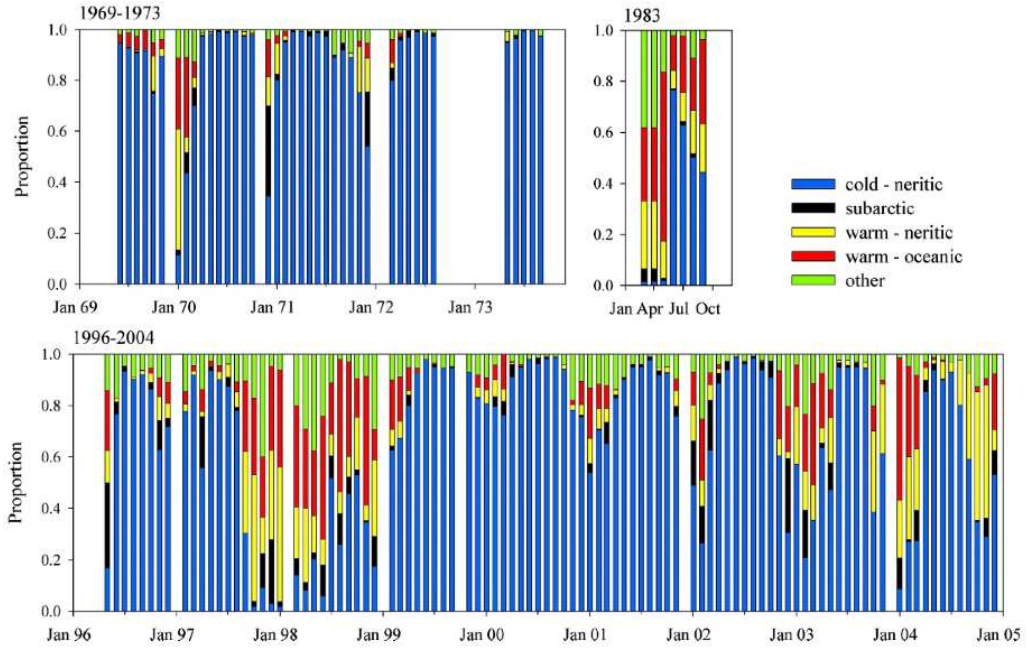

Figure 4.4 - Monthly average fraction of copepod assemblages relative to total copepod biomass. This time series includes the El Niño events of 1969-70, 1982-83, 1997-98 and 2002-03. It is normal to have a greater proportion of warm-water copepods in winter, when the prevailing winds are from the south, than during summer, when winds are from the north (adapted from Hooff and Peterson, 2006).

5. ENSO Impacts in Latin America, 2005 - 2012

To illustrate how ENSO events importantly affect the region of the world that gave the name "El Niño" to us, we consider the 'big picture' impact picture for Latin America and describe the weather anomalies associated with recent ENSO anomalous conditions. It is important to clarify that most of the documented impacts in the region are the result of the interaction of ENSO and the negative phase of the Pacific Decadal Oscillation (PDO). The last decade was characterized by predominant cooler than normal conditions in the South Eastern Pacific, and these modulate

the ENSO influence at local level. The relationships are not clearly understood, and the attribution always will be a challenge, however, this compilation of impacts, which is based on expert reports from the different countries in Latin America, attempts to provide a first view of their magnitude, frequency, and diversity despite the relative moderate ENSO activity during these years.

Severe and persistent climate anomalies in Latin America and the Caribbean are closely linked with inter-annual variability (ENSO). The region comprises equatorial to mid-latitudes environments and a very wide diversity of climate regimes. The responses to different phases of ENSO include severe droughts, extreme rainfalls and temporal shifts in seasonal evolution. Considering the increasing vulnerability in the coastal zone and highlands, ENSO impacts are amplified with subsequent effects in economies and human wellbeing. This section describes climate impacts in Mexico, Central and South America associated with ENSO events during 2005-2012 years. In this period, 16.6% of years were under influence of El Niño (warm ENSO phase), 39.6% were under the influence of La Niña (cold ENSO phase), and 43.7% of those years were neutral. Hence, this last decade evidences the predominance of cooler SST anomalies. There were two warm events: 2006-2007 El Niño (moderate intensity), and 2009-2010 El Niño (stronger intensity but not comparable with 1982-1983). In contrast, there were five cold events: 2005-2006 La Niña (weak), 2007-2008 La Niña (moderate and extended to one year), 2008-2009 La Niña (weak), 2010-2011 La Niña (strong), and 2011-2012 La Niña (moderate).

In general terms, during La Niña occurrence, most of tropical South America to the East of the Andes is warmer than normal with more than normal rainfall in South Eastern Brazil. Conversely, southern South America is affected by rainfall negative anomalies and colder conditions. However, these typical teleconnections could be modulated for other climate variability modes (such us decadal), or more regional factors.

Central American El Niño impacts

El Niño 2006-2007

The 2006-2007 El Niño began in the second half of 2006. It was a short and weak episode, ending in the first quarter of 2007. A slight decrease in hurricane frequency in the Caribbean, and drier conditions than normal over Central America were observed during most of the year. Cold fronts with strong winds and rainfall affecting Guatemala, Honduras and Central Panama were recorded (Ramirez and Fernandez, 2007). Rainy season in Mexico was wetter than normal at the beginning of 2007 (Davydova-Belitskaya, 2007). During the first half of 2006, Brazil experienced a severe drought, which caused losses in 11% soybean and 48% wheat crops (Marengo and Baez, 2008). In contrast, during the 2006-2007 period, extreme rainfall and flooding comparable to the 1997-1998 ones occurred in Southern Brazil and Bolivia (Lopez and Russticucci, 2008).

El Niño 2009-2010

The 2009-2010 El Niño started in the second half of 2009. In July 2009, Mexico had the driest month since 1949 (Davidova-Belitskaya and Romero-Cruz, 2010). Drier than normal conditions were reported in Cuba and Venezuela, with strong impacts on the agriculture and energy

sectors. During 2009, the tropical hurricane frequency was below normal (Amador et al., 2010). Drier than normal conditions were observed in Colombia, Ecuador, northeast Amazonia and Bolivia during the second half of 2009. In Paraguay, strong temperature anomalies were observed (4ºC to 5ºC) while above normal rainfall was reported in Brazil, Paraguay, Uruguay and Peru. These events forced the evacuation of thousands of people.

La Niña impacts

La Niña 2005-2006

The 2005-2006 La Niña started in the last quarter of 2005, and ended in mid-2006. Some related impacts were observed in Mexico with warmer and wetter than normal conditions associated with a high frequency of tropical cyclones, which affects several countries in Central America, especially Guatemala where a third of total population was impacted, as more than 1,000 people killed (Cortez Vazquez, 2006). Most of the Central American countries, especially Honduras, Nicaragua and Costa Rica, also experienced droughts with severe impacts on water resources and agriculture (Grover-Kopec, 2006). During 2005, most of South America evidenced below normal rainfall except for some specific areas in the northeast and southwest of the continent. The temperature was below normal on the Western coast of South America, but above normal on the Caribbean and Atlantic coasts (Rusticucci and Camacho, 2006). During the second half of 2005, Colombia was severely affected by La Niña. Intense and persistent precipitations caused flooding and landslides, which killed about 500 people, and destroyed more than 1,000 houses. Additionally, severe damage in basic infrastructure was reported (Pabon, 2006).

La Niña 2007-2008

La Niña 2007-2008 started in the second half of 2007, and ended in mid-2008. Mexico experienced above normal precipitation associated with an increased frequency of tropical storms and cold fronts. At the end of 2007, Tabasco City registered the worst flooding in the history, with over 80% of its area affected by the flood (Davydova-Belitskaya and Romero-Cruz, 2008). South America experienced very low temperatures in the south of the continent (-22ºC in Argentina and -18ºC in Chile (Marengo and Baez, 2008)), and positive precipitation anomalies between 40% and 60% in the Amazonia. Severe precipitations in Bolivia killed 30 people, and affected up to 25,000 people. More than 10,000 hectares of subsistence crops were destroyed, with more than 30,000.000 USD of losses (Ramirez, 2008). In Brazil, severe rainfalls killed 5 people and affected more than 50,000 people in Rio de Janeiro (Marengo et al., 2009).

La Niña 2008-2009

La Niña 2008-2009 started in the last quarter of 2008, and ended in the first quarter of 2008. It could be considered as an extension of the previous cold episode from 2007-2008. One of the associated impacts was the high frequency of tropical storms in 2008. Mexico evidenced a mean temperature anomaly of 0.7 ºC (Davydova-Belitskaya and Romero-Cruz, 2009). In most of Central America below normal precipitations were observed (Amador et al., 2009) during the first half of 2008. In South America, during 2008, above normal precipitation was reported at the coasts of Suriname, Guyana, Colombia and Ecuador, while in Venezuela, Colombia and southern Peru (Martinez et al., 2009) below normal precipitation was observed. During the first

quarter of 2009, negative precipitation anomalies were reported in Southern Peru (-60%), Bolivia (-62%) and the Ecuadorian coast (-60%). In contrast, La Niña effects in Colombia were associated with positive precipitation anomalies between 40% and 70% (Martinez et al., 2010). During the first quarter of 2009, positive temperature anomalies between 3ºC and 4ºC were observed to the east of the Andes. In contrast, after La Niña finished in mid-2009, negative anomalies up to -3ºC were observed in Southern Brazil (Marengo et al., 2010). During the first months of 2009, positive precipitation anomalies between 25% and 50% were observed in the Amazonia while anomalies up 100% were registered in Northeast Brazil (Marengo, 2010).

La Niña 2010-2011

La Niña 2010-2011 started in mid-2010 and lasted approximately one year. The year 2010 has had a high frequency of tropical storms in the Caribbean (Amador et al., 2011). In August 2010, several tropical depressions coming from the Pacific caused intense rainfall along the southern Mexican coast (Davydova-Belitskaya and Romero-Cruz, 2011). La Niña influence was more evident during the first quarter of 2011, as most of South America reported below normal temperature with highest anomalies between -0.5ºC a -2ºC in Colombia, Ecuador and Peru. Several extreme cold temperatures (up to -20 ºC) were registered in the Bolivian-Peruvian Altiplano (Marengo et al., 2011). Positive precipitation anomalies associated with La Niña were reported in Venezuela (166%), Colombia (156 % to 200%), eastern llanos in Bolivia, central and northern highlands in Peru (400%) and in coastal areas of Ecuador and Peru (0 to 80%) (Martinez-Guingla et al., 2012).

La Niña 2011-2012

La Niña 2011-2012 started in the second half of 2011, and extended to the second half of 2012. In Mexico, the drought was persistent during 2011 jointly with high temperatures that reached an annual average anomaly of 1.1 ºC (second warmest year since 1971). This led to a record on burned areas caused by bushfires, with 956,405 hectares lost (Lobato-Sanchez, 2012). In South America, some of the remarkable impacts of La Niña were the positive precipitation anomalies in Ecuadorian highlands and northern and Central Peru (between 150%-800%) (Martinez-Guingla et al., 2012). During 2012, most of tropical South America to the East of the Andes was warmer than normal with anomalies up to 1ºC. In North of Paraguay and southern Bolivia, the temperature anomalies were up to 3ºC. In January 2012, strong precipitation was recorded in South East Brazil affecting 53 cities and killing 7 people. During the first quarter of 2012, above normal precipitation associated with La Niña were reported in Trinidad and Tobago (184%), Grenada (200%). In March 2012, Colombia was affected by severe flooding in 18 of the 32 departments with more than 66,000 affected people (Marengo et al., 2013). Conversely, the South of South America was affected during the first quarter of 2012 by deficit of precipitation (Bidegain et al., 2013).

6. ENSO effects on the increase of atmospheric carbon dioxide

We have not addressed so far any of the various ways that ENSO can be important in the global scale evolution of planetary conditions. Climate change is on the minds of many, and understanding the persistent and time-varying impacts likely to occur in the future is important. ENSO plays a very significant role in determining the changes in atmospheric carbon dioxide

concentration that are seen each year. In fact, the effects of a strong El Niño can account for nearly as much exchange of carbon between the earth's surface and the atmosphere as anthropogenic activity. The effects of La Niña on the global carbon cycle, on the other hand, typically counteract, to a substantial extent, the effects of anthropogenic carbon emissions. The strong effects of natural variability in the observed atmospheric growth rate are clearly seen in Figure 6.1 (Harrison and Chiodi, 2014), which plots the atmospheric carbon dioxide concentration time series from Mauna Loa (black curve; Keeling et al.,2001) along with the estimated amounts of carbon dioxide emitted by the burning of fossil fuels (Boden et al., 2011), scaled such that the concentration curve would track emissions if all emitted carbon dioxide remained airborne and there were no other sources of variability. Evidently, much of the emitted carbon is re-absorbed by the surface (ocean and land) and the strong year-to-year variability in the observed carbon dioxide concentration is contributed by sources other than fossil fuel consumption.

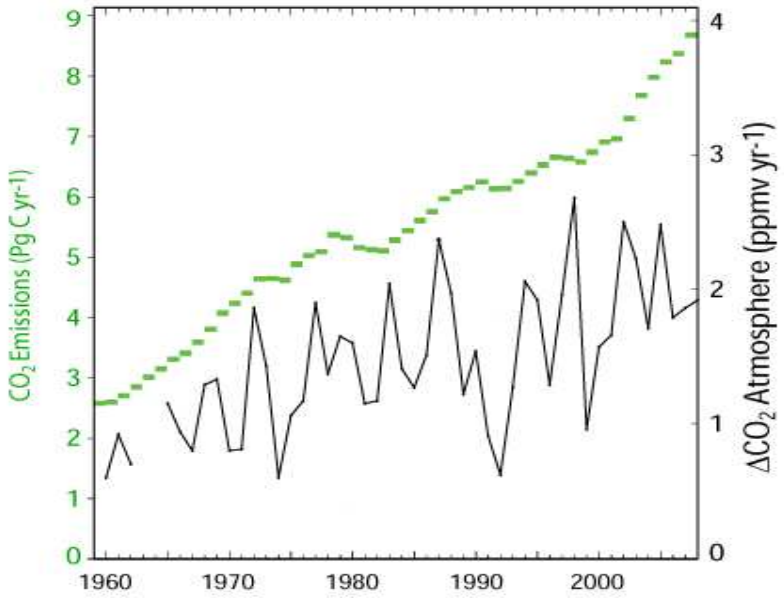

Figure 6.1 - Atmospheric concentration of CO2 (Mauna Loa) and year to year change in concentration. Note strong interannual variability in change of concentration.

Figure 6.2 shows the annual increase in atmospheric carbon dioxide concentration year by year once the trend from fossil fuel emissions is removed and shows the strong similarity of behavior between El Niño years (the conspicuous exception is 1991-92, with the strong Mt Pinatubo explosion). Concentration changes of the opposite-sign, but very similar event by event behavior, are seen during La Niña years. Figure 6.3 shows the composite effects of El Niño and of La Niña events; La Niña effects are smaller than those from El Niño and occur somewhat differently during the year, but still account for a substantial change in the atmospheric growth rate. The La Niña average and El Niño average effects listed in Figure 6.3 are roughly 1/3rd and 2/3rd of the average annual growth rate seen over the last 50 years.

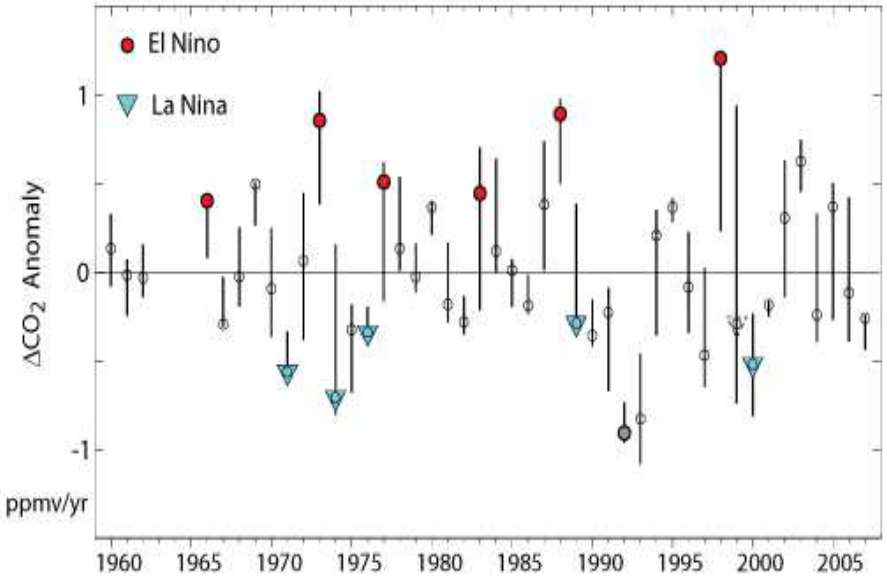

Figure 6.2 - Year to Year change in concentration, with trend removed. El Niño and La Niña years identified.

Clearly, if the statistics of ENSO are to change under global climate change, as has been suggested recently by analysis of the CMIP3 and CMIP5 coupled climate change models, the future trajectory of atmospheric carbon will also be affected.

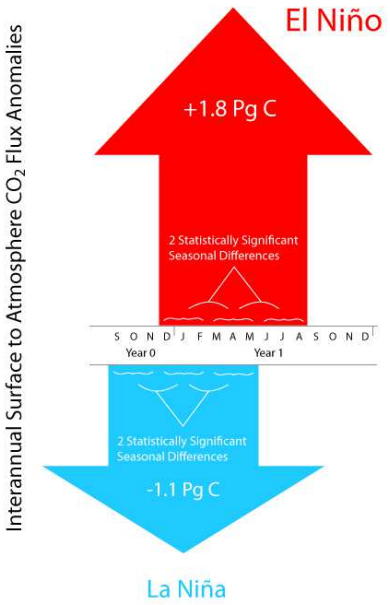

Figure 6.3 - The average effect of El Niño and La Niña years on atmospheric carbon dioxide concentration, and the seasons over which the change takes place.

7. Discussion

We have provided several examples of how ENSO affects conditions that have societal impact. Understanding how to predict ENSO events better as well as how different sorts of ENSO events affect different nations in different seasons, remains very much a work in progress despite the efforts of the ENSO research, prediction and impacts communities. Many societies suffer profound impacts, on average, during El Niño and/or La Niña events. The companion impacts paper to this one (Zebiak et al., 2014) provides examples of impacts on agriculture and health, which we have not addressed here. Other White Papers prepared for this workshop will provide insight into the challenges of better observing, understanding and predicting ENSO events.

ENSO is also connected with other large scale climate anomaly patterns, and these connections are the subject of on-going research. There are well known links to low frequency SSTA variability of the North Pacific, which can be considered from the perspectives of the Pacific Decadal Oscillation or North Pacific Oscillation or the Inter-Pacific Oscillation. There are also links to Indian Ocean patterns of SSTA variability, which can be considered on their own or through the Indian Ocean Dipole perspective.

References:

Amador, J.A., Alfaro, E.J., Rivera, E.R., and Calderon, B. (2009): Central America and the Caribbean (in "State of the Climate in 2008"). Bull. Amer. Meteor. Soc., 90 (8), pp.130-131.

Amador, J.A., Alfaro, E.J., Hidalgo, H.G., Rivera, E.R., and Calderon, B. (2010): Central America and the Caribbean (in "State of the Climate in 2009"). Bull. Amer. Meteor. Soc., 91 (7), pp. 143-144.

Amador, J.A., Alfaro, E.J., Hidalgo, H.G., and Calderon, B. (2011): Central America and the Caribbean (in "State of the Climate in 2010"). Bull. Amer. Meteor. Soc., 92 (6), pp. 182-183.

Ashok, K., Behera, S.K., Rao, S.A., Weng, H., and Yamagata, T. (2007): El Niño Modoki and its possible teleconnection. J.G.R. 112, C11007.

Ashok, K., and Yamagata, T. (2009): The El Niño with a difference. Nature Vol.461, pp. 481-484.

Bidegain, M., Skansi, M., Penalba, O., and Quintana, J. (2013): Southern South America. (in "State of the Climate in 2012"). Bull. Am. Met. Soc. **94** (8).

Botsford. L.W., Castilla, J.C., and Peterson, C.H. (1997): The management of fisheries and marine ecosystems. Science, 277, pp. 509-515.

Bailey, K.M., and Co-authors (1995): ENSO events in the northern Gulf of Alaska, and effects on selected marine fisheries. CalCOFI Rep., Vol. 36, pp. 78-96.

Barber, R.T., and Chavez, F.P. (1983): Biological consequences of El Niño. Science, 222, pp. 1203–1210.

Boden, T.A., Marland, G., and Andres, R.J. (2011): Global, Regional, and National Fossil-Fuel CO_2 Emissions Carbon Dioxide Information Analysis Center, Oak Ridge National Laboratory, U.S. Department of Energy, Oak Ridge, Tenn., U.S.A. (doi 10.3334/CDIAC/00001_V2011).

Botsford, L.W., Castilla J.C., and Peterson, C.H. (1997): The management of the fisheries and marine ecosystems. Science 277, pp. 509-515 (doi: 10.1126/science.277.5325.509).

Camargo, S.J., Emanuel, K.A., and Sobel, A.H. (2007): Use of a genesis potential index to diagnose ENSO effects on tropical cyclone genesis. J. Climate, 20, pp. 4819–4834.

Chan, J. C. L. (1985): Tropical cyclone activity in the northwest Pacific in relation to the El Niño/Southern Oscillation phenomenon. Mon. Wea. Rev., 113, pp. 599–606.

Chavez, F. P., Pennington, J. T., Castro, C. G., Ryan, J. P., Michiaski, R. P., Schlining, B., Walz, P., Buck, K. R., McFadyen, A., and Collins, C. A. (2002): Biological and chemical consequences of the 1997–98 El Niño in central California waters. Prog. Oceanogr, PII: S0079-6611(02) 00050-2.

Chelton, D. B., Bernal, P. A., and McGowan, J. A. (1982): Large-scale interannual physical and biological interaction in the California Current. J. Mar. Res., 40, pp. 1095–1125.

Chiodi, A.M. and Harrison, D.E. (2013): Characterizing warm-ENSO Variability in the Equatorial Pacific – An OLR Perspective. J.Climate 23, pp. 2428-2439, (doi: 10.1175/2009JCLI3030).

Chiodi, A.M. and Harrison, D.E. (2013): El Niño impacts on seasonal U.S. atmospheric circulation, temperature and precipitation anomalies: The OLR-event perspective. *J. Climate, 26(3),* (doi: 10.1175/JCLI-D-12-00097.1, 822–837).

Chiodi, A.M., and Harrison, D.E. (2014): Comment on Qian et al. (2008) – La Niña and El Niño composites of atmospheric CO_2 change. Tellus B 66, 20428, (doi: 10.34027tellusb.v66.20428).

Chu, P.S. (2004): ENSO and tropical cyclone activity. In Hurricanes and Typhoons: Past, Present and Potential. (Editors: Murnane, R.J., and Liu, K.B., Columbia University Press), pp. 297-332.

Cortez Vázquez, M. (2006): Mexico [in “State of the Climate in 2005”]. Bull. Amer. Meteor. Soc., **87 (**6), pp. 66-67.

Davydova-Belitskaya, V., and Romero-Cruz, F. (2008): Mexico [in “State of the Climate in 2007”]. Bull. Amer. Meteor. Soc., 89 (7), pp. 120-121.

Davydova-Belitskaya, V., and Romero-Cruz, F. (2009): Mexico [in “State of the Climate in 2008”]. Bull. Amer. Meteor. Soc., 90 (8), pp. 128-130.

Davydova-Belitskaya, V., and Romero-Cruz, F. (2010): Mexico [in “State of the Climate in 2009”]. Bull. Amer. Meteor. Soc., 91 (7), pp. 142-143.

Davidova-Belitskaya, V., and Romero-Cruz, F. (2011): Mexico, Bull. Am. Met. Soc., 92

Deser, C., and Wallace, J.M. (1987): El Niño events and their relationship to the Southern Oscillation: 1925-1986. J. of Geophys. Res., 92, C13, pp. 14189-14196.

Deser, C., and Wallace, J.M. (1990): Large-scale atmospheric circulation features of warm and cold episodes in the Tropical Pacific. J. Climate, 3, pp. 1254-1281.

Devney, C.A., Short, M., and Congdon, B.C. (2009): Sensitivity of tropical seabirds to El Niño precursors. Ecology 90, pp. 1175-1183.

Di Lorenzo, E., Combes, V., Keister, J.E., Strub, P.T., Thomas, A.C., Franks, P.J.S., Ohman, M.D., Furtado, J.C., Bracco, A., Bograd, S.J., Peterson, W.T., Schwing, F.B., Chiba, S., Taguchi, B., Hormazabal, S., and Parada, C. (2013): Synthesis of Pacific Ocean climate and ecosystem dynamics. Oceanography, Vol. 26 (4), pp. 68-81.

Emanuel, K. (2001): Contribution of tropical cyclones to meridional heat transports by oceans. J. Geophys. Res., 106, pp. 14,771-14,781.

Goddard, L., and Dilley, M. (2005): El Niño - Catastrophe or Opportunity. J. Climate, 18, pp. 651-655.

Gray, W. M. (1984): Atlantic seasonal hurricane frequency. Part I: El Niño and 30 mbQuasi-Biennial Oscillation influences. Mon. Wea. Rev., 112, pp. 1649–68.

Grover-Kopec, E. K. (2006): Central America and the Caribbean [in “State of the Climate in 2005”]. Bull. Amer. Meteor. Soc., **87** (6), pp. 68.

Halpert, M.S., and Ropelewski, C.F. (1992): Surface temperature patterns associated with the Southern Oscillation, J. Climate 5, pp. 577-593.

Harrison, D.E., and Chiodi, A.M. (2014): Multi-decadal variability and trends in the El Niño-Southern Oscillation and Tropical Pacific fisheries implications. Deep-Sea Res. II, (doi: 10.1016/j.dsr2.2013 .12.020).

Harrison, D.E., and Larkin, N.K. (1997): The Darwin Sea Level Pressure record, 1876-1996; Evidence for climate change? Geophysical Research Letters, 24, pp. 1779-1782.

Harrison, D.E., and Larkin, N.K. (1998): El Niño-Southern Oscillation surface temperature and wind anomalies, 1946-*1993.* Rev Geophysics, 36, pp. 353-399.

Harrison, D.E., and Larkin, N.K. (2002): Cold events - Anti-El Niño? In: Glantz, M.H. (Editor), Facts and Speculation about La Niña and Its Societal Impacts. Tokyo, Japan: United Nations University Press*,* pp. 237-241.

Hooff, R. C. and Peterson, W. T. (2006): Copepod biodiversity as an indicator of changes in ocean and climate conditions of the northern California current ecosystem. Limnol. Oceanogr., 51, pp. 2607–2620.

Jaquemet, S., Le Corre, M., and Weimerskirch, H. (2004): Seabird community structure in a coastal tropical environment: Importance of associations with sub-surface predators and of fish aggregating devices (FADs). Mar. Ecol. Prog. Ser. 268, pp. 281–292.

Jordan, R. S. (1991): Impact of ENSO events on the southeastern Pacific region with special reference to the interaction of fishing and climate variability. In: Glantz, M., Katz, R. and Nicholls, N. (eds.), ENSO teleconnections linking worldwide climate anomalies: scientific basis and societal impacts. Cambridge University Press, Cambridge, pp. 401-430.

Keeling, C.D., Piper, S.C., Bacastow, R.B., Wahlen, M., Whorf, T.P., Heimann, M., and Meijer, H. A. (2001): Exchanges of atmospheric CO_2 and $^{13}CO_2$ with the terrestrial biosphere and oceans from 1978 to 2000. I. Global aspects, SIO Reference Series, No. 01-06, Scripps Institution of Oceanography, San Diego.

Kim, H.M., Webster, P.J., and Curry, J.A. (2011): Modulation of North Pacific tropical cyclone activity by three phases of ENSO. J. Climate, 24, pp. 1839-1849.

Kosaka, and Xie (2013): Recent global warming hiatus tied to equatorial Pacific surface cooling. Nature. (doi:10.1038/nature12534).

Landsea, C.W. (2000): El Niño/Southern Oscillation and the Seasonal Predictability of Tropical Cyclones. In El Niño and the Southern Oscillation: Multiscale Variability and Global and Regional Impacts, H.F. Diaz and V. Markgraf, eds., Cambridge University Press, pp. 149-181.

Larkin, N.K., and Harrison, D.E. (2001): Tropical Pacific ENSO Cold Events, 1946-1995; SST, SLP and Surface Wind Composite Anomalies. J. Climate, 14, pp. 3904-3931.

Larkin, N.K., and Harrison, D.E. (2002): ENSO Warm (El Niño) and Cold (La Niña) Event Lifecycles: Ocean surface anomaly patterns, their symmetries, asymmetries, and implications. J. Climate, *15,* pp. 1118-1140.

Larkin, N.K. and Harrison, D.E. (2005): On the definition of El Niño and US seasonal weather anomalies GRL, 32(13), L13705.

Lazo, J., M. Lawson, Larsen, P.H. and Waldman, D.M. (2011): Sensitivity of the US Economy to weather variability, Bull. Am. Met. Soc. (doi: 10.1175/2011BAMS2928.1).

Lehodey, P., Bertignac, M., Hampton, J., Lewis, T., and Picaut, J. (1997): El Niño Southern Oscillation and tuna in the western Pacific. Nature, 389: pp. 715–718.

Lobato-Sanchez, R., Pascual-Ramirez, R., and Albanil-Encarnacion, A. (2012): Mexico. Andes (in “State of the Climate in 2011”). Bull. Amer. Meteor. Soc., 93.

Lopez Carmona, P., and Rusticucci, M. (2008): South America [in “State of the Climate in 2007”]. Bull. Amer. Meteor. Soc., 89 (7), pp. 124-126.

Marengo, J.A., and Báez, J. (2008): Tropical South America, East of the Andes [in “State of the Climate in 2007”]. Bull. Amer. Meteor. Soc., 89 (7), pp. 128-129.

Marengo, J.A., Baez, J., and Ronchail, J. (2009): Tropical South America East of the Andes [in “State of the Climate in 2008”]. Bull. Amer. Meteor. Soc., 90 (8), pp. 134-135.

Marengo, J.A., Alves, L.M., Ronchail, J., and & Baez, J. (2011): Tropical South America, East of the Andes [in “State of the Climate in 2010”]. Bull. Amer. Meteor. Soc., 92.

Marengo, J.A., Ronchail, J., and Alves, L.M. (2013): Tropical South America, East of the Andes [in “State of the Climate in 2012”]. Bull. Amer. Meteor. Soc., 94.

Martinez, R., Pabon, D., Leon, G., Jaimes, E., Quintero, A., and Mascarenhas, A. (2009): Northern South America and the Tropical Andes [in “State of the Climate in 2008”]. Bull. Amer. Meteor. Soc., 90 (8), pp. 133-134.

Martinez, R., A. Mascarenhas, E. Jaimes, G. Leon, A. Quintero and G. Carrasco, 2010: Northern South America and the Tropical Andes [in “State of the Climate in 2009”]. Bull. Amer. Meteor. Soc., 91 (7), S146-S148.

Martinez-Guingla, R., Arevalo, J., Carrasco, G., Jaimes, E., and Leon, G. (2011): Northern South America and the Tropical Andes [in “State of the Climate in 2010”]. Bull. Amer. Meteor. Soc., 92.

McGowan, J. A., Cayan, D. R., and Dorman, L. M. (1998): Climate-ocean variability and ecosystem response in the northeast Pacific. Science, 281, pp. 210–217.

Nicholls, N. (1979): A possible method for predicting seasonal tropical cyclone activity inthe Australian region. Mon. Wea. Rev., 107, pp. 1221–24.

Pabon, J.D. (2006): Northern South America and the Southern Caribbean [in “State of the Climate in 2005”]. Bull. Amer. Meteor. Soc., 87 (6), p. 69.

Pennington, J.T., and Co-authors (2006): Primary production in the eastern Tropical Pacific - A review. Prog. Oceanogr. 69, pp. 285-317.

Pielke, R.A., and Landsea, C.N. (1999): La Niña, El Niño and Atlantic Hurricane Damages in the United States. Bull. Amer. Meteor. Soc., 80, pp. 2027–2033.

Ramírez, P., and Perez Fernández, J. (2007): Central America and the Caribbean [in “State of the Climate in 2006”]. Bull. Amer. Meteor. Soc., 88 (6), pp. 88-89.

Ramirez, P. (2008): Central America and the Caribbean [in “State of the Climate in 2007”]. Bull. Amer. Meteor. Soc., 89 (7), pp. 121-122.

Ropelewski, C.F., and Halpert, M.S. (1987): Global and regional scale precipitation patterns associated with the El Niño/Southern Oscillation Mon. Wea. Rev*.,* 115, pp. 1606-1626.

Ropelewski, C.F., and Halpert, M.S. (1989): Precipitation patterns associated with the high index phase of the Southern Oscillation *J. Climate* 2, pp. 268-284.

Rusticucci, M., and Camacho, J.L. (2006): South America [in “State of the Climate in 2005”]. Bull. Amer. Meteor. Soc., 87 (6), pp. 68-69.

Tang, B. H., and Neelin, J.D. (2004): ENSO Influence on Atlantic hurricanes via tropospheric warming. Geophys. Res. Lett., 31, L24204.

Zebiak, S. E., Orlove, B., Vaughn, C., Munoz, A., Hansen, J., Troy, T., Thomson, M., Lustig, A., and Garvin, S. (2014): Discovering ENSO and Society Relationships. Climate Change (Wiley Interdisciplinary Reviews).

White Paper #3 – ENSO Research: The overarching science drivers and requirements for observations

Kessler, W.S.[1], Lee, T.[2], Collins, M.[3], Guilyardi, E.[4], Chen, D.[5], Wittenberg, A.T.[6], Vecchi, G.[6], Large, W.G.[7], and Anderson, D.[8]

[1] University of Washington, United States
[2] NASA Jet Propulsion Laboratory, United States
[3] University of Exeter, United Kingdom
[4] University of Reading, United Kingdom
[5] Lamont-Doherty Earth Observatory, United States
[6] NOAA Geophysical Fluid Dynamics Laboratory, United States
[7] National Center for Atmospheric Research Earth System Laboratory, United States
[8] NOAA National Climatic Data Center, United States

1. Introduction and history

ENSO is the largest interannual climate signal, with its coupled ocean-atmosphere core in the equatorial Pacific but producing global effects through atmospheric teleconnections. The unpredicted El Niño event of 1982-83 focused attention on this phenomenon and was the impetus for the original development of the tropical Pacific observing system (TPOS) and TAO array in the mid-1980s, under the Tropical Ocean/Global Atmosphere (TOGA) programmeme. ENSO has played two roles in stimulating the observational network and its modeling counterpart: it is a forecast problem with obvious practical benefits, and it is a laboratory for the study of tropical air-sea interaction, which informs the study of other phenomena in other ocean basins.

Before the 1960s, no mechanism had been proposed to connect the well-known SST anomalies known as El Niño on the Peruvian coast with winds and precipitation elsewhere in the basin. Bjerknes (1966) described the fundamental coupled interaction between surface winds and SST gradient, but the mechanism of eastern warming continued to be assumed local until Wyrtki (1975) showed that this signal must be remotely forced by wind anomalies in the west, and thus that ENSO was a basin-scale phenomenon. During the 1980s, models and theory (e.g., Anderson and McCreary, 1984) showed the essential role of equatorial Kelvin and Rossby waves in transmitting the signal across the Pacific, and an explosion of work in the late 1980s explained and fleshed out "delayed oscillator" ideas which established ENSO as a coupled oscillation with a distinct and explainable evolution (Zebiak and Cane, 1987; Battisti and Hirst, 1989; Schopf and Burgman, 2006; and Suarez and Schopf, 1988), although its genesis was (and remains) controversial.

At that time, observation of the subsurface ocean in the tropical Pacific was done primarily by XBTs deployed from merchant ships, producing at best monthly samples on a few meridional lines barely sufficient to detect the relatively slow Rossby waves (Kessler, 1990). Island sea level gauges added higher temporal resolution in a few places (Wyrtki, 1975 and 1981), but the absence of near-equatorial islands in the more than 7000km between the Line Islands (160°W) and the Galapagos (95°W) made it impossible to observe the Kelvin waves. Nevertheless, recognition of the role of these linear wind-driven waves gave some skill in using simple wave models and early GCMs to predict the evolution of El Niño events over a lead time of a few

months (Zebiak and Cane, 1987). These models showed the strong role of ocean memory – mediated by equatorial wave propagation – in guiding the evolving climate of the tropics (Neelin, 1998). The early GCMs, however, proved unable to maintain a realistic mean background state or annual cycle, in either the ocean or atmosphere. The intense feedbacks of the tropical climate meant that small errors in modeling either fluid could quickly "run away" and required assimilated observations to control the background properties. The ad hoc parameterizations of processes that mixed and distributed surface fluxes into the interior ocean continued to require subsurface ocean observations to correct. The sense in the community that great progress was at hand if these needs could be met drove the unprecedented development of the TAO array in the late 1980s (Hayes et al., 1991; McPhaden et al., 1998 and 2010). The success of TAO in turn was a proof of concept for the creation of other basin-scale, multinational arrays (e.g., Argo).

ENSO has continued to propel much of the observational, modeling and theoretical progress of the past 30 years, but despite three decades of focused attention of the climate community, ENSO forecasting skill remains stubbornly slow to improve after the initial advances. In fact, while forecast skill for the full set of retrospective ENSO events has increased slightly, forecast skill for recent events has been lower than for the events prior to the turn of the century (Barnston et al., 2012). Coupled GCMs with far better resolution and more developed physical parameterizations than those of the 1980s have seen improvements in ENSO simulations (Wittenberg et al., 2006; Delworth et al. 2012), but have produced only modest progress in forecast skill (Davey et al., 2002; Turner et al., 2005). Strong hints of decadal or longer modulation of ENSO characteristics complicate the prediction problem, as have the emergence of what might be other "modes" of ENSO. These may be related to changes in the background state that alter the relation between upper ocean heat content and SST (McPhaden, 2012), or they may simply emerge at random from the stochastically-forced and/or chaotic ENSO system (Wittenberg, 2009; Newman et al., 2011ab; Stevenson et al., 2012; Wittenberg et al., 2014).

The overwhelming lesson of the past three decades of ENSO observation is its diversity, the ongoing succession of surprises in the expression of these events. The potential for future surprises in ENSO behavior is high. It appears that the relatively easy issues of wave-carried ocean memory are largely solved, but further advancement will entail diagnosing and explaining the mechanisms of air-sea heat and momentum exchange, in both fluids, which is unlikely to be accomplished by model experiments alone. This situation demands continued attention by the sustained observing system to the physical processes involved in tropical ocean-atmosphere interaction. As we look to the next decade and beyond, we can't predict the next surprises but we can expect that surprises will occur, and we must build a robust observing system that will be ready to detect and diagnose them. We take the point of view that the best way to prepare for new surprises is to observe the underlying physical processes, and thereby to teach models to represent these processes.

2. Unsolved problems of ENSO

2.1 The annual cycle

Winds, SST and zonal currents propagate west along the equator during the annual cycle, while thermocline depth propagates east (Yu and McPhaden, 1999). These facts have been interpreted from several points of view. Xie (1994) proposed a feedback based on wind speed and the resulting evaporative cooling, in which the ITCZ being north of the equator and resulting persistent southerlies are key (also see Mitchell and Wallace, 1992). Yu and McPhaden (1999), on the other hand, highlighted the role of oceanic Kelvin and Rossby waves. The pronounced one cycle per year variability in both ocean and atmosphere, despite the fact that the sun crosses the equator twice a year, indicates the important role of coupled processes, and it remains a non-trivial exercise for coupled models to reproduce the annual cycle. Many of the CMIP5 models either produce an annual cycle that is too strong, or exhibit a spurious semi-annual cycle. The latter may be linked to the double ITCZ still common in these models, which leads to a background state that is more symmetric about the equator than the very asymmetric observed state. Although some improvement to model simulations of the ITCZ can be achieved through increased resolution in the atmosphere and ocean, deficiencies in the ITCZ are seen even at the highest resolutions that can plausibly be used for multi-decadal integrations (Delworth et al., 2012), indicating that improved understanding and parameterizations are needed to improve ITCZ simulation for these long integrations.

Since ENSO appears largely phase-locked to the annual cycle, it is difficult to define, and impossible to prescribe, a "non-ENSO" climatology based on only a few decades of data. The observed phase locking of ENSO, and mechanisms that have been proposed to understand it, indicate a fundamental coupling between the annual cycle of insolation and the evolution of ENSO (Tziperman et al., 1994; Jin et al., 1994; Harrison and Vecchi, 1999; An and Wang, 2001; Spencer, 2004; Lengaigne et al., 2006; Vecchi, 2006; Lengaigne and Vecchi, 2009) – so improvements in the simulation of the mechanisms behind the mean-state and annual cycle are likely to yield improvements in the simulation and prediction of ENSO.

2.2 Low-frequency modulation

Although the basic mechanism of ENSO is contained in the tropical Pacific, there are strong suggestions that epochal changes of ENSO characteristics and predictability can be due to influences from outside, either internal or external to the ocean–atmosphere coupled system. To illustrate the range of possibilities, Trenberth and Hoar (1997) analyzed the abnormal warming during the 1990s and attributed it to anthropogenic global warming, while Gu and Philander (1997) suggested that these decadal changes are part of a natural variability of the mean thermocline in the tropical Pacific Ocean, resulting from a coupled tropical–extratropical interaction. Kirtman and Schopf (1998) also considered the decadal variability as natural, with its magnitude amplified by uncoupled atmospheric "noise". The epochal changes of ENSO have also been related to external factors such as volcanic emissions and solar variability (Mann et al., 2005). Long integrations of coupled GCMs, without any changes in external forcings, can generate multi-decadal epochs of extreme ENSO behavior (Wittenberg, 2009; Stevenson et al., 2012), which may not be predictable (Wittenberg et al., 2014). ENSO modulation, in turn, can affect the decadal-mean state of the tropical Pacific, by blurring and/or stirring the horizontal and vertical thermal gradients in the ocean (Schopf and Burgman, 2006; Ogata et al., 2013). The impact of decadal modulation of ENSO on the mean state of the Pacific combined with changes in observing systems, can affect our ability to detect and attribute changes to the mean-state of

the tropical Pacific, reducing confidence in tests of hypotheses about the influence of radiative forcing on the state of the tropics (e.g., Vecchi et al., 2006, DiNezio et al., 2009, Karanauskas et al., 2009, Seager and Naik, 2012). The predictability of ENSO is modulated as well (Kirtman and Schopf, 1998; Karamperidou et al., 2014; Wittenberg et al., 2014).

One recent issue that has received considerable attention is the ‘pause’ or ‘hiatus’ in global mean surface temperature changes. Several theories have been put forward to explain the hiatus including variations in natural forcing agents (volcanoes, solar), additional heat uptake or redistribution in the ocean (Trenberth and Fasullo, 2012), and atmospheric teleconnections associated with on-going La Niña/negative PDO conditions in the Pacific (Kosaka and Xie, 2013). The accuracy, within which we need to be able to measure changes in ocean heat uptake, in order to explain the pause, challenges the current observing system.

Given the intrinsic modulation of ENSO, long, continuous climate records are needed to characterize ENSO and its sensitivity to external forcings. Observing systems have evolved significantly over the past 150 years, confounding the detection of secular changes in the background state and ENSO (Wittenberg, 2004; DiNezio et al., 2010). Paleo proxy records have been brought to bear on reconstructing past variations in the tropical Pacific mean state and ENSO (Li et al., 2011 and 2013; Emile-Geay et al., 2012ab; McGregor et al., 2013), but these reconstructions are still in their infancy.

2.3 ENSO Diversity - CP vs EP El Niños, or weak vs strong El Niños

The observational era has seen a succession of surprising manifestations of ENSO. The 1982-83 El Niño occurred at a different phase of the seasonal cycle to the accepted consensus description of Rasmussen and Carpenter (1982), which caused experts at the time to deny that it could be an El Niño. The 1986-87 El Niño lasted much longer than had been thought possible. The reappearance of El Niño conditions in early 1993, immediately after the more typical event of 1991-92, contradicted the then-current view that El Niño and La Niña events alternated. The El Niño of 1997-98 grew faster and stronger than could have been imagined before, and the prolonged La Niña conditions that followed have not been explained. In the past decade, the emergence of “Modoki” or Central Pacific El Niños (Ashok and Yamagata, 2009; Kug et al., 2009; Yeh et al., 2009; Takahashi et al., 2011) has confounded forecasters and also remains unexplained.

Gross features of the ENSO cycle can be seen back to the late 1800s in indices such as the Southern Oscillation Index; it is clear that ENSO is subject to decadal or longer apparently-natural modulation. This is expressed in periods of preferred sign of oscillation (e.g., no El Niños in the 1930s, few La Niñas in the 1990s), different phasing with the annual cycle, and different locations of peak anomalies (the occurrence of the "Modoki" or CP El Niños of the 2000s (section 2.3) after decades of peak anomalies near the coast of South America). It is not at all clear what aspects of the background conditions produce this spectrum of behavior. Indeed, both statistical models and coupled GCMs are capable of generating multi-decadal epochs of CP or EP El Niños -- even without changes in external forcings or predictable decadal variations in background climate (Newman et al., 2011b; Wittenberg et al., 2014).

Underlying much of the debate about the diversity of ENSO is continued uncertainty as to whether ENSO is a self-sustained quasi-cyclic oscillation, with irregularity due to "weather noise" (or internal nonlinearities), or if El Niño is a damped event-like phenomenon that requires external forcing as an essential "trigger". It is likely that ENSO exists in a spectrum spanning these states, and its location in the parameter regime may depend on the background state of the Pacific (Fedorov and Philander, 2000; Wittenberg, 2002).

Early theories for ENSO highlighted the role of oceanic equatorially-trapped waves in transmitting thermocline anomalies across the Pacific basin that, when coupled with the Bjerknes atmosphere-ocean feedback, produce quasi-regular oscillations (Battisti and Hirst, 1989; Suarez and Schopf, 1988). As coupled climate and seasonal forecast models were developed, the role of inherent atmospheric variability (e.g., westerly wind bursts) in amplifying individual modes was examined (e.g., Kessler and Kleeman, 2000; Lengaigne et al., 2004; Vecchi et al., 2006a; Gebbie et al., 2007; Zavala-Garay et al., 2008).

More recently, the apparent break in ENSO characteristics following the 1997-98 El Niño, followed by prolonged La Niña conditions and then a series of El Niño events that did not fit the previously-accepted picture has spawned considerable debate about ENSO diversity. There is evidence of more frequent occurrence of warming events that are focused in the central Pacific in the past decade, in contrast to warming events focused in the eastern part of the basin in preceding decades, which had been taken as “typical”. Some authors argue for the existence of physically-distinct modes of variability, positing the existence of the so-called ‘classical’, cold-tongue, or eastern-Pacific El Niño vs. the so-called central-Pacific, warm-pool El Niño or El Niño ‘Modoki’ mode (e.g. Ashok et al., 2007; Kao and Yu, 2009; Kug et al., 2009). This view sees different feedbacks operating in different events, with the CP El Niños tending to be dominated by the zonal advective feedback and the EP events by the Bjerknes or thermocline feedbacks (section 3.4). Model studies suggest that during the El Niño decay phase, EP events decay primarily due to poleward oceanic discharge of equatorial heat content (brought about by strong off-equatorial wind curl), while CP El Niños show a greater role for local surface heat flux damping (Kug et al., 2010; Ren and Jin, 2013; Singh and Delcroix, 2013). Others see these differences merely as manifestations of a continuous spectrum of variability (Giese and Ray, 2011; Newman et al., 2011b; Capotondi and Wittenberg, 2013; Johnson, 2013), arguing that the common view of different physical types is statistically biased by the two extreme events of 1982-83 and 1997-98 (e.g., Takahashi et al., 2011).

Observations and models have shown that the mechanisms in the eastern equatorial Pacific at the end phase of extreme El Niño events can be fundamentally different from those of more moderate El Niños (Vecchi and Harrison, 2006; Vecchi, 2006; Zhang and McPhaden, 2006; Lengaigne and Vecchi, 2009). Sustained and continuous observations documented the unusual coexistence of a very shallow thermocline with extremely warm SSTs in the eastern equatorial Pacific during the height of the 1997-98 El Niño; this was followed by an abrupt termination where the eastern equatorial Pacific SSTs cooled by almost 6°C in a matter of a week or two following the return of the easterlies (McPhaden, 1999; Harrison and Vecchi, 2001; Vecchi and Harrison, 2006; Vecchi, 2006; Zhang and McPhaden, 2006). The co-location of atmospheric and oceanic observations was crucial to understanding the termination of this event, and generalizing it to extreme El Niño events (Vecchi and Harrison, 2006; Vecchi, 2006; Lengaigne

and Vecchi, 2009). Based on the understanding of the mechanisms inherent to the development and termination of extreme El Niño events, there is now a robust projection for an increase in these extreme El Niño events in the decades and century to come (Cai et al., 2014).

Observations by the sustained observing system can contribute to this discussion by diagnosing and quantifying the physical processes that distinguish the feedbacks, and by accurately describing low-frequency changes of the background. Long time series are needed, since understanding the interplay between El Niño and the background state is hampered by the limited duration of the satellite observations and sparse distribution of historical in situ data.

It is also noted that the ENSO cycle in the observational record is prominently skewed, with the cold phase being typically weaker and lasting longer than the warm phase (Kessler, 2002; Hanachi et al., 2003; An and Jin, 2004; Choi et al., 2013), and the spatial patterns of El Niño and La Niña not being mirror images of each other (Hoerling et al., 1997; Burgers and Stephenson, 1999). However, this asymmetry is not consistently represented in present-generation CGCMs. This may have larger significance than just for individual events, as Rodgers et al. (2004) connected the leading EOF pattern of tropical Pacific decadal variability with the El Niño-La Niña asymmetry (Rodgers et al., 2004; Schopf and Burgman, 2006; Ogata et al., 2013).

There is also considerable uncertainty on the physical mechanisms responsible for the asymmetry between El Niño and La Niña. Suggested mechanisms include the nonlinearity in oceanic vertical temperature advection in the eastern Pacific cold tongue (Hanachi et al., 2003; An and Jin, 2004), nonlinear rectification of the Madden-Julian Oscillation (Kessler and Kleeman, 2000), nonlinearities in the dependence of tropical deep convection on the underlying SST (Hoerling et al., 1997) and in the “biological thermostat” effect of phytoplankton in the upper ocean (Timmermann and Jin, 2002), and the positive skewness of the surface zonal wind anomalies in the western tropical Pacific that directly lead to the positive skewness of SST anomalies in the eastern tropical Pacific (Monahan, 2004). The reason for the last mechanism is that the anomalous wind field in the tropical western Pacific is dominated by westerly bursts, which would send down-welling Kelvin waves to the east and warm the SST there, thus, on average, making El Niño stronger than La Niña. A systematic investigation of these processes in a unified, quantitative framework is clearly needed, and there is no substitute for building long time series of winds, upper ocean thermal structure and currents, and surface variables indicating the turbulent and radiative fluxes that will be needed to disentangle these hypotheses.

Overall, the picture is of deep uncertainty about both the diversity of individual events and about the cycle as a whole. We argue that the path forward is to gain insight into the underlying physical processes as the way to resolve these uncertainties.

2.4 Response under ACC

Model forecasts

Estimating the response of ENSO to climate change presents a considerable challenge, both due to the separation of signal from noise and because of multiple, interacting ocean and atmosphere variability at all frequencies. One approach attempts to separate changes of the long-term climate of the tropical Pacific from long-term changes in the variability (e.g., Vecchi

and Wittenberg, 2010; Collins et al., 2010; Watanabe and Wittenberg, 2012; Watanabe et al., 2012; Knutson et al., 2013).

Tropical Pacific SSTs have warmed over the period in which observations or reconstructions are available, but there is still debate over whether they have warmed preferentially in the east relative to the west or vice versa (e.g., DiNezio et al., 2010; Solomon and Newman, 2012). Theory suggests that the tropical trade winds should weaken as a result of the muted response of the hydrological cycle under warming (Held and Soden, 2006; Vecchi et al., 2006), although the role of SST pattern changes may also be implicated (Xie et al., 2010; Tokinaga et al., 2012). The apparent strengthening trend in the trade winds in the last two decades does not fit these theories (L'Heureux et al., 2013; Qiu and Chen, 2013), but evaluation of observed decadal and lower-frequency climate changes is confounded by changing observing systems (Tokinaga et al., 2012ab), and signal-to-noise issues in separating the mean from the variability in both observations and in models.

Future model projections of the mean equatorial climate indicate a peak in warming on the equator with a relatively uniform east-west pattern (Liu et al., 2005; Xie et al. 2010). However, considerable inter-model spread is found, so confidence in this conclusion is low. The ensemble-mean picture also indicates weakening trades, a shoaling and strengthening of the thermocline, a weakening of near-surface currents; but whether observed trends in these fields agree with this model ensemble-mean picture is still a matter of considerable debate (Tokinaga et al., 2012ab).

Future projections of ENSO variability are also still subject to much uncertainty. The recent IPCC AR5 concludes that "… natural modulations of the variance and spatial pattern of El Niño-Southern Oscillation are so large in models that confidence in any specific projected change in its variability in the 21st century remains low." The same conclusion was drawn in the AR4. That ENSO variability might significantly increase or decrease in either magnitude or frequency remains an open question.

For mean changes in the ocean, a 4-dimensional picture of the temperature of the upper levels (e.g. the top few hundred meters) is required to assess how heat is slowly penetrating the ocean, at what rates and in what locations. For mean changes in the atmosphere, the surface wind stresses and surface turbulent and radiative fluxes are required to diagnose and attribute the mean changes below the surface of the ocean.

For changes in ENSO variability, as elsewhere, detection is complicated by the large natural SST variability associated with different flavors of ENSO, the difficulty of separating trends in the mean from trends in ENSO characteristics, and because of SST variability unrelated to ENSO. As models are apparently not resolving these issues despite much work at many institutions, we advocate the documentation and study of changes in the processes and feedbacks in the ENSO cycle: the thermocline feedback, zonal advective feedback, mean current damping, the wind stress-upwelling-SST (Bjerknes) feedback, wind-evaporation-SST (WES) feedback, and the atmospheric damping of SST anomalies (see section 3.4 below). This diagnosis will require coherent information about monthly to seasonal variations in both atmosphere and ocean fields. These include 4-d estimates of ocean temperatures and velocities together with estimates of atmospheric turbulent and radiative fluxes.

The ENSO CO_2 signal and its observed changes

The equatorial oceans are the largest natural source of CO_2 to the atmosphere, contributing about 0.7 Pg C/yr (Takahashi et al., 2009; Wanninkhof et al., 2013); fed by equatorial upwelling, primarily in the eastern Pacific and Atlantic cold tongues (the Pacific is about 70% of the total tropical outgassing). For reference, 0.7 Pg C/yr is about 7% of total CO_2 emissions from anthropogenic sources in 2012 (LeQuere et al., 2013).

Three decades of sampling, mostly during TAO service cruises, have shown strong fluctuations of surface water CO_2 with the ENSO cycle. Tropical Pacific CO_2 emissions increase during La Niña events, and decrease during El Niños, with a magnitude of about ±0.1 Pg C/yr. This is attributed to upwelling transport changes, with stronger upwelling and shallower thermocline depths during La Niña providing a closer communication from the thermocline to the surface. The observed ENSO surface seawater CO_2 signal has a meridional scale of at least ±10° latitude.

Atmospheric pCO_2, by contrast, is well-mixed over broader regions and does not vary spatially nearly as much as the ocean values, thus the equatorial air-sea gradient depends more strongly on the ocean, so air-sea flux variability is driven by oceanic changes. However, the flux also depends on wind speed, which therefore also contributes to increasing CO_2 flux over the cold tongue during La Niña events.

This straightforward picture seemed to describe the observed variability of ocean surface pCO_2 through the El Niño event of 1997-98, with large pCO_2 drops occurring with all the El Niños since observations began in 1981. Since 1999, however, the level of surface water pCO_2 has stepped higher by about 20µatm, and the ENSO-timescale fluctuations are much less evident. As this occurred simultaneously with the apparent change in the physical manifestations of ENSO (e.g., the prolonged La Niña conditions of the 2000s, and largest El Niño SST anomalies observed further west than had been seen over the previous 20 years), it may reflect changes in the location and magnitude of upwelling. The important contribution of ENSO to atmospheric CO_2 variability is the subject of current research (see TPOS WP06).

2.5 ENSO predictability

ENSO has shown the highest predictability among identified climate modes in the Earth's climate system. That seasonal climate prediction is no longer a speculative practice is largely due to the predictability of ENSO and the quantification of ENSO's global impact (Barnston et al., 2003; Goddard et al., 2005). Present ENSO forecast models, despite their vast differences in complexity, exhibit comparable predictive skills, which seem to have plateaued at moderate level (Chen and Cane, 2008), although there are hints of progress (Stockdale et al., 2012). It remains to be seen how predictable ENSO really is and how much room there is for further improvement. To answer these questions, we need to know the underlying physics that produces predictability.

The long-range predictability of ENSO stems from ocean–atmosphere sensitivity in the tropics, the crucial role of the slowly-varying ocean, and the low-dimensional nature of this coupled system. Classic theories consider ENSO as a self-sustaining interannual fluctuation confined to the tropical Pacific, chaotic yet deterministic (Zebiak and Cane, 1987; Battist and Hirst, 1989;

Jin, 1997). Thus its predictability is largely limited by initial error growth, and the potential forecast lead time is likely to be on the order of years (Goswami and Shukla, 1991; Xue et al., 1997). Another strain of thought emphasizes the importance of atmospheric “noise” as triggers for ENSO events (Penland and Sardeshmukh, 1995; Moore and Kleeman, 1999; Thompson and Battisti, 2000). In such a scenario, ENSO is a highly damped oscillation sustained by stochastic forcing, and its predictability is limited more by noise than by initial errors, implying that ENSO events are essentially unpredictable at long lead times.

In principle, predictability can be estimated using twin-model experiments and perturbing the initial conditions, but the answer is model dependent, and existing ENSO models are not realistic enough for this purpose. Present estimates of ENSO predictability are mostly based on retrospective predictions over a relatively small number of events. With so few degrees of freedom, the statistical significance of such estimates is questionable. The uncertainty is worsened by the fact that ENSO predictability is time dependent (Balmaseda et al., 1995; Kirtman and Schopf, 1998). It has been shown that the predictive skill for ENSO varies significantly in the past one and a half centuries, especially at longer lead times (Chen et al., 2004; Tang et al., 2008). The predictability is high for periods dominated by strong and regular ENSO events, but low for periods with fewer and weaker events (Barnston, 2012).

Generally speaking, there are four factors that limit the current skill of ENSO prediction: inherent limits to predictability, gaps in observing systems, model flaws, and suboptimal use of observational data. As discussed above, there is considerable debate on the inherent limits to predictability, but increasing evidence suggests that our current level of predictive skill is still far from those limits and surely there is room for improvement (Chen et al., 2004; Chen and Cane, 2008). Our tasks are then to improve observing systems, models, and data assimilation methods. These call for a continuously sustained, optimally designed TPOS, and process studies that elucidate the physics of ENSO predictability and its low-frequency variability.

3. Processes involved in the above uncertainties

3.1 Equatorial upwelling and rapid atmospheric feedback – scales and fronts

The equatorial cold tongue complex is a region where strong upwelling occurs in the presence of vigorous turbulent mixing; the resulting intimate connection between the thermocline and the surface allows the interaction of basin-scale ocean dynamics and property transports with the equatorial atmosphere that responds sensitively to variations of SST. That sensitivity is demonstrated by the short spatial scales (100km or less) of wind response as southeasterly trade winds cross the SST front on or just north of the equator (Risien and Chelton, 2008). While satellite winds and SST detect the surface front on weekly timescales, SST variability is a convolution of surface fluxes, mixing and upwelling in a complex and time-dependent circulation cell whose dynamics are not well understood. The near-surface, near-equatorial circulation has posed a difficult problem for models, whose representations cannot even be evaluated because existing subsurface observations have been concentrated narrowly on the equator and do not adequately sample properties or currents in the ocean near-surface layer.

These phenomena include equatorial upwelling itself, which is the primary driver of communication between the thermocline and surface. Since the early studies of Cromwell

(1953), Knauss (1963), and Wyrtki (1981), we have known that upwelling transport into the upper layer of the east-central Pacific balances the Ekman transport across ±5° latitude, totaling about 30Sv, with a vertical velocity of a few meters/day (Weisberg and Qiao, 2000; Johnson et al., 2001; Meinen et al., 2001). If we assume that upwelling occurs across the east-central Pacific, and that vertical velocity has a Gaussian structure in latitude, its implied meridional e-folding scale is 50 to 150km. The divergence forcing this upwelling is quite shallow, perhaps 50m thick at most (Johnson et al., 2001). However, we have little information on the time-variability of upwelling. Although zonal pressure gradients in the upper equatorial ocean adjust to changing winds on about 10 day timescales (Cronin and Kessler, 2009), it is not clear that the meridional currents producing divergence and upwelling have the same timescale. Resolving this will require near-surface velocity observations spanning the equator.

Upwelling of cool thermocline water in the east is a key link in the Bjerknes feedback that establishes the mean state of the equatorial Pacific (section 3.4). By producing a zonal SST gradient, eastern upwelling suppresses atmospheric convection in the east and focuses it in the west, driving the trades and Walker Circulation, which is then a positive feedback for the easterlies that cause upwelling. If either upwelling decreases or the temperature of the water it draws from increases, that will tend to weaken the easterlies. This engenders a coupled chain reaction that amplifies the initial anomalies and pushes the system towards an El Niño state (see section 3.4).

The persistence of the sharp front bounding the cold tongue in the north, where strong poleward Ekman currents seem to cross the front, similarly implies a narrow, shallow, vertical circulation along the front. The front, and the tropical instability waves (TIW; section 3.g) that occur along it, are important as a source of heat to the equator from the warmer waters to the north, a meridional heat flux that is comparable in magnitude to that of upwelling (Bryden and Brady, 1989; Kessler et al., 1998). The front and TIW are more intense during La Niña periods and greatly weakened during El Niños, presumably because warming on the equator during El Niño weakens the meridional temperature gradient, and weaker easterlies weaken the shear of the zonal currents across the front.

Thus, processes acting on scales of 100km or less are key mechanisms by which the basin-wide changes in the ocean's vertical structure are communicated to the sensitive overlying atmosphere. While models can now simulate the large-scale ENSO-driven changes to the background vertical structure, especially those mediated by equatorial Kelvin and Rossby waves, models do not yet represent the actual mechanisms or scales by which SST evolution is controlled. Because of positive feedbacks (section 3.4), errors in representing these short-spatial-scale phenomena can grow and corrupt the overall model solutions.

An upper ocean heat budget estimate is a key part of the suite of diagnostics used to interpret changes of the ENSO cycle (Huang et al., 2010; Xue et al., 1997; "Monthly Ocean Briefing", NCEP/CPC). Such diagnostics are essential to understanding and predicting the evolution of ENSO events, yet our present capacity to close the heat budget is extremely limited. To provide an ongoing description of the interaction of upwelling, surface fluxes, horizontal advection and mixing, a credible heat balance should be enabled by the observing system. As we have seen diverse flavors of ENSO that embody different combinations of processes controlling SST (e.g. Kug et al., 2010; see section 2.3), it is essential – in the medium term at least – that the

processes and local consequences of the vertical circulation be directly measured by the sustained observing system at a few representative locations spanning the equator, both for real-time diagnoses and to evaluate model simulations and drive their next generation.

3.2 Mechanisms by which subsurface ocean dynamics drive SST

Knowledge about the mechanisms through which ocean processes affect mixed-layer temperature and provide feedback to the atmosphere are critical to the understanding of ENSO and its decadal variation/modulation. High-frequency measurements of upper-ocean temperature, horizontal currents, and surface meteorological parameters by TAO/TRITON moorings have enabled a great growth of understanding on seasonal and interannual time scales (e.g., Wang and McPhaden, 1999, 2000, and 2001; Cronin and Kessler, 2002), making possible quantification of the roles of the terms of the heat balance on seasonal and interannual timescales (Wang and McPhaden, 1999, 2000, and 2001). Co-located mooring data at (0°, 110°W) was able to characterize the interplay of wind and solar insolation in modulating near-surface stratification and SST (Cronin and Kessler, 2002). However, significant knowledge gaps remain in several aspects:

(1) the contribution by vertical processes (vertical advection, entrainment, vertical mixing, and solar penetration through the water column) is inferred as a residual in observation-based analysis of mixed-layer temperature budget because these processes cannot be resolved by existing measurement techniques;

(2) the heat budget off the equator where there are no current meters is much less certain;

(3) the variation of the heat budget on decadal and longer time scales is not well documented;

(4) the vertical resolution of TAO sampling is too coarse to resolve the variations of mixed-layer depth and properties;

(5) salinity is known to vary on seasonal and interannual (and conceivably on decadal and longer) time scales (Singh and Delcroix, 2013); the relative lack of salinity measurements degrades the estimate of mixed-layer depth and indicates the dispersal of the large precipitation signal in the west Pacific warm pool. Formation of salinity barrier layers could provide yet another feedback that affects the intensity of ENSO events (Maes et al. 2002, and 2005; Maes and Belamari, 2011).

3.3 Atmospheric processes relevant for TPOS observations

The atmosphere is a strong driver of the ocean, and more so than elsewhere tropical oceans force the atmosphere with both local and remote responses. The Atmospheric Boundary layer (ABL) processes of this interaction span a broad spectrum of horizontal scales, with the dominant small scale processes related to convection, clouds and precipitation modulated by the large scale flow, which in turn depends on the small scales. In the vertical too, the free atmosphere and sub-thermocline ocean are connected through small scale processes in both planetary boundary layers. TPOS observations over the large scale of the tropical Pacific have revealed multi-year variability in the background state and ENSO. Of most relevance is the SST

and its gradients, that modeling studies of Lindzen and Nigam (1987) suggest are responsible for observed features of the flow in the ABL. Other important observations are the large scale wind patterns, not only the zonal wind stress of relevance to ENSO, but also the cross equatorial flow that feeds into the convergence zones (e.g. ITCZ). These winds have also been a key reference standard for satellite wind products and their loss would open the door for spurious temporal changes in the combined satellite record.

For decades convection and related clouds and precipitation have remained a daunting challenge for observations and models of the atmosphere, because of their small scales and stochastic nature. Convection itself has a multi-scale character by being driven by low level convergence (dominant in the ITCZ, for example) and by heating from warm SST below. The latter places a premium on measurements of the sensible heat flux as it is the only component of the air-sea heat flux that directly heats the ABL. Evaporation is another, less effective, de-stabilizing flux. Perhaps the most promising prospect for a breakthrough are models that faithfully resolve both the processes and their interactions, but verification of having reached such a state in the tropics will require a series of observational programmes targeted at specific processes. These campaigns would include TPOS elements and utilize the whole of TPOS to set the large scale context.

Perhaps the most compelling argument for coincident and co-located ocean and ABL observations is to discover and diagnose significant correlations between atmospheric properties and the ocean mixed layer, along with their relation to background conditions. The recently observed correlation between small scale SST and near surface wind (Chelton et al., 2000) has important implications for the entrainment of free atmosphere air into the ABL. There may be other significant relationships to be found, and in some cases very long time histories of consistent high frequency observations may be needed to mitigate the statistical problem of sparse spatial sampling of TPOS, and diurnal variability. Discerning the fine details of these processes that connect the upper ocean and lower atmosphere will become more and more critical as forecast systems move toward true fully coupled data assimilation. Present practice of independent atmosphere and ocean assimilation can lead to incompatible initial atmosphere and ocean states, and hence a shock to the subsequent coupled integration. Instead, observations in the atmosphere should be allowed to influence the ocean state, and vice versa, based a priori on observed relationships. Observed air-sea fluxes would also become an integral part of the coupled assimilation/forecast system. Key constraints that could then be imposed within specified limits are conservation of heat and Ekman transports in the ABL that are of equal magnitude, but opposite direction to those in the ocean.

3.4 Large-scale feedbacks driving ENSO variability

Theoretical understanding of ENSO has significantly advanced over the past decades (see Wang and Picaut, 2004). The theoretical framework of the recharge oscillator (Jin, 1997) provides a widely accepted paradigm for ENSO. A linear analysis of the recharge oscillator SST equation provides a simple yet powerful way to evaluate the different mechanisms that amplify or damp ENSO growth.

Damping mechanisms include the thermal damping of SST anomalies by air-sea fluxes and the restoring effect of the mean state (i.e., the fact that advection of temperature anomalies by the

climatological currents tend to reduce those anomalies). The Bjerknes feedback depends on the sensitivity of the atmospheric surface wind responses to ENSO SST anomalies. This atmospheric response to SST anomalies is here referred to as the atmospheric Bjerknes feedback and can be computed from observations. With the associated ocean response the coupling results in amplifying mechanisms through the so-called "ocean feedbacks": the zonal advective feedback, the thermocline feedback and the Ekman pumping feedback, further detailed below.

By focusing on the key processes affecting ENSO dynamics, evaluating these feedbacks from observations will accelerate progress in ENSO understanding and improve its representation in climate models. This evaluation requires coherent multi-decadal time series and is currently constructed from atmosphere and ocean reanalyses. In the tropical Pacific these reanalyses are strongly constrained by TAO in situ measurements which provide a uniquely coherent view of the relevant ocean and surface atmosphere variables over several decades. Evaluation of feedback processes can not only address the question of whether the characteristics of ENSO are changing in a changing climate but, by illuminating the underlying physical processes, also potentially improve the realism of predictions from seasonal to centennial-scale climate projections.

Bjerknes feedback: This is a positive feedback loop acting symmetrically in the ocean and atmosphere that controls the overall state of the tropical Pacific. It maintains the normal background state, but if perturbed can feed back to amplify the original perturbation, and thereby amplifies incipient El Niño or La Niña events. In normal conditions, surface easterlies force both a westward surface equatorial current and Ekman divergence that induces upwelling. The ocean zonal pressure gradient balances the westward wind stress, giving an upward slope of the thermocline towards the east, which means that a given upwelling velocity draws colder water in the east than in the central Pacific where the thermocline is deeper. The resulting zonal SST gradient focuses atmospheric convection in the west and subsidence in the east (the Walker circulation), which enhances the original easterlies in a positive feedback. While this system appears to be stable, the fact that it is maintained by positive feedbacks means that weakening any element weakens the entire system. This insight by Bjerknes (1966) was the first basin-scale theory of ENSO.

Zonal advective feedback: In normal conditions, a westward zonal current carries cool (upwelled) water westward, balanced in the mean by solar heating. If either the wind-driven current or the heating changes so to produce an initial warm anomaly, the winds – and thus currents – over and to the west of the anomaly are weakened. The resulting current anomalies carry warm water eastward, amplifying the original anomaly. It has been argued that the zonal advective mechanism is more effective than upwelling at changing SST in the central Pacific because the background zonal SST gradient is large but thermocline is deeper there so the Bjerknes feedback is less effective. This feedback appears have played a larger role since 2000.

Thermocline feedbacks: A deep-thermocline anomaly in the east Pacific will warm SST - even if upwelling itself remains strong - by reducing the background vertical temperature gradient that upwelling works on. Warm SST tends to produce further warming by either the Bjerknes or

zonal advective feedbacks mentioned above, which will weaken the local winds and self-amplify.

SST/wind stress (Ekman) feedback: A weakening of the wind stress reduces upwelling velocity. Even if the background vertical temperature gradient is strong, this feedback anomalously warms SST as less cold water is pumped upwards. Those positive SST anomalies again act through Bjerknes or zonal advective feedbacks to the further weaken the wind stress.

Wind-evaporation-SST (WES) feedback: Warm SST anomalies induce not only dynamical effects as above but also – by changing wind speed – change the evaporation as well. Near the equator, reduced wind speeds due to a warm SST anomaly also decrease evaporation in a positive feedback. Like the Ekman feedback, the WES feedback can favor westward propagation of equatorial SST anomalies. However, the WES feedback acts somewhat differently for off-equatorial SST anomalies. A subtropical warm SST anomaly tends to induce a cyclonic surface wind, which (in the easterly trade wind regime) tends to reduce wind speeds on the equatorward flank of the SST anomaly – warming the surface by reducing evaporation and resulting in equatorward propagation of the SST anomaly. This feedback has been suggested to play a role in the triggering of ENSO events, by so-called “meridional modes” which propagate off-equatorial anomalies equatorward, where they can affect ENSO (Chiang and Vimont, 2004; Zhang et al., 2009; Dayan et al., 2013; Larson et al., 2013).

Heat flux damping: The heat flux feedback is defined as the regression coefficient between net surface heat fluxes and SST anomalies in the east Pacific. It is usually a negative feedback and is dominated by the shortwave and latent feedbacks. The shortwave feedback changes depending on the stability of the atmosphere. In unstable conditions, higher SST leads to an increase in convection, high clouds, and a decrease in surface shortwave flux: the shortwave feedback is negative in the convective regime. Under stable conditions, higher SST destabilizes the atmospheric boundary layer and prevents the formation of stratiform boundary layer clouds. This leads to an increase in shortwave flux at the surface and the associated feedback is positive in the subsident regime. This shortwave response to SST is, however, complex and non-local; it may be decomposed as the product of (1) the response of large-scale atmospheric dynamics to SST anomalies, (2) the response of clouds to changes in the large-scale circulation, and (3) the characteristics of the shortwave interception by clouds. Several studies have shown that the single largest source of model errors for ENSO in climate models comes from the misrepresentation of this shortwave feedback (e.g., Wittenberg et al., 2006), since it involves multiscale interactions among resolved large-scale motions and parameterized convection, cloudiness, and boundary layer processes. In situ platforms provide an essential component of the observing system, permitting cross-validation and calibration of satellite estimates of clouds and their impacts on the tropical Pacific mean state and ENSO. Estimates of this feedback are hampered by the sparcity of observations, especially of shortwave radiation, but the degree to which OAFlux is a quality product in the equatorial Pacific is mainly thanks to the in situ measurements of the TAO array (Cronin et al., 2006).

3.5 Diurnal cycle and penetration of surface fluxes into ocean

Observations of the ocean mixed layer near the equator show a large diurnal cycle of shear and stratification, both of which affect the vertical transmission of surface fluxes through the ocean.

During the night, with surface radiative cooling destabilizing the water column, the well-mixed layer deepens. As intense daytime solar heating produces shallow stratification, it traps wind-input momentum in a thin near-surface layer, perhaps 10m deep (Schudlich and Price, 1992). During a 7-month study at 2°N,140°W, a mean afternoon jet developed that was 12 cm/s faster in the direction of the wind at 5m than at 25m; this strong shear disappeared at night, despite the fact that the diurnal cycle of winds in the equatorial Pacific is weak (Cronin and Kessler, 2009).

The SST peak occurs in early afternoon, and then cooling begins while the surface is still being heated. One interpretation is that shear at the base of the afternoon mixed layer increases vertical turbulent mixing there, which deepens the sheared layer and hence deepens the penetration of diurnal heating. Later, even after surface heating has ended, the initially shallow stratification and shear continue to propagate downwards, as convection plus the residual shear at the base of the diurnal mixed layer increase vertical turbulent mixing and deepen the layer. This continues through the evening hours, transmitting the previously trapped momentum, heat and possibly freshwater downwards to the main thermocline (Danabasoglu et al., 2006). Strong turbulent dissipation has correspondingly been observed to extend to perhaps 80m depth in the evening, into the upper level of the equatorial undercurrent, before retreating to very shallow depths during the day (Lien et al. 2002), but the source of energy has yet to be partitioned between convection and shear.

The diurnal cycle, therefore, is a strong mediator of the relation between the primary ocean driver of surface heat flux (SST), and the primary upper ocean response (heat content). Further, non-linearity can rectify diurnal variability into the mean, and Bernie et al. (2008) found that diurnal coupling has profound impacts that include large scale variability in the tropics. In principle, models with very high vertical resolution could resolve diurnal mixing processes, but many of the mixing rules are based on unproven analogies with the atmosphere. Therefore, the uncertain results are not generally deemed to justify the substantial increase in computational costs. Alternatively, there are simple schemes (Zeng and Beljaars, 2005) that give an efficient diurnal cycle of SST, but not of shear or salinity stratification. The verification of such schemes is at present primarily indirect using remotely sensed SST.

Thus, it appears that much of the work of heat and momentum transmission to the thermocline in the equatorial Pacific is accomplished by the diurnal cycle. The magnitude and characteristics of the diurnal cycle is dependent on the local cloudiness, wind and precipitation, which vary regionally, seasonally, and with ENSO phase. As well, studies have shown sensitivity to the depth of solar shortwave penetration (e.g. Sweeney et al., 2005; Anderson et al., 2009). The overall picture is that mixing in this region is not a simple stirring of warm surface and colder subsurface waters, but acts through a specific set of downward-propagating dynamics; this implies that momentum transfer to the thermocline and equatorial undercurrent depends on diurnal processes. Since this transfer is key to the Bjerknes and zonal advective feedbacks (section 3.4), and model schemes are not directly verified, observation of the diurnal cycle of temperature, salinity and velocity from the surface to the thermocline should be part of the sustained observing system, at least at some representative locations, both for diagnostics of the above relationships and to spur model improvements that can be verified.

Interestingly, the equatorial Pacific can be sensitive to off-equatorial vertical mixing processes. That the equatorial Pacific background state can be strongly affected by off-equatorial processes – some of which are only crudely represented in models (e.g., the diurnal cycle) – is yet another motivation for an expanded in situ observing system, along with field campaigns to better constrain these dynamical and thermodynamic processes in models.

3.6 Recharge and discharge to subtropics (LLWBCs)

Low latitude western boundary currents (LLWBCs) in the Pacific (namely, the Mindanao Current in the north and the New Guinea and New Ireland Coastal Undercurrents in the south) are the western boundary pathways of the lower limbs of the shallow meridional overturning circulations that connect the tropical and subtropical Pacific Ocean (i.e., the subtropical cells). In the mean, they reinforce the interior geostrophic flow in the pycnocline, bringing colder pycnocline waters from the subtropics to the equator to balance the poleward transports of warmer surface waters by the Ekman currents. On interannual and longer time scales, however, the picture is very different. Satellite and in situ measurements, as well as ocean modeling and assimilation products, suggest that the variations of LLWBC volume transports tend to be anti-correlated to and partially compensate the more dominant variations of the interior transports (Kang and An, 1998; An and Kang, 2000). The causes for the different phasing of the LLWBCs and interior transport are related to two factors:

(1) Propagation of off-equatorial Rossby waves generated by central basin winds to the western boundary (Capotondi et al., 2004).

(2) Anomalous horizontal circulation in the western tropical Pacific due to variations in local Ekman pumping associated with the movement and the strength of the ITCZ and SPCZ (Lee and Fukumori, 2003).

Satellite altimeter data have inadequate resolution near coastlines to capture the complicated structure and tight gradients of the LLWBCs (100km or less), especially in the complex geometry of the Solomon Sea. Argo floats are also limited in sampling these narrow features, as they do not generally sample their cross-shore gradients. The representation of LLWBCs in modeling and assimilation products is dependent on their spatial resolution and the representation of the complicated geometry and bathymetry in these regions (Cheng et al., 2007).

Moreover, volume transports of the LLWBC are primarily a proxy to describe the role of these flows in regulating tropical upper-ocean heat content; the heat that they carry to the west Pacific warm pool is fundamental to the tropical climate evolution. Measurements of both the LLWBCs' transport and temperature are thus necessary to understand their role in ENSO and its decadal and longer variation/modulation; therefore, monitoring the LLWBCs should be an integral part of the ENSO observing system. The international Programmes “Northwestern Pacific Ocean Circulation and Climate Experiment” (NPOCE) and “Southwest Pacific Ocean Circulation and Climate Experiment” (SPICE) are designed to understand the roles of the LLWBCs in tropical Pacific Ocean and climate. However, these experiments are process-oriented. An integration of LLWBC measurements into a long-term monitoring system of the tropical Pacific is necessary to facilitate research on decadal and longer variation/modulation of ENSO.

3.7 Tropical instability waves

Tropical instability waves (TIWs) are an integral element of the coupled ocean-atmosphere system in the Pacific Ocean-atmosphere system. Signatures of the TIWs have been observed by satellites (in SST, SSS, SSH, wind and wind stress, precipitation, and ocean color) (e.g., Legeckis, 1977; Yoder, 1994; Xie et al., 1998; Chelton et al., 2000; Liu et al., 2000; Polito et al., 2001; Lee et al., 2012) and by subsurface ocean measurements (in temperature, salinity, currents, and surface meteorology) (e.g., Qiao and Weisberg, 1995; McPhaden, 1996; Halpern et al., 1998; Lyman et al., 2007). TIW meridional fluxes of heat, freshwater/salt, nutrients, and carbon are comparable to that of upwelling (Bryden and Brady, 1989). They provide a major mechanism of eddy-mean flow interaction in the tropical Pacific Ocean (e.g., Qiao and Weisberg, 1995). The vertical circulation of TIW also facilitates exchanges of heat, freshwater, momentum, and gases between the ocean and atmosphere (e.g., Feely et al., 1994; Xie et al., 1998).

Because of their relatively high frequencies (a dominant period of 17 days near the equator and 33 days off the equator in the Pacific; Lyman et al., 2007; Lee et al., 2012), TIW signals are aliased in Argo sampling (due to its typical 10-day profiling interval) and in the data of some satellites that have less frequent repeat times. On the other hand, the roughly 1500km zonal spacing of TAO mooring pickets is nearly one TIW wavelength, so it is not possible to diagnose TIW properties from the present moored array (but the moorings do resolve the front in detail as it passes (Cronin and Kessler, 2009)).

Since TIW are instabilities, their representation in atmospheric and ocean reanalysis products is hard to correct by assimilation. On the other hand, Vialard et al. (2003) present a more positive view, linking TIWs to the wind forcing. Recent advances in coupled ocean-atmosphere data assimilation (e.g., NOAA/NCEP's CFSR) has improved the representation of TIWs due to the combined use of ocean and atmosphere observations (Wen et al., 2012), demonstrating the utility of simultaneous, co-located, high-frequency measurements of the ocean and the surface meteorology. The representation of TIWs in coupled climate models are related to some model biases (e.g., the cold tongue; Wittenberg et al. (2006) and Delworth et al. (2012) in the context of GFDL's CM2.1 and CM2.5; Bill Large, personal communication in the context of NCAR's CCSM). Enhancing the ability of the Tropical Pacific Ocean Observing System to monitor TIWs would improve our understanding of the roles of TIWs in ENSO and the related impacts on marine biology and the carbon cycle.

4. Observations to resolve these processes

Section 3 above describes a wide variety of processes that contribute to ENSO evolution, some better-understood and becoming well-modeled, others that continue to require ongoing in situ observation to clarify basic facts and enable model advancement. In doing this, we take the viewpoint of future colleagues looking back at the present time: What will they wish we had been measuring in 2014?

4.1 Maintenance of climate time series

Long time series of climate-relevant variables are precious indicators of long-term change. These time series are the only means to document slow variations in the background fields that determine the characteristics of ENSO, and also underpin model bias correction. In situ measurements of geophysical quantities often suffer from poor statistics, and the few existing long time series uniquely reference ongoing data collection.

Through decades of effort, long time series of several climate variables are now available in the equatorial Pacific. Wyrtki (1974, and 1979) developed indices of surface currents from a few island sea level records, building time series back to 1950. These indices proved to be reasonable measures of seasonal and ENSO transport fluctuations when compared to those constructed from in situ temperature profiles (Taft and Kessler, 1991). Nevertheless, although the island sea levels are well-resolved temporally (able to average out tidal fluctuations), they are inherently limited to a small number of locations that in particular do not sample the equator between 160°W and the coast of South America.

Before the TAO array produced reliable and well-resolved temperature profiles across the tropical Pacific, wide use was made of XBT profiles deployed from three quasi-meridional merchant ship lines beginning in the mid-1970s (e.g., Rebert et al., 1985, Kessler, 1990; Picaut and Tournier, 1991). Beginning in the late 1980s and continuing to the present, several of these lines were converted to “high-resolution” lines under WOCE and then CLIVAR, carrying a dedicated observer and deploying XBTs more frequently, roughly every 1/4° (Roemmich and Cornuelle, 1990); data from these lines is adequate to make meaningful averages (for example of eddy properties (Roemmich and Gilson, 2001)). However, the XBT lines are limited to a few widely-separated tracks, and typically sample only once every few months.

The advent of TAO in the mid-1980s, and its completion in the early 1990s (Hayes et al., 1991; McPhaden, 1995), began the era of co-located surface atmospheric and subsurface ocean data, with high temporal resolution and basin-wide coverage. TAO also began the era of real-time and publicly-available data that is now taken for granted. Several sites have been occupied for 30 years, especially on the equator in the east and central Pacific. While the TAO array is described in detail in other white papers of this series, in the ENSO context we note the consistency of sampling over these decades, sampling that was originally designed – in the absence of credible model simulations – to meet the temporal and spatial spectral requirements of detecting the equatorial waves that were then key to progress on the ENSO cycle (Hayes and McPhaden, 1992; Kessler et al., 1996). In the presence of numerous sources of high-frequency signals that can produce aliasing in sparser sampling (e.g., TIWs (section 3.7), westerly wind bursts, as well as tides and internal waves), the highly-resolved sampling of moored measurements makes it possible to confidently extract unaliased low frequency signals. Indeed, one of the early results enabled by TAO’s growing time series was to describe the slowly-varying seasonal cycle in the subsurface eastern equatorial Pacific, and the lack of annual phase consistency between thermocline depth and SST (Gu et al., 1997).

We look forward to the lengthening of the Argo time series of temperature and salinity in the tropical Pacific. As Argo provides excellent zonal resolution that has heretofore been lacking, we expect to see the evolution of many signals – for example those associated with the off-equatorial Rossby waves whose timescales are well-matched to Argo sampling – with added detail and ability to relate them to the overlying winds.

In contrast to this history of carefully maximizing the information content of available data, the climate community has suffered several times from irretrievable losses from observing system changes without adequate documentation of the sampling characteristics of different instruments and techniques. First, the change from bucket to ship-intake SST measurements in the 1940s and 1950s added substantial uncertainty to reconstructions of time series spanning that period (Kaplan et al., 1998). Second, in the transition from broadscale XBT sampling to Argo early in the past decade, insufficient overlap for intercomparison again left a difficult-to-correct uncertainty (Lyman and Johnson, 2008; Wijffels et al., 2008). Third, in situ measurements of near surface winds were affected by a gradual increase in anemometer heights, as the ocean vessels on which they were mounted grew taller over the years (e.g., Wittenberg, 2004, and references therein). As we build time series for future generations, such mistakes must be avoided.

However, we are forced to watch another such mistake unfold today, as the transition of TAO from research lab management to operational status has decimated the array, with data return down below 40% and many moorings practically abandoned. If allowed to continue, this would produce serious gap in the climate record that our future colleagues will see as nothing short of tragic.

One of the most important fields for understanding the tropical Pacific climate and ENSO, is the surface wind stress. Unfortunately, the surface wind stress remains one of the most poorly observed quantities, especially since the 2009 loss of the NASA QuikSCAT satellite, which had for years measured surface wind stresses with unprecedented detail using the SeaWinds scatterometer. In the absence of QuikSCAT, the TAO moored array is one of the last remaining components measuring the all-important surface wind field. Scatterometers, such as ASCAT METOP-A and future instruments require in situ measurements for calibration and validation. The accuracy required in the equatorial region is particularly demanding, and this makes the long-term in situ sampling from the TAO array very important. Generation of a tropical Pacific climate record for future scientific use will critically depend on continuity of future wind-observing systems with ongoing TAO observations.

We are far from understanding either the natural or anthropogenic low-frequency variability of the tropical Pacific and its influence on ENSO characteristics. This variability depends on subtle changes of the underlying background conditions, whose source remains largely unknown. Progress in this area requires consistent long-term observation sufficient to detect small trends without aliasing, either by continuing existing systems, or after a well-understood and well-documented transition of observing techniques.

The difficult question of which existing time series have ongoing value and should be continued, vs. those that might be modified or abandoned, we leave for community discussion.

4.2 Ancillary measurements: shipboard sampling, embedded process studies

The ability to embed temporary process studies, and to build an ongoing suite of shipboard observations, is a significant side-benefit of servicing a large sustained array. The cruises that have maintained TAO have established a substantial database of CTD profiles and repeated ADCP transects. These have drawn an unprecedently clear picture of the zonal current

structure and its seasonal and ENSO variation (Johnson et al., 2002). The regular presence of a research ship has enabled the CO_2 sampling discussed in section 2.4 above, which has documented a large CO_2 flux signal at ENSO and also longer timescales, though whether this is a natural decadal phenomena or anthropogenic signature is not known. These side-benefits have largely evaporated with the transition of TAO to operational status. Fewer CTD profiles are taken, the shipboard ADCP is neglected, and most ancillary measurements are not supported.

As our future colleagues look back from 2025, certainly they will have wanted ongoing surface ocean and atmospheric CO_2 sampling, which is the only means of measuring the ocean's role in recycling natural and anthropogenic carbon, and also serves to check climate model simulations (see TPOS WP06). Whether this sampling is done from ships (i.e., a few times/year, but extending to a wider range of latitudes), or more narrowly near the equator from moorings, remains an open question.

Shipboard ADCP sampling has already shown the ability to resolve the mean, annual cycles and ENSO variations of the zonal (but not meridional; Johnson et al., 2001) currents along a few longitudes, as mentioned above. As the ships traverse the tropical Pacific, they accumulate velocity data that fills in between the few moored velocity sites and improves the climatologies. We note that shipboard ADCP data requires careful processing, and this work at the University of Hawaii is presently unfunded. Research ships servicing the TAO array have been the principal means of deploying Argo floats in the tropical Pacific; with the transition to operations and loss of this opportunity, Argo coverage in the region will decrease unless other means of deployment are found.

Short-term process studies have been enabled by the TAO since its earliest days. The mooring hardware and software are designed to accommodate instrumentation added ad hoc, and the regular service cruises have provided platforms for many process studies (a short list would include TROPIC HEAT, EPOCS NECC, TIWE, JGOFS EqPac, TOGA-COARE, CEPEX, Nauru99, EPIC, NPOCE, SPICE). This facility has largely been a casualty of the transition to operational status, however, but the need and demand is high.

While some observations should be ongoing, other problems can only be attacked with intensive process studies that are necessarily short-term:

- Co-variability of the ocean mixed layer and lower atmosphere winds and precipitation. (Needs a ship with Doppler wind sampling).
- Turbulence measurements to diagnose momentum/property flux penetration into the thermocline and their relation with background currents/thermal structure. (Requires a dedicated cruise).
- Observe the 3-D evolution of the near-equatorial circulation cell (upwelling and the cold tongue front) under varying winds. (Process study embedded in a larger array)
- Clouds, convection, PBL

4.3 Vertical and temporal resolution of temperature sampling

Present TAO moorings typically sample SST and temperature at 11 depths down to 500m, with vertical resolution of 20 or 25m in the upper 100m, at 10-minute intervals. Argo sampling has much better vertical resolution (5m or less), and also measures well-calibrated salinity, but only

every 10 days. These contrasting strengths will each be needed for different aspects of ENSO research.

It remains to be seen how well Argo sampling will resolve the ENSO-related fluctuations of the thermocline, which can only be determined by further study. However, as discussed in section 3.5 above, much of the important dynamics determining the injection of surface momentum and heat fluxes into the ocean occurs in the near-surface layer, which is at present poorly observed and poorly modeled. These dynamics are inherently high-frequency (diurnal), which also implies the need for a significant model development effort that will require observational guidance. Mixed-layer variability is also inherently local, especially in being dependent on the surface flux variability. The next generation of scientists will need us to have made progress in this crucial area. This need can be met by instrumenting the near-equatorial moorings proposed in section 4.d below (1° intervals to ±3° latitude, at a few longitudes) with thermistors at the same depths as the current meters (every 5m down to 50m). These moorings should also have a suite of surface flux measurements (section 4.5), enabling a complete diagnosis of the processes acting on and in the ocean, at several representative cross-equatorial sections.

4.4 Velocity

Ongoing ocean current profiles are made from moorings at five locations on the equator (110°W, 140°W, 170°W, 165°E and 147°E). Because the moorings are subsurface, their data is retrieved only when the mooring is recovered, so is not real-time, but velocity time series from these locations stretch back 20 years at least (though some of these are now failing under operational management). These current profiles are frequently used to validate models, since the velocity structure is a sensitive indicator of vertical momentum mixing. However, the upward-looking ADCPs presently deployed provide useful velocities only deeper than about 30m depth, because bubbles and irregular reflections from surface waves blur the signal (shipboard downward-looking ADCPs have a similar limitation). Thus existing velocity measurements do not adequately sample the ocean mixed layer.

We argued in section 3.1 above that enabling an ongoing upper layer heat balance diagnostic is the key to interpreting changes and mechanisms of ENSO evolution. As near-surface horizontal advection is one of the main processes contributing to SST change (section 3.4), and the model time-dependent velocities now used for this purpose are inconsistent across models and unreliable, real-time near-surface current sampling should be part of the sustained ENSO observing system.

The vertical limb of the equatorial circulation is more challenging to measure, and also much less dependable in models, as it depends on the meridional velocity that whose variability appears more complex than that of the zonal current. The sensitive interaction between downward mixing and upward advection is 0^{th}-order in all theories of ENSO, but its actual operation is very poorly understood. As the principal link through which basin-scale ocean dynamics and property transport communicates with the overlying atmosphere, these challenges must be faced. Observations of the full three-dimensional cell above the EUC core through several seasonal and ENSO cycles are the only means to improve and validate model representations. Therefore, current observations sufficient to estimate vertical velocity from horizontal divergence should be part of the sustained observing system for the next decade.

Since the divergence that drives upwelling occurs primarily in the upper 50m, is largely due to dv/dy, and is surface-intensified, an efficient and economical way to make these measurements would be to add or enhance surface moorings with shallow point current meters, every 5m depth down to 50m, at the equator and 1° intervals to ±3° latitude, at a few representative longitudes in the east-central Pacific.

4.5 Air-sea fluxes

The solar (shortwave) radiation is a standard surface flux measurement of TAO moorings, while downwelling longwave has been measured on a much more limited basis. These fluxes are the dominant ocean heating processes (100s of W/m^2) and hence essential for diurnal cycling, cloud-ocean feedbacks and the climate record, for example. They can be estimated from satellite radiation measurements of the top of atmosphere using radiative transfer equations given atmospheric composition and clouds (e.g. ISSCP-FD), but TAO observations have been critical to correcting biases in solar fluxes. Therefore, basin wide, continuous observations of both these flux components networks is essential to maintain consistency with future satellite estimates, understanding and modeling tropical ocean-atmosphere interaction, as well as to resolve the diurnal cycle.

Observations of surface precipitation have been much more sparse than called for by the science questions involved. In future they should be made whenever and wherever there are available platforms, because oversampling will never be an issue. Depending on location, tropical precipitation can be highly intermittent, can have a prominent diurnal cycle, can be the dominant branch of the hydrological cycle, and can play a critical role in ENSO cycles. Precipitation depends on numerous multi-scale processes, including convection, clouds, convergence, water vapor transport, so it is a powerful diagnostic. Therefore, demand will be for diurnally-resolving observations from all regimes: the high rainfall regions of the ITCZs and western warm pool; the regions of large ENSO related variance; the dry zones of precipitation minima. Such observations would provide key model validation metrics, because the multi-scale and multi-process nature of precipitation makes it difficult to tune or to get right for the wrong reasons. They also offer the prospect of discriminating between the disparate tropical precipitation data sets, including those inferred from satellite measurements and those produced from numerical weather prediction schemes. The range across products can approach a factor of two, so it is problematic to maintain a continuous climate record as the changing observing system (e.g. satellite sensors and algorithms), or data assimilation evolution introduce spurious signals. Although ocean salinity budgets offer limited hopes for constraints, there is no substitute for in situ observations. For some purposes very long time series will be needed to ameliorate the sparse spatial sampling, so the sooner more precipitation time series begin the better.

Turbulent fluxes of momentum, sensible heat and evaporation (latent heat) can be estimated from bulk formulae (see TPOS WP11 for an extensive discussion). The primary bulk parameters are SST, wind, air temperature and humidity the most important TPOS and surface current one of the secondary. They are observed frequently and broadly, hourly accuracy may not be within a factor of two, so direct measurements are needed to resolve the diurnal cycle, and to determine regional empirical bulk coefficients for tropical wind/wave/current conditions. The

accuracy of bulk fluxes would then improve, especially when averaged over fluctuations in these conditions. In contrast, the situation for direct measurements of the turbulent fluxes is more like that of precipitation; measurements are difficult and, therefore sparse, yet long time series of frequent, accurate observations are needed to calibrate bulk estimates from either in situ or satellite based parameters, to reduce spurious signals in the climate record.

4.6 What determines the necessary location of in situ observations?

Tropical Pacific climate exhibits several different regimes in various parts of the basin, which undergo large changes during ENSO events. Characterizing each these regimes, such that each can be better understood and captured in models, should be a major goal of the Tropical Pacific observing system, but may not be well-sampled by broadscale arrays and will require special attention. These regimes include

(1) the waters in a thin strip adjacent to the western coast of South America, where models tend to show warm SST biases, excessive oceanic thermal stratification, too little upwelling, and a deficit of stratus cloud;

2) the eastern equatorial Pacific cold tongue, where the thermocline is shallow, skies are mostly clear, and upwelling is intense;

(3) the southeastern tropical Pacific, where models have too much stratus cloud and/or an unrealistically strong “double” ITCZ in boreal spring;

(4) the LLWBCs, which are an important component in setting the water properties, depth, and intensity of the equatorial thermocline and equatorial undercurrent;

(5) the northern ITCZ, which models often place too far poleward, and whose meridional shifts are critical to ENSO behavior and its interactions with global climate;

(6) the west Pacific warm pool, a regime of atmospheric deep convection that helps to drive a global atmospheric circulation, and the source of the warm waters that spread across the tropical Pacific during El Niño;

(7) the warm pool edge along the equator, a critical zone where complex feedbacks among stochastic westerly wind events, oceanic zonal advection, and possibly salinity barrier layers control the development of ENSO events, and which models usually place too far west.

5. Model-observation process studies and collaboration

5.1 Assessment of model representations of tropical Pacific climate

Coupled climate models continue to be developed with improved resolution, improved parameterisation of unresolved processes and addition of new processes. In addition, the coordination of model simulations and output (e.g. CMIP) mean than models now undergo greater scrutiny and comparison with the limited observational record. A useful evaluation of the current set of CMIP5 models is provided in Chapter 9 of the IPCC AR5 and is summarised here.

Some aspects of the mean climate of the tropical Pacific in models have improved since the previous generation (CMIP3). Cold SST biases in the west Pacific have generally been reduced,

as have westerly biases in the zonal wind stress – although models are still not perfect in the west. Stubborn biases remain in all CMIP5 models. SSTs are generally too cold on the equator across a large area of the central Pacific resulting in a cold tongue that extends too far west (Zheng et al., 2012). SST biases are positive in the east against the coast of South America, linked to insufficient marine stratocumulus in models. The latter has been a subject of a coordinated observational and modeling programmeme (VOCALS - Wood et al., 2011). Biases remain in the thermocline depth and slope and in the structure of the equatorial current system. A persistent error, connected to those above, is the so-called "double ITCZ" problem – models have a tendency to produce an ITCZ in the Southern Hemisphere as well as the north. Also, the seasonal cycle of winds and SSTs in the east tends to be too strong and many models produce a spurious semi-annual cycle. All these biases are linked via coupled processes.

Some improvement is seen in CMPI5 representations of ENSO variability. Fewer models have a tendency for 2-yr ENSO in CMIP5 compared to CMIP3 (Guilyardi, 2006; Guilyardi et al., 2012b). Many models now simulate NINO3 SST variability somewhere in the observed frequency band. The spatial pattern of variability has also improved somewhat, with fewer models showing large excessive variability in NINO4. Some models are able to capture a diversity of ENSO events, including weak central Pacific events and strong east Pacific events (Kug et al., 2010; U.S. CLIVAR Project Office, 2013; Capotondi and Wittenberg, 2013).

However, precipitation variability in NINO4 is generally underestimated. These remaining errors in the NINO4 regions are probably due to the mean cold tongue extending too far west, pushing the sensitivity to feedbacks further west. In terms of simple metrics, the range of errors in the magnitude of variability is reduced in CMIP5, largely due to fewer very bad models. A significant advance has been in the evaluation of ENSO feedback processes in models that tend to show an underestimate of the negative thermal damping and positive bias in the zonal advective and thermocline feedback (Lloyd et al., 2012). Increasing atmospheric and oceanic resolution has also helped, by better resolving tropical convection, the Indonesian Throughflow, the Andes cordillera, and tropical instability waves (Delworth et al., 2012).

5.2 Reducing biases in models

Broadly speaking there are three ways in which observations are used to improve climate models; through the improvement of existing parameterisation schemes and in the development of new schemes, through the model assembly and ‘tuning’ procedure and through the identification and diagnosis of errors which are common to all models and the assessment of how those errors relate to uncertainties in predictions and projections.

5.3 Parameterization development and testing

Parameterisation schemes are self-contained components of models that represent physical or biological processes such as ocean mixing. Typically they are developed off-line from the complete model and are based on our understanding of the process combined with empirical relationships derived from observations or from high-resolution process models. A new development in parameterisation in recent years has been the incorporation of stochastic elements to these schemes. Parameterisation schemes that are important for simulating the tropical Pacific include atmospheric convection and clouds, the atmospheric boundary layer,

ocean mixed layer processes and penetration of shortwave radiation through the water column, and ocean horizontal and vertical mixing and transport by unresolved eddies. Priorities for the improvement and development of schemes are listed in the following section.

5.4 Process studies targeted at particular model weaknesses where progress is likely

The following processes are currently either deficient or absent in the current generation of GCMs so are priority areas for research in both models and observations; they are where models require observational guidance to advance:

- Convection, in particular the diurnal cycle over land and ocean
- Organized convective features, e.g., the Madden-Julian Oscillation
- The diurnal cycle in the ocean mixed layer
- Low-level stratus clouds
- Tropical instability waves, their heat and momentum transport

5.5 Assembling and evaluating model performance

Model assembly and testing typically happens within each modeling center or within the community group when assembling a new version of a model. Each component, complete with new parameterisation schemes, is put together and initial experiments are performed. These test-experiments are compared with observations and previous versions of the model to prove 'fitness-for-purpose' and to show improvements. The priority-level given to different features of the model depends on the modeling group. For example, in building the HadGEM2 model, the Met Office concentrated a lot of effort into improving the climate of the tropical Pacific because of a focus on seasonal-decadal prediction (Martin et al., 2011). Test-versions of models usually require some improvement or tuning, either involving changing parameters within parameterisation schemes, or by revising the structure of the schemes. Here observations of 'processes' and 'emergent properties' are used.

Model intercomparison projects (MIPs): The exchange of model output between modeling groups has revolutionised climate science in recent years and now we have unprecedented knowledge of the performance of models and their response under enhanced greenhouse gases. Models are compared against climatologies of multiple variables and are also used in detection and attribution studies, which can be viewed as a sophisticated form of evaluation. Model evaluation is now an increasingly sophisticated exercise with evaluation exercises digging deeper and deeper into physical and biological processes. Many model errors persist (see Section 5.1 above) but are now diagnosed in a much better 'process-based' approaches, such as computing the BJ stability index (Jin et al., 2006), though these approaches could use further improvement (Guilyardi et al., 2009, 2012a; Graham et al., 2014).

Different observations are required in the three different stages of model improvement. Typically, detailed observations of processes, perhaps collected during dedicated field campaigns, are used to develop parameterisation schemes in (i) and may be used to test emergent processes in (ii). Normally, steps (ii) and (iii) require longer-term observations and typically gridded datasets are employed, perhaps with some gaps in-filled. Increasingly, analysis or re-analysis products are employed.

6. Conclusion and recommendations

We began by noting the societal and scientific importance of ENSO, and have surveyed here an astonishing amount of work by a large community over more than three decades. Although the bulk of this white paper has shown how much we still *don't* know, and how elusive the problems remain, in fact we've solved a lot of the easy problems and are closing in on the hard ones. These hard problems that observations can speak to are often those that fall below the spatial and temporal resolution of GCMs: interacting phenomena in the ocean mixed layer and atmospheric boundary layer – namely, the actual mechanisms that connect and couple the two fluids. We are confident that progress can be made, and that it will result in improved forecasts benefitting many millions. We believe that this progress will come from observing, diagnosing, understanding and teaching models to simulate the *physical processes* that underlie ocean-atmosphere coupling, and that this will have further benefits to much other science. The laboratory of ENSO will continue to illuminate the other tropical oceans.

We recommend:

a) Do not repeat the mistake of changing observational systems without adequate overlap, evaluation and intercomparison (section 4.1).

b) Focus moored observations where moorings' capabilities are needed: where rapid timescales dominate, and where co-located ocean and atmospheric observations are crucial. These are most importantly the near-surface boundary layers, and the near-equator. The moored array should be augmented to provide higher vertical resolution in the ocean mixed layer, with velocities, and to enhance sampling of the ABL.

c) Bring the TAO array back to the research community. The TPOS is not yet a mature system, and continues to serve comprehensive research goals, as well as goals we cannot yet specify; TAO is the backbone that supports almost everything we do. The research community has shown itself more competent at running these arrays than operational groups, and will provide for essential ancillary sampling and embedded process studies.

d) Foster a diverse-platform observing system because ENSO's rich multi-time and space scale variability and interactions requires comparably-diverse kinds of sampling.

e) Support Climate Process Teams to formulate and carry out process studies targeting model weaknesses.

References

Abraham, J.P. and co-authors (2011): A review of global ocean temperature observations: Implications for ocean heat content estimates and climate change. Rev. Geophys., 51(3), 450-483, (doi: 10.1002/rog.20022).

An, S.I., and Kang, I.S. (2000): A further investigation of the recharge oscillator paradigm for ENSO using a simple coupled model with the zonal mean and eddy separated. J. Climate, 13, pp. 1987-1993.

An, S.I., and B. Wang, B. (2001): Mechanisms of locking of the El Niño and La Niña mature phases to boreal winter. J. Climate, 14, pp. 2164–2176.

An, S.I., and B. Wang, B. (2000): Interdecadal change of the structure of the ENSO mode and its impact on the ENSO frequency. J. Climate, 13, 2044-2055.

An, S.I., and Jin, F.F. (2004): Nonlinearity and asymmetry of ENSO. J. Climate, 14, pp. 2399–2412.

Anderson, W., Gnanadesikan, A., and Wittenberg, A. (2009): Regional impacts of ocean color on tropical Pacific variability. Ocean Sci., 5, pp. 313-327, (doi: 10.5194/os-5-313-2009).

Anderson, D.L.T., and McCreary, J.P (1985): Slow propagating disturbances in a coupled ocean atmosphere-model. J. Atmos.Sci. 42, pp. 615-629. An, S.I., and B. Wang, B. (2001): Mechanisms of locking of the El Niño and La Niña mature phases to boreal winter. J. Climate, 14, pp. 2164–2176.

An, S.I., and B. Wang, B. (2000): Interdecadal change of the structure of the ENSO mode and its impact on the ENSO frequency. J. Climate, 13, 2044-2055.

Ashok, K., and Yamagata, T. (2009): The El Niño with a difference. Nature, 461, pp. 481-484.

Ashok, K., Behera, S., Rao, S., Weng, H., and Yamagata, T. (2007): El Niño Modoki and its possible teleconnection. J.Geophys. Res., 112 (C11).

Balmaseda, M.A., Davey, M.K., and Anderson, D.L.T. (1995): Decadal and seasonal dependence of ENSO prediction skill. J. Clim., 8, pp. 2705-2715.

Barnston, A.G., Mason, S.J., Goddard, L., DeWitt, D.G., and Zebiak, S.E. (2003): Increased automation and use of multimodel ensembling in seasonal climate forecasting ath the IRI. Bull.Amer.Meteor.Soc., pp. 1783-1796.

Barnston, A.G., Tippett, M.K., L'Heureux, M.L., Li, S., and Dewitt, D.G. (2012): Skill of real-time seasonal ENSO model predictions during 2002-2011 – is our capability increasing? Bull.Amer.Meteor.Soc., 93, pp. 631-651.

Battisti, D., and Hirst, A. (1989): Interannual variability in a tropical atmosphere ocean model - influence of the basic state, ocean geometry and nonlinearityl. Journal of the Atmospheric Sciences, 46(12), pp. 1687-1712.

Bjerknes, J. (1966): A possible response of the Hadley circulation to variations in the heat supply from the equatorial Pacific. Tellus 18, pp. 820-829.

Bryden, H.L., and Brady, E.C. (1989): Eddy momentum and heat fluxes and their effects on the circulation of the equatorial Pacific Ocean. J. Marine Research, 47, pp. 55-79.

Burgers, G., and Stephenson, D. B. (1999): The ''normality'' of El Niño. Geophys. Res. Lett., 26, pp. 1027–1030.

Cai, W., and coauthors (2013): Greenhouse Warming Leads to Increasing Frequency of Extreme El Niño Events. Nature Climate Change, (in press).

Capotondi, A., and A. Wittenberg, 2013: ENSO diversity in climate models. U.S. CLIVAR Variations, 11, 10-14.

Capotondi, A., Wittenberg, A., and Masina, S. (2006): ENSO diversity in climate models. US CLIVAR Variations, 11, pp. 10.14.

Capotondi, A., Wittenberg, A., and Masina, S. (2006): Spatial and temporal structure of tropical Pacific interannual variability in 20th century coupled simulations. Ocean Modeling, 15, pp. 274-298. (doi: 10.1016/j.ocemod.2006.02.004).

Chang, P. (1996): The role of the dynamic ocean-atmosphere interactions in the tropical seasonal cycle. J. Climate, 9, pp. 2973-2985.

Chelton, D.B. (2001): Observations of coupling between surface wind stress and sea surface temperature in the eastern tropical Pacific. J.Climate, 14, pp. 1479-1498.

Chen, D., Cane, M.A., Kaplan, A., Zebiak S.E., and Huang, D.J. (2004): Predictability of El Niño over the past 148 years. Nature, 428, pp. 733-736.

Chen, D., and Cane, M.A. (2008): El Niño prediction and predictability. J. Comput. Phys., 227, pp. 3625-3640.

Chiang, J. C. H., and Vimont, D.J. (2004): Analogous Pacific and Atlantic meridional modes of tropical atmosphere–ocean variability. J. Climate, 17, pp. 4143–4158, (doi:10.1175/JCLI4953.1).

Choi, K.-Y., Vecchi, G.A., and Wittenberg, A.T. (2013): ENSO transition, duration and amplitude asymmetries: Role of the nonlinear wind stress coupling in a conceptual model. J. Climate, 26, pp. 9462-9476, (doi: 10.1175/JCLI-D-13-00045.1).

Collins, M., An, S.-I., Cai, W., Ganachaud, A., Guilyardi, E., Jin, F.-F., Jochum, M., Lengaigne, M., Power, S., Timmermann, A., Vecchi, G., and Wittenberg, A. (2010): The impact of global warming on the tropical Pacific ocean and El Niño. Nature Geoscience, 3(6), pp. 391-397.

Cromwell, T. (1953): Circulation in a meridional plane in the central equatorial Pacific. J. Mar. Res. 12, pp. 196-213.

Cronin, M.F., Bond, N.A., Fairall, C.W., and Weller, R.A. (2006): Surface cloud forcing in the east Pacific stratus deck, cold tongue, ITCZ complex. J.Climate, 19 (3), pp. 392-409.

Cronin, M.F., and Kessler, W.S. (2002): Seasonal and interannual modulation of mixed layer variability of 0°, 110° W. Deep-Sea Res. I, Vol. 49, pp. 1-17.

Cronin, M.F., and Kessler, W.S. (2009): Near-surface shear flow in the tropical Pacific cold tongue front. J. Phys. Oceanogr., 39, pp. 1200-1215.

Danabasoglu, G., Large, W.G., Tribbia, J.J., Gent, P.R., Briegleb, B.P., and McWilliams, J.C. (2006): Diurnal coupling in the tropical oceans of CCSM3. J. Climate, 19, pp. 2347–2365.

Davey, M.K., and co-authors (2002): STOIC – a study of coupled model climatology and variability in tropical ocean regions. Clim.Dynam., 18, pp. 403-420.

Dayan, H., Vialard, J., Izumo, T., and Lengaigne, M. (2013): Does sea surface temperature outside the tropical Pacific contribute to enhanced ENSO predictability? Climate Dyn., published online, (doi:10.1007/s00382-013-1946-y).

Delworth, T. L., Rosati, A., Anderson, W., Adcroft, A.J., Balaji, V., Benson, R., Dixon, K., Griffies, S.M., Lee, H.C., Pacanowski, R.C., Vecchi, G.A., Wittenberg, A.T., Zeng, F., and Zhang, R. (2012): Simulated

climate and climate change in the GFDL CM2.5 high-resolution coupled climate model. J. Climate, 25, pp. 2755-2781, (doi: 10.1175/JCLI-D-11-00316.1).

DiNezio, P.N., Clement, A.C., and Vecchi, G.A. (2010): Reconciling Differing Views of Tropical Pacific Climate Change. Eos, Trans. AGU, 91 (16), pp. 141-142.

DiNezio, P.N., Kirtman, B.P., Clement, A.C., Lee, S.K., Vecchi, G.A., and Wittenberg, A.T. (2012): Mean climate controls on the simulated response of ENSO to increasing greenhouse gases. J. Climate, 25, pp. 7399-7420, (doi: 10.1175/JCLI-D-11-00494.1).

Emile-Geay, J., Cobb, K., Mann, M., and Wittenberg, A.T. (2013a): Estimating central equatorial Pacific SST variability over the past millennium. Part I: Methodology and validation. J. Climate, 26, pp. 2302-2328, (doi: 10.1175/JCLI-D-11-00510.1).

Emile-Geay, J., K. Cobb, M. Mann, and A. T. Wittenberg, (2013b): Estimating central equatorial Pacific SST variability over the past millennium. Part II: Reconstructions and implications. J. Climate, 26, pp. 2329-2352, (doi: 10.1175/JCLI-D-11-00511.1).

Fedorov, A.V., and Philander, S.G. (2000): Is El Niño changing? Science, 288, pp. 1997-2002.

Feely, R.A., Wanninkhof, R., Cosca, C.E., McPhaden, M.J., Byrne, R.H., Millero, F.J., Chavez, F.P., Clayton, T., Campbell, D.M., and Murphy, P.P. (1994): The effect of tropical instability waves on CO2 species distribution along the equator in the eastern equatorial Pacific during the 1992 ENSO event. Geophys.Res.Lett., 21, pp. 277-280.

Gebbie, G., Eisenman, I., Wittenberg, A.T., and Tziperman, E. (2007): Modulation of westerly wind bursts by sea surface temperature: A semistochastic feedback for ENSO. J. Atmos. Sci., 64, pp. 3281-3295, (doi: 10.1175/JAS4029.1).

Giese, B. S., and Ray, S. (2011): El Niño variability in simple ocean data assimilation (SODA). pp. 1871–2008. J. Geophys. Res., 116, C02024, doi:10.1029/2010JC006695

Goddard, L., and Dilley, M. (2005): El Niño – catastrophe or opportunity. J.Climate, 18, pp. 651-665.

Goswami, B.N., and Shukla, J. (1991): Predictability of a coupled ocean-atmosphere model, J. Clim., 4, pp. 3-22.

Graham, F. S., Brown, J.N., Langlais, C., Marsland, S.J., Wittenberg, A.T., and Holbrook, N.J. (2014): Effectiveness of the Bjerknes stability index in representing ocean dynamics. Climate Dyn., accepted pending minor revisions.

Guilyardi, E. (2006): El Niño-mean state-seasonal cycle interactions in a multi-model ensemble. Climate Dynamics, 26(4), pp. 329-348.

Guilyardi, E., Wittenberg, A.T., Fedorov, A., Collins, M., Wang, C., Capotondi, A., van Oldenborgh, G.J., and Stockdale,T. (2009): Understanding El Niño in ocean-atmosphere general circulation models: Progress and challenges. Bull. Amer. Meteor. Soc., 90, pp. 325-340. (doi: 10.1175/2008BAMS2387.1).

Guilyardi, E., Cai, W., Collins, M., Fedorov, A., Jin, F.F., Kumar, A., Sun, D.Z., and Wittenberg, A.T. (2012a): New strategies for evaluating ENSO processes in climate models. Bull. Amer. Met. Soc., 93, pp. 235-238, (doi: 10.1175/BAM S-D-11-00106.1).

Guilyardi, E., Bellenger, H., Collins, M., Ferrett, S., Cai, W., and Wittenberg, A.T. (2012b): A first look at ENSO in CMIP5. CLIVAR Exchanges, 17, pp. 29-32.

Gu, D., and Philander, S.G.H. (1997): Interdecadal climate fluctuation that depends on exchanges between the tropics and extratropics. Science, 275, pp. 805–807.

Gu, D. F., Philander, S.G.H., and McPhaden, M.J. (1997): The seasonal cycle and its modulation in the eastern tropical Pacific. J. Phys. Oceanogr., 27(10), pp. 2209-2218.

Halpern, D., Knox, R.A., and Luther, D.S. (1988): Observations of 20-day current oscillations in the upper ocean along the Pacific equator. J.Phys.Oceanogr., 18, pp. 1514-1534.

Harrison, D. E., and Vecchi, G.A. (1999): On the termination of El Niño. Geophys. Res. Lett., 26, pp. 1593–1596.

Harrison, D.E., Chiodi, A.M., and Vecchi, G.A. (2009): Effects of surface forcing on the seasonal cycle of the eastern equatorial Pacific. J. Marine Research, 67(6), pp. 701-729.

Hayes, S. P., and co-authors (1991): TOGA-TAO - a moored array for real-time measurements in the tropical Pacific Ocean. Bull. Amer. Meteor. Soc., 72, pp. 339-347.

Hayes, S. P., and McPhaden, M.J. (1992): Temporal sampling requirements for low-frequency temperature variability in the eastern equatorial Pacific Ocean. NOAA Tech. Memo. ERL-PMEL-96, pp. 17-26.

Hannachi, A., Stephenson, D., and Sperber, K., (2003): Probability-based methods for quantifying nonlinearity in the ENSO. Climate Dyn., 20, pp. 241–256.

Held, I. M., and Soden, B.J. (2006): Robust responses of the hydrological cycle to global warming. J. Climate, 19, pp. 5686–5699, (doi:10.1175/JCLI3990.1).

Hoerling, M.P., Kumar, A., and Zhong, M. (1997): El Niño, La Niña, and the nonlinearity of their teleconnections. J. Climate, 10, pp. 1769–1786.

Huang, B., Xue, Y., Zhang, D., Kumar, A., and McPhaden, M.J. (2010): The NCEP GODAS ocean analysis of the tropical Pacific mixed layer heat budget on seasonal to interannual time scales. J.Climate, 23, pp. 4901-4925.

Jin, F.-F., Neelin, J.D., and Ghil, M. (1994): El Niño on the Devil's Staircase: Annual subharmonic steps to chaos. Science, 264, pp. 70–72.

Jin, F. (1997): An equatorial ocean recharge paradigm for ENSO .1. Conceptual model. Journal of the Atmospheric Sciences, 54(7), pp. 811-829.

Jin, F., Kim, S., and Bejarano, L. (2006): A coupled-stability index for ENSO. Geophysical Research Letters, 33(23).

Johnson, G.C., McPhaden, M.J., and Firing, E. (2001): Equatorial Pacific Ocean horizontal velocity, divergence, and upwelling. J.Phys.Oceanogr., Vol.31, pp. 839-849.

Johnson, G.C., Sloyan, B., McTaggart, K., and Kessler, W.S. (2002): Direct measurements of upper ocean currents and water properties across the tropical Pacific Ocean during the 1990's. *Prog.Oceanogr.*, 52(1), pp. 31-61.

Johnson, N. C. (2013): How Many ENSO Flavors Can We Distinguish? J. Climate, 26, pp. 4816–4827, (doi:10.1175/JCLI-D-12-00649.1).

Kang, I.S., and An, S.I. (1998): Kelvin and Rossby wave contributions to the SST oscillation of ENSO. J. Climate, 11, pp. 2461-2469.

Kao, H.Y., and Yu, J.Y. (2009): Contrasting eastern Pacific and central Pacific types of ENSO. J.Climate, 22, pp. 615-632.

Kaplan, A., Cane, M. A., Kushnir, Y., Clement, A. C., Blumenthal, M. B., and Rajagopalan, B. (1998): Analyses of global sea surface temperature 1856-1991. J. Geophys. Res., 103(C9), pp. 18567-18589.

Karamperidou, C., Cane, M.A., Lall, U., and Wittenberg, A.T. (2013): Intrinsic modulation of ENSO predictability viewed through a local Lyapunov lens. Climate Dyn., published online. (doi: 10.1007/s00382-013-1759-z).

Kessler, W.S. (2002): Is ENSO a cycle or a series of events? Geophys.Res.Lett., 29, (doi: 10.1029/2002GL015924).

Kessler, W.S. (1990): Observations of long Rossby waves in the northern tropical Pacific. J. Geophys. Res., 96(C7), pp. 12599-12618.

Kessler, W. S., Spillane, M.C., McPhaden, M.J., and Harrison, D.E. (1996): Scales of variability in the equatorial Pacific inferred from the Tropical Pacific Atmosphere-Ocean buoy array. J.Climate, 9(12), pp. 2999-3024.

Kessler, W.S., and Kleeman, R. (2000): Rectification of the Madden–Julian oscilation into the ENSO cycle. J. Climate, 13, pp. 3560–3575.

Kim, D., J.-S. Kug, I.-S. Kang, F.-F. Jin, and A. T. Wittenberg, 2008: Tropical Pacific impacts of convective momentum transport in the SNU coupled GCM. Climate Dyn., 31, 213-226. doi: 10.1007/s00382-007-0348-4.

Kirtman, B. P. (1997): Oceanic Rossby wave dynamics and the ENSO period in a coupled model. J. Climate, 10, pp. 1690-1704.

Kirtman, B.P., and Schopf, P.S. (1998): Decadal variability in ENSO predictability and prediction. J. Clim., 11, pp. 2804–2822.

Knauss, J.A. (1963): Equatorial current systems. In Hill, M.N. (editor): The Sea, Vol. 2, pp. 235-252.

Knutson, T. R., Zeng, F., and Wittenberg, A.T. (2013): Multi-model assessment of regional surface temperature trends: CMIP3 and CMIP5 20th century simulations. J. Climate, 26, pp. 8709-8743, (doi: 10.1175/JCLI-D-12-00567.1).

Kosaka, Y., and Xie, S. (2013): Recent global-warming hiatus tied to equatorial Pacific surface cooling. Nature, 501(7467), pp. 403-415.

Kug, J.-S., F.-F. Jin, and S.-I. An, 2009: Two types of El Niño events: Cold tongue El Niño and warm pool El Niño. J. Climate, 22, 1499-1515, doi:10.1175/2008JCLI2624.1

Kug, J.-S., Choi, J., An, S.I. Jin, F.F., and Wittenberg, A.T. (2010): Warm pool and cold tongue El Niño events as simulated by the GFDL CM2.1 coupled GCM. J. Climate, 23, pp. 1226-1239. (doi: 10.1175/2009JCLI3293.1).

Larson, S., and Kirtman, B. (2013): The Pacific meridional mode as a trigger for ENSO in a high-resolution coupled model. Geophys. Res. Lett., 40, pp. 3189-3194.

L'Heureux, M., Lee, S., and Lyon, B. (2013): Recent multidecadal strengthening of the Walker circulation across the tropical Pacific. Nature Climate Change, 3(6), pp. 571-576.

Lee, T., and McPhaden, M.J. (2010): Increasing intensity of El Niño in the central-equatorial Pacific. Geophysical Research Letters, 37.

Lee, T., and Fukumori, I. (2003): Interannual to decadal variation of tropical-subtropical exchange in the Pacific Ocean – boundary vs interior pycnocline transports. J.Climate, 16, pp. 4022-4042.

Lee, T., Lagerloef, G., Gierach, M.M., Kao, H.Y., Yueh, S.S., and Dohan, K. (2012): Aquarius reveals salinity structure of tropical instability waves. Geophys.Res.Lett., 39, L12610.

Legeckis, R. (1997): Long waves in the eastern equatorial Pacific, a view of a geostationary satellite. Science, 197, pp. 1177-1181.

Lengaigne, M., Boulanger, J., Menkes, C., Delecluse, P., Slingo, J., Wang, C., Xie, S., and Carton, J. (2004): Westerly wind events in the tropical Pacific and their influence on the coupled ocean-atmosphere system: A review. Earth's Climate: the Ocean-Atmosphere Interaction, 147, pp. 49-69.

Lengaigne, M., Boulanger, J.P., Menkes, C., and Spencer, H. (2006): Influence of the seasonal cycle on the termination of El Niño events in a coupled general circulation model. J. Climate, 19, pp. 1850–1868.

Lengaigne, M., and Vecchi, G.A. (2009): Contrasting the termination of moderate and extreme El Niño events in Coupled General Circulation Models. Climate Dynamics, (doi: 10.1007/s00382-009-0562-3).

Le Quéré, C., and co-authors: The global carbon budget 2013. Earth Syst.Sci.Data Discuss, 6, pp.689-760.

Li, J., S.P. Xie, E. R. Cook, G. Huang, R. D'Arrigo, F. Lui, J. Ma, and X-T. Zheng, 2011: Interdecadal modulation of El Niño amplitude during the past millennium. Nature Climate Change, 1, 114–118.

Li, J., Xie, S.P., Cook, E.R., Morales, M.S., Christie, D.A., Johnson, N.C., Chen, F., D'Arrigo, R., Fowler, M., Gou, X., and Fang, K. (2013): El Niño modulations over the past seven centuries. Nature Climate Change, 3, pp. 822–826, (doi:10.1038/nclimate1936).

Liu, Z., Vavrus, S., He, F., Wen, N. and Zhong, Y., 2005. Rethinking tropical ocean response to global warming: The enhanced equatorial warming. Journal of Climate, 18(22), pp. 4684-4700.

Lloyd, J., Guilyardi, E., and Weller, H. (2012): The Role of Atmosphere Feedbacks during ENSO in the CMIP3 Models. Part III: The Shortwave Flux Feedback. Journal of Climate, 25(12), pp. 4275-4293.

Lyman, J.M., Johnson, G.C., and Kessler, W.S. (2007): Distinct 17- and 33-day tropical instability waves in subsurface observations. J.Phys.Oceanogr., 37, pp. 855-872.

Lyman, J.M., and Johnson, G.C. (2008): Estimating annual global upper-ocean heat content anomalies despite irregular in situ ocean sampling. J. Climate, 21, (doi: 10.1175/2008JCLI2259.1, 5629–5641).

Maes, C., Picaut, J., and Belamari, S. (2002): Salinity barrier layer and onset of El Niño in a Pacific coupled model. Geophys. Res. Lett., 29, (doi:10.1029/2002GL016029).
Maes, C., Picaut, J., and Belamari, S. (2005): Importance of salinity barrier layer for the buildup of El Niño. J. Climate, 18, pp. 104-118.

Maes, C., and Belamari, S. (2011): On the impact of salinity barrier layer in the Pacific ocean mean state and ENSO. SOLA, 7, pp. 97-100, (doi:10.2151/sola.2011-025).

Mann, M., Cane, M.A., Zebiak, S.E., and Clement, A. (2005): Volcanic and solar forcing of El Niño over the past 1000 years. J. Climate, 18, pp. 447–456.

Martin, G.M., and co-authors (2011): The HadGEM2 family of Met Office Unified Model climate configurations. Geoscientific Model Development, 4(3), pp. 723-757.

McGregor, S., Timmermann, A., England, M.H., Elison Timm, O., and Wittenberg, A.T. (2013): Inferred changes in El Niño-Southern Oscillation variance over the past six centuries. Clim. Past, 9, pp. 2269-2284, (doi: 10.5194/cp-9-2269-2013).

McPhaden, M.J. (1995): The Tropical Ocean-Atmosphere (TAO) Array is completed. Bull. Amer. Meteor. Soc., 76, pp. 739-741.

McPhaden, M.J. (1996): Monthly period oscillation in the Pacific North Equatorial Countercurrent. J.Geophys.Res., 101, pp. 6337-6359.

McPhaden, M.J. (2012): A 21st century shift in the relationship between ENSO SST and warm water volume anomalies. Geophys.Res.Lett., 39, L09706.

McPhaden, M.J., Busalacchi, A.J., Cheney, J.R., Donguy, K.S., Gage, D., Halpern, M., Ji, M., Julian, P., Meyers, G., Mitchum, G.T., Niiler, P.P., Picaut, J., Reynolds, R.W., Smith, N., and Takeuchi, K. (1998): The tropical ocean-global atmosphere (TOGA) observing system – a decade of progress. J.Geophys.Res., 103, pp. 14169-14240.

McPhaden, M.J., Busalacchi, A.J., and Anderson, D.L.T. (2010): A TOGA retrospective. Oceanography, 23, pp. 86-103.

Meinen, C.S., and co-authors (2001): Vertical velocities and transports in the equatorial Pacific during 1993-1999. J.Phys.Oceanogr., 31, pp. 3230-3248.

Mitchell, T.P., and Wallace, J.M. (1992): On the annual cycle in equatorial convection and sea surface temperature. J.Climate, 5, pp. 1140-1156.

Monahan, A.H. (2004): A simple model for the skewness of global sea surface winds. J. Atmos. Sci., 61, pp. 2037–2049.

Monahan, A.H. and Dai, A. (2004): The spatial and temporal structure of ENSO nonlinearity. J. Clim., 17, pp. 3026-3036.

Moore, A.M. and Kleeman, R. (1999): Stochastic forcing of ENSO by the intraseasonal oscillation. J. Clim., 12, pp. 1199-1220.

Neelin, J.D., Battisti, D.S., Hirst, A.C., Jin, F.F., Wakata, Y., Yamagata, T., and Zebiak, S.E. (1998): ENSO theory. J.Geophys.Res., 103, pp. 14261-14290.

Newman, M., M. A. Alexander, and J. D. Scott, 2011a: An empirical model of tropical ocean dynamics. Climate Dyn., 37, 1823–1841, doi:10.1007/s00382-011-1034-0.

Newman, M., Shin, S.I., and Alexander, M.A. (2011b): Natural variation in ENSO flavors. Geophys. Res. Lett., 38, L14 705, (doi:10.1029/2011GL047658).

Ogata, T., Xie, S.P., Wittenberg, A.T., and Sun, D.Z. (2013): Interdecadal amplitude modulation of El Niño/Southern Oscillation and its impacts on tropical Pacific decadal variability. J. Climate, 26, pp. 7280-7297, (doi: 10.1175/JCLI-D-12-00415.1).

Penland, C., and Sardeshmukh, P.D., (1995): The optimal growth of tropical sea surface temperature anomalies. J. Clim., 8, pp. 1999-2024.

Picaut, J., and Tournier, R. (1991): Monitoring the 1979-1985 equatorial Pacific current transports with XBTs. J. Geophys. Res., 96, pp. 3263-3277.

Polito, P.S., Ryan, J.P., Liu, W.T., and Chavez, F.P. (2001): Oceanic and atmospheric anomalies of tropical instability waves. Geophys.Res.Lett., 28, (doi: 10.1029/2000GL012400).

Price, J. F., Weller, R.A., and Pinkel, R. (1986): Diurnal cycling: Observations and models of the upper ocean response to diurnal heating, cooling and wind mixing. J. Geophys. Res., 91, pp. 8411–8427.

Qiao, L., and Weisberg, R.H. (1995): Tropical instability wave kinematics – observations from the tropical instability wave experiment. J.Geophys.Res., 100, pp. 8677-8693.

Qiu, B., and Chen, S. (2012): Multidecadal sea level and gyre circulation variability in the northwestern Tropical Pacific Ocean. J.Phys.Oceanogr., 42, pp. 193-206.

Rebert, J.P., Donguy, J.P., Eldin, G., and Wyrtki, K. (1985): Relations between sea level, thermocline depth, heat content and dynamic height in the tropical Pacific Ocean. J. Geophys. Res., 90, pp. 11719-11725.

Ren, H.L., and Jin, F.F. (2013): Recharge Oscillator Mechanisms in Two Types of ENSO. J. Climate, 26, pp. 6506–6523. (doi:10.1175/JCLI-D-12-00601.1).

Risien, C.M., and Chelton, D.B. (2008): A global climatology of surface wind and wind stress fields from eight years of QuikSCAT Scatterometer data. J.Phys.Oceanogr., 38, pp. 2379-2413.

Rodgers, K.B., Friederichs, P., and Latif, M. (2004): Tropical pacific decadal variability and its relation to decadal modulations of ENSO. J. Clim., 17, pp. 3761-3774.

Roemmich, D., and Cornuelle, B. (1990): Observing the fluctuations of t gyre-scale ocean circulation: A study of the South Pacific. J. Phys. Oceanogr., 20, pp. 1919-1934.

Roemmich, D., and Gilson, J. (2001): Transport of heat and thermocline waters in the North Pacific:A key to interannual/decadal climate variability? J. Phys. Oceanogr., 31, pp. 675-691.

Schopf, P. S., and Burgman, R.J. (2006): A simple mechanism for ENSO residuals and asymmetry. J. Climate, 19, pp. 3167–3179.

Schudlich, R.R., and Price, J.F. (1992): Diurnal cycles of current, temperature, and turbulent dissipation in a model of the equatorial upper ocean. J. Geophys. Res., 97, pp. 5409-5422.

Singh, A., and Delcroix, T. (2013): Eastern and Central Pacific ENSO and their relationships to the recharge/discharge oscillator paradigm. Deep Sea Res. Part I: Oceanographic Research Papers, 82, pp. 32-43, (doi:10.1016/j.dsr.2013.08.002).

Solomon, A., and Newman, M. (2012): Reconciling disparate twentieth-century Indo-Pacific ocean temperature trends in the instrumental record. Nature Climate Change, 2(9), pp. 691-699.

Spencer, H. (2004): Role of the atmosphere in seasonal phase locking of El Niño. Geophys. Res. Lett., 31, L24104, (doi:10.1029/2004GL021619).

Stevenson, S., Fox-Kemper, B., Jochum, M., Neale, R., Deser, C., and Meehl, G. (2012): Will there be a significant change to El Niño in the 21st century? J. Climate, 25, pp. 2129–2145, (doi:10.1175/JCLI-D-11-00252.1).

Suarez, M., and Schopf, P. (1988): A delayed action oscillator for ENSO. Journal of the Atmospheric Sciences, 45(21), pp. 3283-3287.

Sweeney, C., Gnanadesikan, A., Griffies, S., Harrison, M., Rosati, A., and Samuels, B. (2005): Impacts of shortwave penetration depth on large-scale ocean circulation heat transport, J. Phys. Oceanogr., 35, pp. 1103–1119.

Takahashi, T., S. C. Sutherland, R. Wanninkhof, C. Sweeney, R. A. Feely, D. W. Chipman, B. Hales, G. Friederich, F. Chavez, A. Watson, D. C. E. Bakker, U. Schuster, N. Metzl, H. Yoshikawa-Inoue, M. Ishii, T. Midorikawa, Y. Nojiri, C. Sabine, J. Olafsson, Th. S. Arnarson, B. Tilbrook, T. Johannessen, A. Olsen, Richard Bellerby, A. Körtzinger, T. Steinhoff, M. Hoppema, H. J. W. de Baar, C. S. Wong, Bruno Delille and N. R. Bates (2009): Climatological mean and decadal changes in surface ocean pCO2, and net sea-air CO2 flux over the global oceans. Deep-Sea Res. II, 56, pp. 554-577.

Takahashi, K., Montecinos, A., Goubanova, K., and Dewitte, B. (2011): ENSO regimes: Reinterpreting the canonical and Modoki El Niño. Geophysical Research Letters, 38.

Taft, B.A., and Kessler, W.S. (1991): variations of zonal current in the central tropical Pacific during 1970 to 1987: Sea level and dynamic height measurements. J. Geophys. Res., 96(C7), pp. 12599-12618.

Thompson, C.J., and Battisti, D.S. (2000): A linear stochastic dynamical model of ENSO. Part I: model development. J. Clim., 13, pp. 2818-2832.

Trenberth, K., and Hoar, T.J (1997): El Niño and climate change, Geophys. Res. Lett., 24, pp. 3057–3060.

Timmermann, A., and Jin, F.F. (2002): Phytoplankton influences on tropical climate. Geophys. Res. Lett., 29, 2104, (doi:10.1029/2002GL015434).

Timmermann, A., Jin, F.F., and Collins, M. (2004): Intensification of the annual cycle in the tropical Pacific due to greenhouse warming. Geophys. Res. Lett., 31, L12208.

Timmerman, H., and co-authors (2005): ENSO suppression due to weakening of the North Atlantic thermohaline circulation. J.Clim., 18, pp. 3122-3139.

Tokinaga, H., S.-P. Xie, A. Timmermann, S. McGregor, T. Ogata, H. Kubota, and Y. M. Okumura, 2012a: Regional patterns of tropical Indo-Pacific climate change: Evidence of the Walker Circulation weakening. J. Climate, 25, 1689-1710. doi:10.1175/JCLI-D-11-00263.1.

Tokinaga, H., Xie, S.P., Deser, C., Kosaka, Y., and Okumura, Y.M. (2012b): Slowdown of the Walker Circulation driven by Indo-Pacific warming. Nature, 491, pp. 439-443. (doi:10.1038/nature11576).

Trenberth, K., and Fasullo, J. (2012): Tracking Earth's Energy: From El Nio to Global Warming. Surveys in Geophysics, 33(3-4), pp. 413-426.

Turner, A.G., Inness, P.M., and Slingo, J.M. (2005): The role of the basic sst in the ENSO-monsoon relationship and implications for predictability. Quart. J. Roy. Meteor. Soc., 131, pp. 781-804.

Tziperman, E., Stone, L., Cane, M.A., and Jarosh, H. (1994): El Niño chaos: Overlapping of resonances between the seasonal cycle and the Pacific Ocean-Atmosphere oscillator. Science, 264, pp. 72–74.

US CLIVAR Project Office (2013): U.S. CLIVAR ENSO Diversity Workshop Report. Report 2013-1, U.S. CLIVAR Project Office, Washington, DC, 20006, pp. 20-32.

Vecchi, G. (2006): The termination of the 1997/98 El Niño. Part II: Mechanisms of tmospheric change. J. Climate, 19, pp. 2647–2664.

Vecchi, G., and Harrison, D.E. (2006): The termination of the 1997/98 El Niño. Part I: Mechanisms of oceanic change. J. Climate, 19, pp. 2633–2646.

Vecchi, G.A. (2006): The termination of the 1997-98 El Niño. Part II: Mechanisms of Atmospheric Change. J. Climate, v.19, pp. 2647-2664.

Vecchi, G.A., and Soden, B.J. (2007): Global warming and th weakening of the tropical circulation. J.Clim., 20, pp. 4316-4340.

Vecchi, G., Soden, B., Wittenberg, A., Held, I., Leetmaa, A., and Harrison, M. (2006): Weakening of tropical Pacific atmospheric circulation due to anthropogenic forcing. Nature, 441(7089), pp- 73-76.

Vecchi, G. A., and Wittenberg, A.T. (2010): El Niño and our future climate: Where do we stand? Wiley Interdisciplinary Reviews: Climate Change, 1, pp. 260-270. (doi: 10.1002/wcc.33).

Vecchi, G. A., Wittenberg, A.T., and Rosati, A. (2006a): Reassessing the role of stochastic forcing in the 1997-8 El Niño. Geophys. Res. Lett., 33, L01706, (doi: 10.1029/2005GL024738).

Vecchi, G. A., Soden, B.J., Wittenberg, A.T., Held, I.M., Leetmaa, A., and Harrison, M.J. (2006b): Weakening of tropical Pacific atmospheric circulation due to anthropogenic forcing. Nature, 441, pp. 73-76, (doi: 10.1038/nature04744).

Wang, W., and McPhaden, M.J. (1999): The surface layer heat balance in the equatorial Pacific Ocean – Part I (Mean seasonal cycle). J.Phys.Oceanorgr., 29, pp. 1812-1831.

Wang, W., and McPhaden, M.J. (2000): The surface layer heat balance in the equatorial Pacific Ocean – Part II (Interannual variability). J.Phys.Oceanogr., 30, pp. 2989-3008.

Wang, W., and McPhaden, M.J. (2001): Surface layer heat balance in the equatorial Pacific Ocean during the 1997-1998 El Niño and the 1998-1999 La Niña. J.Climate, 14, pp. 3393-3407.

Wang, C., and Picaut, J. (2004): Understanding ENSO physics – a review. In Wang, C., Xie, S.P., and Carton, J.A. (editors): Earth's climate – the ocean-atmosphere interaction, AGU, pp. 21-48.

Wanninkhof, R., Park, G.H., Takahashi, T., Sweeney, C., Feely, R., Nojiri, Y., Gruber, N., Doney, S.C., McKinley, G.A., Lenton, A., Le Quéré, C., Heinze, C., Schwinger, J., Graven, H., and Khatiwala, S. (2013): Global ocean carbon uptake – magnitude, variability and trends. Biogeosciences, 10, pp. 1983-2000.

Watanabe, M., and Wittenberg, A.T. (2012): A method for disentangling El Niño-mean state interaction. Geophys. Res. Lett., 39, L14702, (doi: 10.1029/2012GL052013).

Watanabe, M., Kug, J.S., Jin, F.F., Collins, M., Ohba, M., and Wittenberg, A.T. (2012): Uncertainty in the ENSO amplitude change from the past to the future. Geophys. Res. Lett., 39, L20703, (doi: 10.1029/2012GL053305).

Wittenberg, A. T. (2002): ENSO response to altered climates. Ph.D. thesis, Princeton University. Pp. 475-490.

Wittenberg, A. T. (2004): Extended wind stress analyses for ENSO. J. Climate, 17, pp. 2526-2540, (doi: 10.1175/1520-0442(2004)017%3C2526:EWSAFE%3E2.0.CO;2).

Wittenberg, A. T., Rosati, A., Lau, N.C., and Ploshay, J.J. (2006): GFDL's CM2 global coupled climate models, Part III: Tropical Pacific climate and ENSO. J. Climate, 19, pp. 698-722, (doi: 10.1175/JCLI3631.1).

Wittenberg, A. T. (2009): Are historical records sufficient to constrain ENSO simulations? Geophys. Res. Lett., 36, L12702, (doi: 10.1029/2009GL038710).

Wittenberg, A. T., Rosati, A., Delworth, T.L., Vecchi, G.A., and Zeng, F. (2014): ENSO modulation: Is it decadally predictable? J. Climate, in press.

Weng, H., Behera, S.K., and Yamagata, T. (2009): Anomalous winter climate conditions in the Pacific Rim during recent El Niño Modoki and El Niño events. Climate Dynamics, 32, pp. 663-674.

Wood, R., and co-authors (2011): The VAMOS Ocean-Cloud-Atmosphere-Land Study Regional Experiment (VOCALS-REx): goals, platforms, and field operations. Atmospheric Chemistry and Physics, 11(2), pp. 627-654.

Wyrtki, K. (1974): Equatorial currents in the Pacific, 1950 to 1970 and their relation to the trade winds. J.Phys.Oceanogr., 4, pp. 372-380.

Wyrtki, K. (1975): El Niño – the dynamic response of the equatorial Pacific Ocean to atmospheric forcing. J.Phys.Oceanogr. 5 (4), pp. 572-584.

Wyrtki, K. (1979): Sea level variations: Monitoring the breath of the Pacific. Eos Trans. AGU, 60, 25-27.

Wyrtki, K. (1981): An estimate of equatorial upwelling in the Pacific. J.Phys.Oceanogr. 11, pp. 1205-1214.

Xie, S.-P. (1994): On the genesis of the equatorial annual cycle. J. Climate, 7, pp. 2008-2013.

Xie, S.-P., C. Deser, G. A. Vecchi, J. Ma, H. Teng, and A. T. Wittenberg, 2010: Global warming pattern formation: Sea surface temperature and rainfall. J. Climate, 23, 966-986. doi: 10.1175/2009JCLI3329.1

Xie, S.P., Ishiwatari, M., Hashizume, H., and Takeuchi, K. (1998): Coupled ocean-atmospheric waves on the equatorial front. Geophys.Res.Lett., 25, pp. 3863-3966.

Xue, Y., Cane, M.A., and Zebiak, S.E. (1997): Predictability of a coupled model of ENSO using singular vector analysis, Part I: Optimal growth in seasonal background and ENSO cycles. Mon. Wea. Rev., 125, 2043–2056.

Yeh, S.-W., Kug, J.S., Dewitte, B., Kwon, M.H., Kirtman, B.P., and Jin, F.F. (2009): El Niño in a changing climate. Nature, 461, pp. 511-514, (doi:10.1038/nature08316).

Yoder, J.A. and co-authors (1994): A line in the sea, Nature, 371, pp. 689-692.

Zavala-Garay, J., Zhang, C., Moore, A.M., Wittenberg, A.T., Harrison, M.J., Rosati, A., Vialard, J. and Kleeman, R. (2008): Sensitivity of hybrid ENSO models to unresolved atmospheric variability. J. Climate, 21, pp. 3704-3721, (doi: 10.1175/2007JCLI1188.1).
Zebiak, S.E., and Cane, M.A., (1987).: A model El Niño-Southern oscillation. Mon. Wea. Rev., 115, pp. 2262-2278.

Zhang, L., Chang, P., and Ji, L. (2009): Linking the Pacific meridional mode to ENSO: Coupled model analysis. J. Climate, 22, pp. 3488–3505, (doi:10.1175/2008JCLI2473.1).

Zhang, X., McPhaden, M.J. (2006): Wind stress variations and interannual sea surface temperature anomalies in the eastern equatorial Pacific. J. Climate, 19, pp. 226–241.

Zheng, Y., Lin, J., and Shinoda, T. (2012): The equatorial Pacific cold tongue simulated by IPCC AR4 coupled GCMs: Upper ocean heat budget and feedback analysis. Journal of Geophysical Research-Oceans, 117.

White Paper #4 – Operational forecasting systems

Balmaseda, M.A.[1], Kumar, A.[2], Andersson, E.[1], Takaya, Y.[3], Anderson, D., Janssen, P.[1], Martin, M.[4], and Fujii, Y.[1]

[1] European Center for Medium-Range Weather Forecasts, United Kingdom
[2] National Centers for Environmental Prediction, United States
[3] Japan Meteorological Agency, Japan
[4] UK Meteorological Office, United Kingdom
[5] Meteorological Research Institute, Japan

1. Introduction

There is clear demand for reliable weather, marine and climate forecasts at different time scales for a variety of societal applications. The improvement of the observing systems, model development, and computer resources have pushed the operational forecasting activities to expand well beyond the traditional short-range (1-3 days) weather forecast. Current operational forecasting capabilities take advantage of better initialization techniques, incorporate probabilistic methods to cope with the chaotic nature of the atmosphere, and rely on coupled ocean -atmosphere models that can predict the slowly evolving sea-surface-temperature and its impact on the atmosphere, to progressively increase the lead time of forecast horizon.

Medium-range (10-15 days) weather and marine forecasts are now produced operationally in the major forecasting centers, as well as forecasts of climate at seasonal (up to 6-12 months lead time) time scales, and more recently, forecasts at subseasonal time scales (1-2 months lead time), bridging the gap between weather and climate. Figure 1.1 shows schematically the time and spatial scales characteristics of the different forecasting systems. Given the coupled nature of the ocean-atmosphere system, it is expected that the ocean will play an active role in the forecasting systems at all lead-times in the future[1].

Although the observational needs of the different forecasting systems vary, all of them revolve around four main activities: initialization of the ocean and atmosphere for subsequent prediction; model and data assimilation development; forecast verification and, in some cases, calibration of model output; and hindcasts for calibration and skill assessment. Both verification and calibration of forecasts require long ocean and atmosphere reanalyses and reforecasts. The reanalyses are also used for monitoring of the Earth System's climate. This paper discusses the requirements of ocean and boundary layer observations in the tropical Pacific from the perspective of forecasting systems spanning different time-scales: medium range (section 2), seasonal (section 3) and monthly (section 4), organized in order of their maturity. The observational needs for reanalyses, with emphasis on their use for climate monitoring, are discussed in more detailed in section 5. Section 6 provides a summary of recent and future developments, including decadal forecasts, coupled forecasting systems, as well as coupled ocean-atmosphere reanalyses and initialization of forecasting systems. Section 7 presents a summary of general considerations that are common to all the different applications, with

[1] For example, the ECMWF medium range ensemble prediction system has used a coupled ocean-wave-atmosphere model since November 2013.

emphasis on the interpretation of observing system experiments, model error, and the different applications of the observations. The paper ends with a summary of data requirements and specific recommendations (section 8).

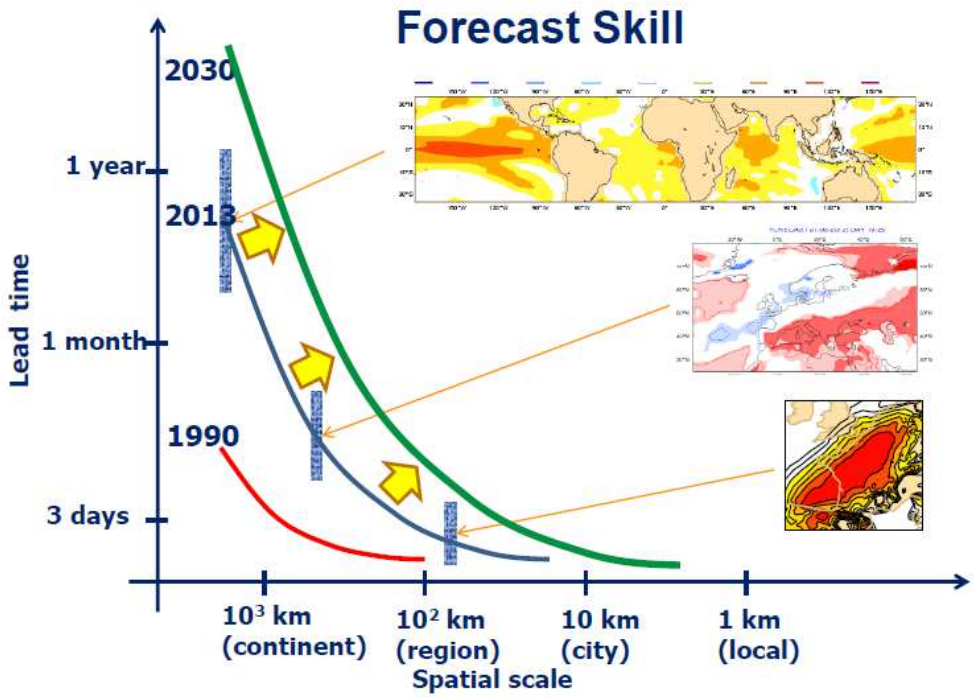

Figure 1.1 - Schematics of the dependence of forecast skill as a function of lead time and spatial resolution. The different size of the vertical bars is indicative of the characteristic averaging time (hours-days, weeks, seasons) for which the forecast is issued.

As such, the scope of the paper outlined above is already too wide, and there are topics not of relevance not explicitly addressed here, but are covered in other white papers. For example, the needs for medium-range high resolution marine forecasting systems are discussed in TPOS-2020 TPOS WP5 (Fujii et al., (2014)). The needs for model development regarding parameterization of atmospheric convection and boundary layer processes, a cross-cutting theme for forecasting activities on all time-scales, are discussed in TPOS WP11 (Cronin et al., 2014). Ocean biochemistry requirements are addressed in a separate paper (TPOS WP6, Mathis et al., 2014). The needs to calibrate and reprocess satellite data are covered in TPOS WP9 (Lindstrom et al., 2014).

To facilitate the discussion of the data needs, Appendix A introduces a naming convention regarding the processing level of the observations, the quality control, and the time-delivery properties.

2. Global Numerical and Wave forecasts at the medium range

Global Numerical Weather Prediction (NWP) models are used to produce medium range weather forecasts (out to 15 days), with a horizontal resolution of typically 15-50 km and a vertical resolution of 10-30 m near the surface increasing to 500 m-1 km in the stratosphere.

There is a strong interest in using NWP model output to predict the risk for extremes or severe and damaging weather events. Statistical approaches based on forecast ensembles are used to predict the probability for extreme or rare events at longer lead times. Such ensembles require good knowledge of the uncertainty in all input data including the observations. Global NWP WP models are also used to provide boundary conditions for regional NWP models.

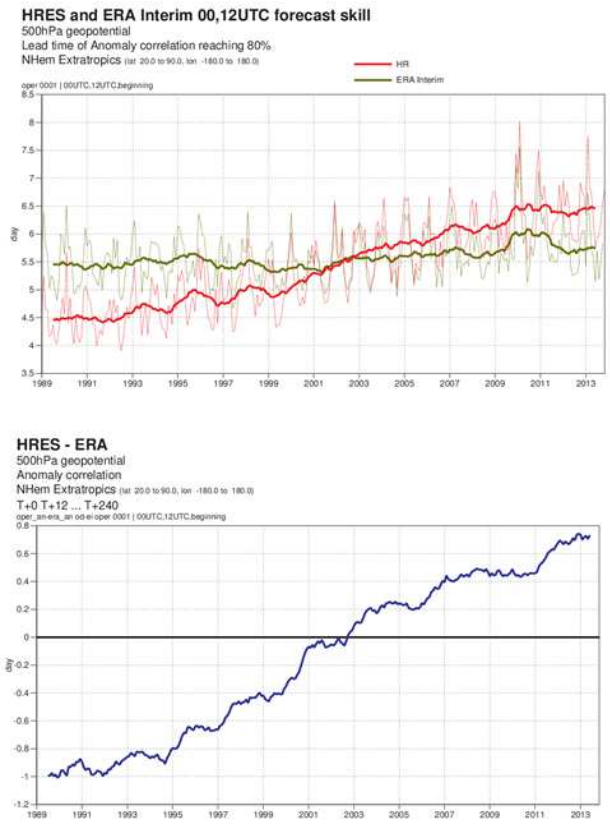

Figure 2.1 - Progress in the ECMWF operational NWP forecast skill since 1989 (OPS, red line) and in ERA-Interim (green line). The skill is measured as the forecast lead time when correlation drops below 80%. The statistics are for the Northern Hemisphere Z500. Progress is about 1 day per decade. The difference between OPS and ERA-Interim (lower panel) filters out changes due to intrinsic predictability of the atmosphere, and highlights progress due to model and data assimilation improvement. The observing system in the 90's is better exploited with the ERA-Interim forecasting system (which was state of the art one decade later) than with the forecasting system used at the time.

Figure 2.1 shows the progress in NWP forecast skill from the ECMWF operational forecasting system (red line, top panel). The metric is the forecast lead time when the anomaly correlation drops below 80% when predicting the geopotential at 500hPa (Z500) in the Northern Hemisphere. The progress is slow but steady (about 1 day per decade). The skill depends very much on the seasonal cycle, and it is convenient to filter the seasonal cycle with a 12-month running mean (red thick line). Another way of filtering out changes in the intrinsic predictability of the atmosphere is to compare with a reference experiment given by forecasts initialized from the ERA-Interim reanalysis system (Dee et al., 2011), which uses a frozen model and data assimilation cycle (the one operational around 2006). The differences between operational and

ERA-Interim show the impact of model and data assimilation development efforts. The observing system in the 90's produces better skill when analyzed with a more advanced forecasting system (typical of the state of the art one decade later). Equally, increases in model resolution and continuous development are incorporated in the operational NWP system, which soon leaves ERa-Interim behind.

To initialize NWP models, an accurate estimate of the complete atmospheric state is required. Observations from surface-based, airborne and space-based platforms are all used to help define this initial state. Reliable error estimates of all observations are needed to estimate the accuracy of the initial state. The observational requirements for global NWP are based on the need to provide an accurate analysis of the complete atmospheric state and the Earth's surface at regular intervals (typically every 6 hours). Through a "data assimilation" system, new observations are used to update and improve an initial estimate of the atmospheric and surface states provided by an earlier short-range forecast. The uncertainty in the initial conditions is generally captured by ensembles of data assimilations.

The key atmospheric model variables for which observations are needed are: 3-dimensional fields of wind, temperature and humidity, and the 2-dimensional field of surface pressure. Also important are surface boundary variables, particularly sea surface temperature, soil moisture and vegetation, ice and snow cover. Of increasing importance in NWP systems are observations of cloud and precipitation. In the latter part of the medium-range, the upper layers of the ocean become increasingly important, and therefore, relevant observations of the ocean are also needed.

The highest benefit is derived from observations available in near real-time; NWP centers derive more benefit from observational data, particularly continuously generated asynoptic data (e.g. polar orbiting satellite data), the earlier they are received, with a goal of less than 30 minutes' delay for observations of geophysical quantities that vary rapidly in time. However, most centers can derive some benefit from data that is up to 6 hours old.

In general, conventional observations have limited horizontal resolution and coverage, but high accuracy and vertical resolution. In situ observations over the ocean or from remote land areas can occasionally be of vital importance. Also, a baseline network of in situ observations is currently necessary for calibrating the use of some satellite data. Observations are more important in some areas than in others; it is desirable to make more accurate analyses in areas where forecast errors grow rapidly, e.g. baroclinic zones and in areas of intense convection, such as the warm pool in the tropical Pacific.

2.1 Surface pressure and surface wind

Over the ocean, ships and buoys provide observations with good frequency. Accuracy is good for pressure and acceptable/marginal for wind. Coverage is generally good but marginal or absent over some areas in the tropics and the Arctic. The coverage in the tropical Pacific has degraded in recent years. Scatterometers on polar-orbiting satellites provide information on surface wind - with global coverage and acceptable horizontal and temporal resolution and accuracy. Scatterometers give information on both wind speed and direction, whereas passive microwave imagers provide information on wind speed only.

Surface pressure is not observed by present or planned satellite systems except for: some contribution from radio occultation data and measurements of differential atmospheric optical depth for a gas of known composition such as oxygen.

2.2 Sea surface temperature

Ships and buoys provide observations of sea surface temperature of good temporal frequency and accuracy. Coverage is marginal or absent over some areas of the Earth, but recent improvements in the in situ network have enhanced coverage considerably. Infrared instruments on polar satellites provide information with global coverage, good horizontal resolution and accuracy, except in areas that are persistently cloud-covered. Here data from passive microwave instruments on research satellites has been shown to be complementary. Observation of the diurnal cycle is becoming increasingly important, for which present and planned geostationary satellites offer a capability.

2.3 Ocean sub-surface variables

In the latter part of the medium-range (~7-15 days), the role of the sub-surface layers of the ocean becomes increasingly important, and hence observations of these variables become relevant. In this respect the requirements of global NWP are similar to those of seasonal and sub-seasonal forecasting (see section 3).

2.4 Sea State

Observations of the sea state from ships have become available since the middle of the nineteenth century. These observations are manually made and concern wave height, period and direction of the wind sea and the swell part of the sea state. The coverage of these observations is marginal over large areas of the Earth. Although ship manual observations have a great historical value, the observations are of marginal accuracy. Increases in accuracy can only be expected when observations by humans are replaced by instruments such as a shipborne wave recorder. The introduction of these will also benefit the observation frequency which is presently every 3 to 6 hours.

Moored buoy provide sea state observations of acceptable frequency (hourly) and acceptable quality. The buoys record the time series of the surface elevation which gives the frequency spectrum and, as a consequence, parameters such as wave height, peak period and several versions of mean period. Certain buoy types are able to give the directional wave spectrum, while buoys from the Canadian network produce estimates of maximum wave height, a parameter which is important for extreme sea states.

The highest quality wave height observations are nowadays provided by altimeters on board of polar orbiters. Although the coverage is global the spatial and temporal resolution is marginal as only along track observations are available. Despite this, these observations have played a major role in the improvement of the physics and numerics of ocean wave models. A number of weather centers use the altimeter wave heights in their wave height analysis.

Information on the low-frequency part of the two-dimensional spectrum can be obtained from Synthetic Aperture Radar (SAR) instruments. The accuracy is good, but horizontal and temporal

resolution is marginal. These observations have been used in the wave analysis of a number of weather centers.

2.5 Data assimilation in the tropics

The Final Report of the Fifth WMO Workshop on the Impact of Various Observing Systems on Numerical Weather Prediction (Andersson et al., 2012) concluded: “Current global observing systems are heavily skewed towards mass observations over wind measurements, especially for the satellite components. And yet many studies presented at the workshop pointed to a higher than average impact of wind observations, both on a component and on a “per-observation” basis. There is a need to invest in enhanced wind observations in the tropics and over the oceans especially.”

A substantial fraction of the tropical large-scale variability can be explained by equatorially trapped waves; the equatorial waves coupled to convection can explain on average 60–70% of the error variance in the tropical atmosphere (Zagar et al., 2005). The largest part of this explained variance is represented by the equatorial Rossby (ER) modes, and a significant percentage pertains to the equatorial inertio-gravity (EIG) modes. Most likely, deep convection, acting as a generator of equatorial wave motion, is the dominant mechanism.

To ensure that the observational information is assimilated mainly in terms of Rossby modes, initialization procedures and methods for generating geostrophically balanced increments have been developed. In the tropics a dominant relationship similar to geostrophy is lacking; the analysis here has thus traditionally been undertaken in the univariate fashion. Consequently, large-scale divergence fields, such as the Hadley and Brewer–Dobson circulations, are analysed nearly univariately. Since the Global Observing System in the tropics relies on mass-field information, uncertainties in the analysed wind field are significant. Furthermore, large-scale motion in the tropics cannot be considered without taking into account inertio-gravity (IG) waves (Browning et al., 2000). In addition, the change of sign of the Coriolis parameter at the equator gives rise to important types of large-scale non-rotational motion, which are absent in the mid-latitude atmosphere: the Kelvin and mixed Rossby–gravity (MRG) modes. Indeed, equatorially trapped Kelvin, MRG and equatorial IG waves have regularly been detected in observations since the 1960s. Observational studies (Wheeler and Kiladis, 1999) identified equatorially trapped wave structures in long-term satellite observations of outgoing long-wave radiation, a proxy for deep tropical cloudiness. The waves have been denoted the ‘convectively-coupled equatorial waves’, as their presence in areas of moist convection implies an interaction between convection and the dynamics. In order to initialize these structures accurately, mass and wind information is required in the areas surrounding the equator, particularly in the tropical Pacific warm pool and surrounding areas.

2.6 Data Withdrawal Experiment: Impact of Winds from Moored Buoys

Traditionally, in situ observations of surface pressure and wind field have played an important role in weather analysis and weather forecasting. Using data assimilation techniques, these observations provide information on the initial state of the forecast, while much can be learned from the validation of the forecast by means of these so-called conventional observations. Nowadays, however, we are facing a different situation because over the past 20 years weather

forecasting centers have introduced a massive amount of satellite data in their analysis systems. The question now is whether in the presence of overwhelming amount of satellite observations the relatively small number of in situ observations can still add information to the weather analysis in the Tropics.

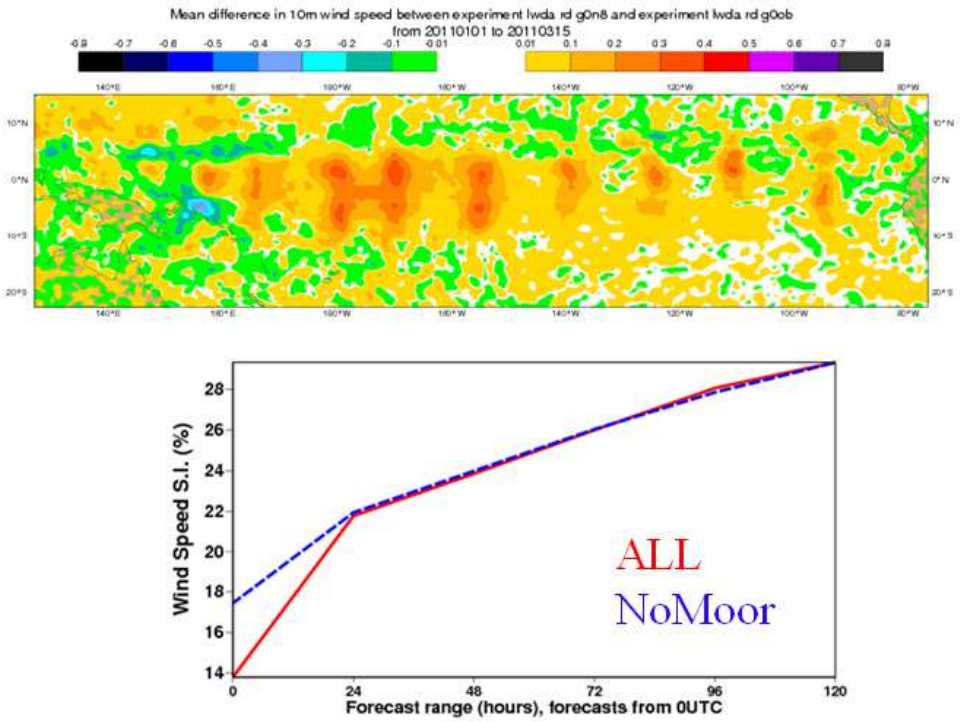

Figure 2.2 - Impact of withdrawing the wind information from the moored buoys in NWP experiments. Experiment ALL is the standard control experiment; experiment NoMoor is equivalent to ALL, but the wind from moored buoys is not used. (Top) Mean differences in analyzed 10m wind speed (ALL - NoMoor), for the period 20110101-20110315, showing that the moorings have a pronounced impact on the analyzed wind speed. (Bottom) Scatter index as a function of forecast lead time, verified against all tropical buoy data. This shows that the information from the moorings is quickly lost in the forecasts.

In order to investigate this, a data denial experiment was performed in which all the pressure and wind vector observations from moored buoys in the Tropics were removed (Bidlot and De Chiara, in preparation). Analysis and forecast results from the data denial experiment were subsequently compared with results from the control experiment, i.e., an experiment which includes all the relevant observations from the Tropics, but has otherwise an identical set-up. Recently weather centers experience a dramatic decrease in the amount of TAO array observations that are received through the GTS. For this reason we had to go back to the year 2011 to have a sufficient number of observations to do a meaningful experiment. Cycle 40R1, which is the latest cycle of the IFS, was chosen for the experimentation and analyses and 10 day forecasts were produced for the period 1 January 2011 until 31 March 2011. The spatial resolution was 40 km (corresponding to a T511 truncation in spectral space) while in the vertical there were 91 levels.

Figure 2.2 (top) shows the systematic difference between analysed surface wind speed from control and data denial experiments, averaged over a 2 1/2 month period. Differences are quite considerable, of the order of 0.4 m/s, and the use of buoy data leads to larger wind speeds in the analysis. It should also be clear from difference patterns where a number of TAO/TRITON moorings are located. This is particularly evident in the west Tropical Pacific. It may come as a surprise that removal of the buoy data in the Tropics has such a big impact on the wind speed analysis. It can be understood by realizing that the TAO array produces good quality wind vector observations on a frequent, hourly basis. They apparently can compete with the scatterometer observations on board polar orbiters as these visit the area where the buoys are located relatively infrequently.

The impact on the wind speed and wave height scores in the Tropical area is, however, fairly limited. This is illustrated by Figure 2.2 (bottom), which shows the scatter index (normalized standard deviation of error) in forecast wind speed, obtained from a comparison with buoy wind speeds. The area is the Tropics. It is evident from this plot that the impact of the Tropical buoy data on the forecast scores for surface winds is already fairly small after one day in the forecast. This also follows from a verification of the forecast wind speed against the control analysis, although in this case there is impact until Day 2 of the forecast. The impression is that the Tropical analysis of wind is not very well-balanced at the initial time, and ingested information is lost rapidly due to initial shocks. As already mentioned in the previous section, unlike the extra-tropics, there is no dominant balance relationship similar to geostrophy. This imbalance is supported by the experience that in the first 12 hours of the Tropical forecast there are signs of spin-down in, for example, the average Tropical wind speed.

Despite the fact that the weather analysis in the Tropics is relatively poor (hence more effort is needed to alleviate the problem with imbalance in the analysis) the in situ observations of surface wind and pressure are considered to be of value for weather forecasting. In a coupled ocean-atmosphere context the observations are potentially of greater value, as parameters such as SST are quite sensitive to errors in the forcing wind field.

3. Seasonal Forecasts

3.1 Description of a Seasonal Forecasting System

Good-quality seasonal forecasts with reliable uncertainty estimates are of great value to society, allowing institutions and governments to plan actions to minimize risks, manage resources, and increase prosperity and security. Human and economic losses that may be caused by adverse climate events can be mitigated with early warning systems (e.g. famine, epidemics) and disaster preparedness. Equally, adequate planning can aid the exploitation of favorable climate conditions.

Seasonal forecasts predict variations in the atmospheric circulation in response to anomalous boundary forcing, changing significantly the probability of occurrence of weather patterns (Palmer and Anderson, 1994). Seasonal forecasting systems are based on coupled ocean-atmosphere general circulation models that predict both the surface boundary forcing and its impact on the atmospheric circulation. The chaotic nature of the atmosphere is taken into account by issuing probabilistic forecasts based on an ensemble of coupled integrations.

An added requirement for seasonal, and in general, extended-range forecast systems is correction for model biases. This step is required as forecast anomalies can easily be of the same magnitude as the model bias, and thus, can be overwhelmed by model errors. The bias correction of real-time forecasts is done by conducting a series of past seasonal hindcasts (also referred to asa reforecasts), which in turn requires initial conditions for a historical period (typically 15-25 years), usually obtained from reanalyses. The reforecasts are also needed for skill assessment for the seasonal forecast system that needs to be conveyed to the user community.

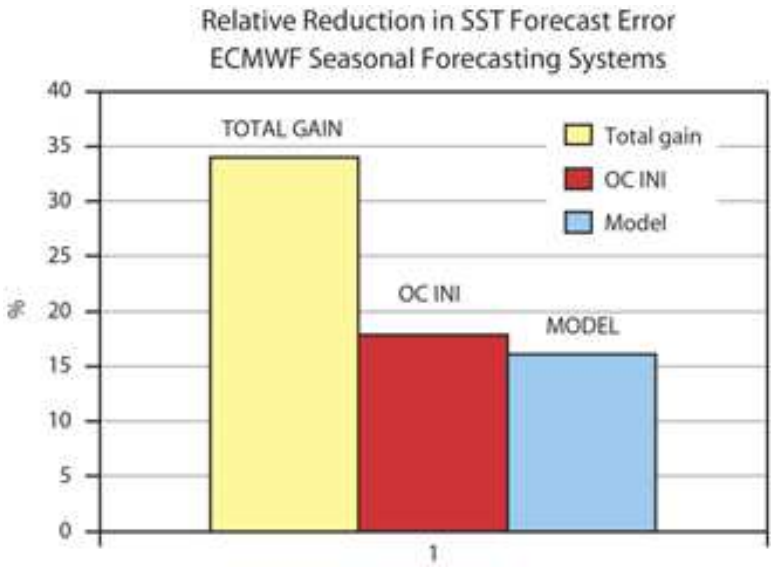

Figure 3.1.Progress in the seasonal forecast skill of the ECMWF operational system since it became operational around 1996. The yellow bar shows the relative reduction in mean absolute error of forecast of SST in the eastern Pacific (NINO3) integrated over the 1-6 months lead time. Contribution from model development (blue bar) and ocean initialization (red bar) are equally important. Developments in ocean and atmosphere models also contribute to the ocean initialization.

Of special importance for seasonal predictions are the variations of the tropical SST in the Pacific sector associated with El Niño Southern Oscillation (ENSO), and is the underpinning of operational seasonal prediction efforts. SST variations associated with ENSO alter the tropical convection and associated changes in heat sources lead to changes in atmospheric circulation. The importance of ENSO in seasonal forecasts is further enhanced by its relatively high potential predictability (Zebiak and Cane, 1987), which is largely inherent equatorial wave dynamics. Thus, the predictability of climate variability on seasonal time-scales depends critically on the adequacy of initial conditions of the ocean. See supplementary figure S1 for an illustration of the equatorial wave dynamics and impact on SST anomalies. However, linear wave dynamics is insufficient to predict the SST outcome, as can be seen in the same figure: not every eastern propagating Kelvin wave leads to an SST anomaly of the expected sign. Figure S1 also shows the wealth of temporal and spatial scales of the SST; especially noticeable is the tropical instability waves (TIW) activity in the Eastern Pacific.

Since seasonal forecasts became operational, their skill has been slowly but steadily increasing. The improvement in skill is equally attributed to better initialization of the ocean and improved

coupled models, as shown in Figure 3.1 from Balmaseda et al. (2010). Improved initialization reflects not only the contribution of the ocean observing system, but also improved atmospheric surfaces fluxes, and better exploitation of the observations by more advanced data assimilation methods and models.

Seasonal forecasts use lower resolution models that those in NWP, mainly because the length of the integration, the number of ensemble members and the need for bias correction and calibration adds to the computational cost. The atmospheric model has a typical resolution of 0.5-1 degree in the horizontal, with 60 to 90 vertical levels. The ocean resolution is typically 1 degree (with equatorial refinement), although in the latest Met Office seasonal forecasting system the ocean resolution is 0.25 degrees (at expense of reducing the reforecast data set). The forecast lead time is typically 6-7 months, sometimes extended up to 12 months. The real-time forecasts require about 40-50 ensemble members. The reforecasts span a period of approximately 30 years, with hindcasts initialized every month using a reduced ensemble (~11-15 members). In total, about 200 years-worth of coupled model integration years are needed for a seasonal forecast at 7 months lead time initialized from a single calendar month. Or in other words, 2400 years-worth of coupled integrations are needed for seasonal forecasts initialized each month.

Seasonal forecasts use both the Near Real Time (NRT) data stream for initialization of real time, and the Behind Real Time (BRT) data stream in the reanalyses needed for the calibration data set. BRT data are also used for verification.

3.2 Ocean Initialization

The simplest way of providing initial conditions is to run an ocean model forced with observed winds and fresh-water fluxes from atmospheric reanalyses and with a strong constraint to observations of SST. Such a 0^{th} order ocean data assimilation system has been shown to generate realistic subsurface ocean structures (Luo et al., 2005; Kumar et al., 2013) in the equatorial Pacific. Although the information about wind forcing (wind stress or surface wind) and SST is essential to initialize seasonal forecasts, it is often not enough. The quality of the models and of surface forcing is not sufficient to provide an accurate estimation of the subsurface ocean state. By assimilating subsurface ocean observations it is possible to reduce the uncertainty in the ocean estimate and improve seasonal forecasts. See supplementary material for a summary of the current ocean observing system used in operational seasonal forecasts.

Figure 3.2 from Balmaseda and Anderson (2009) shows the contribution of ocean and atmospheric observations to the skill of seasonal forecasts, as well as the individual impact of different ocean observing systems. Their results highlight the importance of the surface wind information, and they also show than in the equatorial Pacific all the ocean observing systems contributed to the skill of seasonal forecast. These experiments were conducted with the previous ECMWF seasonal forecasting system (S3), and have been revisited with the new S4 (see below), as well as with a variety of other operational systems (see TPOS WP5). See also section 7.4 for a discussion on limitation of this methodology.

Aside from winds and SST, subsurface temperature observations are the next most important variable for the initialization of seasonal forecasts in the tropical Pacific. Salinity observations

are also important (Yin et al 2011), especially in the mixed layer, and because they contribute to the assimilation of temperature data (by providing better constraints for density field. Altimeter-derived sea-level observations can also be helpful to constrain the upper thermal structure by projection onto the baroclinic ocean density structure. In order to obtain an accurate projection, the model vertical density structure needs to be reasonably realistic, i.e., in situ observations of temperature and salinity are needed. The importance of altimeter-derived data is increasing with increased ocean model resolution. The assimilation of altimeter sea level needs additional information about the geoid which can be derived from gravity missions.

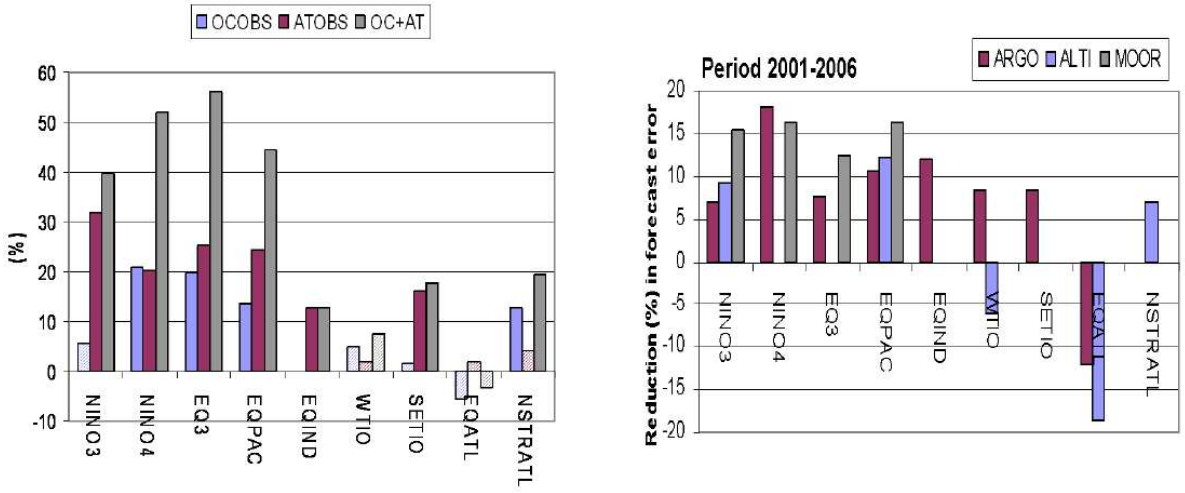

NINO3	5ºS 5ºN, 90-150ºW	EQIND	5ºS-5ºN, 40º-120ºE
NINO34	5ºS-5ºN, 170-120ºW	WTIO	10ºS-10ºN, 50º-70ºW
NINO4	5ºS-5ºN, 160ºE-150ºW	SETIO	10ºS-0ºN, 90º-110ºE
EQ3	5ºS-5ºN, 150ºE-170ºW	EQATL	5ºS-5ºN, 70ºW-30ºE
EQPAC	5ºS-5ºN, 130ºE-80ºW	NSTRATL	5ºN-28ºN, 80ºW-20ºE

Figure 3.2 - Impact of observations in forecast skill for different regions in table above, as measured by the reduction in mean absolute error for the forecast range. (Left) ocean observations (OCOBS), atmospheric observations (ATOBS) and both, for the forecast range 1-3 months, period 1987-2008. (Right) Impact of Argo, altimeter and moorings for the period 2001-2006. Results illustrate the importance of wind information, and also show that in the Equatorial Pacific all observing systems contribute to the skill.

Although the emphasis for initialization of seasonal forecasts is in the upper thermal structure (the upper 300m are more likely to influence the atmosphere on seasonal time scales), it does not mean that only observations of temperature in the upper ocean are needed. A full profile rather than a truncated one also makes a difference in the resulting stability of the water column. Equally, the upper thermal structure is better initialized with T/S profiles rather than only T (Troccoli et al., 2002; Ricci et al., 2005). However the assimilation of temperature and salinity separately (as it is common in variational assimilation methods) may induce problems, especially when the first guess salinity is lower than the observations, and the water column is not very strongly stratified.

There is large uncertainty in the fresh water flux (precipitation, evaporation and river runoff), affecting the surface salinity and mixed layer properties. It is probably the largest source of

uncertainty in the estimation of salinity in the upper 100m. Information about Sea Surface Salinity (SSS) from either in situ measurements close to the surface or from satellite (Aquarius or SMOS) can be useful (TPOS WP9 Lindstrom).

Aside from the biochemistry applications, time and spatially varying ocean color can be used as forcing fields of the ocean models to specify the depth for solar penetration. Ocean model simulations exhibit high sensitivity to ocean color. So far most of the ocean color products consist of climatologies and are not available in real time. A Level 4 (L4, see Appendix) time dependent ocean color maps, delivered in NRT or BRT will be useful.

Assimilation of altimeter-derived sea level (as opposed to sea level anomalies) needs information from the geoid. This is obtained from gravity missions. In addition, gravity missions can provide bottom pressure information, which can be used globally to constrain the non-steric part of global sea level variations. Gravity-derived variations of the global mass field are also useful for verification of ocean reanalyses (Balmaseda et al 2013a), BRT L4 data is desired. Bottom pressure also has the potential to constrain the barotropic mode; however, more experience is needed.

3.3 Weakness of ocean data assimilation

The assimilation of ocean observations in the equatorial wave-guide remains challenging, in spite of progress on data assimilation methods. Preliminary results from the Ocean ReAnalysis Intercomparsion Project (ORA-IP) show large spread in meridional mass and heat fluxes at the Equator (Valdivieso et al., in preparation). Observing system experiments (OSEs) show very little impact of the different observing systems right at the Equator (see TPOS WP5), which is indicative of either redundant information or poor assimilation methods. The relative impact of TAO and Argo at the equator is comparable, although varies among the data assimilation systems.

Fig 3.3 shows results from OSEs conducted with the ECMWF ORAS4 system, where Mooring, Altimeter and Argo are withdrawn from the ocean analyses, once at a time. The figure shows the fit (rms error) of the first-guess to mooring observations during the 10-day assimilation cycle (also called departures) in the Eastern Pacific (EQ1) and in the Western Pacific (EQ3). Since the observations have not yet been assimilated (the comparison is done just before the analysis), they can be considered fairly independent. In both Eastern and Western Pacific withdrawing the moorings increases the rms error. The assimilation of Argo does not seem to improve the fit to the moorings. In fact, in the western Pacific, the fit to the moorings is degraded when Argo is assimilated. These results suggest either that moorings and/or Argo provide different information (for instance, if they are at different locations and there is a lot of spatial structure) or/and that there are problems with the assimilation system. Curiously the assimilation of moorings does not degrade the fit to Argo (not shown).

There are several reasons for the small impact of observing systems at the Equator: i) it is difficult to constrain large scale biases with short spatial decorrelation scales (most of the assimilation methods only use one decorrelation scale) and ii) the equatorial dynamical balance needs longer time scales than the typical ocean assimilation cycle (1-to-10 days). Similar problems to those in the equatorial region are seen in coastal boundary current regions, where

there is no dedicated observing system for the time-being. In the future, both equatorial and boundary current regions may become adequately sampled by Argo (see design plans in TPOS WP10). It can be argued that the observational needs are larger in the areas where model and data assimilation are poor, although it can also be argued otherwise.

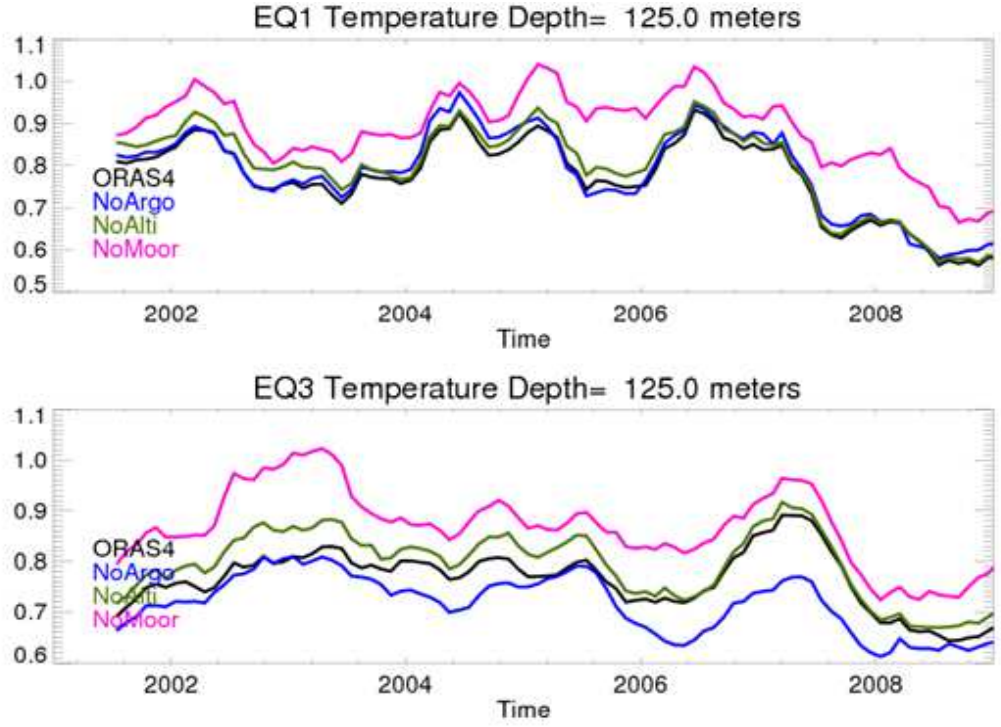

Figure 3.3 - Fit to mooring observations (root mean square error) in the Eastern Pacific EQ1 (top) and Western Pacific EQ3 (bottom) from the 10 days forecasts using the ECMWF ORAS4 data assimilation system (black), and in equivalent data withdrawal experiments NoArgo (blue), NoMoor(pink) and NoAlti (green), where Argo, Moorings and altimeter have been respectively removed. EQ1 (150W-90W, ±5^{o}), EQ3 (150E-170W, ±5^{o}). The verifying mooring observations have not yet being assimilated in any of the experiments. Withdrawing the moorings from the analyses degrades the fit of the 10-day forecast, in both Eastern and Western Pacific. Argo does not improve the fit to the moorings. On the contrary, in the Western Pacific withdrawing Argo improves the fit to the moorings. This can be interpreted as i) Argo and moorings providing different information or ii) sub-optimal data assimilation systems.

In summary, although the information from ocean observations is essential for initialization of seasonal forecasts, its extraction is not always straight forward. There is evidence that the current data assimilation systems are not exploiting the full potential of the observations (see Figure 3.3). Challenging areas are the Western Boundary Currents (WBC) and the Equatorial regions, where the information is quickly lost. Constraining the density field by separate assimilation of temperature and salinity remains difficult, and so is the assimilation of altimeter sea level (both because the methods for projection into subsurface density and because the need of external information in form of geoid or MDT). It is expected that most of these problems will be solved by future developments in data assimilation methods and reduction of model error.

3.4 Model and Data Assimilation Development

Continued deficiencies in ocean and atmospheric models, and their corresponding data assimilation systems have led to ongoing developmental efforts. Model and data assimilation development efforts hinge on observational data sets for (a) validation of model simulations to document biases, and (b) testing and implementing new parameterization and data assimilation schemes. Although model parameterization often falls under the purview of focused field programmes that target a specific process, sustained observations are helpful to evaluate model performance under various climate regimes. A good example is parameterization of stratus cloud decks over the western coast of continental areas (such as the western coast of equatorial South America), that are often associated with warm biases in the ocean models.

Another example of a familiar model error is the equatorial cold-tongue in coupled models. The attribution of the error still remains unresolved. From the ocean perspective, the cold tongue is usually associated with too strong zonal wind stress and/or too much poleward heat transport by the TIW. This could be due to errors in the atmospheric model (deficient resolution or others). In ocean-only simulations, the strong zonal wind stress can be mitigated by taking into account the ocean currents when deriving wind stress from atmospheric analysis winds. But this itself can lead to overcompensation and masking of the errors (there is some inconsistency in this formulation, since the atmospheric analysed winds -produced in uncoupled mode- have not seen the ocean currents). Having measurements of the TIW activity level and heat transports, as well as in situ measurements of surface stress and winds is essential to solve this persistent problem.

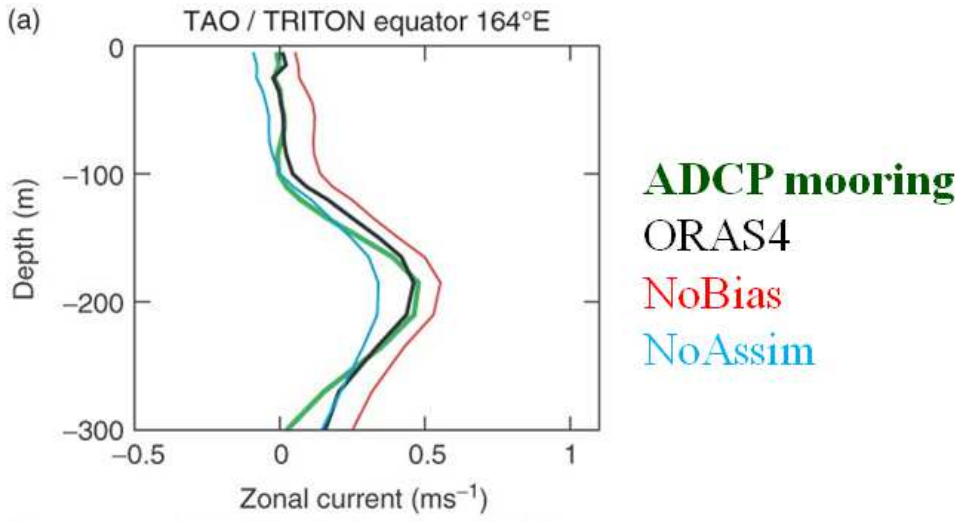

Figure 3.4 – Sub-surface currents for moorings are very valuable to verify ocean reanalyses and develop the data assimilation system.

Ocean currents from moorings have proved very useful in the development of data assimilation (see Figure 3.4). Often the assimilation of density information can lead to spurious circulations, especially at the equator. By looking at the impact on the equatorial undercurrent it is possible to assess if the data assimilation is adequately balanced. This has led to the development of balance constraints for equatorial velocity (second order geostrophic balance, Burgers et al., 2002), and the pressure bias correction suggested by Bell et al. (2004). This latter appears

essential to obtain good velocity fields (Balmaseda et al., 2007). The scheme is quite sensitive to the choice of some parameters, which are tuned by using the currents from moorings.

Another method for validating the ocean data assimilation system is by monitoring error growth. It is easy to overfit the data if the only criterion is the fit of the analysis to the observations. More important is how the information is retained (or how the error grows during the very short forecasts, before the results get contaminated by model error). To this end, and in order to obtain reliable statistics, the sampling of the verifying observations should be homogeneous in space and time. The moorings provide an excellent data set for verification, since they guarantee similar number of observations at the same locations.

Sea level from tide gauges also provide valuable independent information for validation of ocean reanalyses, with the added benefit that some of them span long time-records. These are particularly important for evaluating the quality of the ocean re-analyses prior to the satellite period (Chepurin et al., 2013). Surface currents derived from the combination of altimeter and drifting buoys, such as the OSCAR product (Bonjean and Largelof, 2002) are also used for reanalyses verification.

It can be argued that for model and data assimilation development it is not necessary to have a continuous and permanent observing system in place. However, the errors of model and data assimilation are very flow dependent. Having a reduced data set for model/data assimilation development can lead to over-tuning algorithms for some case studies, which may then not be suitable for other cases. Numerical models, forcing fluxes and observations are also changing, and there is always the need to test new components with the most recent data (for example, it would be difficult to test the assimilation methods for altimeter without a reasonable coverage of in situ observations).

3.5 Bias correction, verification and skill assessment

Seasonal forecasts require bias correction as the anomalies one seeks to predict can often be as large as model biases and can easily overwhelm the signal one strives to predict. The first order calibration is the a-posteriori removal of the mean bias, which depends on the lead time and on the seasonal cycle (Stockdale, 1997). This strategy assumes that the model bias is stationary, but this is not always the case. Figure 3.5 from Kumar et al. 2012 shows that the bias depends on the lead time and the seasonal cycle, a dependency that is accounted for in the a-posteriori removal of the bias. This figure also shows a non-stationary behavior in the bias, with a tendency towards colder (warmer) bias before (after) 1999, contrary to the assumptions in the a-posteriori bias correction. This can lead to complications in bias correction procedures and degradation of forecast skill. Kumar et al. (2012) discuss how changes in the observing system possibly led to non-stationarity in the forecast bias, and sub-optimal forecast skill.

The dominant change in the forecast bias in the CFSv2 system analyzed by Kumar et al. (2012) occurred around 1999, coinciding with the assimilation of AMSU data. Although some of the shifts in the reanalyses time-series can be attributed to the assimilation of AMSU, there are others that may be related to real shifts in nature (Zhang et al., 2012). Long reference time-series of good quality observations representative of the large scale circulation are therefore

needed to be able to distinguish between spurious and real signals. See the section 5 on reanalysis for further discussion on this topic.

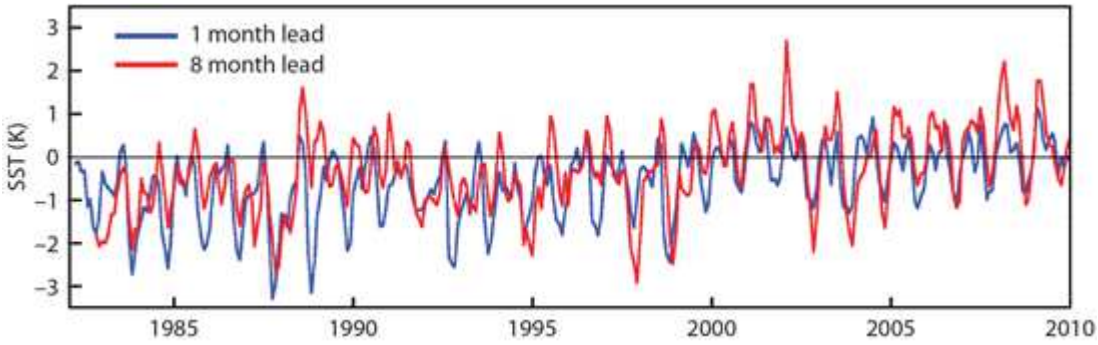

Figure 3.5 - Time evolution of the SST forecast bias in the NCEP CFS version 2. The figure shows the bias at 1-month and 8-months lead time, and it illustrates the non-stationarity of the bias (from Kumar et al., 2012).

For bias-correction and verification of seasonal forecasts, gridded maps (usually monthly means, 1x1 degree) of relevant variables (winds, precipitation, SST, OLR, surface fluxes etc.) are needed. These gridded fields are usually the results of post-processing, either via model-based reanalyses or other gridding algorithms. The quality of the seasonal forecasts will be influenced by the length and the quality of these products. The accuracy of these products is not considered the limiting factor for the forecast quality (with some exceptions such as precipitation, T2m over land, surface fluxes). The length of the temporal record and the stability of the error can be a reason for concern, even for variables like SST. Ideally, one would like records spanning a minimum of 30 years with stable errors and free of spurious variability and trends. These requirements are even stronger when it comes to the seasonal forecasts of extreme events.

3.6 Summary of seasonal forecasts data needs

(See appendix for an explanation of the acronyms used in this section).

Initialization

- Surface winds/wind stress (L4), SST(L2-L3-L4); subsurface temperature/salinity (L2, L2-QC) and sea-level altimeter (L2, L2-QC) are essential variables for initialization;
- Equatorial wave-guide needs intense sampling, which currently is only provided by moorings, but could be better sampled with the new Iridium Argo floats which avoid drift by staying at the surface for only a few minutes;
- Increased horizontal resolution model initialization needs high spatial resolution altimetry;
- SSS, ocean color, heat, freshwater, and turbulent kinetic energy surface fluxes (L3-L4);
- Gravity derived geoids and bottom pressure complementary to altimeter (L3-L4);
- Delivery in two streams: NRT (no more than 24 hours delay) and QC BRT (with delays ranging from a few days to update the current reanalyses, to years or decades, to be used in future reanalyses and verification).

Model and Data Assimilation Development

- Independent data for validation of ocean data assimilation and models: current profiles at the Equator (provided by moorings, L2-QC, L3); sea surface currents (SSC, L4); sea level from tide gauges. Long records. Time series of L2-QC, L3;
- Quality controlled flux data from reference sites (wind, wind stress, long and shortwave radiation, relative humidity, surface temperature, rain gauges). Long time series of L2-QC, L3;
- Controlled profiles of in situ surface and subsurface data for validation of ocean-atmospheric reanalyses and models. Long time-series of L2-QC, L3;
- Processed gridded products of surface fluxes. Long records of L3-L4;
- Indonesian Throughflow transports (heat, salt, volume) time-series;
- Equatorial transports (heat, salt, volume). Time series.

Bias correction, Verification and Skill Assessment

- Long (>30 years) stable ocean-atmospheric and SST reanalyses for initialization of hindcasts;
- Long (>30 years) stable records of end-user related variables (such as surface winds, precipitation, surface temperature, sea-level pressure). Other indirect meteorological variables that can help the calibration and interpretation of forecasts are useful (Z500, OLR). (L3-L4);
- Long records of L2-QC, L3 variables in reference sites;
- Continuous delivery BRT, preferably with delays no longer than 1-3 months, for prompt verification.

4. Sub-seasonal forecasts

Sub-seasonal forecasts are currently produced operationally at various major forecasting centers. Configurations of models range from an uncoupled atmospheric model to coupled ocean-atmosphere models (Table 1). Oceanic observations required for this application may be similar to those for medium-range and/or seasonal forecasts, but there are some differences. Regardless of whether a model is coupled or uncoupled, the sub-seasonal forecast requires ocean analysis (SST or sub-surface analysis) and observations of influence to be consistent in quality over a long period, since the sub-seasonal forecasts also need bias correction based on re-forecasts similar to that for their seasonal counterparts (Section 3). The poor time-consistency of the ocean observations and analysis may hamper a proper calibration and fail to provide opportunity for gains on forecast skill. Furthermore, the sub-seasonal forecasts may be performed with models at a higher resolution (up to ~30 km for the ECMWF monthly forecast system) than seasonal forecasts and the higher resolution models ideally need with higher SST conditions. Hence the incentive to use higher-resolution SST boundary/initial conditions requiring higher-resolution observations by a combination of in situ and satellite measurements.

There is some phenomenological rationale for the requirement of oceanic observation for the sub-seasonal forecast, the primary one may be the Madden-Julian Oscillation (MJO). The MJO is the pronounced variability in an intraseasonal time-scale (30-90 days), accompanying coherent deep convection and large-scale atmospheric circulations in the tropics. The MJO has

a strong influence on tropical weather as well as extra-tropical weather through so-called teleconnections (Cassou, 2008; Mori and Watanabe, 2008; Vitart, 2013). Better representation of the MJO and the teleconnections should lead to better skill of sub-seasonal forecasts (Vitart 2013). Many modeling studies have been conducted to evaluate impacts of ocean coupling in predicting MJO, and indicate that the ocean coupling contributes to improve a representation and forecast skill of MJO (e.g., Klingaman and Woolnough, 2013; Woolnough et al., 2007). Meanwhile in situ and satellite observations have revealed that the MJO is related to the ocean temperature and ocean salinity variations (Anderson et al., 1998; Grunseich et al., 2013; Matthew et al., 2010). Given that the MJO is a coupled atmosphere-ocean phenomenon as the many sensitivity experiments have suggested, better analysis of ocean states should bring better MJO forecasts and sub-seasonal forecasts, at least in principle.

In the traditional ocean data assimilation for seasonal forecasts, the main focus is on relatively large spatial scale and low-frequency variability (i.e. oceanic equatorial Kelvin and Rossby waves and ENSO, Indian Ocean Dipole (IOD)), while the future sub-seasonal forecasting would shed light on the small-scale atmosphere-ocean interaction over tropical instability waves or ocean fronts (Small et al., 2008; Kelly et al., 2010). In the foreseeable future, oceanic observations with finer spatial and time resolutions would be required in order for these phenomena to be analyzed and initialized. Although an oceanic contribution to improving sub-seasonal forecasts has been recognized as mentioned above, an evaluation of the observing system from the sub-seasonal forecast perspective has never been conducted and a research effort should be made to explore the benefit of oceanic observations for sub-seasonal forecasts in the near future.

Table 1 - Operational sub-seasonal prediction systems and utilized ocean observations (as of April 2013).

Institutions	Resolution	Ocean coupling	Ocean observations
ECMWF	TL639L62 (day0-10) TL319L62 (day10-32)	Yes	1,2,3,4,5,6
JMA	TL159L60	No	1,2,3,4
UKMO	N216 (~50km)L85	Yes	1,2,3,4,5,6
NCEP	T126L64	Yes	1,2,3,4,5,6
EC	T63L31/T63L35	Yes	1,2,3,4,5,6
CAWCR	T47L17	Yes	1,2,3,4,5,6
KMA	T106L21	No	
CMA	T63L16	No	
CPTEC	T126L28	Yes	1,2,3,4,5,6
HMCR	1.1x1.4 deg., L28	No	

1: Mooring buoy (in situ, TAO/TRITON/PIRATA) 2: Argo float (in situ)
3: Drifter buoy (in situ) 4: Ship (in situ)
5: Altimeter (satellite) 6: Infrared/Microwave (satellite)

5. Reanalyses

As discussed before, extended-range predictions require calibration of real-time forecast anomalies to reduce the impact of model errors. This is achieved by running the forecast system back in time and developing a database that can be used for quantifying the statistics of model biases, against which real-time forecasts are bias corrected. Running the extended-range forecast system back in time, generally referred to as the reforecast, requires initialized ocean forecasts, and availability of ocean analyses for the initial conditions. This is one of the reasons for conducting the ocean reanalysis going back in time, and which are updated on a periodic basis either after sufficient advancements in models and assimilation systems have been made or when new sets of observations are added in the historical data bases through data mining efforts or improved quality control methodology. Reanalyses (both for the ocean and atmosphere), therefore, are integral components of real-time forecast systems, while at the same time, are extensively used for climate monitoring efforts to place the evolution of the current climate system into a historical context.

Reanalysis efforts, although do not explicitly pertain to real-time ocean and atmospheric observing systems, do provide guidance on (a) the influence of the changing observing system on the analyses and forecasts, and (b) a means of testing the influence of various observing platforms on extended-range forecasts through Observing System Experiments (OSEs), and are briefly discussed next.

Observing systems are in a state of continual evolution either due to development of new technologies, for example, Argo, or due to the phase-out of older observing systems, such as a decline in XBTs (see Figure S3). Such changes in observing systems, even if intended to improve the quality of ocean analysis, can also lead to discontinuities when changes in the ocean observing system interact with the data assimilation. An example could be that as the density of observation increases, the ocean analysis is drawn more towards the observations away from the assimilation system's initial guess state (which is based on the model forecast). If the initial guess state (that is obtained by a forward integration of the assimilation model has biases), then a sudden appearance of a new observing system in a data void region can create a spurious jump in the analyses from a model state towards in situ observations. Similar discontinuities could occur due to changes in the QC systems or changes in the correction to raw observations, such as XBT fall rate correction (Wijffels et al., 2006), or the reported pressure sensor biases in the Argo floats (Lymann et al., 2006). Influence of such changes in the reanalysis can subsequently affect the forecast biases, so invalidating one of the fundamental assumptions of forecast calibration (Figure 3.5). Such discontinuities in the historical analysis, and their influence on the reforecasts, also provide valuable lessons for the real-time analysis of the ocean state that can occur due to ongoing changes in the observing system, and care needs to be taken in the design and evaluation any of tropical Pacific observing system.

Reanalyses also provide an opportunity for conducting OSEs, whereby influence of a particular observational platform on ocean analysis and subsequent forecast skill can be assessed. The importance of OSEs in the context of TPOS 2020 is of obvious importance for the design of observing system to provide adequate initial states for operational forecasting systems for different time-scales. Reanalysis based on OSEs are also a means of quantifying the accuracy

requirements for the observing system in the context of forecasts. Although OSEs represent a computationally expensive exercise, primarily due to requirements of doing an extensive set of reforecasts to obtain results that are statistically significant (for more discussion see white paper 5), it is recommended that a robust OSE activity involving multiple operational forecasting centers should be maintained to inform the design and assessment of the current and future configuration of the tropical Pacific observing system. In summary, although the reanalysis efforts may not be of direct relevance to the real-time observing systems, they encompass a set of tools that are of value for assessing and informing the design of the tropical Pacific observing system.

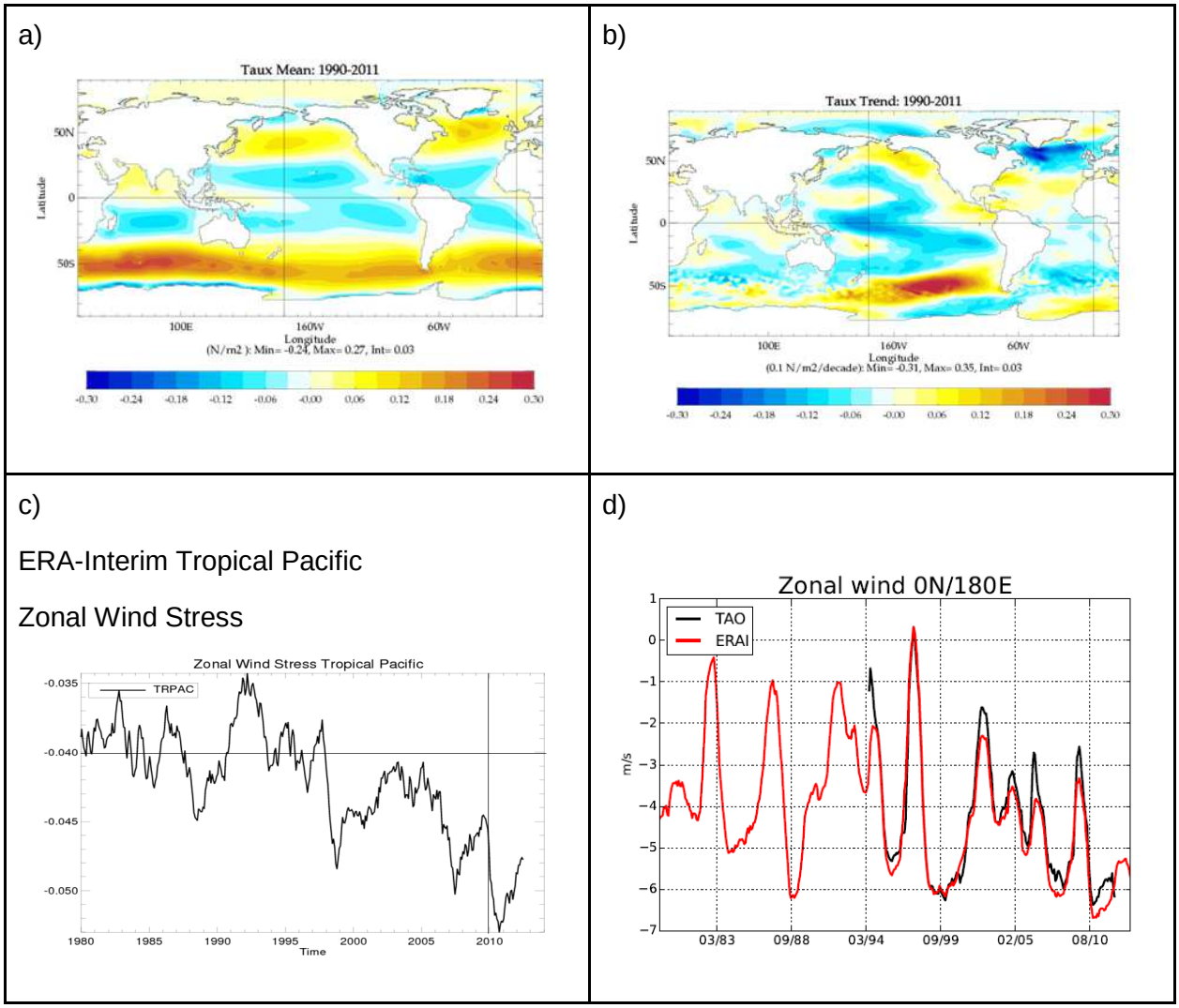

Figure 5.1 - a) Mean zonal mean stress from Era-Interim (EI) (1990-2011). b) Linear trend of EI zonal mean stress for the same period. c) Time series of EI zonal wind stress in the Tropical Pacific and d) EI and TAO zonal wind at 0N-180E.

Atmospheric reanalyses are undoubtedly a great asset for climate research and forecasts applications. They are so widely used that often are taken as truth. Atmospheric reanalyses, as well as the oceanic reanalyses, can present spurious signals due to changes in the observing system (Zhang et al., 2012; for instance, see section 3 above). When changes in the observing

system coincide with real changes in climate variability, the true and spurious signals are difficult to disentangle. This is the case for the interesting changes in tropical Pacific winds after the 1998-1999 La Niña event.

Figure 5.1 shows the maps of zonal wind stress from ERA-Interim (mean and linear trend, top), and corresponding time-series averaged over the tropical Pacific. Pronounced changes can be seen in the zonal wind, consistent with changes in the gyre circulation. The time-series shows that the trend is punctuated by intense easterly episodes (1999, 2006-2007, 2009-2010). After 2009 (with the end of Quickscat) no scatterometer winds are assimilated in ERA-Interim. Establishing if the changes in the reanalysis wind stress are robust is vital for the understanding and prediction of climate. For instance, Balmaseda et al. (2013) and England et al. (2014) argue that wind variability is instrumental for the ocean heat uptake. Backscatter from altimeter also detected some extreme signals in the surface winds around 2010, but doubts were cast about the calibration (Abdalla, personal communication). The record from scatterometer winds is often too discontinuous to provide a reliable assessment. The TAO moorings offer a more consistent picture, although of limited spatial extent (De Boisseson et al., in preparation). The implications for the observing system are obvious: there is a clear need for good quality reference long time series, stable in time and representative in space. Spatial sampling to obtain this representativeness needs to be evaluated.

6. Future Developments

6.1 Decadal predictions

Decadal forecasting is a rapidly evolving field. External forcing influences the predictions throughout, but the initial state influenced by natural variability also plays an important role in the evolution of coupled system on shorter lead time, e.g., in the first six-to-nine years. Hawkins and Sutton (2009), Meehl et al. (2013) discuss the importance of initialization to produce time-evolving predictions of regional climate. The analysis of multi-model ensemble results suggesting that some aspects of decadal variability like the mid-1970s shift in the Pacific, the mid-1990s shift in the western Pacific, and the early-2000s hiatus, are better represented in initialized hindcasts compared to uninitialized simulations. The difference between initialized and non-initialized forecasts becomes more evident when using the multi-model ensemble than in any individual forecasting system. The tropical Pacific appears as one of the regions with real predictive skill at 1-2 year lead times arising from the initialization of the ocean (Pohlmann et al., 2013).

Some of the decadal forecasting systems rely on information from existing atmospheric and ocean reanalyses (the later produced for seasonal forecasts) for initialization. This information is used directly, by nudging the coupled model (anomaly or full field) or by forcing an ocean model with atmospheric fluxes. Some systems use a specific data assimilation system designed for decadal forecasts, such as the Met Office system (Smith and Murphy, 2007). A key difference of initialized decadal predictions from initialized predictions on shorter time-scales is the need for ocean observations into the deeper ocean.

From the Tropical Pacific perspective, the observational needs for decadal forecasting are similar to those of seasonal, except the need for even longer and stable observational records is

stronger, both for initialization and verification. At decadal timescales the deeper ocean (below 500m) also plays a role and observations up to 2000m are considered important. Results from synthetic observing system experiments suggest that even observations below 2000m are likely to play a role, especially in the prediction of the Atlantic Meridional Overturning Circulation. Initializing the large scale modes of decadal variability such as the PDO may be important.

6.2 Coupled forecasting Systems: thermal and dynamic coupling

Whenever the term coupled ocean-atmosphere system is used, the thermodynamic coupling in the tropics springs to mind, where the atmosphere responds to the SST values and its gradients. And indeed, the benefits of the ocean-atmosphere thermal coupling in the tropics for MJO and NWP prediction have been demonstrated (De Boisseson et al. 2012, Janssen et al. 2013, for instance). However, there are other processes in the air-sea interaction related to the momentum transfer that have potential impact on the resulting SST.

Evidence is growing that ocean wave dynamics plays an important role in the evolution of currents and temperatures of the upper ocean, suggesting that it makes sense to develop a tightly coupled ocean-wave, ocean circulation model. The first indication came from the theoretical work of Craig and Banner (1994) and the experimental work of Terray et al. (1996) that highlighted the prominent role of breaking waves in the upper-ocean mixing of momentum and heat. Monin-Obukhov similarity is based on the balance between production and dissipation of turbulent kinetic energy and breaking waves generate so much additional turbulence that large deviations from similarity occur resulting in enhanced mixing. Additional sea state effects that are relevant for the upper ocean are the generation of turbulence by Langmuir circulation (McWilliams and Restrepo, 1999; Grant and Belcher, 2009) and the Stokes-Coriolis force (Hasselmann, 1970; McWilliams and Restrepo, 1999). Furthermore, although it is well-known that ocean waves experience refraction in the presence of spatially uniform currents, it is perhaps less well-known that by Newtons third law this implies that there will be a sea-state dependent force exerted on the ocean (Garrett, 1976). In return, it should be emphasized that ocean circulation also affects the sea state, through for example current refraction and through Doppler shifting. In an inhomogeneous current system the refraction may lead to focusing of wave energy, triggering the generation of freak waves.

The development and validation of a coupled ocean, ocean-wave, and atmosphere system is a very interesting development, and opens the door to better exploitation of the observations. Data on the ocean and atmosphere boundary layer, as well as on sea-state, are of vital importance in order to validate and further develop these coupled systems. An example of the use of in situ data in the development of a mixed layer model, including sea state effects, is given in Janssen (2012).

6.3 Coupled Data Assimilation

A recent focus for development is the implementation of coupled ocean-atmosphere-land-sea ice data assimilation (CDA) systems which are expected to improve forecasts at various time ranges (from medium range out to seasonal and decadal). These developments, initiated with the weakly coupled reanalyses at NCEP (Saha et al., 2010), are gaining momentum at different operational and research centers (Met Office, ECMWF, BMRC, JMA-MRI, NASA). Observations

of the air-sea interface are crucial to better understand the important coupled processes which should be represented in the CDA systems. Observations in the boundary layers of both the atmosphere and ocean can help to constrain these coupled processes in this important area.

CDA is an important approach to improving the forecast skills for the phenomena in which the air-sea interaction plays an essential role. Fujii et al. (2009) demonstrated that distribution and variability of precipitation in the tropics are improved in their weakly CDA run, in which ocean observation data alone is assimilated into a coupled model, compared to an AMIP run (i.e., a free simulation of the atmospheric model using the observed SST temperature). They found that the negative feedback between the change of SST and atmospheric convective activity is not properly represented in the AMIP run due to the prescribed SST, but it is recovered in the CDA run (see the negative correlation between SST and precipitation around the Philippine Sea in the CDA run (see Figure 6.1). They also showed that the negative feedback improves the precipitation fields and atmospheric circulations.

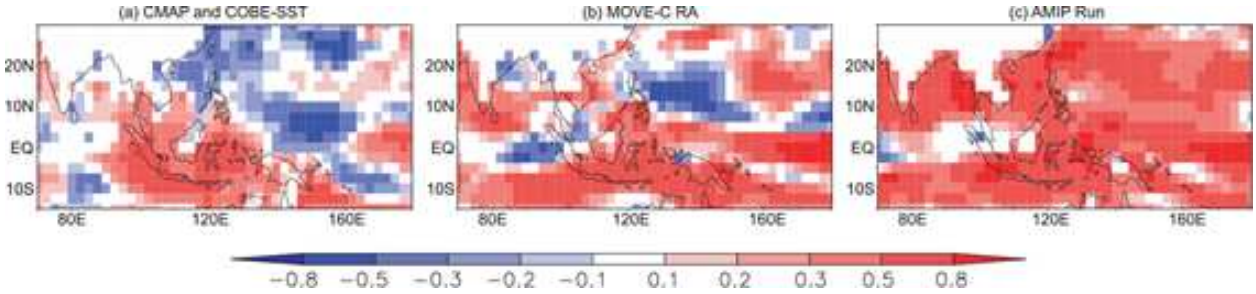

Figure 6.1 - Maps of the Correlations between SST and precipitation in summer (June-August) calculated from (a) CMAP and the gridded SST data in JMA, (b) the weekly CDA run, (c) the AMIP run (adjusted from Fujii et al., 2009).

A few international meetings have taken place to discuss progress in this area, one of which was organized jointly by WGNE and GODAE OceanView in March 2013. A series of white papers are being developed following that meeting and the current status of those is described at www.godae-oceanview.org/outreach/meetings-workshops/task-team-meetings/coupled-prediction-workshop-gov-wgne-2013/white-papers.

It is envisaged that in the near future the SST analysis and initialization will be carried out with such CDA systems. L2 SST bias-corrected data will become necessary (as opposed to using a gridded L4 SST product), frequently enough to be able to represent the diurnal cycle.

One of the most challenging aspects of CDA is the formulation of the error covariance between the variables involved in the air sea interaction. Balance relationships between variations in the ocean mixed layer and in the atmospheric boundary layer are needed. These can be obtained from model integrations, but verification data are needed. From this perspective, ocean and atmosphere observations collocated in a single column are considered very valuable. No systematic studies have been carried out as yet to assess directly the impact of tropical moored buoy data on these systems. However, the tropical moored buoys are expected to provide a very useful input to develop and improve these coupled systems.

7. General considerations

7.1 Different lives of an observation

It is perhaps not always realized how often and in how many ways an observation or set of observations is used. The most immediate way is in weather and climate forecasting via the analyses used to initiate short range high resolution (~4km) weather forecasts up to 2 days, moderate resolution (20km) forecasts up to 10 days, ensembles of medium resolution forecasts up to 15 days, ensembles of intraseasonal forecasts (40km) up to 30 days, seasonal forecasts (80km) up to a year, and in the future, as decadal forecasts become more mature, to multi-annual time scales.

A completely different stream would use the same observations, not in near-real-time analyses, but in delayed reanalyses. These are used for validation and model bias correction and calibration, whereby some aspects of model deficiencies can be corrected. Calibration is applied in some way to all forecasts from days to years.

An interesting feature of reuse of data is that it influences not just real-time forecasts of today but will influence forecasts for many years into the future. Additionally much greater use can be made of observations today than was possible when they were taken 10, 20, 50, etc. years ago. This results from the improvements in models and in analysis procedures.

A third stream of use of an observation is in scientific research, ranging from improving parameterisation of physical processes to greater understanding of major phenomena such as the Intraseasonal Oscillation and ENSO.

Finally, an aspect of the sustained observing system often overlooked, is its contribution to the forecast verification. There is a lot of experience gained during the routine monitoring and verification of forecasts (or learning from errors). Verification is essential to identify different sort of errors, and it often sets the directions for model development.

7.2 Panorama for TPOS 2020

7.2.1 Ready-Get Set-Go

The IRI and the Red Cross have been advocating an approach to the use of forecasts of many timescales, in order to improve their use for society. The idea is a simple one. Use the seasonal forecasts to provide an outlook of potential major climatic anomalies, several months in advance, so that steps can be taken to start getting ready. The next stage (the GET SET stage) is to use intraseasonal forecasts which will start to refine the nature of the anomaly and refine the probability of what happening where. This is refined further through the use of medium range forecasts in the GO stage.

7.2.2 Interpretation of climate and decadal signals

As well as expanding the forecast capabilities from the seasonal to daily timescales, as illustrated with the Ready-Get Set-Go example, TPOS 2020 should be ready to serve the needs for climate monitoring and decadal forecasting. There is increasing need to detect and predict decadal variability. Indeed, the Pacific basin has received a lot of attention in relation with the

recent hiatus of the surface warming. Quoting the feature news of Nature (16th January 2014), “And here, the spotlight falls on the Equatorial Pacific”.

7.3 Continuous but steady progress

There is a perception that progress in seasonal forecasting has plateaued and that there has been little progress in the last few years. We think that this not the case. While it is generally accepted that seasonal forecasting is a more difficult problem than was initially conceived in the early days of TOGA (1985-1994) progress is being made, albeit more steady than revolutionary, but if experience in weather forecasting is anything to go by, this is hardly surprising.

Figures 2.1 and 3.1 show progress over the years from the ECMWF medium range and seasonal systems respectively. Progress is being made on two fronts. Not only is the RMS error of the forecasts being reduced (the usual measure of skill), but the forecasts are becoming more reliable in that the growth in the ensemble spread now matches the growth of error; the forecasts are no longer far too confident with the observed values lying frequently outside the ensemble, when retrospectively verified.

What may be less reliably known is if there is increased skill in predicting the evolution of large events. There are only two in the period with better observations (82/3 and 96/7). With a sample of only two events it is difficult to validate the models reliably. Attempts are being made to use more extended atmospheric reanalyses, going back a hundred years buoyed by the encouraging results from simpler models (Chen et al., 2003). Our best approach is to understand processes and improve the various parameterisations used in the models. Here too, there appears to be steady progress.

7.4 On the Observing System Experiments

Observing system experiments (OSEs), or Observing system simulation experiments (OSSEs) provide a mechanism for obtaining guidance on the potential importance of an observing system (or even on specific measurements or measurement sites). The strategy consists of performing analyses with and without the observing system. In the case of OSSEs the observing system does not exist and observations must be simulated. This could be because the system is still in planning or has been withdrawn or reduced as in the case of TAO/TRITON (TT). We will not consider OSSEs further.

The first check is to compare analyses with and without the observation system, to gauge the impact on the analyses. Examples of this were given in Figure 3.3 and in TPOS WP5. In Figure 3.3, it was shown that the analyses without TT were noticeably less accurate at mooring sites when the TT data are not used, especially in the west Pacific.

A second check is to compare the forecasts from analyses made with and without the observing system. Because the atmosphere is chaotic and the models used to make forecasts are imperfect, any forecast system must consist of an extensive set of ensembles. It is thus not possible to verify the impact on a single forecast. In fact to obtain reliable statistics it is necessary to run the forecasts over many realizations spanning many years. This is very costly and so only limited sets of forecasts are feasible. Examples of OSEs are given in Figure 3.2 and also in TPOS WP5.

One could argue that to identify the effect of TAO/TRITON on say the prediction of Nino3.4 SST, one might need an ensemble of at least 3 members, ideally run every month for 10 years (the bigger the effect, the smaller the set needed to establish statistical reliability). More chaotic variables such as 2m temperature (T2m) in the extratropics, or precipitation, need considerably more ensemble members, since the spread of the PDF (Probability Distribution Function) of the target variable is larger and the shift in the mean of the PDF likely to be small compared with its width (Kumar and Hoerling, 1995). A greater effect might be expected in the tails of the distribution but the models are likely to be less reliable here.

Evaluating the significance of OSEs is difficult as the results are likely to be model dependent. For example fig 3.2 , obtained using ECMWF S3 shows an important role for TT based on the 2001-6 period (this period was chosen as the study aimed to compare the relative importance of TT and ARGO and 2001-6 was the then period of ARGO coverage). Later results using ECMWF S4 do not confirm this result. The reason has not yet been investigated but could be because the analysis system involving atmospheric analyses and reanalyses as well as ocean reanalyses has improved (or deteriorated) or because the longer period suggests the earlier results were not as statistically reliable as thought.

There is a further complication; the impact on the analysis is complex and never investigated in its entirety. For example, TT provides not just ocean observations but also surface meteorology (vector winds and humidity) which can influence the atmospheric analyses (see section 2.6). In the OSEs discussed here and in TPOS WP5, the effect of TT winds on reanalyses is not considered. Further, because of flaws in the atmospheric and oceanic models, systematic errors are present. Attempts to deal with these are usually included in the analysis system through a bias correction. However, this bias is based on an operational system in which the bias will have been evaluated over a substantial period of time, maybe 20 years or more, and so the bias estimate will have knowledge, albeit implicit, of the observing system whose importance is being evaluated. Without the observing system, the bias estimate would likely be less accurate. Since bias is perceived to be important (see Balmaseda et al., 2007) in improving the quality of the analyses and forecasts, and the bias would be less accurate if one withdrew the observing system while evaluating the bias, it is likely that the importance of the observing system being tested is underestimated. On the other hand the bias may be caused by the observing system, resulting from say a mismatch between the wind forcing and the observed thermocline depth (for example, see Bell et al., 2004; and Balmaseda et al., 2007). For these various reasons, blind interpretation of OSEs is not encouraged. They should be carried out using several models to see if a consistent picture emerges. But this may not be sufficient. Analysis systems are flawed (analysis is a very complex process). One example of this is shown in Figure 3.3 lower panel, when the fit to the verifying data actually improves when a data stream, in this case ARGO, is removed. It could be that ARGO and TT are inconsistent, but a more likely interpretation is that the data assimilation system is not using the data in an optimum way. One should note, however, that correcting errors like this is unlikely to be straightforward. Progress will undoubtedly be made, but on a scale of decades rather than years.

In summary, OSEs are a useful and essential tool for assessing the importance of an observation system and their use, particularly multi-model approach, should be encouraged, but they must be interpreted with caution.

8. Data Requirements and Recommendations

There are different aspects of a forecast system (initialization, system development, verification and calibration) that require observational information. Methodology for objective evaluation of the observing system only exists for the initialization, in terms of so-called “forecast sensitivity” evaluation, or from more ad-hoc Observing System Experiments (OSES). Even then, it is not always easy to extract useful information. In NWP there is routine forecast evaluation, but the metrics are not targeted to the boundary layer or surface variables. At seasonal and monthly forecasts range, the size of sample to be evaluated is smaller, and it is harder to establish statistical significance. Some ad-hoc OSES are conducted to evaluate in the initialization and forecast for seasonal time scales. But results are generally not very conclusive; vary a lot from different systems; and appear to be influenced by model error, rendering the evaluation quite difficult. To our knowledge, there has not been any evaluation of the observing system with forecasting systems at monthly time scales. In any case, this sort of evaluation targets only the impact of observations on the initialization of forecasts, but it can not measure the impact of the observations on the other components of a forecasting system (such as verification or model development).

TPOS WP5 offers a thorough list of observing system requirements from the ocean initialization perspective. Specific requirements for NWP are also captured by the relevant WMO expert groups. Rather than duplicating these documents, in what follows we provide a discussion of the relevant attributes of any observing system, including data delivery, accuracy, stability, resilience, temporal sampling and span, spatial sampling and coverage, including focus areas, and variables for the ocean, for waves, and for atmosphere boundary layer.

8.1. Data Streams

Regarding the delivery of data, operational centers would need at least 2 streams of data delivery: real time stream via GTS, to be used for the initialization of forecasts, and a BRT quality-controlled data stream. The latter is used for a variety of applications, which allow for longer delay times. Close-to-real-time reanalyses used for monitoring and the backbone of a seasonal forecasting system can accept delays of around 10-15 days to receive better processed data (such as better orbit specification for altimeter sea level or bias-corrected Argo salinity data). Verification of current forecasts need data (either station or L2) arriving with a delay or about 1-3 months. Delays of years or decades are accepted for re-processed data, or observations recovered from data mining.

8.2 Accuracy

It is difficult to provide hard set values for accuracy and precision of the observations. Indeed, these will depend very much on the application, and it is likely to vary in time as the models get better. Given that model error is still large, the requirements for verification will be more relaxed than for assimilation. Requirements for model development may vary, and in some cases very precise observations may be needed. From the assimilation perspective, it is important that the observations are unbiased. It is better to have larger random errors in the observations than smaller systematic biases. It is also important that the errors are stable in time, and homogeneous in space. If this is not possible, models to parameterize these errors should be

provided. Currently, the instrument error of most in situ observations is small compared with the representativeness error (which is determined by the model unresolved spatial and temporal scale). One possibility is to require that the observation random error should not exceed a percentage of the variability that the forecast system is trying to predict (say 1-5%).

8.3 Stability

An important requirement for the observing system is continuity and stability in time. Although changes leading to improvement are of course welcome, exploring new ways of obtaining efficient measurements should not compromise more traditional but critical observations. Well established observing systems should only be abandoned when there is clear evidence that they are redundant, or that the needs they were serving can be catered by alternative means. One should bear in mind that for calibration of seasonal forecasts requires stable data records of about 30 years. The longer the record, the better the calibration of extreme events is performed. For decadal forecasting and climate monitoring, records of 50-100 years are required.

8.4 Resilience

The observing system needs to be robust and resilient to guarantee that the needs of operational services are met. This implies some degree of redundancy, to cover for failure of individual components. It may also be advisable to formulate a priority list for sites and observations that need to be maintained in critical situations.

8.5 Spatial sampling, coverage and focus areas

The equatorial region appears challenging for both atmospheric and ocean models. The question is whether regions where forecasting systems do not make good use of observations should be more, or on the contrary less, sampled. The Equator is a key region for the earth's climate and for monthly to seasonal forecasts. From that point of view it should be sufficiently sampled. Ocean models also have problems with western boundary currents, which are also key for the ocean circulation and air-sea interaction.

The robust broad scale sampling of in situ temperature and salinity achieved by Argo should be maintained, and if possible enhanced. The sampling of the deep ocean below 2000m is needed for advancing decadal forecasts, reanalyses of the global ocean, and ocean model development.

Enhanced sampling of the ocean and atmosphere boundary layer should be considered, both for model development and for coupled data assimilation. The enhancement includes higher vertical and temporal resolution, as well as the existence of reference flux sites sampling different regimes. More specific studies are needed to establish the needs for a sustained observing system of the ocean-atmosphere boundary layer.

The high resolution spatial sampling of surface variables achieved by satellite instruments (SST, SSH, SSS, ocean color, surface winds) is needed, and it is likely to have higher impact as the model resolution increases.

8.5 Temporal sampling

The temporal sampling is not independent of the spatial sampling. Currently global coverage of the ocean at 3 x 3 degrees is achieved by Argo every 10 days, but this should be increased if possible. Equally, daily global coverage at, say, 2 x 2 degree of SSH by satellite altimeter would be desirable. Satellite altimetry does not yet resolve the diurnal cycle. The temporal sampling by the moored array (daily and sub-daily) is very valuable.

General guidelines for temporal sampling would be: 1-3 hours sampling for ocean-atmosphere boundary layer process. Daily sampling for in situ subsurface (upper 1000m) at a spatial resolution of 200km-1000km (depending on the region). Below 2000m, monthly samplings may be adequate, but more specific studies are needed.

8.6 Essential variables

The following variables are considered necessary (see also TPOS WP5)

- Ocean subsurface [T(z),S(z),U(z)]
- Ocean surface [SST, SSS, Surface Currents], as well as SSH, Geoid, and Bottom pressure
- Atmosphere Surface and BL: surface winds, T2m, humidity, SLP, and precipitation
- Waves: wave height, wave period, wave spectrum
- Multivariate (collocated at same location), direct or derived: heat flux, humidity flux, wind stress, TKE profile, ocean-atmosphere boundary layer high resolution soundings.

References

Anderson et al. (1998): Surface buoyancy forcing and the mixed layer of the Western Pacific warm pool: Observations and 1D model results, J. Clim., 9, pp. 3056–3085.

Andersson, E., and Yoshiaki, S. (Editors) (2012): Final Report of the Fifth WMO Workshop on the Impact of Various Observing Systems on Numerical Weather Prediction. WIGOS WMO Integrated Global Observing System Technical Report 2012-1.

Balmaseda, M.A., Dee, D., Vidard, A, and Anderson, D.L.T. (2007a): A multivariate treatment of bias for sequential data assimilation: application to the tropical oceans. Q. J. R. Meteorol. Soc. 133: pp. 167–179.

Balmaseda, M., and Anderson, D. (2009): Impact of initialization strategies and observations on seasonal forecast skill, Geophys. Res. Lett., 36, L01701, (doi:10.1029/2008GL035561).

Balmaseda, M. & Co-Authors (2010): "Role of the Ocean Observing System in an End-to-End Seasonal Forecasting System" in Proceedings of OceanObs'09: Sustained Ocean Observations and Information for Society (Vol. 1), Venice, Italy, 21-25 September 2009, Hall, J., Harrison, D.E. & Stammer, D., Eds., ESA Publication WPP-306, doi:10.5270/OceanObs09.pp.03.

Balmaseda, M. A., Trenberth, K.E., and Källén, E. (2013): Distinctive climate signals in reanalysis of global ocean heat content, Geophys. Res. Lett., 40, pp. 1754–1759, (doi:10.1002/grl.50382).

Bell, M. J., Martin, M. J., and Nichols, N. K. (2004): Assimilation of data into an ocean model with systematic errors near the equator. Q. J. R. Meteorol. Soc., 130, pp. 873-893.

Bonjean, F., and Lagerloef, G.S.E. (2002): Diagnostic Model and Analysis of the Surface Currents in the Tropical Pacific Ocean. J. Phys. Oceanogr., 32, pp. 2938–2954.

Browning, G. L., Kreiss, H.O., and van de Kamp, D.W. (2000): "Comments on "Observations of a Mesoscale Ducted Gravity Wave"." *Journal of the atmospheric sciences* 57.4 (2000): pp. 595-598.

Burgers, G., Balmaseda, M.A., Vossepoel, F.C., van Oldenborgh, G.J., and Leeuwen, P.J. (2002): Balanced ocean data assimilation near the equator. J Phys Ocean, 32, pp. 2509-2519.

Cassou (2008): Intraseasonal interaction between the Madden–Julian Oscillation and the North Atlantic Oscillation, Nature, 455, pp. 523-527.

Chepurin, G. A., Carton, J.A., and Leuliette, E. (2014): Sea level in ocean reanalyses and tide gauges, J. Geophys. Res. Oceans, 119, (doi:10.1002/2013JC009365).

Craig, P.D. and Banner, M.L. (1994): Modeling wave-enhanced turbulence in the ocean surface layer. J. Phys. Oceanogr. 24, pp. 2546-2559.

De Boisséson, E., Balmaseda, M. A., Vitart, F., and Mogensen, K. (2012): Impact of the sea surface temperature forcing on hindcasts of Madden-Julian Oscillation events using the ECMWF model, Ocean Sci. Discuss., 9, pp. 2535-2559, (doi:10.5194/osd-9-2535-2012).

Dee, D.P., Uppala, S.M., Simmons, A.J., Berrisford, P., Poli, P., Kobayashi, S., Andrae, U., Balmaseda, MA, Balsamo, G., Bauer, P., Bechtold, P., Beljaars, A.C.M., van de Berg, L., Bidlot, J., Bormann, N., Delsol, C., Dragani, R., Fuentes, M., Geer, A.J., Haimberger, L., Healy, S.B., Hersbach, H., Hólm, E.V., Isaksen, L., Kållberg, P., Köhler, M., Matricardi, M., McNally, A.P., Monge-Sanz, B.M., Morcrette, J.J., Park, B.K., Peubey, C., de Rosnay, P., Tavolato, C., Thépaut, J.N., and Vitart, F. (2011): The ERA-Interim reanalysis: Configuration and performance of the data assimilation system. Q. J. R. Meteorol. Soc. 137: pp. 553–597.

England, M.H. (2014): "Recent intensification of wind-driven circulation in the Pacific and the ongoing warming hiatus." Nature Climate Change 4.3 (2014): pp. 222-227.

Fujii, Y., Nakaegawa, T., Matsumoto, S., Yasuda, T., Yamanaka, G., and M. Kamachi (2009): Coupled climate simulation by constraining ocean fields in a coupled model with ocean data. J. Climate, 22(20), pp. 5541-5557, (doi:10.1002/jgrc.20094).

Garrett, C. (1976): The generation of Langmuir circulations by surface waves- A feedback mechanism. J. Mar. Res., 34, pp. 117-130.

Grant, A.L.M. and Belcher, S.E. (2009): Characteristics of Langmuir Turbulence in the Ocean Mixed layer, J. Phys. Oceanogr. 39, pp. 1871-1887.

Grunseich et al. 2013: The Madden-Julian oscillation detected in Aquarius salinity observations, Geophys. Res. Lett., 40, 20, 5461–5466

Hasselmann, K., 1970. Wave-driven inertial oscillations. Geophys. Fluid Dyn. 1, pp. 463-502.

Hawkins E, and Sutton R. (2009): The potential to narrow uncertainty in regional climate predictions. Bull Am Meteor Soc 90: pp. 1095–1107.

Janssen, P.A.E.M. (2012): Ocean wave effects on the daily cycle in SST. J. Geophys. Res, 117, C00J32, 24 pp., (doi:10.1029/2012JC007943).

Janssen, P.A.E.M., Breivik, O., Mogensen, K., Vitart, F., Balmaseda, M.A., Bidlot, J.R., Keeley, S., Leutbecher, M., Magnusson, L., and Molteni, F. (2013): Air-sea interaction and surface waves. ECMWF Technical Memorandum 712. 34 pages. Kelly et al. 2010: Western Boundary Currents and Frontal Air–Sea Interaction: Gulf Stream and Kuroshio Extension. J. Clim., 23, pp. 5644–5667.

Klingaman, and Woolnough (2013): The role of air–sea coupling in the simulation of the Madden–Julian oscillation in the Hadley Center model, Quart. J. Roy. Meteorol. Soc. accepted.

Kumar, A., and Hoerling, P.M. (1995): Prospects and Limitations of Seasonal Atmospheric GCM Predictions. Bull. Ame. Meteor. Soc., 76, pp. 335-345.

Kumar, A., Chen, M., Zhang, L., Wang, W., Xue, Y., Wen, C., Marx, L., and Huang, B. (2012): An analysis of the non-stationarity in the bias of sea surface temperature forecasts for the NCEP climate forecast system (CFS), version 2. Mon Wea Rev 140:3003–3016, (doi:10.1175/MWR-D-11-00335.1).

Kumar, A., Wang, H., Xue, Y., and Wang, W. (2014): How much of monthly subsurface temperature variability in equatorial pacific can be recovered by the specification of sea surface temperatures? J. Climate, 27, pp. 1559-1557.

Luo, J.-J., et al. (2005): Seasonal Climate Predictability in a Coupled OAGCM Using a Different Approach for Ensemble Forecasts. Journal of climate 18.

Lyman, J. M., Willis, J.K., and Johnson, G.C. (2006): Recent cooling of the upper ocean, Geophys. Res. Lett., 33, L18604, (doi: 10.1029/2006GL027033).

Magnusson, L., Balmaseda, M.A., and Molteni, F. (2012b): On the dependence of ENSO simulation on the coupled model mean state. Clim Dyn., (doi: 10.1007/s00382-012-1574-y).

Magnusson, L., Alonso-Balmaseda, M., Corti, S., Molteni, F., and Stockdale, T. (2012): Evaluation of forecast strategies for seasonal and decadal forecasts in presence of systematic model errors. *Climate Dynamics*, pp. 1-17.

Matthew et al. (2010): Ocean temperature and salinity components of the Madden–Julian oscillation observed by Argo floats, Clim. Dyn., 35, 7-8, pp. 1149-1168.

McWilliams, J.C., and Restrepo, J.M. (1999): The wave-driven ocean circulation. J. Phys. Oceanogr. 29, pp. 2523-2540.

Molteni, F., Stockdale, T., Balmaseda, M.A., Balsamo, G., Buizza, R., Ferranti, L., Magnusson, L., Mogensen, K., Palmer, T.N., and Vitart, F. (2011): 'The new ECMWF seasonal forecast system (System 4)'. Tech. Memo. 656. ECMWF: Reading, UK.

Mori, and Watanabe (2008): The growth and triggering mechanisms of the PNA: a MJO-PNA coherence. J. Meteorol. Soc. Jpn. 86, pp. 213–236.

Palmer, T. N., and Anderson, D. L. T. (1994): The prospects for seasonal forecasting-A review paper. *Quartly. J. Roy. Met. Soc. 120,* pp. 755-793.

Saha, S., Moorthi, S., Pan, H.L., Wu, X., Wang, J., Nadiga, S., Tripp, P., Kistler, R., Woollen, J., Behringer, D., Liu, H., Stokes, D., Grumbine, R., Gayno, G., Wang, J., Hou, Y.T., Chuang, H.Y., Juang, H.M.H., Sela, J., Iredell, M., Treadon, R., Kleist, D., Van Delst, P., Keyser, D., Derber, J., Ek, M., Meng, J., Wei, H., Yang, R., Lord, S., Van Den Dool, H., Kumar, A., Wang, W., Long, C., Chelliah, M., Xue, Y., Huang, B., Schemm, J.K., Ebisuzaki, W., Lin, R., Xie, P., Chen, M., Zhou, S., Higgins, W., Zou, C.Z., Liu, Q., Chen, Y., Han, Y., Cucurull, L., Reynolds, R.W,. Rutledge, G., Goldberg, M. (2010): The NCEP climate forecast system reanalysis. Bull. Am. Meteorol. Soc. 91: pp. 1015–1057.

Ricci, S., Weaver, A.T., Vialard, J., and Rogel, P. (2005): Incorporating temperature-salinity constraints in the background-error covariance of variational ocean data assimilation. Mon. Wea. Rev. 133: pp. 317–338.

Small et al. (2008): Air-sea interaction over ocean fronts and eddies. Dyn. Atmos.-Ocean, 45, pp. 274-319.

Smith, D. M., and Murphy, J.M. (2007): An objective ocean temperature and salinity analysis using covariances from a global climate model, J. Geophys. Res. 112, C02022.

Stockdale T. (1997): Coupled ocean-atmosphere forecast in the presence of climate drift. Mon Wea Rev 125: pp. 809–818.

Terray, E.A., Donelan, M.A., Agrawal, Y.C., Drennan, W.M., Kahma, K.K., Williams, A.J., P.A. Hwang, P.A., Kitaigorodskii, S.A. (1996): Estimates of Kinetic Energy Dissipation under Breaking Waves. J. Phys. Oceanogr. 26, pp. 792-807.

Troccoli, A., and Haines K. (1999): Use of Temperature–Salinity relation in a data assimilation context. J. Atmos. Oceanic Technol. 16: pp. 2011–2025.

Vitart (2013): Evolution of ECMWF sub-seasonal forecast skill scores. Quart. J. Roy. Meteorol. Soc., accepted.

Wheeler, M., and Kiladis, G.N. (1999): Convectively Coupled Equatorial Waves: Analysis of Clouds and Temperature in the Wavenumber–Frequency Domain. *J. Atmos. Sci.*, **56**, 374–399.

Wijffels, S., Willis, J., Domingues, C.M., Barker, P., White, N.J., Gronell, A., Ridgway, K., Church, J.A. (2009): Changing expendable bathythermograph fall rates and their impact on estimates of thermosteric sea level rise. J. Climate 21: pp. 5657–5672.

Woolnough et al. (2007): The role of the ocean in the Madden-Julian Oscillation: Implications for MJO prediction. Quart. J. Roy. Meteorol. Soc., 133 (622), pp. 117-128.

Yin, Y., Alves, O., and Oke, P.R. (2011): An ensemble ocean data assimilation system for seasonal prediction. Mon. Wea. Rev.139, pp. 786-808.

Žagar, N., Andersson, E., and Fisher, M. (2005): Balanced tropical data assimilation based on study of equatorial waves in ECMWF short-range forecast errors. Q. J. R. Meteorol. Soc. 131, pp. 987-1011.

Zhang, L., Kumar, A., and Wang, W. (2012): Influence of changes in observations on precipitation: A case study for the Climate Forecast System Reanalysis (CFSR), J. Geophys. Res.117, D08105.

Zebiak, S.E., and Cane, M.A. (1987): "A Model El Niño–Southern Oscillation". Mon. Wea. Rev. 115 (10): pp. 2262–2278.

Appendix A

A.1 Naming convention used in this paper

To facilitate the discussion of the data needs it is helpful to introduce a naming convention regarding the processing level of the observations, the quality control, and the time-delivery properties.

For the processing level we follow the remote sensing convention, which classifies the data in different levels (L0 to L4) as described in the Appendix A.2. This will also be used for in situ data. L0 data is not usually required in the applications mentioned in this paper. For operational forecasting we will be talking about level 1 (L1) to level 4 (L4). Most of the in situ data used in operational forecasting are L2 (intended geophysical variables (IGV) at measurement location and time. When the data have been gridded (such as some Argo gridded products), binned in time, and sometimes combined with other data sources, it becomes L3. These can have regions or periods of time with missing data. If a further degree of processing takes place, the data can become L4. This is the case of analyses conducted with models via data assimilation, or when derived geophysical variables (DGV) are produced by some sort of geophysical constraint (such as geostrophic transports, or Argo derived velocities, or surface currents from altimeter). Some derived variables such as section transports or surface fluxes derived from bulk formulae are available only at precise locations, and no gridding algorithm has taken place. We will refer to these products as L3-D (D for Derived), to distinguish them from the more direct L2-QC and gridded L4 products.

Table A1 - Naming convention for data streams according to the delivery time and processing level. IGV is for Intended Geophysical Variable and DGV is for Derived Geophysical Variable. See text for other acronyms.

Product Level	Processing	Use	Examples
L2	IGV No Gridded	Real Time Initialization (Analyses)	Data acquired via GTS
L2-QC	IGV-QC No Gridded Time series possible	Reanalyses. Verification. Model development	WOA/EN3 data set.
L3	IGV Binned. Areas with missing data permitted. Time series possible	Analyses and Reanalyses Verification. Model development	Gridded sea-level maps from altimeter. Ocean Color climatology.

L3-D	DGV Binned. Areas with missing data permitted. Time series possible	Analyses and Reanalyses. Verification. Model development	Transports. Fluxes from bulk-formulae at observation points
L4	IGV/DGV Gridded. Time series possible	Analyses and Reanalyses. Verification. Model Development	Surface fluxes from Reanalyses. Surface currents from reanalyses

For many operational applications L2 data is expected to be delivered in near real-time (traditionally within 3 hours in meteorology and say within 24 hours for ocean applications) following a protocol that allows its automatic acquisition and usage, often under the auspices of the WMO. We will refer to this data stream as NRT. The L2 data can have some degree of quality controlled (QC), such as bias correction, black-listing, and others. We will refer to this as L2-QC. The QC often takes place in specialized data processing centers, and this may result in a delay in the delivery, even when the QC is done on a routine/operational basis. We can refer to this data stream as BRT, since it arrives behind real-time, but it can still be used in operational delayed products such as reanalyses. The delay time application of observed data depends very much of the application, and will be specified whenever is needed. When L2-QC data from a fixed location are further treated to provide time-series with the data binned at adequate time-intervals (daily, monthly), the product becomes L3 or L3-timeseries. Note that the L3 data can still have regions or period where the data is missing. Finally, there can be very sophisticated QC and processing procedures (especially some of L4 data), without specific delivery time requirements.

A.2 Levels of processing of remote sensing data

In remote sensing the data is classified in different levels (Level 0 to Level 4) according to the degree of processing:.

- L0: Reconstructed, unprocessed instrument and payload data at full resolution, with any and all communications artifacts (e. g., synchronization frames, communications headers, and duplicate data) removed.

- L1a: Reconstructed, unprocessed instrument data at full resolution, time-referenced, and annotated with ancillary information, including radiometric and geometric calibration coefficients and georeferencing parameters (e.g., platform ephemeris) computed and appended but not applied to the L0 data (or if applied, in a manner that L0 is fully

recoverable from L1a data).

- L1b: These are L1a data that have been processed to sensor units (e. g., radar backscatter cross section, brightness temperature, etc.); not all instruments have L1b data; L0 data is not recoverable from L1b data.

- L2: Derived geophysical variables (e. g., ocean wave height, soil moisture, ice concentration) at the same resolution and location as L1 source data.

- L3: Variables mapped on uniform space-time grid scales, usually with some completeness and consistency (e. g., missing points interpolated, complete regions mosaicked together from multiple orbits, etc.).

A.2 Illustration of Equatorial Dynamics and Time Scales

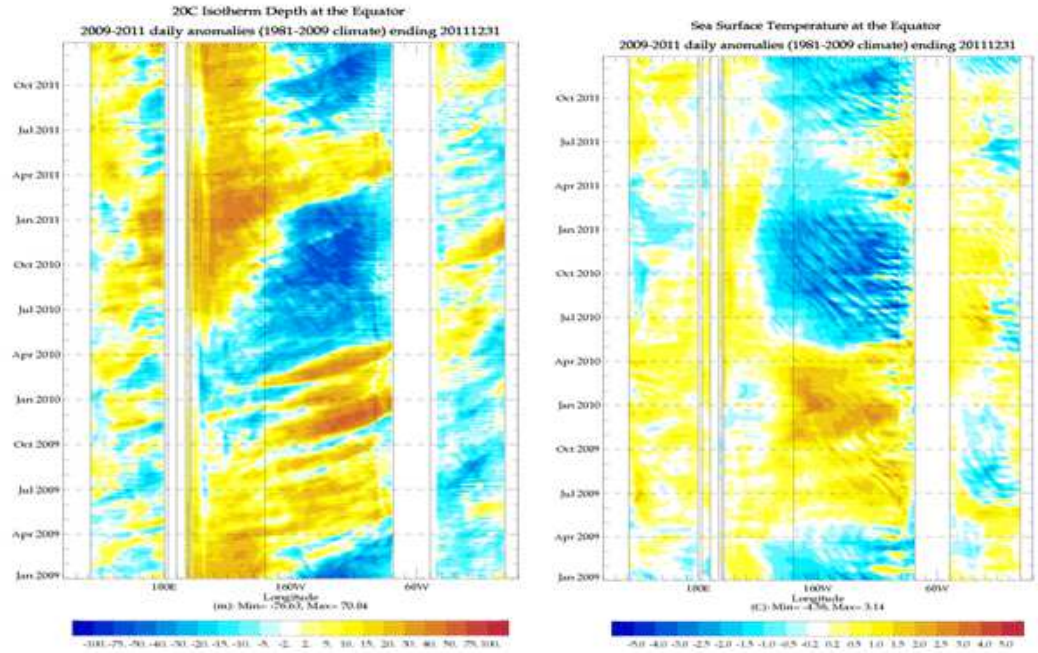

Figure S1 - Longitude-time diagrams of equatorial thermocline depth (left) and SST (right) anomalies. The thermocline depth is represented by the depth of the 20 degree Isotherm (D20). The anomalies are computed respect the 1989-2008 climatology. The eastward propagation of equatorial Kelvin waves is visible in D20 usually preceding the appearance of SST anomalies in the Eastern Pacific (from the ORAS4 ocean reanalysis (Balmaseda et al., 2013)). The figure also shows that a thermocline anomaly associated with an individual Kelvin wave does not always translate into a large scale SST anomaly, as it happened in the "failed" El Niño of 2011, when in spite of a substantial propagation of the thermocline anomalies the warm SST anomaly was very short lived, and the El Niño did not materialized. The figure also shows the variability associate with the westward propagating Tropical Instability Waves in Eastern Pacific.

Ocean Observing System

Supplementary Figure S2 shows schematically the different components of the ocean observing system and their availability in time. SST observations are essential for seasonal forecasts. Most of the initialization systems also use subsurface temperature from XBT's (Expendable bathythermograph), CTDs (Conductivity, Temperature and Depth) usually from scientific cruises, moored buoys (TAO/TRITON in the Pacific, PIRATA in the Atlantic, RAMA in the Indian Ocean) and Argo floats. Salinity (mainly from Argo and CTDs), and altimeter-derived sea-level anomalies (SLAs, since approximately 1993) are also assimilated. The latter usually need a prescribed external Mean Dynamic Topography (MDT), which can be derived indirectly from gravity missions such as GRACE (Gravity Recovery and Climate Experiment) and, in the near future, GOCE (Gravity field and steady-state Ocean Circulation Explorer). Supplementary figure S3 shows the time evolution of the number of temperature and salinity observations, as well as the typical spatial distribution. The figure shows the large increase in observations associated to the advent of Argo. The properties of spatial and temporal sampling varies substantially between instruments: the XBTs usually follow commercial ship routes, CTDs are associated

with intense scientific missions, the moored array samples the equatorial oceans at few selected fix positions; Argo, is only observing system that sample uniformly the subsurface of the ocean, measuring temperature and salinity up to depth of 2000m. Altimeter sea-level (not shown) also samples the surface of the ocean quite uniformly, but a good relation between sea level variations and subsurface structure is only possible in regions of strong stratification (the tropics).

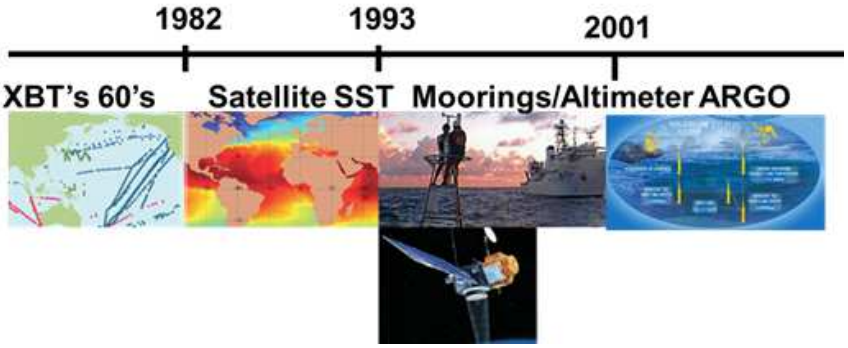

Figure S2 - Time evolution of the ocean observing system by instrument.

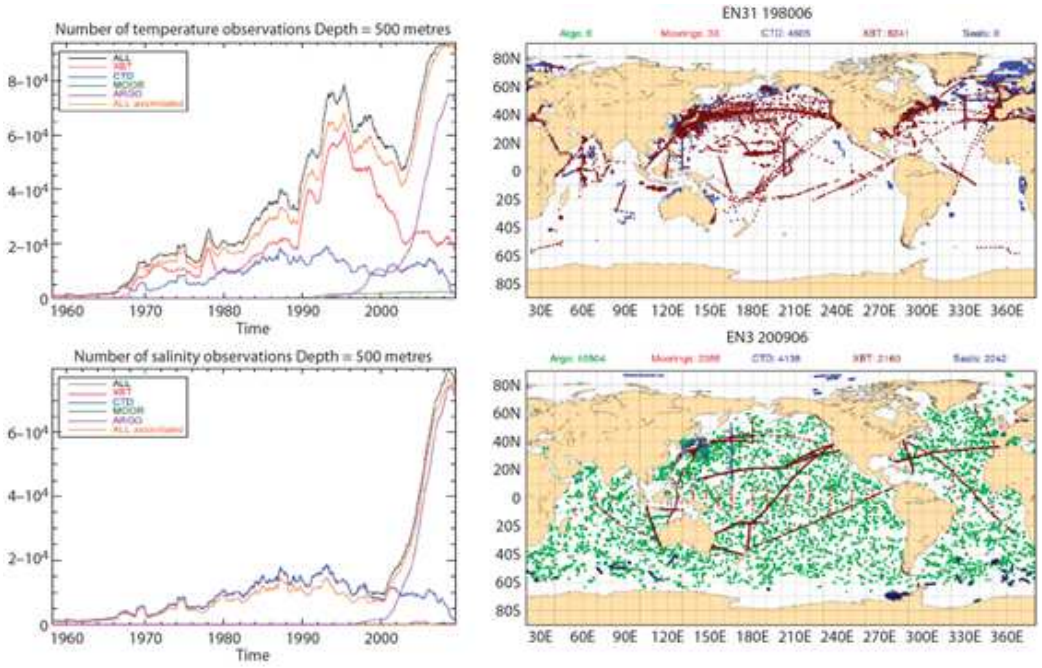

Figure S3 - (left) Number of temperature (top) and salinity (bottom) observations within the depth range 400m-600m as a function of time per instrument type. The black curve is the total number of observations. The orange curve shows the number of assimilated observations. (right) Typical observation coverage in June 1980 (top) and in June 2005 (bottom). Note that the color coding for the instruments is not the same in the left and right panels.

White Paper #5 – Evaluation of the Tropical Pacific Observing System from the data assimilation perspective

Fujii, Y.[1], Cummings, J.[2], Xue, Y.[3], Schiller, A.[4], Lee, T.[5], Balmaseda, M.A.[6], Remy, E.[7], Masuda, S.[8], Alves, O.[9], Brassington, G.[10], Cornuelle, B.[11], Martin, M.[12], Oke, P.[4], Smith, G.[13], and Yang, X.[14]

[1] Meteorological Research Institute, Japan
[2] Naval Research Laboratory, United States
[3] NOAA Climate Prediction Center, United States
[4] CSIRO Marine and Atmospheric Research, Australia
[5] Jet Propulsion Laboratory, United States
[6] European Center for Medium-Range Weather Forecasts, United Kingdom
[7] Mercator-Ocean, France
[8] Research Institute for Global Change, JAMSTEC, Japan
[9] Center for Australian Weather and Climate Research, Australia
[10] Bureau of Meteorology, Australia
[11] Scripps Institution of Oceanography, United States
[12] Met Office, United Kingdom
[13] Environment Canada, Canada
[14] NOAA Geophysical Fluid Dynamics Laboratory, United States

1. Introduction

Ocean Data Assimilation (DA) systems are tools to synthesize ocean observation data using the numerical ocean models, and widely applied as the primary method for transforming the data into information which can be used effectively by society. Conversely, the capacity of ocean DA systems inevitably depends on the extent to which the observing system satisfies the requirements of the DA systems. If an observing system does not satisfy these requirements, the system cannot provide effective information to society, which implies observational data are abandoned without being converted into effective information. Thus, it is essential for observing systems to satisfy the requirements of the DA systems. Moreover, quantifying the impacts of observational data on products of the systems is equivalent to evaluating the impact of the observations on society.

This white paper introduces the current status and achievement of ocean DA systems using the Tropical Pacific Observing System (TPOS), and summarizes requirements of the DA systems for the TPOS and the impacts of TPOS on the products of the systems. In this paper, we mainly focus on observations of physical parameters for the ocean interior, that is, temperature, salinity, and current velocity (including at the surface), and SSH because ocean DA systems generally calculate the time-evolution of those parameters. Although atmospheric observations at the surface affect ocean DA systems since they are often employed for estimating the atmospheric forcing data for the systems, we leave most discussions on those data to the white paper led by TPOS WP4. The white paper led by Mathis discusses on biogeochemical observations (TPOS WP6).

The purposes of ocean DA systems can roughly be classified into three categories. The first purpose is for ENSO monitoring and Seasonal-to-Interannual (S-I) forecasting, the second is for

short-to-medium range (generally less than 1 month) ocean forecasting, and the third is for climate research, including estimations of the ocean state and variability in the climate time-scale and decadal predictions. In this paper, we discuss the current status and requirements of ocean DA systems, and impacts of the observations on those systems associated with each purpose separately, although many systems are being used for multiple purposes and over multiple time scales.

This paper is organized as follows. First, we introduce the current status and achievements of ocean DA systems and discuss their requirements in section 2. The variety of the observing system evaluation studies for TPOS is given in section 3. A summary follows in section 4.

2. Current status, achievements, and requirements

2.1 Seasonal-interannual forecasting

Ocean DA systems as well as a Coupled ocean-atmosphere General Circulation Model (CGCM) are essential components of general S-I forecasting systems in operational centers Since most predictability for S-I forecasts comes from ENSO, the estimation of the tropical Pacific Ocean state is vital for S-I forecasting systems. Ocean DA systems are also employed in operational centers for monitoring equatorial wave activity, variability of the equatorial thermocline, and other oceanic phenomena associated with ENSO.

Deployment of TAO array under the Tropical Ocean and Global Atmosphere (TOGA) programme initially realized the operational monitoring of the ocean interior state in the equatorial Pacific using ocean DA systems in the early 1990s (e.g., Ji et al., 1995). In this early stage, the DA systems assimilated temperature profiles alone. Assimilation of SSH data started in the mid 1990s after the launch of the TOPEX/Poseidon satellite. Subsequently the rapid increase of Argo floats after 2000 motivated updates to the DA systems in order to assimilate salinity globally from Argo. Consequently most current ocean DA systems for S-I forecasting (hereafter, SIDA systems) have the capacity to assimilate salinity profiles imposing a multivariate (mainly T-S) balance relationship (summarized in Fujii et al., 2011).

Current SIDA systems in operational centers generally use Ocean General Circulation Models (OGCM) with resolution typically 1˚ but with some equatorial refinement in the horizontal and about 10 m resolution in the vertical in the upper ocean. The resolution is restrained because of the large computational burden for S-I forecasting. The UK Met Office, however, has started to use a 1/4˚-resolution ocean model for the ocean DA system and the ocean component of the CGCM for S-I forecasting (MacLachlan et al. 2014). The majority of the systems currently apply 3DVAR assimilation schemes (e.g., NCEP, JMA, and ECMWF). However, other sophisticated assimilation schemes are also used in other institutes (e.g., EnOI is adopted in ABoM; Yin et al., 2011). Although most systems are forced by sea surface fluxes estimated from atmospheric DA fields which are separately calculated, the ocean DA system in NCEP is coupled with an atmospheric DA system on line (i.e., it is a weakly coupled DA system) and SST in the ocean DA fields also affects atmospheric DA results (Saha et al., 2010). Development toward coupled DA has also started in other centers. Retrospective long-term (typically 20-30 years) ocean DA runs are often performed with SIDA systems in operational centers for validation and calibration of SI forecasting systems, and called “reanalyses”. This can be used for estimating forecast

biases in order to correct forecasts for model error, and for skill assessment Reanalyses are also used in climate research (see subsection 2.3).

SST data are assimilated in SIDA systems as essential data because SST anomalies over the whole tropical Pacific are important features of El Niños and La Niñas, and directly affect the atmospheric global circulation and climate. SIDA systems generally use SST data whose resolution and sampling intervals are typically 1˚ and 1 day. This resolution and interval generally seems to be sufficient for reconstructing the variability associated with ENSO. Horizontal distribution of SST is effectively observed from satellites and calibrated using in situ observations including the data from the mooring buoys. Gridded datasets of observed SST are provided from several operation centers (see Cronin et al., 2014, TPOS WP10).

Assimilation of subsurface temperature observations is also essential for ENSO monitoring and S-I forecasting because variations of thermocline depths are considered to play important roles in the ENSO mechanism. In particular, there is a general consensus that baroclinic Kelvin wave activity along the equator frequently affects occurrences of El Niños and La Niñas. Considering the horizontal scale of these phenomena, required sampling intervals in the zonal and meridional directions are 500-1000 km, and around 200 km, respectively. The meridional interval is smaller due to the stretched structure of waves in the zonal direction, but it is still not so demanding. The TAO/TRITON array was originally designed considering these requirements, and assimilating temperature profile data from the TAO/TRITON array is thus considered to be effective for detecting thermocline changes associated with ENSO. However, the vertical sampling interval (20-50 m around the thermocline) may not be sufficient to detect the thermocline depth accurately. Considering the typical vertical resolutions of SIDA systems, a vertical interval around 10 m is desirable. In contrasts, the sampling interval of TAO/TRITON array in the temporal direction (1 hour) is very short compared to the time scale of target phenomena. Time-averaging is often performed before assimilating into the systems in order to reduce high frequency noise and the number of observation data. Thus, the advantage of TAO/TRITON array (i.e., high frequency of data) is not fully utilized in current SIDA systems.

Temperature profiles observed by Argo floats, which are also major components of data assimilated into SIDA systems, complement the TAO/TRITON data. These have higher vertical and zonal resolutions (1 m, and 300 km), and their temporal sampling interval is reasonable for ENSO. However, the meridional sampling interval is somewhat larger than TAO/TRITON array, and currently few floats stay in the vicinity of the equator due to the equatorial divergence of the near surface current. Argo floats are, thus, less suitable than TAO/TRITON array for detecting the baroclinic wave activities along the equator (see TPOS WP10 for ARGO floats with improved equatorial performance).

Variability of the thermocline depth can be also detected by SSH observations, and therefore the majority of SI systems assimilate SSH data from satellites. The sampling interval across the SSH satellite paths is 100-300 km (the interval along the paths is much smaller) and the temporal interval is 10-40 days. These intervals seem to be reasonable for detecting ENSO-scale variability. However, the impacts of assimilating SSH is generally small because the information from SSH observation duplicates that from subsurface temperature data by TAO/TRITON and Argo floats, and because the complicated vertical structure in the equatorial region makes it difficult to infer the vertical distribution of the temperature anomaly from SSH

that offers vertically integrated information on the temperature field alone. Assimilation of altimeter SSH needs support from sub-surface temperature and salinity profiles.

Considering the possibility that Tropical Instability Waves (TIW) and other complex structures in the far western equatorial Pacific (e.g., New Guinea current systems) affect ENSO (e.g., Ueki et al., 2003; Menkes et al., 2006), observed temperature or SSH data with higher resolution may have some potential. Although the high resolution data cannot be employed for the current lower resolution SIDA systems, it could be better exploited with the use of higher resolution ocean models (a resolution of 1/4˚ is the target for SI forecasts for the coming years).

The importance of near-surface salinity fields for ENSO prediction has been discussed in the last 20 years (e.g., Roemmich et al., 1994; Maes et al., 2005). It affects SST through the stability of stratification (e.g., the barrier layer), and the advection of warm water (e.g. fresh water jet). These features are particularly important around the equatorial salinity front due to the large variability of the salinity fields there. Most ATLAS buoys observe SSS, while TRITON buoys observe SSS and subsurface salinity. However, these data are not enough for SIDA systems to reproduce the salinity fields around the front whose horizontal scale is 100-200 km. Vertical resolution is also insufficient for reproducing the influence of salinity fields on SST and near-surface temperature.

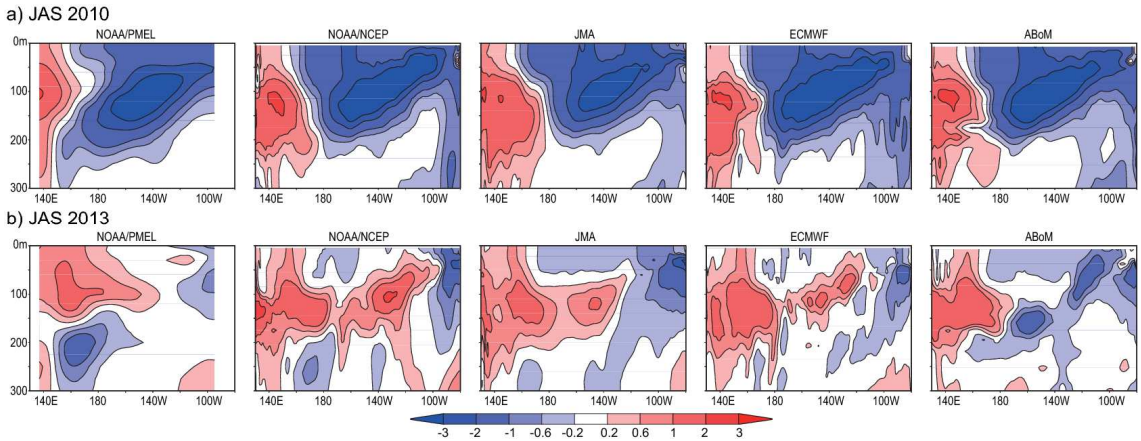

Figure 2.1 - Temperature anomaly (unit: ˚C) distribution averaged in a) July-September 2010, and b) July-September, 2013 in the equatorial vertical section in the Pacific in the objective analysis from the TAO/TRITON data produced by NOAA/PMEL and the operational DA results of NOAA/NCEP, JMA, ECMWF, ABoM. The anomaly is calculated as the deviation from the WOA09 for the objective analysis, and those from the monthly climatology of each system in 1989-2007 for the DA results.

Argo floats are powerful for observing salinity profiles. Their horizontal resolution is still insufficient, and the number of data is relatively low around the equator. But its vertically high-sampling profiles have substantial impacts on the reproduction of the salinity fields. SSH data also has an ability to detect the salinity variability when temperature profiles are well observed by other measurements and salinity has large variability (e.g., Fujii and Kamachi, 2003). Assimilation of satellite SSS observation has started only recently and its impact is still being assessed. Although the accuracy of the SSS observations (more than 0.2 PSU for monthly mean) does not satisfy the requirements for DA (favorably less than 0.1PSU in 10-day mean), it

may support the detection of the SSS variability associated with ENSO, and migration of the SSS fronts.

Data from ship observations are too sporadic spatially and temporally and cannot detect the basin-wide variability of the thermocline depth, nor the salinity fields. However, snapshots of the vertical section from the ship observation are useful to grab the image of the structures of temperature and salinity fields. These images promote our understanding and also useful to validate the DA results. Ocean current data is assimilated in few ocean DA systems because of severe contamination by tidal components and shorter-time scale variation, and the difficulty of controlling oceanic state by assimilating current data alone. However, they are often adopted as valuable independent data for validating assimilation results (see section 2.4).

The drastic decrease of observations from the TAO array started from 2011. In August 2013, the distribution of data from the TAO array becomes very sporadic in the central and eastern equatorial pacific. In contrast, the data from floats seems to be distributed densely enough to partly compensate the decrease of TAO data. However, Figure 2.1, in which the equatorial Pacific temperature anomaly fields are compared among the objective analysis from the TAO/TRITON data produced by NOAA/PMEL (http://www.pmel.noaa.gov/tao/jsdisplay/) and the operational DA results of NOAA/NCEP (Behringer and Xue, 2004), JMA (Fujii et al., 2012), ECMWF (Balmaseda et al., 2013a), and ABoM (Yin et al., 2011), shows the increased diversity among the objective analysis (without ocean model) and data assimilation results compared to those in 2010 resulting from the lack of TAO array data. In 2010, all results show similar anomaly pattern that is typical for the La Niña period. In contrast, assimilation results indicate different longitudes for the position of the eastern tip of the warm anomaly, which ENSO forecasters particularly focus on in order to judge the possibility of emergence of the anomaly at the surface. Moreover, the objective analysis field is most doubtful due to the small number of available data. Thus the lack of TAO array data currently makes a tough situation for ENSO forecasters, which indicates that the TAO array data along the equator has indispensable information for SIDA systems. NOAA/NCEP, JMA, and ECMWF plan to start routine near-real time intercomparison of the tropical Pacific subsurface temperature fields from their operational SIDA systems, such as shown above currently.

2.2 Seasonal-interannual forecasting

The launch of the TOPEX/Poseidon satellite in 1992 realized the possibility of monitoring/forecasting variability of western boundary currents and meso-scale eddies by an ocean DA system. Subsequently, a variety of ocean DA systems for short-to-medium range ocean forecasting (hereafter, OFDA systems) have been developed in operational centers and research institutes in several countries. The implementation of GODAE (1998-2008) and its follow-on programme, GODAE Ocean View (2009-current), underpin these developments in the last 15 years.

OFDA systems operated in some centers or groups, such as MERCATOR (Lellouche et al., 2013), the Canadian Meteorological Center (Smith et al. 2013), UKMO (Blockley et al., 2013), US Navy (see sub subsection 3.2.2), and ABoM (Brassington et al., 2012), include the tropical Pacific in their target domain. Those OFDA systems generally assimilate in situ temperature and salinity data including those observed by TAO/TRITON array and ARGO floats, and SST and

SSH from satellites in their eddy-permitting/resolving ocean models (typically 1/4° to 1/12° horizontal resolution). A variety of assimilation schemes (OI, 3DVAR, EnOI, EnKF, etc.) are used in those systems. Most OFDA systems are forced by sea surface fluxes estimated by atmospheric DA system. Typically forecasts of 5-days to 1-month are performed routinely with those systems. Most OFDA systems serve as the backbone for a variety of applications of ocean security, search and rescue, monitoring of marine eco-systems, etc. A couple of OFDA systems also provide the ocean initial conditions for coupled models in S-I forecasting. Retrospective ocean DA runs or Reanalyses are often performed with OFDA systems for validation of the system, as well as SIDA systems.

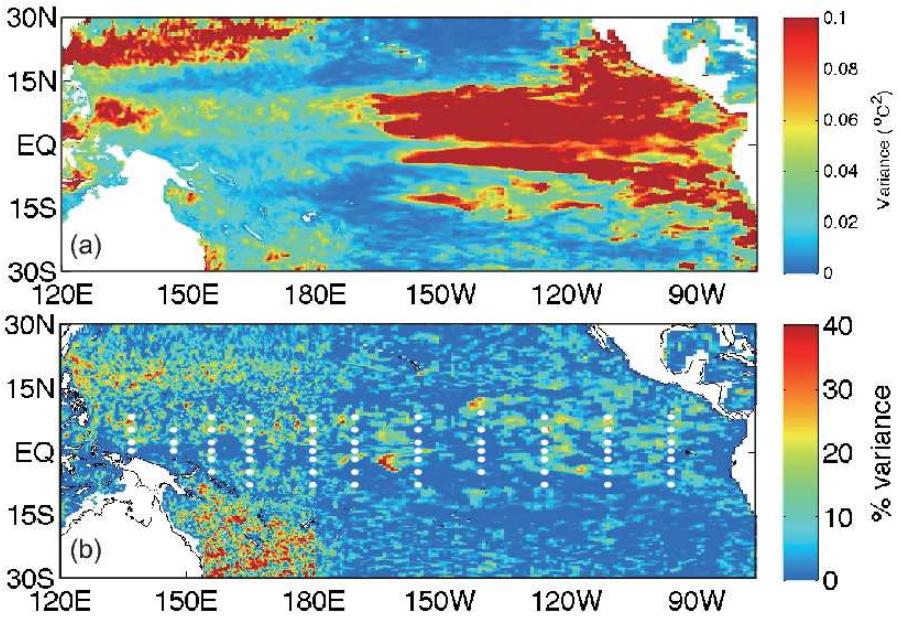

Figure 2.2 - (a) Time-averaged variance of 100-m-depth temperature among 0-3-day lead time forecasts from different ensemble members. (b) The percentage reduction in the time-averaged variance shown in (a) compared with the time-averaged variance of 100-m-depth temperature among 4-7-day lead time forecasts (equivalent to the background field for the data assimilation). The positions of the mooring buoys constituting the TAO/TRITON array are superimposed. The variance is calculated from the lagged ensemble assimilation and prediction runs of OceanMAPS. The averaging is performed for the period of from March 1st to August 31st in 2012 (adjusted from Brassington et al., 2014).

OFDA systems require TAO/TRITON data, as well as ARGO profiles, for constraining the ocean heat content, stratification and circulation in the tropics. However, observations with a higher resolution than that of current in situ observing systems seem to be favorable for those systems because they are generally designed to reproduce the variability associated with meso-scale eddies, and because the eddy activities (e.g., TIW, the Mindanao eddy, etc.) are very vigorous in the northern Tropical Pacific. This requirement is partly satisfied by satellite observations of SSH and SST, but they are still not sufficient. It is also important to note that most OFDA systems do not use sub-daily high frequency measurements of TAO/TRITON array but assimilate daily mean fields of the temperature and salinity measurements. Recently, several institutes also direct their efforts toward developing a coupled DA and prediction system based

on OFDA and atmospheric NWP systems for improving short-to-medium range forecasting of the atmosphere and ocean, especially coupled phenomena such as tropical cyclones and MJO.

In Figure 2.2, we show the uncertainty of data-assimilated fields and its growth in the prediction mode in the operational system in ABoM called OceanMAPS (Brassington et al., 2012, 2014; and Brassington, 2013) as an example of the current status of OFDA. OceanMAPS implements a 4-member lagged ensemble data assimilation run where each member is initialized using observation data every 4 days, and the timings of the initialization lagged 1-3 days behind those for other members. A 12-day prediction run (including 5-day hindcast) is also performed from every initialized fields of every ensemble member. The horizontal resolution of the system is 0.1°×0.1° for the region 90° E-180° and 75° S-20° N, and 0.1°×0.9° for the central and eastern tropical Pacific east of 180°.

Uncertainty of 100-m-depth temperature in the system is large in the eastern tropical Pacific and also in the far-western tropical Pacific, and relatively small between 140°E and 170°W (Figure 2.2a). This distribution has a similarity with the distribution of the climate variance of temperature at this depth. The uncertainty is relatively high in the zonal band around 8°N due to activities of TIW. Figure 2.2b indicates the percentage reduction in the uncertainty of the initialized field compared with the background hindcast. The percentage reduction becomes large at points where data assimilation constrains the ocean state substantially. Large values are concentrated east of Australia and in the zonal band between 15-20° N west of 180˚, but also interspersed in the area covered by the TAO/TRITON array, especially in the western Pacific between 0°-10° N, and the NINO3 region. A closer look reveals that some areas where the percentage reduction is large are collocated with mooring buoys, which implies that temperature observations by the mooring buoys are essential for constraining the ocean state around there.

2.3 Ocean state estimations and decadal forecasts

The development of in situ and satellite observing systems, such as those under the global XBT Programme, the TOGA-TAO Programme, the World Ocean Circulation Experiment (WOCE), and satellite observing systems (esp. altimetry such as the TOPEX/Poseidon), have spurred the efforts of ocean state estimation (a term used here loosely that includes the so-called ocean reanalysis) that gear towards climate research. NOAA GFDL first produced a decade-long reanalysis of the global ocean aiming to facilitate the study and prediction of seasonal-interannual variability (Rosati et al., 1995). A Simple Ocean Data Assimilation (SODA) system was developed (Carton et al., 2000) to produce a reanalysis of the (near) global ocean using historical data since 1960. The Estimating the Circulation and Climate of the Ocean (ECCO) Consortium, formed in 1998 as part of the WOCE synthesis activity, began to produce dynamically consistent estimates of the ocean state and surface fluxes (e.g., Stammer et al., 2002), satisfying the conservations laws described by the underlying models. The NOAA/GFDL effort (and the later NOAA/NCEP GODAE effort) has a tropical Pacific focus while SODA and ECCO have (near) global scope. There have been various efforts outside the US as well, including developments of reanalyses through SIDA and OFDA systems (See sub sections 2.1 and 2.2), for example, ECMWF (Balmaseda et al., 2013a), MERCATOR (Ferry et al., 2012) and CERFACS (Weaver et al., 2003) in France, INGV in Italy (Masina et al., 2011), and K-7 in Japan

(Masuda et al., 2003). Ocean state estimation products have been applied to various topics of oceanographic research, including sea level variability (e.g., Wunsch et al., 2007), water-mass pathways (e.g., Fukumori et al., 2004), the subtropical cells in the Pacific (e.g., Lee and Fukumori, 2003), mixed-layer heat balance (e.g., Kim et al., 2007), estimating surface fluxes and river runoff (e.g., Stammer et al., 2004), and interannual and decadal variability of the ocean heat content (e.g., Balmaseda et al., 2013b).

Recently, weakly coupled assimilation efforts have been made by NOAA/NCEP (the CFSR, Saha et al., 2010). These efforts assimilate atmospheric and oceanic data in the atmosphere and ocean models separately but use the coupled model to communicate the influence of the atmospheric and oceanic observations through the first-guess field instead of simultaneous assimilation of atmospheric and oceanic data in the coupled models. Nevertheless, the use of ocean and atmospheric data from in situ (e.g., the TAO/TRITON array) and satellite systems has improved some aspects of the estimation compared to the stand-alone atmospheric and ocean estimation. For example, Wen et al. (2012) showed that the weakly coupled assimilation in CFSR results in a more realistic representation of the atmospheric and oceanic signature of the tropical instability waves in the Pacific, which is a coupled ocean-atmosphere feature. A fully coupled ocean-atmosphere DA effort was made by Japan's K-7 group (Sugiura et al., 2008), showing an impact on the hindcast of the 1997-98 El Niño, and by NOAA/GFDL (ECDA, Zhang et al., 2007; Chang et al., 2013).

Long time series of physically well-balanced ocean states are also necessary for 'decadal' predictions which focus on time scales of several years to a few decades. Decadal prediction, in which a CGCM is initialized using observation-based information and integrated for a decade, is included in the CMIP5 protocol (Taylor et al., 2012) and the results are evaluated in IPCC 5th assessment report (AR5). The feasibility of decadal predictions over the North Atlantic, and the relationship with the Atlantic Meridional Overturning Circulation (AMOC) have been investigated (e.g., Dunstone and Smith, 2010; Pohlmann et al., 2013a). Successful decadal prediction for the Pacific Decadal Oscillation (PDO), and the recent hiatus in surface warming are also reported (e.g., Mochizuki et al., 2010; Guemas et al., 2013).

Relatively low resolution (around 1˚) is usually adopted for the ocean part of a CGCM used in decadal prediction systems. One strategy for initializing the ocean part of the CGCM is to force the ocean model variables toward independently analyzed ocean fields, including ocean reanalyses and other ocean state estimations, usually by nudging. Some systems also force atmospheric variables toward an atmospheric reanalysis. This strategy can be considered as a simple version of coupled data assimilation in the sense that coupled model dynamics is used to propagate the information of ocean and atmospheric data within the coupled model. In this strategy, the analysis fields are often used in the form of anomalies and are called "anomaly initialization method" compared to initialization using full fields. Feasibility of extending the SI forecasts, in which ocean observations are directly assimilated into the ocean part of the forecasting model by the SIDA system, to a decadal lead time is also explored in several studies (e.g., Doblas-Reyes et al., 2011), as well as initialization by a fully coupled ocean-atmosphere DA (e.g., Mochizuki, personal communication). Which strategy is most effective for decadal forecasts is currently a subject of active research (e.g., Magnusson et al., 2013; Smith et al., 2013). Although most decadal prediction systems are developed and exploited in research

mode, UKMO has implemented decadal predictions operationally using the system named “DePreSys” (Smith et al., 2007).

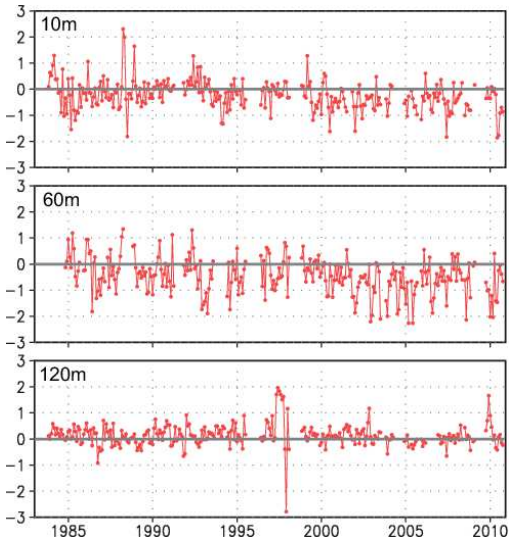

Figure 2.3 - Time series of the difference between temperature (°C) in the reanalysis using the JMA operational near-global ocean DA system and that observed by a TAO mooring at 10, 60 and 120 m depths at 0°-110°W between 1983-2010.

In situ temperature and salinity profile data and sea level anomalies derived from satellite altimetry are assimilated in most ocean state estimations, and also utilized directly or indirectly in most decadal predictions. These applications require particularly accurate observation data in order to detect small climate signals. Observing systems stably sustained for a long period are also desirable for long-term ocean state estimation and decadal prediction because changes in observing systems induce temporal discontinuities in the estimated ocean fields and discrepancies in decadal prediction skill between the periods before and after the change. TAO/TRITON mooring data provide valuable long time-series and an important constraint for those applications. The multiple-parameter measurements of oceanic and atmospheric variables by the tropical mooring arrays have been important in the evaluation of the ocean state estimation systems and the corresponding heat budget analysis. As the community is moving towards coupled data assimilation, the ocean and surface meteorology measurements from the tropical mooring array will become more and more important.

2.4 Use of TAO/TRITON for validation

TAO/TRITON data are also regularly used for calibration of DA systems, including SIDA and OFDA systems and those for climate research. Figure 2.3 shows an example of validation using TAO data for the temperature field in a reanalysis using the operational near-global DA system in JMA (Fujii et al., 2012). Figure 2.3 indicates that temperature at 60 m depth has relatively large errors compared with that at 10 and 120 m depth at 0°-110° W. It also indicates existence of a cold bias at 10 and 60 m depths after 2000. Appearance of this bias may be caused by a qualitative change of wind stress forcing fields provided by the atmospheric DA system. It also shows that the temperature at 120 m depth derivates considerably from the observation data

around the periods of the strong El Niños in 1997-1998 and 2009-2010, probably because the model cannot represent large variations associated with the events. This kind of information cannot be obtained without comparing the simulation fields with a long time observation record. The long time series provided by TAO/TRITON moorings are, thus, extremely valuable to validate long-term simulations such as ocean reanalysis which cover several decades and include interannual variability of the tropical ocean.

The TAO current data are also often exploited for validation although they are assimilated in few ocean DA systems. Figure 2.4 shows an example in MERCATOR. The representation of the tropical currents is a known weakness in the old global 1/4° system in MERCATOR. To assess the improvement of the currents, the zonal velocity profiles in the old and new systems are compared with the current measurements at TAO bouys. The figure demonstrates that the zonal currents are strengthened and agree with the TAO measurements much better in the new system. The TAO current data are, thus, valuable as independent data for validating ocean DA fields.

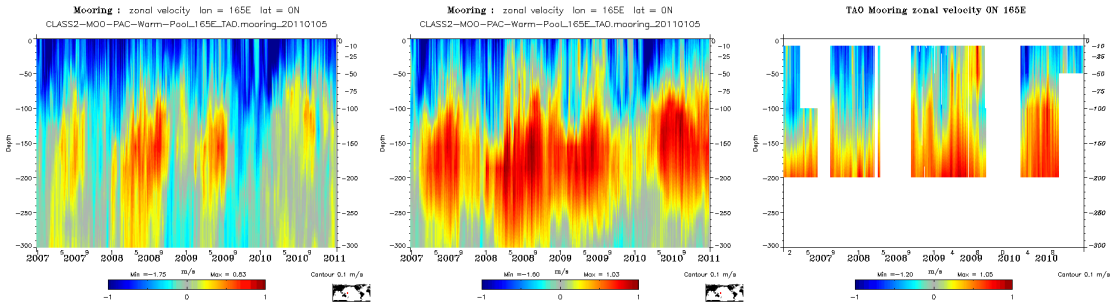

Figure 2.4 - Comparison of the evolution of the currents (ms^{-1}) at 0°-165°E for the old (left panel) and new (middle panel) global 1/4° system in MERCATOR with the TAO mooring data (right panel).

3. Observing system evaluations

3.1 Evaluation for seasonal-interannual forecasting

3.1.1 Observing system experiments at NOAA (NCEP and GFDL)

The Climate Programme Office of NOAA called for a coordinated OSE at NCEP and GFDL to assess impacts of TPOS for the S-I forecasting. At NCEP, the operational seasonal forecast model, referred to as Climate Forecast System version 2 (CFSv2) (Saha et al., 2013), is used. Although the operational version of CFSv2 is initialized by a weakly coupled ocean and atmosphere reanalysis (see sections 2.1 and 2.3), for the OSE project discussed here, this was not done and an ocean-alone data assimilation system, referred to as global ocean data assimilation system (GODAS; Beheringer and Xue, 2004) was used instead. In situ temperature and salinity profiles are assimilated in the reference run. The model SST is nudged strongly to the NOAA daily OI SST (Reynolds et al., 2007). At GFDL, an ensemble coupled data assimilation (ECDA) system (Zhang et al., 2007) was developed by applying an ensemble-based filtering algorithm to the GFDL's fully coupled climate model, CM2.1, which is one of two GFDL CMIP3 models (Delworth et al., 2006). In situ temperature and salinity profiles, winds,

sea level pressure and temperature data from the NCEP reanalysis 2, and the weekly OISST are assimilated in the reference run.

To assess the relative roles of the TAO/TRITON and Argo data in constraining the upper ocean thermal structure and improving ENSO forecasts, four OSE runs were performed, which assimilated (a) no ocean profiles (referred to as CTL), (b) all ocean profiles (the reference runs; referred to as ALL), (c) all ocean profiles except the mooring profiles (referred to as noMoor), and (d) all except the Argo profiles (referred to as noArgo). Since SSH observations are not assimilated in any OSE run, we use it to validate the model SSH. The impacts of ocean observations on SSH anomalies are quantified using RMSE against altimetry data. Figure 5 indicates that the impacts of moorings (red bar) are generally weak, and they improve RMSE by 10% in NINO3 of GODAS and by 3-5% in the equatorial indices of ECDA. In contrast, the impacts of Argo (green bar) are much larger. They improve RMSE by 15-19% in GODAS and 8-11% in ECDA. In off equatorial regions, the impacts of Argo are strongly positive. The impacts of all in situ profiles (blue bar) are strongly positive in all areas. The results suggest that in situ ocean observations are absolutely critical in constraining model errors in the whole tropical Pacific, and it is mostly critical in the eastern Pacific (NINO3 region). RMSE in NINO3 is reduced by 37% in GODAS and 60% in ECDA.

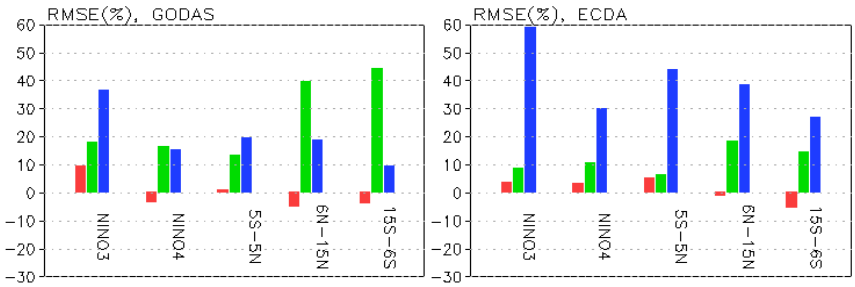

Figure 3.1 - Impacts on RMSE of SSH anomalies in 2004-2010. Shown are RMSE difference normalized by RMSE of ALL for GODAS (left) and ECDA (right). Red: ALL minus noMoor (impacts of Mooring bouys); Green: ALL minus noArgo (impacts of Argo); Blue: ALL minus CTL (impacts of all in situ profiles).

In order to evaluate the impacts of in situ observations on the skill of hindcasts, hindcast experiments were initialized from the four OSEs around January 1, April 1, July 1 and October 1 during 2004-2011. From each start time, an ensemble of 6 (10) coupled forecasts with perturbed initial conditions is integrated up to 12 months ahead using CFSv2 (CM2.1). The monthly forecast SSTs are first smoothed with a 3-month-running mean. SST anomalies are then derived by removing the model climatology calculated separately for each initial month and lead month in 2004-2011. The hindcast skill is measured by RMSE against the weekly OI SSTs that are calculated for all initial months and all years, but for lead months from 0 to 4 (L0-L4) and from 5 to 9 (L5-L9) separately.

The impacts of TAO/TRITON on seasonal forecast skill of equatorial Pacific SST are consistently positive in both models (red bars in Figure 6). The RMSE is reduced by 10-25% in equatorial SST indices (NINO3, NINO4, NINO3.4 and TPAC) in both models. Argo data are beneficial too, but the amplitude of RMSE reduction is generally smaller than for TAO/TRITON. The moorings and Argo have the largest positive impacts on the eastern tropical Indian Ocean

(SETIO) SST in both models. The Argo has the largest positive impacts on the tropical Atlantic SST.

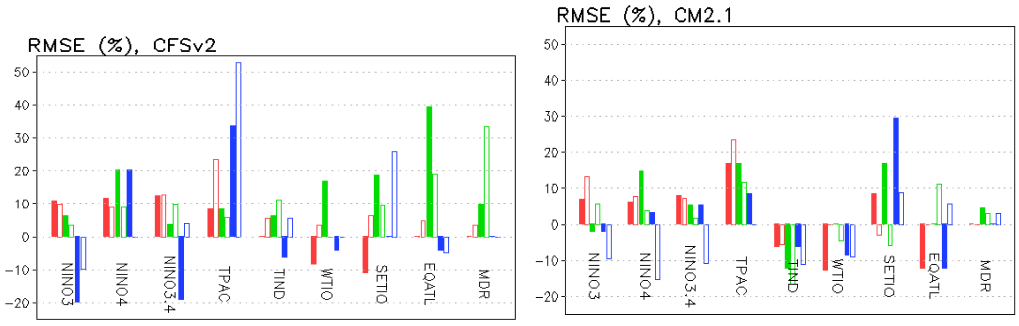

Figure 3.2 - Hindcast skill of RMSE difference normalized by RMSE of ALL for CFSv2 (left) and CM2.1 (right) for various SST indices. Red bar: ALL minus noMoor; Green bar: ALL minus noArgo; Blue bar: ALL minus CTL. Filled (unfilled) bars are skill for L0-L4 (L5-L9). The RMSE are calculated with seasonal mean SST anomalies between model and observations for all initial months, all years (2004-2011) and lead month L0-L4 and L5-L9 separately. RMSEs are calculated for NINO3 (5^{o}S-5^{o}N, 150^{-}90^{o}W), NINO4 (5^{o}S-5^{o} N, 160^{o} E-150^{o} W), and NINO3.4 (5^{o} S-5^{o} N, 170-120^{o} W) regions, tropical Pacific (TPAC; 20^{o} S-20^{o} N, 120^{o} E-80^{o} W), tropical Indian (TIND; 20^{o}S-20^{o} N, 30-120^{o} E), western tropical Indian (WTIO; 10^{o} S-10^{o} N, 50-70^{o}E), and south eastern tropical Indian (SETIO; 10^{o} S-0^{o}, 90-110^{o} E) Oceans, equatorial Atlantic (EQATL; 5^{o} S-5^{o} N, 70^{o} W-30^{o} E), and Main Developing Region (MDR; 10-20^{o}N, 80-20^{o}W).

Model drift is still very large (not shown), which may diminish the benefits of all in situ profiles in some cases (blue bars). For CFSv2, the model drift varies considerably with initial times, so it is hard to remove model systematic bias. For CM2.1, both the model drift and the impacts of in situ profiles on hindcast skill are strong functions of initial months - impacts can be positive, neutral or negative depending on initial months. We conclude that model drifts are still a big obstacle for models to fully utilize the benefits from all in situ profiles.

3.1.2 Observing system experiments at JMA/MRI

JMA/MRI also conducted a series of OSEs to evaluate the relative impact of Argo floats and TAO/TRITON buoys on the ocean DA fields and ENSO forecasts using an operational seasonal forecasting system (Fujii et al., 2011 and 2014). The system adopted the nearly-global ocean DA system, MOVE-G (Fujii et al., 2012), for the ocean initialization, in which a multivariate three-dimensional variational analysis scheme, MOVE, is employed to assimilate satellite SSH, gridded SST, and in situ temperature and salinity profiles, including data form Argo, XBT, and moorings.

Impacts of TAO/TRITON and Argo data on the ocean heat content in the equatorial Pacific in the DA system is quantified using seven OSE runs, namely, noArgo (the same as in 3.1.1), Argo20, Argo40, Argo60, Argo80 (20, 40, 60, 80% of Argo data and all available data from other than Argo are assimilated), noTTA80 (TAO/TRITON data and 20% of Argo data are withheld), and TTeqA80 (TAO/TRITON data out of 2.5˚S-2.5˚N and 20% of Argo data are withheld). The accuracy of these runs is evaluated by the RMSE against the 20% of Argo float profiles that are withheld from all OSE runs (Figure 3.3). This figure clearly demonstrated that the impact of Argo data on salinity is larger than that on temperature. The impacts of Argo are largest in the NINO3

region and smallest in the TRITON region. It also indicates that the accuracy monotonically improves with increasing number of assimilated Argo floats from 0% to 80% for both temperature and salinity in NINO3 and NINO4 regions, indicating that any further increase in the number of Argo floats has the potential to further improve the accuracy of the DA system there. The accuracy of the run without TAO/TRITON (noTTA80) is roughly similar to the ARGO40 run in NINO3 and NINO4 regions, implying impacts of TAO/TRITON is similar to 40% of Argo data. Accuracy of the salinity field is not degraded even if data from extra-equatorial buoys outside of 2.5˚S-2.5˚N are withheld (TTeqA80) in the 2 regions, although those data have some impacts on temperature there. The impact of TAO/TRITON data is as large as (larger than) that of 80% of Argo data in the TRITON region, and the data from extra-equatorial buoys also have some impact.

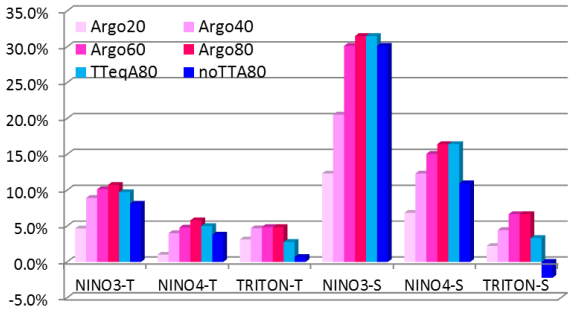

Figure 3.3 - Reduction of the RMSE of the 0-300m averaged temperature (T) and salinity (S) averaged in NINO3, NINO4, and TRITON (5˚S-5˚N, 120-160˚E) regions in OSE experiments from the RMSE of noArgo normalized by the RMSE of noArgo. The RMSEs are calculated for the period of 2004-2010.

We also quantified the impact of TAO/TRITON and Argo data on the forecasts of NINO3 and NINO4 SST indices using four OSE runs, namely, ALL, noArgo (the same as in 3.1.1), noTT (TAO/TRITON data are withheld), and TTeq (TAO/TRITON data outside of 2.5˚S-2.5˚N are withheld). We performed 13-month, 11-member ensemble hindcasts from each OSE run using the coupled model. The hindcasts were started from the end of January, April, July, and October in 2004-2011. TAO/TRITON data reduces the RMSE of the NINO3 and NINO4 indices for lead month from 1 to 4 (L1-4) by 3.5% and 5.8%, respectively (Figure 3.4).

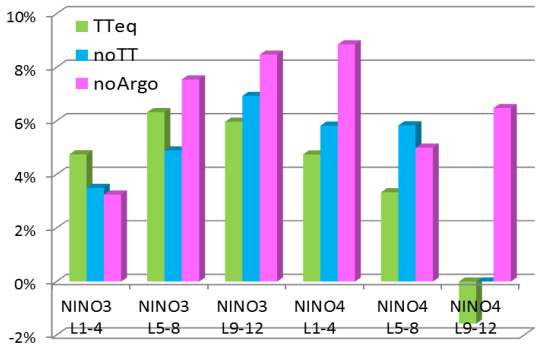

Figure 3.4 - Increase of the RMSE of the NINO3 and NINO4 SST indices in the hindcasts from TTeq, noTT, and noArgo from the RMSE in the hindcasts from ALL normalized by the RMSE in the hindcasts from ALL for L1-4m L5-8, and L9-12. Forecast biases are estimated for each lead month and for each OSE separately, and removed from the forecasted values.

The impact on NINO3 increases for lead time month from 5 to 8 (L5-8) and from 9 to 12 (L9-12). In contrast, the impact on NINO4 is not changed for L5-8 and disappears for L9-12. Assimilating equatorial buoy data (2.5˚S-2.5˚N) alone (TTeq) increases the RMSEs by 3-6% compared to ALL, except for NINO4 for L9-12. It should be noted that the RMSEs in TTeq are larger than noTT for NINO3 for L1-4 and L5-8, which may indicate the importance of assimilating equatorial and extraequatorial (outside of 2.5˚S-2.5˚N) buoys simultaneously, especially for relatively short lead time forecasts of the NINO3 index. Impacts of Argo are larger than those of TAO/TRITON on both NINO3 and NINO4 for all lead times except for NINO3 indices for L1-4 and NINO4 for L5-8. The impact of Argo on NINO3 is enhanced with increasing lead time, but for NINO4 the impact is not monotonic being smaller for L5-8 than for shorter and longer lead times.

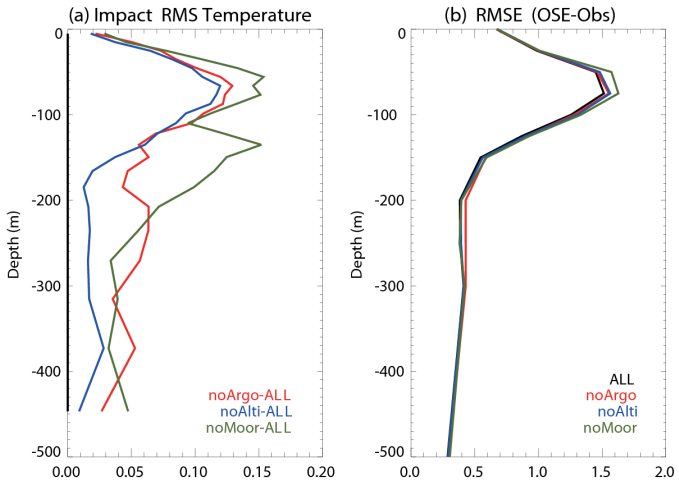

Figure 3.5 - Profiles of the (a) RMSD for temperature in the equatorial Pacific between OSEs and (b) the RMSE for temperature in the eastern equatorial Pacific (90-130˚W, 5˚S-5˚N), computed by comparing the temperature in each OSE with all in situ observations.

3.1.3 Observing system experiments at ECMWF

A series of OSEs has been performed using ECMWF's ocean reanalysis ORAS4 (Balmaseda et al., 2013a), which is used to initialize the operational monthly and seasonal forecasts. Here, we introduce the results of four OSE runs, i.e., ALL, noMoor, noArgo (the same as in 3.1.1), and noAlti (SSH data are withheld). Figure 3.5 presents the profile of the RMSD between each OSE and ALL and the profile of the RMSD between all OSEs and the in situ observations.

The former represents the data impact on the analysis; the latter represent the data impact on the error. We find that in the eastern tropical Pacific, whenever any data type is withheld, the fit to in situ temperature profiles degrades. This indicates that all data types contribute some unique information to the data assimilating system. It should, however, be noted that all OSE runs adopt a bias correction scheme, which applies correction to temperature, salinity, and in the equatorial wave-guide, corrections to the pressure gradient. The mean seasonal cycle of the bias correction is estimated a-priori from a previous data assimilation experiment, and therefore implicitly includes information from all observing systems. A supplemental run assimilating all

data without the bias correction indicated that the bias correction has the largest impact, illustrating the role of the observations in correcting the mean.

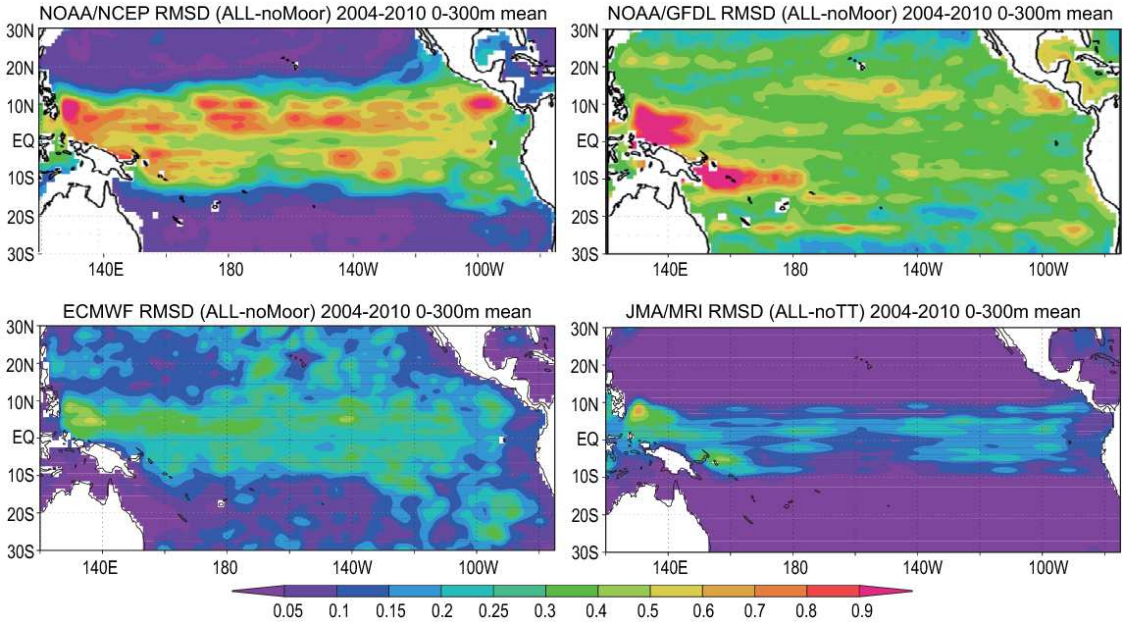

Figure 3.6 - 0-300 m averaged RMSD of temperature (˚C) between ALL and noMoor/noTT in 2004-2011 (2004-2010) for NCEP and GFDL (ECMWF and JMA/MRI).

Although the initial conditions from ALL, noArgo, noAltim and noMoor have been used to initialize seasonal forecasts, using the current operational ECMWF seasonal forecasting system S4, it was not possible to measure a significant contribution of individual observing systems. This is contrary to the results reported by Balmaseda and Anderson, (2009), who used a similar methodology to evaluate the impact of the observing system in the then ECMWF operational seasonal forecast system S3. They found that all the observing systems contributed to the skill of ENSO prediction. The reasons for the lack of impact are under investigation. Possibilities are i) too limited sample in a forecasting system with large ensemble spread; ii) the impact of the observing system in the mean state through the bias correction is not accounted for.

3.1.4 Observing system experiments at ECMWF

Results of OSEs depend on the quality and characteristics of the ocean DA systems used as well as the forecasting model. Therefore it is desirable to examine the consistency among the results of OSEs in different centers. For this purpose, an evaluation of OSE results in NOAA (NCEP and GFDL), JMA/MRI, and ECMWF has been initiated using common metrics. Figure 3.6 shows an example of the intercomparison. The averaged RMSD of temperature between ALL and noMoor/noTT in 0-300 m is relatively large in the far western equatorial Pacific, and around 8˚S-160˚E. These are probably regions where the model accuracy is relatively low. The differences are also large in the zonal band along 5˚ N particularly for the OSEs in NCEP and JMA/MRI, probably due to energetic eddy activity. Through this initiative we aim to estimate some general impacts of the observing system which do not depend strongly on the DA systems used and are thus likely to be more robust.

3.2 Evaluation for short-to-medium range ocean forecasting

3.2.1 Near-real time OSE (GODAE Ocean View OSEval Task Team Initiative)

Under GODAE Ocean View, the Observing System Evaluation (OSEval) Task Team has advocated the development and application of tools and techniques that quantify the impact of ocean observations on OFDA systems. It has also encouraged studies that evaluate observational impacts on SIDA systems and ocean state estimations for climate research. The team also intends to issue observation impact statements that provide feedback and requirements to observation agencies through evidence of the impacts of the observations, mainly on operational systems.

In order to achieve routine monitoring of current observing systems, the OSEval Task Team plan to set up Near-Real Time (NRT) OSEs. NRT OSEs consist of the nominal operational forecast system and a second system where a single observation component of the observing system is withheld. By comparing the results of the run excluding a particular observation with the operational run, the impact of the withheld observation type on the forecast system is assessed. NRT OSE experiments were performed in 2011 with the UK Met Office's operational ocean forecasting system (Lea et al., 2013).

Following this GODAE Ocean View initiative, NRT OSEs were conducted over successive months of the 2013 year by Mercator Ocean. The operational 1/4° global ocean system (Lellouche et al., 2013) is setup for those experiments. During March 2013, TAO/TRITON/RAMA temperature and salinity observations are withheld from the analysis. However, in 2013, some of the TAO mooring observations are not available. The operational ocean analysis and forecasting system used for those experiments is based on a 1/4° global ocean model configuration. The assimilated observations are satellite SSH data, the AVHRR SST maps and the in situ temperature and salinity profiles. No current data are assimilated. A 3D-Var T/S bias correction computed with in situ model-observation misfits available 3 months prior to the analysis is applied below the thermocline. The effect of withholding a part of the in situ data set will then be underestimated for simulations shorter than 3 months due to the memory of this bias correction.

Different observation based statistics and ocean state quantities are compared between the 2 simulations to evaluate the impact of assimilating data from the tropical moorings. Model observation error statistics are computed over the month for both experiments. TAO/TRITON and RAMA observation misfits are included. Figure 3.7 (left) shows that significant differences are found for the mean and RMS temperature misfits in the NINO3 region at the thermocline depth. The higher level of error, RMS or mean, is clearly at the thermocline depth, which is shallower when going eastward. The assimilation of the TAO observation reduces the RMS and means of temperature errors. Under the thermocline, the bias correction is still active and takes into account innovations from the previous 2 months.

Figure 3.7 (right) shows the temperature differences at 100 m depth on the last day of the 1-month experiments. Important differences are visible at and around the moorings and can reach 2°C. Salinity differences are found within the thermocline and can reach 0.5 PSU at the surface (not shown). After one month, changes have already propagated away from the mooring points

through ocean tropical dynamics. The SST data probably prevent larger differences in temperature close to the surface; the surface salinity is much less constrained by data assimilation. The number of salinity data is also much smaller than the temperature data from TAO moorings. These results are generally consistent with Lea et al. (2013).

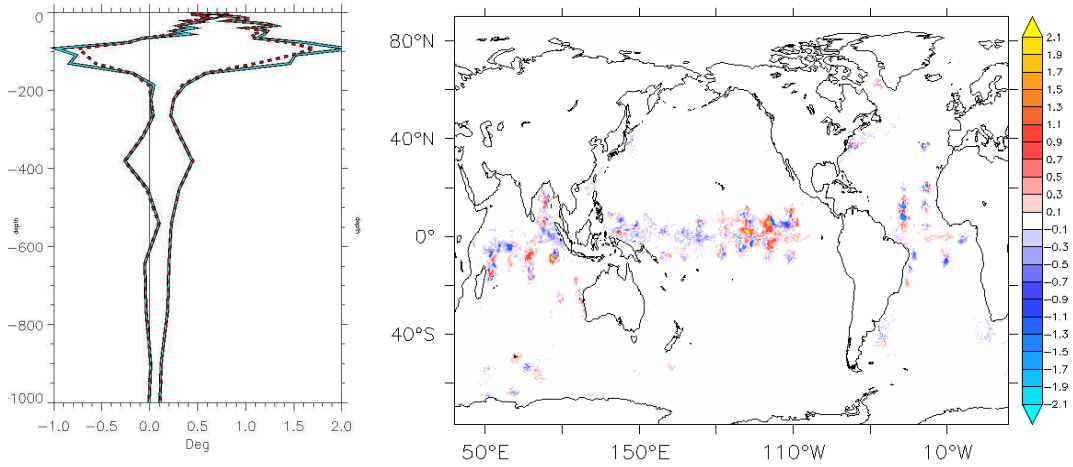

Figure 3.7 – (left) Mean and RMS observation-analysis error to in situ temperature observations in the Nino 3 region with the TAO assimilated in red, without in blue; (right) Temperature differences on the last day of the 1-month experiments with and without TAO observations assimilated at 100 m depth.

Further investigation and longer simulations will be required to fully assess the impact on the analysis and forecast of the 1/4° global ocean of the assimilation of the temperature and salinity data from the tropical mooring arrays Because TAO data return was already low in 2011, a year prior to 2011 should be chosen to have a higher return data rate. The results highly depend on the assimilation system, the physical model and observation error a priori specification. Those quantities are not always well known. One month does not allow a full assessment of the observation impact but does give some indication.

3.2.2 Evaluation of forecast sensitivities using an adjoint model

Assessment of the contribution of each observation assimilated by the Navy Coupled Ocean Data Assimilation (NCODA) 3DVAR (Cummings and Smedstad, 2013) on the forecast performance of global Hybrid Coordinate Ocean Model (HYCOM; equatorial resolution of ~1/12º) is achieved by the adjoint-based observation sensitivity technique (Langland and Baker 2004). The technique computes the variation in a measure of the forecast error due to the assimilated data through the adjoint model. Results presented here are from the Pacific domain of global HYCOM cycling with NCODA 3DVAR for the 16 September to 30 November 2012 time period.

Figure 3.8 shows the geographic variation of the impacts of assimilating temperature and salinity profile observation data types on reducing HYCOM 48-hour forecast error. Note that profile levels are treated as independent observations in the assimilation. Figure 3.8 indicates that the majority of temperature profile observations assimilated show beneficial impacts, although non-beneficial impacts are seen in some Argo. Assimilation of salinity observations,

however, is always beneficial. Figure 3.8 presents the summed observation impacts for the different profile observing systems.

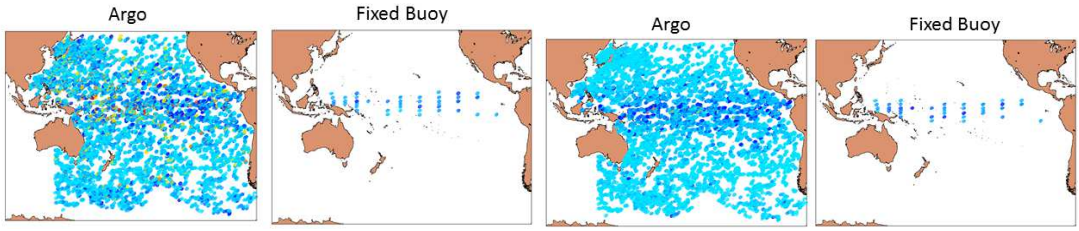

Figure 3.8 - Observation impact of temperature (left 2 panels) and salinity (right 2 panels) observations assimilated in global HYCOM on 48 hours forecasts. Magnitude of the forecast error reduction (increase) from assimilation of the observation is shown as a negative (positive) value. Each point represents the combined impacts of all depth level observations in the vertical profile. Units are °C and PSU.

The summations have been normalized by the number of observations to facilitate the intercomparison since temperature observations are dominated by synthetic temperature profiles derived from satellite SSH measurements and salinity observations are dominated by Argo. The results show that impacts of temperature and salinity from all observing systems are beneficial, with the most beneficial observing system assimilated being the tropical fixed moorings. Figure 3.9 compares Argo and the fixed buoy arrays as a function of 5° latitude bands on a per observation basis. The greatest impact of Argo is in the tropics (±10° latitude), with impact magnitudes of Argo temperature and salinity similar to those of the tropical moorings at those latitudes.

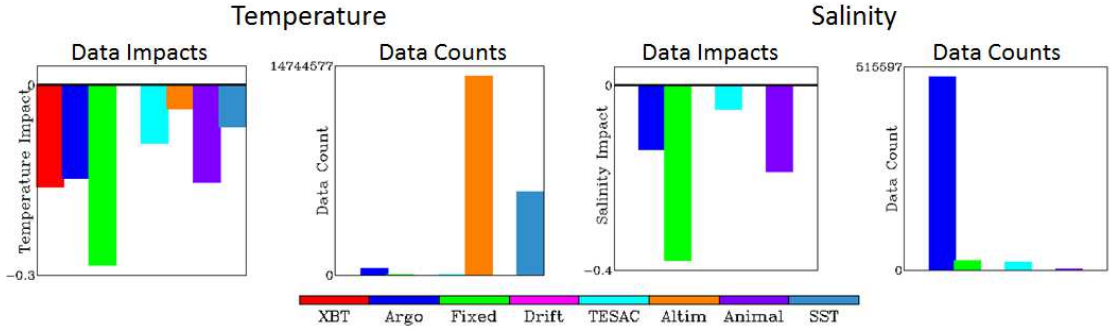

Figure 3.9 - Temperature (°C) and salinity (PSU) observation impacts on 48 hours forecasts normalized by the number of observations and partitioned by observing system. Includes all observations assimilated, i.e., XBT, Argo, Fixed Buoy (Fixed), Drifter (Drift), TESAC, synthetic temperature profiles derived from satellite SSH, Animal sensor, and satellite SST retrievals. Negative data impact values indicate beneficial observing systems.

It is shown that the greatest data impacts for reducing forecast error in the Pacific basin of global HYCOM are for observations in the tropics. This result is an indication that HYCOM model errors are greatest in the tropical Pacific and continued routine observing is needed there to adequately constrain the model. It is shown that on a per observation basis the impact of Argo and tropical moorings are equivalent at low latitudes. Argo has the advantage over the moorings of providing improved vertical sampling. An advantage for the moorings is much

higher frequency observing than Argo. Daily profiles are available from the moorings, which matches the 24 hour HYCOM assimilation update cycle interval. The two observing systems are thus complementary.

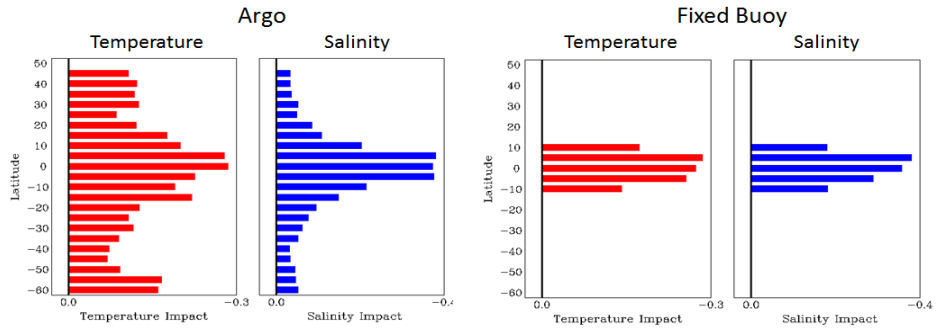

Figure 3.10 - Per observation data impacts on 48 hours forecasts of Argo and fixed buoy arrays for temperature (°C) and salinity (PSU) and partitioned by 5° latitude bands.

3.3 Evaluation for climate research

3.3.1 Evaluation for ocean state estimation

Beside the fact that most of SIDA and OFDA are applicable to some ocean state estimation for climate research, we here focus on the 4DVAR systems that enable us to estimate a dynamically consistent ocean state, in particular, over a long-term (several months to several decades) in a single optimization (e.g., Stammer et al., 2002). The accuracy of such estimation at a specific time depends on various aspects of observed information, not only of that time but also of the past and future time within the assumed assimilation time-window.

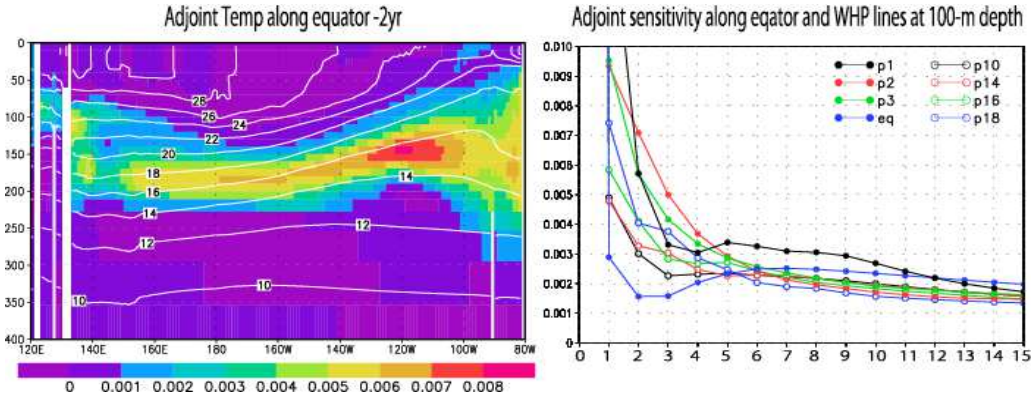

Figure 3.11 – (left) Sensitivity of changes (units in K) in water temperature at the WHP lines at 100-m depth in the Pacific Ocean in the vertical section along 0.5°N at –2 years. Temperature (˚C; white color contours) of the background ocean state is superimposed; (right) Temporal evolution of the sensitivity averaged for each WHP hydrographic line at 100 m depth normalized to the initial value at year 0. The horizontal axis denotes the retrospective period from 0 to –15 years in reverse chronological order.

A data synthesis system applying the smoothing scheme, in particular, requires sustainable monitoring during the time-window in order to obtain a suitable ocean climate state. Here, we show an application of adjoint sensitivity analysis (e.g., Fukumori et al., 2004) to ocean

observing system evaluation (e.g., Köhl and Stammer, 2004).

A 4DVAR ocean-state estimation system with 1°×1° resolution, developed as a part of the JAMSTEC–Kyoto University collaborative programme (the K7 consortium, Masuda et al., 2013), is used to evaluate an ocean observing system for improved long-term ocean-state estimation (Masuda et al., 2014). The adjoint model in the system is applied to identify the sensitivity of temperature at 100 m depth located along the equator and some of the World Ocean Circulation Experiment Hydrographic Programme (WHP) lines in the Pacific Basin to the retrospective ocean state estimation. The obtained sensitivity values show possible contributions of the hydrographic observations along the lines to the retrospective state estimation. The sensitivity thus corresponds to the possible change in temperature taking place at the lines at an allocated model time (defined as year zero) when temperature changes at an arbitrary grid point at an arbitrary time in the past.

Figure 3.11 (left) shows a vertical cross section of the sensitivity in the equatorial region at –2 years. It is apparent that the sensitivity values of 100 m temperature changes are almost lost in the upper 100 m and mostly distributed in the lower part of the thermocline around 150 m. This is because mixed layer dynamics dominate the changes in temperature above 100 m on time-scales less than 2 years in this central region. This implies that sustainable observations at 100 m along the equator could be required for retrospective ocean-state reconstruction for relatively short-term climate change, and that a hydrographic observation at 100 m can contribute to better representation of the thermocline if a 2-year period is chosen for the assimilation window.

Here we assess a rate of decrease in the sensitivity values to make best use of repeat surveys. Figure 3.11 (right) shows the sensitivity values averaged within each hydrographic line at 100 m. These values show the impact of assumed observations at year zero on the retrospective ocean state estimation within the lines at the depth when tracing back 15 years. The rate of decrease of the sensitivity during the retrospective period largely depends on the geographical location. The rates show that equatorial ocean is a key region to be intensively monitored since the local memory of the ocean properties is shorter than that in other regions. This kind of analysis enables us to provide unique information on the effectiveness of an ocean observing system on the retrospective ocean-state estimation although the detailed values of estimated sensitivity depend on the model platform.

In the real ocean, meso-scale eddies and various small-scale fluctuations sometimes play a role in determining ocean properties. These influences can be evaluated by applying the adjoint approach to a higher resolution model (e.g., Hoteit et al., 2010) or through ensemble sensitivity analysis (e.g., Torn and Hakim, 2008). A regional assimilation effort at SIO also aims to quantify the impact of moored observations of temperature, salinity, and velocity under the influence of meso-scale eddies using the ECCO adjoint (4DVAR) assimilation system (resolution 1/3 to 1/6˚).

3.3.2 Evaluation for decadal predictions

Impacts of TPOS on decadal predictions have not been substantially evaluated yet since it is a relatively new science field. However, Doblas-Reyes et al. (2011) investigated impacts of ocean observation data on decadal predictions using a version of the ECMWF coupled forecast

system. They performed three decadal hindcast experiments, namely XBT-C, NoOcObs (with and without initialization using ocean observation data), and Assim (Same as XBT-C but the correction of XBT bias is not applied).

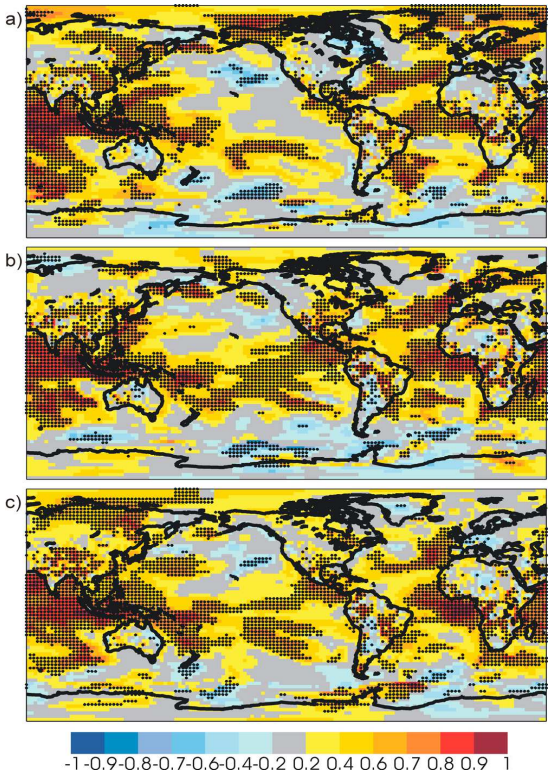

Figure 3.12 - Ensemble mean correlation for near-surface air temperature with respect to the GHCN/ERSST/GISS data set for winter (December to February) over the forecasts period 2 to 5 years of the (a) NoOcObs, (b) XBT-C, (c) Assim experiments. Three member ensemble reforecasts for the period 1960-2005 have been used. The black dots depict the grid points where the correlation is significantly different from zero with 95% confidence (adjusted from Doblas-Reyes et al., 2011).

Figure 3.12 shows improvement of prediction skill for 2 to 5 year lead time over the tropical Pacific by assimilating ocean observation data, which implies the importance of TPOS for decadal prediction. Furthermore, a substantial improvement was obtained by correcting XBT bias. This result indicates that the accuracy of ocean observation data is a crucial factor for decadal prediction.

More recently, Polhmann et al. (2013b) demonstrated improved decadal prediction skill over the equatorial Pacific in the first 3-5 years of the prediction by using ocean and atmosphere initialization, which is consistent with the result of Doblas-Reyes et al. (2011), introduced above.

4. Summary

This white paper reviewed the current status and achievements of ocean DA systems and discussed their requirements for the tropical Pacific observing system including the TAO/TRITON array and Argo floats. It also summarizes past and current studies to evaluate impacts of those observation data.

Temperature data from TAO/TRITON array are assimilated in most ocean DA systems, and essential for constraining the ocean heat content, stratification and circulation in the tropics. The intercomparison of the temperature fields along the equator among the DA systems for Seasonal-to-Interannual (S-I) forecasting in NCEP, JMA, ECMWF, ABoM reveals that the recent decrease of TAO/TRITON data severely affects the accuracies of the analyzed fields making it more difficult to issue reliable forecast statements. TAO/TRITON data are also essential for validating ocean DA products.

Observing system evaluation studies always have their limitations. For example, impacts of observing system evaluated through OSEs depend strongly on the quality and characteristics of both the ocean DA systems and the forecasting models used. In particular, current coupled models still have large errors and biases, and there is, thus, a high possibility that observation impacts are severely diminished due to them. It should be also noted that OSE and other observing system evaluation studies can evaluate only the impacts of data that are assimilated in the DA system. Some of the surface meteorology and current meter data from TAO/TRITON moorings are not assimilated, but withheld for evaluation and validation. Some systems do not assimilate salinity data. As such, evaluation through OSEs in which temperature (and salinity) data are withheld will under-estimate the impact of the TAO/TRITON array.

Table 4.1 – Requirements of SIDA systems for TPOS in 2020.

Variable	Accuracy	Vertical	Horizontal	Temporal
SST	0.05K	-	Global/ 0.25˚	more than 20 years/ daily
Ocean Temperature	0.05K	0-250m/ 10m 250-1000m/ 50m	Tropics/ 2˚×10 as the baseline	more than 20 years/ 1-5-daily
SSS	0.1PSU	-	Global/ 2˚	more than 20 years/ 10-daily
Salinity	0.02PSU	0-250m/ 10m 250-1000m/ 50m	Tropics/ 2˚×10˚ as the baseline	more than 20 years/ 1-5-daily
SSH	3cm	-	Global/ 1˚	more than 20 years/ 10-daily
Currents	2cm/s	0-250m/ 20m 250-1000m/ 100m	Tropics/ 5˚×20˚	more than 20 years/ 10-daily

In spite of the limitations above, positive impacts of TAO/TRITON are evaluated in most studies introduced in this paper. Although the evaluated impacts depend on the studies, the impacts are

generally around the same level with, and sometimes larger than those of Argo in the equatorial Pacific. Several studies also indicate that profiles from Argo floats cannot compensate the loss of TAO/TRITON data. We, thus, assume that a further loss of data will lead to a degradation of the forecast skill in the tropical Pacific and will have a detrimental impact on many applications based on ocean DA systems.

Table 4.2 – Requirements of OFDA systems for TPOS in 2020.

Variable	Accuracy	Vertical	Horizontal	Temporal
SST	0.05K	-	Global/ 0.1˚	more than 5 years/ daily
Ocean Temperature	0.05K	0-250m/ 10m 250-1000m/ 50m	Global/ 2˚	more than 5 years/ daily
SSS	0.1PSU	-	Global/ 1˚	more than 5 years/ daily
Salinity	0.02PSU	0-250m/ 10m 250-1000m/ 50m	Global/ 2˚	more than 5 years/ daily
SSH	3cm	-	Global/ 0.1˚	more than 5 years/ daily
Currents	2cm/s	0-250m/ 20m 250-1000m/ 100m	several important points (including western boundary currents)	more than 5 years/ daily

We are assured that continued deployment and maintenance of the tropical mooring arrays in all of the ocean basins is highly desirable. However, given funding constraints, a re-prioritization of the design of the mooring arrays might be appropriate and timely, taking into account the complementarity of other observing systems such as Argo. This effort should be aided by an internationally coordinated multi-model effort in (tropical) observing system evaluation and design.

The basic requirements of ocean DA systems for TPOS in 2020 are summarized in Tables 4.1-4.3. The recent crisis of the TAO array provides the rationale for commencing new studies in evaluating the tropical Pacific observing system. Follow-up of these studies will be carried out by the GODAE Ocean View OSEval task team.

Table 4.3 – Requirements of DA systems for ocean state estimations and decadal predictions for TPOS in 2020.

Variable	Accuracy	Vertical	Horizontal	Temporal
SST	0.05K	-	Global/ 1˚	more than 20 years/ 10-daily
Ocean Temperature	0.002K	0-250m/ 10m 250-1000m/ 50m 1000-bottom/ 250m	Global/ 2˚	more than 20 years/ 10-daily
SSS	0.1PSU	-	Global/ 2˚	more than 20 years/ 10-daily
Salinity	0.002PSU	0-250m/ 10m 250-1000m/ 50m 1000-bottom/ 250m	Global/ 1˚	more than 20 years/ 10-daily
SSH	3cm	-	Global/ 1˚	more than 20 years/ 10-daily
Currents	2cm/s	0-250m/ 20m 250-1000m/ 100m 1000-bottom/500m	several important points (including western boundary currents)	more than 20 years/ 10-daily

References

Balmaseda, M. A., and Anderson, D.L.T. (2009): Impact of initialization strategies and observations on seasonal forecast skill. Geophy. Res. Lett. 36, L01701, (doi:10.1029/2008GL035561).

Balmaseda, M. A., Mogensen, K., and Weaver, A.T. (2013a): Evaluation of the ECMWF ocean reanalysis system ORAS4. Q. J. R. Meteorol. Soc., 139, pp. 1132-1161.

Balmaseda, A.B., Trenberth, K.E., and Källén, E. (2013b): Distinctive climate signals in reanalysis of global ocean heat content. Geophys. Res. Lett., 40, pp. 1754-1759. (doi:10.1002/grl.50382).

Behringer, D., and Xue, Y. (2004): Evaluation of the global ocean data assimilation system at NCEP: The Pacific Ocean. Preprints, Eighth Symposium on Integrated Observing and Assimilation System for Atmosphere, Ocean, and Land Surface, Seattle, WA, Amer. Meteor. Soc. 2.3. Available online at https://ams.confex.com/ams/84Annual/webprogramme/Paper70720.html.

Blockley, E. W., Martin , M.J., Guiavarc'h , C., Lea, D.J., McLaren , A.J., Mirouze, I., Peterson, A.K., Ryan, A.G., Sellar, A., Storkey, D., Waters, J., and While, J. (2013): Recent development of the Met Office operational ocean forecasting system: an overview and assessment of the new Global FOAM forecasts. Submitted to GMD.

Brassington, G. B. **(**2013): Multicycle ensemble forecasting of sea surface temperature, Geophys. Res. Lett., 40, (doi:10.1002/2013GL057752).

Brassington, G. B., Freeman, J., Huang, X., Pugh, T., Oke, P.R., Sandery, P.A., Taylor, A., Andreu-Burillo, I., Schiller, A., Griffin, D.A., Fiedler, R., Mansbridge, J., Beggs, H., and Spillman, C.M. (2012): Ocean Model, Analysis and Prediction System (OceanMAPS): version 2, CAWCR Technical Report, No. 052, pp. 110.

Brassington, G. B., Fujii, Y., Schiller, A., and Oke, P.R. (2014): Assessing the impact of the ocean observing system in the western tropical Pacific Ocean based on a spectral analysis of a multicycle prediction system, GRL (in prep).

Carton, J. A., Chepurin, G., and Cao, X. (2000): A simple ocean data assimilation analysis of the global upper ocea 1950-95. Part I: Methodology. J. Phys. Oceanogr. 30, pp. 294-309.

Chang, Y.-S., Zhang, S., Rosati, A., Delworth, T.L., and Stern, W.F. (2013). An assessment of oceanic variability for 1960-2010 from the GFDL ensemble coupled data assimilation. Clim. Dyn., 40, pp. 775–803, (doi:10.1007/s00382-012-1412-2).

Cummings, J. A., and Smedstad, O.M. (2013): Variational Data Assimilation for the Global Ocean. Chapter 13, pp. 303-343. In, *Data Assimilation for Atmospheric, Oceanic & Hydrologic Applications (Vol. II).* S. Park and L. Xu (eds). (doi:10.1007/978-3-642-35088-713), Springer-Verlag, Berlin, Heidelberg.

Delworth, T. L., et al. (2006): GFDL's CM2 global coupled climate models. part I: Formulation and simulation characteristics. J. Clim., 19, pp. 643–674.

Doblas-Reyes, F. J., Balmaseda, M.A., Weisheimer, A., and Palmer, T.N. (2011): Decadal climate prediction with the European Center for Medium-Range Weather Forecasts coupled forecast system: Impacts of ocean observations. J. Geophys. Res., 116, D19111, (doi:10.1029/2010JD015394).

Dunstone, N. J., and Smith, D.M. (2010): Impact of atmosphere and sub-surface ocean data on decadal climate prediction. Geophys. Res. Lett., 37, L02709, (doi:10.1029/2009GL041609).

Ferry, N., Parent, L., Garric, G., Bricaud, C., Testut, C.E., Le Galloudec, O., Lellouche, J.M., Drevillon, M., Greiner, E., Barnier, B., Molines, J.M., Jourdain, N.C., Guinehut, S., Cabanes, C., and Zawadzki, L.

(2012): GLORYS2V1 global ocean reanalysis of the altimetric era (1992-2009) at meso scale. Mercator Quarterly Newsletter, 44, January 2012, pp. 29-39.

Fukumori, I., Lee, T., Cheng, B., and Menemenlis, D. (2004): The origin, pathway, and destination of Niño-3 water estimated by a simulated passive tracer and its adjoint. J. Phys. Oceanogr., 34, pp. 582–604.

Fujii, Y., and Kamachi, M. (2003): Three-dimensional analysis of temperature and salinity in the equatorial Pacific using a variational method with vertical coupled temperature-salinity empirical orthogonal function modes. J. Geophys. Res., 108(C9), 3297, (doi:10.1029/2002JC001745).

Fujii, Y., Kamachi, M., Matsumoto, S., and Ishizaki, S. (2012): Barrier layer and relevant variability of the salinity field in the equatorial Pacific estimated in an ocean reanalysis experiment. Pure and Appl. Geophys., 169, pp. 579-594, (doi:10.1007/s00024-011-0387-y).

Fujii, Y., Kamachi, M., Nakaegawa, T., Yasuda, T., Yamanaka, G., Toyoda, T., Ando, K., and S. Matsumoto (2011): Assimilating Ocean Observation data for ENSO monitoring and forecasting. Climate Variability - Some Aspects, Challenges and Prospects, Ed: A. Hannachi, InTech, Rijeka, Croatia; pp. 75-98, (doi: 10.5772/30330).

Fujii, Y., Ogamwa, K., Ando, K., Yasuda, T., and Kuragano, T. (2014): Evaluating the impacts of the tropical Pacific Observing system on the ocean analysis fields in the global ocean data assimilation system for operational seasonal forecasts in JMA. To be submitted to J. Operational Oceanogr.

Guemas, V., Dablas-Reyes, F.J., Andreu-Burillo, I., and Asif, M. (2013): Retrospective prediction of the global warming slowdown in the past decade. Nature Climate Change, 3, pp. 649-653, (doi: 10.1038/NCLIMATE1863).

Hoteit, I., Cornuelle, B., and Heimbach, P. (2010): An eddy-permitting, dynamically consistent adjoint-based assimilation system for the tropical Pacific: Hindcast experiments in 2000. J. Geophys. Res-Oceans*.,* 115, (doi:10.1029/2009jc005437).

Ji, M., Leetmaa, A., and Derber, J. (1995): An ocean analysis system for seasonal to interannual climate studies. Mon. Wea. Rev., 123, pp. 460–481.

Kim, S.-B., Lee, T., Fukumori, I., (2007): Mechanisms controlling the interannual variation of mixed layer temperature averaged over the NINO3 region. J. Clim., 20, pp. 3822-3843.

Köhl, A., Stammer, D. (2004): Optimal observations for variational data assimilation. J. Phys. Oceanogr., 34, pp. 529–542.

Langland, R., and Baker, N. (2004): Estimation of observation impact using the NRL atmospheric variational data assimilation adjoint system. *Tellus,* 56A, pp. 189–201.

Lea, D. J., Martin, M.J., and Oke, P.R. (2013): Demonstrating the complementarity of observations in an operational ocean forecasting system. Q. J. R. Meteorol. Soc., In press.

Lellouche, J.-M., Le Galloudec, O., Drévillon, M., Régnier, C., Greiner, E., Garric, G., Ferry, N., Desportes, C., Testut, C.-E., Bricaud, C., Bourdallé-Badie, R., Tranchant, B., Benkiran, M., Drillet, Y., Daudin, A., and De Nicola, C. (2013): Evaluation of global monitoring and forecasting systems at Mercator Océan, Ocean Sci., 9, pp. 57-81, (doi:10.5194/os-9-57-2013).

Lee, T., and Fukumori, I. (2003): Interannual to decadal variation of tropical-subtropical exchange in the Pacific Ocean: boundary versus interior pycnocline transports. J. Climate. 16, pp. 4022-4042.

MacLachlan, C., Arribas, A., Peterson, D., Maidens, A., Fereday, D., Scaife, A.A., Gordon, M., Vellinga, M., Williams, A., Comer, R.E., Camp, J., and Xavier, P. (2014): Global Seasonal Forecast System 5 (GloSea5): a high resolution seasonal forecast system. To be submitted to Q. J. Roy. Meteor. Soc.

Maes, C., Picaut, J., and Belamari, S. (2005): Importance of salinity barrier layer for the buildup of El Niño, J. Climate, 18, pp. 104--118.

Magnusson, L., Balmaseda, M.A., Corti, S., Molteni, F., and Stockdale, T. (2013): Evaluation of forecast strategies for seasonal and decadal forecasts in presence of systematic model errors. Clim. Dyn,, 41, pp. 2393-2409.

Masina, S., Pietro, P.D., Storto, A., and Navarra, A. (2011): Global ocean re-analyses for climate applications. Dyn. Atmos. Oceans, 52, pp. 341-366.

Masuda, S., Awaji, T., Sugiura, N., Ishikawa, Y., Baba, K., Horiuchi, K., and Komori, N. (2003): Improved estimates of the dynamical state of the North Pacific Ocean from a 4 dimensional variational data assimilation. Geophys. Res. Lett., 30, 16, 1868, (doi:10.1029/2003GL017604).

Masuda, S., Sugiura, N., Hosoda, S., Osafune, S., Ishikawa, Y., and Awaji, T. (2014): Effective ocean observing systems toward an improved ocean state estimation. Submitted to Deep Sea Res part 1.

Menkes, C. E. R., Vialard, J.G., Kennan, S.C., Boulanger, J.P., and Madec, G.V. (2006): A Modeling Study of the Impact of Tropical Instability Waves on the Heat Budget of the Eastern Equatorial Pacific. J. Phys. Oceanogr., 36, pp. 847-865.

Mochizuki, T., Ishiia, M., Kimoto, M., Chikamoto, Y., Watanabe, M., Nozawa, T., Sakamoto, T.T., Shiogama, H., Awajia, T., Sugiura, N., Toyoda, T., Yasunaka, S., Tatebe, H., and Mori, M. (2010): Pacific decadal oscillation hindcasts relevant to near-term climate prediction, Proc. Natl. Acad. Sci. U. S. A., 107, pp. 1833–1837, (doi:10.1073/pnas.0906531107).

Pohlmann, H., Smith, D.M., Balmaseda, M.A., Keenlyside, N.S., Masina, S., Matei, D., and Rogel, P. (2013): Predictability of the mid-latitude Atlantic meridional overturning circulation in a multi-model system. Clim. Dyn., 41, pp. 775-785.

Pohlmann, H., W. A. Müller, K. Kulkarni, M. Kameswarrao, D. Matei, F. S. E. Vamborg, C. Kadow, S. Illing, and J. Marotzke., (2013b): Improved forecast skill in the tropics in the new MiKlip decadal climate predictions. Geophys. Res. Lett. 40, pp. 5798-5802.

Reynolds, T., Smith, T.M., Liu, C., Chelton, D.B., Casey, K.S., and Schlax, M.G. (2007): Daily high-resolution blended analyses for sea surface temperature. J. Climate, 20, pp. 5473–5496.

Roemmich, D., Morris, M., Young, W.R., and Donguy, J.R. (1994): Fresh equatorial jet. J. phys. Oceanogr. 24, pp. 540-558.

Rosati, A., Gudgel, R., and Miyakoda, K. (1995): Decadal analysis produced from an ocean data assimilation system. Mon. Wea. Rev. 123, pp. 2206-2228.

Saha, S., and Coauthors (2010): The NCEP Climate Forecast System Reanalysis. Bull. Amer. Meteor. Soc., 91, pp. 1015–1057.

Saha, S., and Coauthors (2013): The NCEP Climate Forecast System Version 2. J. Climate, published online. (doi: 10.1175/JCLI-D-12-00823.1).

Smith, D. M., Cusack, S.A., Colman, W., Folland, C.K., Harris, G.R., and Murphy, J.M. (2007): Improved surface temperature prediction for the coming decade from a global climate model. Science, 317, pp. 796-799.

Smith, D. M., Eade, R., and Pohlmann, H. (2013): A comparison of full-field and anomaly initialization for seasonal to decadal climate prediction. Clim. Dyn. 41, 11-12, pp. 3325-3338.

Smith, G.C., Roy, F., Belanger, J.M., Dupont, F., Lemieux, J.F., Beaudoin, C., Pellerin, P., Lu, Y., Davidson, F., and Ritchie, H. (2013): Small-scale ice-ocean-wave processes and their impact on coupled environmental polar prediction. Proceedings of the ECMWF-WWRP/THORPEX Polar Prediction Workshop, 24-27 June 2013, ECMWF Reading, UK.

Stammer, D., Wunsch, C., Giering, R., Eckert, C., Heimbach, P., Marotzke, J., Adcroft, A., Hill, C.N., and Marshall, J. (2002): Global ocean circulation during 1992–1997, estimated from ocean observations and a general circulation model. J. Geophys. Res., 107, C9, pp. 3118.

Stammer, D., Ueyoshi, K., Köhl, A., Large, W.B., Josey, S., and Wunsch, C. (2004): Estimating Air-Sea Fluxes of Heat, Freshwater and Momentum Through Global Ocean Data Assimilation. J. Geophys. Res., 109, C05023, (doi:10.1029/2003JC002082).

Sugiura, N., Awaji, T., and Masuda, S. (2008): Development of a four-dimensional variational coupled data assimilation system for enhanced analysis and prediction of seasonal to interannual climate variations. J. Geophys. Res., 113, (doi:10.1029/2008JC004741).

Taylor, K.E., Stouffer, R.J., and Meehl, G.A. (2012): An Overview of CMIP5 and the experiment design." Bull. Amer. Meteor. Soc., 93, 485-498, (doi:10.1175/BAMS-D-11-00094.1).

Torn, R.D., and Hakim, G.J. (2008): Ensemble-based sensitivity analysis. Mon. Wea. Rev., 136, 663–677, (doi: 10.1175/2007MWR2132.1).

Ueki, I., Y. Kashino, and Kuroda, Y. (2003): Observation of current variations off the New Guinea coast including the 1997–1998 El Niño period and their relationship with Sverdrup transport. J. Geophys. Res., 108, C7, 3243, (doi:10.1029/2002JC001611).

Vecchi, G. A., et al. (2013): Multiyear predictions of north atlantic hurricane frequency: Promise and limitations. J. Climate, 26, pp. 5337–5357.

Weaver, A. T., Vialard, J., and Anderson, D.L.T. (2003): Three- and four-dimensional variational assimilation with a general circulation model of the tropical Pacific Ocean. Part I: Formulation, internal diagnostics, and consistency, checks. Mon. Wea. Rev., 131, pp. 1360-1378.

Wen, C., Xue, Y., and Kumar, A. (2012): Ocean–Atmosphere Characteristics of Tropical Instability Waves Simulated in the NCEP Climate Forecast System Reanalysis. J. Climate, 25, pp. 6409–6425. (doi:10.1175/JCLI-D-11-00477.1).

Wunsch, C., Ponte, R.M., and Heimbach, P. (2007): Decadal trends in sea level patterns: 1993-2004. J. Clim., 20, pp. 5889-5911.

Yin, Y., Alves, O., and Oke, P. (2011): An Ensemble Ocean Data Assimilation System for Seasonal Prediction, Mon. Wea. Rev. 139, pp. 786-808.

Zhang, S., Harrison, M.J., Rosati, A., and Wittenberg, A. (2007): System design and evaluation of coupled ensemble data assimilation for global oceanic climate studies. Monthly Weather Review, 135(10), pp. 3541-3564.

White Paper #6 – Tropical Pacific biogeochemistry: status, implementation and gaps

Mathis, J.T.[1], Feely, R.A.[1], Sutton, A.[1], Carlson, C.[2], Chai, F.[3], Chavez, F.[4], Church, M.[5], Cosca, C.[1], Ishii, M.[6], Mordy, C.[1], Murata, A.[7], Resing, J.[1], Strutton, P.[8], Takahashi, T.[9], and Wanninkhof, R.[10]

[1] NOAA Pacific Marine Environmental Laboratory, United States
[2] University of California, Santa Barbara, United States
[3] University of Maine, United States
[4] Monterey Bay Aquarium Research Institute, United States
[5] University of Hawai'i, United States
[6] Meteorological Research Institute, Japan
[7] Marine Science and Technology Center, Japan
[8] University of Tasmania, Australia
[9] Columbia University, United States
[10] NOAA Atlantic Oceanographic and Meteorological Laboratory, United States

1. Introduction

The oceans play an important role in the climate system as a large sink for anthropogenic carbon dioxide (CO_2), and, thereby partially mitigate the large-scale effects of humankind's CO_2 emissions into the atmosphere. As a whole, the oceans take up approximately 2.6±0.5 Pg C $year^{-1}$ of the 8.6±0.4 Pg C $year^{-1}$ that are emitted from the burning of fossil fuels. As such, the oceans absorb about 24 million tons of CO_2 every day or roughly 4 kg per day for every person on Earth.

Estimates of the net sea-air CO_2 flux based on measurements of partial pressure of CO_2 (pCO_2) in near-surface seawater and in the marine boundary air show that the extra tropics are major oceanic sinks of atmospheric CO_2 and the tropics are major sources. The tropical ocean is the ocean's largest natural source of CO_2 to the atmosphere and the annual contribution of CO_2 to the atmosphere from the oceanic equatorial belt is estimated to be between 0.6–1.0 Pg C (Takahashi et al., 1999, 2002, 2009; Wanninkhof et al., 2013). Despite comprising a net source of CO_2 to the atmosphere, equatorial waters are characterized by relatively high rates of primary productivity and serve as globally significant regions of biologically-fueled carbon sequestration to the deep sea. However, changes in ocean circulation patterns along with regional and global-scale climate processes may significantly impact the biogeochemistry of equatorial regions and alter the uptake rates of CO_2 on decadal or longer time-scales. Given the role that this region plays in determining atmospheric CO_2 concentrations, it is critical to determine;

- Will the ocean carbon sinks keep pace with increasing anthropogenic CO_2 emissions?
- How does oscillation between El Niño/La Niña events impact the delivery of nutrients to the mixed layer and the production, transport and fate of biogenic carbon?

Here, we provide the justification for answering these questions and lay the groundwork for how to carry out the necessary observations as part of the Tropical Pacific Observing System (TPOS) 2020 effort.

2. Background

2.1 The role of the Tropical Ocean in the Global Carbon Cycle

The mean circulation of the equatorial Pacific Ocean is characterized by upwelling that brings cold nutrient- and carbon-rich water to the surface along the equator east of about 160°W during non-El Niño periods. The primary source of the upwelled water along the equator is the narrow Equatorial Undercurrent (EUC), which flows eastward across the basin. This mean circulation and its seasonal variations are significantly modulated on interannual and decadal time scales by two prominent modes of natural variability: (1) the El Niño-Southern Oscillation (ENSO) cycle; and (2) the Pacific Decadal Oscillation (PDO). The warm El Niño phase of the ENSO cycle is characterized by a large-scale weakening of the trade winds, decrease in upwelling of carbon dioxide (CO_2) and nutrient-rich subsurface waters and a corresponding warming of the sea surface temperature (SST) in the eastern and central equatorial Pacific (McPhaden et al., 1998). Carbon-14 (C-14) data suggest that the high-CO_2 water of the EUC originates in the pole-ward edge zone of the subtropical gyres (possibly both in the northern and southern hemispheres).

The bomb C-14 concentration in the atmosphere peaked around 1965. This was detected in the 100-meter deep western equatorial Pacific water about 8 years later and propagated eastward via the undercurrent reaching the Galapagos area about 13 years after the atmospheric peak (Mahadevan, 2001). This suggests that the pCO_2 in the upwelling waters during La Niña events includes the atmospheric CO_2, which was absorbed by high-latitude low-pCO_2 waters in the past decade, as well as the CO_2 respired from biogenic debris released back into the atmosphere during the La Niña events. Thus, CO_2 in the upwelling water in the equatorial Pacific is a complex mixture of CO_2, which may vary with time reflecting physical and biological responses to climate change.

El Niño events occur roughly once every 2–7 years and typically last about 12–18 months. The opposite phase of the ENSO cycle, called La Niña, is characterized by strong trade winds, cold tropical SSTs, and enhanced upwelling of CO_2-rich water along the equator (Figure 2.1). El Niño and La Niña are associated with dramatic shifts in the atmospheric pressure difference between the eastern and western Pacific (referred to as the Southern Oscillation) that have major impacts on the climate variability worldwide (McPhaden, 1999) and on the sources and sinks for CO_2 in the atmosphere and oceans. The PDO has been characterized either in terms of fluctuations over a broad band of periods between 10–70 years (Minobe, 2000), or in terms of abrupt temporal “regime” shifts in climate conditions and ecosystems over large parts of the basin (Mantua et al., 1997) with the most recent of these regime shifts occurring in 1976–1977, 1988–1989, and 1998 (Trenberth et al., 1996; Watanabe and Nitta, 1999; Beamish et al., 1999; Hare and Mantua, 2000; McPhaden and Zhang, 2002; Chavez et al., 2003; Takahashi et al., 2003; McPhaden and Zhang; 2004).

For example, both Hare and Mantua (2000) and Wang et al. (2006) found evidence for the 1989 regime shift from time-series of a number of physical, biological and chemical parameters in the North Pacific. In the tropics, the 1976–1977 regime shift was characterized by a slowdown of the shallow meridional overturning circulation and a warming of the sea surface by nearly 1°C in the cold tongue region of the eastern and central equatorial Pacific Ocean (McPhaden and

Zhang, 2002). The most recent shift, which occurred in the 1997–1998 period, was characterized by an enhancement of the meridional transport and a slight decrease in SST (McPhaden and Zhang, 2004). On the other hand, based on a coupled atmosphere-ocean model, Rodgers et al. (2004) suggested that nonlinearities in ENSO variability can play an important role in determining the structure of tropical Pacific variability on decadal time scales. Thus, it is still open to debate whether the decadal modulation of ENSO is a cause of, or effect of, the PDO.

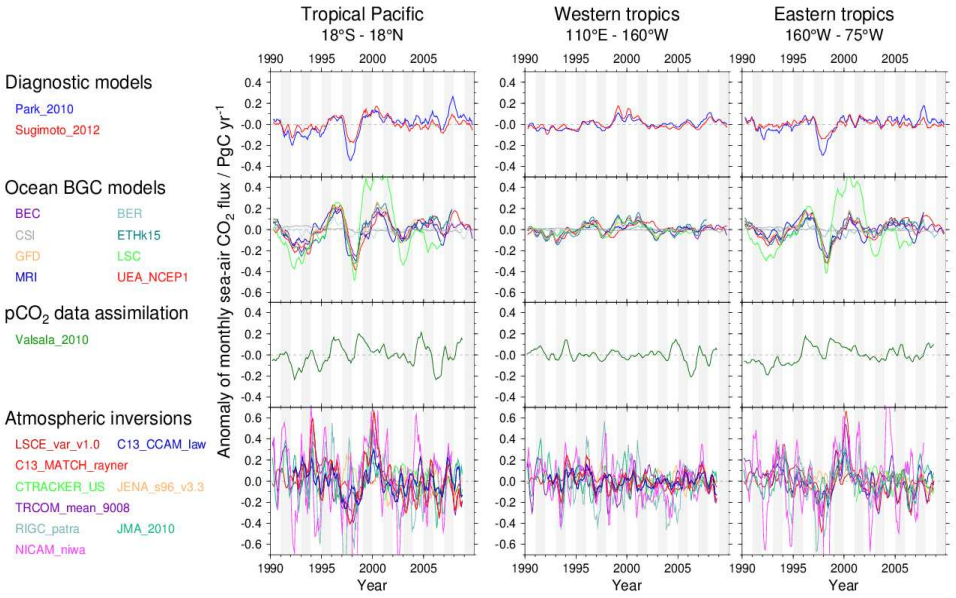

Figure 2.1 – Trends of sea-air CO_2 flux anomalies (5-month running mean, positive is flux out of the ocean) in the tropical Pacific (18°S – 18°N) for 1990-2009 (after Ishii et al., 2014).

For example, both Hare and Mantua (2000) and Wang et al. (2006) found evidence for the 1989 regime shift from time-series of a number of physical, biological and chemical parameters in the North Pacific. In the tropics, the 1976–1977 regime shift was characterized by a slowdown of the shallow meridional overturning circulation and a warming of the sea surface by nearly 1°C in the cold tongue region of the eastern and central equatorial Pacific Ocean (McPhaden and Zhang, 2002). The most recent shift, which occurred in the 1997–1998 period, was characterized by an enhancement of the meridional transport and a slight decrease in SST (McPhaden and Zhang, 2004). On the other hand, based on a coupled atmosphere-ocean model, Rodgers et al. (2004) suggested that nonlinearities in ENSO variability can play an important role in determining the structure of tropical Pacific variability on decadal time scales. Thus, it is still open to debate whether the decadal modulation of ENSO is a cause of, or effect of, the PDO.

Table 2.1 – Net sea-air CO_2 flux (Pg C yr^{-1}) by ocean basin and latitude band (updated from Takahashi et al., 2009).

Latitude Band	Pacific	Atlantic	Indian	Southern	Global
N of 50°N	-0.03	-0.26	-	-	-0.29
14°N-50°N	-0.50	-0.22	+0.02	-	-0.69
14°S-14°N	+0.48	+0.10	+0.10	-	+0.68
14°S-50°S	-0.41	-0.20	-0.41	-	-1.02
50°S-62°S	-	-	-	-0.05	-0.05
Total	-0.46	-0.58	-0.29	-0.05	-1.37
% of Uptake	34	42	21	3	100

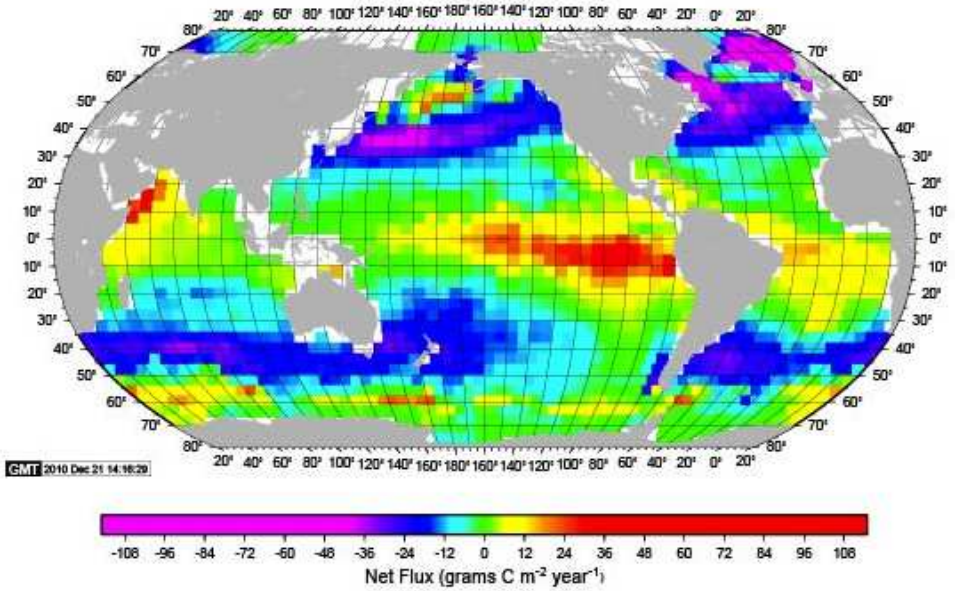

Figure 2.2 - Climatological mean sea-air CO_2 flux (g C m^{-2} yr^{-1}) for the reference year 2000 (non-El Niño conditions), updated after Takahashi et al., 2009.

2.2 Interannual and decadal variability of sea-air CO_2 fluxes

As a direct consequence of the extensive amount of physical, chemical and biological research of the tropical oceans over the past 30-40 years, it is well known that this region, particularly the

central and eastern equatorial Pacific, exhibits a large amount of spatial and temporal variability in ocean biogeochemical processes and properties. Much of this variability appears attributable to tightly coupled ocean-climate interactions in this region. Interannual to decadal scale variations in trade wind forcing control the strength of upwelling in this region, resulting in modification to air-sea CO_2 fluxes (Figure 2.2), nutrient supply, and ultimately biological productivity in the region. As a result, pCO_2 and sea-to-air CO_2 fluxes demonstrate large variability over interannual to decadal time scales (Feely et al., 1999, 2002, 2006; Ishii et al., 2004, 2011, 2014; Takahashi et al., 2003, 2009; Wanninkhof et al., 2013; Sutton et al., 2014).

Studies based on the long time-series measurements of chemical and biological measurements collected from ships and moorings associated with the Pacific Tropical Atmosphere Ocean (TAO) mooring array have delineated that the central and eastern equatorial Pacific are major sources of CO_2 to the atmosphere (Table 2.1) during non-El Niño and La Niña periods; it is near neutral during strong El Niño periods, and a weak source during weak El Niño periods. On decadal time scales, the Pacific Ocean has undergone major physical and biological regime shifts commonly referred to as the Pacific Decadal Oscillation (PDO), which has been documented on the basis of extensive physical and biological data (Trenberth et al., 1996; Hare and Mantua, 2000; McPhaden and Zhang, 2002; Chavez et al., 2003; McPhaden and Zhang; 2004; Chavez et al., 2011). While the causes and effects of these regime shifts have been investigated in recent years, only a few long-term studies of its effect on primary productivity, CO_2 chemistry, and nutrient supply in the equatorial Pacific have been conducted (Takahashi et al., 2003; Feely et al., 2006; Chavez et al., 2011; Ishii et al., 2014). Such studies demonstrate the sensitivity of these regions to climate variability, including documenting long-term (decadal-scale) changes in primary production and the growth rate of CO_2 in surface waters and an overall decline in pH, referred to as ocean acidification (Sutton et al., 2014).

While ENSO drives much of the interannual variability in the outgassing of CO_2 in the equatorial Pacific, the PDO, the strength of ENSO events, and the location of the SST anomalies during El Niño events also play important roles. During the strong El Niño events of 1982-1983 and 1997-1998, upwelling ceased at the Equator along with CO_2 outgassing as the pCO_2 in surface waters reduced to equilibrium with respect to the atmosphere (Chavez et al., 1999; Feely et al., 1987, 1999, 2002, 2006). In fact, in early 1998, moored pCO_2 measurements from the central equatorial Pacific showed that the region became a weak sink of CO_2 (Chavez et al., 1999). Weaker El Niño events have dominated in the period since, and some suggest that a PDO regime shift after the 1997-1998 El Niño has caused increasing trade winds, shallower thermocline, rebound of the shallow meridional overturning circulation, and increasing frequency of La Niña events (Chavez et al., 2003; Feely et al., 2006; Ishii et al., 2009, 2014; McPhaden, 2012; McPhaden and Zhang, 2004; Peterson and Schwing, 2003; Takahashi et al., 2003; Sutton et al., 2014; Feely et al., in preparation; Cosca et al., in preparation). In addition, El Niño events post 1997-1998 have been central Pacific (CP) events (also referred to as “date line”, “warm pool”, or “El Niño-Modoki” events), where the largest SST anomalies occur in the central Pacific instead of in the eastern Pacific during traditional El Niño events (Ashok et al., 2007; Kao and Yu, 2009; Kug et al., 2009; Larkin and Harrison, 2005). These events impact the distribution of sea surface conditions across the equatorial Pacific, influencing seawater pCO_2 and SST conditions and the outgassing flux of CO_2 to the atmosphere particularly during El Niño events.

Since this regime shift, CO_2 outgassing by the ocean has increased ~25-30% (Feely et al., in preparation).

2.3 Primary production and nutrient dynamics

The equatorial Pacific is a globally significant region of ocean production, with rates of net primary productivity estimated between 9 and 14 Pg C yr^{-1}. Moreover, export production, the fraction of organic matter production that escapes upper ocean remineralization and hence contributes to biological carbon sequestration, has been estimated ~0.7-2.5 Pg C yr^{-1} (Chavez and Barber 1987; Behrenfeld et al. 2006). Gravitational settling of particulate organic matter, physical redistribution (via mixing, advection and subduction) of dissolved organic carbon, and zooplankton vertical migration are the prominent mechanisms driving vertical fluxes of organic matter from the well-lit upper ocean across the thermocline. The upper ocean waters of the eastern and central regions of the equatorial Pacific have been broadly characterized as high nutrient-low chlorophyll (HNLC) habitats, where concentrations of inorganic macronutrients (specifically nitrate) are perennially elevated. The HNLC condition implies the physical supply of nutrients to the upper ocean (primarily via upwelling in equatorial waters) exceeds the rate of biological removal of these nutrients.

Various factors have been identified as controlling phytoplankton consumption of macronutrients in this region and hence limiting export production in the equatorial Pacific; these include trophodynamic processes (*i.e.* grazing control of phytoplankton biomass) and nutrient supply and availability, most notably including the supply of iron (Landry et al., 2011; Coale et al. 1996; Behrenfeld et al., 1996). Thus, understanding the sensitivity of biological carbon drawdown in this region to changes in ocean-climate will require detailed, time-resolving measurements of air-sea interactions, vertical and Aeolian nutrient supply, and primary production and phytoplankton biomass.

Primary productivity in the tropical Pacific is regulated both by macronutrients (e.g., nitrate) and by trace nutrients with iron (Fe) most often being the limiting nutrient in the open ocean. Fe is transported to most of the open ocean by atmospheric transport of aerosols from the continents to the surface ocean. However, near the equator there is little transport of aerosol Fe and additional sources are required to sustain primary productivity. Transport of iron from the western to eastern Pacific by the EUC is one possible source (Ryan et al., 2006; Slemons et al., 2010). Models suggest that western Pacific sources of dissolved iron delivered via the EUC are important in sustaining annually integrated equatorial Pacific primary production; short term variations in this Fe source do not appear to constrain the timing of modeled central and eastern Pacific plankton blooms (Gorgues et al., 2010), but the ecological impact in the eastern Pacific from long- and short-term variability in equatorial undercurrent iron sources remains to be shown.

To date, a single study conducted over a 45 day interval has documented this transport; in that study the maxima in Fe in the eastern tropical Pacific was just below the core of the undercurrent (~200m). If this maximum is perpetually at this depth then the depth of the thermocline and strength of the equatorial upwelling that are important in the release of nutrients to the euphotic zone of the eastern Pacific are even more important for transporting the limiting trace nutrient Fe into the photic zone. Meanwhile, waters in the EUC are generally < 1 year old

and reflect the variability of its source waters on both short and long time scales. How this variability is superimposed upon thermocline depth and strength of upwelling is largely unknown and remains an important question. However, the depth and magnitude of the source must play a role in the depth of Fe transport within the EUC and it has been suggested that this has directly affected primary productivity (Ryan et al., 2006). This variability depends in some ways on the seasonal and interannual variability of the major western boundary currents feeding the EUC (e.g., the New Guinea Coastal Undercurrent (Cresswell, 2000). Sources of Fe include sediment resuspension, riverine runoff, hydrothermal activity and anthropogenic sources like subaerial and eventually submarine mining. Ultimately, the modulation and variability of Fe input and mobilization within the pathways of these source currents and the subsequent transport of these iron-enriched waters might act as a throttle on productivity in the central and eastern equatorial Pacific and may also act to regulate carbon export from this region.

While new monitoring efforts have helped to reduce uncertainties in the sea-air flux of CO_2, large uncertainties remain in our understanding of the export flux of particulate organic carbon (POC) from the euphotic zone to the interior of the ocean – ranging from ~4-6 Pg C yr^{-1} (Gehlen et al., 2006; Henson et al., 2010; Moore et al., 2004; Lutz et al., 2007; Siegel et al., 2014) to ~10-12 Pg C yr^{-1} (Dunne et al., 2007; Gehlen et al., 2006; Laws et al., 2000) (Figure 2.3). Even higher values are necessary to balance rates of heterotrophic respiration in the deep ocean (e.g. Burd et al., 2010). These uncertainties are driven by differences in the methods used to determining the export ratio (e.g. f-ratio, ^{234}Th), the parameterization of sparse data sets that are globally extrapolated using satellite SST, and the influence of environmental and biological factors on sinking rates of POC (e.g. fraction of diatoms, packaging effects, biogenic minerals that may act as ballast; Armstrong et al., 2002; François et al., 2002) among other factors.

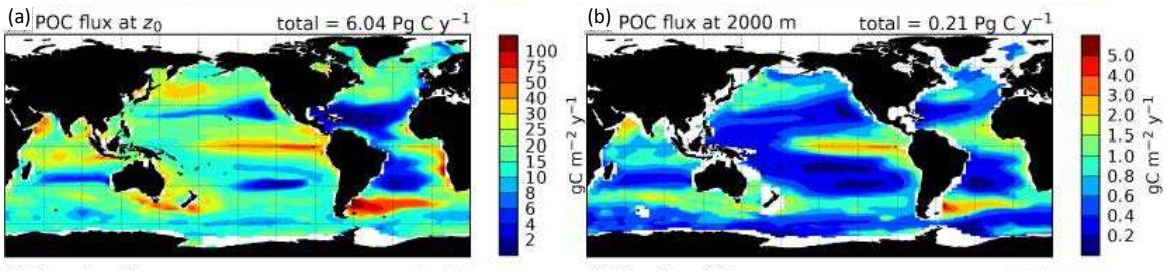

Figure 2.3 – Modeled flux of POC at a) the export depth (Z0) and b) 2000 m (Lima et al., 2014). The export depth was computed as the depth where POC production is 1% if maximum POC production in the water column, and varied from 50-300 m in the global ocean.

Some of the highest rates of POC export are found in the eastern tropical Pacific (Figure 2.3; Siegel et al., 2014), where shoaling of the nutricline (Figure 2.4) supports very high rates of primary production (as reviewed by Pennington et al., 2006). In this region, both Fe and $Si(OH)_4$ influence new and export production of diatoms – with Fe regulating the production of organic matter, and $Si(OH)_4$ regulating silicification, i.e. frustual thickness (Brzezinski et al., 2008).

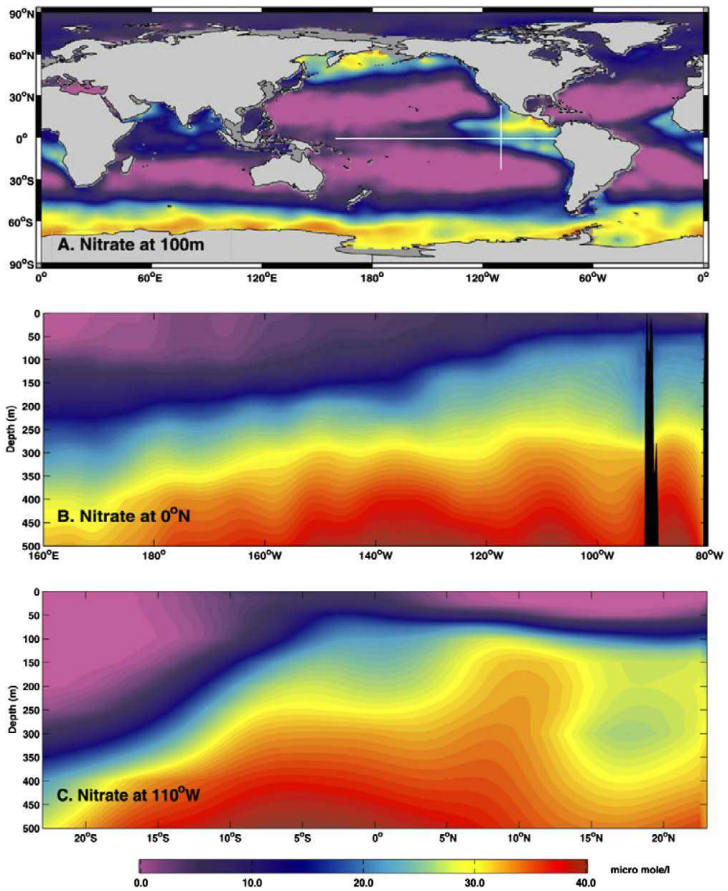

Figure 2.4 – Distribution of nitrate in the eastern tropical Pacific as shown by Pennington et al., 2006. (a) Global 100 m nitrate. The white lines indicate the positions of panels B and C. 100 m nitrate is near zero in the subtropical gyres and at the western boundaries, at high latitudes, and in the eastern tropical Pacific; (b) vertical section of nitrate along the equator. The equatorial thermocline tilt causes near-surface nitrate to be higher in the east; (c) vertical section of nitrate on 110°W showing basin-scale nutricline shoaling across the equator associated with the subtropical gyre circulation.

As the nutrient supply and export production is sustained by southeasterly trade winds, the ENSO cycle plays a major role in controlling the export flux of biogenic carbon out of the euphotic zone. A synthesis of the Joint Global Ocean Flux Study (JGOFS) in the equatorial Pacific during 1992 revealed that the export flux of total organic carbon was four-times higher during the fall non-El Niño period as compared with the Spring El Niño event (Quay, 1997). Behrenfeld et al. (2006) observed strong correspondence between fluctuations in ENSO and satellite derived net primary production in this region, with subdecadal scale increases in net primary production during cold phase ENSO cycles, with reduced rates of productivity occurring during warm phases. Recent studies by Chavez et al. (2011) have also demonstrated that primary production is also affected by the changes in the physical dynamics of upwelling and thermocline mixing processes during the warm and cold phases of the ENSO cycle (Figure 2.5). Their results show that the biogenic carbon fluxes are directly responding to the phasing of the ENSO cycle by taking up more nutrients into phytoplankton during the cold phase of the ENSO cycle when upwelling is strong and nutrient inputs are highest. In the same manner, the primary production appears to be increasing over the past several years, consistent with the recent PDO

shift to cooler conditions and more extensive upwelling (Chavez et al., 2011). In addition, dissolved organic carbon (DOC) is thought to contribute ~20% to carbon export in the global ocean (Hansell et al., 2009).

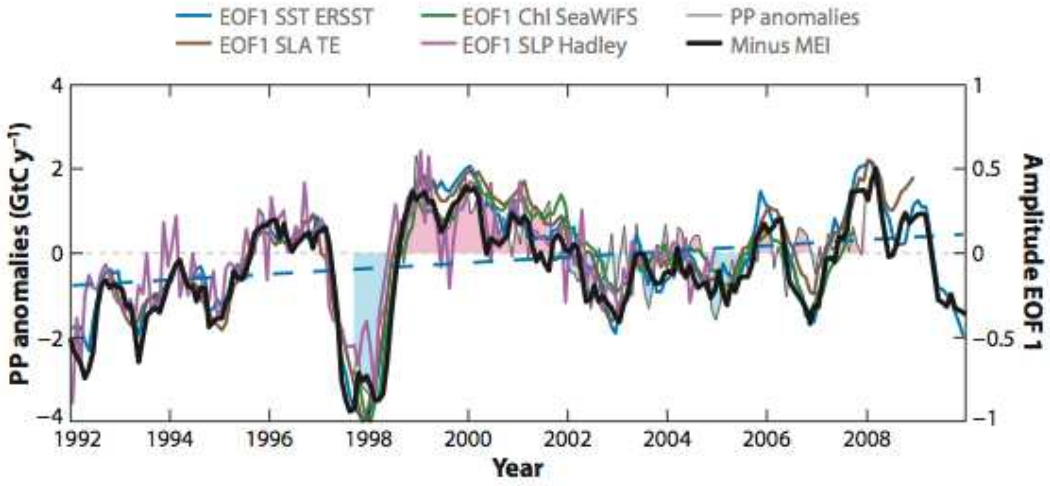

Figure 2.5 – Global primary production anomaly (PPA) and first empirical orthogonal function (EOF) modes of sea surface temperature (SST), sea level anomaly (SLA), sea level pressure (SLP), chlorophyll (logChl), and the normalized multivariate ENSO index (MEI).

Dissolved organic matter (DOM) represents one of the largest exchangeable reservoirs of organic material on earth. At ~662 ±32 Pg (10^{15} g) C (Hansell et al., 2009), dissolved organic carbon (DOC) exceeds the inventory of organic particles in the oceans by 200 fold, making it one of the largest of the bioreactive pools of carbon in the ocean, second only to dissolved inorganic carbon. Photoautotrophic production fixes CO_2 to organic matter, which in turn serves as a substrate that fuels the oceanic food web. As that organic matter is produced and processed within the oceanic food web a portion is released into the dissolved organic matter (DOM) pool. Most of the freshly produced DOM is consumed rapidly by heterotrophic microbes but some escapes remineralization or is further transformed into recalcitrant forms of DOM that accumulates and can persist in the oceanic water column for months (semi-labile DOM) to millennia (refractory DOM) (Carlson, 2002; Hansell and Carlson, 2012; Benner and Herndl, 2011; Goldberg et al., 2011). The recalcitrant DOM pools are biogeochemically relevant because they can be physically transported via ocean currents and mixing, thus contributing significantly to vertical and horizontal export of organic carbon, nitrogen within the oceanic water column (Hansell et al. 2009; Letscher et al., 2013).

As described above, the Equatorial Pacific is a significant source of CO_2 to the atmosphere, but it also contributes considerably to the global ocean's new production. Estimates of new production within the equatorial Wyrtki box (5°N – 5°S) range between 0.61 Pg C y^{-1} (Wang et al., 2006) and 1.9 Pg C y^{-1} (Chavez and Barber, 1987) or ~ 5- 20 % of global new production (~10 Pg C y^{-1}; Chavez and Toggwelier, 1995). New production is partitioned between particulate organic matter (POM) and DOM each of which has a vastly different effect on export of organic matter in this system. Using mass balance techniques Hansell et al. (1997) estimated that vertical POM flux dominated organic matter removal from the surface waters accounting for approximately 80% of net community production in equatorial Pacific with the balance

accumulating as DOM in the surface waters. The DOM that escaped rapid microbial remineralization and accumulated in the surface water was available for horizontal advection from the equatorial Pacific into the subtropical gyres (Figure 2.6). Estimates of poleward advection of DOM from the Wyrtki box range from a low range of 0.7 – 0.18 Pg C y^{-1} (Hansell et al. 1997) up to 0.4 Pg C y^{-1} (Archer et al., 1997) as DOC and 0.03 Pg N y^{-1} as DON (Hansell et al., 1997). The build up of semi-labile DOC in the subtropical gyres (Figure 2.6) as a result of autotrophic production in the gyres as well as horizontal advection of DOM from the equatorial Pacific can be exported into the interior by Ekman convergence of surface waters and downwelling of DOC-rich waters to a few hundred meters depth.

Techniques have greatly improved over the past two decades with regard to DOM analyses and the US Repeat Hydrography programme has allowed for the first ever high-resolution ocean DOM maps and inventory. Yet, there is still a paucity of DOM data especially in the equatorial Pacific. It would be beneficial to obtain measurements in this important region to better estimate the role of DOM in both horizontal and vertical export from this important oceanic region.

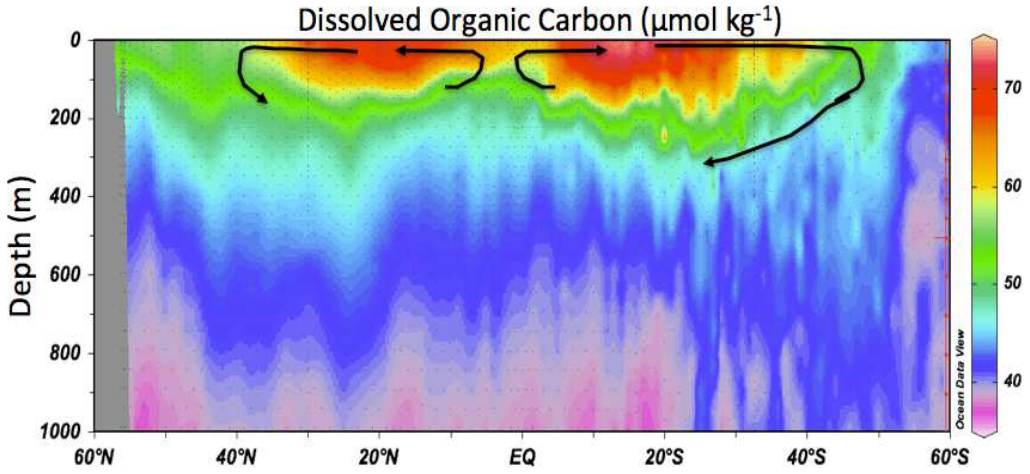

Figure 2.6 – Distribution of DOC (µmol kg^{-1}) along P16 meridional transect (150°W) in the Pacific basins. This Figure depicts accumulation of DOC in the surface waters of the equatorial Pacific of which a portion is redistributed poleward by wind-driven circulation. This horizontal export contributes to DOC build-up in the subtropical gyres (PDW), which can then lead to vertical export into the interior via intermediate water formation. The arrows represent generalized water circulation. Data for this graph are available at http://ushydro.ucsd.edu/data_centers.htm.

Sustained observations in the equatorial Pacific have been critical to improving our understanding of the ENSO cycle and its interaction with other modes of large-scale climate variability in this region and around the globe (McPhaden et al., 2006). While many global biogeochemical models, ocean carbon cycle models, and atmospheric inversions are able to capture the interannual variability of sea-air CO_2 fluxes in the equatorial Pacific (Rayner et al., 1999; Jones et al., 2001; Patra et al., 2005; Le Quéré et al., 2010), separating natural variability from global change impacts and understanding how these phenomena will interact in the future is challenging. Climate change predictions in the equatorial Pacific include warming sea surface temperatures, weakening trade winds, and a shoaling thermocline; however, it is unclear

whether the frequency or intensity of ENSO events may change (Vecchi et al., 2006; Collins et al., 2010). Some researchers link an increased frequency of CP El Niño events to anthropogenic climate change (Yeh et al., 2009), while others suggest the observed increase since 1997–1998 is part of a natural variation of the climate system (McPhaden et al., 2011; Newman et al., 2011). Continued investigation into the interannual, decadal, and multi-decadal dynamics that impact the equatorial Pacific is key to understanding how ENSO and CO_2 outgassing in this region may change in the future.

3. Time series of biogeochemical observations in the equatorial Pacific

While the basin-scale understanding of biogeochemical processes is principally derived from repeat hydrographic cruises, our present understanding of the sea-air CO_2 flux in the equatorial Pacific is primarily derived from very high-quality surface carbon measurements on research cruises, volunteer observing ships and moorings coupled with satellite measurements of SST and winds from which flux algorithms have been derived (Cosca et al., 2003; Feely et al., 1999, 2002, 2006; Ishii et al., 2004, 2011, 2014; Takahashi et al., 2003, 2009; Wanninkhof et al., 2013; Figure 3.1). These data sets have been integrated into the community-wide data product Surface Ocean CO_2 Atlas (SOCAT; Pfeil et al., 2013; Bakker et al., 2014) and the Takahashi pCO_2 data product (Takahashi et al. 2013, CDIAC) for the tropical ocean and also have been used to validate models of carbon dioxide fluxes and variability over the last few decades (Doney et al., 2009; Le Quéré et al., 2009; Fay and McKinley, 2013). Two major conclusions have resulted from the synthesis and modeling research on the tropical and global data sets:

1. The tropical Pacific is the major natural source of CO_2 from the ocean to the atmosphere, contributing nearly 70% of the global flux to the atmosphere.

2. Interannual variability of the sea-air CO_2 flux in the tropical Pacific is also the major source of CO_2 flux variability in the global oceans (Doney et al., 2009; Ishii et al 2014). These two facts emphasize the strong need for sustained observations of carbon system parameters in this region.

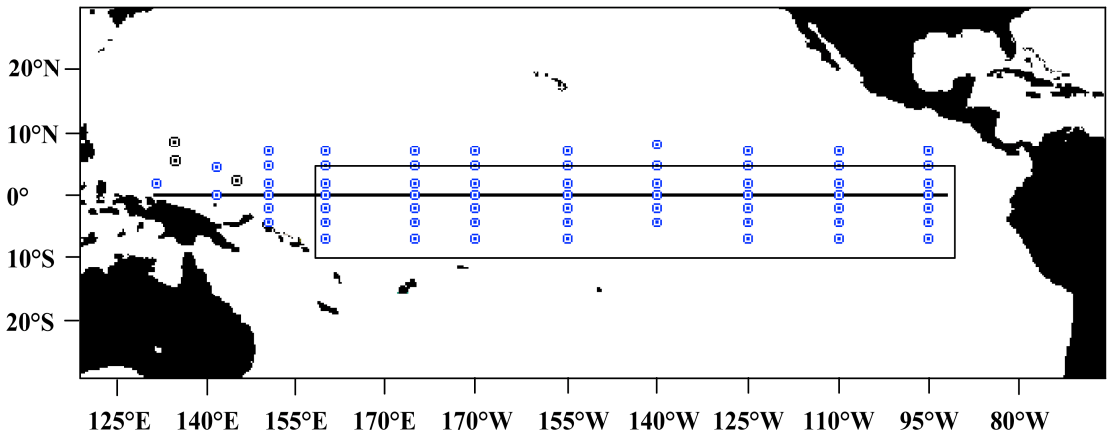

Figure 3.1 – Locations of the TAO/TRITON buoys. Moored pCO_2 data is collected mostly along the equator, shown as the dark line. Underway surface ocean pCO_2 measurements have been collected on surface ships as part of the bi-annual servicing of the TAO array.

4. Current and emerging technology

4.1 Underway vessel observations

Sea surface pCO_2 observations have been made on research vessels servicing the TAO/TRITON array since 1982. These automated underway systems are designed to continuously measure seawater and atmospheric pCO_2 onboard ships of opportunity with a high degree of precision (±0.5 µatm) and accuracy (±2 µatm). In this method, seawater is equilibrated with air in a chamber, dried, and pumped through a non-dispersive infrared (NDIR) analyzer. Each measurement is calibrated *in situ* against three or four gas reference standards certified by the World Meteorological Organization (WMO). Oxygen and nutrient sensors have not yet been integrated into the underway measurements made in the Tropical Pacific. These measurements are critically important in constraining the spatial variability of surface pCO_2 values. Accordingly, automated underway pCO_2 systems should be installed and maintained on all vessels servicing the TAO/TRITON array.

4.2 Mooring observations

The ENSO observing system in the equatorial Pacific includes moored autonomous pCO_2 ($MAPCO_2$) systems deployed on 6 of the 7 flux reference sites along the equator (0°, 110°W; 0°, 125°W; 0°, 140°W; 0°, 155°W; 0°, 170°W; and 0°, 165°E) and a mooring in the warm water pool of the western equatorial Pacific (8°S, 165°E; Figure 3.1). The $MAPCO_2$ system collects marine boundary air and surface seawater xCO_2 (the mole fraction of CO_2 in air in equilibrium with sea surface temperature) measurements every three hours and is similar to the underway method utilizing a pCO_2 equilibrator and Non-Dispersive Infra-Red (NDIR) analyzer. Each measurement is calibrated *in situ* against a WMO certified gas reference standard. Based on laboratory tests and field intercomparisons at PMEL and other institutions, estimates of uncertainty for air and seawater pCO_2 measurements are better than 1 and 2 µatm, respectively. The data from the $MAPCO_2$ systems have provided new insights (e.g. Sutton et al., 2014) into the seasonal cycles and the trends in annual CO_2 fluxes.

4.3 Repeat hydrography measurements

Ship-based hydrography is the only method for obtaining discrete high-quality carbon, oxygen, and nutrient measurements over the full water column and in areas of the ocean inaccessible to other platforms. Global hydrographic surveys have been carried out every decade since the 1980s through research programmes such as GEOSECS, WOCE/JGOFS, CLIVAR and GO-SHIP. Repeat hydrographic lines that have crossed the TOA/TRITON array are: P13, P14, P15, P16, P17, and P18. During these cruises, observations of pCO_2 (ship's underway system) provide additional spatial context for the moored $MAPCO_2$ systems and discrete sampling of dissolved inorganic carbon (DIC) and total alkalinity (TA) are used to determine changes in water column carbon inventories, shoaling of the lysocline and provide insight into other biogeochemical processes.

Repeat measurements of limiting trace nutrients in the equatorial Pacific are required to better elucidate the role that they play in regulating primary productivity and carbon export in this broad region of the ocean. However, given the course spatial resolution and sparse temporal

resolution, many questions still remain. Samples collected from *in situ* sampling devices placed on moorings would allow understanding of temporal variability in macro- and micronutrient supply (particulate and dissolved) within the EUC and would thus help constrain the effects of short term variability in the supply as both a throttle on primary productivity and on net productivity in the eastern tropical Pacific. The use of nitrate sensors on autonomous vehicles would identify regions where macronutrients are readily available and thus areas where primary productivity is likely limited by Fe and/or other trace nutrient metals. Long-term records over significant spatial scales would aid in targeting regions for more extensive, ship-based studies, aimed at understanding this process. Establishing an area for ship-based time series studies will be essential if we are to fully understand the physical and chemical forcing on primary productivity and carbon export.

In the future, improved understanding of the distribution and magnitude of source waters to the EUC and their geochemical make-up will be essential. This information will aid in constraining whether longer-term shifts in primary productivity are the result of longer-term shifts in the geochemical make-up of the source waters. A fuller geochemical examination of this region will be required to accomplish this.

4.4 Satellite observations

While it is not possible to measure surface ocean pCO_2 from satellite, estimates of phytoplankton biomass and primary productivity have been made continuously from August 1997 by SeaWiFS, MODIS and other satellite ocean color missions. These observations have proved essential for filling in gaps between ship and mooring data, and Chavez et al (1999) showed excellent agreement for chlorophyll observations across all three platforms. Recent work (Hales et al, 2012) has demonstrated the use of multiple satellite-measured parameters for estimating surface ocean pCO_2, as did Cosca et al. (2003) for *in situ* measurements. Because of the strong relationship between upwelling (and its SST signature), productivity and pCO_2, the equatorial Pacific is a region that holds promise for future work linking pCO_2 to satellite observations. Continued observations of surface pCO_2 from moorings and vessel underway systems will allow for further improvement of the empirical relationships between SST and salinity, which will be necessary for satellite pCO_2 algorithm development.

5. Potential expansion of CO_2 and biogeochemical measurements

The autonomous carbon sensors described in sections 4.1 and 4.2 provide climate quality (uncertainty < 2 µatm) seawater pCO_2 measurements. However, since these instruments were developed to measure sea-air flux, they can only be operated at the ocean surface and are not adaptable to subsurface drifters or gliders. There has been some success in developing algorithms to predict ocean acidification parameters in coastal environments using temperature, salinity, and oxygen, which can be measured on subsurface platforms, but these algorithms are not reliable in surface waters largely due to heat and oxygen fluxes to the atmosphere that do not have an associated carbon signature (Juranek et al. 2009, 2011; Alin et al., 2012). The algorithms developed by Feely et al. (2006) to predict seawater pCO_2 based on SST and SSS are robust, but must be validated using underway-data with sufficient spatial (i.e., spanning the Tropical Pacific) and temporal resolution (i.e., capturing seasonal and ENSO variability). These

surface seawater pCO_2 algorithms must be recalculated every 5-10 years in order to reevaluate the influence of changing atmospheric CO_2 on the surface ocean. These facts clearly demonstrate the need for continued direct observations of the carbon parameters as well as underlying biogeochemistry. However, as ship-time becomes more costly, it will be necessary to develop more robust, reliable and accurate autonomous sensors and platforms.

5.1 Experiments and pilot studies necessary for new observations

One of the most promising new technologies that could supplement existing platforms and perhaps reduce some of ship-time needs is the carbon wave glider (Figure 5.1). This platform is designed to conduct autonomous, basin-scale ocean transits for long-durations (up to 6 months). The wave glider has to date been tested extensively in coastal environments with pCO_2, pH, and nitrate sensors at the surface and temperature and oxygen at 6 m depth on the subsurface, energy-harvesting vanes. Because the $MAPCO_2$ systems that are used on the moorings have been integrated into the wave gliders is it possible for them to return the same climate-quality pCO_2 data and provide data inter-comparison with the moorings and underway *p*CO2 measurements from vessels. In order to assess the carbon wave glider in a high energy, open ocean environment, a 3-6 month pilot-study experiment in the equatorial Pacific is necessary. Comparison to proven technology and standardized methods (i.e., underway pCO_2, mooring pCO_2, and bottle samples) should be used to validate the wave glider carbon system and biogeochemical sensors. Accordingly, this pilot-study should be done in conjunction with either a repeat hydrography cruise or a mooring servicing cruise where underway and discrete measurements can be made. In the future, faster autonomous platforms that have larger payloads such as the Sail Drone should be adapted to make pCO_2 and related biogeochemical measurements. These drones can cover larger areas of the ocean and carry more sensors with greater endurance.

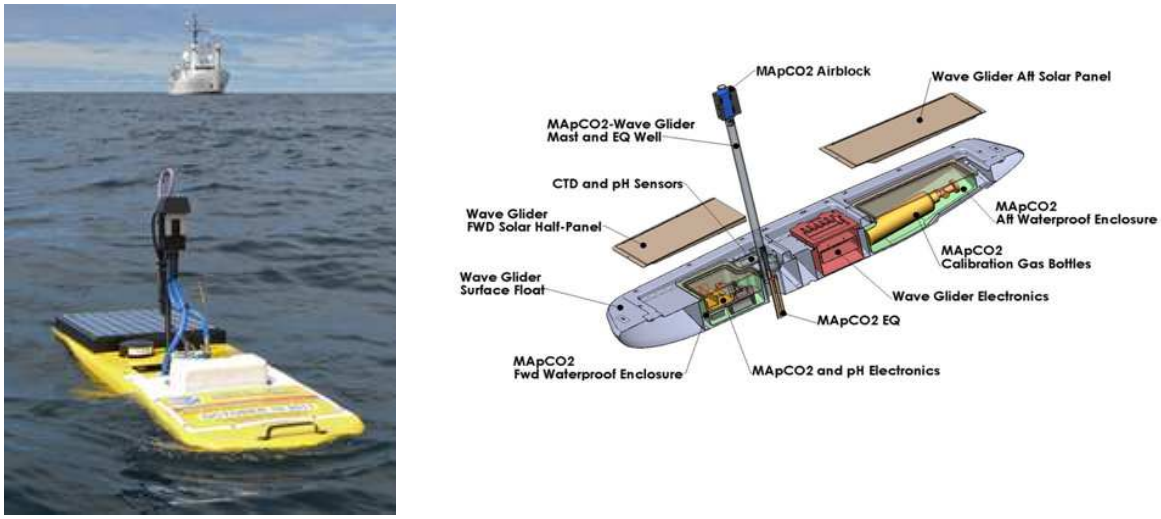

Figure 5.1 – Carbon wave glider with integrated $MAPCO_2$ system.

A more robust and immediate capability that should be added to the existing mooring array and vessel-mounted underway systems operating in the region are autonomous sensors for

dissolved oxygen and inorganic nitrate. In both cases, existing sensor technology has reached the stage where continuous measurements can be made with high precision during a 12-month deployment period. The addition of these new sensors would provide valuable insights into the seasonal nutrient delivery into the mixed layer and give an indication of the intensity and duration of primary production. Other "off-the-shelf" technologies that could greatly supplement the existing mooring array are the remote access sampler (RAS) and sediment traps. The RAS has the ability to collect 96 (8 per month) discrete water samples at fixed depths. The data could be used to calibrate moored sensors as well as provide increased temporal resolution for parameters such as Fe, silicate and DOM, which can't be measured autonomously. Sediment traps can also provide discrete estimates of particles fluxes out of the surface ocean and are important indicators of primary production that can be related to satellite data.

Finally, a significant effort should be made to outfit ARGO floats with biogeochemical sensors. At present, the only biogeochemical sensors that have been tested on these platforms are dissolved oxygen and pH. While both have been limited by hysteresis effects and calibration issues, the performance and reliability of these sensors is improving. Further efforts should be made to incorporate other measurements, particularly nitrate into these sensor packages. Additionally, Slocum gliders that can profile the water column provide another autonomous platform where oxygen, nitrate and pH sensors can be incorporated. While an order of magnitude more expensive than an ARGO float, the Slocum's can carry a greater payload and have some navigation capability. Another emerging sensor package is the Carbon Prawler that integrates carbon and biogeochemical measurements. These systems can be deployed on a mooring and by moving up and down the wire can profile the water column. The Prawler's can also be deployed on CTD casts during repeat hydrography cruises and provide high-resolution profiles of the water column. When properly integrated, the combination of moorings, underway ship-based observations, repeat hydrographic measurements, gliders, floats, RAS, and satellite data streams can provide a four-dimensional picture of carbon biogeochemistry in the equatorial Pacific Ocean.

6. Recommendations for TPOS 2020

Based upon the discussion within this White Paper, we make the following overall recommendation for the TPOS of 2020:

1. Long climate and pCO_2 records should be continued at the existing TAO/TRITON locations.
2. The research vessels that are used to maintain the observing system should be treated as a platform within the observing system itself, making standard measurements along repeat tracks (e.g. CTD, pCO_2, dissolved oxygen, nitrate, pH, etc.) and deployment of moorings, floats and gliders.
3. The TPOS array should integrate multi-disciplinary observations. Data should be freely provided for all users. The array should be designed to provide data needed to observe ENSO events through their full life cycle; to force, initialize, and validate numerical models; to assess uncertainties in numerical models and satellite products; to calibrate

remotely measured variables; to develop and test parameterizations needed for models and satellite products; and to better understand the climate system.

4. Interdisciplinary process and pilot studies should be built around the infrastructure of the TPOS. New platforms such as wave gliders, remote access water samplers, and sediment traps should be added to the existing array and new sensors (e.g. pCO_2, pH, dissolved oxygen, nitrate, pH, etc.) should be added to existing assets.

7. Conclusion statement

Decades of work and millions of observations have shown that the tropical Pacific is the major natural source of CO_2 from the ocean, contributing nearly 70% of the global flux to the atmosphere. Data synthesis and modeling efforts have confirmed that interannual variability of the sea-air CO_2 flux in the tropical Pacific is the major source of CO_2 flux variability in the global oceans. Much of the CO_2 flux is controlled by the underlying physical and biogeochemical processes in the region, which are impacted by decadal and longer time-scale ocean and climate processes. Given its role in global climate and potential impacts to ocean resources and billions of people around the world the TPOS must be maintained at a level commensurate with its importance.

References:

Alin, S. R., Feely, R.A., Dickson, A.G., Hernández-Ayón, J.M., Juranek, J.W., Ohman, M.D., and Goericke, R. (2012): Robust empirical relationships for estimating the carbonate system in the southern California Current System and application to CalCOFI hydrographic cruise data (2005–2011), Journal of Geophysical Research: Oceans, 117(C5), C05033.

Archer, D., Peltzer, E.T., and Kirchman, D.L. (1997): A timescale for dissolved organic carbon production in equatorial Pacific surface waters. Global Biogeochem. Cycles 11, pp. 435-452.

Ashok, K., Behera, S.K., Rao, S.A., Weng, H., and Yamagata, T. (2007): El Niño Modoki and its possible teleconnection, Journal of Geophysical Research: Oceans, 112(C11).

Beamish, R. J., Noakes, D.J., McFarlane, G.A., Klyashtorin, L., Ivanov, V.V., and Kurashov, V. (1999): The regime concept and natural trends in the production of Pacific salmon, Canadian Journal of Fisheries and Aquatic Sciences, 56(3), pp. 516-526.

Behrenfeld, M.J., Bale, A.J., Kolber, Z.S., Alken, J., Falkowski, P.G. (1996): Confirmation of iron limitation of phytoplankton photosynthesis in the equatorial Pacific Ocean Nature, 383, pp. 508–511.

Behrenfeld, M. J., O'Malley, R.T., Siegel, D.A., McClain, C.R., Sarmiento, J.L., Feldman, G.C., Milligan, A.J., Falkowski, P.G., Letelier, R.M., and Boss, E.S. (2006): Climate-driven trends in contemporary ocean productivity, Nature, 444(7120), pp. 752-755.

Benner, R., and Herndl, G. (2011): Bacterially derived dissolved organic matter in the microbial carbon pump. In: "Microbial Carbon Pump in the Ocean" (Jiao, N., Azam, F., Sanders, S., Eds.), pp. 46-48.Science/AAAS, Washington, DC.

Brzezinski, M.A., Dumousseaud, C., Krause, J.W., Measures, C.I., and Nelson, D.M. (2008): Iron and silicic acid concen- trations together regulate Si uptake in the equatorial Pacific Ocean. Limnol. Oceanogr. 53: pp. 875–89.

Burd, A. B., Hansell, D.A., Steinberg, D.K., Anderson, T.R., Aristegui, J., Baltar, F., Beaupre, S.R., Buesseler, K.O., DeHairs, F., Jackson, G.A., Kadko, D.C., Koppelmann, R., Lampitt, R.S., Nagata, T., Reinthaler, T., Robinson, C., Robinson, B.H., Tamburini, C., and Tanaka, T. (2010): Assessing the apparent imbalance between geochemical and biochemical indicators of meso- and bathypelagic biological activity: What the @$#! is wrong with present calculations of carbon budgets?, Deep Sea Res., Part II, 57, pp. 1429–1592.

Carlson, C.A. (2002): Production and Removal Processes. In: "Biogeochemistry of Marine Dissolved Organic Matter" (Hansell, D.A., Carlson, C.A., Eds.), pp. 91-151.Academic Press, San Diego.

Chavez, F.P., and Barber, R.T. (1987): An estimate of new production in the equatorial Pacific. Deep-Sea Res. 34, pp. 1229-1243.

Chavez, F., and Toggweiler, J. (1995): Physical estimates of global new production: the upwelling contribution. In: "Upwelling in the Ocean: Modern Processes and Ancient Records" (Summerhayes, C., Emeis, K., Angel, M., Smith, R., Zeitzschel, B., Eds.), pp. 313-320. John Wiley and Sons, New York.

Chavez, F. P., Strutton, P.G., Friederich, G.E., Feely, R.A., Feldman, G.C., Foley, D.G., and McPhaden, M.J. (1999): Biological and Chemical Response of the Equatorial Pacific Ocean to the 1997-98 El Niño, Science, 286(5447), pp. 2126-2131.

Chavez, F. P., Ryan, J., Lluch-Cota, S.E., and Ñiquen, M.C. (2003): From Anchovies to Sardines and Back: Multidecadal Change in the Pacific Ocean, Science, 299(5604), pp. 217-221.

Chavez, F. P., Messié, M., and Pennington, J.T. (2011): Marine Primary Production in Relation to Climate Variability and Change, Annual Review of Marine Science, 3(1), pp. 227-260.

Coale, K.H., Fitzwarter, S.E., Gordon, R.M., Johnson, K.S., and Barber, R.T. (1996): Control of community growth and export production by upwelled iron in the equatorial Pacific Ocean Nature, 379 (1996), pp. 621–624.

Collins, M., et al. (2010): The impact of global warming on the tropical Pacific Ocean and El Niño , Nature Geosci, 3(6), pp. 391-397.

Cosca, C.E., Feely, R.A., Boutin, J., Etcheto, J., McPhaden, M.J., Chavez, F.P. and Strutton, P.G. (2003): Seasonal and interannual CO2 fluxes for the central and eastern equatorial Pacific Ocean as determined from fCO2-SST relationships. J. Geophysical Research 108(C8): 3278, (doi:3210.1029/2000JC000677).

Cresswell, G. (2000): Coastal currents of northern Papua New Guinea, and the Sepik River outflow. Marine and freshwater research, 51, 553–564. Retrieved from http://www.publish.csiro.au/?paper= MF99135.

Doney, S. C., Lima, I., Feely, R.A., Glover, D.M., Lindsay, K., Mahowald, N., Moore, J.K., and Wanninkhof, R. (2009): Mechanisms governing interannual variability in upper-ocean inorganic carbon system and air–sea CO2 fluxes: Physical climate and atmospheric dust, Deep Sea Research Part II: Topical Studies in Oceanography, 56(8–10), pp. 640-655.

Dunne, J. P., Sarmiento, J.L., and Gnanadesikan, A. (2007): A synthesis of global particle export from the surface ocean and cycling through the ocean interior and on the seafloor, Global Biogeochem. Cycles, 20, (doi:10.1029/2006GB002907).

Fay, A. R., and McKinley, G.A. (2013): Global trends in surface ocean pCO_2 from in situ data, Global Biogeochemical Cycles, 27(2), pp. 541-557.

Feely, R. A., Gammon, R.H., Taft, B.A., Pullen, P.E., Waterman, L.S., Conway, T.J., Gendron, J.F., and Wisegarver, D.P. (1987): Distribution of chemical tracers in the eastern equatorial Pacific during and after the 1982–1983 El Niño/Southern Oscillation event, Journal of Geophysical Research: Oceans, 92(C6), pp. 6545-6558.

Feely, R. A., Wanninkhof, R., Takahashi, T., and Tans, P. (1999): Influence of El Niño on the equatorial Pacific contribution to atmospheric CO_2 accumulation, Nature, 398(6728), pp. 597-601.

Feely, R. A., Boutin, J., Cosca, C.E., Dandonneau, Y., Etcheto, J., Inoue, H.Y., Ishii, M., Le Quéré, C., Mackey, D.J., McPhaden, M., Metzl, N., Poisson, A., and Wanninkhof, R., (2002): Seasonal and interannual variability of CO2 in the equatorial Pacific, Deep Sea Research Part II: Topical Studies in Oceanography, 49(13-14), pp. 2443-2469.

Feely, R. A., Takahashi, T., Wanninkhof, R., McPhaden, M.J., Cosca, C.E., Sutherland, S.C., and Carr, M.E. (2006): Decadal variability of the air-sea CO2 fluxes in the equatorial Pacific Ocean, J. Geophys. Res. 111.

Gehlen, M., Bopp, L., Emprin, N., Aumont, O., Heinze, C., and Ragueneau, O. (2006): Reconciling surface ocean productivity, export fluxes and sediment composition in a global biogeochemical ocean model Biogeosciences, pp. 521–537

Goldberg, S., Carlson, C., Brzezinski, M., Nelson, N., and Siegel, D. (2011): Systematic removal of neutral sugars within dissolved organic matter across ocean basins. Geophys. Res. Lett. 38, (doi:10.1029/2011GL048620).

Gorgues, T., Menkes, C., Slemons, L., Aumont, O., Dandonneau, Y., Radenac, M., and Moulin, C. (2010): A 1998 phytoplankton blooms in the equatorial Pacific Revisiting the La Nin. Deep-Sea Research Part I, 57(4), pp. 567–576. (doi:10.1016/j.dsr.2009.12.008).

Hales, B., Strutton, P.G., Saraceno, M., Letelier, R.M., Takahashi, T., Feely, R., Sabine, C., and Chavez, F.P. (2012): Satellite-based prediction of pCO2 in coastal waters of the eastern North Pacific. Progress in Oceanography 103: pp. 1-15.

Hansell, D.A., Carlson, C.A., Bates, N.R., and Poisson, A. (1997): Horizontal and vertical removal of organic carbon in the equatorial Pacific Ocean: a mass balance assessment. Deep-Sea Res. II 44, pp. 2115-2130.

Hansell, D.A., Carlson, C.A., Repeta, D.J., and Shlitzer, R. (2009): Dissolved organic matter in the ocean: A controversy stimulates new insights. Oceanography 22, pp. 202-211.

Hare, S. R., and Mantua, N.J. (2000): Empirical evidence for North Pacific regime shifts in 1977 and 1989, Progress In Oceanography, 47(2–4), pp. 103-145.

Hansell, D.A., Carlson, C.A., and Schlitzer, R. (2012): Net removal of major marine dissolved organic carbon fractions in the subsurface ocean. Global Biogeochem. Cycles 26, (doi:10.1029/2011GB004069).

Henson, S. A., Sarmiento, J. L., Dunne, J. P., Bopp, L., Lima, I., and Doney, S. C. (2010): Detection of anthropogenic climate change in satellite records of ocean chlorophyll and productivity. Biogeosciences, 7, pp. 621–640.

Ishii, M., Saito, S., Tokieda, T., Kawano, T., Matsumoto, K., and Inoue, H.Y. (2004): Variability of surface layer CO2 parameters in the western and central equatorial Pacific, in Global Environmental Change in the Ocean and Land, edited by M. Shiyomi, H. Kawahata, H. Koizumi, A. Tsuda and Y. Awaya, pp. 59–94, TERRAPUB.

Ishii, M., Inoue, H.Y., Midorikawa, T., Saito, S., Takayuki, T., Sasano, D., Nakadate, A., Nemoto, K., Metzl, N., Wong, C.S., and Feely, R.A. (2009): Spatial variability and decadal trend of the oceanic CO2 in the western equatorial Pacific warm/fresh water, Deep Sea Research Part II: Topical Studies in Oceanography, 56(8-10), pp. 591-606.

Ishii, M., Kosugi, N., Sasano, D., Saito, S., Midorikawa, T., and Inoue, H.Y. (2011): Ocean acidification off the south coast of Japan: A result from time series observations of CO2 parameters from 1994 to 2008, J. Geophys. Res., 116(C6), C06022.

Ishii, M., Feely, R.A., Rodgers, K.B., Park, G.-H., Wanninkhof, R., Sasano, D., Sugimoto, H., Cosca, C.E., Nakaoka, S., Telszewski, M., Nojiri, Y., Mikaloff Fletcher, S.E., Niwa, Y., Patra, P.K., Valsala, V., Nakano, H., Lima, I., Doney, S.C., Buitenhuis, E.T., Aumont, O., Dunne, J.P., Lenton, A., and Takahashi, T. (2014): Air-sea CO2 flux in the Pacific Ocean for the period 1990 - 2009, Biogeosciences,

Juranek, L. W., Feely, R.A., Peterson, W.T., Alin, S.R., Hales, B., Lee, K., Sabine, C.L., and Peterson, J. (2009): A novel method for determination of aragonite saturation state on the continental shelf of central Oregon using multi-parameter relationships with hydrographic data, Geophys. Res. Lett., 36.

Kao, H.-Y., and Yu, J.Y. (2009): Contrasting Eastern-Pacific and Central-Pacific Types of ENSO, Journal of Climate, 22(3), pp. 615-632.

Kug, J.-S., Jin, F.F., and An, S.I. (2009): Two Types of El Niño Events: Cold Tongue El Niño and Warm Pool El Niño, Journal of Climate, 22(6), pp. 1499-1515.

Landry, M.R., Selph, K.E., Taylor, A.G., Décima, M., Balch, W.M., and Bidigare, R.R. (2011): Phytoplankton growth, grazing and production balances in the HNLC equatorial Pacific. Deep-Sea Research II 58, pp. 524–535.

Larkin, N. K., and Harrison, D.E. (2005): On the definition of El Niño and associated seasonal average U.S. weather anomalies, Geophysical Research Letters, 32(13).

Laws, E. A., P. G. Falkowski, W. O. Smith, H. Ducklow, and McCarthy, J.J. (2000): Temperature effects on export production in the open ocean, Global Biogeochem. Cycles, 14, pp. 1231–1246.

Le Quere, C., M. R. Raupach, J. G. Canadell, and G. Marland (2009): Trends in the sources and sinks of carbon dioxide, Nature Geosci, advance online publication.

Le Quéré, C., Takahashi, T., Buitenhuis, E.T., Rödenbeck, C., and Sutherland, S.C. (2010): Impact of climate change and variability on the global oceanic sink of CO2, Global Biogeochemical Cycles, 24(4).

Letscher, R.T., Hansell, D.A., Carlson, C.A., Lumpkin, R., and Knapp, A.N. (2013): Dissolved organic nitrogen in the global surface ocean: Distribution and fate. Global Biogeochem. Cycles.

Lima, I.D., Lam, P.J., and Doney, S.C. (2014): Dynamics of particulate organic carbon flux in a global ocean model. Biogeosciences, 11, pp. 1177–1198.

Lutz, M. J., Caldeira, K., Dunbar, R.B., and Behrenfeld, M.J. (2007): Seasonal rhythms of net primary production and particulate organic carbon flux to depth describe the efficiency of biological pump in the global ocean, J. Geophys. Res., 112, C10011, (doi:10.1029/2006JC003706).

Mahadevan, A. (2001): An analysis of bomb radiocarbon trends in the Pacific. Marine Chem., 73, pp. 273-290.

Mantua, N. J., Hare, S.R., Zhang, Y., Wallace, J.M., and Francis, R.C. (1997): A Pacific Interdecadal Climate Oscillation with Impacts on Salmon Production, Bulletin of the American Meteorological Society, 78(6), pp. 1069-1079.

McPhaden, M. J., Busalacchi, A.J., Cheney, R., Donguy, J-R., Gage, K.S., Halpern, D., Ji, M., Julian, P., Meyers, G., Mitchum, G.T., Niiler, P.P., Picaut, J., Reynolds, R.W., Smith, N., and Takeuchi, K. (1998): The Tropical Ocean-Global Atmosphere observing system: A decade of progress, Journal of Geophysical Research: Oceans, 103(C7), pp. 14169-14240.

McPhaden, M. J. (1999): Genesis and Evolution of the 1997-98 El Niño, Science, 283(5404), pp. 950-954.

McPhaden, M. J., and Zhang, D. (2002): Slowdown of the meridional overturning circulation in the upper Pacific Ocean, Nature, 415(6872), pp. 603-608.

McPhaden, M. J., and D. Zhang (2004), Pacific Ocean circulation rebounds, Geophys. Res. Lett., 31(18), L18301.

McPhaden, M. J., Zebiak, S.E., and Glantz, M.H. (2006): ENSO as an Integrating Concept in Earth Science, Science, 314(5806), pp. 1740-1745.

McPhaden, M. J., Lee, T., and McClurg, D. (2011): El Niño and its relationship to changing background conditions in the tropical Pacific Ocean, Geophys. Res. Lett., 38(15), L15709.

McPhaden, M. J. (2012): A 21st century shift in the relationship between ENSO SST and warm water volume anomalies, Geophys. Res. Lett., 39(9), L09706.

Minobe, S. (2000): Spatio-temporal structure of the pentadecadal variability over the North Pacific, Progress In Oceanography, 47(2-4), pp. 381-408.

Moore, J.K., Doney, S.C., and Linday, K. (2004): Upper ocean ecosystem dynamics and iron cycling in a global three-dimensional model. Global Biogeochemical Cycles, Vol 18, (doi: 10.1029/2004GB002220).

Newman, M., Shin, S.I., and Alexander, M.A. (2011): Natural variation in ENSO flavors, Geophysical Research Letters, 38(14).

Patra, P. K., S. Maksyutov, M. Ishizawa, T. Nakazawa, T. Takahashi, and Ukita, J. (2005): Interannual and decadal changes in the sea-air CO2 flux from atmospheric CO2 inverse modeling, Global Biogeochemical Cycles, 19(4), GB4013.

Pennington, J.T., Mahoney, K.L., Kuwahara, V.S., Kolber, D.D., Calienes, R., and Chavez, F.P. (2006): Primary production in the eastern tropical Pacific: a review. Progress in Oceanography 69 (2–4), pp. 285–317.

Peterson, W. T., and Schwing, F.B. (2003): A new climate regime in northeast pacific ecosystems, Geophys. Res. Lett., 30.

Pfeil, B., et al. (2013): A uniform, quality controlled Surface Ocean CO2 Atlas (SOCAT), Earth Syst. Sci. Data, 5(1), pp. 125-143.

Quay, P. (1997): Was a carbon balance measured in the equatorial Pacific during JGOFS?, Deep Sea Research Part II: Topical Studies in Oceanography, 44(9–10), pp. 1765-1781.

Rayner, P. J., Law, R.M., and Dargaville, R. (1999): The relationship between tropical CO2 fluxes and the El Niño‐Southern Oscillation, Geophys. Res. Lett., 26(4), pp. 493-496.

Rodgers, K. B., Friederichs, P., and Latif, M. (2004): Tropical Pacific Decadal Variability and Its Relation to Decadal Modulations of ENSO, Journal of Climate, 17(19), pp. 3761-3774.

Ryan, J. P., Ueki, I., Chao, Y., Zhang, H., Polito, P. S., and Chavez, F. P. (2006): Western Pacific modulation of large phytoplankton blooms in the central and eastern equatorial Pacific. Journal of Geophysical Research, 111(G2), G02013. (doi:10.1029/2005JG000084).

Siegel, D.A., Buesseler, K.O., Doney, S.C., Sailley, S.F., Behrenfeld, M.J., and Boyd, P.W. (2014): Global assessment of ocean carbon export by combining satellite observations and food-web models. Global Biogeochemical Cycles. (doi: 10.1002/2013GB004743).

Slemons, L. O., Murray, J. W., Resing, J., Paul, B., and Dutrieux, P. (2010): Western Pacific coastal sources of iron, manganese, and aluminum to the Equatorial Undercurrent. Global Biogeochemical Cycles, 24(3), pp. 1–16. (doi:10.1029/2009GB003693).

Sutton, A. J., Feely, R.A., Sabine, C.L., McPhaden, M.J., Takahashi, T., Chavez, F.E., Friederich, G.E., and Mathis, J.T. (2014): Natural variability and anthropogenic change in equatorial Pacific surface ocean pCO2 and pH, Global Biogeochemical Cycles, 2013GB004679.

Takahashi, T., Feely, R.A., Weiss, R.F., Wanninkhof, R.H., Chipman, D.W., Sutherland, S.C., and Takahashi, T. (1997): Global air-sea flux of CO2: An estimate based on measurements of sea–air pCO2 difference, Proceedings of the National Academy of Sciences, 94(16), pp. 8292-8299.

Takahashi, T., et al. (2002): Global sea–air CO2 flux based on climatological surface ocean pCO2, and seasonal biological and temperature effects, Deep Sea Research Part II: Topical Studies in Oceanography, 49(9–10), pp. 1601-1622.

Takahashi, T., Sutherland, S.C., Feely, R.A., and Cosca, C.E. (2003): Decadal Variation of the Surface Water PCO2 in the Western and Central Equatorial Pacific, Science, 302(5646), pp. 852-856.

Takahashi, T., et al. (2009): Climatological mean and decadal change in surface ocean pCO2, and net sea-air CO2 flux over the global oceans, Deep Sea Research Part II: Topical Studies in Oceanography, 56(8-10), pp. 554-577.

Takahashi, T., Sutherland, S.C., and A. Kozyr, A. (2013): Global Ocean Surface Water Partial Pressure of CO2 Database: Measurements Performed During 1957-2012 (Version 2012), ORNL/CDIAC-160, NDP-088(V2012). Carbon Dioxide Information Analysis Center, Oak Ridge National Laboratory, U.S. Department of Energy, Oak Ridge, Tennessee, (doi: 10.3334/CDIAC/OTG.NDP088(V2012)).

Trenberth, K. E., and Hoar, T.J. (1996): The 1990–1995 El Niño-Southern Oscillation Event: Longest on Record, Geophysical Research Letters, 23(1), pp. 57-60.

Vecchi, G. A., Soden, B.J., Wittenberg, A.T., Held, I.M., Leetmaa, A., and Harrison, M.J. (2006): Weakening of tropical Pacific atmospheric circulation due to anthropogenic forcing, Nature, 441(7089), pp. 73-76.

Wang, X., Christian, J.R., Murtugudde, R., and Busalacchi, A.J. (2006): Spatial and temporal variability in new production in the equatorial Pacific during 1980–2003: Physical and biogeochemical controls. Deep-Sea Res. II 53, pp. 677-697.

Wanninkhof, R., et al. (2013): Global ocean carbon uptake: magnitude, variability and trends, Biogeosciences Discuss., 9(8), pp. 10961-11012.

Watanabe, M., and Nitta, T. (1999): Decadal Changes in the Atmospheric Circulation and Associated Surface Climate Variations in the Northern Hemisphere Winter, Journal of Climate, 12(2), pp. 494-510.

White Paper #7 - A Tropical Pacific Observing System in relation to biological productivity and living resources

Chavez, F.P.[1], Hobday, A.J.[2], Strutton, P.[3], Gierach, M.[4], Radenac, M.H.[5], Chai, F.[6], Lehodey, P.[7], Evans, K.[2], and Guevara, R.[8]

[1] Monterey Bay Aquarium Research Institute, United States
[2] CSIRO Marine and Atmospheric Research, Australia
[3] University of Tasmania, Australia
[4] NASA Jet Propulsion Laboratory, United States
[5] LEGOS, France
[6] University of Maine, United States
[7] CLS, France
[8] Instituto del Mar del Peru, Peru

1. Introduction

The tropical Pacific Ocean is remarkable for a variety of reasons. It is the most variable region of the oceans on interannual to centennial time scales (McPhaden et al., 2006; Chavez et al., 2011) and this ocean variability influences climate globally (Rasmussen and Wallace, 1983). It is also the largest natural source of carbon dioxide to the atmosphere, supplying up to 1 petagram (Pg) of carbon annually to the atmosphere (Feely et al., 2002; Chavez et al., 1999). Changes in primary production (PP) in the tropical Pacific dominate global anomalies in PP, resulting in decreases of an order of 3 Pg carbon per year during the large 1997-98 El Niño to increases of 2 Pg per year during La Niña (Chavez et al., 2011; Messie and Chavez, 2012); this interannual variability is on the same order as that observed globally by terrestrial primary producers (Field et al., 1998; Zhao and Running, 2010). The southeastern tropical Pacific supports the largest single species fishery in the world, the Peruvian anchoveta (*Engraulis ringens*) (Chavez et al., 2008). The western and central Pacific Ocean support 60% of global commercial catches of tuna that contributes up to 40% of national Gross Domestic Product (GDP) for countries in the region (order of 7 billion US dollars annually). These and other living marine resources fluctuate dramatically from the resulting physical variability (Barber and Chavez, 1983; Chavez et al., 2008; Williams and Terawasi, 2013). Given the importance of the region in driving global climate variability and the significance of resources throughout the region, it is of great value to society to have a well-designed and sustained observing system that provides a wide variety of information on the state of this large ocean ecosystem. This overview focuses on how a tropical Pacific observing system (TPOS) can support science and management of ocean ecosystems. Given that the existing TPOS is currently returning a reduced amount of information and the real prospects of continued declines we reconsider requirements for biologists, and recommend improvements given emerging technologies.

2. Biological dynamics

Dynamics in ocean physics in the tropical Pacific Ocean can be directly tied to variations in biological production regionally and globally (Figure 1; Chavez et al., 2011; Messie and Chavez, 2012, 2013). ENSO to multi-decadal variations with multiple nomenclatures, permeate through to biological productivity and living marine resources. In the following sections we discuss

processes, features and variations that impact biology at: 1) the interannual to centennial time scales; 2) the local or regional scale; and 3) the global scale.

The interannual to centennial time scales –The El Niño and La Niña cycle, often combined with their atmospheric counterpart the Southern Oscillation, and referred to as ENSO are presently the dominant mode of ocean variability in the tropical Pacific and globally (Philander, 1990; McPhaden et al., 2006; Desser et al., 2010; Messie and Chavez, 2011). The theory behind ENSO and its impact on biology are relatively well developed (Philander, 1990; McPhaden et al., 2006; Barber and Chavez, 1983). At the core are basin-scale changes in the depth of the thermocline (and nutricline, the region that separates nutrient poor waters at the surface to nutrient rich waters at depth) that are initiated in the western equatorial Pacific by anomalous winds. Atmospheric teleconnections propagate additional changes in ocean conditions. The character of ENSO varies from event to event and perhaps even on decadal to multi-decadal time scales (Takahashi et al., 2011); the past decades have seen the emergence or prominence of ENSO Modoki (Modoki is Japanese for like but not the same) or central Pacific ENSO (Figure 2.1).

Interest in decadal to multi-decadal variations was first spurred by the observations that some important fish populations vary dramatically over these time scales; as a result an additional family of recurring climatic phenomena have been identified over the past several decades (Mantua et al., 1997; Chavez et al., 2003; DiLorenzo et al., 2008). Those that are particularly germane to the Pacific include the multi-decadal Pacific Decadal Oscillation (Mantua et al., 1997), also referred to as the Interdecadal Pacific Oscillation (Power et al., 1999) or the El Viejo/La Vieja cycle (Chavez et al., 2003), and the decadal North Pacific Gyre Oscillation (DiLorenzo et al., 2008), which appears related to Modoki (Messie and Chavez, 2011). Robust theory behind these fluctuations is still emerging but their improved understanding and prediction lies at the core of a new TPOS.

Centennial variability in the tropical Pacific associated with changes from the medieval warm period (900-1300) to the Little Ice Age (LIA, 1400-1800) to the present warm period has been elucidated from paleo (cores in anoxic sediments, corals, etc.) proxies (Newton et al., 2006; Gutierrez et al., 2009; Sachs et al., 2009; Conroy et al., 2010; Mann et al., 2010; Chavez et al., 2011). The general picture that emerges is that during the LIA the Walker circulation in the atmosphere was shutdown in the tropical Pacific as a result of a southward migration of the mean position of the InterTropical Convergence Zone (ITCZ) across the equator (Sachs et al, 2009). This resulted in a flattening of the equatorial thermocline (normally deep in the west, shallow in the east and as a result the typical surface nutrient enrichment, anoxic conditions and abundant populations of anchoveta along the coast of Peru disappeared during LIA but returned with a bang after 1820 (Gutierrez et al., 2009).

Human activities have changed the concentration of elements in the atmosphere with potential impacts on temperature, climate and biological productivity. Human activities on living marine resources are more direct, through exploitation. Humans are also altering water quality in the oceans, most notably by the absorption of carbon dioxide derived from the burning of fossil resulting in so-called ocean acidification. Recent declines in subsurface oxygen concentrations may also be tied to a warmer planet (Stramma et al., 2007). Here we refer to these declines collectively as global change since climate change includes the natural variations described

above. Global change presents an emerging challenge to the sustainable management of living marine resources in the ocean, and robust information is essential to ensure future sustainability. Climate, water quality and harvest affect stocks of living marine resources, populations of non-target, dependent species and the ecosystem. To provide relevant advice we need an improved understanding of oceanic ecosystems and better information to parameterise the models that forecast the impacts of global change (Nicol et al., 2013).

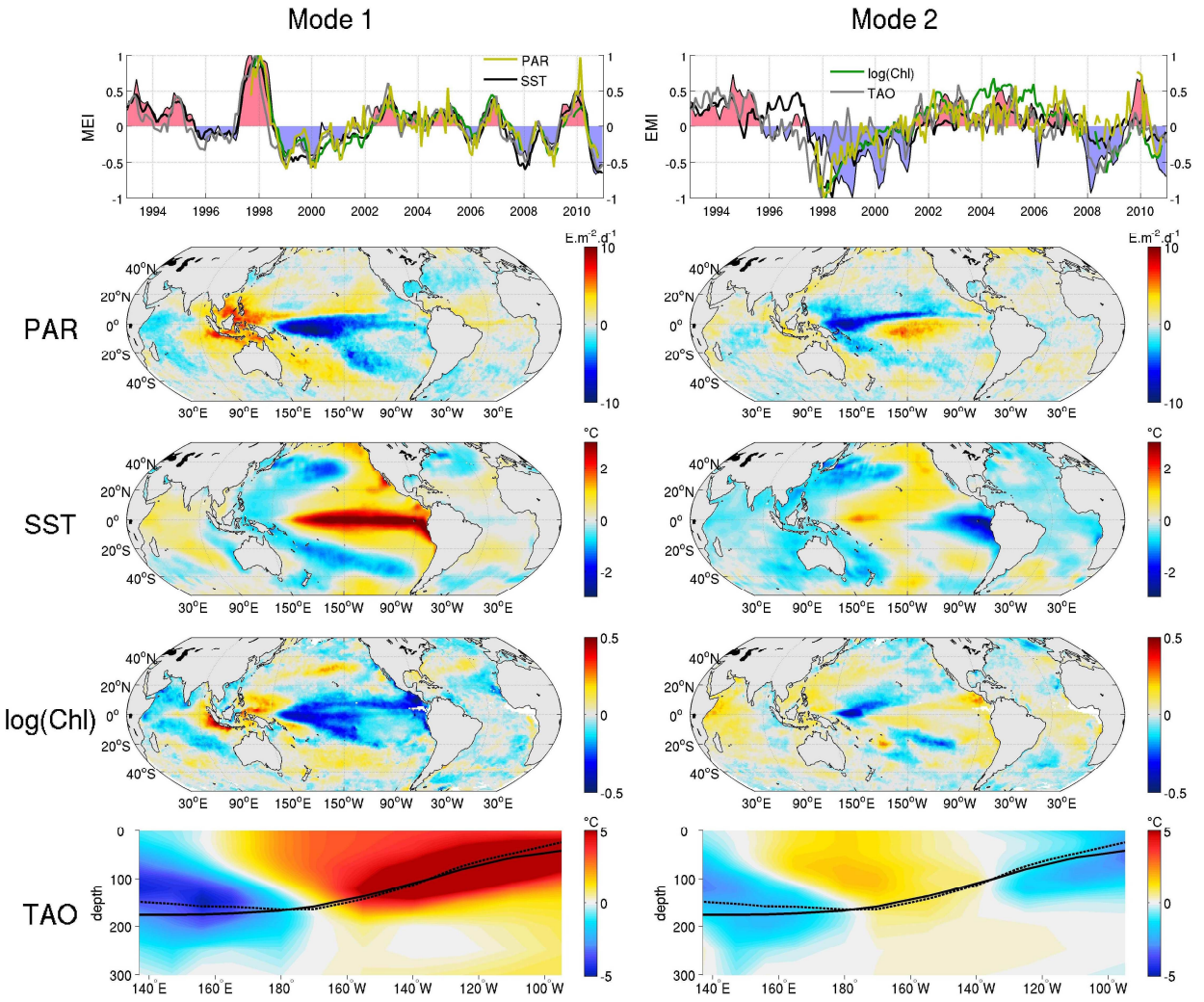

Figure 2.1 - Time series (top) of the Multivariate ENSO Index (MEI, left) and the ENSO Modoki Index (EMI, right) (shaded) together with the first (left) and second (right) principal components of global fields of Photosynthetically Active Radiation (PAR, equivalent to precipitation/cloudiness), Sea Surface Temperature (SST) and Chlorophyll (Chl). Also included are principal component time series (one, left and three, right) for equatorial TAO temperatures. Below the time series are the spatial distributions of the Empirical Orthogonal Functions (EOFs) of the first (left) and second (right) modes. The variations in the atmosphere (PAR), ocean (SST, TAO temperature), and atmosphere are synchronous across the two modes (and the ENSO indices) showing that they are intimately related. Figures redrawn from Chavez et al., 2011; Messie and Chavez, 2012; and Messie and Chavez, 2013.

The regional scale -There are well-known processes and features that influence and are diagnostic of biological productivity and its variability in the tropical Pacific. The dominant is thermocline dynamics (Cane, 1983; Barber and Chavez, 1983). This dynamic is directly linked to the atmosphere via the trade winds, which drive the accumulation of heat and water in the western Pacific raising the thermocline in the east and deepening it in the west (Philander, 1990). Since the thermocline and nutricline are linked, high levels of nutrients and carbon dioxide reach the surface in the east but are kept at depth in the west creating a east (more productive)/west (less productive) gradient in biological productivity (Barber and Chavez, 1983; Chavez et al., 1999). Surprisingly tuna populations thrive in the so-called oligotrophic warm pool (Lehodey et al., 1997); episodic enhanced productivity in the lee of islands or close to the western boundary may support these populations but further research is required. Periodically this east-west dynamic is perturbed by the phenomena described above. During El Niño (and El Viejo) the thermocline and nutricline are deepened in the east while rising in the west Barber and Chavez, 1983). The thermocline dynamics and the trades set up the western Pacific warm pool and the eastern/central Pacific cold tongue whose size and character are also modulated by climate (Chavez et al., 1999). A perplexing feature of the cold tongue is the reduced biological productivity relative to the input of macro nutrients such as nitrate leading a condition referred to as high nitrate/nutrient low chlorophyll (HNLC). This condition could also be referred to as high CO_2 low chlorophyll (HCLC) since the reduced biological productivity can be directly linked to the large natural source of CO_2 to the atmosphere. The favored hypothesis is that the HNLC condition is a result of iron deficiency (Martin et al., 1996) associated with weak input from the atmosphere. Periodically the Equatorial Undercurrent (EUC) delivers increased levels of iron to the cold tongue, resulting in large and unusual blooms of phytoplankton (Chavez et al., 1999; Ryan et al., 2002). It is hypothesized that during these times the EUC recruits this iron from the continental shelves in the New Guinea region, a behavior that may also be climate modulated. The front that sets up between these the warm pool and cold tongue, as well as other fronts between warm and cold features such as the North Equatorial Counter Current (NECC) and the South Equatorial Current (SEC), the so-called Equatorial Front (EF) are locations of enhanced biological activity. Along the EF Tropical Instability Waves are generated creating spectacular features that are clearly visible from space.

The global scale – Fast moving waves (Kelvin, 200 km per day) generated by the westerly wind anomalies in the western Pacific propagate thermocline anomalies from the western to the eastern Pacific ocean. Upon reaching the eastern Pacific these waves propagate poleward expanding the tropical dynamics to higher latitudes. A complex set of slower travelling waves (Rossby, Yanai, etc.) propagate back towards the western Pacific. In the atmosphere, teleconnections change the intensity and position of low and high pressure systems globally. These oceanic and atmospheric processes result in global biological impacts of tropical variability.

THE USER COMMUNITY AND HOW THEY USE THE EXISTING TPOS

The user community is broad from managers to scientists. These include:

1) Scientists are interested in:

- Primary production
- Zooplankton
- Fish
- Large Marine Vertebrates

2) Industry interested in:

- The harvest of living marine and terrestrial resources

3) Managers interested in:

- Regulation of harvest of living marine and terrestrial resources
- Conservation of marine life
- Ocean health

3. TPOS user examples

Remote Sensing

Remote sensing of ocean color from space began in 1978 with the successful launch of NASA's Coastal Zone Color Scanner (CZCS). Since then multiple ocean color sensors have been launched (e.g., MODIS, SeaWiFS, MERIS, HICO, VIIRS) and still more are planned for the near future by various space agencies. The significance of ocean color sensors is the ability to provide a continuous, global view of near surface ocean bio-optical properties to the Earth science community, from which chlorophyll-a (chl-a), inorganic and organic matter, colored dissolved organic matter, primary production, phytoplankton functional types, and other biological variables are derived. While remotely sensed ocean color data are informative of biological activity on the ocean surface, what is happening subsurface, and the physical or chemical mechanisms responsible for the biological responses remains unclear. Thus, in situ observations are necessary in coincidence with satellite data to fill in the gaps and to validate ocean color estimates.

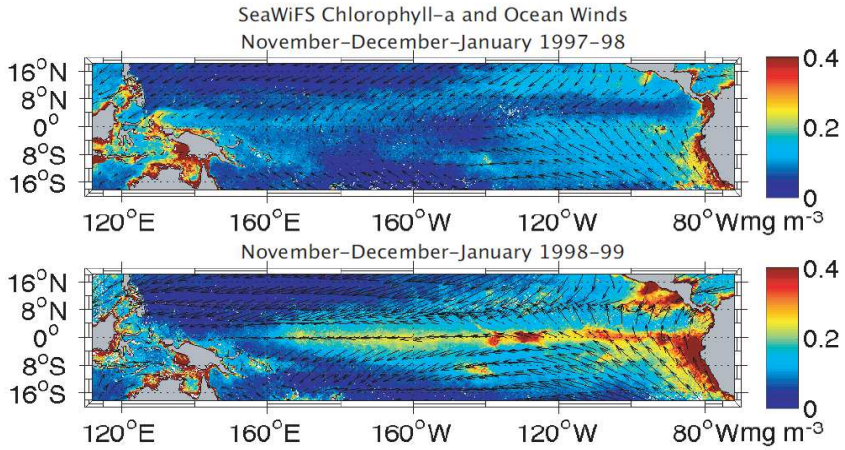

Figure 3.1 - November-December-January (NDJ) averaged SeaWiFS chl-a in the equatorial Pacific Ocean for the (top) 1997-98 El Niño and (bottom) 1998-99 La Niña overlaid with Cross-Calibrated Multi-Platform (CCMP) ocean surface wind vectors.

For a short duration in the late 1990s, biological and chemical sensors (i.e., continuous pCO_2 analyzers, three biospherical irradiance meters, nitrate analyzers, and PAR sensors) were added by MBARI to several TAO buoys that permitted researchers to directly and continuously monitor biological productivity improving our understanding of biophysical coupling from interannual (ENSO events) to intra-seasonal (tropical instability waves) timescales (e.g., Chavez et al., 1998; Chavez et al., 1999; Strutton et al., 2001). Taking advantage of the spatial coverage of satellite sensors, past studies have illustrated a decrease (increase) in near surface phytoplankton biomass and productivity in the eastern Pacific during El Niño (transition and La Niña) events in association with weakened or possibly reversed (enhanced) trade winds (Figures 2.1 and 3.1). The vertical dimension of TAO data, such as the 20°C isotherm depth and depth profiles of temperature and zonal currents, allows monitoring subsurface variations that contribute to understanding the surface biological observations.

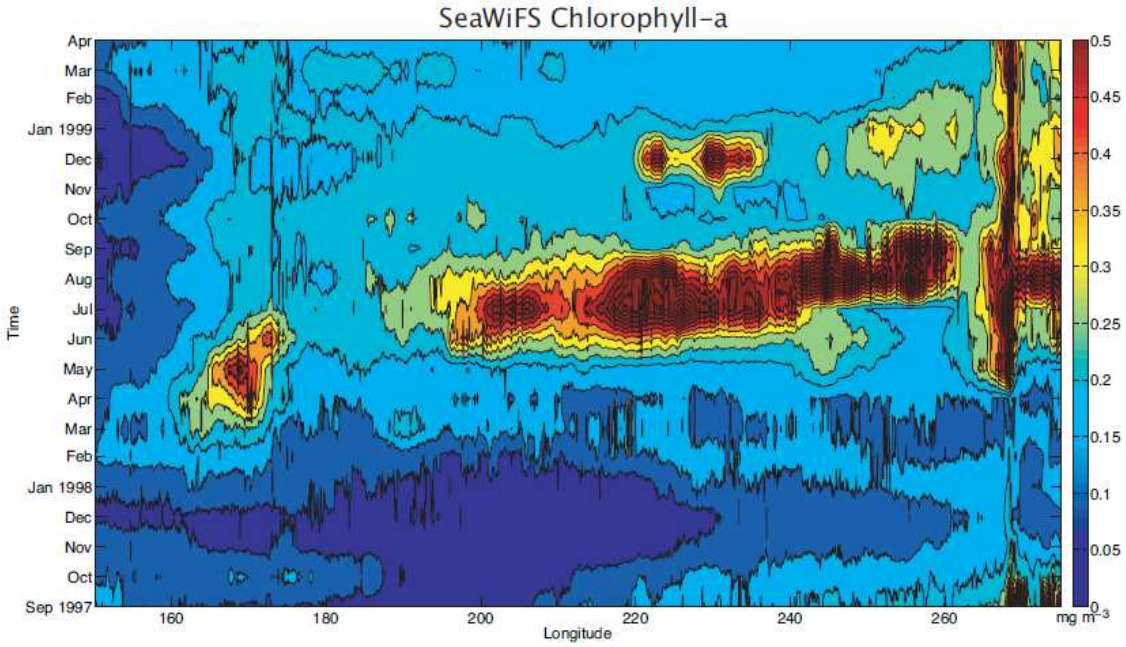

Figure 3.2 - 2°N–2°S averaged SeaWiFS chl-a (mg m^{-3}) in the equatorial Pacific Ocean from September 1997 – April 1999, showing the 1997-98 El Niño, 1998 transition (or recovery), and 1998-99 La Niña.

The depth of the 20°C isotherm is generally used as a proxy for the thermocline and nutricline, whereas maximum eastward velocities are used as proxies for the Equatorial Undercurrent, which is an important nutrient source for the equatorial Pacific. TAO data has shown that the thermocline and nutricline deepen (shoal) and the EUC is suppressed (enhanced) in the eastern Pacific during El Niño (La Niña), both of which decrease (increase) the flux of nutrients to the euphotic zone reducing (increasing) phytoplankton biomass and productivity observed at the surface by satellites (Figures. 3.1-3.3). The scenarios provided above are classic examples of the biophysical response to El Niño and La Niña events. However, the frequency and intensity of ENSO events are highly variable, eliciting different physical and thereby biological responses. Such variability has led to the idea of two flavors of El Niño: the classic, Eastern Pacific (EP) El Niño with surface anomalies spreading from the South American coast to the central basin and the Central Pacific (CP) El Niño (Kao and Yu, 2009), otherwise known as the dateline El Niño

(Larkin and Harrison, 2005), El Niño Modoki (Ashok et al., 2007), or warm-pool El Niño (Kug et al., 2009), with anomalies restricted to the central basin. TAO data in concert with satellite observations are extremely important to our understanding of how biology, the physical environment, and their coupling will respond to ENSO variability in the equatorial Pacific. Numerous scientific articles have illustrated the need for such coincident observations including, but not limited to: Chavez et al., 1998 and 1999; Gierach et al., 2012 and 2013; Messié et al., 2006; Messié and Chavez, 2012 and 2013; Radenac et al., 2001, 2012, and 2013; Ryan et al., 2002 and 2006; Strutton et al., 2001; Turk et al., 2001 and 2011; Wilson and Adamec, 2001.

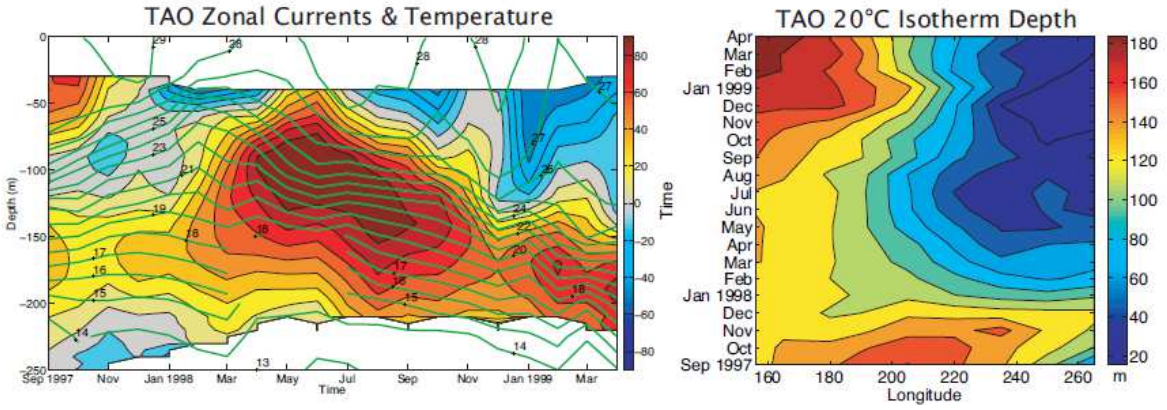

Figure 3.3 - (left) Subsurface zonal currents (cm s^{-1}) and temperature (°C; green contours) from the TAO array at 0°N, 165°E, and (right) 2°N–2°S averaged TAO array 20° isotherm depth (m) in the equatorial Pacific Ocean from September 1997 – April 1999, showing the 1997-98 El Niño, 1998 transition (or recovery), and 1998-99 La Niña.

Existing TPOS observations of the physical and biological/biogeochemical environment have been extremely important in the validation of past and present satellite observations, as well as filling in information about subsurface conditions that are incapable from satellite. However, improvements are necessary to the existing TPOS framework to usher in the next era of satellite observations and further our understanding of the ocean processes/dynamics in the Pacific. Upcoming satellite missions, including the NASA Pre-Aerosol, Cloud and ocean Ecosystem (PACE) mission, will usher in a new era in ocean color. PACE will address outstanding ocean science questions, such as separating absorbing components, assessing ocean particle abundances and living carbon stocks, nutrient stressors, and phytoplankton functional groups. Such problems have been difficult to address given limited capabilities of earlier satellite sensors (e.g., CZCS, SeaWiFS, MODIS, VIIRS), but PACE proposes advanced global remote sensing capabilities, such as hyperspectral imaging with extended spectral coverage. TPOS should incorporate instruments that can provide calibration/validation capabilities and help explore the refined science goals/questions of PACE (e.g., hyperspectral measurements of down-welling irradiance and upwelling radiances, and phytoplankton composition) and other future satellite missions. Overall, the future TPOS framework should continue and expand upon key physical observations, incorporate biological and biogeochemical observations at multiple sites for continuous duration, and provide observations with gap-free temporal resolution.

The Peruvian anchoveta fishery

Fishing is an important activity for Perú, since it generates order of 2 billion dollars annually, with interesting perspectives for growth. However, this activity is affected in a recurring manner by climate variations that disrupt the dynamics of marine living resources that support it (Figure 5), in particular the abundance of anchoveta (*Engraulis ringens*) (Barber and Chavez, 1983). This species supports harvests on the order of 5 to 6 million tons per year which is primarily used to produce fish meal and oil, utilized in a variety of ways by humans. More recently the anchoveta has started to be consumed directly. El Niño events of varying intensities not only affect the fishing industry but also the climate throughout the country and therefore the entire Peruvian economy. Extreme rainfall in northern and central Peru cause floods and destroy services including transportation. Large El Niño events like 1982/83 and 1997/98 caused losses of the order of 3 to 4 billion dollars.

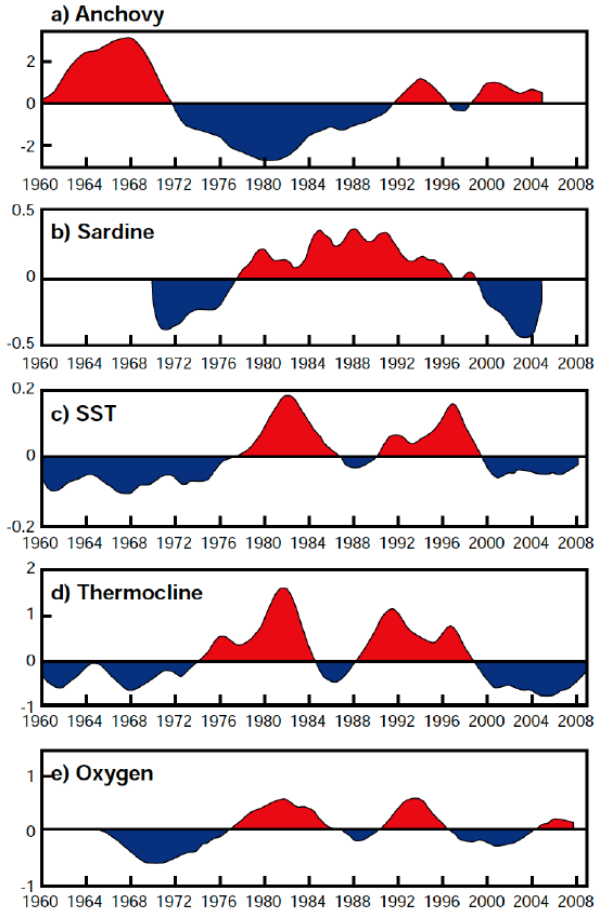

Figure 3.4 - Time series of anomalies in fish catch (anchoveta and sardine) compared to anomalies in a series of environmental variables (Empirical Orthogonal Function of sea surface temperature (SST) in the Peru domain, depth of the 15°C isotherm close to the coast of Peru and surface oxygen off Peru). There is clear alignment of the positive anomalies in the sardine catch with the positive anomalies in the environmental parameters for about 20 years. The negative anchoveta catch anomalies are of the same length but begin and end earlier (Figure by Purca, S., IMARPE).

The tight coupling between ocean variability and the biological processes of the species that support the fishing industry have driven the Instituto del Mar del Peru (IMARPE) to develop an observation strategy geared at monitoring for El Niño. The strategy seeks to observe climate driven changes in real time to provide scientific and technical information for fisheries management and other government activities. The ability to provide real time information to the managers improved dramatically in the 1990s when information from the TAO array was provided over the internet. This information has not only led to a better understanding of these climatic phenomena but also to better forecasts. On a monthly to seasonal basis IMARPE utilizes TAO data to schedule their field activities. Given Peru's location at the eastern terminus of the Pacific basin the TAO data provides timely information regarding the arrival of down-welling Kelvin waves since these can be forecast and followed 8 to 10 weeks prior to their arrival to the Peruvian coastal ocean. The waves affect the not only the availability of anchoveta but also that of the jack mackerel (*Trachurus murphyi*), the horse mackerel (*Scomber japonicus*) and the jumbo squid (*Dosidicus gigas*). Eastern Pacific TAO buoys provide information about the Equatorial Undercurrent, an important ventilator of the anoxic waters off Peru. This ventilation regulates the abundance and distribution of the hake (*Merluccius gayi peruanus*). The real time TAO data is also used by a consortium of western South American countries (Colombia, Ecuador, Peru and Chile), under an organization called de Estudio Regional del Fenómeno El Niño (ERFEN), which supports a wide variety of government activities, including disaster preparedness. On longer time scales the variability of anchovies and sardines can be directly related to variations in the large scale physical environment (Figure 3.4).

Tuna and the Pacific

Tunas and billfishes are particularly valuable (Collette et al., 2011), with worldwide ex-vessel values approaching $9 billion in the 1990s, exceeded only by the value of the world's small pelagic and demersal fisheries (Sumaila et al., 2007) (see Figure 3.5).

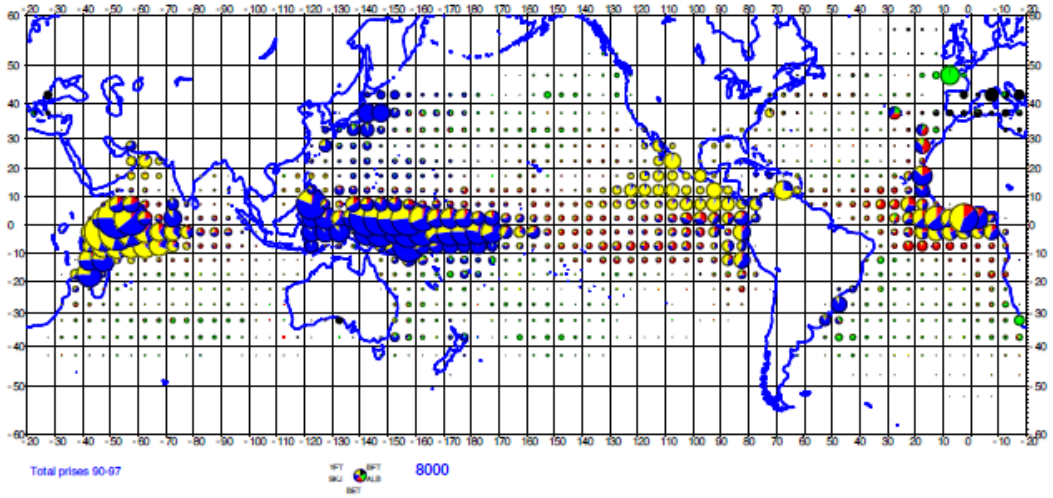

Figure 3.5 - Total global tuna (skipjack, yellowfin, bigeye, albacore and Bluefin) catch from 1990-97. Evident are the large tropical concentrations (Figure by Fonteneau, A.).

WCPO tuna fisheries were worth about $4 billion in 2007 (Reid 2007; Parris 2010a). Tuna fisheries comprised about 11% of the GDP of the region's 22 island nations in 1999, and half of total export value (Gillett et al. 2001). Moreover, Pacific Island Countries and Territories (PICTs) typically derive 5-8% of wage employment from tuna fisheries and related industries. As noted by Gillett et al. (2001), "for people of the Pacific, tuna is not only a key resource but often *the* key resource."

Despite being regarded as a low productivity region, the equatorial warm pool region in the western Pacific Ocean supports the world's largest tuna fishery (50-60% of global catches). Tuna fisheries are central to socio-economic security in many PICTs, providing income and employment. The western equatorial region of the Pacific around Papua New Guinea/the Solomons Islands is a key region driving physical features and productivity within the warm pool region and these processes have impacts across the whole Pacific basin, particularly in association with ENSO. Although central to ecosystem productivity, the dynamics of the western warm pool region are poorly understood and satellite imagery and ocean models currently are not able to capture physical and biological processes in the area effectively. This has flow-on implications for understanding the impacts of climate variability and change on tuna populations. Fisheries oceanographers seek an improved understanding of the circulation and dynamics of water masses in western warm pool region and their coupling to the biogeochemistry of the water column.

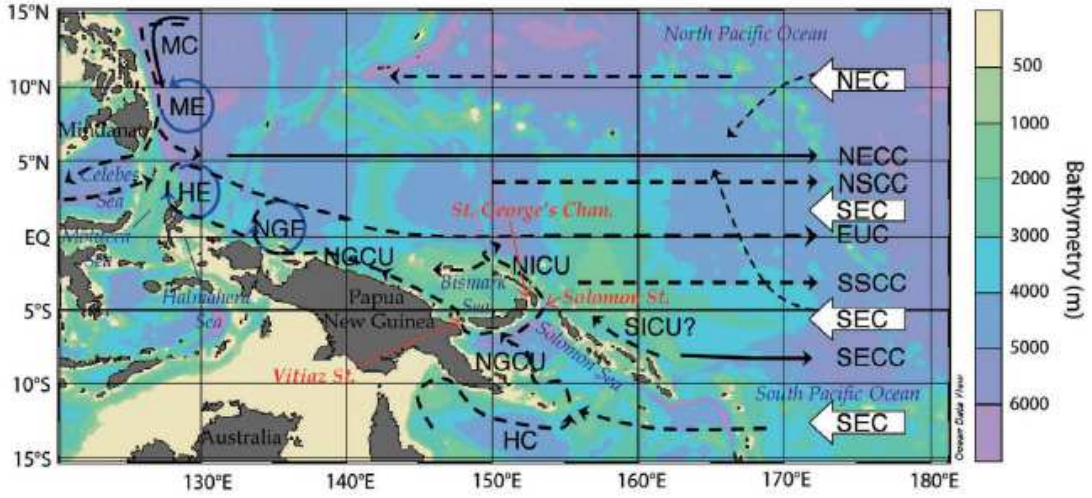

Figure 3.6 - Schematic map of major currents in the equatorial western Pacific region.

The physical oceanography of the western equatorial Pacific Ocean is dominated by a number of major ocean currents including the North Equatorial Current (NEC), the South Equatorial Current (SEC) and the sub-surface Equatorial Under-Current (EUC; Figure 3.6). The NEC and SEC are driven by prevailing easterly trade winds, and as water moves from the eastern to the western Pacific, a thick layer of warm water (>29°C) known as the warm pool is formed (Lehodey et al., 2011; Figure 3.7). The thermal stratification of the warm pool delimits subsurface nutrients from the surface, resulting in the warm pool being largely nutrient depleted. As both the NEC and SEC encounter islands, and eventually the western edge of the basin, they bifurcate into a number of currents some of which, particularly the New Guinea Coastal

Undercurrent (NGCUC) and the Mindano Current contribute to the warm pool and EUC (Ganachaud et al., 2011). Along the equatorial Pacific, the EUC transports water eastward from north of Papua New Guinea (PNG) to the coast of South America where it upwells into the SEC.

Water transported by the EUC is considered to contribute significantly to equatorial thermocline waters and is suspected to modulate ENSO. The EUC is the primary source of upwelled biologically available iron in the photic layer and variability of biological productivity in the region is driven by variability in this iron supply (Ryan et al. 2006). Iron is thought to derive mainly from the NGCUC and is potentially determined by sedimental release along the continental slope north of PNG and hydrothermally.

Oceanic fisheries and particularly tuna fisheries in the western and central Pacific are intimately linked to the western Pacific warm pool. Close to 60% of global tuna catches in 2009 were caught in the western and central Pacific Ocean, around 95% of which were caught in the EEZs of countries situated in the warm pool region (Lehodey et al., 2011). Distributions of tuna follow inter-annual variability in the warm pool associated with ENSO which lead to large fluctuations in catches within country EEZs (Figure 3.7). Variation in productivity associated with ENSO also has flow-on effects on tuna abundances (Lehodey et al., 2011), which then flow-through to neighboring fisheries including Australian fisheries. The distribution of such large tuna populations in a region largely considered as oligotrophic appears to be a paradigm and the physical and biological processes that support such large tuna populations in the region are not well understood.

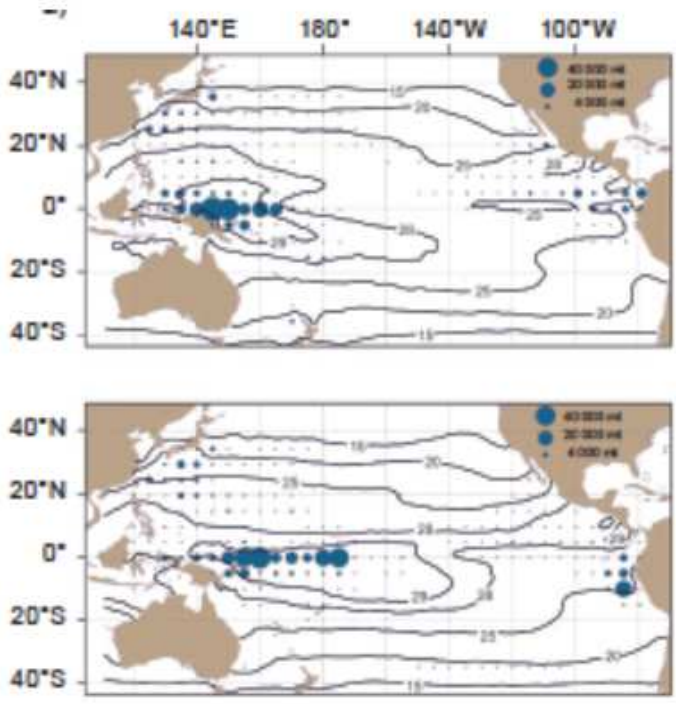

Figure 3.7 - Catches of skipjack tuna and mean sea surface temperatures during a La Niña (top) and El Niño (bottom). The 29°C contour depicts the area of the warm pool (taken from Lehodey et al., 2011).

Tropical tuna fisheries provide a vital contribution to the development goals of PICTs, with many depending heavily on the benefits derived from these fisheries. License fees from distant water fishing nations operating in the region contribute as much as 40% of government revenue and domestic tuna fishing fleets and local fish processing can account for up to 20% of national gross domestic product. Tuna resources provide an important source of jobs and opportunities to earn income and there are active plans to domesticate more of the benefits associated with tuna resources, increasing local job opportunities (Bell et al., 2011).

Given the importance of tuna to countries in the region, there is a need to understand the physical and biological processes that support tuna populations and the impacts of both short and longer-term variability in these. Satellite imagery does not fully capture the physical and biological processes driving productivity as many of the processes occur below the ocean surface layer and the present state of ocean models do not fill this void which requires *in situ* observations (Le Borgne et al. 2011). The ability to provide robust projections of ecosystems and their influence on tuna populations is therefore limited and recent assessment of the vulnerability of oceanic fisheries to climate change have highlighted these limitations (Lehodey et al., 2011). Improved observations and models and, in association, improved projections of tuna stocks, are required by regional fisheries management organizations and agencies to assess the socio-economic implications of changes in tuna catches and adjust preliminary recommended adaptations (Bell et al., 2011b) to minimize any risks and maximize opportunities.

Key features of uncertainty that could be resolved by an improved observing array include:

1. circulation in the far western Pacific, including the EUC origins, which has flow-on effects for understanding the climate of the equatorial Pacific, and in turn, global climate.
2. transport and distributions of trace metals and macro and micro-nutrients, particularly coupling of water mass dynamics and biogeochemistry

with this understanding, gained from improved observations, the fisheries oceanographers can then begin to determine the;

3. coupling of food webs supporting tuna populations to the biogeochemistry of the western warm pool region and in particular transfer of energy from nutrients to plankton to zooplankton to nekton
4. composition and structure of food webs supporting tuna populations, particularly estimates of the relative abundance of key functional groups in the food web of the western warm pool region

Ecosystem Modeling

Information collected by the physical TPOS has been of great value for validation of the emerging next generation ecosystem models (Figure 3.8). These models are now being used to develop operational models for tuna management for example (Figure 3.9). What is currently missing is validation information for chemistry and biology. Even a limited amount of such information would serve to greatly improve our existing models.

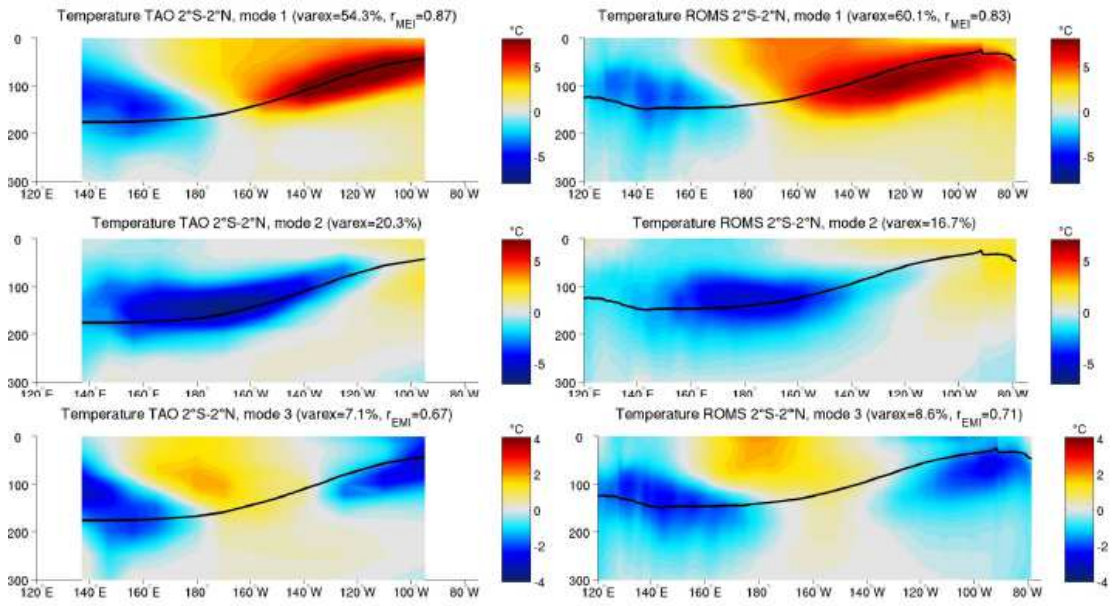

Figure 3.8 - Comparison of data from the TPOS and the output of a coupled physical-biological model. Shown are the first 3 EOFs of temperature (left – data; right –model).

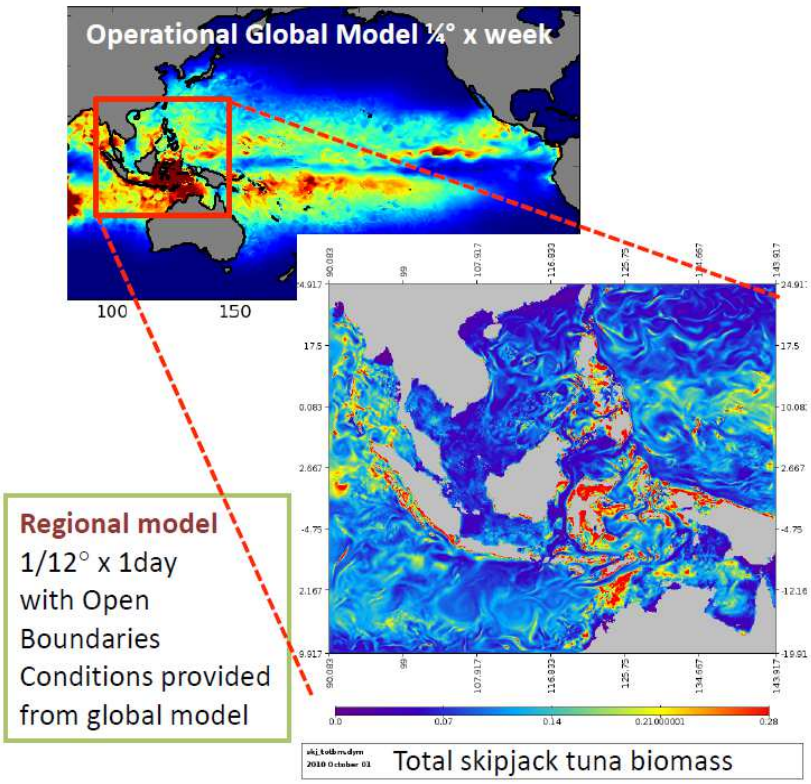

Figure 3.9 - Example of a coupled global and regional model utilized for real time management of tuna stocks in the western Pacific.

4. A biological TPOS – requirements and how to achieve them

The biological and fisheries community routinely utilizes existing physical information (i.e., surface winds, and currents, temperature and salinity with depth) from the present TPOS. Ideally and in the future this information would be daily to weekly gap-free temporal resolution over the entire tropical Pacific with order of 5-10 degree latitude spatial resolution, higher in some areas. A future TPOS would also benefit greatly by the addition of vertically distributed bio-optical, chemical, and ecological observations at a subset of locations to: 1) validate satellite measurements; 2) initialize and validate ecosystem models; and 3) be extrapolated over the entire tropical Pacific using physical *in situ* observations, remote sensing and modeling. In the following sections we assume that physical observations, including those from remote sensing (winds, sea level, SST, salinity, ocean color) will be available at about the resolution described above and focus on the measurements and locations that might be augmented with bio-optical, chemical and ecological sensors and samplers. We build on the biogeochemistry white paper. We try to avoid specifying a particular platform unless it is felt that there are no other options.

A biological TPOS for 2020 should support both operational (what is ready) and evolving/needed technologies (important information but not presently ready for operations). The use by the biology and fisheries communities is as follows:

1) Utilize information provided by the in situ physical and remote sensing observing system to: a) Determine the state of the tropical Pacific and direction of change (e.g. warming or cooling); b) Assimilate information into numerical models with embedded ecosystems to produce nowcasts and forecasts; c) Use the information in statistical models that predict biological fields.
2) At strategic locations augment the physical TPOS with biogeochemical and ecological measurements to calibrate/validate: a) remote sensing products; b) Ecosystem models; c) Statistical models that utilize the physical information to predict biological fields. The payoff for these is great likely improving estimates from physics alone by 50-100%.
3) Implement a technology development effort to develop critical sensors and systems (i.e. iron, eDNA, etc,) that can be added to the TPOS; this requires that the TPOS be designed/implemented with expansion capabilities.

The desired outputs:

1) Remote sensing calibration/validation of ocean color
2) Concentrations of chemical elements (nutrients) that drive primary production or determine the distribution of animals (e.g. oxygen)
3) Rates of primary production and the composition of the primary producers
4) The growth and distribution of forage species (zooplankton to small pelagic fish)
5) The growth and distribution of large marine vertebrates (living marine resources to endangered charismatic species)

How might these be achieved?

1) Vertically distributed hyperspectral measurements of down-welling irradiance and upwelling radiances at order of 20 locations in the tropical Pacific.

2) Vertically distributed concentrations of oxygen, nitrate and pH at order of 40 locations in the tropical Pacific. Investment in autonomous sensors for iron.
3) Vertically distributed concentration of chlorophyll and samples for the analysis of: a) Triple isotopes of oxygen; b) Composition of the primary producers (and the entire food web via environmental DNA) at order of 20 locations in the tropical Pacific.
4) Acoustic estimates of forage species biomass from fixed and moving platforms.
5) Tracking of tagged large marine vertebrates.
6) Regional and basin-wide ecosystem models.

What platforms could be instrumented to supply these data?

1) Ships – important to consider this part of a TPOS. Certain biological and biogeochemical measurements can only be made from these platforms.
2) Moorings – bio-optics, nutrients, carbon, samples, acoustics
3) Argo floats – bio-optics, nutrients, carbon
4) Gliders (profiling and wave – other ASVs)/Long Range AUVs – bio-optics, nutrients, carbon, samples, acoustics
5) Large Marine Vertebrates – tags, T, S

There is a requirement for broad-scale TPOS information for biology and biogeochemistry. This broad-scale coverage can be achieved by collection of data from a subset of the physical TPOS and development of basin-wide and regional relations/models that link physics with biogeochemistry and biology. The regional focus would include:

1) The eastern to central Pacific cold tongue, where biological productivity is enhanced and variability is greatest.
2) The eastern boundary where the production of small pelagic fish is enhanced. The boundary regions in general are regions of enhanced production of living marine resources.
3) The western Pacific oligotrophic warm pool where the chlorophyll maximum is deepest, requiring subsurface measurements for accurate estimates of primary production. Tuna populations are enhanced in this region as well.
4) The region north or on the Equatorial Front.

5. Conclusions/recommendations

There are clear needs for biogeochemical and biological information from the tropical Pacific across a wide variety of time and space scales. The requirements are diverse and include:

1) The physical state and direction of change. Multi-decadal variations with strong ecological imprints are particularly challenging.
2) The biogeochemical state and direction of change.
3) The ecological state and direction of change.
4) The synthesis of information for decision making purposes regarding biology and biogeochemistry.

The recommendations are:

1) Have adequate physical information to: a) Determine the state of the Tropical Pacific Ocean; b) Assimilate into numerical models with embedded ecosystems and utilize model simulations; c) Develop algorithms that predict biological fields.
2) At strategic locations augment the physical TPOS with biogeochemical and ecological measurements to calibrate/validate: a) remote sensing products; b) Ecosystem models; c) Algorithms that utilize the physical information to predict biological fields.
3) Implement a technology development effort to develop critical sensors and systems (i.e. iron, eDNA, etc,) that can be added to the TPOS; this requires that the TPOS be designed/implemented with expansion capabilities.

References

Ashok, K., Behera, S.K., Rao, S.A., Weng, H., and Yamagata, T. (2007): El Niño Modoki and its possible teleconnection, J. Geophys. Res., 112, C11007, (doi:10.1029/2006JC003798).

Bell, J.D., Reid, C., Batty, M.J., Allison, E.H., Lehodey, P., Rodwell, L., Pickering, T.D., Gillett, R., Johnson, J.E., Hobday, A.J., and Demmke, A. (2011): Implications of climate change for contributions by fisheries and aquaculture to Pacific Island economies and communities. pp. 733–801 in Bell, J.D., Johnson, J.E., and Hobday, A.J. (editors): Vulnerability of tropical Pacific fisheries and aquaculture to climate change. Secretariat of the Pacific Community. Available for download at www.spc.int.

Chavez, F.P., Strutton, P.G., and McPhaden, M.J. (1998): Biological-physical coupling in the central equatorial Pacific during the onset of the 1997-98 El Niño, Geophys. Res. Lett., 25, pp. 3543-3546.

Chavez, F.P., Strutton, P.G., Friederich, G.E., Feely, R.A., Feldman, G.C., Foley, D.G., and McPhaden, M.J. (1999): Biological and chemical response of the equatorial Pacific Ocean to the 1997-98 El Niño, Science, 286, (doi:10.1126/science.286.5447.2126).

Chavez, F., Messié, P.M., and Pennington, J.T. (2011): Marine primary production in relation to climate variability and change. Annual Review of Marine Science, 3; pp. 227–60, (doi:10.1146/annurev.marine. 010908.163917).

Gierach, M. M., Lee, T., Turk, D., and McPhaden, M.J. (2012): Biological response to the 1997-98 and 2009-10 El Niño events in the equatorial Pacific Ocean. Geophys. Res. Lett., 39, L10602, (doi:10.10.29/2012GL051103).

Gierach, M. M., Messié, M., Lee, T., Karnauskas, K.B., and Radenac, M.H. (2013): Biophysical Responses near Equatorial Islands in the Western Equatorial Pacific Ocean during El Niño/La Niña Transitions. Geophys. Res. Lett., (doi:10.1002/2013GL057828).

Kao, H.-Y., and Yu, J.Y. (2009): Contrasting eastern-Pacific and central- Pacific types of ENSO, J. Clim., 22, pp. 615–632, (doi:10.1175/ 2008JCLI2309.1).

Kug, J.-S., Jin, F.F., and An, S.I. (2009): Two types of El Niño events - Cold tongue El Niño and warm pool El Niño, J. Clim., 22, pp.1499–1515, (doi:10.1175/2008JCLI2624.1).

Larkin, N. K., and Harrison, D.E. (2005): Global seasonal temperature and precipitation anomalies during El Niño autumn and winter, Geophys. Res. Lett., 32, L16705, (doi:10.1029/2005GL022860).

Le Borgne, R., Allain, V., Griffiths, S.P., Matear, R.J., McKinnon, A.D., Richardson, A.J., and Young, J.W. (2011): Vulnerability of open ocean food webs in the tropical Pacific to climate change. pp. 189 – 249 in Bell, J.D., Johnson, J.E., and Hobday, A.J. (editors): Vulnerability of tropical Pacific fisheries and aquaculture to climate change. Secretariat of the Pacific Community. Available for download at www.spc.int.

Lehodey, P., Hampton, J., Brill, R.W., Nicol, S., Senina, I., Calmettes, B., Pörtner, H., Bopp, L., Ilyina, T., Bell, J.D., and Sibert, J. (2011): Vulnerability of oceanic fisheries in the tropical Pacific to climate change. pp. 433 – 492 in Bell, J.D., Johnson, J.E., and Hobday, A.J. (editors): Vulnerability of tropical Pacific fisheries and aquaculture to climate change. Secretariat of the Pacific Community. Available for download at www.spc.int.

Lehodey, P., Hampton, J., Brill, R.W., Nicol, S., Senina, I., Calmettes, B., Pörtner, H.O., Bopp, L., Ilyina,,T., Bell, J.D., and Sibert, J. (2011): Vulnerability of oceanic fisheries in the tropical Pacific to climate change. pp. 433-492 in Bell, J.D., Johnson, J.E., and Hobday, A.J. (editors): Vulnerability of tropical Pacific fisheries and aquaculture to climate change. Secretariat of the Pacific Community. Available for download at www.spc.int.

McPhaden, M.J. (1993): TOGA-TAO and the 1991-93 El Niño Southern Oscillation Event, Oceanography, 6(2), pp. 36-44.

McPhaden, M.J. (1999): Genesis and Evolution of the 1997-98 El Niño, Science, 283, pp. 950-954.

McPhaden, M.J., Busalacchi, A.J., and Anderson, D.L.T. (2010): A TOGA Retrospective, Oceanography, 23, pp. 86-103.

Messié, M., Radenac, M.H., Lefevre, J., and Marchesiello, P. (2006): Chlorophyll blooms in the western Pacific at the end of the 1997-1998 El Niño: The role of the Kiribati Islands. Geophys. Res. Lett., 33, L14601, (doi:10.1029/2006GL026033).

Messié, M., and Chavez, F.P. (2012): A global analysis of ENSO synchrony - The oceans' biological response to physical forcing, J. Geophys. Res., 117, C09001, (doi:10.1029/2012JC007938).

Messié, M., and Chavez, F.P. (2013): Physical-biological synchrony in the global ocean associated with recent variability in the central and western equatorial Pacific, J. Geophys. Res. Oceans, 118, pp. 3782–3794, (doi:10.1002/jgrc.20278).

Nicol, S. J., Allain, V., Pilling, G.M., Polovina, J., Coll, M., Bell, J.D., Dalzell, P., Sharples, P., Olson, R., Griffiths, S., Dambacher, J.M., Young, J., Lewis, A., Hampton, J., Molina, J.J., Hoyle, S., Briand, K., Bax, N., Lehodey, P., and Williams, P. (2013): An ocean observation system for monitoring the affects of climate change on the ecology and sustainability of pelagic fisheries in the Pacific Ocean. Climatic Change; (doi:10.1007/s10584-012-0598-y).

Radenac, M.H. (2001): Modeled and observed impacts of the 1997-1998 El Nino on nitrate and new production in the equatorial Pacific, J. Geophys. Res., 106, pp. 26879-26898.

Radenac M.H., Léger, F., Singh, A., and Delcroix, T. (2012): Sea surface chlorophyll signature in the tropical Pacific during Eastern and Central Pacific ENSO events, Journal of Geophysical Research, 117, C04007, (doi:10.1029/2011JC007841).

Radenac M.H., Messié, M., Léger, F., and Bosc, C. (2013): Oligotrophic and non-oligotrophic waters in the equatorial Pacific warm pool as observed from space, Remote Sensing of Environment, 134, pp. 224-233, (doi:10.1016/j.rse.2013.03.007).

Ryan, J.P., Polito, P.S., Strutton, P.G., and Chavez, F.P. (2002): Unusual large-scale phytoplankton blooms in the equatorial Pacific. Prog. Oceanogr., 55, pp. 263-285.

Ryan, J.P., Ueki, I., Chao, Y., Zhang, H., Polito, P.S., and Chavez, F.P. (2006): Western Pacific modulation of large phytoplankton blooms in the central and eastern equatorial Pacific. J. Geophys. Res., 111, G02013, (doi:10.1029/2005JG000084).

Strutton, P.G., Ryan, J.P., Chavez, F.P. (2001): Enhanced chlorophyll associated with tropical instability waves in the equatorial Pacific, Geophys. Res. Lett., 28, pp. 2005-2008.

Turk, D., McPhaden, M.J., Lewis, M.R., and Busalacchi, A.J. (2001): Remotely-sensed biological production in the Tropical Pacific during 1992-1999. Science, 293, pp. 471-474.

Turk, D., Meinen, C.S., Antoine, D., McPhaden, M.J., and Lewis, M.R. (2011): Implications of changing El Niño patterns for biological dynamics in the equatorial Pacific Ocean. Geophys. Res. Lett., 38, L23603, (doi: 10.1029/2011GL049674).

Weng, K. C., Glazier, E., Nicol, S.J., and Hobday, A.J. (in review): Fishery Management, Development and Food Security in the Western and Central Pacific in the Context of Climate Change. Deep Sea Research II.

Wilson, C., and Adamec, D. (2001): Correlations between surface chlorophyll and sea surface height in the tropical Pacific during the 1997-1999 El Niño - Southern Oscillation event. J. Geophys. Res., 106, 31, pp. 175-188.

White Paper #8a – Regional applications of observations in the eastern Pacific: Western South America

Takahashi, K.[1], Martinez, R.[2], Montecinos, A.[3], Dewitte, B.[4], Gutiérrez, D.[5], and Rodriguez-Rubio, E.[6]

[1] Instituto Geofísico del Perú, Lima, Perú
[2] Centro Internacional para la Investigación del Fenómeno El Niño, Guayaquil, Ecuador
[3] Departamento de Geofísica, Universidad de Concepción, Concepción, Chile
[4] Laboratoire d'Etudes en Géophysique et Océanographie Spatiales, Toulouse, France
[5] Instituto del Mar del Perú, Callao, Perú
[6] Instituto Colombiano del Petróleo, Piedecuesta, Santander, Colombia

1. Introduction

El Niño is the main source of climate variability in the tropical Pacific ocean and it is particularly dramatic along the western coast of South America, where monthly sea surface temperature anomalies during the peak of the 1982-83 and 1997-98 events have been on the order of 9°C. The local warming favors a southward displacement of the ITCZ, which results in dramatic increase in rainfall on the coasts of northern Peru, Ecuador, producing significant losses in infrastructure and economical activities associated with flooding. Also, the tropicalization of the coastal upwelling environment of Peru and Chile produces disruptive effects on the ecosystem and associated fisheries. Decadal variability in the equatorial Pacific is closely linked to variability along western South America. Recent manifestations include the abrupt warming around 1976 throughout the eastern Pacific, which was followed by a cool period since the late 1990s. Similar to El Niño, this variability also impacts climate along the coast and the marine ecosystems. The dynamics of this variability, however, is poorly understood at present. A similar issue is related to climate change, and its potential influence associated with equatorial dynamics and local air-sea interactions along the coast. These relationships are not well understood at present.

Key needs in the region are the enhancement of subsurface monitoring in the far eastern equatorial Pacific and along the coast of South America, and the reduction of long-standing biases in the mean and the variability in climate models in the eastern Pacific, guided by process understanding, to provide reliable climate forecasts on intraseasonal to decadal scales, and climate change projections for the eastern Pacific and its feedbacks and impacts on global climate.

2. Applications of ocean observations

Scientific applications:

- Improve the understanding of critical processes in the equatorial eastern Pacific that will lead to the improvement in the understanding and modeling of ENSO, decadal variability and climate change in this region. This is particularly important in the light of long-standing errors in the eastern Pacific in climate models and the associated challenges in representing ENSO diversity. Key processes are ocean temperature advection, turbulent ocean mixing, dissipation and dispersion oceanic equatorial waves, atmospheric

convection in the ITCZ and convectively-coupled wave-like atmospheric disturbances, meridional ocean-atmosphere coupled mechanisms, and the role of the wind mountain gaps between the Caribbean and Pacific in equatorial ocean-atmosphere dynamics.

- Monitoring of CO_2, pH, chlorophyll and oxygen, and associated oceanic transports and air-sea fluxes in the near-equatorial eastern Pacific and coastal zone in order to improve the understanding of large marine ecosystems dynamics in the context of climate variability and change.

Operational applications:

- Near real-time monitoring of intraseasonal equatorial Kelvin wave propagation across the basin and along the coasts of western South America (e.g. SST, sea level and thermocline depth). This information, together with forecasts from international centers, feeds the analysis that national institutions make for the assessment of local potential effects of ENSO-related anomalies in the eastern Pacific.
- Monitoring of upper ocean water masses (temperature, salinity, and other tracers) in the eastern Pacific on monthly to seasonal timescales to attribute causality of climatic anomalies (e.g. associated with the southward displacement of the equatorial front or shutdown of coastal upwelling) to water transports (horizontal advection) or more local processes (mixing, vertical advection, cloudiness). Continuity and quality control of long term series by regional institutions and buoys (TAO and Stratus) are prioritary for assessing decadal variability.
- Near real-time monitoring of coastal and eastern Pacific winds (i.e. local forcing of coastal ocean conditions) on meteorologically synoptic timescales. In addition to the equatorial zonal winds and the southeasterly trades, northerly gap winds in the far-eastern Pacific are also important.
- Real-time diurnal-cycle-resolving observations in the ocean subsurface thermal structure, sea surface temperature and 3D atmosphere structure (wind, temperature), with emphasis on the eastern tropical Pacific, for assimilation and validation of operational seasonal forecast model systems.
- Near real-time monitoring of intraseasonal atmospheric equatorially propagating disturbances (e.g. MJO or convectively coupled Kelvin waves) for medium-range weather forecasting for western South America and forecasting potential forcing of equatorial ocean Kelvin waves. In addition to remote sensing (e.g. OLR), in situ daily profiling of atmospheric variables along the equator will be valuable, particularly in the eastern Pacific where convective coupling is generally weak.
- Near real time and long term monitoring of surface-ocean and coastal waves for assimilation (and validation) into operational wave forecast and warning systems. Long term monitoring is also needed for a climatologically characterization of surface waves and their extremes for planning in the coastal and offshore (i.e. navigation, fishing and oil/gas offshore activities) regions.
- Monitoring of ocean biogeochemical variables on seasonal timescales to identify environmental changes for marine ecosystems management and associated fisheries.

These will be the basis for medium and long term adaptation strategies and international coordinated efforts.

- Near real-time monitoring of precipitation, both *in situ* and through high resolution 3D remote sensing (e.g. Global Precipitation Mission), in the eastern Pacific, including western South America, is needed for assessment of ENSO-related impacts and potentially for assimilation into forecast systems and their validation. Both types of data should be considered complementary and inter-dependent.

3. Scientific questions/main drivers

3.1 Role of the eastern Pacific in ENSO Diversity

Great progress in El Niño research has been made under the TOGA programme and it is believed that an understanding of the essential mechanisms has been achieved (e.g. Wallace et al., 1998; Neelin et al., 1998). However, in the recent decade there has been renewed interest in understanding the differences among individual ENSO events. As noted by Wallace et al. (1998): "Descriptions based on a single index do not do justice to the complexity of the climate variability over the equatorial Pacific", and Trenberth and Stepaniak (2001) proposed that at least two indices should be used for describing ENSO evolution. This extra degree of freedom and, particularly, the associated effect on the longitudinal position of the maximum SST anomalies has been the focus of recent work (e.g. Larkin and Harrison, 2005; Ashok et al., 2007; Kug et al., 2009). This approach is particularly relevant considering that the recent decade appears to have experienced a larger relative frequency of El Niño events with their SST maxima located in the central Pacific (e.g. Kug et al., 2009; Lee and McPhaden, 2010), although it is unclear whether this reflects a long-term trend (Ray and Giese, 2012).

A different interpretation of the record suggests that the extraordinary El Niño events of 1982-83 and 1997-98 corresponded to a nonlinear ENSO regime, different from all the other El Niño events (Takahashi et al., 2011; Dommenget et al., 2012; Takahashi and Dewitte, 2014). In addition to their generally large magnitude, these events featured disproportionally large SST anomalies in the Niño 1+2 regions (Takahashi et al., 2011) and a different temporal evolution to the “canonical” El Niño, which precluded the recognition of the onset of the 1982-83 event at that time (Wallace et al., 1998). However, only two extraordinary events have been observed in modern times, and only the 1997-98 event was measured comprehensively by the TAO array. Furthermore, despite their similarities, these two events presented some substantial differences between them, so that the observational constraints on some subtle aspects of their common dynamics are not tight (Takahashi and Dewitte, 2014).

A way of gaining some insight into what made these events different is to analyze simulations by models that reproduce some of the key observed features and verifying the relevant mechanisms with observations. For instance, an analysis of the GFDL CM2.1 model, which reproduces in detail many aspects of both observed extraordinary events, indicates that atmospheric and oceanic non-linearities are at the heart of the existence of the two El Niño regimes (Takahashi and Dewitte, 2014). Two types of nonlinear processes are considered the leading potential sources of asymmetries in El Niño/La Niña.

Firstly, it has been proposed that positive nonlinear ocean advection in the eastern Pacific

enhances El Niño and reduces La Niña, particularly through vertical advection (Jin et al., 2003; An and Jin, 2004) and this idea has been used to devise simple mathematical models that reproduce burst-like El Niño events (An and Jin, 2004; Timmermann et al., 2003). However, newer reanalysis products indicate that this vertical nonlinear advection is actually negative, but that the zonal nonlinear advection makes up for this and produces a net positive nonlinear advection (Su et al., 2010). These analyses are all based on reanalysis products that provide a complete 4D depiction of the state variables yet, if observed data is not assimilated into them; the result would be dependent on underlying the ocean general circulation models. The discrepancy in the sign in nonlinear vertical advection among reanalysis products can be traced to the sign of the equatorial vertical velocity anomalies in the Pacific east of 95W (Su et al., 2010), but this variable is not directly measured (and therefore is not assimilated into the reanalysis) so the contribution of this process to ENSO asymmetry and regimes remains an open question.

The other key nonlinearity is related to the existence of a threshold SST above which atmospheric deep convection is active (e.g. Graham and Barnett, 1987). This nonlinearity has been formulated in a variety of ways in ENSO models, where it accounts for a nonlinear response of surface wind stress to SST anomalies (e.g. Zebiak, 1986). This can explain not only the asymmetry between El Niño and La Niña (Dommenget et al., 2012; Choi et al., 2013) but, if the threshold is substantially above the climatological values, this can explain the existence of two different El Niño regimes, with one of them corresponding to the extraordinary events (Takahashi et al., 2011; Takahashi and Dewitte, 2013). However, observational evidence of the latter is limited to the sampling of only two events. Empirically, the response of convection to SST anomalies is known to depend on the basic atmospheric state (Zebiak, 1986; Xiang et al., 2013), yet the nature of this dependence and how the changes on long time-scales will influence the convective feedback on ENSO is not straightforward.

It has been proposed that decadal changes in the air-sea coupling in the eastern Pacific (Choi et al., 2010) and westward shift in the mean equatorial Pacific atmospheric low-level convergence (Xiang et al., 2013) resulted in the observed changes in ENSO characteristics, i.e. with reduced variability in the eastern Pacific in the recent decade, leading to an ENSO SST pattern maximizing in the central Pacific. On longer timescales, Vecchi and Soden (2007a) showed that climate change effects on tropical convection through SST could be non-local, i.e. changes in the tropical SST pattern can also have an effect comparable to the changes in local SST. On the other hand, climate model projections show that increased atmospheric moisture associated with warming will lead to larger precipitation anomalies during El Niño, even if the related SST variability does not change (Power et al., 2013).

Although El Niño research has adopted the ENSO paradigm, El Niño events local to the far eastern Pacific, characterized by coastal warming and heavy rainfall in northern Peru and Ecuador as they were initially identified (Carrillo, 1891; Carranza, 1893; Murphy, 1926), can be substantial and not strongly linked to the basin-scale mode (e.g. Deser and Wallace, 1987). For example, the El Niño event in 1925 (Murphy, 1926) had very strong impacts associated with heavy rainfall along the coasts of Peru and Ecuador due to a southward displacement of the ITCZ like has not been seen ever since, while the central Pacific was anomalously cool (Takahashi et al 2014). Meridional ocean-atmosphere dynamics in the eastern Pacific appear to

have played a role at least as important as the well-known zonal processes (i.e. equatorial zonal winds and oceanic waves, etc.). Additionally, meridional processes originating in the southeast Pacific associated with surface winds and heat ocean-atmosphere exchange could penetrate into the equatorial eastern Pacific and affect ENSO (Toniazzo, 2010; Zhang et al., 2014ab), similarly to the air-sea coupled process already documented for the Northern subtropical Pacific (Chiang and Vimont, 2004, Vimont et al., 2003).

3.2 The equatorial Kelvin wave in the eastern Pacific

The equatorial Kelvin wave is a salient feature of the tropical Pacific dynamics at a variety of timescales (from intraseasonal to interannual) because it transfers rapidly (in a few months) and efficiently the variability from the western Pacific to the eastern Pacific. For this reason, the equatorial Kelvin wave is also inherently tied to the ENSO dynamics through its effect on both the zonally averaged heat content in the equatorial Pacific and the advection processes, acting both as a trigger and a time-integrator for ENSO. It is also the main oceanic conduit by which the South American west coast is impacted by the tropical climate due to the coast behaving as an extension of the equatorial wave guide. Although variations in sea level, thermocline and current in the equatorial Pacific can be interpreted to a large extent from linear theory, due to the anisotropy for the mean state (thermocline, SST, currents), a number of processes have the potential to modify the characteristics of the equatorial Kelvin wave (flux, phase speed, amplitude, vertical structure).

TAO data have been key for documenting/monitoring the variability in current and thermocline depth associated to the intraseasonal to interannual Kelvin wave (McPhaden and Taft, 1988; Kessler et al., 1995; Johnson and McPhaden, 1993; Kessler and McPhaden, 1995ab; McPhaden et al., 1998). However, progress in our understanding of the role of the Kelvin wave on ENSO dynamics has been permitted by the satellite altimetric data that provides the sufficient horizontal resolution for an estimated separation into Rossby and Kelvin waves (Perigaud and Dewitte, 1996; Boulanger and Menkes, 1995; Boulanger and Fu, 1996), allowing for testing ENSO theories (see Neelin et al. (1998) for a review) that confers to the reflections of equatorial waves on the meridional boundaries a key role. Sea level anomalies has been also shown to be a good proxy of anomalous heat content in the equatorial band (Meinen and McPhaden, 2000), which determines to a larger extent the evolution and amplitude of ENSO (Jin, 1997). Although the interannual Kelvin wave has a clear signature on SST and is well observed through altimetric data, the intraseasonal Kelvin wave has its largest influence on subsurface temperature (in the vicinity of the thermocline) with a weak signature on SST (Mosquera et al., 2014) and is less easily diagnosed from weekly satellite data due to its stronger dissipation.

Because the thermocline slopes from west to east, the vertical structure of the equatorial waves is not homogeneous in space (Dewitte et al., 1999), which implies that the Kelvin wave may experience a change in amplitude, phase speed, vertical and meridional structure as it reaches the eastern Pacific (Dewitte et al., 2003) or a strong dispersion through scattering of energy (Busalacchi and Cane, 1988; Dewitte et al., 1999). At intraseasonal timescales, the equatorial Kelvin wave can be also impacted by Tropical Instability Waves (TIW) (Giese and Harrison, 1999) that produces mixing (Luther and Johnson, 1990). In return, the Kelvin wave can also

affect the instability conditions (if the mean flow is weak) on which the TIWs depends. The Kelvin wave can also partially reflect as Rossby waves which may subsequently trigger TIWs (Allen et al., 1995). The scattering of energy of the Kelvin wave has been studied previously mainly theoretically (Busalacchi and Cane, 1988; Giese and Harrison, 1990). Dewitte et al. (1999) using a multimode ocean model suggested that modal dispersion could explain the large eastward increase in the contribution of the higher-order baroclinic modes to zonal currents and sea level in the eastern Pacific (east of 120°W) at interannual timescales, implying a change in dynamical regime in the eastern Pacific compared to free non-dispersive low-order propagating wave dynamics as in the central Pacific, Such modal dispersion process remains largely undocumented from observations although satellite data reveals an eastward change of the dominant frequency (from ~60 $days^{-1}$ to ~120 $days^{-1}$) of the intraseasonal Kelvin wave (Cravatte et al., 2003) suggestive of energy scattering of the long waves.

The motivation for better understanding the dissipation process of the equatorial Kelvin at intraseasonal timescales arises also from the observations that the recent decades have been characterized by a relatively steeper mean thermocline, favorable for the of wave energy in the central Pacific. Recent El Niño events (i.e. Central Pacific events) are characterized by an increased variance of the intraseasonal Kelvin wave activity in the central Pacific (Gushchina and Dewitte, 2012; Mosquera et al., 2014) at their peak phase, suggesting that the intraseasonal Kelvin wave may be linked to Central Pacific El Niño dynamics. So far the study of the intraseasonal equatorial Kelvin wave and its role on ENSO has been somewhat limited to its potential in triggering a local Bjerknes feedback prior to the development of ENSO (Lengaigne et al., 2004; Kessler and Kleeman, 2000; Kleeman et al., 2003), which applies to extreme El Niño events. Intraseasonal Kelvin wave activity is linked to the MJO activity that favors the development of Westerly Wind Bursts. In previous studies (Hendon et al., 2007; McPhaden et al., 2007; Lengaigne et al., 2004), MJO (and associated intraseasonal Kelvin wave) activity was shown to be anomalously active prior to the development of El Niño (6 to 7 month ahead the peak phase). However, as mentioned earlier, extreme El Niño events are very few over the instrumental record (2 events, 1982/83 and 1997/98), so that such relationship may apply mostly for Eastern Pacific events although Bergman et al. (2001) indicate that the MJO was abnormally inactive prior to the 1982/83 El Niño.

The “stochastic” nature of the intraseasonal Kelvin wave and its tied relationship to ENSO calls for monitoring parameters that allows for its derivation/estimation. Whereas, within the assumption that the ocean reduces to a unique active surface layer, satellite data do provide estimate of the amplitude and evolution of the intraseasonal equatorial Kelvin wave, they have not been used to understand the processes that impact its propagating characteristics, because the latter depends largely on the vertical structure variability of currents and temperature. The TAO array has provided such information so far. However, it is not clear to which extent the available information can be used for inferring the characteristics of the equatorial Kelvin wave in the far eastern Pacific and its dispersion due to the rather coarse vertical resolution of the existing array and lack of data east of 95W.

Long wave dissipation has been modeled by a Rayleigh friction in most simple model studies and a wide range of estimates of the time decay for such effective friction have been used (from 6 months to 30 months). The rather wide range of values reflects that the decay time scales of

equatorial waves are frequency dependent. Upper ocean wave dissipation has been studied in the frame of linear theory assuming that the vertically propagating variability through the thermocline accounts for the loss of energy that has a surface expression onto sea level (Kessler and McPhaden, 1993; Dewitte and Reverdin, 2000). Such process is hardly detectable from available observations because of the paucity of the data below the thermocline and the relatively low vertical resolution. The study of such process would also greatly benefit from the implementation of high-vertical resolution thermal profiling in the eastern Pacific where the annual and interannual Rossby wave is detectable below the thermocline. Dissipation can be accounted for by non-linear processes that are potentially at work in the eastern Pacific due to the strong vertical current shear associated to the equatorial undercurrent (EUC), the sharp SST front north of the equator associated to the cold tongue and a driver of TIW activity, the maximum zonal gradient of the thermocline (located ~120°W) potentially producing modal dispersion of the waves (Mosquera et al., 2014), and local-air sea interactions. Wave damping in the eastern Pacific will result in all cases from the accumulation of warmer water (weaker stratification) where the Kelvin waves are damped. So far the study of these processes has been mostly based on the experimentation with ocean models confronted to TAO observations (Cravatte et al., 2006; Benestad, 1997; Mosquera et al., 2014). The better understanding of these processes (that are resolution-dependent) would require high-vertical resolution and high-frequency measurements (microstructure, internal waves) which have been only available in the past from dedicated cruises (3 main experiments in the eastern Pacific since 1979) and now from the Argo data (although the equatorial divergence does not ease the dense sampling of such processes). The modeling community would greatly benefit from such measurements in order to develop useful parameterizations of diapycnal fluxes in the equatorial upwelling region and to improve the realism of the mean vertical stratification of the eastern equatorial Pacific as simulated in current generation CGCMs (Figure 3.1).

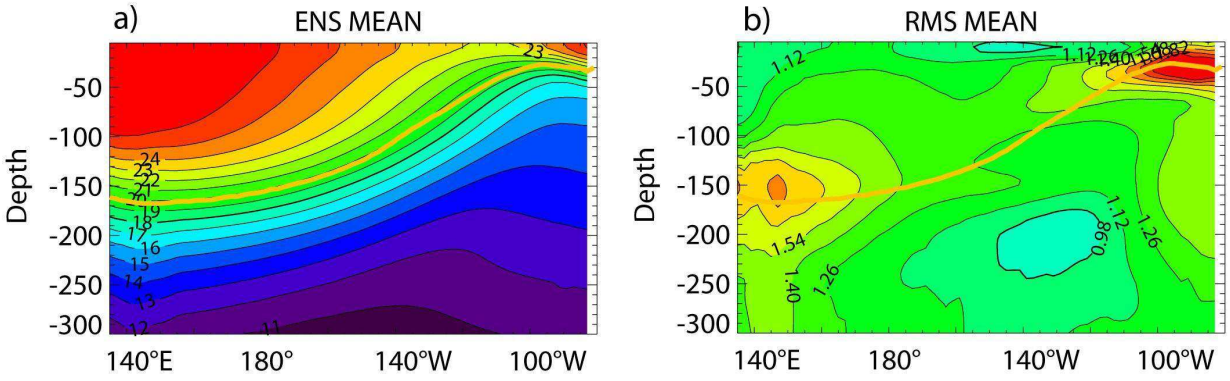

Figure 3.1 - (a) Ensemble mean (15 CMIP3 models) of vertical temperature and (b) the dispersion (RMS) among models. The ensemble mean thermocline depth is overplotted (orange thick line).

3.3 The thermocline feedback in the eastern Pacific

The magnitude and interaction of the mechanisms by which the thermocline fluctuations connects to the SST in the eastern pacific (called “thermocline feedback” in ENSO studies) remain largely unknown and depend on the complex of processes that connects the thermocline to the surface. These processes are parametrized as a whole in intermediate complexity

coupled model. In the OGCMs, also parametrized into the mixing terms, they are highly dependent on both horizontal and vertical resolution. Due to the large dispersion in the representation of the thermocline in current generation coupled models in the eastern tropical Pacific (cf. Figure 1), there is a large uncertainty on how these models can predict the change in ENSO statistics. The thermocline feedback in the eastern Pacific is crucially influential on the evolution of ENSO and determines its stability (An and Jin, 2001). Quantifying its “strength” requires estimating the details of the heat budget in the eastern Pacific in the upper ~50m since it implicitly accounts for various processes, including vertical diffusion/entrainment and linear vertical advection. So far the thermocline feedback in the eastern Pacific has not been explicitly estimated observationally although it is a key parameter for ENSO dynamics. Current estimate relies on oceanic reanalysis in which TAO data have been assimilated and consists in either the estimate of the regression coefficient between SST and thermocline depth anomalies or the derivation of ad-hoc parametrizations (Zebiak and Cane, 1987). There is also indication of a marked zonal variation of the thermocline feedback within the eastern Pacific region (e.g. Niño 3 region), particularly with a sharp decrease east of the Galapagos Island associated with the higher SST there.

There have been some speculations concerning a possible connection between the cold tongue and the upwelling off Peru, which would imply a relation between the thermocline feedback and the Peru upwelling, although a model experiment suggests otherwise (Kessler et al. 1998). In order to refine our understanding of such process and to validate the ocean models in this region, observations of upwelling in full three dimensional context are necessary, which the TAO data have allowed so far, although the current design of the network (i.e. low meridional resolution) have limitations for inferring the 3-D circulation of the “tropical cells” (McCreary and Lu, 1994) or details of the ramification of the EUC east of the Galapagos Islands (Montes et al., 2010). New instrumentation (e.g. gliders and Argo floats) and high-resolution oceanic model could help documenting the meridional variability of the circulation in the eastern Pacific and its role in modulating the equatorial stratification, which can provide guidance for adapting the TAO mooring array spacing.

3.3 Coastal dynamical and biogeochemical processes

The carbon, nitrogen and oxygen cycles are closely related in the Peru-Chile upwelling system (PCUS) (Lam et al., 2009). Coastal upwelling and the relatively shallow position of the thermocline allow an efficient upward advection of nutrients from the nutrient/CO_2-rich subsurface waters, releasing CO_2 during the active upwelling and triggering strong phytoplankton growth when upwelling relaxes. The large productive area associated to this Eastern Boundary Upwelling System, overlaps to some extent with the southeastern Pacific oxygen minimum zone (OMZ) that impinges the continental margin (Pennington et al., 2006; Helly and Levin, 2004). Due to the predominant oxygen-deficiency in the subsurface waters and the high concentrations of organic matter, high rates of anaerobic ammonium oxidation and water column denitrification occur in the water column, causing that this region be one of the most important areas of Nitrogen loss in the global ocean (Lam et al., 2009). Over the shelf and upper slope, the main oxygen sources are the Peru–Chile undercurrent, which is mainly fed by the eastward equatorial subsurface currents (Montes et al., 2011), and the turbulent diffusion from the surface; while the main sink is the oxygen consumption by the high respiratory demand

of the particulate organic matter settling from surface waters (Codispoti et al., 1989; Fossing, 1990; Pennington et al., 2006; Schunk et al., 2013).

This general pattern exhibits latitudinal and mesoscale variations along the PCUS, associated with the distance to the Equator, the position of upwelling cells relative to the south Pacific anticyclone, and the extension of the continental shelf, among other factors. ENSO-driven impacts vary in intensity as well, and local and regional forcing gain in importance nearshore and poleward.

The classical description of biogeochemical impacts associated with El Niño involves the disruption of coastal upwelling-related fertilization of surface waters due to the deepening of the thermocline, associated with the intensification of the poleward undercurrent and the propagation of coastal trapped waves from the Equator from the early phases of the events (Huyer et al., 1991; Morales et al, 1999, Gutiérrez et al., 2008). The same process ventilates the subsurface waters, while the reduction of primary productivity results in lesser oxygen consumption in the water column, leading to a net oxygenation of the system. In addition, coastal trapped waves propagating during non-El Niño conditions also trigger shallow subsurface oxygenation episodes (Gutiérrez et al., 2008). So far, the El Niño impacts on the nutrient cycles have not been quantified, but certainly the subsurface oxygenation and the decreased productivity should modify the nutrient ratios in the upwelling source waters, while in parallel diminish the export production to the seafloor and offshore, as well as the release rates of nitrous oxide and CO_2 to the atmosphere.

On the other hand, in the eastern tropical Pacific, a different seasonal upwelling mechanism occurs along the central American coast from December through March, where wind jets cross the physiographic gaps of central America existing at the Gulf of Tehuantepec, Gulf of Papagayo and the Isthmus of Panama (Chelton et al., 2000) producing oceanic upwelling due to Ekman pumping, increasing the subsurface oxygen and nutrient availability and producing a surface chlorophyll bloom as was observed in the Colombian Pacific Ocean (Rodríguez-Rubio and Stuardo, 2002; Rodríguez-Rubio et al., 2003). This particular process, and its relationship with the wind field and ocean and coastal currents, is also influenced by the ENSO and is involved in ocean-atmosphere feedbacks (Chiang and Vimont, 2004; Xie et al., 2005).

Understanding the coupling between physical and biogeochemical processes along the west coast of South America has major practical consequences. The PCUS is the most productive in the world (e.g., Alheit and Bernal, 1993; Chavez et al., 2008) and supports the large fishing industry of Chile and Peru. According to the hypothesis of the “optimal environmental window” (Cury and Roy, 1989), both La Niña-like conditions (stronger mixing and advection) and El Niño-like conditions (weaker upwelling) would be negative for small pelagic fish larval recruitment. But if El Niño signature changes towards a dominance of Central Pacific El Niños (Yeh et al., 2009), the net effect would be more complex to predict. Paleoceanographic records evidence multi-decadal changes in oxygenation, productivity and fish production along the Peru-Chile coast, associated to past warmer or cooler periods. During the Little Ice Age (ca. 1500 – 1800 AD), an overall reduction of fish productivity off central Peru occurred while the OMZ weakened, with little effect off northern Chile. By the mid- to late nineteenth century, a period of more frequent El Niño events (Ortlieb, 2000; Gergis and Fowler, 2009) was associated to a reduction of anchovy and increase of sardines off central Peru, with lower effect off northern Chile

(Gutiérrez et al., 2009; Valdés et al., 2008), suggesting a poleward displacement of the anchovy population nucleus. Using projected surface winds from regional numerical downscaling (Fuenzalida et al., 2007). Aiken et al. (2011) studied larval dispersion and meridional connectivity off central Chile under intensified favorable upwelling winds, suggesting a potential reorganization of coastal communities at the end of this century. Moreover, Yáñez et al. (2013) found large discrepancies in the anchovy landings in northern Chile under different climate scenarios through the XXI century. For instance, by 2050 the annual landing would increase (~4%) or decrease (~20%) if a cooling or warming condition is verified in northern Chile, respectively.

3.4 Convective processes in the eastern Pacific and ENSO

The atmospheric circulation in the deep tropics is strongly tied to moist convection. In the eastern Pacific, the latter is primarily organized by the ITCZ, that features a zonal band of convective systems to the north of the equator and that constitutes the regional component of the upward branch of the Hadley circulation. Seasonally, the latitude of the eastern Pacific ITCZ varies, approximately in synchrony with the highest SST (e.g. Mitchell and Wallace, 1992), although the two should be viewed as part of strongly coupled system (e.g. Xie and Philander, 1994; Takahashi and Battisti, 2007ab) seasonally driven by insolation. On interannual timescales, variability in precipitation in this region is dominated by ENSO and can also be characterized as meridional displacements of the ITCZ according to the SST anomalies, but also providing nonlinear feedbacks into the ENSO system (Lloyd et al., 2012; Dommenget et al., 2012; Takahashi and Dewitte, 2014). With future climate change, the increase in atmospheric moisture content could lead to an intensification of the precipitation rates in rainy regions such as the ITCZ (Held and Soden, 2006), although the climate models indicate also a southward displacement of the ITCZ (IPCC WG1, 2013). Recently, analyses of global climate models indicate that, with future climate change, El Niño would produce stronger rainfall anomalies even if the SST statistics were unchanged (Power et al., 2013; Cai et al., 2014). Also, climate change scenarios indicate that future changes in upwelling-favorable winds off Peru are strongly linked to the changes in precipitation (Belmadani et al., 2013).

However, the climate model deficiencies are large in the eastern Pacific and calls for considering these results with caution. In particular, global climate models suffer from the so-called “double ITCZ syndrome”, which results in strong positive rainfall biases in the southeastern Pacific and appears to be associated with the frequency of deep convective events in the atmospheric models (Bellucci et al., 2010). The problem persists even in the end-of-the-line CMIP5 models (IPCC WG1, 2013). On the other hand, observations of the eastern Pacific ITCZ are lacking and its basic structure is not well known. Satellite based measurements indicate that the vertical structure convective heating is maximum in the mid-upper troposphere (Schumacher et al., 2004), but Reanalysis products indicate that the ascent is shallow (Back and Bretherton, 2006), consistent with the direct observations of a strong shallow overturning circulation in this region (Zhang et al., 2004). The vertical structure of the latent heating is of particular importance to ENSO since it has substantial influence on the surface wind response that is key for the Bjerknes feedback (Nigam et al., 2000; Nigam and Chung, 2000; Wu, 2003).

Given the uncertainties in reanalysis and remote sensing, observational estimates of profiles of

latent heating, which can be obtained from radiosonde networks, or vertical velocity, which can be directly measured with wind-profiling radars (e.g. Gage et al., 1991) are required. In the case of the latter, however, these are restricted to equatorial islands (e.g. Galapagos and Christmas islands), so would only measure the ITCZ during strong El Niño events. On the other hand, field campaigns like EPIC (Raymond et al. 2004) would provide invaluable information, but the determination of the mean vertical velocity profiles would require a field campaign design with several radiosounding stations around the ITCZ over periods long enough to average out the high-frequency variability.

Additionally, warm conditions in the eastern Pacific may allow equatorial weather systems such as the Madden-Julian Oscillations and convectively coupled Kelvin waves to propagate farther into the east (Straub and Kiladis, 2001), thus providing an enhancement of stochastic forcing of ENSO (e.g. Jin et al., 2007). It is necessary to carry out observational verification of this process and the characterization of the dynamics of these systems in order to improve ENSO representation. Continuous wind and thermodynamic profiling from equatorial islands would allow observing these systems even when the convective signal is weak, particularly over the equatorial cold tongue, which would be useful for monitoring and forecasting purposes.

3.5 Decadal variability and climate change in the tropical-south Pacific

Since Nitta and Yamada (1989) and Trenberth (1990) noticed the presence of interdecadal fluctuations in the observed climate records, their importance has increased dramatically dramatically due in part to the difficulty to separate their regional manifestation from climate change of anthropogenic origin. Certainly, all the different interdecadal climate modes defined since the 1990s are the result of internal climate variability, in which the ocean plays a key role. In the Tropical-South Pacific region the most important interdecadal mode is the Interdecadal Pacific Oscillation (IPO; e.g., Power et al., 1999), or the ENSO-like interdecadal variability (Zhang et al., 1997), that resembles the typical ENSO pattern but with a broader latitudinal scale in the eastern Pacific (e.g., Garreaud and Battisti, 1999). The interdecadal variability along the west coast of South America was first recognized in fisheries fluctuations in Peru (Pauly and Tsukayama, 1987), Chile (Yanez, 1991) and Colombia (Díaz-Ochoa *et al*., 2004). However, there is a few studies based on observed atmospheric and oceanic in Perú and Chile (Montecinos et al., 2003), and recently in Colombia (Rodriguez-Rubio, 2013).

Clarke and Lebedev (1999) showed that decadal and longer changes of the thermocline depth off California are mainly driven by low-frequency strengthening and weakening of the equatorial Pacific trade winds. They suggested that this mechanism should be responsible for decadal and longer fluctuations along the western coast of the Americas. Accordingly, Pizarro and Montecinos (2004) found that the thermocline depth and SST anomalies off Ecuador, Peru and Chile, which are positively correlated at interdecadal timescales, change along with the equatorial wind anomalies. Specifically, their estimation of the thermocline depth in the eastern tropical Pacific, which is proportional to the integral of the zonal wind stress along the equatorial Pacific (Clarke and Lebedev, 1999), presents similar evolution and amplitude in comparison with the observed thermocline along the western coast of South America.

On the basis of multivariate analysis of the SST-sea level pressure (SLP) coupled interdecadal variability in the tropical South Pacific region, Montecinos and Pizarro (2005) compared three

mechanisms explaining SST variability along the western coast of South America: the equatorial wind driven mechanism of Clarke and Lebedev (1999), the advection mechanism of White and Cayan (1998), and the local upwelling mechanism of Tourre et al. (2001). According to their results, positive (negative) SST interdecadal anomalies in the eastern equatorial Pacific and along the western coast of South America are explained by westerly (easterly) equatorial wind stress anomalies that would force deeper (shallower) thermocline depths in the region, while south of 30°S the local northerly (southerly) alongshore wind stress anomalies reinforce the positive (negative) SST anomalies driven remotely, through coastal upwelling fluctuations. These results were derived from the analysis of numerical simulations of the interface elevation anomalies with a reduced gravity model forced by observed wind stress (Montecinos et al., 2007). Also, these authors shown that, in the eastern equatorial Pacific, interface elevation anomalies are negatively correlated with SST at interdecadal timescales.

As a result of the external forcing, the global mean surface temperature exhibits positive trends (warming) since the beginning of the XX century, with an interruption from 1940s to 1970s (e.g., Vose et al., 2012). Natural forcing, in particular the increased solar radiation, can explain most of the warming in the first part of the XX century (e.g., Stott et al., 2000; Meehl et al., 2004; 2009a), while anthropogenic forcing appears to be responsible for the warming observed since late 1970s (e.g., Hegerl et al., 2007; Meehl et al., 2009a). The expected surface warming in the tropics is not uniform (Meehl et al., 2007). The IPCC projections for the XXI century show local minimum warming in the Southeastern tropical Pacific, the South tropical Atlantic, and the North tropical Atlantic (e.g., Vecchi and Soden, 2007a; Leloup and Clement, 2009). In particular, Leloup and Clement (2009) suggest the increasing efficiency of latent heat flux as responsible for the minimum warming, yet it would not be applicable in areas where the projected wind speed increases, as the southeastern Pacific (Garreaud and Falvey, 2009). On the other hand, most model simulations suggest that the response of tropical Pacific to radiative forcing would resemble an El Niño-like warming pattern (e.g., Held and Soden, 2006; Vecchi and Soden, 2007b), although a La Niña-like cooling pattern could also be expected theoretically (Clement et al., 1996; An and Im, 2013). So far, the observational evidences are ambiguous (e.g., Vecchi et al., 2008).

In the context of the global anthropogenic warming, observational evidence shows a noticeable cooling trend in the Southeastern Pacific since late 1970s (Trenberth et al., 2007; Falvey and Garreaud, 2009; Schulz et al., 2011; Gutiérrez et al., 2011a) in contrast with warming immediately inland. Vargas et al. (2007) and Gutierrez et al. (2011b) have extended back in time the evidence of the coastal cooling since late XIX century based on paleo-temperature estimations from sediments at 23°S and 14°S, respectively. According to Gutierrez et al. (2011b), the cooling trend increases since 1950s despite the interdecadal variability present in the region (e.g., Garreaud and Battisti, 1999; Montecinos et al., 2003). This negative sea and air surface temperature trends in the Southeastern Pacific, from tropics to mid-latitudes, is not simulated by coupled global models (Falvey and Garreaud, 2009). On which degree the observed cooling trend is related with the intensification of the Eastern Pacific OMZ (Stramma et al., 2010) is still an open question. Although in the latest years there have been reports of sulphidic events reaching the surface waters off the Central Peruvian coast (Schunk et al., 2013; G. Lavik, pers. comm.), so far there is not a conclusive result on existing long-term trends

for the subsurface oxygenation along the Peru-Chile coast.

A plausible factor for explaining the cooling trend is an intensification of the alongshore wind stress and the associated coastal upwelling enhancement. The coastal winds could be increasing due to an intensification of the South Pacific subtropical anticyclone (Falvey and Garreaud, 2009), increasing land-sea pressure gradient due to the land warming (Bakun, 1990; Narayan et al., 2010) or the increasing land-sea thermal contrast due to reduced mean low-cloud cover (Vargas et al., 2007). In climate change models, the increase in the winds off central Chile is associated with changes in the anticyclone, but changes off Peru, on which models do not agree, is associated with changes in the oceanic rainfall distribution (Belmadani et al., 2013). The remote response of the coastal thermocline to enhanced zonal equatorial Pacific wind stress at low frequency timescales (Pizarro and Montecinos, 2004; Montecinos et al., 2007) or the increase occurrence of Central Pacific El Niño in the recent decades (Dewitte et al., 2012) are other sources of cooling. Also, changes in the northward advection of subantarctic water have been argued to explain observed cooling (and freshening) trend during the 1990s (e.g., Schneider et al., 2007). On the other hand, local processes such as an increase in cloudiness associated with cold advection or low level stability (Klein and Hartmann, 1993; Takahashi, 2005) or enhanced evaporation associated with subsidence (Takahashi and Battisti, 2007; Xie et al., 2010) could also play a role. To this respect, Schulz et al. (2011) shown that, for northern Chile, the cloudiness exhibited a strong decrease since the 1970s.

On a broader scale, away from the coast of South America, decadal variability in the southeast Pacific has been characterized in terms of local ocean-atmosphere interactions involving SST, cloudiness, wind speed, and evaporation (Clement et al., 2009; Okumura, 2013). Due to the meridional asymmetry of the eastern Pacific climate relative to the equator, this southeastern Pacific variability can influence the equatorial Pacific more easily than the north Pacific and can therefore lead to further teleconnections through changes in the equatorial convection and through the oceanic equatorial waveguide (Okumura, 2013; Zhang et al., 2014ab). Although ocean dynamics in the southeast Pacific itself do not appear to be important for this mechanism, characterizing and monitoring the changes in the ocean thermal structure will be necessary for modeling and prediction efforts on decadal timescales.

Monitoring the eastern equatorial Pacific on decadal timescales is also important in terms of global climate change, as has been suggested in relation to the reduced global warming rate of the last two decades. The model experiments of Kosaka and Xie (2013) suggest that one important process behind this was the intensification of the eastern Pacific cold tongue. An observational confirmation of the mechanism would require adequate data for a heat budget calculation over decadal timescales, but in this region upwelling and mixing are key processes and their estimation would require knowledge of vertical velocities and turbulence, which are not standard variables.

3.6 Seasonal and intraseasonal prediction

The history of physically based seasonal climate forecasts is relatively short and strongly linked to the ability to predict sea surface temperatures (SST) in the El Niño region. The first physically based model forecast of equatorial Pacific Ocean temperatures was produced only in the mid-1980s (Cane et al., 1986). The growing ability to predict El Niño led to a cascade of efforts for

developing and improving the seasonal climate forecasts and attempting to make those useful to society (Goddard et al., 2011). El Niño is the overall dominant influence in regional climate variability worldwide, though other modes of sea surface temperature variability can be more important in some regions (Folland et al., 1991).

On the other hand, although many operational climate models were able to predict an El Niño event in 1997, they all underestimated its magnitude (Barnston et al., 1999; Landsea and Knaff, 2000). This issue is particularly notorious in the prediction of the eastern Pacific SST anomalies, which were the largest during this event, as they were in 1982-1983 (e.g. Takahashi et al., 2011), and even the most recent climate models can not hindcast this correctly, as shown in Figure 3.2 for the NOAA CFS v2 model. In this model, it is interesting that not only the Niño 1+2 hindcasts for the 1982-1983 and 1997-1998 events were underestimated by the ensemble mean by a half, with none of the members predicting the right amplitude, but forecast of the central Pacific 2009-2010 event (Lee and McPhaden, 2010) called for the same magnitude in Niño 1+2 as for the extreme eastern Pacific ones. Thus, the CFS v2 forecast did not distinguish among the very different spatial patterns of these events, despite assimilating data from TAO TRITON, satellite, etc. Although unpredictable westerly wind bursts could have played a role degrading the forecasts (e.g. Lengaigne et al., 2004), this model failed to maintain the warm conditions in the eastern Pacific even when the event was underway. Other GCMs (not shown) share a similar problem in their hindcasts. This suggests that either the model physics are inadequate, resulting in errors in the mean state and feedback processes, and/or important measurements are missing for initialization. Considering that recent research into El Niño suggests that the extreme events are qualitatively different from the others, possibly corresponding to a different dynamical regime (Takahashi et al., 2011; Takahashi and Dewitte, 2014), then the sampling by the TAO array of the subsurface ocean dynamics and surface meteorology, limited to only one extreme El Niño (1997-98), may not be enough to adequately identify all of the relevant mechanisms. In any case, enhanced observations in the far eastern Pacific are likely to be necessary to improve prediction in this region.

On intraseasonal timescales, the monitoring of equatorial Kelvin waves is a key source of predictability of coastal conditions due to their finite travel time to the South America of two or three months. These waves can impact the coastal sea surface temperature and trigger heavy rainfall, as was the case of the wave pulse forced in December 2001 (McPhaden, 2004) that, even though it did not trigger a large-scale El Niño, resulted in warning and flooding in northern Peru in March 2002 (Takahashi, 2004). Additionally, the modulation of the subsurface environment affects the coastal marine ecosystem (Echevin et al., 2014). On the other hand, coastal winds also play an important role in modulation the coastal conditions on intraseasonal timescales (Dewitte et al., 2011).

With respect to decadal variability, several studies have suggested that the south Pacific can be considered an important component of the system in the tropical Pacific, although the mechanisms are diverse, e.g. tropical/subtropical interactions (Giese et al., 2002, Luo et al., 2003), equatorial/coastal wave dynamics (Power and Colman, 2006; Montecinos et al., 2005 and 2007) or thermodynamic ocean response to stochastic forcing (Okumura, 2013). However, studies of decadal Pacific predictability have focused mainly in the northern and equatorial regions due to a large extent to the lack of long-term data in the south Pacific (e.g. Meehl et al.,

2010). Monitoring decadal variability in the southeast Pacific is a key need for improving understanding and predictive capacities over these timescales.

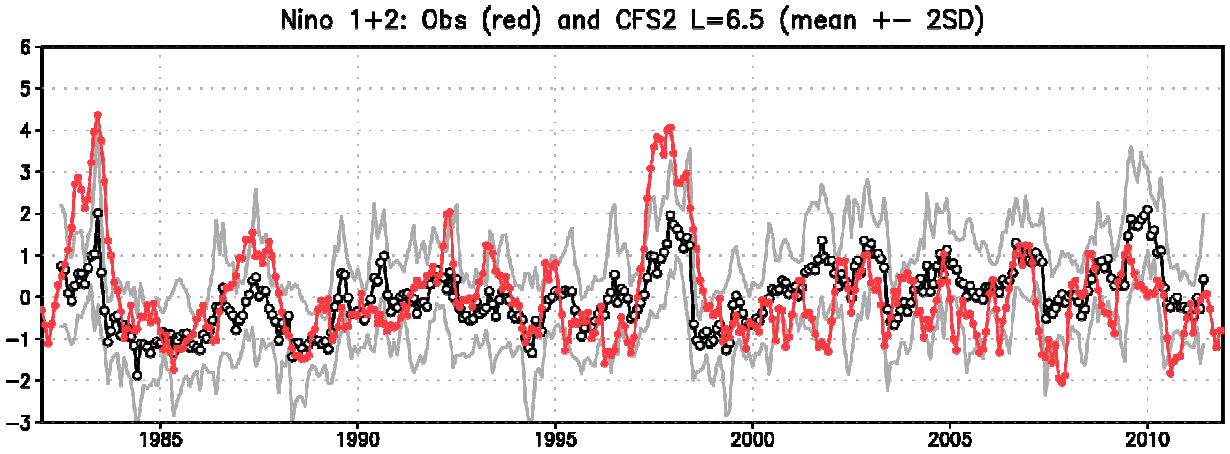

Figure 3.2 - Observed Niño 1+2 SST anomaly (red) and NOAA CFS2 6.5-lead forecast ensemble mean (black) and ensemble spread (2 standard deviations, grey).

3.7 Extreme surface waves climate and the long-term variability

The extreme surface wave climate is of paramount importance for: (i) off-shore and coastal engineering design, (ii) ship design and maritime transportation, or (iii) analysis of coastal processes. Monitoring such events and identifying the synoptic patterns that produce extreme waves is necessary to understand the wave climate for a specific location. Thus, a characterization of these weather patterns may allow the study of the relationships between the magnitude and occurrence of extreme wave events and the climate system (Izaguirre et al., 2012).

Alterations in wave climate are also often related to climate pattern variability. This variability as well as long-term trends has been an issue of research in recent years around the world but in the region of Latin America an understanding of wave climate and its variability is scant (Reguero et al., 2013). On the other hand, a strong correlation between the significant wave height and the Southern Oscillation Index (SOI), and both directional components of the wave energy flux and the SOI shows that the El Niño-Southern Oscillation (ENSO) variability has a strong influence on the wave climate of the Pacific (Hemer et al., 2011), however the ENSO influence in the wave climate on the eastern tropical and south Pacific is not well know. Furthermore, model-based projections indicate that the western coast of South America would be among the regions with largest relative increase in significant wave heights with climate change (Hemer et al., 2013).

Hence, an integrated network of surface wave measurements in the eastern Pacific is needed to monitor extreme wave events, perform the analyses of the effects of climate variability in this region and validate the wave models that are commonly used for short-term forecasting and climate scenarios.

3.8 Regional impacts and applications

In terms of impacts, western South America experiences different and even opposing influences from El Niño, depending on the geographical location and the seasonality of the associated SST anomalies. For instance, there is a direct effect of the coastal warming on the occurrence of rainfall along the western tropical coast of South America as a result of the local destabilization of the lower atmosphere and larger moisture content, particularly during the seasonally warm months (Horel and Cornejo-Garrido, 1986; Goldberg et al., 1987; Poveda and Mesa, 1997; Takahashi, 2004). On the other hand, anomalous warming in the central equatorial Pacific in austral summer tends to reduce rainfall in the tropical Andes (Aceituno, 1988; Poveda and Mesa, 2000; Lagos et al., 2007; Lavado and Espinoza, 2013; Takahashi et al., 2014). For instance, cool central Pacific conditions were present during the 1925 El Niño and this is believed to have enhanced substantially the rainfall along the coast of Peru and Ecuador (Takahashi et al 2014). In the austral winter, rainfall maxima changes latitudinal in central Chile associated with teleconnection effects from the central Pacific (Aceituno, 1988; Montecinos and Aceituno, 2003).

Thus, the differences in warming and cooling patterns along the equator associated with ENSO diversity have very important practical consequences for impacts in western South America, as it implies different behavior, even opposed, among El Niño regions. Although a single-mode view of ENSO implied that these two types of effects were expected to occur simultaneously, after the 1997-1998 El Niño the coast of South America has experienced atypically low SST variability and, hence, the coastal impacts of ENSO have been small. In Peru, this prompted the official committee for El Niño forecast (ENFEN) to define an operational index based on Niño 1+2 (ENFEN, 2012) to establish the presence of El Niño or La Niña in the eastern Pacific, while simultaneously considering more conventional ENSO indices such as SOI or NOAA's ONI in order to monitor the central Pacific El Niño/La Niña and its teleconnection effects. Using this index, in mid-2012, ENFEN were able to announce El Niño conditions in the eastern Pacific to Peruvian users (ENFEN, 2012b), while the international community was still expecting to see whether the central Pacific would warm.

During and after El Niño 1997-1998, the increasing access to web based products and the real time monitoring with TAO, determined a significant change in the way of Western South America countries monitor ENSO. The comprehensive monitoring done by National institutions and local scientists in the region to El Niño 1997-1998, combined with coastal observation networks along the coast, research cruises and weather stations in the continental areas, lead to different ways to estimate impacts and further evolution of the SST (Zambrano, 2000). In the framework of the ERFEN programme (Programmea para el Estudio Regional del Fenómeno El Niño en el Pacífico Sudeste) under the Permanent Commission for the South Pacific (CPPS), the western South America countries (Colombia, Ecuador, Peru, Chile) have implemented specialized groups for the assessment and forecasting of ENSO-related ocean-atmosphere conditions and potential impacts, which are then integrated into a regional assessment. ENFEN in Peru is an example of one of such national groups, which directly analyzes TAO/TRITON data, ocean reanalysis, global climate model forecasts and even a linear shallow water model forced by observational wind products (Mosquera, 2009) for intraseasonal prediction of coastal conditions. Similarly, in Ecuador, due to the urgency to provide advice to decision makers, in 1997, INOCAR developed a very simple model to foresee the SST evolution based on a

spectral correlation model using the strong and linear relationship between sea level anomalies, the depth of thermocline and consequently SST anomalies in the Ecuadorian sea. This model was able to represent fairly well the SST anomalies and predict the potential trends months ahead (Martínez et al., 2000). The information provided contributed with the analysis and climate forecasts at moments where the seasonal forecast was not implemented in most of the countries in the region.

Regional Climate Outlook Forums are an innovative concept developed and supported as part of the WMO Climate Information and Prediction Services (CLIPS) project in partnership with the National Meteorological and Hydrological Services (NMHSs), regional climate institutions and other agencies. The RCOFs have completed about 12 years of successful operation in different sub-regions of Africa, in parts of South America and in the Andean region. Regional Climate Outlook Forums in various forms and sizes are now in operation serving more than 10 sub-regions around the world, and concerted efforts are being made to extend the concept to several other regions. Despite the challenges of resources and human and infrastructural capacities, some of the RCOFs have achieved remarkable progress in regional networking and user liaison, and have contributed substantially to capacity-building and user awareness (Martínez et al., 2010).

National and regional capacities are varied, but are certainly inadequate to face the task alone. Built into the RCOF process is a regional networking of the climate service providers and stakeholders including user sector representatives. Participating countries recognize the potential of climate prediction and seasonal forecasting as a powerful development tool to help populations and decision-makers face the challenges posed by climatic variability and change. In parallel, NMHSs and some decision-makers have come to realize the potential benefits to be gained and have played larger roles in the processes. Ownership now lies largely with national and regional players, but there is a continuing need for support at all levels to ensure that the momentum gained to date is maintained (Goddard et al, 2011). For all this process, data provided by TAO and satellite derived data are key to provide suitable predictors for regional expert assessments and statistical models which could be for some seasons and transition periods more accurate and useful than numerical prediction (Martinez et al, 2011).

Regional Climate Outlook Forums bring together national, regional and international climate experts, on an operational basis, to produce regional climate outlooks based on input from NMHSs, regional institutions, Regional Climate Centers (RCCs), Global Producing Centers of long-range forecasts (GPCs) and other climate prediction centers. Through interaction with sectoral users, extension agencies and policy makers, RCOFs assess the likely implications of the outlooks on the most pertinent socio-economic sectors in the given region and explore the ways in which these outlooks may be used. Regional Climate Outlook Forums also review impediments to the use of climate information and the experiences and successful lessons regarding applications of past RCOF products in an effort to enhance sector-specific applications. In many cases the RCOFs are followed up by national forums to develop detailed national-scale climate outlooks and risk information including warnings for communication to decision-makers and the public at large.

Since 2003, the International Research Center on El Niño (CIIFEN), with WMO sponsorship, assumed the coordination of the Climate Outlook Forum for Western South America

(WCSACOF). The seasonal forecast for the region is produced monthly as a result of a consensus discussion, conducted by e-mail, among all the NMHSs. All the members share a common methodology and several parameters have been agreed upon and are being refined from year to year. This consensus forecast is widely disseminated by e-mail to more than 15 000 users across Central and South America and contacts on other continents. This approach has increased the understanding of the climate information management process, and the organizations have established a regional/national basis for early warning and risk management systems (Martínez, 2009).

However, although the coordination and dissemination mechanisms have being strengthened in the past few years, an outstanding remaining limitation is the scarcity of international-level scientists working in the far-eastern Pacific research that is necessary for improving the quality of the information produced, but which involves substantial challenges that have baffled the international scientific community for long and that are also not priority issues for countries away from this region. Collaborative participation of the eastern far-Pacific countries in TPOS activities in this region is a key way by which their scientific capabilities can be enhanced.

4. Data requirements

- High zonal (dx = 500km), meridional (dy = 200km), vertical (dz = 10m) and temporal (dt = 1 day) resolution subsurface temperature measurements are needed between 110°W and the coast of South America within 10° of the equator in order to characterize the propagation, modal dispersion and effective dissipation of Kelvin waves and to characterize the vertical gradients of the shallow thermocline and its vertical displacements.
- Continuity of the TAO array surface meteorology and subsurface temperature measurements in the equatorial (8°S, 5°S, 2°S, Eq, 2°N, 5°N, 8°N) eastern Pacific (125°W, 110°W, 95°W). The preservation of long and homogeneous records is necessary for the characterization of decadal variability and climate change.
- Coastally-trapped wave monitoring requires a coordinated network of sea level and subsurface temperature and current measurements along the coast of South (and Central) America, approximately every 5° latitude on a daily timescale. High vertical resolution (dz=5m in the upper 100 m) would be needed due to the shallow thermocline.
- Alongshore coastal wind measurements are necessary in order to assess the local forcing of the ocean. The strong diurnal cycle would need to be adequately sampled and alongshore variability associated with local topography needs to be considered.
- Vertical velocity estimates in the equatorial eastern Pacific (near 90°W) are necessary to estimate vertical thermal advection, which is a key component of the heat budget in this region. This is needed also for estimating the thermocline ENSO feedback and to quantify the nonlinear advection ENSO feedback. The estimates would need to resolve the intraseasonal timescales observed in Kelvin and tropical instability waves. Vertical resolution should match that of the temperature measurements (dz = 10m in the upper 200m) with a precision on the order of 1cm/day.

- Zonal velocities associated with the equatorial current system near 95°W (8°S-2°N) are important to assess the transport of water properties towards the coast of South America and for monitoring the contribution to zonal advection associated with ENSO and the equatorial Kelvin wave. Intraseasonal timescales should be resolved.
- Surface heat flux measurements on the eastern Pacific TAO/TRITON buoys and at locations along the coastal upwelling region on intraseasonal to decadal timescales are necessary for the upper ocean heat budget as a tool for determining feedback mechanisms and validating coupled models.
- Estimations of subsurface vertical turbulent heat fluxes on equatorial eastern Pacific buoys (e.g. 110°W, 95°W) are necessary for closing the heat budget, for estimating the thermocline ENSO feedback and to validate numerical ocean models.
- Long-term measurements of surface winds and heat fluxes and upper ocean vertical thermal structure in the data-sparse southeast Pacific (e.g. Stratus buoy) are needed to characterize the meridional dynamics that can influence the equatorial Pacific and the decadal variability in this region.
- Periodic measurements of dissolved oxygen, pH, PAR, surface chlorophyll-a, turbidity, nitrates, phosphates and silicates in the eastern equatorial Pacific and along the coasts are necessary for monitoring the effect of biogeochemical variability on seasonal to decadal timescales.
- Measurements of surface air-sea gas fluxes in equatorial and coastal regions.
- Wind stress fields resolving the diurnal cycle over the tropical Pacific are needed to adequately characterize atmospheric component of ENSO and decadal variability.
- Characterization of the atmospheric vertical velocity and/or latent heating profiles in the ITCZ on monthly timescales in the eastern Pacific are necessary to validate models for the atmospheric role of ENSO, particularly during strong El Niño.
- Hourly precipitation rates on the TAO/TRITON array and coastal locations to provide ground truth to remote sensing products (e.g. Global Precipitation Mission) and to validate models.
- Diurnal cycle-resolving profiles of equatorial atmospheric temperature, humidity, height and winds for the study of boundary layer processes, equatorial convectively coupled waves and the ITCZ.
- Hourly and long-term measurement of surface wave characteristics (significant height, period, and directional spectrum) that impact the western coast of South America to characterize their dynamics (sea and swell) and their variability on intraseasonal to decadal timescales.

5. Observational strategies

- Near real-time daily subsurface temperature data along the equatorial waveguide is key to monitor the propagation of equatorial Kelvin waves into the far eastern Pacific in support of intraseasonal forecasts for coastal conditions in western South America.

TAO/TRITON is an essential source of data for Equatorial Ocean monitoring and is key for providing long-term continuous records, but has some limitations:

a) It only extends to 95°W to the east, so it cannot observe the propagation and dispersion of Kelvin waves as the thermocline becomes shallower and then deeper towards the coast.

b) The system requires constant maintenance and is therefore vulnerable to funding limitations: 9 out of 10 buoys in the far-eastern equatorial Pacific (110°W-95°W, 5°S-5°N) stopped reporting subsurface temperature data between March and August 2012 when maintenance was suspended (Figure 5.1), and the completeness of the 100 m-depth temperature data was below 40% in the 2012-2013 period for 7 out of these 9 buoys (Figure 5.2).

c) Even though TOA/TRITON contains a relatively large number of buoys, it does not have redundant measurements, particularly in the eastern Pacific where strong zonal and meridional gradients in the circulation exist and the data from different latitudes are needed to separate Kelvin and Rossby modes.

d) Vertical resolution in the far-eastern Pacific (95°W) is too low (approx. dz = 20m for 0-140m) for thermocline displacements and Kelvin wave dispersion. Need approximately 10m down to a 200m depth.

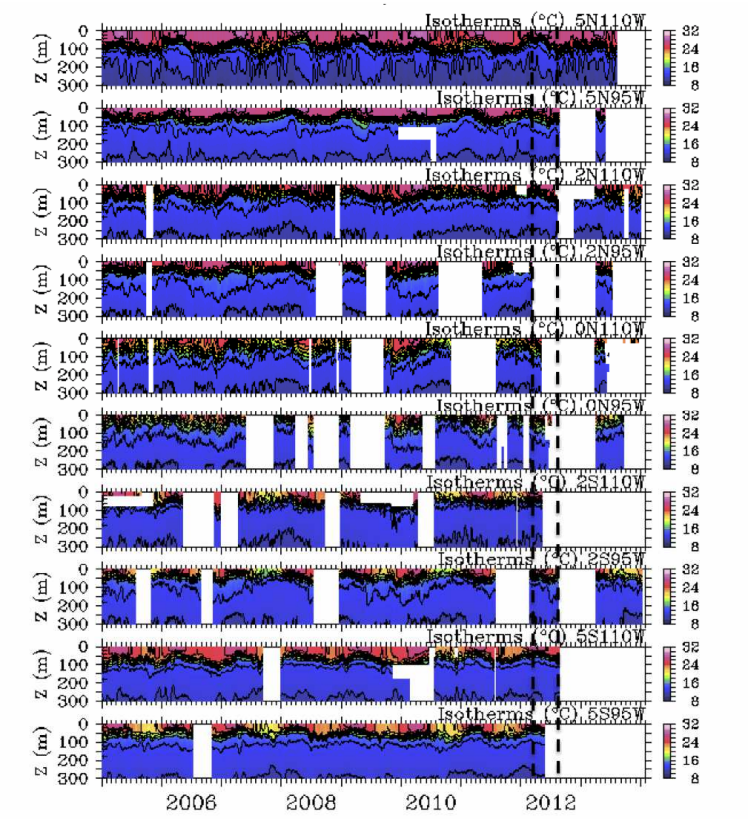

Figure 5.1 - 5-day mean TAO subsurface temperature measurements in the far-eastern equatorial Pacific (110W-95W, 5S-5N). Dashed lines indicate March and August 2012 (from http://www.pmel.noaa.gov/tao).

- Some possible strategies for strengthening the subsurface physical and biogeochemical observing system in the far-eastern equatorial Pacific are:

  a) Establish partnerships with regional institutions to maintain the existing easternmost buoys (110°W, 95°W).

  b) Add an additional buoy line at 85°W (10°S-10°N), equipped with physical and biogeochemical sensors. However, high exposure to vandalism would make the sustainability challenging.

  c) Deploy Iridium-equipped ARGO drifters equipped with biogeochemical sensors (oxygen, pH) in the region 95°W-80°W, 10°S-10°N with high meridional resolution (2°) and sampling rate of at least one profile every 3 days per drifter.

  d) Operate gliders equipped with biogeochemical sensors in a continuous monitoring mode in the region 95°W-80°W, 10°S-10°N. However, the required dense spatial and temporal sampling, the need for permanent human resources, and the large size of the region, would be limiting considerations for this approach.

- TOPEX/JASON data does provide adequate meridional resolution, but meridional structures of different vertical modes present subtle differences on sea level, so this should be considered complementary to the buoys. Additionally, the temporal resolution is too low for adequate monitoring of intraseasonal Kelvin waves.

- ALTIKA will provide high-resolution sea level that could be used for coastal wave propagation.

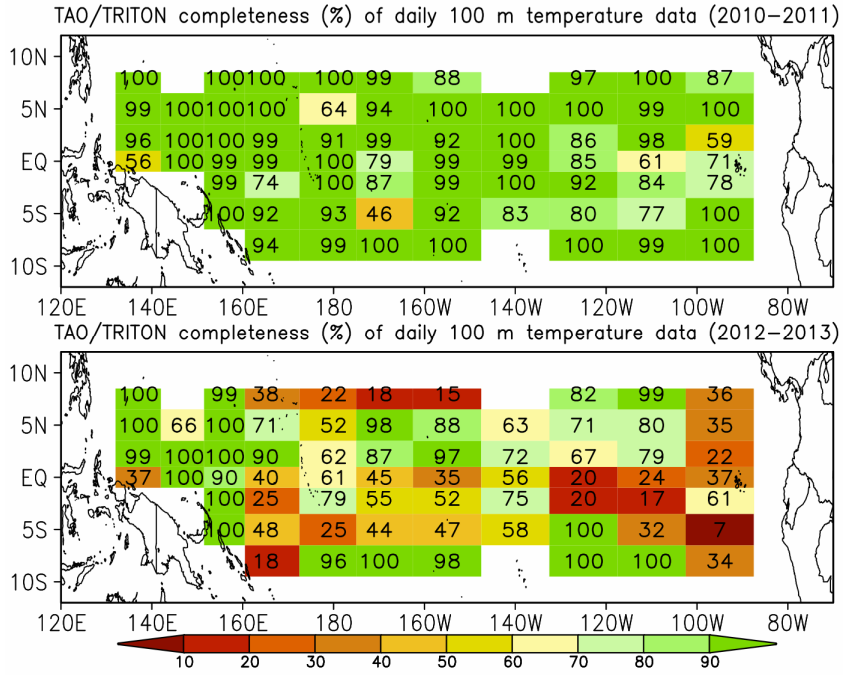

Figure 5.2 - Completeness (%) of daily 100 m-depth temperature TAO/TRITON data for the 2010-2011 (top) and 2012-2013 (bottom) periods (data from http://www.pmel.noaa.gov/tao/data_deliv/deliv.html).

- Along the coast of South America, high-frequency subsurface temperature and salinity, surface meteorology and air-sea fluxes measurements are also needed for near real-time monitoring and research. Given the strong problem of vandalism, surface buoys are not recommended. Some options are:

  a) Oil drilling platforms near the equatorial coasts (excellent opportunity for thermodynamic profiling although measurements of currents could be compromised by the platforms themselves).
  b) Small islands that disturb minimally the air-flow (corrections could be estimated with a modeling approach).

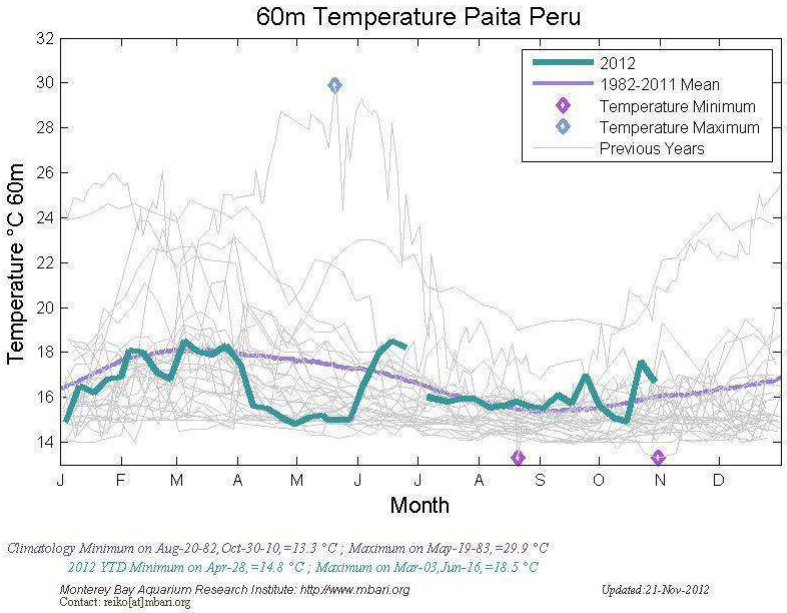

Figure 5.3 - Weekly 60 m-depth temperature off the coast of Paita, Peru (5S) maintained by MBARI from 1982 to the present (from: http://www.mbari.org/bog/Projects/Peru/peruhome.htm).

  c) Shallow subsurface moorings with data collected weekly using small crafts or connected with cables to the coast.
  d) Continuous operation of gliders near the coasts (an advantage is that they could be withdrawn when fishing activities pose a risk)
  e) Near-coastal (0-100 m) periodic CTD measurements using very small crafts (a cheap approach been proven reliable by the continuous weekly measurements supported by MBARI off Paita (5S) since 1982 to date, see Figure 5.3).

6. Data and Information delivery

The dissemination system for TAO/TRITON through the PMEL website is excellent, although it could use some improvements. The quick-view figure feature should be treated as a data delivery component for real-time applications and it would be useful to allow for more customization (interpolation options, contouring, averaging) and more explicit warnings in case of buoy problems.

It is highly desirable that other real-time components of the monitoring system, e.g. Argo drifter data, satellite data, and the regional observations (e.g. sea level, coastal temperature, etc.) are available in a similar fashion, ideally through a single integrated portal and common file formats (e.g. NetCDF), even if each observing subcomponent maintains particularities in their data processing. Data quality and other metadata should be easily accessible and common standards and protocols should be implemented.

7. Potential synergies and opportunities with countries in western South America

- Since 2003, the SE Pacific countries (Colombia, Ecuador, Peru and Chile), established the GOOS Regional Alliance for the South Eastern Pacific (GRASP). It has a Strategic Plan which could be updated and discussed in line with the TPOS new challenges and objectives. http://www.grasp.cpps-int.org/
- Considering the annual efforts that SE Pacific countries develop to conduct regional cruises each year (since 1997), this cooperation mechanism could be a good opportunity as support of TPOS, particularly for buoys maintenance, and as platforms for addressing critical gaps in research. http://www.cpps-int.org/index.php/el-nino-y-la-oscilacion-del-sur/erfen/crucero-regional.html
- The potential interaction and coordination between Global and regional programmes requires a considerable effort, time and resources mobilization. Regional organizations such as CPPS (http://www.cpps-int.org/index.php/el-nino-y-la-oscilacion-del-sur/erfen/crucero-regio-nal.html) and CIIFEN could make a significant contribution to hasten cooperation mechanisms with TAO-TRITON, integrate and exchange data and enhance the TPOS.
- Since 2001 to 2009, relevant efforts of IOC-UNESCO were developed in the region to enhance the ocean data exchange and evolve the traditional observing systems to near real time systems. These efforts are still ongoing, but not well connected with the research community at regional and global scale.
- Galapagos Islands (Ecuador), Hormigas Island (Peru) and oil drilling platforms, are strategic places to concentrate observations and multipurpose platforms. In addition, there is increasing interest of local and international organizations to enhance ocean and atmosphere observation systems that can be taken as an opportunity for the new design of TPOS.
- SE Pacific countries have increased their near real time gauges and coastal stations. However the data exchange is still limited as well as ocean modeling for operational and research purposes. Potential tradeoffs could be explored to get a better and more collaborative TPOS which involves to SE Pacific countries.

8. General Recommendations

- Explore bilateral or regional cooperation mechanisms for ship employment as contribution to TPOS, particularly for the maintenance of TAO buoys and/or other components of the observational system.

- Define a road map for a high level cooperation mechanism between TAO/TRITON and GRASP.
- Ensure the continuity of the TAO array into the far eastern Pacific equatorial waveguide (to 95°W) and implement high-density ARGO monitoring farther to the east with comparable latitudinal resolution to characterize intraseasonal Kelvin wave propagation across the zonal thermocline gradients.
- Promote and support a sustained real-time coastal network of sea level, SST, and wind measurements based on national systems to be incorporated into TPOS.
- Promote and support a network of sustained coastal measurements of subsurface temperature, currents, biogeochemistry, and surface heat/momentum/gas fluxes. The data should be made available as part of TPOS at least monthly.
- Include biogeochemical sensors in the eastern Pacific TAO buoys and Argo drifters.
- Explore synergies between SE Pacific region scientific networks with GEWEX.
- Organize an international meeting in SE Pacific region with the support of International agencies, IOC, WMO and JCOMM to define the road map to the enhancement of TPOS in the Eastern Pacific region including the presence of financial institutions. Explore bilateral or regional cooperation mechanisms for ship employment as contribution to TPOS, particularly for the maintenance of TAO buoys and/or other components of the observational system.

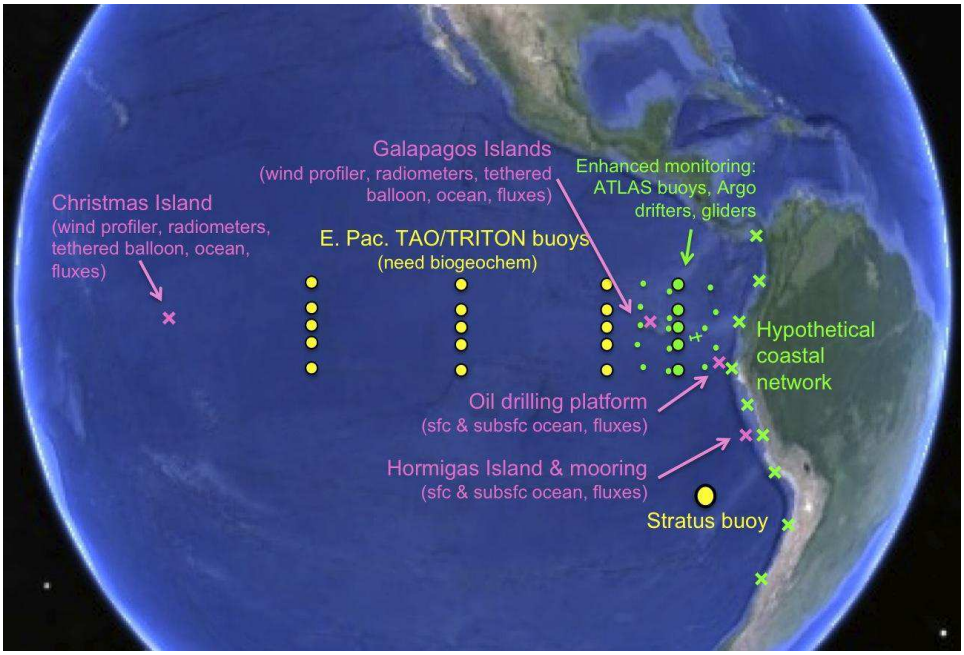

Figure 8.1 - Potential components of the enhanced observing system in the far-eastern Pacific for addressing needs of western South America.

References

Aiken, C. M., Navarrete, S.A., and Pelegrí, J.L. (2011): Potential changes in larval dispersal and alongshore connectivity on the central Chilean coast due to an altered wind climate, J. Geophys. Res., 116, G04026, (doi:10.1029/2011JG001731).

Alheit, J., and Bernal, P. (1993): Effects of physical and biological changes on the biomass yield of the Humboldt Current ecosystem. In Large Marine Ecosystems: Stress, Mitigation, and Sustainability, pp. 53–68. Ed. by K. Sherman, L. M. Alexander, and B. D. Gold. American Association for the Advancement of Science, Washington, D.C.

Alory, G., Maes, C., Delcroix, T., Reul, N., and Illig, S. (2012): Seasonal dynamics of sea surface salinity off Panama: The far Eastern Pacific Fresh Pool, J. Geophys. Res. 117, C04028, (doi:10.1029/2011JC007802).

An, S.I., and Im, S.H. (2013): Blunt ocean dynamical thermostat in response of tropical eastern Pacific SST to global warming. Theoretical and Applied Climatology, (doi:10.1007/s00704-013-1048-0).

An S.I., and Jin, F.F. (2004): Nonlinearity and asymmetry of ENSO. J Clim 17:2399-2412.

Arntz, W. E., and Tarazona, J. (1990): Effects of El Niño 1982-83 on benthos, fish and fisheries off the South American Pacific coast. Global Ecological Consequences of the 1982–83 El Nino—SouthernOscillation.

Back, L. E., and Bretherton, C. S. (2006): Geographic variability in the export of moist static energy and vertical motion profiles in the tropical Pacific. Geophys. Res. Lett. 33 (17), L17810.

Bakun, A. (1990): Global climate change and intensification of coastal ocean upwelling. Science, 247, pp. 198-201.

Barber, R.T., and Chavez, F.P. (1983): Biological consequences of El Niño. Science, 222, pp. 1203-1210.

Barnston, A. G., Glantz, M. H., and He, Y. (1999): Predictive skill of statistical and dynamical climate models in SST forecasts during the 1997–98 El Niño episode and the 1998 La Niña onset. Bull. Amer. Met. Soc. 80 (2), pp. 217-243.

Barnston, A., Tippett, M., L'Heureux, M., Li, S., DeWitt, D. (2012): Skill of Real-Time Seasonal ENSO Model Predictions during 2002-11: Is Our Capability Increasing? Bull. Amer. Met. Soc., (doi:10.1175/BAMS-D-11-00111.1).

Barber, R. T., and Chávez, F. P. (1983): Biological consequences of El Niño. Science 222, 1203-1210.

Belmadani, A., Echevin, V., Codron, F., Takahashi, K., Junquas, C. 2013: What dynamics drive future wind scenarios for coastal upwelling off Peru and Chile? Climate Dynamics doi:10.1007/s00382-013-2015-2

Bellucci A, Gualdi S, Navarra A, 2010: The double-ITCZ syndrome in coupled general circulation models: The role of large-scale vertical circulation regimes. J. Climate 23 (5), 1127-1145.

Benestad, R.E., 1997: Intraseasonal Kelvin waves in the Tropical Pacific, D.Phil thesis, Oxford University, pp. 244.

Bergman J. W., Hendon, H.H., and Weickmann, K.M. (2001): Intraseasonal air-sea interactions at the onset of El Niño. J Climate 14: pp. 1702–1719.

Busalacchi, A. J., and Cane, M.A. (1988): The effect of varying stratification on low-frequency equatorial motions. J. Phys. Oceanogr., 18, pp. 801-812.

Cai, W., Borlace, S., Lengaigne, M., van Rensch, P., Collins, M., Vecchi, G., Timmermann, A., Santoso, A., McPhaden, M., Wu, L., England, M., Wang, G., Guilyardi, E., and Jin, F. F. (2014): Increasing frequency of extreme El Nino events due to greenhouse warming. Nature Climate Change, (doi:10.1038/NCLIMATE2100).

Carranza, L. (1891): Contra-corriente marítima, observada en Paita y Pacasmayo. Boletín de la Sociedad Geográfica de Lima, 1 (9), pp. 344-345.

Castro-González, M., Molina V., Rodríguez-Rubio E., and Ulloa, O. (2014): The first report of a microdiverse anammox bacteria community in waters of Colombian Pacific, a transition area between prominent oxygen minimum zones of the eastern tropical pacific.. Submitted to Environmental Microbiology.

Chavez, F.P., Bertrand, A., Guevara-Carrasco, R., Soler, P., and Csirke, J. (2008): The northern Humboldt Current System: brief history, present status and a view towards the future. Progress in Oceanography, 79: pp. 95-105.

Chelton, D. B., Freilich, M.H., and Esbensen, S.K. (2008): Satellite observations of the wind jets off the Pacific Coast of Central America. Part II: Relationships and dynamical considerations, Mon. Wea. Rev., 128, pp. 2019–2043.

Chiang, J.C.H., and Vimont, D.J. (2004): Analogous Pacific and Atlantic meridional modes of tropical atmosphere.ocean variability. J. Climate, 17, pp. 4143-4158.

Choi, J., An, S. I., Kug, J. S., and Yeh, S. W. (2010): The role of mean state on changes in El Niño's flavor. Clim. Dyn. (doi:10.1007/s00382-010-0912-1).

Choi, K.Y., Vecchi, G.A., and Wittenberg, W.T. (2013): ENSO transition, duration, and amplitude asymmetries: Role of the nonlinear wind stress coupling in a conceptual model. J. Climate, 26, pp. 9462–9476.

Clarke, A. J., and Lebedev, A. (1999): Remotely driven decadal and longer changes in the coastal Pacific waters of the Americas, J. Phys. Oceanogr., 29, pp. 828 – 835.

Clement, A. C., Seager, R., Cane, M.A., and Zebiak, S.E. (1996): An ocean dynamical thermostat. J. Climate, 9, pp. 2190–2196.

Codispoti, L.A., Barber, R.T., and Friederich, G.E. (1989): Do nitrogen transformations in the poleward undercurrent off Peru and Chile have a globally significant influence? In: Neshyba, S.J., Mooers, N.K., Smith, R.L., Barber, R. (Eds.), Poleward Flows Along Eastern Ocean Boundaries. Coastal and Estuarine Studies. Springer-Verlag, pp. 281–310.

Cravatte, S., Picaut, J., and Eldin, G. (2003): Second and first baroclinic Kelvin modes in the equatorial Pacific at intraseasonal timescales, Journal of Geophysical Research-Oceans, 108(C8).

Cravatte, S., Madec, G., Izumo, T., Menkes, C., and Bozec, A. (2007): Progress in the 3-D circulation of the eastern equatorial Pacific in a climate ocean model, Ocean Modeling, 17(1), pp. 28-48.

Cury, P., and Roy, C. (1989): Optimal environmental window and pelagic fish recruitment success in upwelling areas. Canadian Journal of Fisheries and Aquatic Sciences, 46: pp. 670-680.

Dalsgaard, T., Thamdrup, B., and Canfield, D.E. (2005): Anaerobic ammonium oxidation (anammox) in the marine environment. Res Microbiol 156: pp. 457-464.

Dekaezemacker, J., Bonnet, S., Grosso, O., Moutin, T., Bressac, M., and Capone, D.G. (2013), Evidence of active dinitrogen fixation in surface waters of the eastern tropical South Pacific during El Niño and La Niña events and evaluation of its potential nutrient controls,Global Biogeochem. Cycles, 27,

(doi:10.1002/gbc.20063).

Deser, C., and Wallace, J.M. (1987): El Niño events and their relation to the Southern Oscillation. J. Geophys. Res. 92 (C13), pp. 14189-14196.

Dewitte B., Reverdin, G., and Maes, C. (1999): Vertical structure of an OGCM simulation of the equatorial Pacific Ocean in 1985-1994.J. Phys. Oceanogr., 29, pp. 1542-1570.

Dewitte B., and Reverdin, G. (2000): Vertically propagating annual and interannual variability in an OGCM simulation of the tropical Pacific in 1985-1994. J. Phys. Oceanogr., 30, pp. 1562-1581.

Dewitte, B., Illig, S., Renault, L., Goubanova, K., Takahashi, K., Gushchina, D., Mosquera, K., Purca, S., 2011: Modes of covariability between sea surface temperature and wind stress intraseasonal anomalies along the coast of Peru from satellite observations (2000–2008). J. Geophys. Res. 116, C04028, (doi:10.1029/2010JC006495).

Dewitte B., Illig, S., Parent, L., duPenhoat, Y., Gourdeau, L., and Verron, J. (2003): Tropical Pacific baroclinic mode contribution and associated long waves for the 1994-1999 period from an assimilation experiment with altimetric data. J. Geophys. Research, 108 (C4), pp. 3121-3138.

Dewitte, B., Vasquez, J., Goubanova, K., Illig, S., Takahashi, K., Cambon, G., Purca, S., Correa, D., Gutierrez, D., Sifeddine, A., and Ortlieb, L. (2012): Change in El Niño flavors over 1958-2008: Implications for the long-term trend of the upwelling off Peru, Deep-Sea Research II, (doi:10.1016/j.dsr2.2012.04.011).

Díaz-Ochoa, J., Rodríguez-Rubio., E., Alvarez-León, R. (2004): Oscilaciones quasi-bienales de un índice del reclutamiento del camarón Litopenaeus occidentalis con relación a la variabilidad climática del Pacífico oriental tropical. En: Contribuciones al Estudio de los Crustáceos del Pacífico Este 3, Publisher: Instituto de Ciencias del Mar y Limnología, UNAM., Editors: M.E. Hendrickx, pp.17-29 .

Dommenget, D., Bayr, T., and Frauen, C. (2012): Analysis of the non-linearity in the pattern and time evolution of El Niño southern oscillation. Clim. Dyn., (doi:10.1007/s00382-012-1475-0).

Falvey, M., and Garreaud, R.D. (2009): Regional cooling in a warming world: Recent temperature trends in the southeast Pacific and along the west coast of subtropical South America (1979–2006). J. Geophys. Res., 114 (D04102), pp. 1–5. (doi:10.1029/2008JD010519).

Flores, R., Tenorio, J., Dominguez, N. (2009): Variaciones de la extensión Sur de la Corriente Cromwell frente al Peru entre los 3–14 S. Boletín Instituto del Mar del Peru 24 (1–2), pp. 45–55.

Fossing, H., 1990. Sulfate reduction in shelf sediments in the upwelling region off central Peru. Continental Shelf Research 10 (4), pp. 355–367.

Fuenzalida H., Aceituno, P., Falvey, M., Garreaud, R., Rojas, M., and Sanchez, R. (2007): Study on climate variability for Chile during the 21st century [in Spanish], technical report, Natl. Environ. Comm. Santiago.

Gage, K. S., Balsley, B. B., Ecklund, W. L., Carter, D. A., and McAfee, J. R. (1991): WInd-profiler research in the tropical Pacific. J. Geophys. Res. 96, pp. 3209-3220.

Galán, A., Molina, V., Thamdrup, B., Woebken, D., Lavik, G., Kuypers, M.M.M., and Ulloa, O. (2009): Anammox bacteria and the anaerobic oxidation of ammonium in the oxygen minimum zone off northern Chile. Deep-Sea Res II 56(16): pp. 1021-1031.

Galán, A., Molina, V., Belmar, L., Ulloa, O. (2012): Temporal variability in phylogenetic characterization of planktonic anammox bacteria in the coastal upwelling ecosystem off central Chile. Progr in Oceanogr 92-95: pp. 110-120.

Garces-Vargas, J., Schneider, W., Abarca del Rıo, R., Martinez, R., and Zambrano, E. (2005): Inter-annual variability in the thermal structure of an oceanic time series station off Ecuador (1990–2003) associated with El Nino events, Deep-Sea Res. Pt. I, 52, pp. 1789–1805.

Garreaud, R. D., and Battisti, D.S. (1999): Interannual (ENSO) and interdecadal (ENSO-like) variability in the Southern Hemisphere tropospheric circulation. J. Climate, 12, pp. 2113-2122.

Garreaud, R., and Falvey, M. (2009): The coastal winds off western subtropical South America in future climate scenarios. Int. J. Climatol., 29, 543–554, (doi:10.1002/joc.1716).

Gergis, J., and Fowler, A. (2009): A history of ENSO events since A.D. 1525: Implications for future climate change, Clim. Change, 92, 343–387, (doi:10.1007/s10584-008-9476-z).

Giese, B. S., and D. E. Harrison, D.E. (1990): Aspect of the Kelvin wave response to episodic wind forcing. J. Geophys. Res., 95, pp. 7289-7312.

Goldberg, R. A., Tisnado, G., and Scofield, R. A. (1987): Characteristics of extreme rainfall events in north-western Peru during the 1982– 1983 El Niño period, J. Geophys. Res.,92,C14, pp. 14225–14241.

Graham, N. E., and Barnett, T. P. (1987): Sea surface temperature, surface wind divergence, and convection over tropical oceans. Science 238 (4827), pp. 657-659.

Gutiérrez, D., and collaborators (2009): Rapid reorganization in ocean biogeochemistry off Peru towards the end of the Little Ice Age, Biogeosciences, 6, pp. 835–848, (doi:10.5194/bg-6-835-2009).

Gutiérrez, D., and collaborators (2011b): Coastal cooling and increased productivity in the main upwelling zone off Peru since the mid-twentieth century, Geophys. Res. Lett., 38, L07603, (doi:10.1029/2010GL046324).

Gutiérrez, D., Enríquez, E., Purca, S., Quipúzcoa, L., Marquina, R., Flores, G. and Graco, M. 2008. Oxygenation episodes on the continental shelf of central Peru: Remote forcing and benthic ecosystem response. Progress in Oceanography, 79, pp. 177-189.

Gutiérrez, D., Bertrand, A., Wosnitza-Mendo, C., Dewitte, B., Purca, S., Peña, C., Chaigneau, A., Tam, J., Graco, M., Echevin, V., Grados, C., Fréon, P., and Guevara-Carrasco, R. (2011a): Sensibilidad del sistema de afloramiento costero del Perú al cambio climático e implicancias ecológicas. Revista Peruana Geo-Atmosférica, 3: pp. 1-26.

Hegerl, G. C., and collaborators (2007): Understanding and attributing climate change, in Climate Change 2007, edited by S. Solomon et al., pp. 663 – 745, Cambridge Univ. Press, Cambridge, U. K.

Held, I. M., and Soden, B.J. (2006): Robust responses of the hydrological cycle to global warming. J. Climate, 19, pp. 5686–5699.

Helly, J.J., and Levin, L. A. (2004): Global distribution of naturally occurring marine hypoxia on continental margins. Deep Sea Research I, 51: pp. 1159–1168.

Hemer, M., Katzfe, J., and Hotan. C. (2011): The wind-wave climate of the Pacific Ocean. Report for the Pacific Adaptation Strategy Assistance Programme Department of Climate Change and Energy Efficiency. CSIRO, 120 pp.

Hemer, M.A., Fan, Y., Mori, N., Semedo, A., and Wang, X.L. (2013): Projected changes in wave climate from a multi-model ensemble, Nature Climate Change 3, 471, (doi:10.1038/nclimate1791).

Horel, J. D. and Cornejo-Garrido, A. G. (1986): Convection along the coast of northern Peru during 1983: Spatial and temporal variation of clouds and rainfall, Mon. Wea. Rev., 114, pp. 2091–2105.

Huyer, A., Knoll, M., Paluszkiewicz, T., and Smith, R. (1991): The Peru Undercurrent: a study in

variability. Deep Sea Research Part A. Oceanographic Research Papers. Volume 38, Supplement 1, pp. 247–271.

IPCC WG1 (2013): Climate Change 2013: The Physical Science Basis. http://www.ipcc.ch/report/ar5/wg1/.

Izaguirre, C., Menéndez, M., Camus, P., Méndez, F., Mínguez, R., and Losada, I. (2012): Exploring the interannual variability of extreme wave climate in the Northeast Atlantic Ocean. Ocean Modeling, Vol, 59-60, pp. 31-40.

Jin, F.F., An, S.I., Timmermann, A., Zhao, J. (2003): Strong El Niño events and nonlinear dynamical heating. Geophys Res Lett 30 (3) 1120, (doi:10.1029/2002GL016356).

Jin, F.-F., Lin, L., Timmermann, A., and Zhao, J. (2007): Ensemble-mean dynamics of the ENSO recharge oscillator under state-dependent stochastic forcing. Geophys. Res. Lett. 34, L03807.

Karamperidou, C., Di Nezio, P.N., and Jin, F.F. (2014): The response of ENSO flavors to orbital forcing. Paleoceanography, submitted.

Kessler, W.S., and McPhaden, M.J. (1995b): The 1991-93 El Niño in the central Pacific. Deep Sea Res II 42: pp. 295–333.

Kessler WS, McPhaden MJ (1995a) Oceanic equatorial waves and the 1991-93 El Niño. J Climate 8: pp. 1757–1774.

Kessler, W.S., McPhaden, M.J., and Weickmann, K.M. (1995) Forcing of intraseasonal Kelvin waves in the equatorial Pacific. J Geophys Res 100(C6): pp. 10613–10631.

Kessler, W.S., and Kleeman, R. (2000): Rectification of the Madden–-Julian oscillation into the ENSO cycle. J Climate 13: pp. 3560–3575.

Kirtman, B.P., Shukla, J., Balmaseda, M.A., Graham, N., Penland, C., Xue, Y., Zebiak, S. (2000): Current status of ENSO forecast skill. Report to CLIVAR (http://grads.iges.org/ellfb/WGSIP/report.htm).

Kirtman and coauthors (2013): The North American Multi-Model Ensemble (NMME) for Intra-Seasonal to Interannual Prediction. Submitted to Bull. Amer. Met. Soc.

Klein, S., and Hartmann, D.L. (1993): The seasonal cycle of low stratiform clouds. J. Climate, 6, pp. 1587–1606.

Kosaka, Y., and Xie, S. P. (2013): Recent global-warming hiatus tied to equatorial Pacific surface cooling, Nature, (doi:10.1038/nature12534).

Lagos, P., Silva, Y., Nickl, E., and Mosquera, K. (2008): El Niño–related precipitation variability in Perú. Adv. Geosciences, (doi:10.5194/adgeo-14-231-2008).

Lam, P., Lavik, G., Jensen, M., van de Vossenberg, J., Schmid, M., Woebken, D., Gutierrez, D., Amann, R., Jetten, M., and Kuypers, M. (2009): Revising the nitrogen cycle in the Peruvian oxygen minimum zone. Procceedings of the National Academy of Sciences USA, 106: pp. 4752–4757.

Landsea, C.W., and Knaff, J.A. (2000): How much skill was there in forecasting the very strong 1997–98 El Niño? Bull. Amer. Met. Soc., 81 (9), pp. 2107-2119.

Lavado, W. C., and Espinoza, J. C. (2013): Impactos de El Niño y La Niña en las lluvias del Perú (1965-2007). Rev. Brasileira de Met., in review.

Lee, T., and McPhaden, M.J. (2010): Increasing intensity of El Niño in the central-equatorial Pacific. Geophys. Res. Lett. 37 (14), pp. L14603.

Leloup, J., and Clement, A. (2009): Why is there a minimum in projected warming in the tropical North Atlantic Ocean?. Geophys. Res. Lett., 36, L14802, (doi:10.1029/ 2009GL038609).

Lengaigne, M., Guilyardi, E., Boulanger, J. P., Menkes, C., Delecluse, P., Inness, P., Cole, J., and Slingo, J. (2004): Triggering of El Niño by westerly wind events in a coupled general circulation model. Clim. Dyn. 23, pp. 601–620.

L'Heureux, M., Lee, S. and Lyon, B. (2012): Recent multidecadal strengthening of the Walker circulation across the tropical Pacific. Nature Climate Change, 3: pp. 571-57.

Lloyd, J., Guilyardi, E., and Weller, H. (2012): The role of atmosphere feedbacks during ENSO in the CMIP3 models. Part III: The shortwave flux feedback. J Clim. (doi:10.1175/JCLI-D-11- 00178.1).

Martellini, B., Tamy, J., and Quispe, C. (2007): Modelo empírico para previsión de la temperatura superficial del mar peruano. Rev. Peru. Biol., 14(1), pp. 101-108.

Maturana, J., Bello, M., and Manley, M. (2004): Antecedentes históricos y descripción del fenómeno El Niño, Oscilación del Sur. In: Avaria S, J Carrasco, J Rutllant, & E Yáñez (eds). El Niño-La Niña 1997-2000, pp. 13-27. Comité Oceanográfico Nacional, Valparaíso.

McPhaden, M.J. (2008): Evolution of the 2006–2007 El Niño: The role of intraseasonal to interannual time scale dynamics. Adv. Geosci., 14, pp. 219–230.

McPhaden, M.J., and Taft, B.A. (1988): Dynamics of seasonal and intraseasonal variability in the eastern equatorial Pacific, J Phys Oceanogr 18: pp. 1713–1732.

Meehl, G. A., Washington, W.M., Ammann, C., Arblaster, J.M., Wigley, T.M.L., and Tebaldi, C. (2004): Combinations of natural and anthropogenic forcings and twentieth-century climate. J. Climate, 17, pp. 3721–3727.

Meehl, G. A., and collaborators (2007): Global climate projections, in Climate Change 2007, edited by S. Solomon et al., pp. 747 – 846, Cambridge Univ. Press, Cambridge, U. K.

Meehl, G. A., Hu, A., and Santer, B.D. (2009a): The mid-1970s climate shift in the Pacific and the relative roles of forced versus inherent decadal variability. J. Climate, 22, pp. 780–792.

Meehl, G.A., and collaborators, 2009b: Decadal prediction: can it be skillful? Bull. Amer. Met. Soc., 90, pp. 1467-1485, (doi:10.1175/2009BAMS2607.1)

Meehl, G., Hu, A., and Tebaldi, C. (2010): Decadal prediction in the Pacific region, J. Climate 23 (11), pp. 2959-2973, (doi:10.1175/2010JCLI3296.1).

Mitchell, T., and Wallace, J. M. (1992): The annual cycle in equatorial convection and sea surface temperature. J. Climate 5, 10, pp. 1140-1156.

Montecinos, A., and Aceituno, P. (2003): Seasonality of the ENSO-related rainfall variability in Central Chile and associated circulation anomalies. J. Climate 16, pp. 281-296.

Montecinos, A., and Pizarro, O. (2005): Interdecadal sea surface temperature-sea level pressure coupled variability in the South Pacific Ocean, J. Geophys. Res., 110, C08005, (doi:10.1029/2004JC002743).

Montecinos, A., Purca, S., Pizarro, O. (2003): Interannual-to-interdecadal sea surface temperature variability along the western coast of South America. Geophys. Res. Lett., 30, pp. 1570, (doi:10.1029/2003GL017345).

Montecinos, A., Leth, O. and Pizarro, O. (2007): Wind-driven interdecadal variability in the eastern tropical and South Pacific, J. Geophys. Res. 12 (C4), 8 pp, (doi:10.1029/2006JC003571).

Montes, I., Colas, F. Capet, X., and Schneider, W. (2010): On the pathways of the equatorial subsurface currents in the eastern equatorial Pacific and their contribution to the Peru-Chile undercurrent. Journal of Geophysical Research, 115: C09003. (doi:10.1029/2009JC005710).

Moore, A. M., and Kleeman, R. (1999): Stochastic forcing of ENSO by the intraseasonal oscillation. J. Clim. 12, pp. 1199–1220.

Morales, C.E., Hormazabal, S.E., and Blanco, J.L. (1999): Interannual variability in the mesoscale distribution of the depth of the upper boundary of the oxygen minimum layer off northern Chile (18–241S): implications for the pelagic system and biogeochemical cycling. Journal of Marine Research 57, pp. 909–932.

Mosquera, K. (2009): Variabilidad intra-estacional de la onda de Kelvin ecuatorial en el Pacífico (2000-2007): Simulación numérica y datos observados. M.Sc. Thesis in Physics (Geophysics), Universidad Nacional Mayor de San Marcos.

Mosquera-Vásquez, K., Dewitte, B., Illig, S., Takahashi, K., and Garric, G. (2013): The 2002-03 El Niño: Equatorial waves sequence and their impact on sea surface temperature, Journal of Geophysical Research, Oceans, (doi:10.1029/2012JC008551).

Mosquera-Vásquez, K., Dewitte, B., and Illig, S. (2014): The Central Pacific El Niño intraseasonal Kelvin wave. Journal of Geophysical Research, Oceans, submitted.

Mulder, A., Van de Graaf, A,A., Robertson, L.A., and Kuenen, J.G. (1995): Anaerobic ammonium oxidation discovered in a denitrifying fluidized bed reactor. FEMS Microbiol Ecol 16: pp. 177-184.

Murphy, R. C. (1926): Oceanic and climatic phenomena along the west coast of South America during 1925. Geographical Review, 16 (1), pp. 26-54.

Narayan, N., Paul, A., Mulitza, S., and Schulz, M. (2010): Trends in coastal upwelling intensity during the late 20th century, Ocean Sci., 6, pp. 815–823, (doi:10.5194/os-6-815-2010).

Neelin, J., Battisti, D.S., Hirst, A.C., Jin, F.F., Wakata, Y., Yamagata, T., and Zebiak, S. (1998): ENSO theory. J. Geophys. Res. 103 (C7) 14261.

Nigam, S., Chung, C., and DeWeaver, E. (2000): ENSO diabatic heating in ECMWF and NCEP–NCAR Reanalyses, and NCAR CCM3 simulation. J. Climate 13, pp. 3152-3171.

Nigam, S., and Chung, C. (2000): ENSO surface winds in CCM3 simulation: Diagnosis of errors. J. Climate 13, pp. 3172-3186.

Nitta, T., and Yamada, S. (1989): Recent warming of tropical sea surface temperature and its relationship to the Northern Hemisphere circulation, J. Meteor. Soc. Japan, 67, pp. 375-382.

Ortlieb, L. (2000): The documentary historical record of El Niño events in Peru: An update of the Quinn record (sixteenth through nineteenth centuries), in El Niño and the Southern Oscillation: Variability, Global and Regional Impacts, edited by H. Diaz and V. Markgraf, pp. 207–295, Cambridge Univ. Press, Cambridge, U. K.

Pauly, D., and Tsukayama, I. (Eds.) (1987): The Peruvian anchoveta and its upwelling ecosystem: Three decades of change. ICLARM Studies and Reviews, 351 pp.

Pennington, J.T., Mahoney, K.L., Kuwahara, V. S., Kolber, D., Calienes, R., and Chavez, F.P. (2006): Primary production in the eastern tropical Pacific: A review. Progress in Oceanography, 69: pp. 285-317.

Perez, C. L., Moore, A. M., Zavala-Garay, J., and Kleeman, R. (2005): A comparison of the influence of additive and multiplicative stochastic forcing on a coupled model of ENSO. J. Clim. 18, pp. 5066–5085.

Périgaud, C., and Dewitte, B. (1996): El Niño-La Niña events simulated with the Cane and Zebiak's model and observed with satellite or in situ data. Part I: Model data comparison. J. Climate, 9, pp. 66-84.

Pizarro, O., and Montecinos, A. (2004): Interdecadal variability of the thermocline along the west coast of South America. Geophys. Res. Lett., 31, L20307, (doi:10.1029/ 2004GL020998).

Poveda, G., and Mesa, O.J. (1997): Feedbacks between hydrological processes in tropical South America and large-scale oceanic–atmospheric phenomena. J. Climate, 10, pp. 2690–2702.

Poveda, G., and Mesa, O.J. (2000): On the existence of Lloró (the rainiest locality on earth): Enhanced ocean–atmosphere–land interaction by a low-level jet. Geophys. Res. Lett., 27, pp. 1675–1678.

Power, S., Casey, T., Folland, C., Colman, A., and Mehta, V. (1999): Interdecadal modulation of the impact of ENSO on Australia. Clim. Dyn., 15, pp. 319-324.

Power, S., Delage, F., Chung, C., Kociuba, G., and Keay, K. (2013): Robust twenty-first-century projections of El Niño and related precipitation variability, Nature, (doi:10.1038/nature12580).

Ray, S., and Giese, B. S. (2012): Historical changes in El Niño and La Niña characteristics in an ocean reanalysis. J. Geophys. Res. 117, C11007, (doi:10.1029/2012JC008031).

Raymond, D. J., and Coauthors (2004): EPIC2001 and the coupled ocean–atmosphere system of the tropical east Pacific. Bull. Amer. Meteor. Soc., 85, pp. 1341–1354.

Reguero, B.G., Méndez, F.J., and Losada, I.J. (2013): Variability of multivariate wave climate in Latin America and the Caribbean. Global and Planetary Change, Vol 100, pp. 70-84.

Rodríguez-Rubio, E., and Stuardo, J. (2002): Variability of photosynthetic pigments in the Colombian Pacific Ocean and its relationship with the wind field using ADEOS-I data. Journal of Earth System Science, 111(3), pp. 227– 236.

Rodríguez-Rubio, E., Schneider, W., and Abarca del Río, R. (2003): On the seasonal circulation within the Panama Bight derived from satellite observations of wind, altimetry and sea surface temperature, Geophys. Res. Lett., 30(7), 1410, (doi:10.1029/ 2002GL016794).

Rodríguez-Rubio, E. (2013): A multivariate climate index for the western coast of Colombia. Adv. Geosci., 33, 21-26. (doi:10.5194/adgeo-33-21-2013).

Saba, V.S., Santidrian-Tomillo, P., Reina, R.D., Spotila, J.R., Musick, J.A., Evans, D.A., Paladino, F.V. (2007): The effect of the El Niño Southern Oscillation on the reproductive frequency of eastern Pacific leatherback turtles. J Appl Ecol 44: pp. 395–404.

Schneider, W., Fukasawa, M., Garcés-Vargas, J., Bravo, L., Uchida, H., Kawano, T., Fuenzalida, R. (2007): Spin-up of South Pacific subtropical gyre freshens and cools the upper layer of the eastern South Pacific Ocean. Geophysical Research Letters 34(24), L24606. (doi: 10.1029/2007GL031933).

Schulz, N., Boisier, J.P., and Aceituno, P. (2011): Climate change along the arid coast of northern Chile. Int. J. Climatol., 32, 1803-1814, (doi: 10.1002/joc.2395).

Schumacher, C., Houze, R.A., and Kraucunas, I. (2004): The tropical dynamical response to latent heating estimates derived from the TRMM precipitation radar. J. Atmos. Sci. 61, pp. 1341-1358.

Schunck, H., Lavik, G., Desai, D.K., Großkopf, T., and Kalvelage, T. (2013): Giant Hydrogen Sulfide Plume in the Oxygen Minimum Zone off Peru Supports Chemolithoautotrophy. PLoS ONE 8(8): e68661. (doi:10.1371/journal.pone.0068661).

Shaffer, G., Pizarro, O., Djurfeldt, L., Salinas, S., and Rutllant, J. (1997): Circulation and low- frequency variability near the Chilean coast: Remotely forced fluctuations during the 1991-92 El Niño, J. Phys.

Oceanogr., 27, pp. 217-235.

Stott, P. A., Tett, S.F.B., Jones, G.S., Allen, M.R., Mitchell, J.F.B., and Jenkins, G.J. (2000): External control of 20th century temperature by natural and anthropogenic forcings. Science, 290, pp. 2133–2137.

Stramma, L., Johnson, G.C., Sprintall, J., and Mohrholz, V. (2008): Expanding oxygen-minimum zones in the tropical oceans. Science 320: pp. 655-58.

Straub, K. H., and Kiladis, G. N. (2001): Observations of a convectively coupled Kelvin wave in the eastern Pacific ITCZ. J. Atmos. Sci. 59, pp. 30-53.

Su, J., Zhang, R., Li, T., Rong, X., Kug, J.S., and Hong, C. (2010): Causes of the El Niño and La Niña amplitude asymmetry in the equatorial eastern Pacific. J Clim 23 (3), 605-617. (doi:10.1175/2009JCLI2894.1).

Stramma, L., Schmidtko, S., Levin, L., and Johnson, G.C. (2010): Ocean oxygen minima expansions and their biological impacts. Deep Sea Research Part I: Oceanographic Research Papers, 57(4): pp. 587-595.

Straub, K. H., and Kiladis, G. N. (2001): Observations of a convectively coupled Kelvin wave in the eastern Pacific ITCZ. J. Atmos. Sci. 59, pp. 30-53.

Takahashi, K. (2004): The atmospheric circulation associated with extreme rainfall events in Piura, Peru, during the 1997—1998 and 2002 El Niñ̃o events. Ann. Geophys. 22: pp. 3917–3926

Takahashi, K. (2005): The annual cycle of heat content in the Peru Current region. J. Climate 18, pp. 4937-4954, (doi:10.1175/JCLI3572.1).

Takahashi, K. , and Battisti, D.S. (2007): Processes controlling the mean tropical Pacific precipitation pattern. Part I: The Andes and the eastern Pacific ITCZ. J. Climate 20, pp. 3434-3451, (doi:10.1175/JCLI4198.1).

Takahashi, K., Montecinos, A., Goubanova, K., and Dewitte, B. (2011): ENSO regimes: Reinterpreting the canonical and Modoki El Niño, Geophys. Res. Lett. (doi:10.1029/2011GL047364).

Takahashi, K., and Dewitte, B. (2013): Strong and moderate El Niño regimes in the GFDL CM2.1 model. Submitted to Clim. Dyn.

Takahashi, K., Martinez, A. G., and Mosquera, K. (2014): The strong far-eastern El Niño in 1925-1926, revisited. To be submitted to Clim. Dyn.

Timmermann, A., Jin, F.F., and Abshagen, J. (2003): A nonlinear theory for El Niño bursting, J Atmos Sci 60 (1), pp. 152-165.

Toniazzo, T. (2010): Climate variability in the south-eastern tropical Pacific and its relation with ENSO: a GCM study. Clim. Dyn. 34, pp. 1093-1114, (doi:10.1007/s00382-009-0602-z).

Tourre, Y. M., Rajagoplan, B., Kushnir, Y., Barlow, M., and White, W.B. (2001): Patterns of coherent decadal an interdecadal climate signals in the Pacific Basin during the 20th Century, Geophys. Res. Lett., 28, pp. 2069 – 2072.

Trenberth, K. E. (1990): Recent observed interdecadal climate changes in the Northern Hemisphere, Bull. Amer. Meteor. Soc., 71, pp. 988-993.

Trenberth, K.E., and Caron, J.M. (2000): The Southern Oscillation revisited: Sea level pressures, surface temperatures, and precipitation. J. Climate 13, pp. 4358-4365.

Trenberth, K., and Hoar, T. (1996): The 1990–1995 El Niño - Southern Oscillation Event: Longest on Record. Geophys. Res. Lett.23 (1), pp. 57-60.

Trenberth, K.E., and Shea, D.J. (1987): On the evolution of the Southern Oscillation. Mon. Wea. Rev. 115, pp. 3078-3096.

Trenberth, K. E., and Stepaniak, D. P. (2001): Indices of El Niño evolution. J. Climate 14 (8) pp. 1697-1701.

Trenberth, K. E., and collaborators (2007): Observations: Surface and atmospheric climate change, in Climate Change 2007, edited by S. Solomon et al., pp. 253 – 336, Cambridge Univ. Press, Cambridge, U. K.

Ulloa, O., Escribano, R., Hormazabal, S., Quinones, R.A., Ramos, M., and Gonzalez, R.R. (2001): Evolution and biological effects of the 1997–98 El Nino in northern Chile. Geophysical Research Letters 28 (8), pp. 1591–1594.

Valdes, J., Ortlieb, L., Gutiérrez, D., Marinovic, L., Vargas, G., and Sifeddine, A. (2008): A 250 years – sedimentary record of Sardine and Anchovy scale deposition in Mejillones Bay, 23 S, Northern Chile, Prog. Oceanogr., 79: pp. 198–207.

Vargas, G., Pantoja, S., Rutllant, J.A., Lange, C.B., and Ortlieb, L. (2007): Enhancement of coastal upwelling and interdecadal ENSO - like variability in the Peru–Chile Current since late 19th century, Geophys. Res. Lett., 34, L13607, (doi:10.1029/2006GL028812).

Vecchi, G. A., and Soden, B.J. (2007a): Effect of remote sea surface temperature change on tropical cyclone potential intensity, Nature, 450, pp. 1066 –1070, (doi:10.1038/nature06423).

Vecchi, G. A., and Soden, B.J. (2007b): Global warming and the weakening of tropical circulation. J. Climate, 20, pp. 4316–4340.

Vecchi, G. A., Clement, A., and Soden, B.J. (2008): Examining the tropical Pacific's response to global warming. Eos, Trans. Amer. Geophys. Union, 89, pp. 81–83.

Vimont, D.J., Wallace, J.M., and Battisti, D.S. (2003): The Seasonal Footprinting Mechanism in the Pacific: Implications for ENSO. J. Climate, 16, pp. 2668–2675.

Vose, R. R., and collaborators (2012): NOAA's merged land-ocean surface temperature analysis. Bull. Amer. Met. Soc., 93, pp. 1677–1685. (doi:10.1175/BAMS-D-11-00241.1).

Wallace, J.M., Rasmusson, E.M., Mitchell, T.P., Kousky, V.E., Sarachik, E.S., and von Storch, H. (1998): On the structure and evolution of ENSO-related climate variability in the tropical Pacific: Lessons from TOGA. J. Geophys. Res. 103 (C7), pp. 14241-14259.

Waylen, P., and Poveda, G. (2002): El Niño–Southern Oscillation and aspects of western South American hydro-climatology. Hydrol. Process. 16, pp. 1247-1260, (doi:10.1002/hyp.1060).

White, W. B., and Cayan, D.R. (1998): Quasi-periodicity and global symmetries in interdecadal upper ocean temperature variability, J. Geophys. Res., 103, pp. 21,335 – 21,354.

Xiang, B., Wang, B., and Li, T. (2012): A new paradigm for the predominance of standing Central Pacific Warming after the late 1990s. Clim Dyn. (doi:10.1007/s00382-012-1427-8).

Xie, S.-P., and Philander, S. G. H. (1994): A coupled ocean-atmosphere model of relevance to the ITCZ in the eastern Pacific. Tellus, 46A, pp. 340-350.

Xie, S.-P., Deser, C., Vecchi, G.A., Ma, J., Teng, H., and Wittenberg, A.T. (2010): Global warming pattern formation: Sea surface temperature and rainfall, J. Climate 23, pp. 966-986.

Xie S.-P., Xu, H., Kessler, W. S., and Nonaka, M. (2005): Air–sea interaction over the eastern Pacific warm pool: gap winds, thermocline dome, and atmospheric convection. J. Climate, 18, pp. 5-20.

Yanez, E. (1991): Relationships between environmental changes and fluctuating major pelagic resources exploited in Chile (1950 – 1988), in Long-term variability of pelagic fish populations and their environment, edited by T. Kawasaki, S. Tanaka, Y. Toba, and A. Taniguchi, pp. 301 – 309, Pergamon Press, Great Britain.

Yáñez E., Barbieri, M.A., Plaza, F., and Silva, C. (2013): Climate change and fisheries in Chile. In: Behnassi M., Shelat K., Hayashi K., Syomiti M. (eds.), Vulnerability of Agriculture, Water and Fisheries to Climate Change: Toward Sustainable Adaptation Strategies. Springer, in press.

Yeh, S., Kug, J.S., Dewitte, B., Kwon, M.H., Kirtman, B.P., and Jin, F.F. (2009): El Niño in a changing climate, Nature, 461, pp. 511-515.

Wu, Z. (2003): A shallow CISK, deep equilibrium mechanism for the interaction between large-scale convection and large-scale circulations in the tropics. J. Atmos. Sci. 60, pp. 377-392.

Zebiak, S.E. (1986): Atmospheric convergence feedback in a simple model for El Niño. Mon Wea Rev 114:pp. 1263-1271.

Zebiak, S.E., and Cane, M.A. (1987): A model El Niño-Southern Oscillation. Mon. Wea. Rev. 115, pp. 2262-2278.

Zhang, C., McGauley, M., and Bond, N.A. (2004): Shallow meridional circulation in the tropical eastern Pacific. J. Climate, 17 (1), pp. 133-139.

Zhang, H., Clement, A., and Di Nezio, P. (2014a): The South Pacific Meridional Mode: A Mechanism for ENSO-like Variability. J. Climate, 27, pp. 769–783, (doi:10.1175/JCLI-D-13-00082.1).

Zhang, H., Deser, C., Clement, A., and Tomas, R. (2014b): Equatorial signatures of the Pacific Meridional Modes: Dependence on mean climate state, Geophys. Res. Lett., (doi:10.1002/2013GL058842).

Zhang, Y., Wallace, J.M., and Battisti, D.S. (1997): ENSO-like interdecadal variability: 1900 – 93. J. Climate, 10, pp. 1004-1020.

Zheng, Y., Kiladis, G.N., Shinoda, T., Metzger, E.J., Hurlburt, H.E., Lin, J., and Giese, B.S. (2010): Upper-Ocean Processes under the Stratus Cloud Deck in the Southeast Pacific Ocean. Journal of Physical Oceanography 40:1, pp. 103-120.

Zheng, J., T. Shinoda, J.L. Lin, and Kiladis, G.N. (2011): Sea surface temperature biases under the stratus cloud deck in the Southeast Pacific ocean in 19 IPCC AR4 coupled general circulation models. J Clim, 24, pp. 4139–4164. (doi: http://dx.doi.org/10.1175/2011JCLI4172.1).

Zelle, H., Appeldoorn, G., Burgers, G., and van Oldenborgh, G.J. (2004): The relationship between sea surface temperature and thermocline depth in the eastern equatorial Pacific, J. Phys. Oceanogr., 34, pp. 643 – 655.

White Paper #8b – The Tropical Pacific Observing System and the Pacific Islands

Wiles, P.[1], Murphy, B.[2], Ngari, A.[3], White, R.[4], Berdon, J.[5], Hampton, J.[6], and Pahalad, J.[2]

[1] Secretariat of the Pacific Regional Environment Programmeme, Samoa
[2] Bureau of Meteorology, Australia
[3] Cook Islands Meteorological Service, Cook Islands
[4] Republic of the Marshall Islands Weather Service Office, Marshall Islands
[5] Chuuk Weather Service Office, Federated States of Micronesia
[6] Secretariat of the Pacific Community, New Caledonia

1. Introduction

The daily lives of the ~10 million people living on the Pacific Islands are affected by weather and climate variability. Two examples are; low lying atolls usually have little natural water storage due to the their thin groundwater lenses, which means that agriculture and drinking water resources are vulnerable to low rainfall and wave overtopping from the ocean; and steep, high islands often experience high erosion during heavy tropical downpours and can suffer severe property damage and loss of life during resulting floods.

The Tropical Pacific Observing System (TPOS) provides immense value to the Pacific Islands. Most of this benefit comes via analysis products derived from the TPOS such as seasonal climate predictions which can enable Pacific Islands to plan for events such as drought, heavy rainfall and extreme sea level. Most benefit in the Pacific Islands from the TPOS comes from processed products, with only weather forecasters and researchers accessing raw data.

2. Benefits from the TPOS for Pacific Islands

Few of the Pacific Islands access raw data from the Tropical Pacific Observing System however all of the islands receive substantial benefit via products from the system. Examples are seasonal climate outlooks (of rainfall, temperature and sea level), weather forecasting (including wave conditions and aviation forecasting), cyclone warnings, fisheries management, tsunami warnings, and monitoring and prediction of climate change in the region. The products developed from the TPOS and the components they use are discussed below, and summarized in Table 2.1.

Table 2.1 – Seasonal climate outlooks produced for the Pacific Islands.

Product	Audience	Method	Outlooks of
United States NOAA ENSO Update	US Affiliated Pacific Islands		Rainfall, SST?, Sea Level
Australian BoM SCOPIC	Independent Pacific Islands,	ENSO indices	Rainfall, SST
New Zealand NIWA Island Climate Update	Independent Pacific Islands,	TPOS observations and dynamical models	Rainfall, SST

2.1 Seasonal climate outlooks

The Pacific Ocean is a key driver of global climate, predominantly through the processes of El Niño and La Niña, also known as ENSO (Collins et al., 2010). The Pacific Islands are situated at the core of this climate engine, and are particularly affected by ENSO. For example, records extending over the past 73 years show that during the dry season, rainfall on Tarawa Atoll, the capital of Kiribati, is correlated to the Niño 3.4 Index and Southern Oscillation Index with coefficients of 0.81 and -0.74 respectively (Australian Bureau of Meteorology et al., 2011).

Predictions of rainfall, temperature and sea level are produced by Pacific Island climate services in collaboration with development partners. These seasonal predictions are founded on the TPOS, particularly using data from the TAO/TRITON array, satellites (TRMM, SST) and met stations. The three main development partners are the U.S. National Oceanic and Atmospheric Administration (NOAA), the New Zealand National Institute of Water and Atmospheric Research (NIWA) and the Australian Bureau of Meteorology (BoM) as outlined in Table 2.1. Of the three seasonal prediction tools, the NIWA *Island Climate Update* (www.niwa.co.nz/climate/icu) goes into the most detail of data from the TPOS. Monthly teleconferences between NIWA, Pacific Island (PI) NMS, NOAA and BoM discuss the state of the tropical Pacific based on surface and subsurface data from the TAO/TRITON array, satellite data, and model output. Three month outlooks for rainfall and temperature within specific country areas are produced.

The BoM Seasonal Climate Outlooks in Pacific Island Countries (SCOPIC) programmeme holds a monthly Online Climate Outlook Forum (OCOF) with good attendance by PI NMS. Each of the participating Pacific Island countries runs a statistical comparison of past rainfall (and other parameters) against the relevant oceanic Niño index and uses recent SST analyses to provide 3 month rainfall outlooks for their particular regions within country. BoM is also providing experimental seasonal climate outlooks for the Pacific from the POAMA dynamical seasonal prediction model. The NOAA Pacific ENSO Applications Center (PEAC) ENSO Update provides a comprehensive overview of current and projected ENSO conditions (http://www.prh.noaa.gov/peac/update.php). Forecasts of sea surface temperature, rainfall and sea level are then produced for each of the US Affiliated Pacific Islands (USAPI).

Current activities in the Pacific aim to link climate forecasts from the National Meteorological Services to sectoral responses. For example, water management for electricity and town supply in Samoa, and seasonal agricultural planning in Vanuatu. Seasonal climate outlooks in the Pacific region also have health applications, such as predicting the risk of vector-borne disease outbreaks. Dynamical seasonal prediction model output is also used to inform these seasonal climate outlooks in the Pacific. The skill of these models is dependent on the accuracy of initializing ocean analyses, requiring surface and sub-surface temperature and salinity. However, at present model error dominates over analysis uncertainty; this will change as models improve. The forecasts from the dynamical models can only be applied to local-scale sites through statistical downscaling that requires individual station data. For all numerical models (used for seasonal prediction, weather forecasting and climate change projections), the TPOS data is essential for forecast verification, calibration of satellite data included in analyses, model development and improving model parametrization.

2.2 Weather forecasting

Given the proximity of the observing array to the islands themselves, the real time data return is invaluable for providing boundary conditions for numerical weather predictions (NWP). The primary data sources for this are the surface wind conditions gathered from meteorological stations in the Pacific Islands along with data from TAO-TRITON array and satellite remote sensing. However, subsurface ocean data from the Argo array also contributes significantly to the long term accuracy of the NWPs (Andersson and Sato, 2012; Balmaseda et al., 2007; Dunstone and Smith, 2010). Tropical Cyclone (TC) forecasting is a special case of NWP, and provides obvious benefits to the Pacific Islands in predicting the timing and intensity of possible landfall. NWP skill in predicting TC tracks and intensities is strongly dependent on the accuracy of initialized winds, which across the Pacific are provided from scatterometer data. NWP is moving towards coupled modeling, so in future ocean initialization (particularly SST) will become important, with expected improvements in TC prediction.

2.3 Sea level monitoring and prediction

Sea level is of particular concern to all Pacific Islands. Low lying atolls are obviously very vulnerable, but the high islands also usually have most of their critical infrastructure located at the coast. The Pacific ENSO Applications for Climate (PEAC) center provides sea level forecasts for the USAPI with a three month lead time, using statistical models. Experimental products have been developed by the Pacific Australia Climate Change Science and Adaptation Planning Programme (at BoM) using the POAMA seasonal prediction model to give sea level outlooks up to 7 months ahead (Miles et al., 2013; Cottrill et al., 2013). The New Zealand National Institute of Water and Atmospheric research (NIWA) is also developing statistical products for sea level forecasting.

Sea level varies noticeably with ENSO; sea level generally rises (falls) in the western (central/eastern) Pacific during La Niña and falls (rises) in the western (central/eastern) Pacific during El Niño with considerable consequences (Australian Bureau of Meteorology et al., 2011). For example, the two main population centers of the Republic of Marshall Islands, Majuro and Ebeye, regularly suffer coastal inundation during king tides that coincide with La Niña conditions. Over the past couple of years, high sea swell has occurred with these extreme water levels, leading to severe inundation, property damage and contamination of aquifers. Monitoring of sea level is of particular concern to Pacific Island states, and is undertaken primarily by tide gauge networks operated by the UH Sea Level Center and the Australian Bureau of Meteorology along with satellite altimetry. However to gain a deeper understanding of sea level, subsurface temperature and salinity data is vital. The TAO-TRITON array provides a slice of this information across the equator, and the Argo array extends these observations to the majority of the Pacific Islands that are beyond the ± 8° latitudinal extent of TAO-TRITON.

2.4 Fisheries

A substantial proportion of both formal income and subsistence food for Pacific Island communities comes from fisheries. Data from the TPOS underlies the Ocean Global Circulation

Models that are used by the region to model tuna populations, and extremely warm water or low tides can damage shallow coral reefs that are the foundation for many coastal fisheries.

The TAO-TRITON buoys also act as de-facto Fish Aggregating Devices (FADs) which has positive and negative implications. The increased concentration of tuna around the buoys means that researchers can tag fish much more efficiently; however, this also attracts fishing activity which can damage the buoys. Working with fisheries management agencies in the Pacific may help to alleviate this problem.

Many components of the TPOS feed in to the ocean models used for tuna modeling, and warning products for coral bleaching are based on satellite SST data (Liu et al., 2013) and forecasts from seasonal prediction models (Cottril et al., 2013). As noted in the sea level section, products for extreme water levels are currently being developed. High resolution data for monitoring around Pacific islands, for example to monitor coral bleach risk, is provided by the BoM and CSIRO Bluelink project, a high resolution analysis and short term ocean forecast that uses data from satellite altimetry, the Argo array and satellite SST.

2.5 Tsunami monitoring

The majority of destructive tsunamis in the Pacific are generated by earthquakes. Landslides are an additional generation mechanism that may cause localized damage; however these often occur with no method of detection (Dominey-Howes and Goff, 2012). The magnitude and depth of the generating earthquake are used to provide an initial model of tsunami propagation and threat across the Pacific, along with existing knowledge of the orientation of the fault line. These forecasts are theoretical until they have been validated against data collected from tide gauges and the DART buoy system (IOC-UNESCO, 2011).

2.6 Climate change

Communities in the Pacific Islands are among the most vulnerable to climate change (Duncan, 2012) being particularly sensitive to changes in sea level, rainfall patterns and temperature. Planning for adaptation to climate change is dependent on insights into how climate works and is expected to change. Identifying optimum adaptation strategies that ensure the best protection for communities relies on long term observations from land based stations, ocean observation arrays and upper air networks. Often external donor funding focuses on mitigation and adaptation to climate change at the policy and planning level without investing in the observation networks and their accompanying data needed to ensure these are effective. Enhanced understanding of current and past climate is critical to informing policy makers about future climate scenarios; however this is frequently not adequately considered (Australian Bureau of Meteorology et al., 2011). Climate records in the Pacific (ocean and atmosphere) are also vital for evaluating climate model performance, to drive model improvement and to understand model biases and the limitations of climate change projections (Brown et al., 2012).

Sustained, long term data series are required to distinguish between slow climate trends and climate variability. Several platforms are now building the long time series needed, such as TAO-TRITON, the tide gauge network and satellites. More recent innovations such as Argo

have enabled monitoring of critical subsurface changes in the ocean that were not possible a decade ago and will greatly enhance our understanding over time.

2.7 Wave monitoring and prediction

Waves play a significant role on the Pacific Islands. Day to day activities such as subsistence and commercial fishing are affected by sea state, and reliable forecasts are needed to help communities plan their activities. In addition to the inundation events described in the Marshall Islands above, similar events have taken place recently in the Cook Islands, Fiji and Tonga.

Winds from global atmospheric models, assimilating data from the TPOS are used to drive basin scale wave models such as NOAA's WaveWatch III. However, the lack of observations in the region between New Zealand and Hawai'i means that there is little verification of the model. Anecdotal evidence has noted that there are discrepancies with the amplitude and timing of wave trains arriving in the Pacific.

2.8 Upper atmosphere observations and forecasting

Global models depend on availability of upper air data in the Pacific Ocean region for accuracy. All models used for day to day weather prediction display diminished skill when this data is not included in the model initialization. The limited accuracy of models can literally mean the difference between life and death when decisions are made in hazardous weather events such as tropical cyclones. In the same vein, the aviation industry is critical to the social and economic well being of the region and upper air data is vital for safe and dependable air services. Aviation is the main mode of international passenger transport in the Pacific, and carries a substantial amount of cargo both to and from the islands. The Pacific Islands play a key role providing information to the GCOS Upper Air Network (GUAN), however many of these stations are no longer active due to financial costs.

3. Summary and future needs

It is important to note that Pacific Island communities are reliant on the services founded on data from the TPOS. The use of these services in the Pacific save lives through warnings of extreme weather events, aid planning for seasonal extremes like drought, extreme sea level and health risk, and inform longer term adaptation planning to climate change impacts. Continued maintenance and development of the TPOS system is needed to support these services and to implement new products. Much of this is built on the research discussed in other white papers.

There are emerging needs and technologies that should be taken into account when considering the future of the TPOS. Examples of these are;

- Ocean Acidification is expected to have drastic consequences for coral reefs, pelagic fisheries and the Pacific Island communities that depend on them by the middle of this century. However, there are few sustained observations of marine carbonate chemistry and ecosystem response to the changes already being experienced. This baseline information is vital if management options are to be considered to mitigate this threat.

- The inclusion of biological monitoring components that can be interfaced into the existing physical systems. An example is the acoustic monitoring of fish abundance from TAO-TRITON moorings to investigate tuna behavior in response to ENSO.
- Higher sea levels are already causing issues on Pacific Islands, particularly when they coincide with a significant sea-swell. Nevertheless, models lack observations of wave conditions to calibrate against.
- The development of new technologies, such as wave powered gliders and sensors on submarine cables, open opportunities for new observations in the Pacific, and more cost effective methods of continuing existing observations.

Table 3.1 – Products used by the Pacific Islands and the components of the TPOS that contribute to them.

	TAO/ TRITON	Argo	XBT	Satellite	Tide gauge	Wave buoy	DART
Seasonal Predictions	X	X		X			
Weather forecasting	X	X		X		X	
Sea Level		X	X	X	X		
Fisheries	X	X		X		X	
Cyclone Forecasting				X	X	X	
Waves				X		X	
Tsunami warning					X		X
Climate Change	X	X	X	X	X	X	

Acknowledgements

Many colleagues have provided valuable advice for this paper, including Australian Bureau of Meteorology scientists Harry Hendon, Oscar Alves, Eric Schultz, Elaine Miles, Andrew Charles, Peter Steinle, Sheng Guo, and Justin Freeman, Lindsay Chapman from SPC, Nicolas Faucherau from NIWA, Pene Lefale from NZ Met Service, and SPREP staff Neville Koop and Kaniaha Salesa Nihmei.

References:

Andersson, E., Sato, Y. (2012): WIGOS WMO Integrated Global Observing System Final Report of the Fifth WMO Workshop (Sedona, United States) on the Impact of Various Observing Systems on Numerical Weather Prediction (Technical No. 2012-1).

Australian Bureau of Meteorology, CSIRO (Australia), Pacific Climate Change Science Programme (PCCSP), International Climate Change Adaptation Initiative (ICCAI) (2011): Climate change in the Pacific scientific assessment and new research. CSIRO Publishing, Collingwood, Vic.

Balmaseda, M.A., Anderson, D., and Vidard, A. (2007): Impact of Argo on analyses of the global ocean: IMPACT OF ARGO. Geophys. Res. Lett. 34.

Brown, J.N., Brown, J.R., Langlais, C., Colman, R., Risbey, J.S., Murphy, B.F., Moise, A., Sen, G.A., Smith, I., Wilson, L., Narsey, S., Grose, M., Wheeler, M.C. (2013): Exploring qualitative regional climate projections: a case study for Nauru. Climate Research, 58, pp. 165-182.

Collins, M., An, S.-I., Cai, W., Ganachaud, A., Guilyardi, E., Jin, F.-F., Jochum, M., Lengaigne, M., Power, S., Timmermann, A., Vecchi, G., and Wittenberg, A.T. (2010): The impact of global warming on the tropical Pacific Ocean and El Niño. Nat. Geosci. 3, pp. 391–397.

Cottrill, A., Hendon, H.H., Lim, E.-P., Langford, S., Shelton, K., Charles, A., McClymont, D., Jones, D., and Kuleshov, Y., (2013): Seasonal Forecasting in the Pacific Using the Coupled Model POAMA-2. Weather Forecast. 28, pp. 668–680.

Dominey-Howes, D., and Goff, J. (2012): Tsunami Risk Management in Pacific Island Countries and Territories (PICTs): Some Issues, Challenges and Ways Forward. Pure Appl. Geophys. 170, pp. 1397–1413.

Duncan, D. (2012): Freshwater under Threat: Pacific Islands, United Nations Environment Programmeme, Bangkok. SOPAC.

Dunstone, N.J., and Smith, D.M. (2010): Impact of atmosphere and sub-surface ocean data on decadal climate prediction: Initialisation for Decadal Prediction. Geophys. Res. Lett. 37.

IOC-UNESCO (2011): Intergovernmental Coordination Group for the Pacific Tsunami Warning and Mitigation System (ICG/PTWS). Twenty-fourth Session. IOC-UNESCO, Beijing, China.

Liu, G., Rauenzahn, J., Heron, S., Eakin, M., Skirving, M., Christensen, T., Strong, A., and Li, J. (2013): NOAA Coral Reef Watch 50 km Satellite Sea Surface Temperature-Based Decision Support System for Coral Bleaching Management (NESDIS No. 143). NOAA, Washington D.C.

Miles, E., Spillman, C.M., Church, J., and McIntosh, P. (2013): Seasonal Prediction of Global Sea-Level Anomalies using an Ocean-Atmosphere Dynamical Model. Climate Dynamics, in review.

White Paper #9 – Satellite views of the Tropical Pacific

Lindstrom, E.[1], Bourassa, M.[2], Chelton, D.[3], Corlett, G.[4] , Durland, T.[3], Farrar, T.[5], Janssen, P.[6], Lagerloef, G.[7], Lee, T.[8], Minnett, P.[8], O'Neill, L.[3], and Willis, J.[8]

[1] NASA Headquarters, United States
[2] Florida State University, United States
[3] Oregon State University, United States
[4] University of Leicester, United Kingdom
[5] Woods Hole Oceanographic Institute, United States
[6] European Center for Medium-Range Forecasts, United Kingdom
[7] Earth and Space Research, United States
[8] Jet Propulsion Laboratory, United States

1. Introduction

Satellites are an integral component of the Tropical Pacific Observing System (TPOS). Oceanographic satellite missions have been providing measurements for a suite of oceanographic variables such as sea surface temperature (SST), salinity (SSS), and height (SSH), as well as significant wave height (SWH), ocean surface wind speed and wind stress, precipitation, ocean mass, and variables related to ocean color (e.g., Chl). Combinations of satellite measurements also provide estimates of ocean surface currents and surface heat fluxes. These satellite observations have provided measurements of the tropical Pacific that are complementary to in situ observations. For example, satellite altimetry and gravimetry in combination with Argo have enabled a comprehensive study of sea level and the relative contribution of steric and mass contributions. Satellites and mooring data together have greatly facilitated the estimation of upper ocean heat balance.

Satellites provide a unique vantage point to observe the tropical Pacific in many aspects. They have overall more uniform spatio-temporal sampling than *in situ* systems to capture oceanographic features. As such, they can help decipher eddy and large-scale signals from in situ data such as measurements by Argo floats. The extensive spatial sampling also allows the calculation of spatial derivative fields important for the study of ocean and atmospheric circulation and air-sea interaction such as SST gradients and the surface wind stress curl and divergence. The more extensive (often global) coverage of satellites facilitates studies of large-scale teleconnections and impacts. On the other hand, in situ data extend the interpretation of satellite data by providing information about vertical structure below the sea surface. They also help improve satellite observations by providing independent measurements critical to the calibration and validation of many satellite measurements. High-frequency measurements of some in situ data (e.g., mooring and meteorological measurements) also help de-alias signals that may not be adequately sampled by satellites (e.g., diurnal signals).

This whitepaper summarizes the major contributions of satellites in studying the circulation and climate variability of the tropical Pacific (section 2), the advantages of the satellites and their complementarity to *in situ* observations (section 3), the unique capabilities of satellite observations of the ocean (section 3), and the need for the enhancement of future satellite observing systems to complement the design of the future tropical Pacific observing system (section 4).

2. Major contributions of satellites in observing the tropical Pacific

A diverse array of Earth-observing satellites has provided measurements of the globe, including the tropical Pacific for several decades. The current missions, along with missions already completed (e.g., TOPEX/Poseidon, JASON-1, NSCAT), have provided comprehensive measurements of several variables, including sustained measurements of SST for more than three decades, SSH for more than two decades, ocean surface wind speed for nearly three decades, and ocean surface vector winds for two decades. The upcoming missions continue and enhance the legacy of oceanographic satellite missions by extending the temporal record and by providing measurements with better sampling and/or accuracy (e.g., SWOT, RapidSCAT, and Sea and Land Surface Temperature Radiometer (SLSTR)).

The past and ongoing oceanographic satellite missions have made significant accomplishments. The major achievements related to ocean and climate research are summarized below and organized by different time scales. Although not discussed here, these satellite measurements have made important contributions to the improvement of models and climate prediction and to the study and forecast of shorter time-scale phenomena (covered by other whitepapers). The discussion here focuses on satellite measurements related to the physical state of the ocean, including meteorological forcing. Ocean color measurements are described in another whitepaper led by Dr Francisco Chavez.

Recommendation: Ensure all components, including satellites, *in situ*, models, data and information management are considered part of the observing system.

2.1 Intraseasonal variability

A spectrum of intraseasonal variability revealed by satellites

There are many different dynamical phenomena that occur at intraseasonal periods (20-100 days) in the tropical Pacific Ocean and the overlying atmosphere. In the ocean, the most prominent of these are tropical instability waves (TIWs) and equatorial Kelvin waves. Prominent modes of atmospheric intraseasonal variability include convectively coupled Kelvin waves and the Madden-Julian Oscillation (MJO). Intraseasonal variability in both the atmosphere and ocean stand out as prominent features in most data records in the tropical Pacific, and these various forms of intraseasonal variability have thus been the subject of intensive study with in situ and satellite measurements. We focus here on the uses and limitations of satellite measurements for studying and monitoring intraseasonal variability in the ocean; representative examples of the use of satellite observations for study of atmospheric intraseasonal variability include Madden and Julian (1994), Wheeler and Kiladis (1999), and Roundy and Frank (2004).

Several distinct types of oceanic variability co-exist with intraseasonal periods, including eastward propagating Kelvin waves, and shorter-wavelength, westward-propagating variability such as TIWs. A relatively clear separation of these processes is often achieved through examining the spectrum of oceanic variability in the zonal-wavenumber-frequency domain. Examination of the zonal-wavenumber/frequency spectrum is also helpful because the most common theoretical approaches to Kelvin waves and TIWs are carried out in the zonal-wavenumber/frequency domain. As is discussed further below, spectra of different oceanic properties tend to highlight different wavenumber-frequency bands; we will examine the zonal-

wavenumber/frequency spectrum of SSH (Perigaud, 1990; Zang et al., 2002; Wakata, 2007; Farrar, 2008; Shinoda et al., 2009; Farrar, 2011). The zonal-wavenumber/frequency spectrum of SSH exhibits two broad regions of elevated SSH variance, one corresponding to eastward propagating Kelvin waves at small, positive zonal wavenumbers (wavelengths exceeding 50° longitude), and one corresponding to TIWs and other westward-propagating variability with zonal wavelengths of about 9-30° (Figure 2.1). The SSH spectrum shown in Figure 2.1 (after Farrar, 2011) was estimated using data from the AVISO gridded altimetry product over the period 1993-2006 and almost the full width of the equatorial Pacific (149°E-88°W).

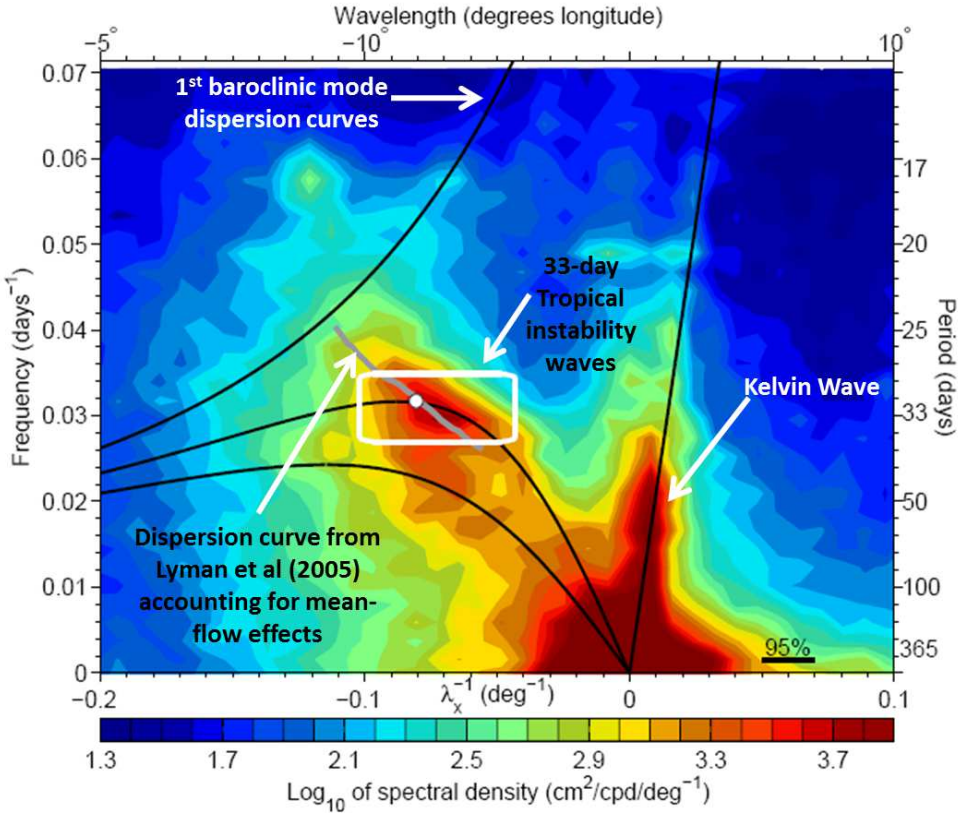

Figure 2.1 - Zonal-wavenumber/frequency spectrum of SSH, averaged over 7°S-7°N (after Farrar, 2011), using data from 1993-2006 and almost the full width of the Pacific (149°E-88°W). At periods of 20-100 days, there are two broad regions of elevated SSH variance, one corresponding to eastward propagating Kelvin waves at small, positive wavenumbers (wavelengths exceeding 50°), and one corresponding to TIWs and other westward-propagating variability having zonal wavelengths of about 9-30°. The TIW spectral peak in SSH near 33-day periods (white box) has wavelengths of 12-17°. The four black curves are the theoretical dispersion curves for the first-baroclinic-mode Kelvin, Rossby, and mixed Rossby-gravity waves. The grey line depicts a theoretical dispersion curve for the unstable TIW mode, and the white circle indicates the fastest growing wavelength (from Lyman et al., 2005). The 95% confidence interval should be measured against the color scale; a difference of two contour intervals is significant at 95% confidence.

TIWs provide a natural starting point for a discussion of the use of satellite measurements for the study of intraseasonal variability because they were first discovered in satellite infrared SST measurements in the Pacific (Legeckis, 1977). TIWs arise from instabilities of the equatorial

current system (Philander, 1976; Luther and Johnson, 1990; Lyman et al., 2005), and are clearly visible in satellite SST measurements as a meandering of the northern side of the equatorial cold tongue near 2°N. More recently, microwave SST measurements were used to show that TIWs also cause SST signals on the southern side of the equatorial cold tongue, near 2°S (Chelton et al., 2000; Figure 2.2).

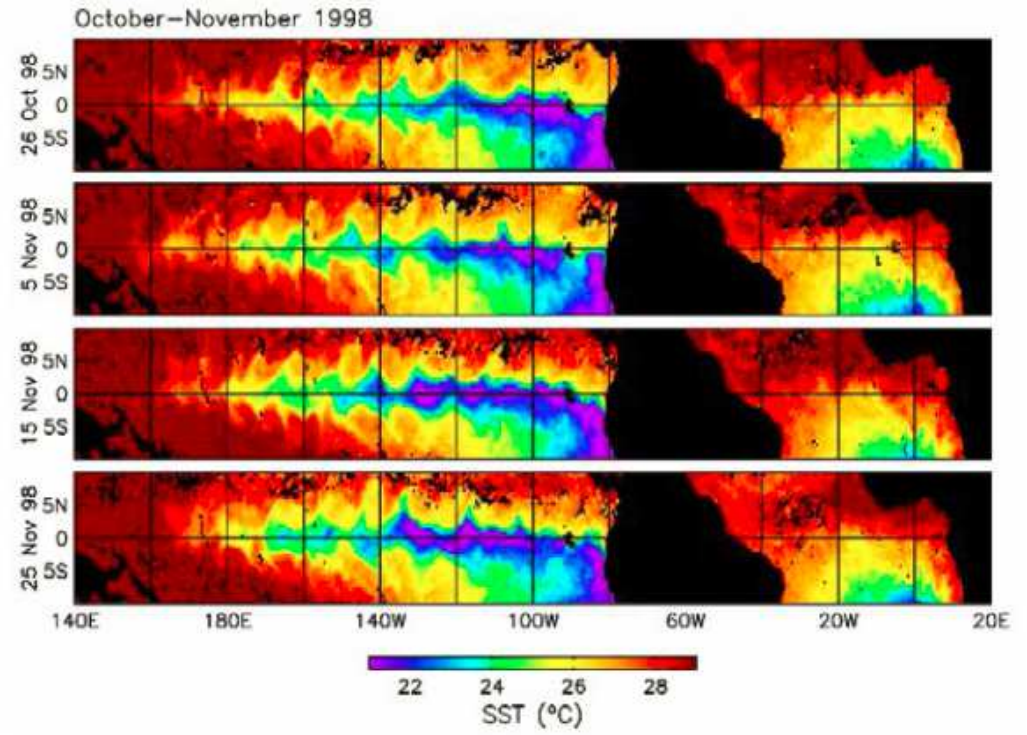

Figure 2.2 - SST measurements from the Microwave Imager onboard the Tropical Rainfall Measuring Mission (TRMM) satellite. Tropical instability waves produce the cusp-shaped patterns along the northern and southern SST fronts of the tongue of cold water on the equator (Chelton et al., 2000).

The discovery of TIWs in the late 1970's stimulated a great deal of subsequent theoretical and observational work to understand their generation mechanisms, properties, and consequences. Descriptions of the properties of TIWs have varied widely: TIWs have been reported to occur at periods of 14-50 days, zonal wavelengths of 7-25°, and to have maximum amplitude at locations ranging from the equator to 6°N (Qiao and Weisberg, 1995). Observational studies of TIWs have typically characterized them as a fairly narrowband phenomenon, but this apparently conflicts with the broad range of wavenumbers and frequencies reported. For example, Halpern et al. (1988) characterized the TIW signal in meridional velocity measurements on the equator as a narrowband fluctuation with a period of 20 days, while Lyman et al. (2005) found a clear maximum in SSH variability at periods of about 33 days.

When the various wavenumbers and frequencies that have been reported or theoretically predicted for TIWs are plotted over the spectrum shown in Figure 2.1, it becomes apparent that the various estimates collectively span the range of wavenumber-frequency space that exhibits energetic SSH variability in the 7°S-7°N latitude band (Figure 2.3). Figure 2.3 includes the wavenumber-frequency estimates summarized in Table 1 of Qiao and Weisberg (1995) and

some more recent estimates from Chelton et al., (2000), Donohue and Wimbush (1998), McPhaden (1996), and Lyman et al., (2005, 2007). The figure shows boxes, lines, and points depending on whether each study provided a range of wavenumbers and/or frequencies or simply stated a single wavenumber and frequency. Not surprisingly, previous studies using SSH measurements (Perigaud, 1990; Lyman et al., 2005) identified TIW wavenumbers and frequencies around the spectral peak in SSH seen near 33-day periods. Those studies, and other SSH-based studies by Farrar (2008, 2011) and Shinoda et al. (2009) also determined the peak TIW variability to occur near 5°N. At the other extreme of the reported frequency range, in situ equatorial velocity measurements have tended to yield shorter reported periods, near 20 days, and they have tended to see the strongest signals in meridional velocity on the equator (e.g., Halpern et al., 1988). Satellite SST and in situ temperature measurements have tended to yield estimates in between these two extremes and have also tended to identify maximum variability as occurring near 2°N. One interpretation of these disparate observations is that there is TIW variability that resembles mixed Rossby-gravity waves, which have a relatively weak SSH signal and a strong signal in equatorial meridional velocity, and other variability that resembles first-meridional-mode (and perhaps second-meridional-mode) equatorial Rossby waves, with a stronger off-equatorial SSH signal (Lyman et al., 2007).

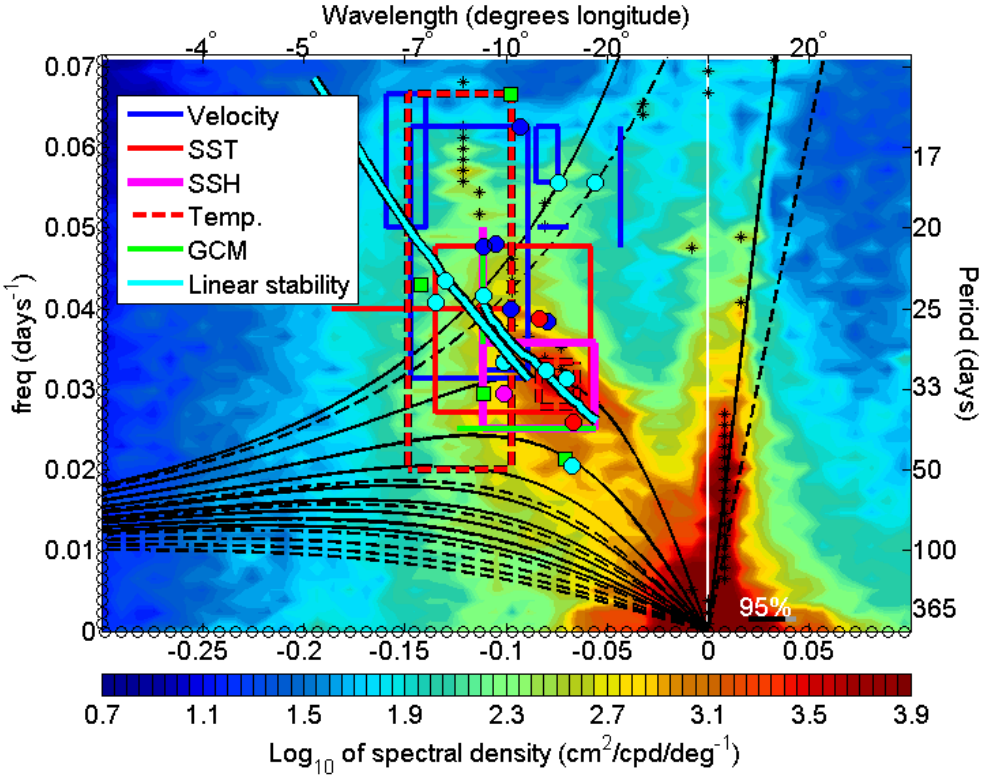

Figure 2.3 - A zonal-wavenumber/frequency spectrum of SSH similar to the one in Figure 2.1, but averaged over 5°S-5°N. Previous estimates of the wavenumbers and frequencies of tropical instability waves (TIWs) are indicated, where a box indicates that a particular study provided a range of wavenumbers and frequencies, a line indicates a range of frequencies or wavenumbers, and a point indicates that a single wavenumber-frequency value was given. “SST” and “SSH” are from satellite observations, and “Velocity” and “Temp” are from moored in situ measurements.

Previous studies of TIWs using satellite observations were mostly based on SST, SSH, wind, and ocean color. SSS observations from the Aquarius/SAC-D satellite mission have provided an unprecedented opportunity to study the salinity structure associated with TIWs. The studies by Lee et al. (2012) demonstrated the capability of Aquarius data in detecting tropical Pacific TIWs and the complementarity between SSS and other satellite observations in studying the TIWs. In particular, SSS provide the strongest propagating signature of tropical Pacific TIWs near the equator where the salty South Pacific waters meet the freshwater waters under the ITCZ, forming a relatively large meridional SSS gradient. In contrast, the meridional gradient of SST is weaker near the equator and is the strongest near the northern edge of the cold tongue near 2N, where TIW signature in SST is strongest. For SSH, the strongest signature is further north near the center latitudes of the tropical instability vortices. Aquarius data are not only able to detect TIWs, but reveal new features of the TIWs not previously reported from SST and SSH observations. The dominant westward propagating speed of TIWs near the equator is approximately 1 m/s, which nearly twice as fast as the approximately 0.5 m/s dominant speed reported from SST and SSH data, typically off the equator. This is because the dominant periods of TIWs near and away from the equator are 17 and 33 days, and are associated with the projection of instabilities onto the Yanai mode and the Rossby mode, respectively (Lyman et al., 2007). Satellite SSS allows a better characterization of TIWs near the equator because of the relatively large meridional SSS gradient near the equator (in contrast to the strong SST gradient away from the equator near the cold-tongue edges). The new discovery has important implications to eddy-mean flow interaction and eddy-induced mixing.

Kelvin waves are the other major form of intraseasonal variability in the tropical Pacific Ocean. These waves are visible in Figures 2.1 and 2.3 as a low-wavenumber band of high variance along the first-baroclinic-mode Kelvin wave dispersion curve. They dominate the variance of SSH and other fields at 30-90-day periods and have received considerable attention (e.g., Enfield, 1987; McPhaden and Taft, 1988; Johnson, 1993; Johnson and McPhaden, 1993; Kessler et al., 1995; Kessler and McPhaden, 1995; Hendon et al., 1998; Kutsuwada and McPhaden, 2002; Zang et al., 2002; Cravatte et al., 2003; Roundy and Kiladis, 2006; Farrar, 2008). The waves are forced by intraseasonal wind fluctuations (e.g., from the MJO) in the western and central Pacific (Kessler et al., 1995; Hendon et al., 1998).

Air-sea coupling associated with tropical instability waves

Satellite observations of SST and surface vector winds have provided a clearer understanding of air-sea interaction in the eastern tropical Pacific than could be obtained from TAO mooring data or model wind fields. SST anomalies on scales shorter than ~1000 km modify the turbulent mixing and pressure field within the marine atmospheric boundary layer. This results in local changes in surface winds and stress from imbalances between the turbulent stress divergence and pressure gradient forces that generate accelerations of surface winds from cool to warm water and decelerations from warm to cool water. This coupling between SST and surface stress is easily identified in association with tropical instability waves (TIWs) (e.g., Liu et al., 2000; Chelton et al., 2001; Polito et al., 2001; Hashizume et al., 2002; Chelton, 2005). The divergence of the surface stress is found to be a linear function of the downwind component of the SST gradient; the curl of the surface stress is likewise found to be a linear function of the crosswind component of the SST gradient (Chelton et al., 2001). Wind stress divergence and

curl anomalies propagate westward in lock step with the downwind and crosswind SST anomalies associated with the westward propagating TIWs (Chelton et al., 2001; Chelton, 2005). This SST influence on surface wind stress fields is evident in model winds such as the operational ECMWF analyses of 10-m winds, but with coarser resolution and with air-sea coupling that is too weak by about a factor of two (Chelton, 2005).

Because the wind stress curl is correlated with the crosswind SST gradient, the feedback effects of Ekman upwelling are strong where the winds blow parallel to isotherms. This SST-induced Ekman upwelling consists of order-1 perturbations of the large-scale background Ekman upwelling. Since their persistence time scales are weeks or longer, the small-scale features in the wind stress curl field are important to the ocean circulation. For example, a zonal band of strong wind stress curl just north of the equatorial cold tongue that is established in the time-averaged wind stress curl field from the influence of SST on surface wind stress (Chelton et al., 2001) significantly increases the transport of the northern branch of the South Equatorial Current (Kessler et al., 2003).

The ramifications of this 2-way coupling have been investigated by Pezzi et al. (2004) from an ocean model of TIWs in the Pacific Ocean with empirical coupling consistent with the satellite observations. The coupling resulted in a modest (~10%) but significant negative feedback on TIWs that reduced the temperature and meridional velocity variability and dampened the growth rate of the TIWs. The net effects of these changes were to decrease the meridional fluxes of heat and momentum, thereby altering the mean state in a manner that resulted in moderate cooling of the equatorial cold tongue and strengthening of the Equatorial Undercurrent. Similar results have been obtained from a full-physics coupled model that was run for 7 years to investigate TIWs in the Atlantic (Seo et al., 2007b).

Another empirically coupled model of the tropical Pacific Ocean concludes that the feedback effects of TIW-induced SST variations of the wind stress field may also be important to El Niño-Southern Oscillation (ENSO) variability (Zhang and Busalacchi, 2008; 2009). The cooling of the equatorial cold tongue by the 2-way coupling can modulate the amplitude and timing of transitions between the El Niño and La Niña phases of the ENSO cycle. The TIW-induced coupling between SST and wind stress may therefore contribute to the observed irregularity of ENSO variability.

2.2 Seasonal variability

Satellite observations have also enhanced the knowledge about the variability of the tropical Pacific Ocean on seasonal time scales. One particular example is the quasi-annual equatorial Rossby wave in the tropical Pacific Ocean. The classical theory for equatorially trapped waves, in which the equations of motion for a given vertical mode are linearized about a state of rest on an equatorial beta plane, yields an orthogonal basis set of meridional modes with latitudinal structures of the pressure and the two components of velocity that can be expressed in terms of linear combinations of Hermite functions (e.g., Moore and Philander, 1977). At low frequencies, the first vertical mode, first meridional mode that is often presumed to account for most of the westward propagating variability has a phase speed of ~0.9 m/s. The pressure perturbations associated with this theoretical mode are symmetric about the equator. This latitudinal structure is not observed in the Pacific Ocean. Studies of annual variability in subsurface thermal data

and in altimeter data consistently find asymmetric latitudinal structure with larger amplitude north of the equator. These studies also consistently find a westward propagation speed about half as fast as predicted by the classical theory.

The observed latitudinal asymmetry (Figure 2.4) has been variously attributed to sampling errors in the observational data, a superposition of multiple meridional Rossby wave modes, asymmetric forcing by the wind, and forcing by cross-equatorial southerly winds in the eastern Pacific. Chelton et al. (2003) showed that, when the equations of motion are linearized about mean zonal currents typical of the equatorial Pacific, the latitudinal pressure structure for the first meridional mode is distorted in a manner that agrees well with altimeter measurements of SSH variability (Chelton et al, 2003; Durland et al., 2011). The classical double-peaked symmetric structure becomes one in which the northern peak is roughly twice as large as the southern one as a consequence of the modification of the potential vorticity gradient by meridional shear in the equatorial current system. The mean currents for this study were derived from ADCP data obtained during cruises to service the TAO-TRITON moorings.

The background mean currents also decrease the westward phase speed of the first meridional mode, improving the consistency with the observations. This is partly through eastward advection by the Equatorial Undercurrent, and partly through a decrease in the background potential vorticity gradient at the peaks of the South Equatorial Current, which coincide with the latitudes where the first-mode meridional velocity has extrema (Durland et al., 2011).

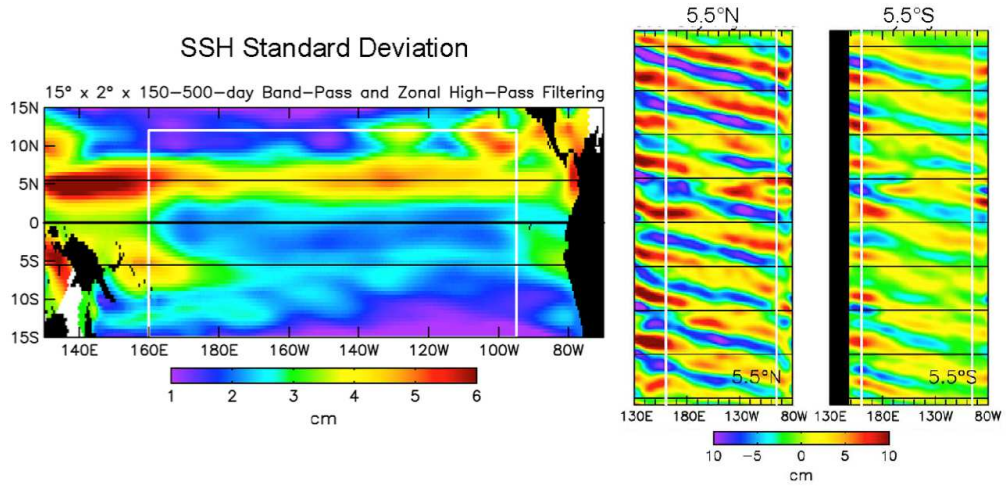

Figure 2.4 - Standard deviation of seasonal SSH in the tropical Pacific (left) and the propagation of the seasonal SSH at 5.5°N and 5.5°S (right), showing strong latitudinal asymmetry of the quasi-annual Rossby waves and phase speed that are much slower than that predicted by linear theory, suggesting the roles of wind forcing and ocean currents.

The fact that equatorial winds do not exhibit a westward phase propagation at the latitude of the largest SSH peak initially led to some confusion as to the whether the wave is directly forced throughout the basin. Durland and Farrar (2012) showed that the efficiency of the wind forcing depends on how the meridional structure of the zonal wind projects onto the meridional structure of the zonal velocity field associated with the free wave. In contrast to the SSH eigenfunction that has extrema at about 5°N and 5°S, the eigenfunction of zonal velocity for the

first meridional mode has an extremum on the equator in the classical theory. When the effects of mean currents are taken into account, the zonal velocity extremum becomes displaced only slightly north of the equator. Although the annual zonal winds on the equator are considerably weaker than those in the ITCZ and SPCZ, the annual harmonic of zonal wind stress in the equatorial Pacific calculated from the satellite scatterometer-based climatology of Risien and Chelton (2008) exhibits a westward phase propagation within a few degrees of the equator, where it can project well onto the oceanic mode that crosses the basin in roughly one year. The phase speed of the zonal wind varies with latitude and longitude, but on the equator between 100°W and 170°E, it averages about 0.47 m/s, in rough agreement with the phase speeds estimated from altimeter data by Chelton et al. (2003) for the annual SSH variability. The evidence based on altimeter and scatterometer data thus strongly suggests an oceanic wave that is resonantly forced by the zonal winds across the entire equatorial Pacific. This agrees with conclusions of pre-satellite studies of the vertically propagating annual Rossby wave (Lukas and Firing, 1985; Kessler and McCreary, 1993), although these studies were unable to account successfully for the latitudinal asymmetry in the variability.

Questions remain regarding details of latitudinal and longitudinal variability in the measured SSH phase speed. Variations in the zonal wind propagation speed are likely to be important. It is also possible that a superposition of meridional modes plays a role. Durland et al. (2011) showed that the mean currents of the equatorial Pacific also produce an asymmetry in the eigenfunctions of the second meridional mode, and that the westward phase speed of this mode is increased by the mean currents. This is in contrast to the 1st meridional mode, for which the phase speed is decreased by the mean currents, as noted above. The phase speeds of the two gravest meridional modes are thus brought closer together in the mean-current-modified system, and the likelihood is increased that the annual winds could resonantly excite both modes simultaneously. Such a mode superposition would alter the observed phase speed at particular latitude, and lead to discrepancies between observed phase speeds at different latitudes, which are at least qualitatively consistent with the analysis of altimeter data by Chelton et al. (2003).

2.3 Interannual variability

In addition to the contribution to the understanding of the seasonal cycle to which ENSO events are phase-locked, satellite observations of SST, SSH, surface currents, and wind have become indispensable resources to monitor, understand, and even predict interannual variability of the tropical Pacific. For example, satellite observations have provided a multi-variable, basin-scale view of the evolution of El Niño, La Niña, and their transitions, and the associated ocean-atmosphere interaction (e.g., Picaut et al., 1996, McPhaden et al., 1998). Satellite-derived ocean surface currents (OSCAR, http://oscar.noaa.gov) were used to show that the first EOF of the surface currents leads that of SST by 2-3 months in the tropical Pacific (Figure 2.5), suggesting the important role of ocean currents in regulating ENSO-related SST (Lagerloef et al., 2003; Lumpkin et al., 2013).

Satellite observations have also improved the understanding of ENSO diversity in the past three decades, such as the different behaviors of the so-called central- and eastern-Pacific El Niño and their low-frequency change (e.g., Lee and McPhaden 2010). The strongest central-Pacific

El Niño thus far occurred in 2009-10 (Lee and McPhaden 2010). It had a substantial impact on the South Pacific and West Antarctica (Lee et al., 2010, Boening et al., 2011).

Satellite-derived SSH and wind stress data have been used to characterize the structure and variability of the lower branch of the so-called subtropical cell (STC), i.e., a shallow overturning cell that connects the tropical and subtropical oceans (e.g., Lee and Fukumori, 2003). SSH differences between the eastern and western boundary are used as a proxy for the net meridional geotrophic transport in the pycnocline, which is the lower branch of the STC. The structure of SSH and wind stress curl in the western tropical Pacific suggest near anti-correlated variability of pycnocline geostrophic flow near the western boundaries and in the interior, with the former being more dominant. This feature is due to the anomalous horizontal circulation generated by wind stress curl in the western tropical Pacific, as shown from satellite-based estimates of wind stress curl associated with the variability of the Intertropical Convergence Zone (ITCZ) and the South Pacific Convergence Zone (SPCZ). The boundary and interior flow of the Pacific STC therefore play opposite roles in regulating the interannual variability of upper ocean heat content in the tropical Pacific Ocean.

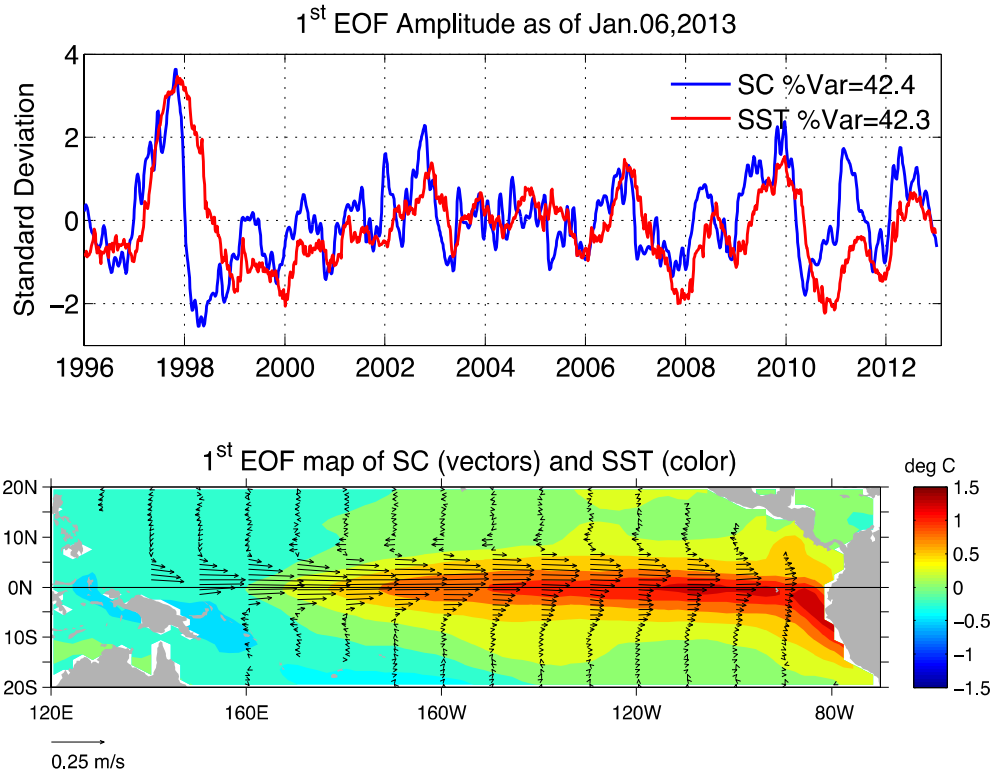

Figure 2.5 - The time series (upper) and spatial structure (lower) of the first EOF of non-seasonal ocean surface current and SST in the tropical Pacific, showing the 2-3 month lead time of the surface current over SST (after Lumpkin et al., 2013).

Satellite observations of SST are essential in the study of interannual variability of the mixed-layer heat balance because they enable the calculation of horizontal gradient of SST needed in the calculation of the horizontal heat advection in addition to the related estimate of SST

tendency (e.g., Wang and McPhaden, 2000; Zhang and McPhaden, 2010).

2.4 Decadal and longer variability

Despite the relatively short temporal records, satellite observations have provided important observations and insights about decadal variability in the tropical Pacific. Satellite observations of SSH and wind stress reveal a near coherent decadal change over much of the Indo-Pacific region (including the subpolar North Pacific and the Southern Ocean) since the early 1990s that is substantially stronger than that observed previously (Lee and McPhaden 2008). Satellite observations of zonal wind stress and the SSH difference between the eastern and western boundaries allow an estimate of the decadal variability of the strengths of the upper and lower branches of the STC, respectively. Based on these, Lee and McPhaden (2008) suggest that the STCs of the Pacific and Indian Ocean are linked by an atmospheric bridge (through the oscillation of the Walker Circulation) and an ocean tunnel (via the connection of the Indonesian Archipelago). The Pacific and Indian Ocean STCs oscillate out of sync during this period, thus playing opposite roles in controlling the upper ocean heat content of the Indo-Pacific domain. This has strong implications to ocean-atmosphere coupling of the Indo-Pacific region on decadal time scales (at least during the period of the satellite observations).

Satellite observations of SST in the past three decades reveal a statistically significant increasing trend of the amplitude of El Niño in the central Pacific, which the amplitude nearly doubled in the past three decades (Lee and McPhaden, 2010). This is associated with the more frequent occurrence of a stronger central-Pacific El Niño. The trend of El Niño amplitude in the central equatorial Pacific is in stark contrast to the amplitude of eastern-Pacific El Niño that shows no significant trend. Lee and McPhaden (2010) also showed that, while the El Niño amplitude in the central-Pacific has been increasing over the past three decades, no significant trend is found in La Niña amplitude and SST during neutral years in this region. Therefore, the increasing amplitude of El Niño in this region contributed to the well-observed increasing trend of the background SST.

3. Unique vantage point from space and complementarity with in situ observations

Satellite systems have important advantages in observing the tropical Pacific in several aspects. For instance, the overall more uniform spatio-temporal sampling of satellite observations in comparison with in situ data helps decipher large-scale and eddy variability captured by in situ data such as Argo floats (e.g., Willis et al., 2003; Willis 2010).

The relatively more uniform and dense spatial sampling of many satellite observations compared with in situ observations allows the calculation of spatial derivative fields. Satellite SST, SSS, and wind-stress gradients can be computed with much finer spatial resolutions than those obtained from in situ data, facilitating the analysis of mixed-layer heat and salt budgets and ocean dynamics. The importance of derivative SST and wind stress fields for studies of air-sea interaction was discussed in Sec. 2.1. In the case of SSS, the Aquarius satellite launched in 2011 has revealed much finer salinity gradients than those estimated from the Argo data (Figure 3.1).

The extensive (often global) spatial coverage of satellite observations is critical to studies of basin-to-global-scale teleconnections and the related impacts. For example, Lee et al. (2010) illustrated the teleconnection between the tropical Pacific (especially during the 2009-10 central-Pacific El Niño) and the Southern Ocean and Antarctica (including the SST near the Wilkins Ice Shelf). Boening et al. (2012) documented the large effect of the 2011 La Niña on globally averaged sea level and the relation to the record-flooding event in Australia.

Complementarity between satellite and in situ observations has been shown by a large number of studies. In particular, in situ data have played important roles in many applications of satellite data, primarily by providing information about subsurface variability that cannot be obtained from satellites. For example, satellite data from altimeters and GRACE have been used in combination with in situ Argo data to study the nature of sea level changes, in particular, the steric and mass contributions (e.g., Willis et al. 2003; Willis et al. 2008). SST derived from satellites, and the TOGA-TAO arrays have been used to produce the widely used blended OISST (e.g., Reynolds et al., 2007). Other examples of this complementarily were discussed in section 2.

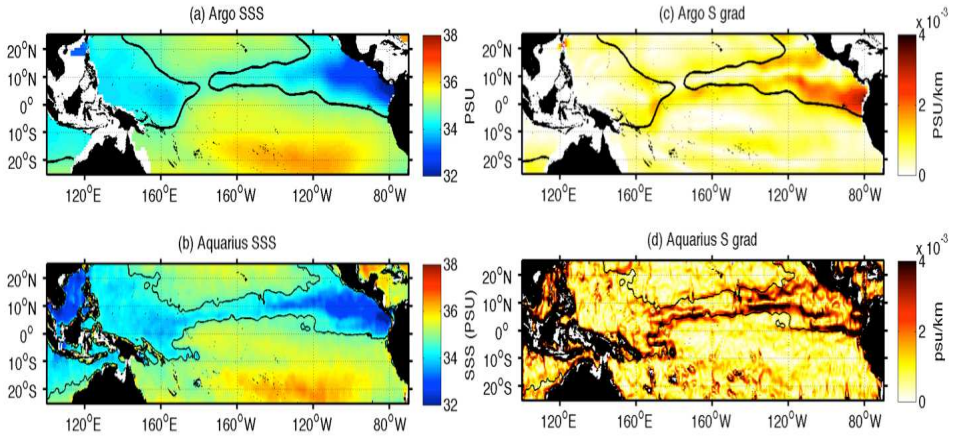

Figure 3.1 - Aquarius SSS gradients reveal intense frontal structures that are not evident in Argo OI maps. The dark contour is the 34.6 isohaline (Courtesy of Lagerloef, G., and Kao, H.).

Despite their relatively uniform spatio-temporal coverage, satellite observations have a number of limitations. For example, satellite observations are prone to high-frequency aliasing between temporal samples, in contrast to mooring observations that have high frequency sampling. Satellite infrared observations are prone to large sampling errors in the tropics from missing data because of the persistent cloud cover in many regions that obscures the sea surface at infrared wavelengths. As summarized below, infrared estimates of SST are also subject to measurement errors from several sources of atmospheric contamination of the measurements. Satellite microwave measurements are much less affected by atmospheric contamination. Moreover, because clouds are transparent at microwave frequencies, sampling errors are also less for microwave data than for infrared data. Sampling errors can nonetheless be an issue in microwave data because of affects of rain contamination. As discussed below, temporally and spatially averaged microwave data are therefore biased toward non-raining conditions.

In situ data, including measurements from the TAO-TRITON array, have historically been an

important component for the global calibration and validation of a suite of satellite data (e.g., SST, SSS, wind, precipitation). High-frequency mooring observations may be used to de-alias high-frequency signals not adequately captured by satellites (e.g., diurnal variability), at least regionally near the moorings. The following discussion illustrates some examples of the use of in situ data for the calibration and validation of satellite data.

3.1 SST validation

Satellite measurements of SST by infrared sensors, especially in the tropics, have a significant sampling issue because cloud cover obscures the sea surface at infrared wavelengths. In cases of low-level clouds, especially at nighttime, a large source of error in infrared estimates of SST is errors in the cloud masking algorithms. In such cases, clouds are difficult to detect because they often have a temperature very similar to that of the sea surface. Infrared SST retrievals are also subject to large errors from water vapor, which is a bigger problem in the tropics than anywhere else in the world ocean. Infrared estimates of SST are also contaminated by aerosols (which occur for a variety of reasons, including volcanic eruptions, dust storms and smoke from agricultural and forest burning). Aerosol concentrations are often large in the tropics. Since the tropics are especially prone to all of these sources of errors, TAO data have been very useful for improving infrared SST retrieval algorithms.

Satellite microwave measurements are much less affected by atmospheric effects. Whereas atmospheric transmittance is typically less than 50% and sometimes less than 10% at the wavelengths used for infrared estimates of SST, it is more than 97% at microwave frequencies, even in conditions of very high water vapor. As noted above, however, microwave measurements cannot be made in raining conditions. In most cases, it is easy to identify and therefore flag rain contaminated microwave data. The biggest problem is thus that the data gaps result in sampling errors, as opposed to the combined measurement and sampling errors in the infrared data. Although the data gaps in microwave data are much less of a concern than data gaps from cloud cover in the infrared measurements, they are nonetheless significant.

The most stringent accuracy and stability requirements on satellite-derived SSTs are imposed by climate research and monitoring purposes (Interim SST Science Team White Paper, 2010; Kaiser-Weiss et al., 2012). Over scales of order 100km, the absolute accuracy requirement is ± 0.1K and the stability requirement is ±0.04 K decade^{-1} (Ohring et al. 2005; Kaiser-Weiss et al., 2012). Not only is it very challenging to achieve these accuracies using either in situ or satellite measurements, it is also very difficult to demonstrate whether these targets have been met. The generation of Climate Data Records (CDRs) requires contributions from several satellite instruments over time (NRC, 2000; NRC, 2004). The generation of temperature CDRs is greatly facilitated by the fact that temperature is one of the seven base units of the Système International d'Unités (SI) to which measurements should be referenced (BIPM, 1995); this provides the basis for combining measurements from several different sources.

Assessing uncertainties by simple comparisons between SST fields from different satellite instruments does not necessarily satisfy the accuracy and stability requirements, even for the case of multiple instruments on satellites that are contemporaneous or have temporally overlapping missions. One exception is the use of measurements from the ATSR and AATRS series ((Advanced) Along-Track Scanning Radiometer; see below) to bias correct

contemporaneous AVHRR (Advanced Very High Resolution Radiometer) SSTs (O'Carroll et al., 2012). There are several approaches to validating the satellite retrievals of SST using independent measurements, with each source of validating data having their own strengths and weaknesses (Minnett, 2010). The most plentiful source of validating data is the drifting buoy array that comprises about a thousand buoys reporting near surface temperature per day (Figure 3.2); the depths of the drifting buoy measurements are typically 0.2 - 0.3 m.

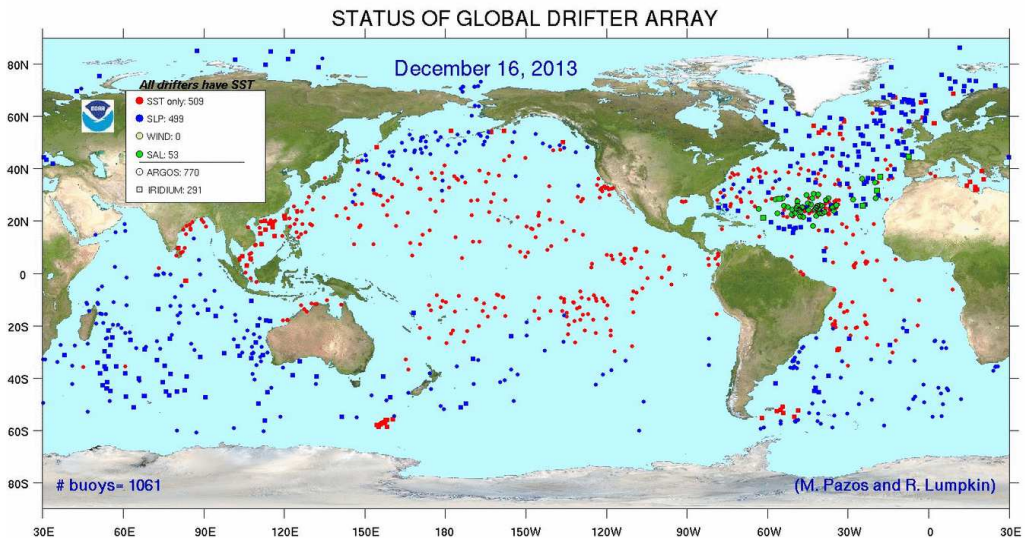

Figure 3.2 - Distribution of drifting buoys, all of which report near surface temperature.

The accuracy of SST from drifters is in the range 0.15 – 0.4 K (O'Carroll et al., 2008; Xu and Ignatov, 2010; Merchant et al., 2012) and therefore has uncertainties greater than the CDR requirements. There are efforts underway, through the Group for High Resolution SST (GHRSST) and the Data Buoy Cooperation Panel (DBCP), to improve the accuracy of the temperatures measured from drifters by about an order of magnitude.

The Global Tropical Moored Buoy Array (GTMBA) near-surface thermometers are calibrated before and after deployment and have a stated accuracy of 0.01K (Gentemann et al. 2004). Therefore, at least in principle, the GTMBA temperatures can make a useful contribution to the assessment of satellite-derived SST uncertainties in the tropical Pacific; modeling is required to remove the effects of diurnal heating and the thermal skin layer between the surface and the drifting buoy measurement depth (Embury and Merchant, 2012a; Embury et al., 2012b).

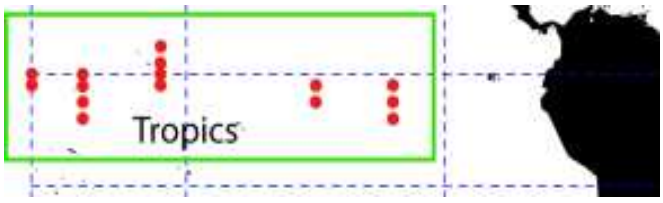

Figure 3.3 - Location of 'primary' GTMBA moorings identified by Merchant et al. (2012) as being suitable for assessing the stability of the ATSR and AATSR SST record.

The pre-deployment calibration of thermometers on the Argo profilers is rigorous and the

instrument is designed to be very stable. Thus, the near-surface temperatures from Argo, especially from the “unpumped” sensors, have the potential to contribute to the assessment of satellite-derived SSTs (Castro et al., 2014).

Only one assessment of stability capable of being informative at the level required by Ohring et al. (2005) has been published (Merchant et al., 2012) which assesses the stability of the (A)ATSR satellite SSTs relative to the GTMBA measurement. Only GTMBA buoys with a minimum of 120 months of data in the period 1991–2009 were used, and only buoys that passed strict quality control procedures were accepted. The resulting set of ‘primary’ GTMBA for stability assessment is shown in Figure 3.3.

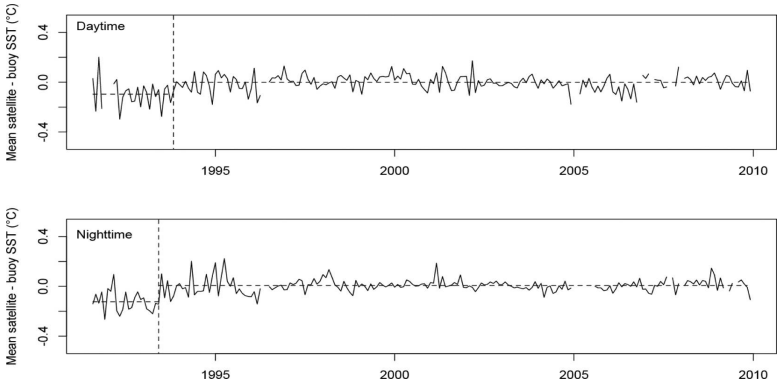

Figure 3.4 - Time series of monthly mean SST differences between ARC and GTMBA SSTs (taken from Merchant et al., 2012). See manuscript for further details and explanation of plot.

The monthly mean composite time series for daytime and nighttime (A) ATSR SST_{1m} data minus co-located GTMBA SSTs shown in Figure 3.4. The 95% confidence intervals for the trends are -0.0026 to 0.0015 K yr^{-1} (daytime) and -0.0018 to 0.0019 K yr^{-1} (nighttime). These results suggest that the (A) ATSR SSTs meet the target stability required by Ohring et al. (2005) in the tropics from 1994 onward. The use of the GTMBA for stability assessment is now an essential part of activities to analyze long-term satellite derived SST records. As such the GHRSST Climate Data Assessment Framework (CDAF) has this as a core activity. Such analyses are highly dependent on the long-term continuity of the GTMBA, particularly at the locations with the longest available data records such as the locations emphasized in Figure 3.4.

The paucity of measurements from drifting buoys in the tropics apparent in Figure 3.3 is a persistent feature. Figure 3.5 shows the global distribution of the difference between the 11µm brightness temperature measured by Visible Infrared Imaging Radiometer Suite (VIIRS) and in situ temperatures measured from drifting and moored buoys in confidently cloud-free conditions for most of the *Suomi* National Polar-orbiting Partnership (S-NPP) mission (January 2012-September 2013). It is clear that for much of the equatorial regions, the only in situ data are from the GTMBA – this is especially apparent in the Pacific Ocean.

The ITCZ poses particular challenges to the measurement of SST, because of the persistence of the clouds obscuring the surface to infrared radiometers, and rainfall contaminating the passive microwave measurements (Figure 3.6). There is a pronounced sampling minimum in the equatorial Pacific and Tropical Warm Pool regions, which underscores the need for

continuing GTMBA measurements.

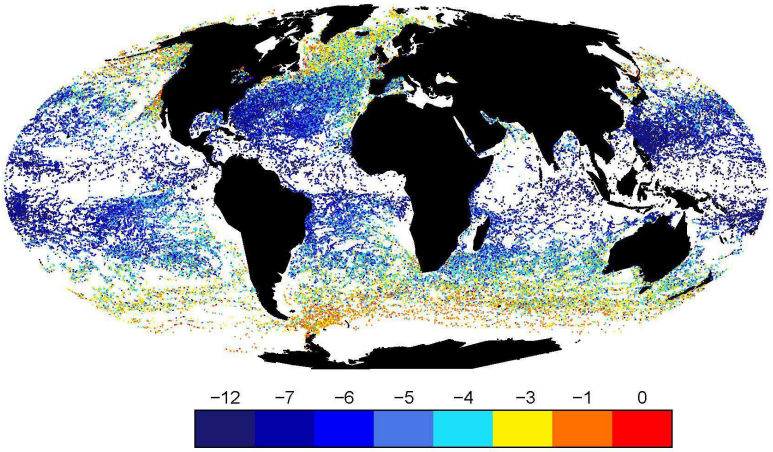

Figure 3.5 - VIIRS night-time temperature deficit at 11 µm, with reference to drifting and moored buoys. January 2012 to September 2013.

The effects of the cloud obscuration in infrared SST fields can be mitigated to some extent by temporal or spatial averaging, but the effects of sampling errors cannot be entirely eliminated in regions of persistent clouds. Figure 3.7 shows the consequences of clouds for daytime and night-time measurements. These are averages for January, April, July, and October 2011. The effects of spatial and temporal averaging are different, but a persistent feature is a negative bias in the equatorial regions in the eastern Pacific and eastern Atlantic Oceans.

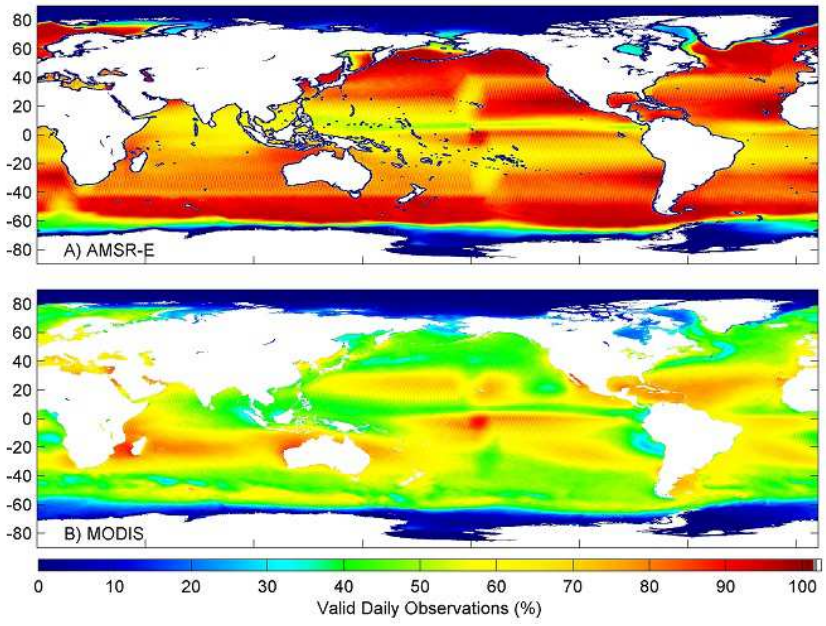

Figure 3.6 - Global distributions of the long-term fraction of SST retrievals in microwave measurements (AMSR-E top) and infrared measurements (Aqua MODIS, bottom) (figure provided by Gentemann, C.L., Remote Sensing Systems).

These are associated with equatorial upwelling and TIWs on the zonally aligned fronts to the north and south of the upwelling features. Clouds form preferentially on the warm sides of the fronts (Legeckis, 1977) leading to persistent and significant negative biases from sampling errors in the satellite-derived infrared SSTs.

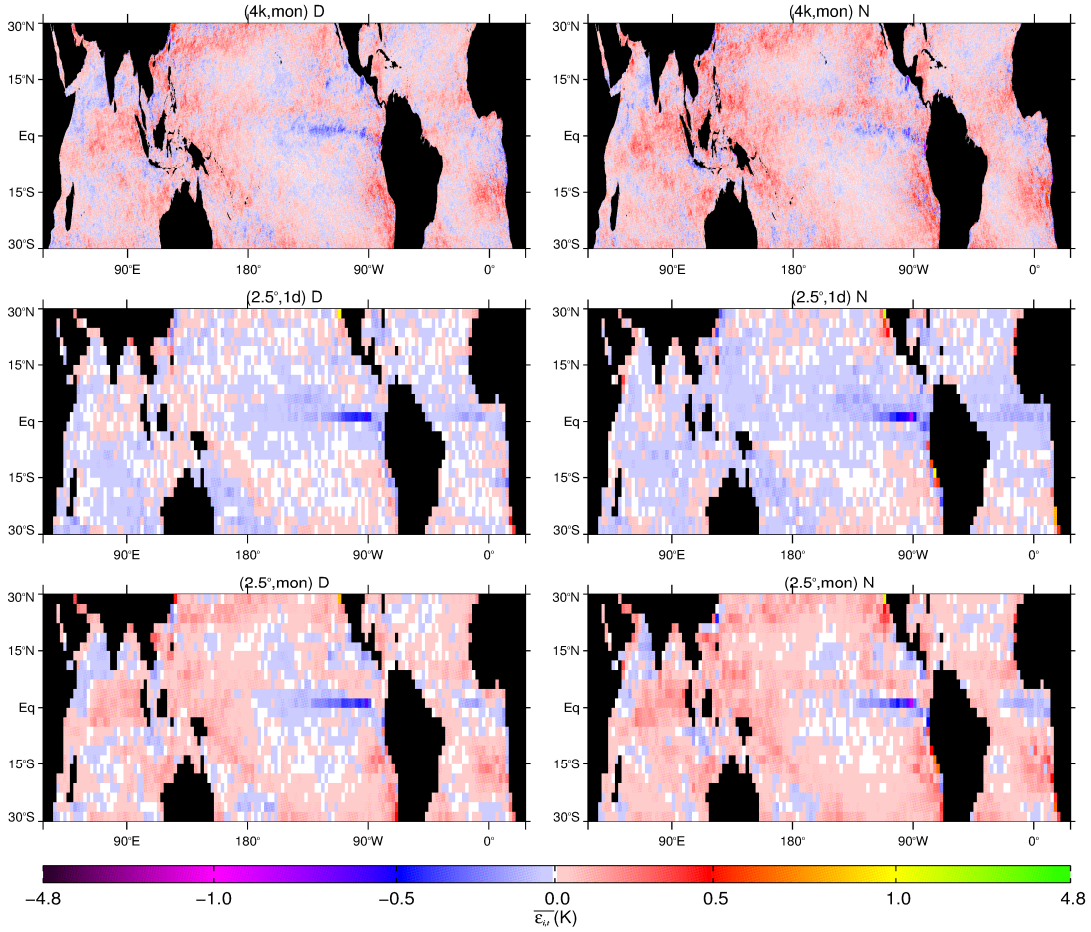

Figure 3.7 - Sampling errors introduced by clouds in infrared SSTs during the day (left) and at night (left). The top row shows the mean errors in monthly averaged daily fields at 4 km spatial resolution; the middle row shows the effects of spatial averages to 2.5^{o} grid cells, and the bottom row shows spatially and temporally averaged fields. Note the color scale is non-linear (from Lui and Minnett, 2013).

GTMBA near-surface temperature measurements have been shown to provide valuable information for the assessment of uncertainties and stability of satellite-derived SSTs. The equatorial regions are absent in the measurements from drifting buoys and even the next generation of drifters that are expected to provide more accurate measurements will not render the GTMBA data unnecessary for satellite SST validation. The ITCZ results in poorer sampling in both infrared and microwave SSTs than in many other ocean regions, and the effects of clouds introduce significant errors in spatially and temporally averaged fields. Despite their respective limitations, satellite and in situ SST measurements are complementary to each other to provide indispensible resources for the climate research community.

3.2 Altimeter and scatterometer calibration and validation

There is a clear need to maintain and even enhance the observing system over the global oceans and in particular over the Tropical Oceans. At the moment, weather centers all over the world are experiencing a dramatic decrease in the amount of in situ tropical Pacific observations received through the Global Telecommunication System (GTS). Although it is often assumed currently that ample quantities of satellite observations are available for initialization and validation of weather and marine (i.e. both ocean-wave and ocean circulation) forecasts, in situ observations still play a crucial role. Firstly, subsurface observations can only be obtained from in situ observations. Secondly, in situ observations of air temperature, humidity, surface pressure and surface vector wind in the Tropical Pacific play an important role in weather analysis and in short-term weather forecasts. This is discussed extensively in the TPOS 2020 whitepaper on Operational Forecasting Systems. Thirdly, as discussed below, in situ observations play a vital role in the development of a reliable geophysical model function (GMF) for satellite estimates of surface winds. Two examples are discussed next to illustrate this point, namely the development of GMFs for altimeter wind speeds and for scatterometer vector winds based on the efforts by the Royal Netherlands Meteorological Institute (KNMI). Finally, using a triple collocation technique which involves the collocation of three independent estimates of the truth, e.g. model forecast winds, scatterometer or altimeter winds and in situ wind observations, allows estimation of the random error of each of the three collocated wind products. The availability of independent in situ observations therefore gives important information on the quality of model and satellite products.

3.3 Development of a GMF for Altimeter and Scatterometer winds

Altimeters and scatterometers transmit microwave radiation to the wind-roughened ocean surface and measure the backscattered power. Altimeters are nadir-looking instruments, for which specular reflection of transmitted power leads to an inverse relation between backscatter and wind speed. Scatterometers, on the other hand, operate at oblique incidence angles in which the dominant scattering mechanism is the resonant interaction of the incident microwaves with short ocean ripple waves satisfying the Bragg resonance condition. These short waves are usually in equilibrium with the surface wind. Even though the physics of these backscatter processes are fairly well understood, wind retrievals from radar backscatter for both altimeter and scatterometer rely on empirical algorithms. A number of established approaches empirically relate radar backscatter to wind speed in the case of altimeters (e.g., Abdalla, 2012) and to the wind vector in the case of scatterometers (e.g., Hersbach, 2010; Ricciardulli and Wentz, manuscript in preparation).

3.4 Triple Collocation Analysis Using Satellite and In situ Data

In the development of the GMF's the implicit assumption has been made that the in situ observations or the model represent the truth. This is not necessarily the case, even for in situ observations and therefore this assumption needs to be checked.

The observation error consists of several components. The instrumental error usually only gives a small contribution to the total error. More significant are the representation error and errors caused by the finite distance and time between to observations. The plausible reasons for

model error have already been indicated.

When comparing several types of data it is desirable to have an idea about the size of the error. For example, when calibrating one instrument against another it is important to know their errors because the calibration constants depend on them. An example of linear regression is discussed by Marsden (1999). Furthermore, data assimilation requires knowledge of the weights given to the observations and to the first-guess field. These weights typically depend on the ratio of the first-guess error and the observation error. Therefore the resulting analysis will depend on this ratio as well.

The need for estimating errors from different data sources was noted by Stoffelen (1998). He proposed to use a triple collocation method to calibrate observations of winds from the Scatterometer using winds from buoys, model winds and winds from the ERS-1 Scatterometer. If the errors of these data sources are uncorrelated it can be shown that the random error for each of them can be obtained. Assuming that one data source (e.g. the buoy winds) gives an unbiased estimate of the truth, the systematic errors of the other two can be obtained as well.

In a similar vein, Caires and Sterl (2003) applied a triple collocation method to estimate and calibrate winds and wave heights from the ERA40 analysis effort. In a somewhat different context, Tokmakian and Challenor (1999) estimated errors in the mean sea-level anomalies of model and the ERS-2 and Topex-Poseidon satellites. The triple collocation method has recently also be applied to validate the retrieval of soil moisture from Scatterometer data over land (Scipal et al., 2008). For a further discussion of the method, including some applications, see Janssen et al. (2007). Abdalla et al. (2011) have extended this approach to estimate the errors in Altimeter wind and wave products as function of wind speed and wave height respectively. The overall statistics are as follows: the Envisat, Jason-1, buoys and 1-day forecast random error are 0.9, 1.0, 1.2, and 1.0 m/s while the scatter index (defined as the random error normalized with the mean value) for significant wave height for Envisat, Jason-1, buoys and first-guess wave height are 6%, 8%, 9% and 8%. These results suggest, on the one hand, that present day wind-wave forecasting is of high quality, while, on the other hand it should be clear that in situ observations still play a vital role in assessing the quality of satellite and wind-wave model products. Finally, the high quality of the Satellite wind products should be stressed, in particular the Altimeter wind speed product and the Scatterometer wind vector. Combining the results from the comparison of the Advanced Scatterometer (ASCAT) wind speed with ECMWF winds, which typically gives a standard deviation of error of about 1.3 m/s (Hersbach, 2010), with the present estimate of the ECMWF wind speed error of 1 m/s, and suggests a quite low standard deviation error of about 0.6 m /s. This is in agreement with earlier results of Stoffelen (1998). In summary, the triple collocation method demonstrates the complementary use of satellite and in situ data in error analysis. A triple collocation analysis involving satellite and in situ data is also used in the validation and error analysis of Aquarius-derived SSS.

3.5 QuikSCAT calibration and validation

QuikSCAT has provided an uninterrupted 10+ year record of vector winds over most of the rain and ice-free global ocean spanning the period July 19, 1999 to Nov 21, 2009. Compared to TAO winds, the rain-free QuikSCAT winds exhibited unprecedented accuracy. Distributions of the rain-free 10-m equivalent neutral wind (ENW) from QuikSCAT and all TAO buoys (solid and

dashed lines in Figure 3.8 a-b, respectively) collocated in space and time over the complete QuikSCAT data record agree well. The percentage of QuikSCAT wind direction observations with absolute differences >90° are limited to light winds where there are relatively few observations (Figure 3.8 c). Between 3 and 9 m s^{-1}, the mean QuikSCAT wind speeds match very closely with the buoy wind speeds, as shown from the binned scatterplot in Figure 13d. For wind speeds greater than 9 m s^{-1}, the QuikSCAT wind speeds are biased low compared to those from TAO (winds with speed higher than 9 m s^{-1} is often associated with rain in this region). The root-mean-square (RMS) differences between collocated QuikSCAT and TAO wind directions and wind speeds are shown in Figure 3.8 e-f, respectively, as a function of buoy wind speed. The RMS difference of wind direction shows a strong dependence on wind speed, with differences largest for small wind speeds, while decreasing rapidly as the wind speed increases. For the whole range of wind speeds, the overall RMS difference of wind direction is 26°, while restricted to wind speeds greater than 3 m s^{-1}, the RMS difference is 16°. The RMS wind speed differences also exhibit a significant dependence on wind speed, with the smallest RMS differences occurring between 6 and 9 m s^{-1}. Over the full range of wind speeds, the RMS difference in the 10-m ENW speed is 0.90 m s^{-1} for all buoys locations. Where both the buoys and QuikSCAT measure winds, they agree very well.

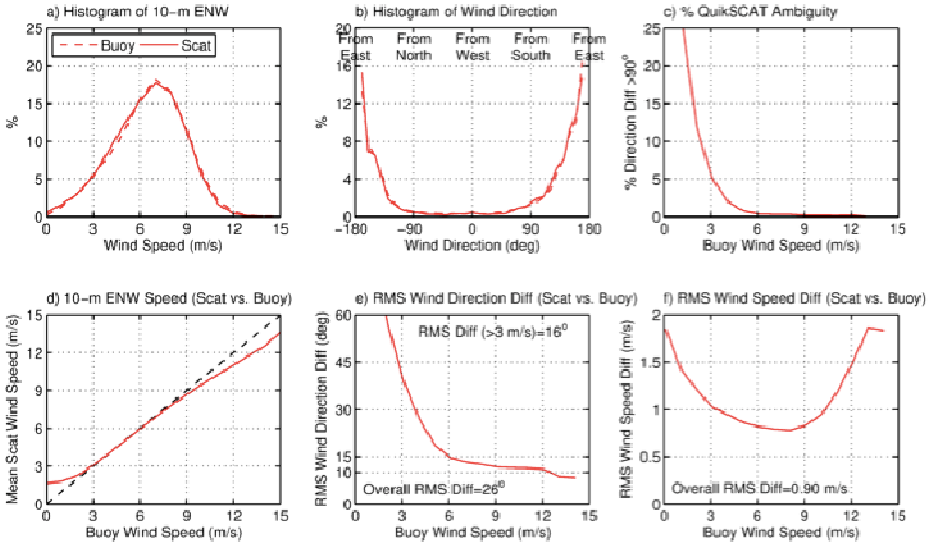

Figure 3.8 - Statistics for the comparison between collocated QuikSCAT and TAO 10-m ENW for all buoy locations over the 10+ year period July 19, 1999-Nov 21, 2009: (a) Histograms of wind speed (a) and direction (b) from QuikSCAT (solid) and TAO (dashed); (c) Percentage of QuikSCAT wind observations within each wind speed bin whose absolute wind direction differed from TAO by >90°; (d) QuikSCAT wind speed (y-axis) bin-averaged as a function of TAO wind speed (x-axis); RMS difference between QuikSCAT and TAO wind direction (e) and wind speed (f) on the y-axis as functions of buoy wind speed (x-axis). Only rain-free QuikSCAT wind observations were used in computing these statistics.

Rain can limit full utilization of QuikSCAT surface winds since rain degrades the ability of Ku-band scatterometers such as QuikSCAT and OSCAT to retrieve accurate vector winds over the ocean. Rain is relatively frequent in the western equatorial Pacific and along the ITCZ and western SPCZ, contaminating more than 30% of wind observations, as demonstrated in Figure 14a, which shows the percentage of rain-flagged QuikSCAT wind observations over the 10-yr

period Aug 1999-Jul 2009. The northern and western TAO moorings (squares in Figure 3.9 a) are well placed to measure winds in these rainy locales that are not measured accurately by satellite. Rarely does rain occur over the equatorial cold tongue and the southeast equatorial Pacific (<5% of the time). Such locations will be important for training wind retrieval algorithms to account for rain and to determine when rain corrections can be done effectively. Figure 3.9 b-e show that rain frequency has strong seasonal variability over most of the TAO moorings.

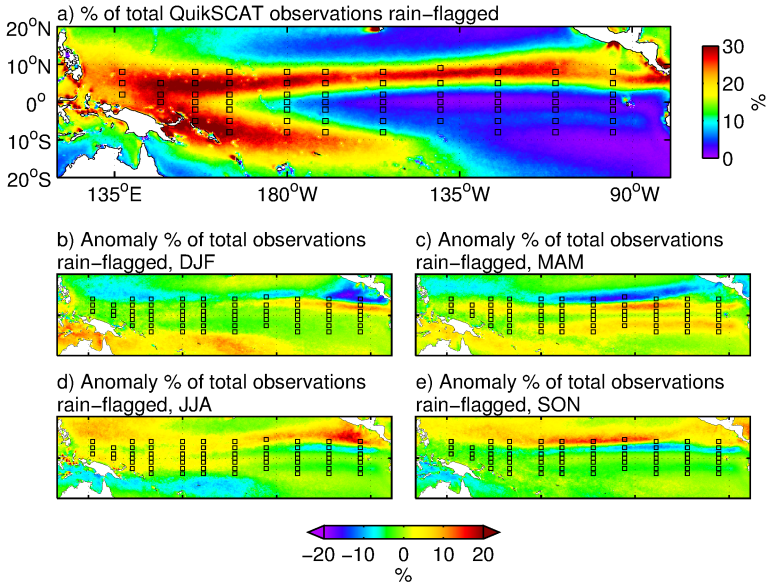

Figure 3.9 - (a) Map of the QuikSCAT rain-flag frequency over the 10-yr period August 1999-July 2009 from the Remote Sensing Systems (RSS) QuikSCAT version 4 dataset. (b-e) Seasonal anomalies of the QuikSCAT rain-flag frequency relative to total field in panel (a). Rain is determined from the QuikSCAT-only rain flag and collocated radiometer rain rate provided in the RSS dataset. The squares in each panel show the locations of the individual buoys in the TAO/TRITON array.

In light of the strong spatial and temporal rain variability, in situ TAO wind measurements are valuable in the tropical Pacific since anemometers provide all-weather sampling of surface winds. To demonstrate possible sampling limitations of scatterometer winds due to rain, the all-weather sampling capabilities of the TAO winds are exploited by computing the ratio of variances of rain-free and all-weather time series of zonal U10n and meridional V10n wind components at each buoy location shown in Figure 3.9. Figure 3.10 a,b shows this variance ratio as a function of time-scale. For time-scales less than 5 days, the rain-free time series contain significantly less variance than the all-weather time-series, while for longer than 5 days, the rain-free and all-weather variances are nearly equal. TAO wind measurements thus provide important information on temporal variability on time-scales less than 5 days that is degraded significantly in rain-free sampling, such as provided by most QuikSCAT wind datasets.

As shown in Figure 3.10 c-d, the variance reduction from rain-free sampling is strongly related to rain frequency for periods less than 3 days (black points); frequent rain strongly reduces measured wind variance. For rain frequencies greater than 20%, rain-free sampling captures only about half of the variance of the full all-weather time series. Even relatively modest occurrences of rain, 5% for example, reduces the measured wind variance to only about 80% of

the all-weather wind variance. Rain still affects wind variability on time-scales of 3-5 days (red points), although less so; for periods greater than 5 days (green points), the variance ratios approach unity for the whole range of rain frequencies encountered. The effect on time-scales less than 5 days is a consequence of the intermittent nature of precipitating weather disturbance in the tropics.

In addition to the variance reduction at time-scales less than 5 days, cross-correlations between the rain-free QuikSCAT and TAO wind components are reduced below 0.8 on time-scales less than 5 days (Figure 3.10 e-f). Winds for both platforms are highly correlated for longer time-scales, however. Part of the drop-off in correlation for shorter time-scales is due to random instrument errors for each platform, but part is also due to errors in the satellite rain-flag, which is known to misidentify rain-contaminated grid cells (e.g., Weissman et al., 2012).

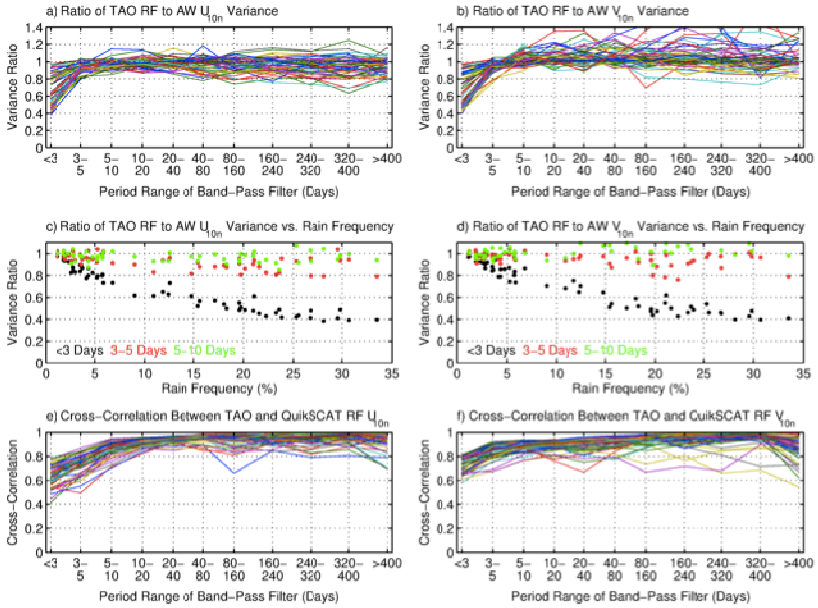

Figure 3.10 - Wind statistics computed over the 10-yr period August 1999-July 2009: (panels a-b) The ratio of temporal variance between rain-free (RF) and all-weather (AW) TAO equivalent neutral wind (ENW) components as a function of band-pass filtered time period. Each line corresponds to each of the buoys shown in Figure 2.2. (panels c-d) Ratio of TAO rain-free to all-weather wind variances as a function of rain-frequency for each buoy. Black points denote periods less than 3 days, red points are periods of 3-5 days, and green points are periods of 5-10 days. Each point represents an individual buoy. (panels e-f) Cross-correlation coefficients between the rain-free TAO and QuikSCAT ENW components as a function of band-pass filtered period. Each line corresponds to a different buoy. In all panels, only TAO winds collocated in time and space with QuikSCAT observations were used, and rain occurrence was determined from the QuikSCAT rain flag.

Despite that this analysis is based on the worst-case assumption of no useful data during rain, qualitatively similar problems exist within the JPL v3 QuikSCAT wind dataset for which corrections for rain were attempted. While this analysis demonstrates some limitations of rain-free sampling by QuikSCAT, it also shows that QuikSCAT provides accurate surface wind measurements for time-scales greater than approximately 5 days compared to those from TAO. Analysis of many of the wind-forced phenomena in the equatorial Pacific discussed earlier, such

as ENSO, MJO, and TIWs, thus are not affected greatly by the rain-free QuikSCAT wind sampling.

In addition to the Cal/Val of the QuikSCAT wind fields, the satellite wind-SST interaction discussed in Section 2 has also been compared with that from the TAO mooring array (O'Neill 2012). The metric used for the comparison relies on the slope of the linear response of the surface wind speed to SST perturbations along the equator. Figure 16 shows a bar chart comparing the ENW coupling coefficients estimated from both QuikSCAT and TAO (brown and green bars, respectively); these were estimated by binning the ENW and SST differences between pairs of buoys located along 2°S, 2°N, and the equator at 5 different longitudes. The coupling coefficients between QuikSCAT and the TAO buoys agree to within 10-30% at these locations, providing an independent verification of the QuikSCAT ENW response to SST.

The response of the QuikSCAT ENW may be due to either SST-induced changes to the actual wind speed, or to changes in surface layer stability that can change the surface stress without a change in wind speed. To determine the importance of each effect, the coupling coefficients for the response of the in situ buoy wind speed to SST are shown by the grey bars in Figure 3.11. These are about 20% smaller than the ENW coupling coefficients, which indicates that the wind response to SST observed by satellite is caused mainly by the response of the actual surface wind speed to SST rather than a simple adjustment of the surface layer stability. The in situ wind measurements from the TAO buoys thus provided an important clarification to the mechanisms involved in the satellite wind response to SST.

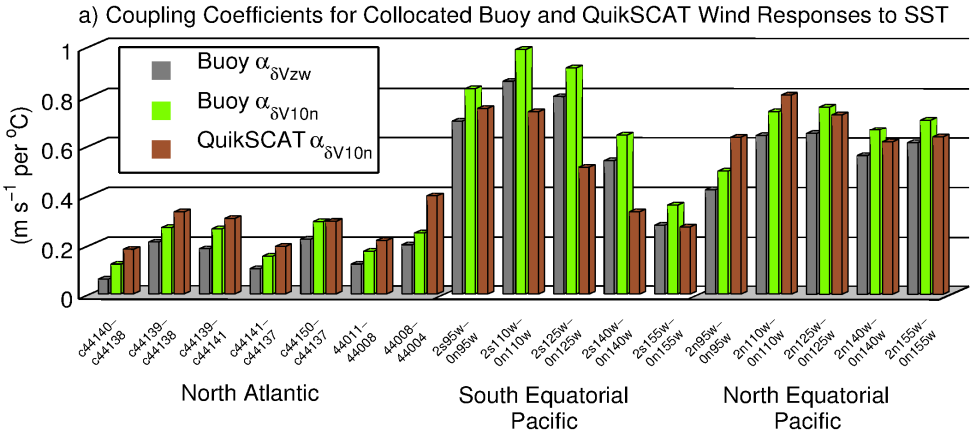

Figure 3.11 - Bar chart showing the coupling coefficients for the linear response of the 10-m ENW from QuikSCAT (brown) and the TAO buoys (green) to SST from the buoy pairs collocated spatially and temporally with the QuikSCAT ENW and AMSR-E SST. The grey bars show the linear coupling coefficients for the response of the in situ TAO winds to SST following the same procedure.

Recommendation: Ensure satellites are considered an integrated component of the tropical Pacific observing system. This should minimally include calibration/validation synergies with in situ systems, science and operational application contributions, and their role in tracking global climate teleconnections.

4. Enhancement of future satellite observing systems to complement the design of the future TPOS

Satellites are an important element of the integrated tropical Pacific observing system. Despite the significant achievement of satellite observations in the past few decades in understanding the variability of the tropical Pacific Ocean and related climate variability, there are several areas where improvement are required in order to advance these understanding further and to improve the prediction of tropical Pacific climate variability. These include (1) the improvement of spatial and temporal sampling, (2) maintaining the continuity of satellite observations of Essential Ocean Variables (EOVs) and Essential Climate Variables (ECVs), and (3) expanding the variables measured from space (such as ocean surface current and mixed-layer depth). As an example of enhance of spatial sampling, the planned Surface Water Ocean Topography (SWOT) mission is designed to provide high-resolution SSH measurements that will revolutionize our ability to study meso- and sub-mesoscale variability of the ocean (in addition to its capability to capture terrestrial water bodies). The RapidSCAT, scheduled for launch to the International Space Station in June 2014, along with other scatterometers currently in orbit (e.g., ASCAT, OSCAT) and for the future will allow the study of diurnal wind in the tropics. JASON-3 and GRACE Follow-on continue the measurements of sea level and gravity beyond TOPEX/Poseidon, JASON-1 and -2, and GRACE. These future measurements will significantly bolster the capability of the integrated tropical Pacific observing system.

Recommendation: TPOS design should plan for the improved observations at air-sea interface resulting from approved satellite missions of the coming decade.

5. Conclusion

As an integral component of the tropical Pacific observing system, satellites have provided measurements for a suite of variables (SST, SSS, SSH, wind and wind stress, precipitation, significant wave height, and related derived products such as ocean surface current). These measurements and products have the great advantage and benefit of providing global context and uniform spatio-temporal sampling. They have significantly advanced our understanding of the tropical Pacific Ocean and related climate variability. Satellite observations are complementary to in situ observations in many ways. They help decipher signals that are not adequately resolved or covered in space and time by in situ observations. Together they provide a much more complete view of the three-dimensional structure of the ocean circulation and greatly benefit the study of air-sea interaction. Blended satellite and in situ observations (e.g., SST and in the future, blended SSS) provide important value-added products that are important to the climate research community. In situ and satellite observing systems work in tandem to illuminate phenomena of interest to both science and applications. Recent decades of research and applications demonstrate the value and synergy of a tropical Pacific observing system that takes advantage of latest satellite and in situ measurement technologies. Any new “design” of a tropical Pacific observing system must incorporate satellite remote sensing capabilities into the system.

References

Abdalla, S., Janssen, P.A.E.M., and Bidlot, J.R. (2011): Altimeter near real time wind and wave products: Random error estimation. Mar. Geod., 34, pp. 393-406.

Abdalla, S. (2012): Ku-Band Radar Altimeter Surface Wind Speed Algorithm. Mar. Geod., 35 (S1), pp. 276-298.

Boening, C., Willis, J.K., Landerer, F.W., Nerem, R.S., and Fasullo, J. (2012): The 2011 La Niña - So Strong, the Oceans Fell. Geophys. Res. Lett., 39, L19602, (doi:10.1029/2012GL053055).

BIPM (1995) : Comptes rendus de la 20^{e} Conférence Générale des Poids et Mesures, (CGPM). (Available at http://www.bipm.org/en/CGPM/db/20/1).

Caires, S., and Sterl, A. (2003): Validation of ocean wind and wave data using triple collocation. J. Geophys. Res., 108 (C3), pp. 3098, (doi:10.1029/2002JC001491).

Castro, S. L., Wick, G.A., and Buck, J.J.H. (2014): Comparison of diurnal warming estimates from unpumped Argo data and SEVIRI satellite observations. Remote Sens. Environ. 140(0): pp. 789-799.

Chelton, D. B., Wentz, F.J., Gentemann, C.L., de Szoeke, R.A., and Schlax, M.G. (2000): Satellite microwave SST observations of transequatorial tropical instability waves. Geophys. Res. Lett., 27, pp. 1239-1242.

Chelton, D. B., Esbensen, S.K., and Schlax, M.G. (2001): Observations of coupling between surface wind stress and sea surface temperature in the eastern Tropical Pacific. J. Climate, 14, pp. 1479-1498.

Chelton, D. B., Schlax, M.G., Lyman, J.M., and Johnson, G.C. (2003): Equatorially trapped Rossby waves in the presence of meridionally sheared baroclinic flow in the Pacific Ocean. Progress in Oceanography, 56, pp. 323-380.

Chelton, D. B. (2005): The impact of SST specification on ECMWF surface wind stress fields in the eastern tropical Pacific. J. Climate, 18, pp. 530-550.

Cravatte, S., Picaut, J., and Eldin, G. (2003): Second and first baroclinic Kelvin modes in the equatorial Pacific at intraseasonal timescales. J. Geophys. Res. 108, (doi: 10.1029/2002JC001511).

Donlon, C., Robinson, I.S., Reynolds, M., Wimmer, W., Fisher, G., Edwards, R., and Nightingale, T.J. (2008): An Infrared Sea Surface Temperature Autonomous Radiometer (ISAR) for Deployment aboard Volunteer Observing Ships (VOS). J. Atmos. Oceanic Tech., 25(1): pp. 93-113.

Donohue, K., and Wimbush, M. (1998): Model results of flow instabilities in the tropical Pacific Ocean. J. Geophys. Res., 103, (doi: 10.1029/98JC01912).

Durland, T. S., Samelson, R.M., Chelton, D.B., and de Szoeke, R.A. (2011): Modification of long Rossby wave phase speeds by zonal currents. J. Phys. Oceanogr., 41, pp. 1077-1101.

Durland, T. S., and Farrar, J.T. (2012): The wavenumber-frequency content of resonantly excited equatorial waves. J. Phys. Oceanogr., 42, pp. 1834-1858.

Embury, O., and Merchant, C.J. (2012a): A reprocessing for climate of sea surface temperature from the along-track scanning radiometers: A new retrieval scheme. Remote Sens. Environ. 116(0), pp. 47-61.

Embury, O., Merchant, C.J., and Filipiak, M.J. (2012b): A reprocessing for climate of sea surface temperature from the along-track scanning radiometers: Basis in radiative transfer. Remote Sens. Environ. 116(0): pp. 32-46.

Enfield, D. B. (1987): The intraseasonal oscillation in eastern Pacific sea levels: How is it forced? J. Phys. Oceanogr., 17, pp. 1860-1876.

Farrar, J. T. (2008): Observations of the dispersion characteristics and meridional sea-level structure of equatorial waves in the Pacific Ocean. J. Phys. Oceanogr., 38, pp. 1669-1689.

Farrar, J. T. (2011): Barotropic Rossby waves radiating from tropical instability waves in the Pacific Ocean. J. Phys. Oceanogr., 41, pp. 1160-1181.

Gentemann, C. L., Wentz, F.J., Mears, C.A., and Smith, D.K. (2004): In situ validation of Tropical Rainfall Measuring Mission microwave sea surface temperatures. J. Geophys. Res., 109(C4): C04021.

Halpern, D., Knox, R.A., and Luther, D. (1988): Observations of the 20-day period meridional current oscillations in the upper ocean along the Pacific equator. J. Phys. Oceanogr., 18, pp. 1514-1543.

Hashizume, H., Xie, S.P., Liu, W.T., and Takeuchi, K. (2001): Local and remote atmospheric response to tropical instability waves: A global view from space. J. Geophys. Res., 106, pp. 10173–10185.

Hersbach, H. (2010): Comparison of C-Band Scatterometer CMOD5.N Equivalent Neutral Winds with ECMWF. J. Atmos. Oceanic Technol., 27, pp. 721-736.

Interim Sea Surface Temperature Science Team (2010): Sea Surface Temperature Error Budget: White Paper. Available at http://www.sstscienceteam.org/white_paper.html

Johnson, G. C. (1993): A deep inertial jet on a sloping bottom near the equator. Deep-Sea Res. I, 40, 1781-1792, (doi:10.1016/0967-0637(93)90032-X).

Hendon, H. H., Liebmann, B., and Glick, J.D. (1998): Oceanic Kelvin waves and the Madden-Julian Oscillations. J. Atmos. Sci., 55, pp. 88-101.

Janssen, P.A.E.M., Abdalla, S., Hersbach, H., and Bidlot, J. (2007): Error estimation of buoy, satellite and model wave height data. J. Atmos. Oceanic Technol., 24, pp. 1665-1677.

Johnson, G. C., and McPhaden, M.J. (1993): Effects of a 3-dimensional mean flow on intraseasonal Kelvin Waves in the Equatorial Pacific Ocean. J. Geophys. Res., 98, pp. 10185-10194.

Kaiser-Weiss, A., Vazquez, J., and Chin, M. (2012): GHRSST User Requirements Document (URD), Version 2.0. National Center for Earth Observation, Dept. Meteorology, University of Reading, Reference D-06 URD_v02, 42 pp.

Kessler, W. S. and McCreary, J.P. (1993): The annual wind-driven Rossby wave in the sub-thermocline equatorial Pacific. J. Phys. Oceanogr., 23, pp. 1192-1207.

Kessler, W. S. and M. J. McPhaden, 1995: Oceanic equatorial waves and the 1991-93 El Niño. J. Climate, 8, 1757-1774.

Kessler, W. S., McPhaden, M.J., and Weickmann, K.M. (1995): Forcing of intraseasonal Kelvin waves in the equatorial Pacific. J. Geophys. Res., 100, pp. 10613-10631.

Kessler, W. S., Johnson, G.C., and Moore, D.W. (2003): Sverdrup and Nonlinear Dynamics of the Pacific Equatorial Currents. J. Phys. Oceanogr., 33, pp. 994–1008.

Kutsuwada, K., and McPhaden, M.J. (2002): Intraseasonal Variations in the Upper Equatorial Pacific Ocean prior to and during the 1997–98 El Niño. J. Phys. Oceanogr., 32, pp. 1133–1149.

Lagerloef, G.S.E, Lukas, R., and Bonjean, F. (2003): El Niño tropical Pacific Ocean surface current and temperature evolution in 2002 and outlook for early 2003. Geophys. Res. Lett., 30, (doi:10.1029/2003GL017096).

Lee, T., and M. J. McPhaden, 2008: Decadal phase change in large-scale sea level and winds in the Indo-Pacific region at the end of the 20th century. Geophys. Res. Lett., 35, L01605, doi:10.1029/2007GL032419.

Lee, T., and McPhaden, M.J. (2010): Increasing intensity of El Niño in the central-equatorial Pacific. Geophys. Res. Lett., 37, L14603, (doi:10.1029/2010GL044007).

Lee, T., Hobbs, W., and Willis, J. (2010): Record warming in the South Pacific and western Antarctica associated with the strong central-Pacific El Niño in 2009-10. Geophys. Res. Lett., 37, L19704, (doi:10.1029/2010GL044865).

Lee, T., Lagerloef, G., Gierach, M.M., Kao, H.Y., Yueh, S.S. and Dohan, K. (2012): Aquarius reveals salinity structure of tropical instability waves. Geophys. Res. Lett., 39, L12610, (doi:10.1029/2012GL052232).

Legeckis, R.V. (1977): Long waves in the eastern equatorial ocean. Science, 197, pp. 1177–1181.

Liu, W. T., Xie, T.X., Polito, P.S., Xie, S.P., and Hashizume, H. (2000): Atmospheric Manifestation of Tropical Instability Wave Observed by QuikSCAT and Tropical Rain Measuring Mission. Geophys. Res. Lett., 27, pp. 2545-2548.

Lui, Y., and Minnett, P.J. (2013): Sampling Errors in Satellite Derived Sea Surface Temperature for Climate Data Records. Presented at 14th Science Team Meeting of the Group for High Resolution Sea-Surface Temperature. Woods Hole. 17 – 21 June 2013.

Lukas, R., and Firing, E. (1985): The annual Rossby wave in the Central Equatorial Pacific Ocean. J. Phys. Oceanogr., 11, pp. 55-67.

Lumpkin, R., Goni, G., and Dohan, K. (2013): Surface Currents, in "State of the Climate in 2012". Bull. Amer. Meteor. Soc., 94, S62-S65. (doi: 10.1175/2013BAMSStateoftheClimate.1).

Luther, D. S., and Johnson, E.S. (1990): Eddy energetics in the Upper Equatorial Pacific during the Hawaii-to-Tahiti Shuttle Experiment. J. Phys. Oceanogr., 20, pp. 913-944.

Lyman, J. M., Chelton, D.B., de Szoeke, R.A., and Samelson, R.M. (2005): Tropical Instability Waves as a Resonance between Equatorial Rossby Waves. J. Phys. Oceanogr., 35, pp. 232–254.

Lyman, J. M., Johnson, G.C., and Kessler, W.S. (2007): Distinct 17- and 33-Day Tropical Instability Waves in Subsurface Observations. J. Phys. Oceanogr., 37, pp. 855–872.

Madden, R. A., and Julian, P.R. (1994): Observations of the 40–50-day tropical oscillation—A review. Mon. Wea. Rev, 122, pp. 814–837.

McPhaden, M. J. (1996): Monthly period oscillations in the Pacific North Equatorial Countercurrent. J. Geophys. Res., 101, 6337-6359, (doi:10.1029/95JC03620).

McPhaden, M. J., and Taft, B.A. (1988): Dynamics of Seasonal and Intraseasonal Variability in the Eastern Equatorial Pacific. J. Phys. Oceanogr., 18, pp. 1713–1732.

McPhaden, M. J., Busalacchi, A.J., Cheney, R., Donguy, J.R., Gage, K.S., Halpern, D., Ji, M., Julian, P., Meyers, G., Mitchum, G.T., Niiler, P.P., Picaut, J., Reynolds, R.W., Smith, N., and Takeuchi, K. (1998): The Tropical Ocean-Global Atmosphere observing system: A decade of progress. J. Geophys. Res., 103, pp. 14169-14240.

Merchant, C. J., Embury, O., Rayner, N.A., Berry, D.I., Corlett, G.K., Lean, K., Veal, K.L., Kent, E.C., Llewellyn-Jones, D.T., Remedios, J.J., and Saunders, R. (2012): A twenty-year independent record of sea surface temperature for climate from Along Track Scanning Radiometers. J. Geophys. Res. 117.

Minnett, P. J. (2010): The Validation of Sea Surface Temperature Retrievals from Spaceborne Infrared Radiometers. Oceanography from Space, revisited. V. Barale, J. F. R. Gower and L. Alberotanza, Springer Science+Business Media B.V.: pp. 273-295.

Minnett, P. J., and Corlett, G.K. (2012): A pathway to generating Climate Data Records of sea-surface temperature from satellite measurements. Deep Sea Res. Part II, 77–80(0): pp. 44-51.

Minnett, P. J., Knuteson, R.O., Best, F.A., Osborne, B.J., Hanafin, J.A., and Brown, O.B. (2001): The Marine-Atmospheric Emitted Radiance Interferometer (M-AERI), a high-accuracy, sea-going infrared spectroradiometer. J. Atmos. Oceanic Tech., 18(6): pp. 994-1013.

Moore, D. W., and Philander, S.G.H. (1977): Modeling of the Tropical Ocean Circulation. In “The Sea,” Vol. 6, pp. 319–361 (Goldberg et al., ed.). Wiley, New York.

NRC (2000): Issues in the Integration of Research and Operational Satellite Systems for Climate Research: II. Implementation. Washington, DC, National Academy of Sciences.

NRC (2004): Climate Data Records from Environmental Satellites. Washington, DC. National Academy of Sciences.

O'Carroll, A. G., Eyre, J.R., and Saunders, R.W. (2008): Three-Way Error Analysis between AATSR, AMSR-E, and In Situ Sea Surface Temperature Observations. J. Atmos. Oceanic Tech., 25(7): pp. 1197-1207.

O'Carroll, A. G., Blackmore, T., Fennig, K., Saunders, R.W., and Millington, S. (2012): Towards a bias correction of the AVHRR Pathfinder SST data from 1985 to 1998 using ATSR. Remote Sens. Environ. 116(0): pp. 118-125.

Ohring, G., Wielicki, B., Spencer, R., Emery, B., and Datla, R. (2005): Satellite Instrument Calibration for Measuring Global Climate Change: Report of a Workshop. Bull. Amer. Meteor. Soc., 86(9): pp. 1303-1313.

Pezzi, L. P., Vialard, J., Richards, K., Menkes, C., and Anderson, D. (2004): Influence of ocean-atmosphere coupling on the properties of tropical instability waves. Geophys. Res. Lett., 31, (doi: 10.1029/2004GL019995).

Picaut, J., Loualalen, M., Menkes, C., Delcroix, T., and McPhaden, M.J. (1996): Mechanism of the Zonal Displacements of the Pacific Warm Pool: Implications for ENSO. Science, 274, pp. 1486-1489.

Perigaud, C. (1990): Sea level oscillations observed with Geosat along the two shear fronts of the Pacific North Equatorial Countercurrent. J. Geophys. Res., 95, pp. 7239-7248.

Philander, S. G. H. (1978): Instabilities of zonal equatorial currents, Part 2. J. Geophys. Res., 83, pp. 3679-3682.

Polito, P., Ryan, J., Liu, W.T., and Chavez, F.P. (2001): Oceanic and Atmospheric Anomalies of Tropical Instability Waves. Geophys. Res. Lett., 28, pp. 2233-2236.

O’Neill, L. W. (2012): Wind Speed and Stability Effects on Coupling between Surface Wind Stress and SST Observed from Buoys and Satellite. J. Climate, 25, pp. 1544-1569.

Qiao, L., and Weisberg, R.H. (1995): Tropical instability wave kinematics: Observations from the Tropical Instability Wave Experiment. J. Geophys. Res., 100, pp. 8677–8693.

Reynolds, R. W., Smith, T.M., Liu, C., Chelton, D.B., Casey, K., and Schlax, M.G. (2007): Daily high-resolution-blended analyses for sea surface temperature. J. Climate, 20, pp. 5473–5496.

Rice, J. P., J. J. Butler, B. C. Johnson, P. J. Minnett, Maillet, K.A., Nightingale, T.J., Hook, S.J., Abtahi, A., Donlon, C.J., and Barton, I.J. (2004): The Miami 2001 Infrared Radiometer Calibration and Intercomparison: 1. Laboratory Characterization of Blackbody Targets. J. Atmos. Oceanic Tech., 21, pp. 258-267.

Risien, C. M., and Chelton, D.B. (2008): A Global Climatology of Surface Wind and Wind Stress Fields from Eight Years of QuikSCAT Scatterometer Data. J. Phys. Oceanogr., 38, pp. 2379-2413.

Roundy, P. E., and Frank, W.M. (2004): A Climatology of Waves in the Equatorial Region. J. Atmos. Sci., 61, pp. 2105–2132.

Scipal, K., Holmes, T., de Jeu, R., Naeimi, V. and Wagner, W. (2008): A possible solution for the problem of estimating the error structure of global soil moisture data sets. Geophys. Res. Lett., 35, L24403, (doi:10.1029/2008GL035599).

Seo, H., Jochum, M., Murtugudde, R., Miller, A.J., and Roads, J.O. (2007): Feedback of Tropical Instability-Wave-Induced Atmospheric Variability onto the Ocean. J. Climate, 20, pp. 5842–5855.

Shinoda, T., Kiladis, G.N., and Roundy, P.E. (2009): Statistical representation of equatorial waves and tropical instability waves in the Pacific Ocean. Atmos. Res., 94, pp. 37–44.

Stoffelen, A. (1998): Error modeling and calibration: Towards the true surface wind speed. J. Geophys. Res. 103, pp. 7755-7766.

Tokmakian, R., and Challenor, P.G. (1999): On the joint estimation of model and satellite sea surface height anomaly errors. Ocean Modeling, 1, pp. 39-52.

Wakata, Y. (2007): Frequency-wavenumber spectra of equatorial waves detected from satellite altimeter data. J. Oceanogr., 63, pp. 483–490.

Wang, W. M., and McPhaden, M.J. (2001): Surface layer temperature balance in the Equatorial Pacific during the 1997–98 El Niño and 1998–99 La Niña. J. Climate, 14, pp. 3393–3407.

Weissman, D. E., Stiles, B.W., Hristova-Veleva, S.M., Long, D.G., Smith, D.K., Hilburn, K.A., and Jones, W.L. (2012): Challenges to Satellite Sensors of Ocean Winds: Addressing Precipitation Effects. J. Atmos. Oceanic. Tech., 29, pp. 356-384.

Wheeler, M., and Kiladis, G.N. (1999): Convectively Coupled Equatorial Waves: Analysis of Clouds and Temperature in the Wavenumber–Frequency Domain. J. Atmos. Sci., 56, pp. 374–399.

Willis, J. K., Roemmich, D., and Cornuelle, B. (2003): Combining altimetric height with broadscale profile data to estimate steric height, heat storage, subsurface temperature, and sea-surface temperature variability, J. Geophys. Res., 108 (C9), pp. 3292.

Willis, J. K., Chambers, D.P. and Nerem, R.S. (2008): Assessing the Globally Averaged Sea Level Budget on Seasonal to Interannual Time Scales. J. Geophys. Res., 113, C06015, (doi:10.1029/2007JC004517).

Willis, J. K. (2010): Can In situ Floats and Satellite Altimeters Detect Changes in Atlantic Ocean Overturning? Geophys. Res. Lett., 37, L06602, (doi:10.1029/2010GL042372).

Wimmer, W., Robinson, I.S., and Donlon, C.J. (2012): Long-term validation of AATSR SST data products using shipborne radiometry in the Bay of Biscay and English Channel. Remote Sens. Environ. 116(0): pp. 17-31.

Xu, F., and Ignatov, A. (2010): Evaluation of in situ sea surface temperatures for use in the calibration and validation of satellite retrievals. J. Geophys. Res., 115(C9): C09022.

Zang, X., Fu, L.L., and Wunsch, C. (2002): Observed reflectivity of the western boundary of the equatorial Pacific Ocean. J. Geophys. Res., 107, 3150, (doi:10.1029/2000JC000719).

Zhang, R.-H., and Busalacchi, A.J. (2008): Rectified effects of tropical instability wave (TIW)-induced atmospheric wind feedback in the tropical Pacific. Geophys. Res. Lett., 35, L05608. (doi:10.1029/2007GL033028).

Zhang, R.-H., and Busalacchi, A.J. (2009): An Empirical Model for Surface Wind Stress Response to SST Forcing Induced by Tropical Instability Waves (TIWs) in the Eastern Equatorial Pacific. Mon. Wea. Rev., 137, pp. 2021–2046.

Zhang, X. and McPhaden, M.J. (2010): Interannual surface layer heat balance in the eastern equatorial Pacific and its relationship with local atmospheric forcing. J. Climate, 23, pp. 4375–4394.

White Paper #10 – In situ temperature, salinity, and velocity observations

Roemmich, D.[1], and Cravatte, S.[2]

[1] Scripps Institution of Oceanography, United States
[2] Institut de Recherche pour le Développement (IRD), Center IRD de Nouméa, New Caledonia

and Delcroix, T.[3], Gasparin, F.[1], Hu, D.[4], Johnson, G.C.[5], Kessler, W.S.[5], Lumpkin, R.[6], Reverdin, G.[7], Sprintfall, J.[1], and Wijjfels, S.[8]

[3] LEGOS/CNES, Université de Toulouse, France
[4] Institute of Oceanology, Chinese Academy of Sciences, China
[5] NOAA Pacific Marine Environmental Laboratory, United States
[6] NOAA Atlantic Oceanographic and Meteorological Laboratory, United States
[7] Université Pierre et Marie Curie, France
[8] CSIRO Marine and Atmospheric Research, Center for Australian Weather and Climate Research, Australia

1. Establishing Observing System Requirements

The observing system requirements for *in situ* temperature, salinity, and velocity (T,S,V) are set by the space/time scales of phenomena that are to be resolved in applications. The process of observing system design is an iterative one, as improved understanding of the requirements is balanced with new technologies that make more comprehensive observations practical. Observing system design is a compromise between what is required and what is feasible from economical and/or logistical perspectives. Observing system designs relevant to the tropical Pacific Ocean are described for TAO/TRITON (Hayes et al., 1991; Anonymous, 2002), the Argo Programme (Argo Steering Team, 1998), the Global Drifter Programme (Dohan et al., 2010), and the Expendable Bathy-Thermograph (XBT) Networks (Goni et al., 2010).

Here we consider two classes of observing system requirements for *in situ* T,S,V. The first are for broadscale observations that span the spatial domain of the tropical Pacific Ocean, and are relevant from a climate observing system perspective (sections 1.1, 2, 3.1). The second are for high resolution observations that are needed in specific sub-domains, or for specific processes (sections 1.2 and 3.2). Some observations in this second class will be part of the sustained observations networks, and others are useful to progress the observing system design. These "high-resolution observations" include measurements in the western boundary regions, the equatorial band, and the surface mixed layer. The applications to be served by both classes of observations include basic research, operational modeling and prediction, ocean/climate assessment, and education. These span a broad range of space and time-scales, including mesoscale to basin scale processes, intraseasonal to interannual variability (ENSO research and prediction), decadal fluctuations (including decadal variability of ENSO), and multi-decadal climate change.

1.1 Broadscale T,S,V observations

As a step toward establishing the requirements for broadscale observations, and recognizing that conclusions from other TPOS 2020 White Papers will help in this regard, Table 1.1 and 1.2 provide provisional data requirements for *in situ* T, S, and V, by describing what is needed for different processes to be observed in the tropical Pacific. The separation of broadscale T, S variability into upper ocean and deep ocean components is an artificial one, based on technology and cost limitations. Deep measurements are indispensable for multi-decadal variability, since deep warming plays a significant role in total ocean budgets for energy and sea level (Purkey and Johnson, 2010). Seasonal to interannual variability also extends into the deep ocean, though the importance of deep ocean observations in prediction applications is yet to be tested. Increased cost of full depth profiles relative to upper ocean profiles may impose limits on observed time-scales in the deep ocean.

Table 1.1 – Observing system variable requirements for T, S, and V.

Variable	*Application Area(s)*	*Magnitude of signal*	*Depth Coverage/ Resolution*	*Spatial Coverage/ Resolution*	*Temporal Coverage/ Resolution*
T,S,V	Mesoscale variability	SSS: 0.2 – 0.4 (1)	?	0.25°x0.25°	5 days
T,S	Intraseasonal variability		3 vertical modes	5°x0.5°	5 days
T,S	ENSO research and forecasting	SSS: 0.2 – 0.4 (2)	15m 0 - 500m, higher near sea surface (5)	1.5°x1.5°	1 month
V, SSS	Climate model validation		15m 0 - 500m	Equatorial sites + SPCZ (6)	5 days
T,S, SSS	Climate variability	SSS: 0.2 – 0.5 (3,4)	Sea surface to 2000m	200 km	1 month
T,S	Multi-decadal trends		All water column	500 km	1 month (> 30 years)
T,S,V	LLWBCs and ITF		To 2000m at least or to the bottom ITF passages: >sill depth	10 km ITF: major passages	10 days ITF: 5 days (intraseasonal signals)

Here we do not distinguish between *in situ* temperature and salinity sampling requirements. As with temperature, salinity is an essential climate variable, necessary to estimate density, and especially important in regions including the western Pacific Warm Pool and the shallow thermocline of the eastern tropical Pacific. Salinity is essential for documenting multidecadal change, and useful in forecasting systems (e.g. Hackert et al., 2011).

Table 1.2 – Present observing system designs.

Observing Element	*Variable (s)*	*Random Error*	*Horizontal Coverage/ Resolution*	*Vertical Coverage/ Resolution*	*Temporal Coverage/ Resolution/ Observing Cycle*	*Timeliness*
TAO/TRITON Moored Array	T, S, V		15° longitude 2-3° latitude, 8°S-8°N	~12 depths, 0-500 m	hourly	
Repeat Hydrography	T, S, V and other	T .001 °C S .002	1/2 degree along track; sparse tracks	Top-to-bottom (GO-SHIP); 1-2 dbar resolution	variable	RT: 6 weeks DM: ½ yr
Argo Programme	T, S profiles V_{1000}	T .005°C S 0.01	3° x 3° (plus regional enhancements)	0-2000 dbar, 1 - 5 dbar res.	10 days (plus regional enhancements)	RT: 24 hours DM: 1 year
Global Drifter Programme	SST, SLP (subset), SSS (subset)	T 0.1°C 0.05°C for subset	5° x 5° (plus regional enhancements)	N/A	Approximately hourly	RT: 24 hours DM: 1/3 yr
VOS Sea Surface Salinity Network	SSS, SST	S .05 (with bucket sampling) T: 0.01	3 km along track; variable across track	0 – 10 m	1-3 month intervals	RT: 24 hours DM: 1 yr
High Resolution XBT Network	T profiles	T 0.2°C Z 2%	10 – 20 km in WBCs	0 – 800 m, 2 m res.	3 month intervals	RT: 24 hours DM: 1/3 yr

Many of the tropical signals have long zonal scales (> 10^6 m) relative to mid-latitude mesoscale variability and longer time scales (> a month), and thus the tropical ocean is easier to observe (in terms of space and timescales) than the higher latitudes. One of the major sources of aliasing is Tropical Instability Waves (TIWs), with 17-30-day period. The small space scales of the TIWs and their complex structures make them quite challenging to observe, and despite their importance for the climate, it is not possible with the present observing system to diagnose adequately their properties. The intraseasonal Kelvin waves (50 to 120-day period), on the other hand, are a realistic and important phenomenon to be observed, perhaps the most demanding tropical phenomenon for broadscale observations. If the observing system requirements for T,S,V are based on these scales of intraseasonal variability, then the larger/slower seasonal-to-interannual signals will also be adequately observed.

As with temperature and salinity, ocean current is an Essential Climate Variable and an Essential Ocean Variable (http://ioc-goos-oopc.org/obs/ecv.php). Broadscale systematic observations of current in the tropical Pacific are provided by a number of networks including the Global Drifter Network, Argo, TAO/TRITON moorings, and TAO/TRITON servicing cruise

data. All of these datasets have serious limitations in spatial, depth, and/or temporal sampling. For example, Dohan et al. (2010) noted that the GOOS/GCOS sampling requirement of “one Sea Surface Velocity measurement per month per 5° x 5° box is inadequate for any surface circulation calculation beyond climatology”. This objective was inherited from the SST calibration requirement, and does not take into consideration the scales of surface current features. Argo sampling of 1000-m depth velocity provides nearly an order of magnitude more estimates on a yearly basis, but is still inadequate except on long timescales. Mean velocity fields in the tropical Pacific at the sea surface (Maximenko et al., 2008) and at 1000 m (Cravatte et al., 2012) have complex spatial structure. The GOOS/GCOS requirement should be reevaluated for the modern observing system, taking into consideration velocity information indirectly provided by sea surface height, geostrophic shear, and ocean vector winds.

1.2 High resolution T,S,V observations

As noted above, some parts of the ocean, including boundary currents, the Indonesian Throughflow (ITF), the equator, and the surface mixed layer, are not adequately sampled by broadscale observations, and require dedicated observational networks. For the most part, they require a combination of observation types (see section 3.2)

The wind-driven shallow meridional overturning circulation (MOC) is an important component of seasonal to multi-decadal variability in the tropical Pacific mass and heat budgets. While the interior ocean elements of the shallow MOC are observed by the broadscale networks, the low latitude western boundary currents (LLWBCs) that represent an important part of the MOC remain poorly observed by sustained systems. Another critical element of the tropical Pacific mass and heat budgets is the Indo-Pacific exchange of waters via the ITF. Present observational technologies do not permit sampling of the full latitude/longitude/depth/ time structure of the tropical WBC and ITF regions at the required resolution of order 10 km and 10 days. Instead, and in contrast to the areal-mode of sampling addressed in the broadscale networks, boundary current and inter-basin exchange observations are mostly done in line-modes. That is, transects across the WBCs, LLWBCs, and the ITF are obtained by line-mode networks including shipboard hydrography, XBT, gliders, and moorings. These four *in situ* observational types provide a mixture of spatial, depth, and temporal sampling characteristics (see section 3.2). Integrated designs such as Ganachaud et al., (2008) and Hu et al., (2014), merging multiple *in situ* and satellite systems offer promise for sustained observations of the western boundary region. The equator is another important dynamical boundary that requires some enhancement of resolution in T,S,V relative to the off-equator ocean interiors.

In addition to the high horizontal and temporal resolution required for the western boundary region and the ITF, some applications also have requirements for high vertical resolution that are not met by all observational networks. These include studies of ocean mixing and the surface layer, where vertical resolution of 1 dbar or better is required for air-sea exchange estimates with short time-scales that resolve diurnal variability of the T,S stratification. In both applications, high vertical resolution observations may also be needed from broadscale systems and there may be specific regions where high vertical (and temporal) resolution is required.

1.3 Accuracy

Errors in observations of subsurface T(z), S(z) come from both the T,S measurements and the depth or pressure measurements. The vertical temperature gradient averaged over the tropical Pacific ranges from .001°C/dbar at 2000 dbar to 0.07°C/dbar in the shallow thermocline, but may be higher for individual profiles. With pressure errors in shipboard and low-power float and glider CTDs of <1 dbar to 2 dbar (respectively) and temperature errors of <.001°C to .002°C, the pressure errors dominate over temperature errors in the upper ocean for estimating T(z). It is essential to quantify and if possible correct systematic pressure or depth errors in order to ensure consistency in long time-series and consistency between observational networks.

The most demanding application, and hence requirement setting, for T(z), S(z) measurement accuracy is the estimation of long-term climate change. The upper ocean (0-2000 m, volume average) has warmed by .002°C/year (Levitus et al., 2012). Global warming rates decrease with depth in the upper ocean but remain positive over the full water column, with a second maximum of 0.0008 °C/year (Purkey and Johnson, 2010, Figure 2.9c) at 4500 m in the abyss. Combined errors due to spatial coverage and measurement accuracy must be small enough on multi-year time-scales to observe these signals. Wijffels et al. (2008) showed that correction of systematic depth errors in XBT data removed spurious decadal variability in 50-year estimates of global thermosteric sea level and hence ocean heat content.

In conclusion, modern shipboard and low-power float and glider CTDs provide adequate accuracy in T(z) for multi-year estimates of global temperature change, as well as for the larger signals of interannual to decadal variability on a regional basis. A similar conclusion can be drawn for S(z), with the condition that slow drift in salinity is adjusted through Delayed-Mode quality control procedures. The importance of correcting systematic pressure (or depth) errors is underlined, both for historical XBT observations and for modern autonomous pressure sensors.

2. The present sustained networks

2.1 TAO/TRITON moorings

Temperature, salinity, and velocity data are measured by moorings of the TAO/TRITON array [McPhaden et al., 1998] at 11 longitudes across the Pacific from 137°E to 95°W and nominally at latitudes of ±8°, ±5°, ±2°, and the equator (Figure 2.1). Temperature data are generally measured at 11 or 12 depths at all mooring locations between 500 m and the surface, more closely spaced in the vertical in the upper water to resolve the mixed layer and the thermocline, and more coarsely spaced at depth, where thermal gradients and variability are smaller. Salinity is measured from the surface to 500 m at the same depths as temperature on all TRITON moorings, in the western Pacific where barrier layers (Lukas and Lindstrom, 1991) are important. Salinity is measured near the surface from all TAO moorings, and along with subsurface temperature between 120 m and the sea surface at many of the TAO moorings along the equator. Velocity is nominally measured near-surface at all TRITON moorings, and along the equator in the upper few hundred meters at 147°E, 165°E, 170°W, 140°W, and 110°W.

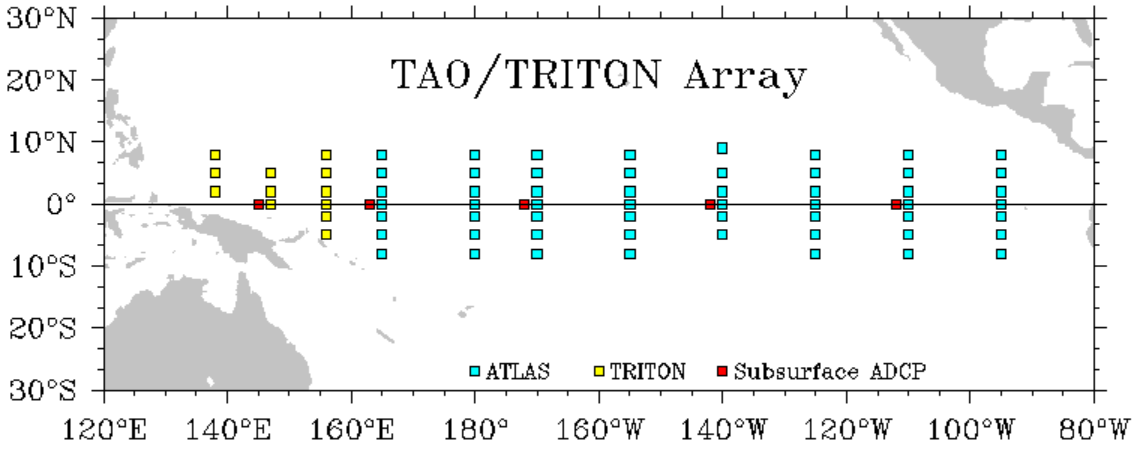

Figure 2.1 – Mooring locations for the TAO/TRITON array.

The vertical spacing of the subsurface moored temperature data is generally adequate to resolve the vertical thermocline structure, but without much redundancy. The lateral spacing of moorings is sufficient to resolve the structure of the thermocline for many timescales, including seasonal and ENSO timescales; it is marginally sufficient for sampling intraseasonal Kelvin waves (Kessler et al., 1996) but greatly insufficient to resolve the small structures and frontal characteristics of the TIWs. Daily temporal resolution is important for avoiding aliasing, although longer intervals (up to five days) between sampling could be sufficient for resolving many phenomena (Kessler et al., 1996). It is worth noting that hourly time series from moorings can also be used for specific process studies, such as surface layer studies (near surface stratification, SST diurnal cycle).

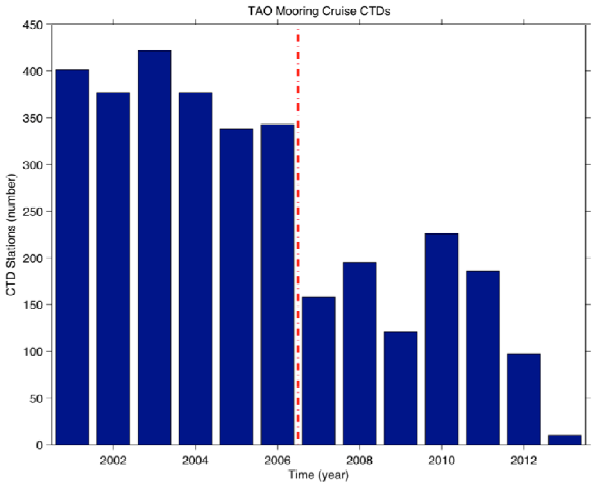

Figure 2.2 – Numbers of CTD casts taken during TAO cruises in each year from 2001-2013 (blue bars). The transition from PMEL to NDBC responsibility for the TAO mooring maintenance cruises (vertical red dashed line) in 2006 is shown. Nominally 366 CTD stations should have been occupied per year, time and equipment allowing.

While the TRITON mooring measurements continue to have a good data return, the TAO moorings have degraded considerably. The TAO array operated at 80–90% data returns from 46–55 moorings in the years just prior to 2006, when maintenance of the array transitioned from NOAA research (PMEL) to Weather Service management operations (NDBC). After the transition was mostly completed at the end of 2006 through 2011 the data return was usually closer to 80% than 90%, with from 45–54 moorings reporting. However, starting in 2012, data return dropped precipitously, falling to around 40% from 31–38 moorings in 2013, as the ship that had been maintaining TAO the array was laid up and not replaced.

TAO/TRITON data, including subsurface temperature, salinity, and velocity data, are used for a broad range of applications, including oceanographic research, climate studies, fisheries studies, and operational and reanalysis products related to oceanography and meteorology. A bibliography of TAO/TRITON research is found at (http://www.pmel.noaa.gov/tao/proj_over/pubs/taopubsr.shtml).

2.2 Repeat hydrography from TAO/TRITON cruises and GO-SHIP

Shipboard temperature, salinity, and pressure (CTD) profiles, and velocity (shipboard ADCP) data have been collected during TAO mooring maintenance cruises along the eight TAO longitudes and similarly along the three TRITON longitudes. Station spacing for TAO CTDs is nominally 1° poleward of ±3° latitude, and 0.5° equatorward of that. CTD data have been collected regularly along TAO longitudes in the eastern equatorial Pacific since 1979, before the pilot moored array was established along 110°W in 1984, with collection generally expanding westward as did the array. Since the array was fully established in 1994, but prior to the transition to operations, CTD transects were often continued north of the northernmost moorings, often to 12°N, to sample the equatorial current system. Data were collected from the surface to 1000 dbar, and deeper when time allowed.

During the six-year period between 2001 and 2006, when PMEL was leading the effort, on average 376 CTD profiles per year were collected during TAO mooring maintenance cruises (Figure 2), more than the nominal target of 366 profiles owing to collection of data north of mooring locations. After the transition to operations and NDBC leadership, data collection fell immediately, with an average of 164 profiles per year collected for the six-year period between 2007 and 2012 (44% of the data collection rate over the previous six years), with no data collected north of the northernmost moorings at each longitude. In 2013, a total of only 10 CTD profiles were collected during TAO maintenance cruises.

Shipboard velocity data were collected using an ADCP, with the first useable data obtained in 1991 (Johnson and Plimpton, 1999). Early ADCP instrumentation profiled only to 300–400 dbar, but an upgrade in 2004 allowed velocity data to be collected to pressures of 600–800 dbar from the NOAA Ship Ka'imimoana, since laid up in 2012. Having recent TAO mooring maintenance cruises on other ships without ADCP instrumentation has sometimes prevented velocity data collection entirely. Additionally, there has been no funding for SADCP data processing within TAO since the 1990s, so the data sets are processed as practicable by J. Hummon and E. Firing at the University of Hawaii.

The shipboard CTD and ADCP data have provided climatological estimates of current velocities, water-properties, and transports across the upper tropical Pacific Ocean, their seasonal cycles (Johnson et al., 2002b), and the effects of ENSO on tropical currents (Johnson et al., 2000). These data are very useful in describing and quantifying narrow features such as the subsurface countercurrents (Rowe et al., 2000). These features are invisible to satellites or surface drifters, and not well resolved by Argo except perhaps in the time-mean (e.g. Taguchi et al., 2012). The shipboard TAO/TRITON data have been widely used for evaluating ocean models and the ocean components of climate models. These data have also provided a divergence-based estimate of equatorial upwelling (Johnson et al., 2001) and direct measurements of the subsurface meridional velocities associated with the tropical cell (Perez et al., 2010).

Additional full-depth repeat hydrographic stations have been collected across the tropics at nominal longitudes of 137°E, 149°E, 165°E, 170°W (in the southern hemisphere only), 150°W, and 110°W at roughly decadal intervals starting with WOCE in the 1990s and now as part of the international GO-SHIP programme (http://www.go-ship.org/). Station spacing is nominally 0.5° of latitude, reduced to 0.33° equatorward of ±3°. Full-depth velocity data are collected using a lowered ADCP. These data and others have been used to document large-scale warming of the bottom waters, including the equatorial Pacific (Kouketsu et al., 2011). High quality shipboard CTD data are invaluable for calibrating salinity data from the CTD sensors on Argo floats, which may drift or shift from their pre-deployment calibration after time (Owens and Wong, 2009). Shipboard CTD data must be collected world-wide on a regular basis as a necessary condition for attaining sufficient accuracy of the Argo salinity data set.

In the equatorial-wave guide, full-depth CTD and velocity data are also very useful for studying the propagation of energetic and prominent planetary waves. The propagation of an annual Rossby wave in the equatorial Pacific has been traced across the basin from the surface to 3000 m using temperature profiles (Kessler and McCreary, 1993). Full-depth velocity data collected across the Pacific (Firing et al., 1998) have revealed equatorial deep jets and currents, distinct from the annual signal.

2.3 The Argo Programme

The original design of the Argo array (Argo Science Team, 1998) called for a profiling float in each 3° x 3° square, collecting 0-2000 dbar T,S profiles and 1000 dbar velocity estimates every 10 days. Argo achieved its initial global target of 3000 floats in 2007, and the present array includes 3600 active floats. The enormous impact of Argo on subsurface T, S observations in the tropical Pacific (15°S - 15°N) is illustrated in Figure 2.3. The World Ocean Database contains about 37,000 shipboard T, S profiles to at least 1000 m (Figure 2.3), with the distribution of profiles biased toward the coasts and the northern hemisphere. The median number of these profiles per 1° square is 3, and there are many areas with none. In contrast, Argo has so far obtained 150,000 T, S profiles (and trajectories) in the same tropical Pacific domain, with more uniform spatial distribution, and median of 32 profiles per 1° square. Argo coverage is systematic and regular over the domain. The tropical Pacific (15°S - 15°N) contains 4310 1° ocean squares, so the original Argo design requires about 17,500 profiles per year. In 2012 there were 18,455 profiles (Fig 3), and 43% of the 1° squares contained at least 4 profiles

that year. Further gains in uniformity of coverage are limited by the availability of float deployment opportunities. Array divergence is an issue for older model floats spending about 10 hours on the sea surface, but much less so for new floats with bidirectional communications, spending about 15 minutes on the sea surface.

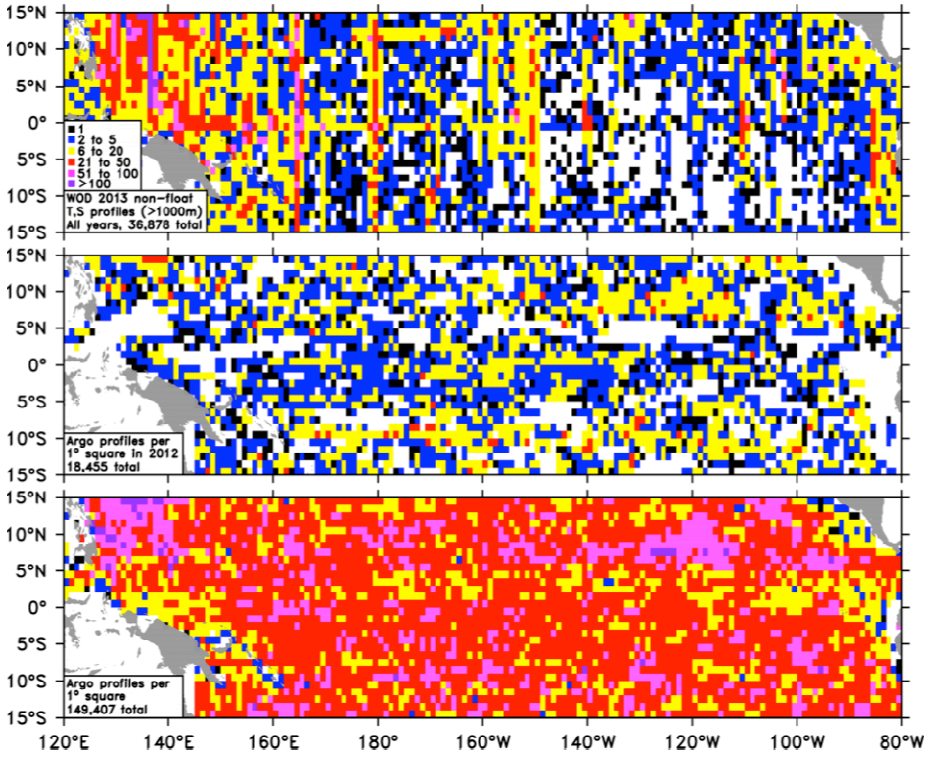

Figure 2.3 – (top) World Ocean Database, all years, non-Argo T,S profiles > 1000 m, per 1° square (36,878 total); (middle) Argo profiles per 1° square in 2012 only (18,455 total); (bottom) Argo profiles per 1° square in the tropical Pacific Ocean (149,407 total).

The OceanObs'09 Conference produced community recommendations for enhancement of the Argo array. These were further discussed at Argo's 4th Science Workshop in 2012, and endorsed by the Argo Steering Team in 2013 (though sustaining the original design of Argo is the top priority). Recommended enhancements impacting the tropical Pacific include denser sampling in western boundary regions and along the equator. A draft map of the revised Argo design is shown in Fig 4. In 2013, a float deployment cruise on RV Kaharoa added 75 floats in the western boundary region of the South Pacific. In late 2013-2014 a deployment of 50 floats along the full length of the Pacific equator will double Argo coverage there. Fig 4 shows the present density of Argo coverage, where 4 floats = 100% represents the "original design" metric for sampling in the 6° x 6° boxes shown in this figure.

Argo's broadscale coverage of the tropical Pacific (Figure 2.4) provides accurate estimates of the mean and annual cycle, for the period 2006 to the present, of T and S in the upper 2000 dbar, and velocity at 1000 dbar. To demonstrate how well Argo captures tropical variability, we use gridded altimetric sea surface height (SSH, AVISO weekly 1/3°) as a well-sampled proxy for steric height. In Figure 2.5, a linear regression of gridded steric height onto SSH in the central

equatorial Pacific captures 91% of the variance in the 2006 – 2012 time-series. When this record is separated into low frequency (100-day running mean) and intraseasonal (full minus 100-day running mean) components, the linear regression captures 95% and 79% of the variance respectively. Thus, Argo coverage captures nearly all the low frequency variability (seasonal to interannual) in the tropics. It is less effective for intraseasonal variability, but with the enhanced resolution from the denser sampling described above the estimate of intraseasonal variability will be further improved.

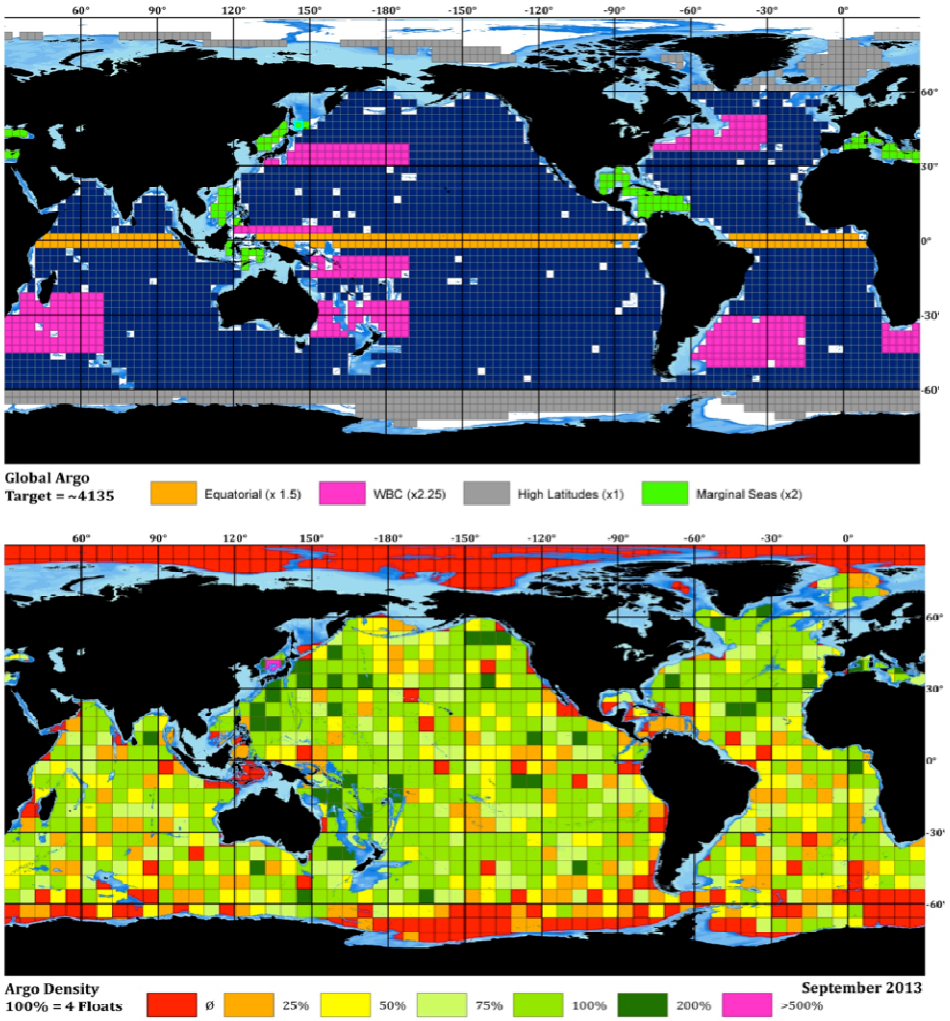

Figure 2.4 – (top) Draft map of recommended regions for enhanced Argo coverage, including western boundary regions and the equatorial band; (bottom) present coverage in 6° x 6° relative to Argo's original design (4 floats = 100%) (Source: Argo information center).

Another community recommendation for Argo is extension of the depth of profiles from the present 2000 dbar limit to full ocean depth profiling. Prototype Deep Argo floats have been deployed using 4000 dbar and 6000 dbar float models. Additional prototype deployments are planned for 2014, including testing of a new ultra-stable 6000 dbar float CTD. Deployment of pilot arrays of Deep Argo floats is expected to begin in 2015. A design for global sampling of

Deep Argo floats will be considered when the capabilities, costs, and support level for the instrument are better known.

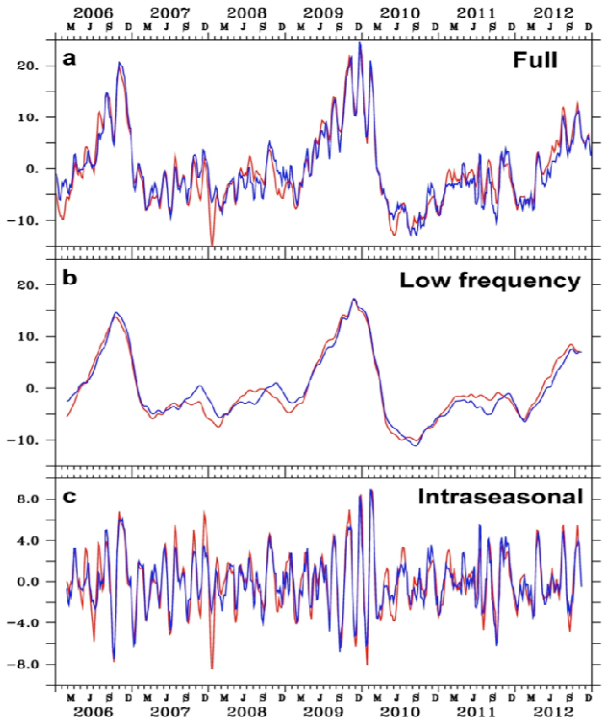

Figure 2.5 – a) SSH (red line, cm, AVISO, after Ducet et al., 2000) averaged over 160° W to 150° W, and 1.5° S to 1.5° N, linear regression of Argo steric height (blue line, cm, 10-day resolution, after Roemmich and Gibson, 2009) onto SSH; b) same but low-pass filtered with 100-day running mean; c) same but using the difference between the full time series and the low pass filtered series.

All Argo data are made publicly available within about 24 hours of collection via the GTS and the internet (2 mirrored Global Data Assembly Centers). A delayed-mode version of the data is available within about a year, including adjustments for salinity drift and pressure error. Trajectory and technical files are also available, and allow the computation of Argo subsurface drift at the parking depth.

2.4 The Global Drifter Programme

The network of drogued drifters (at 15-m) in the tropical Pacific is shown in Figure 2.6 (left). Surface velocity from drifters is a valuable source of current information, used as a mean current reference for altimetric height products, and recently in ocean data assimilation using drogued drifters (e.g., Lumpkin and Pazos, 2007). Drifter velocities have been used to quantify monthly variations in equatorial divergence and the surface current response to El Niño events (Lumpkin and Johnson, 2013, see Figure 2.7). Because Figure 2.6 is for the most recent quarter (July-September 2013), it reveals the large gap in the central equatorial Pacific where drifter observations are sparse due to equatorial divergence and lack of reseeding opportunities from TAO servicing cruises. Eastern equatorial observations were collected by some drifters deployed from volunteer ships transiting into the Pacific basin from the Panama Canal, while the westernmost equatorial Pacific was well-sampled by current meters on TRITON moorings. It is

clear that a large fraction of the region is not meeting the GOOS/GCOS (1999) requirement (Figure 2.6, right), evaluated here using both drifters and moored current meter sites of TAO/TRITON. The region was better sampled in earlier years (see http://www.aoml.noaa.gov/phod/ soto/gsc/reports.php); returning to coverage meeting the 1999 requirements will require resumption of TAO servicing cruises, or an alternate to repeatedly deploy drifters across a broad swath of the Tropical Pacific.

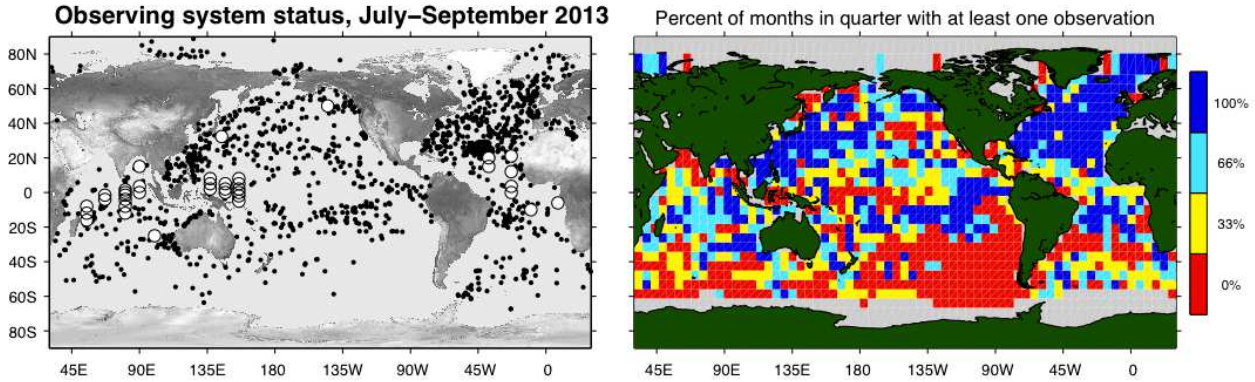

Figure 2.6 – (left) Location of drogued drifters (black dots), and moored near-surface current meter observations (circles) during the quarter July-September 2013; (right) percent of months in the quarter satisfying the GOOS/GCOS requirements for sea surface velocity.

The Eulerian velocity measurements from moorings and Lagrangian measurements from drifters are complementary, but not redundant. With respect to depth, moored acoustic current meters on the Global Tropical Moored Buoy network are placed at 10m depth, while the center of a drifter's drogue is at 15m. More fundamentally, the Eulerian measurements at a mooring are ideal for studies at a site - for example, calculating the impact of heat/salt advection on the mixed layer budget in combination with satellite-based measurements of lateral gradients - while the Lagrangian measurements of a drifter are capable of measuring dispersion, stirring and total derivative (including advective terms) of properties.

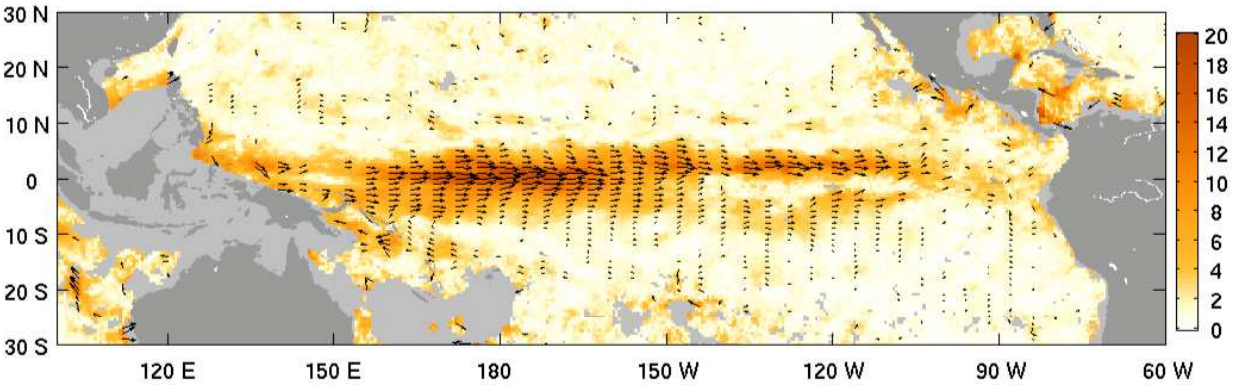

Figure 2.7 – Velocity of drifter-derived currents regressed onto the Southern Oscillation Index (SOI) (colors in cm/s) shown for SOI = -1 (moderate El Niño) with directions (black arrows) indicated for a subset of grid points. Arrows are not shown where their magnitude is not significantly different from zero. Light grey areas have less than 365 drifter days per bin (29 per square degree) (adapted from Lumpkin and Johnson, 2013).

Because they drift, Lagrangian measurements cover a broad area and contribute the vast majority of the 5° x 5° degree bins quantified in maps such as Figure 2.6. The value of Eulerian measurements is underrepresented in such maps, but moored measurements are the most cost-effective way to maintain observations in regions of surface divergence such as the equator. Surface drifters in the tropical oceans are also providers of SST data and are the main source of validation/correction of satellite-based SST products. Some surface drifters also have been equipped to measure surface salinity; these were first used during TOGA-COARE, with large-scale deployments initiated in 2012 in the tropical Atlantic. Prior to the Atlantic SPURS campaign of 2013, this augmentation had been mostly done on an exploratory or dedicated experiment fashion due to the high additional cost of the measurement, and the average time of usable data on any drifter is only 6 months to a year because of salinity sensor fouling and drift. These approximately hourly data can be used to resolve diurnal cycles, explore the response of surface salinity to rainfall and complement other near-surface data.

2.5 The Volunteer Observing Ship Sea Surface Salinity Network

Sea Surface Salinity (SSS) is also an essential climate variable (ECV). Its scientific relevance has been recognized and endorsed in the Oceanobs09 conclusions (Lagerloeff et al., 2010). The Tropical Pacific underway SSS and SST network includes data collected from Voluntary Observing Ships (VOS) and from oceanographic Research Vessels (RV). The VOS data in the tropical Pacific Ocean originated from the French SSS Observation Service (http://www.legos.obs-mip.fr/observations/sss/), dating back to 1969, and presently involves the efforts of international participants through the Global Ocean Surface Underway Data (GOSUD) project (http://www.gosud.org). These *in situ* SSS observations are a critical and quasi-unique source for observing and understanding small scale SSS variability (Figure 2.9). They are also essential for understanding the impact of river discharge on the ocean, evaluating satellite salinity observations (SMOS and Aquarius), and understanding hydrological changes among other physical processes (see http://www.legos.obs-mip.fr/observations/sss/publications/refereed).

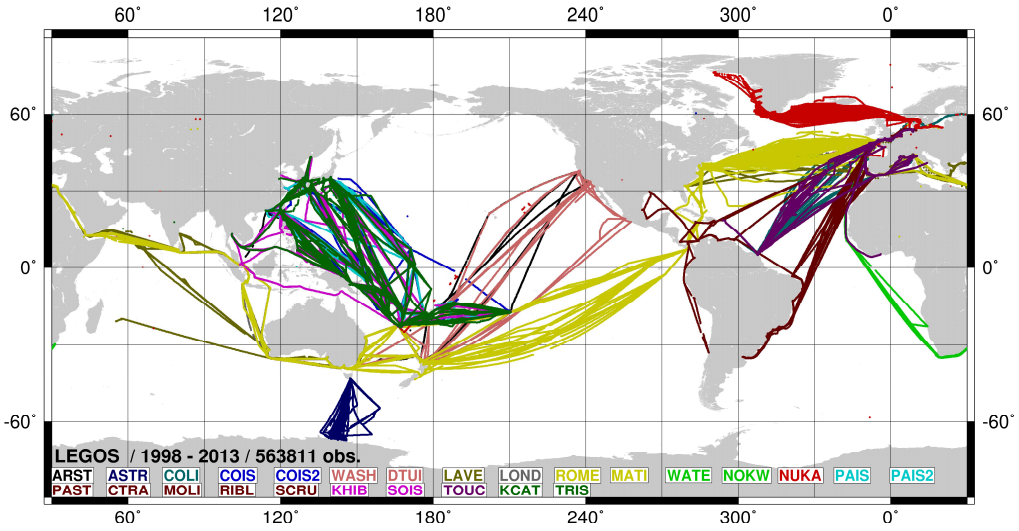

Figure 2.8 – Number of SSS observations per 1° longitude and 1° latitude, expressed in decimal logarithm scale, as obtained from TSG on VOS during 1998-2013.

On average, the contributing ships provide one to three SSS sections per season along a regular track (Figure 2.8). The SSS (& SST) measurements are mainly based on SeaBird SBE-21 TSG instruments located as close as possible to the ship's engine water intake. Most SSS measurements are collected at 15 second intervals, and a 5-minute median value is transmitted in real time, yielding spatial resolution of the order of 1-2 km. The 5-minute real time data are mainly designed to remotely check the on-board TSG systems, as well as for operational oceanography, and their use is not recommended for research purposes since they cannot be properly validated. The real time SSS data received are collected daily via ftp by CORIOLIS, which is the Global Data Acquisition Center for GOSUD.

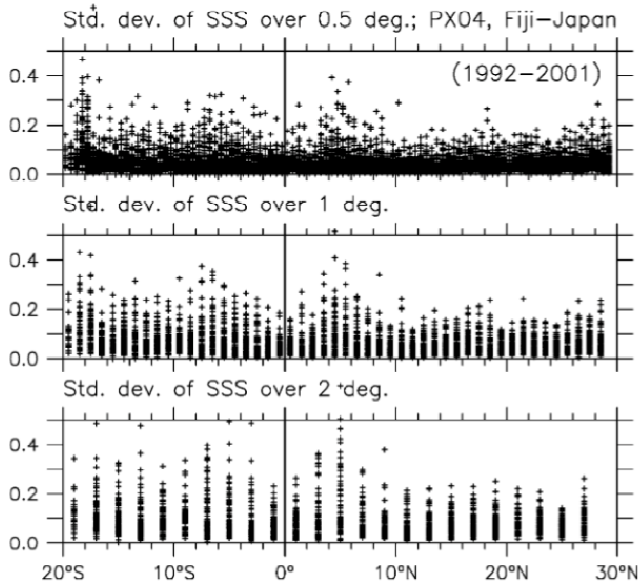

Figure 2.9 – Distribution of the standard deviation values of SSS computed over 0.5°, 1° and 2° latitudes for all 1992-2001 voyages along the Fiji-Japan shipping track (PX04) (from Delcroix et al., 2005).

Delayed mode quality control is made with simultaneous water samples, collocated Argo floats and/or CTD measurements. Once quality controlled, the estimated accuracy of SSS is of order 0.02 pss-78. The delayed mode data are made available from the French SSS Observation Service website, and also archived and made available via the CORIOLIS web site for the international GOSUD network.

2.6 The XBT Networks

The XBT Networks have undergone major evolutions in the past 15 years (Smith et al., 2001, Goni et al., 2010, Figure 2.10) in response to the implementation of the Argo Programme and to changes in the commercial shipping industry. The Argo Programme has replaced the previous broadscale XBT network, allowing XBT sampling to focus on line-modes while Argo provides the areal coverage. The line-modes include Frequently Repeated XBT (FRX) lines, with 18 or more transects per year at low spatial resolution (typically ~100-150 km), and High Resolution XBT (HRX) lines, with 4 transects per year at high spatial resolution (10-15 km in boundary currents). The shipping industry continues evolving to larger ships travelling on fewer routes,

increasing the challenge of maintaining exactly repeating transects on oceanographically important routes. Recognizing that the highest value of HRX transects is in sampling the oceans' boundary currents (and fine-scale features in the ocean interior), the HRX network is re-focusing again, toward boundary current observations, particularly along transects with existing long time-series. The present HRX Network in the Pacific and Indian Oceans (Figure 2.10) is similar in scope to the network in the Atlantic.

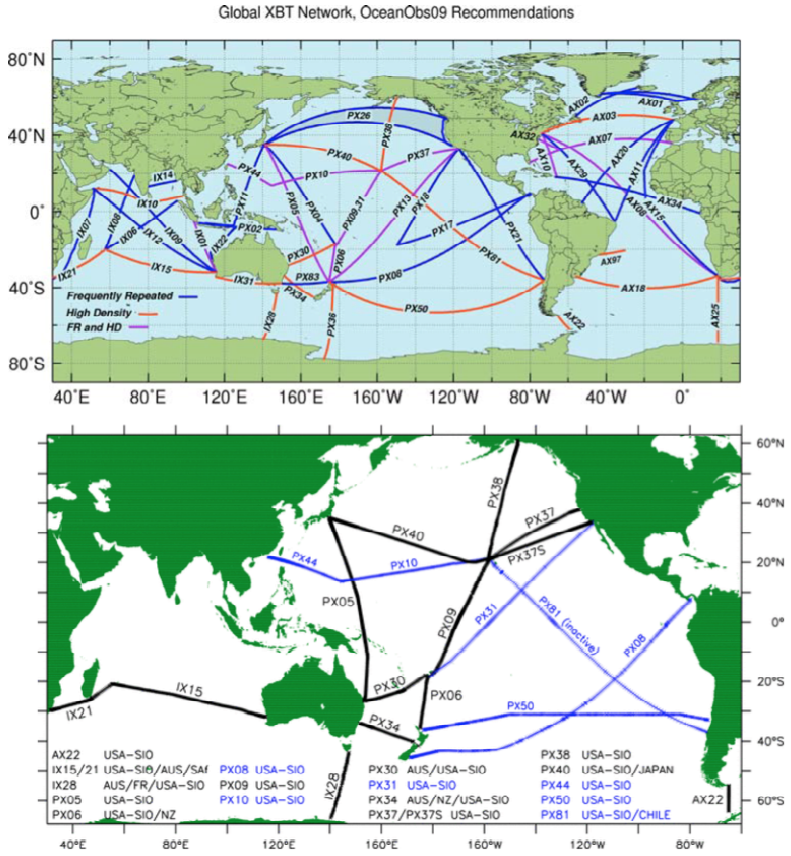

Figure 2.10 – (top) Recommended line-mode sampling from OceanObs'09 (Goni et al., 2010); (bottom) present configuration of the high resolution XBT Network in the Pacific and Indian Ocean. Blue lines are presently inactive, as the network refocuses on boundary current observations.

HRX data are released in near real-time via the GTS and archived by the NODC. As with other line-mode datasets, the primary uses of HRX data are as transects. Transect data are made available on websites of the data providers, but availability in the form of transects (rather than as collections of profiles) through global data centers would increase usage.

3. Integration of networks

3.1 Integration of broadscale networks

The broadscale networks, building on different instrument technologies, have fundamentally different sampling characteristics. It is these contrasts in spatial and temporal coverage and

resolution that can be exploited for integrating the total information content of the datasets. For example, the moored observations of the TAO/TRITON network provide high temporal resolution at widely-spaced fixed point locations, while the Argo array provides denser spatial coverage at lower frequency and at varying locations. Each of these datasets can reveal what is missed by the other – the moorings documenting temporal aliasing by Argo's 10-day cycling, and the floats showing the spatial patterns missed by the moored array. In the same way, Eulerian surface velocity measurements from moorings and Lagrangian velocity measurements from drifters are complementary, as noted in section 2.4. Drifters provide a broader spatial coverage, and moorings allow continuous time series, especially at the equator where drifters diverge.

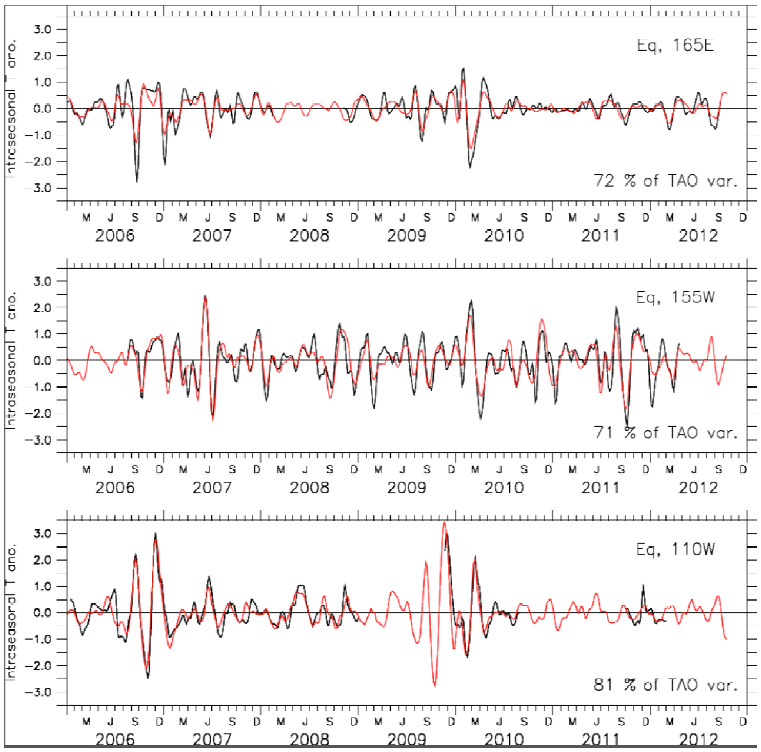

Figure 2.11 – TAO time series (black), 10 day-running mean, of 100 m temperature at 3 equatorial locations, compared with Argo data interpolated to the same locations (red).

An important first step in system integration is analysis of the individual datasets and comparisons to quantify their respective biases. For some variables, such as SSS, it can be challenging to mix data from different instruments, with different depth, accuracy, and coverage, without biasing the resulting mixed product. In that case, careful simultaneous data comparisons (VOS TSG and concurrent Argo profiles or CTDs) are needed to validate the different datasets, evaluate their differences and possibly readjust the data to finally obtain a consistent long interannual SSS gridded product (Delcroix et al., 2011). Similarly, producing climate-quality Argo salinity data requires comparisons with shipboard CTD data that have been carefully calibrated to international standards (Wong et al., 2003). Another important step is analysis of the individual datasets and comparisons to quantify their respective limitations. In Figure 11, Argo temperature at 100 m depth is interpolated to mooring locations in the western, central,

and eastern equatorial Pacific. The Argo records are then filtered with a 100-day running mean to separate low frequency and intraseasonal variability, for comparison with moored data at the same locations. For the low frequency variability, which has large spatial scales, Argo captures over 90% of the variance of the moored records. The intraseasonal signals are more challenging due to their shorter spatial scales (Kessler et al., 1996), and Figure 2.11 shows that Argo captures only 71 – 81% of the intraseasonal variance in the moored time-series.

The key to observing system integration is accurate knowledge of the spatial and temporal statistics (autocovariance) of T,S,V in the tropical Pacific (e.g. Meyers et al., 1991, Kessler et al, 1996), as well as the covariances linking T,S,V with related observations. The interannual timescale of ENSO, and its strong decadal modulations, require multi-decadal time series for estimating covariances. At present, remaining uncertainties in the statistics result in substantial differences in the estimated optimal interpolation (OI) mapping errors. In Figure 2.12, OI error maps are displayed for the TAO/TRITON array, with 2.12a using the functional fit to the autocovariance from Roemmich and Gilson (2009).

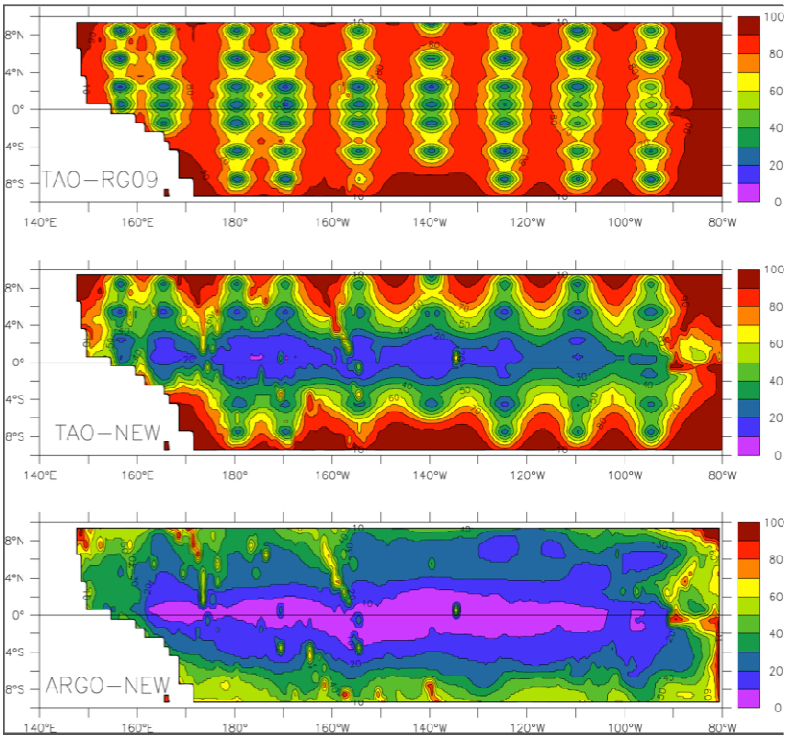

Figure 2.12 – Optimal interpolation fractional mapping error variance (%) for a) TAO/TRITON spatial coverage, using the Roemmich and Gilson (2009) covariance, b) TAO/TRITON coverage, using the Gasparin et al. (2014) covariance, and for c) Argo spatial coverage using Gasparin et al. (2014) covariance.

This representation and similar ones by Ducet et al. (2000) and Kessler et al. (1996) decay more rapidly (meridionally and zonally) than the present (extended) Argo dataset indicates, and so they produce larger errors than indicated by comparisons with independent datasets that are withheld from the mapping (e.g. Figures 2.5 and 2.11). Figure 2.12b is based on a functional covariance with realistic scales based on Argo data (Gasparin et al., 2014, in preparation), and the same is used to estimate mapping errors based on Argo coverage in Figure 2.12c. A

general characteristic of OI is that small differences in the covariance function can make large differences in estimated errors (Figure 2.12). OI error maps are very sensitive to details of the covariance. Thus, for applications requiring accurate error estimates, such as array design and evaluation, extensive datasets are needed to develop accurate representation of the covariance function, and independent (withheld) data are important for confirming that error estimates are realistic.

All of the broadscale *in situ* networks are sparsely sampled, but their resolution can be augmented through integration with satellite observations. The key synergies in the ocean observing system (e.g., Roemmich et al, 2010), are those linking subsurface T,S,V with SSH and with air-sea exchanges of momentum, heat, and freshwater (e.g. Willis et al., 2003; Willis and Fu, 2008; Ridgway and Dunn, 2010; Rio et al., 2011). Variability in SSH is dominated by subsurface density (mainly temperature), and the global, systematic character of satellite altimetry makes it powerful in combination with subsurface datasets to amplify their space/time resolution. One approach (e.g., Guinehut et al., 2012) has been to project SSH and SST variability onto subsurface T(z) anomalies as a first guess of the time-varying field, then using temperature profile data for an OI estimate based on this first guess. A more general approach would utilize all datasets containing T(z) information, which might include wind stress and air-sea heat flux as well as SSH and T(z) profiles. As long as accurate estimates are available of the covariances of these data with T(z), improved estimation of the vertical and horizontal structure of temperature or density fields can be made. S(z) is more weakly correlated with SSH than T(z), and so resulting estimates are strongly dependent on the existence of salinity profile data. A further step in dataset integration is through the use of ocean data assimilation models. The same statistics of the underlying datasets are required, but in addition, dynamical consistency imposed by the model can add information and value to the statistically based analyses. Both the multivariate approach (*in situ* plus satellite combinations) and ocean data assimilation modeling are powerful tools for amplifying the scope/domain/resolution of broadscale datasets. However, caution is warranted, and independent datasets should be maintained that are sufficient to assess the skill and limitations of these powerful methods.

3.2 Integration of networks observing the WBC systems and ITF

The LLWBCs - the New Guinea Coastal Undercurrent (NGCU) and the Mindanao Current - are essential elements of the shallow MOC supplying waters of low to mid-latitude origin to the equatorial Pacific. On ENSO timescales, the LLWBCs have been shown to partially compensate the interior transport variability, and are thus key components for the recharge/discharge of the equatorial warm water volume. As such, their properties, and their transport of mass, heat and freshwater should be monitored continuously in order to complete the Tropical Pacific Observing System. In the same way, the poleward western boundary currents - East Australian Current (EAC) and Kuroshio - that influence the climate of the mid-latitudes are not well resolved. The variability of the South Equatorial Current (SEC) and North Equatorial Current bifurcations into equatorward LLWBCs and poleward WBCs are poorly observed. Flowing close to the coast, and concentrated in narrow jets, the boundary currents are not adequately sampled by the broadscale networks, and require dedicated observations, and integration across networks.

Currently, observations of the western boundary regions are being made in the context of specific programmes, and some for limited time periods. The feasibility of sustained regional observing systems is being tested and demonstrated. Contributions to Western Boundary Current observations include full-depth moorings, repeated gliders surveys, end-point moorings and Pressure Inverted Echo Sounders (PIES, Send et al., 2010), HR-XBT transects, and shipboard repeat hydrography.

- Moorings are useful for monitoring transports, temperature and salinity of boundary currents in locations where they are sufficiently confined by the bathymetry for adequate sampling by a small number of fixed point measurements. Along coasts where the offshore extent of the boundary current is not well defined, or in larger straits, a line of moorings can be deployed, and integrated with regional or basin-wide observations.
- Underwater gliders (Davis et al., 2002) provide, at a moderate cost, repeated transects of the WBCs, measuring T, S along their route, and vertically integrated velocity. They are able to cross strong currents, albeit with irregular routing, and to sample close to the coast and in shallow waters. Their sampling (typically of 4-km horizontal resolution and to 1000-m depth) resolves the small scales of the boundary currents. Their slow speed and irregular paths pose issues for analyses.
- End-point moorings and PIES: density profiles spanning the boundary current and bottom pressure sensors can provide fluctuations of horizontal integrals of mass transport over large distances, but do not resolve the internal structure.
- HR XBT repeated transects can also help to sample the boundary currents. In some locations such as the EAC off Brisbane a combination of HR XBT, gliders, and moorings, sampled along a common transect, can overcome the limitations of the individual networks.

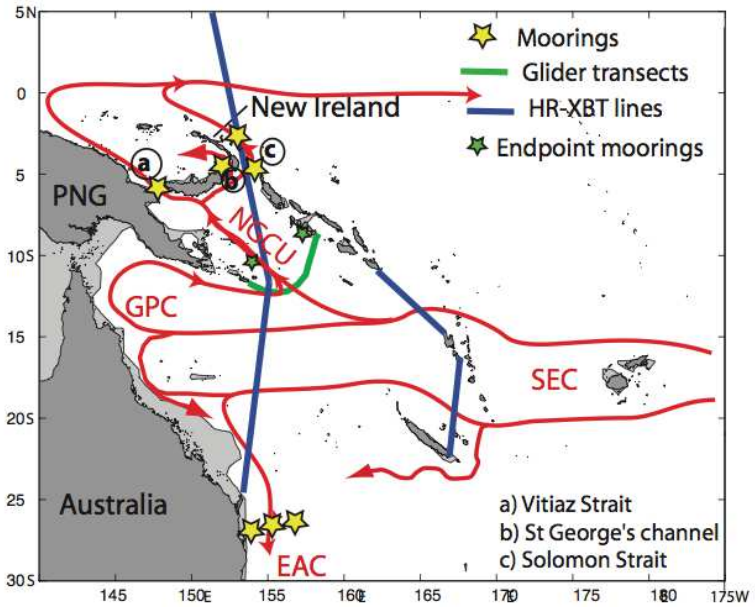

Figure 2.13 – Schematic view of the thermocline circulation in the Southwestern Pacific, and observational network in the context of the SPICE project (NGCU = New Guinea Coastal Undercurrent; GPC = Gulf of Papua Current; SEC = South Equatorial Current; EAC = East Australian Current).

A combination of these approaches can meet the challenges posed by the complex western boundary regions (Ganachaud et al., 2013, Figure 2.13). Integrated planning such as this will define the regional sustained observing system. Here we describe observations in the southwest tropical Pacific and ITF. Those in the northwest tropical Pacific are described briefly below and in greater detail in a separate contribution (Hu et al., 2014, Figure 2.14).

Presently, the circulation of the southwest Pacific is being observed (Figure 2.13) using moored arrays, glider transects, HR-XBT transects, and hydrography. Moorings equipped with ADCP, current meters, and T, S sensors were deployed in July/August 2012 in Vitiaz Strait, Solomon Strait and St. George's channel) (Eldin et al., 2013) to sample the flow exiting the Solomon Sea toward the equator. Two additional moorings, designed for duration of 1.5 years, have been deployed east of New Ireland to sample the New Ireland Coastal Undercurrent. Since 2007, gliders have measured the transport across the south entrance of the Solomon Sea, with four to eight crossings annually (Davis et al., 2012). The Solomon Sea glider transects are supplemented by Pressure Inverted Echo Sounders across the entrance of the Solomon Sea to provide horizontal integrals of mass transport at high temporal resolution.

To monitor the EAC transport, moorings were deployed in April 2012 off Brisbane (Figure 2.13, http://www.imos.org.au/), close to HR-XBT Line PX30. HR-XBT transects also allow a monitoring of the SEC transport and of its bifurcation. The SECARGO line samples the transport between New Caledonia and Vanuatu (Maes et al., 2011). Line PX05 extends northward from Brisbane, crossing the East Australian Current (EAC), the SEC, the Gulf of Papua Current (GPC), and the central Solomon Sea, exiting very close to New Ireland at 5°S. Thus, the net transport across this line is equal to the combined flow through Vitiaz Strait and St George's Channel (Figure 2.13). Other HRX lines in the tropical Pacific domain sample the upstream Kuroshio (PX44), and zonal flows in the central tropical Pacific (PX09).

Another critical element of the tropical Pacific circulation is the leakage of mostly warm and fresh tropical waters from the Pacific to the Indian Ocean through the Indonesian seas via the ITF. The ITF forms the only low latitude oceanic pathway for the global thermohaline circulation, and plays important roles in the interbasin transfer of heat and freshwater. Intense mixing occurs in the Indonesian seas, leading to water mass transformations. The interbasin exchange consists of several filaments that pass through the complex bathymetry of the Indonesian seas, making measurement of the total ITF logistically challenging. The observing system for the ITF has included moored arrays, frequently repeated XBT lines, pressure recorders, and repeat hydrography. There are no Argo floats in interior Indonesian seas presently, but this is technically feasible and important for global interannual heat and freshwater content.

During the 2004-2006 INSTANT programme, a moored array measured the major components of the full-depth ITF simultaneously through the inflow passage Makassar Strait (Gordon et al., 2008), and the exit passages of Lombok, Ombai and Timor (Sprintall et al., 2009). Since INSTANT, ITF transport measurements have mostly continued (with a gap from August 2011 – August 2013) in Makassar Strait through a single ADCP and current meter mooring, designed to resolve the full-depth transport, with recovery and redeployment planned in 2015. The deepest outflow passages of Ombai and Timor are instrumented by an array of moorings along a Jason altimeter track that crosses the Australian Northwest Shelf. This includes 3 moorings on the shelf, 3 tall moorings at the eastern end of the Timor trench and a single mooring in Ombai

Strait, all resolving full depth velocity, with discrete temperature and salinity sensors and PIES. These moorings were deployed in 2011, with next planned turn-around in mid-2014, and data are available through the IMOS web data portal (http://imos.aodn.org.au/imos/). Other discrete moorings in individual passage are planned for deployment by the Chinese Academy of Sciences (2013-2018).

Three frequently repeated XBT transects represent the longest continuous time series of temperature profiles and geostrophic velocity/transport within the Indonesian Seas (Wijffels et al., 2008). The IX1 line spans between southwestern Australia and Java while PX2 crosses the lower Banda Sea to the shelf break off northwest Australia. Both these transects were established around 1984. Line IX22 was established a few years later, and samples from the Australian northwest shelf across the Savu Sea and the Banda Sea. All three lines are subject to strong ageostrophic internal tide variability.

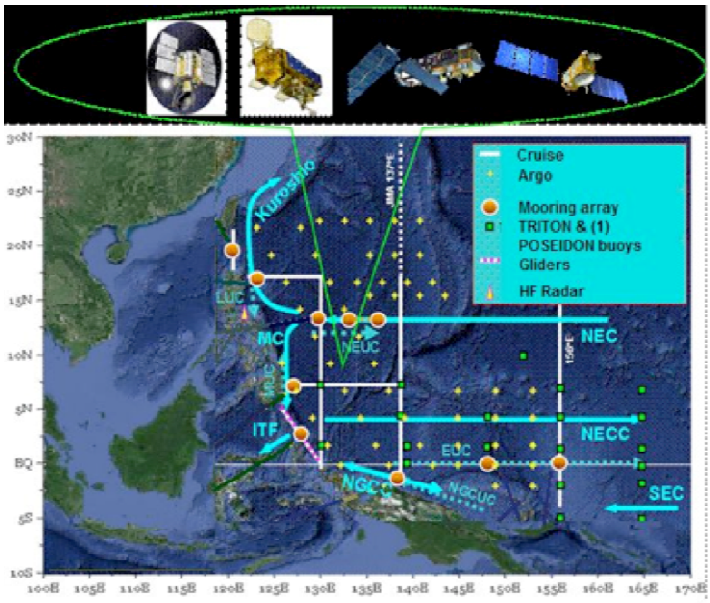

Figure 2.14 – Schematic view of the circulation in the Northwestern Pacific, and observational network in the context of the NPOCE Project (Hu et al., 2014).

The western tropical North Pacific is a critical crossroads for ocean circulation, linking the equatorial and subtropical North Pacific, communicating with the southern hemisphere along a range of density levels and with the Indian Ocean via the ITF. The Mindanao Current is the primary pathway for subtropical North Pacific waters to reach equatorial latitudes. This low latitude WBC system may play significant roles in ENSO variability through source waters for equatorial upwelling in the shallow MOC, and in the process of tropical Warm Water Volume recharge and discharge. However, understanding of these roles is limited by a lack of observations. In order to mitigate this limitation, the NPOCE observational framework (Hu et al., 2014 and Figure 2.14) is focused on the North Equatorial Current bifurcation into the poleward Kuroshio and the equatorward Mindanao Current (and ITF). Repeat hydrographic transects and moored arrays along historically sampled lines (8°N, 18°N, and 130°E) are the central elements for observing each of these three circulation components. In addition, glider transects, and enhanced areal sampling by Argo floats and surface drifters are included on a regional basis.

4. Gaps

4.1 Sustained WBC region and ITF observations

As discussed in Section 3.2, there are short-term (a few years) observations in the boundary current regions and the ITF, but the primary multi-decadal sustained observations of these currents are provided by the XBT networks. These transects have serious limitations (temporal resolution, 0-800 m in depth, no salinity or velocity). The WBCs usually extend deep, and integrate forcing over the entire basin; their variability thus includes a wide range of phenomena, and requires a frequent sampling. Moreover, their narrow width (around 100 km) also requires a sampling at 25 km resolution or higher. Sustained observing systems in these regions should be designed and implemented for full-depth coverage of T, S, V in order to resolve volume, heat, and freshwater transport variations on timescales of a season and longer. These systems are essential to close the basin-wide Meridional Overturning Circulations, including western boundary currents and interior circulations, and the low latitude Indo-Pacific exchange. Sustained systems may include glider and HR-XBT transects, repeat hydrography, Argo floats, moorings, and satellite altimetry. They would require international collaboration to share costs, and in particular ship time.

A key conclusion from the community consensus on sustained ocean observations, including both OceanObs'99 (Smith et al., 2001) and OceanObs'09 (Fisher et al., 2010), was that sustained boundary current and inter-basin exchange observations are primary missing elements of the global ocean observing system. Work already underway in the western boundary region of the tropical Pacific in the context of NPOCE and SPICE programmes is a valuable starting point for the global system. However, there is not yet a plan for sustaining observations currently funded by time-limited national projects. In the ITF region, observations are being maintained by individual programmes in the Makassar inflow and Lesser Sunda Island outflow passages. Additional observations are needed in the northeastern Indonesian seas to record the primary inflow from the Southern Hemisphere that provides the major salt contribution to the ITF.

4.2 Deep ocean broadscale observations

The present Argo array spans only the upper ocean, 0 – 2000 m, due to technology limitations. Broadscale observations of the deep ocean are obtained by the GO-SHIP repeat hydrography programme, but these transects are overly sparse spatially and temporally. Research and operational drivers for systematic observations of the deep ocean include closure of global and regional budgets for heat, freshwater, and sea level. Away from the equatorial waveguide and from the boundary currents, deep ocean interest is mainly focused on decadal and longer timescales, including the mean circulation and its variability. However, there remains much to understand concerning the intraseasonal, seasonal and interannual variability of the deep ocean components, including ENSO-related equatorial waves.

Prototype Deep Argo floats have been deployed demonstrating the capability of profiling to 6000 m. Low power ultra-stable CTDs are also under development to meet accuracy requirements for deep ocean temperature and salinity decadal variability and multi-decadal change. Design and implementation of a deep component of Argo is needed, based on the practical capabilities and

endurance of deep floats and CTDs as well as on the sampling requirements for decadal variability.

4.3 Near-equatorial velocity

Present direct velocity observations (surface drifters, Argo float trajectories, equatorial moored ADCP, TAO/TRITON cruise shipboard ADCP) do not resolve the near-equatorial meridional and zonal structure and temporal variability of the mixed-layer (ageostrophic + geostrophic) velocity. Equatorial upwelling – the horizontal divergence of the surface layer transport – is a critical process for the tropical Pacific Observing System. It is a dominant term of the cold tongue heat budget at ENSO timescales, and thus should be monitored. Conventional observational techniques have not proven adequate for this objective, except perhaps in estimating the long-term mean, for which consistent credible estimates have been provided using different techniques (Bryden and Brady, 1985; Johnson et al. 2001). Estimates of upwelling variability require dedicated process studies, such as mooring deployments at higher latitudinal resolution than the present TAO array (e.g., Weisberg and Qiao, 2000), in order to determine the requirements for sustained observations.

4.4 Mixed-layer variability in relation to air-sea fluxes

Near-surface observations are needed of the vertical structure of T, S, whose changes must balance the air-sea exchanges of heat and freshwater. Balances of air-sea flux and ocean storage are important on timescales as short as diurnal. On longer timescales the advection of heat and freshwater anomalies also becomes increasingly important in the budgets. Due to the large range of spatial and temporal scales involved, a combination of *in situ* observational systems may be required, potentially including moorings, Argo floats, and gliders in addition to high resolution satellite observations. For the observing system, at any location where fixed-point time series of air-sea fluxes of heat and freshwater are maintained, there should be subsurface T(z) and S(z) observations that resolve diurnal variability and that have vertical resolution in the surface layer sufficient for calculation of heat and freshwater storage. In addition, the observing system requires measurements of the velocity and of the horizontal gradients of T(z) and S(z), in order to evaluate the advective terms in the heat and freshwater balance.

4.5 Eastern boundary regions

Eastern boundary regions, including the far eastern equatorial band, the Peru-Chile upwelling systems, and the Costa Rica dome, are not adequately sampled by the current in situ networks (compare Figures 2.1, 2.4, 2.6). Moreover, they are regions of strong eddy activity and of small-scale processes that complicate their monitoring. Yet, they are regions of great societal and ecological importance. Understanding how equatorial signals (such as ENSO) are transmitted by way of equatorial and coastal Kelvin waves to the eastern boundary is fundamental in regard to their climatic impacts. Important physical phenomena remain poorly documented: among them vertical advection in the far east during ENSO events, the fate of the equatorial undercurrent and Tsuchiya jets and the Peru upwelling waters sources (Takahashi et al., 2014, TPOS WP8). The role of eddies in redistributing biological properties would also require

dedicated observations. Observational networks should be tested in the region to improve our understanding of these issues and help to define which regional sustained observing system would be needed.

5. Data and information systems

In the global broadscale *in situ* networks, data and information systems have developed around the individual networks, including TAO/TRITON (http://www.pmel.noaa.gov/tao/index.shtml), the Argo Programme (http:/www.argo.net), repeat hydrography (Go-Ship: http://www.go-ship.org/), the HR XBT programme (http://www-hrx.ucsd.edu), the Global Drifter Programme (GDP, http://www.aoml.noaa.gov/phod/dac), and the VOS SSS data (http://www.legos.obs-mip.fr/observations/sss/). The data management teams of these networks deserve credit for high data quality and ease in data delivery. A persistent issue is the chronic underfunding of the data management systems. Where there are identified issues of interoperability, effort has been expended to resolve these. For example, Delayed-Mode Quality Control of Argo profile data requires timely access (6-12 months) to the best quality shipboard hydrographic data. Progress on this issue is ongoing. Most of the broadscale networks have open data policies that ensure public availability of all data in near real-time (TAO/TRITON, Argo, GDP, VOS). Open data policies are a key element in the sustained observations programmes, allowing maximum utilization of the data in both research and operational reanalysis and forecasting applications.

There is a gap in the distribution and availability of SSS, SST, and ADCP data collected underway during scientific cruises. Most research vessels steaming in the TPO are fitted with TSG and SADCP instruments which, in principle, can collect SSS, SST and velocity data while in transit between port calls or hydrographic stations. These data, once compiled, can be usefully used to provide velocity or SSS climatologies (e.g. Johnson et al., 2002b; Dutrieux et al., 2009; Cravatte et al., 2011). The data acquisition and quality control procedures are however not systematic. There is clearly a need to centralize all underway SST and SSS data in a unique data portal, and international efforts should be made to collect, validate and archive all underway SSS and SST data derived from RVs. Similarly, SADCP data need a careful processing before being made publicly available (through the Joint Archive for Shipboard ADCP, http://ilikai.soest.hawaii.edu/sadcp/), and this data processing is currently unfunded.

In addition to the basic datasets, the data management systems also provide a range of data products, some of which have noteworthy utility. Widely disseminated data products in the tropical Pacific include Niño sea surface temperature indices, thermocline depth, and warm water volume. These products and indices have been developed to characterize the ENSO state of the tropical Pacific and for testing ideas about the genesis and evolution of ENSO episodes. Other noteworthy data products are the gridded global versions of Argo temperature and salinity data (http://www.argo.ucsd.edu/Gridded_fields.html), gridded SSS products from various datasets (http://www.legos.obs-mip.fr/observations/sss/) and the drifter velocity climatology (Lumpkin and Johnson, 2013; http://www.aoml.noaa.gov/phod/dac/dac_meanvel.php). These gridded datasets have greatly increased the accessibility of *in situ* data for research and education applications, and have amplified the number of research publications that utilize the data. Other useful delayed-time products are the global datasets of subsurface Argo velocities (YoMaHa05 from Yoshinari et al., 2006; and ANDRO from Ollitrault

and Rannou, 2013). The Argo Programme is in the process of upgrading trajectory and technical files, to make estimates of drift velocity more accurate and accessible to users, but manpower limitations in data management are a limiting factor.

The high-resolution datasets collected in the western boundary, ITF, and equatorial regions are, for the most part, readily available from the data providers. However, there is a need to fully document and co-ordinate the consistency of data quality control, since these data sets are generally maintained and made available by individual investigators. As the suite of high-resolution sustained observations is not fully defined, so the data systems are still under development. Argo's data management system has been a model emulated by other observational networks, and inclusive data management systems have been developed or are emerging for fixed point moored time-series data (Ocean Sites), repeat hydrography, and ocean gliders. In total, the data management systems provide access to the high-resolution datasets. However, if the primary utility of the high-resolution data is for regional observations including multiple data types, then consideration is needed for joint distribution of all datasets needed for a particular boundary current or other high-resolution phenomenon. In addition, data products that integrate the high-resolution datasets are needed.

6. Potential tradeoffs for a more efficient observing system

In Section 3 it was noted that *in situ* T,S,V observations can be augmented by related satellite datasets, including wind stress, sea surface height, sea surface temperature and sea surface salinity, and through constraints imposed by ocean dynamics in data assimilation modeling. Here we offer a cautionary note with regard to these powerful approaches. If the observing system now appears to have redundancies, in most cases these are complementary datasets that are essential for independent checking and assessment of system performance. An example was provided (Figure 2.11) to show the skill level in mapping intraseasonal variability along the equator from broadscale Argo data. Moored time-series data were essential to validate mapping accuracy, due to the level of uncertainty in formal error estimates. Equivalently one might use Argo data to assess the accuracy of spatial maps based on TAO/TRITON measurements. The Tropical Pacific Observing System has a long, well-documented history of combining fixed-point time series with broadscale variable-location observations, beginning with the XBT networks. The latter approach was improved by implementation of the Argo Programme, providing higher resolution than was possible with broadscale VOS XBT profiling, as well as much greater measurement accuracy and depth range, and the addition of salinity profiles and 1000 m trajectories. While Argo has increased the capabilities of the TPOS overall, it has not obviated the need for fixed-point time series measurements. In the future, the need for economies may diminish the use of large ships in support of the TPOS, but it should not upset the scientific balance of contrasting observational approaches. Greater efficiency is to be found not in reduced observations but in new technologies and improved cost effectiveness. Sustaining multi-decadal time series observations, and particularly in the equatorial region, should be a given for TPOS 2020.

References

Anonymous (2002): International Workshop for Review of the Global Tropical Moored Buoy Network. Workshop Report GCOS No. 77, GOOS No. 122, ICPO No., Seattle WA, June 2002.

Argo Science Team (1998): On the design and implementation of Argo - An initial plan for a global array of profiling floats. International CLIVAR Project Office Report 21, GODAE Report 5. GODAE International Project Office, Melbourne, Australia, 32 pp.

Brandt, P., Funk, A., Hormann, V., Dengler, M., Greatbatch, R.J., and Toole, J.M. (2011): Interannual atmospheric variability forced by the deep equatorial Atlantic Ocean, Nature, 473(7348), pp. 497-U237, (doi:10.1038/nature10013).

Bryden, H. L., and Brady, E.C. (1985): Diagnostic model of the three- dimensional circulation in the upper equatorial Pacific Ocean. J. Phys. Oceanogr., 15, pp. 1255–1273.

Cravatte, S., Ganachaud, A., Duong, Q., Kessler, W.S., Eldin, G., and Dutrieux, P. (2011): Observed circulation in the Solomon Sea from SADCP data, Prog. Oceanogr, 88(1–4), pp. 116–130.

Cravatte, S., Kessler, W., and Marin, F. (2012): Intermediate zonal jets in the tropical Pacific Ocean observed by Argo floats. Journal of Physical Oceanography, 42, pp. 1475–1485. (doi: 10.1175/JPO-D-11-0206.1).

Davis, R., Kessler, W., and Sherman, J. (2012): Gliders measure Western Boundary Current transport from the South Pacific to the Equator. Journal of physical Oceanography 42, 2001–2013. (doi: 10.1175/JPO-D-12-022.1).

Delcroix, T., McPhaden, M., Dessier, A., and Y. Gouriou, Y. (2005): Time and space scales for sea surface salinity in the tropical oceans. Deep Sea. Res. 52/5, pp. 787-813.

Delcroix, T., Alory, G., Cravatte, S., Correge, T., and McPhaden, M.J. (2011): A gridded sea surface salinity data set for the tropical Pacific with sample applications (1950-2008). Deep-Sea Research Part I-Oceanographic Research Papers, 58, pp. 38-48.

Dohan, K., and Co-Authors (2010): "Measuring the Global Ocean Surface Circulation with Satellite and In Situ Observations" in *Proceedings of OceanObs'09: Sustained Ocean Observations and Information for Society (Vol. 2),* Venice, Italy, 21-25 September 2009, Hall, J., Harrison, D.E. & Stammer, D., Eds., ESA Publication WPP-306, doi:10.5270/OceanObs09.cWP.23

Ducet, N., Le Traon, P.Y., and Reverdin, G. (2000): Global high resolution mapping of ocean circulation from TOPEX/Poseidon and ERS-1 and -2. Journal of Geophysical Research 105 (C8), pp. 19477–19498.

Dutrieux, P. (2009): Tropical Western Pacific Currents and the Origin of Intraseasonal Variability Below the Thermocline, PhD in Oceanography, University of Hawaii, Honolulu, Hawaii, USA.

Eldin, G., Ganachaud, A., Cravatte, S., and Jeandel, C. (2013): Pandora cruise provides an unprecedented description of the solomon sea, CLIVAR Newsletter Exchanges, 61 (18), pp. 24–25.

Firing, E., Wijffels, S.E., and Hacker, P. (1998): Equatorial subthermocline currents across the Pacific, Journal of Geophysical Research-Oceans, 103(C10), 21413-21423, (doi:10.1029/98jc01944).

Ganachaud et al. (2013): Ocean circulation of the Southwest Pacific: new insights from the Southwest Pacific Ocean and Climate Experiment (SPICE), submitted to JGR.

Ganachaud, A., and Co-Authors (2008): Southwest Pacific Ocean Circulation and Climate Experiment (SPICE)—Part II. Implementation Plan. International CLIVAR Project Office, CLIVAR Publication Series No. 133, NOAA OAR Special Report, NOAA/OAR/PMEL, Seattle,WA, 36 pp.

Goni, G., and Co-Authors (2010): "The Ship of Opportunity Programme" in Proceedings of OceanObs'09: Sustained Ocean Observations and Information for Society (Vol. 2), Venice, Italy, 21-25 September 2009, Hall, J., Harrison, D.E. & Stammer, D., Eds., ESA Publication WPP-306, (doi:10.5270/OceanObs09. cWP.35).

Gordon, A.L., Sprintall, J., Van Aken, H.M., Susanto, D., Wijffels, S., Molcard, R., Ffield, A., Pranowo, W., and Wirasantosa, S. (2010): The Indonesian Throughflow during 2004-2006 as observed by the INSTANT programme, Dynamics of Atmosphere and Oceans, 50, pp. 115-128.

Gordon, A., and Co-Authors (2010): "Interocean Exchange of Thermocline Water: Indonesian Throughflow; "Tassie" Leakage; Agulhas Leakage" in Proceedings of OceanObs'09: Sustained Ocean Observations and Information for Society (Vol. 2), Venice, Italy, 21-25 September 2009, Hall, J., Harrison, D.E. & Stammer, D., Eds., ESA Publication WPP-306, (doi:10.5270/OceanObs09.cWP.37).

Guinehut, S., A. L. Dhomps, G. Larnicol, and P. Y. Le Traon, 2012: High resolution 3-D temperature and salinity fields derived from in situ and satellite observations, Ocean Sci., 8(5), 845-857, http://www.ocean-sci.net/8/845/2012/

Hackert, E., Ballabrera-Poy, J., Busalacchi, A.J., Zhang, R.H., and Murtugudde, R. (2011): Impact of sea surface salinity assimilation on coupled forecasts in the tropical Pacific, J. Geophys. Res., 116, C05009, (doi:10.1029/2010JC006708).

Hayes, S.P., Mangum, L.J., Picaut, J., Sumi, A., and Takeuchi, K. (1991): TOGA TAO: A moored array for real-time measurements in the tropical Pacific Ocean. Bulletin of the American *Meteorological Society*, 72, pp. 339-347.

Hu, D., Wu, L., Wang, F., Yuan, D., Chen, D., Tian, J., Chen, Z., and Hu, S. (2014): On the Northwestern Pacific Ocean Circulation and Climate. White Paper, TPOS 2020 Workshop, La Jolla California, January 2014.

Johnson, E. S., and Plimpton, P.E. (1999): TOGA/TAO shipboard ADCP data report, 1991–1995. NOAA Data Report ERL PMEL-67, NTIS: PB2002-101766, NOAA/Pacific Marine Environmental Laboratory, 23 pp.

Johnson, G. C., Kunze, E., McTaggart, K.E., and Moore, D.W. (2002a): Temporal and spatial structure of the equatorial deep jets in the Pacific Ocean, Journal of Physical Oceanography, 32(12), pp. 3396-3407, (doi:10.1175/1520-0485(2002)032<3396:tassot>2.0.co;2).

Johnson, G. C., McPhaden, M.J., and Firing, E. (2001): Equatorial Pacific ocean horizontal velocity, divergence, and upwelling, Journal of Physical Oceanography, 31(3), pp. 839-849, (doi:10.1175/1520-0485(2001)031<0839:epohvd>2.0.co;2).

Johnson, G. C., McPhaden, M.J., Rowe, G.D., and McTaggart, K.E. (2000): Upper equatorial Pacific Ocean current and salinity variability during the 1996-1998 El Niño-La Niña cycle, Journal of Geophysical Research-Oceans, 105(C1), pp. 1037-1053, (doi:10.1029/1999jc900280).

Johnson, G. C., Sloyan, B.M., Kessler, W.S., and McTaggart, K.E. (2002b): Direct measurements of upper ocean currents and water properties across the tropical Pacific during the 1990s, Progress in Oceanography, 52(1), pp. 31-61, (doi:10.1016/s0079-6611(02)00021-6).

Johnson, G. C., and Zhang, D.X. (2003): Structure of the Atlantic Ocean equatorial deep jets, Journal of Physical Oceanography, 33(3), pp. 600-609, (doi:10.1175/1520-0485(2003)033<0600:sotaoe>2.0.co;2).

Kessler, W. S., and J. P. McCreary (1993), The annual wind-driven Rossby-wave in the subthermocline equatorial Pacific, Journal of Physical Oceanography, 23(6), pp. 1192-1207, (doi:10.1175/1520-0485(1993)023<1192:tawdrw>2.0.co;2).

Kessler, W., Spillane, M., McPhaden, M., and Harrison, D.E. (1996): Scales of variability in the equatorial Pacific inferred from the Tropical Atmosphere-Ocean buoy array. Journal of Climate, 9, pp. 2999 – 3024.

Kouketsu, S., et al. (2011): Deep ocean heat content changes estimated from observation and reanalysis product and their influence on sea level change, Journal of Geophysical Research-Oceans, 116, 16, (doi:C0301210.1029/2010jc006464).

Lagerloef, G., and Co-Authors (2010): "Resolving the Global Surface Salinity Field and Variations by Blending Satellite and In Situ Observations" in Proceedings of OceanObs'09: Sustained Ocean Observations and Information for Society (Vol. 2), Venice, Italy, 21-25 September 2009, Hall, J., Harrison, D.E. & Stammer, D., Eds., ESA Publication WPP-306, (doi:10.5270/OceanObs09.cWP.51).

Levitus, S., and Co-Authors (2012): World ocean heat content and thermosteric sea level change (0–2000 m), 1955–2010, *Geophysical Research Letters,* 39, L10603, (doi:10.1029/2012GL051106).

Lukas, R., and Lindstrom, E. (1991): The mixed layer of the western equatorial Pacific ocean, Journal of Geophysical Research-Oceans, 96, pp. 3343-3357.

Lumpkin, R., and Pazos, M., (2007): Measuring surface currents with Surface Velocity Programme drifters: the instrument, its data, and some recent results. Chapter 2 of "Lagrangian Analysis and Prediction of Coastal and Ocean Dynamics", ed. A. Griffa, A. D. Kirwan, A. Mariano, T. Ozgokmen and T. Rossby, Cambridge University Press.

Lumpkin, R., and Johnson, G. (2013): Global Ocean Surface Velocities from Drifters: Mean, Variance, ENSO Response, and Seasonal Cycle. *J.* Geophys. Res.-Oceans, 118(6), pp. 2992-3006.

Maximenko, N. A., Melnichenko, O.V., Niiler, P.P., and Sasaki, H. (2008): Stationary mesoscale jet-like features in the ocean, *Geophysical Research Letters*, 35, L08603, (doi:10.1029/2008GL033267).

McPhaden, M. J., et al. (1998), The tropical ocean global atmosphere observing system: A decade of progress, Journal of Geophysical Research-Oceans, 103(C7), 14169-14240, (doi:10.1029/97jc02906).

Meyers, G., Phillips, H., Smith, N., and Sprintall, J. (1991): Space and time scales for optimal interpolation of temperature – Tropical Pacific Ocean. Progress in Oceanography, 28, pp. 189 – 218.

Ollitrault, M., and Rannou, J.R. (2013): ANDRO: An Argo-Based Deep Displacement Dataset. Journal Of Atmospheric And Oceanic Technology, 30(4), pp. 759-788. (doi:10.1175/JTECH-D-12-00073.1).

Owens, W. B., and Wong, A.P.S. (2009): An improved calibration method for the drift of the conductivity sensor on autonomous CTD profiling floats by theta-S climatology, Deep-Sea Research Part I-Oceanographic Research Papers, 56(3), pp. 450-457, (doi:10.1016/j.dsr.2008.09.008).

Perez, R. C., Cronin, M.F., and Kessler, W.S. (2010): Tropical Cells and a Secondary Circulation near the Northern Front of the Equatorial Pacific Cold Tongue, Journal of Physical Oceanography, 40(9), pp. 2091-2106, (doi:10.1175/2010jpo4366.1).

Purkey, S. G., and Johnson, G. C. (2010): Warming of global abyssal and deep Southern Ocean waters between the 1990s and 2000s: Contributions to global heat and sea level rise budgets. Journal of Climate 23, pp. 6336-6351.

Rio, M. H., Guinehut, S., and Larnicol, G. (2011): New CNES-CLS09 global mean dynamic topography computed from the combination of GRACE data, altimetry, and in situ measurements, J. Geophys. Res., 116, C07018, (doi:10.1029/2010JC006505).

Roemmich, D., and Co-Authors (2010): "Integrating the Ocean Observing System: Mobile Platforms" in Proceedings of OceanObs'09: Sustained Ocean Observations and Information for Society (Vol. 1), Venice, Italy, 21-25 September 2009, Hall, J., Harrison, D.E. & Stammer, D., Eds., ESA Publication WPP-

306, (doi:10.5270/OceanObs09.pp.33).

Roemmich, D., and Gilson, J. (2009): The 2004–2008 mean and annual cycle of temperature, salinity, and steric height in the global ocean from the Argo Programme. Progress in Oceanography, (doi:10.1016/j.pocean.2009.03.004).

Rowe, G. D., Firing, E., and Johnson, G.C. (2000): Pacific equatorial subsurface countercurrent velocity, transport, and potential vorticity, Journal of Physical Oceanography, 30(6), pp. 1172-1187, (doi:10.1175/1520-0485(2000)030<1172:pescvt>2.0.co;2).

Sabine, C. L., et al. (2004): The oceanic sink for anthropogenic CO2, Science, 305(5682), pp. 367-371, doi:10.1126/science.1097403.

Smith, N., and Co-Authors (2001): The upper ocean thermal network. From: Observing the Oceans in the 21st Century, C. Koblinsky and N. Smith, Eds, Bureau of Meteorology, Melbourne, pp 259-284.

Sprintall, J., Wijffels, S.E., Molcard, R., and Jaya, I. (2009): Direct estimates of the Indonesian Throughflow entering the Indian Ocean, Journal of Geophysical Research 114, C07001, (doi: 10.1029/2008JC005257).

Taguchi, B., Furue, R., Komori, N., Kuwano-Yoshida, A., Nonaka, M., Sasaki, H., and Ohfuchi, W. (2012): Deep oceanic zonal jets constrained by fine-scale wind stress curls in the South Pacific Ocean: A high-resolution coupled GCM study, Geophys. Res. Lett., 39, L08602, (doi:10.1029/2012GL051248).

Tanhua, T., Waugh, D.W., and Bullister, J.L. (2013): Estimating changes in ocean ventilation from early 1990s CFC-12 and late 2000s SF6 measurements, Geophysical Research Letters, 40(5), pp. 927-932, (doi:10.1002/grl.50251).

Weisberg, R. H., and Qiao, L. (2000): Equatorial upwelling in the central Pacific estimated from moored velocity profilers. J. Phys. Oceanogr., 30, pp. 105–124.

Wijffels, S. E., Willis, J., Domingues, C.M., Barker, P., White, N.J., Gronell, A., Ridgway, K., and Church, J.A. (2008): Changing expendable bathythermograph fall rates and their impact on estimates of thermosteric sea level rise, Journal of Climate, 21, pp. 5657– 5672.

Wijffels, S.E., Meyers, G., and Godfrey, J.S. (2008): A 20-yr average of the Indonesian Throughflow: Regional Currents and the interbasin exchange, Journal of Physical Oceanography, 38, pp. 1965-1978.

Willis, J.K., Roemmich, D., and Cornuelle, B. (2003): Combining altimetric height with broadscale profile data to estimate steric height, heat storage, subsurface temperature and sea-surface temperature variability, J. Geophys. Res., 108,(C9) 3292, (doi:10.1029/2002JC001755).

Willis, J. K., and Fu, L.L. (2008): Combining altimeter and subsurface float data to estimate the time-averaged circulation in the upper ocean, J. Geophys. Res., 113, C12017, (doi:10.1029/2007JC004690).

Wong, A. P. S., Johnson, G.C., and Owens, W.B. (2003): Delayed-mode calibration of autonomous CTD profiling float salinity data by theta-S climatology, J. Atmos. Oceanic Technol,, 20, pp. 308–318, (doi:10.1175/1520-0426(2003)020<0308:DMCOAC>2.0.CO;2).

Yoshinari, H., Maximenko, N.A., and Hacker, P.W. (2006): YoMaHa'05—Velocity data assessed from trajectories of Argo floats at parking level and at the sea surface. IPRC Tech. Note 4, 16 pp.

Zilberman, N., Roemmich, D., and Gille, S. (2013): The mean and the time variability of the shallow Meridional Overturning Circulation in the tropical South Pacific Ocean. Journal of Climate, 26, pp. 4069 – 4087.

White Paper #11 – Wind stress and air sea fluxes observations: status, implementation and gaps

Cronin, M.F.[1], Bourassa, M.[2], Clayson, C.A.[3], Edson, J.[4], Fairall, C.[5], Feely, D.[1], Harrison, D.E.[1], Josey, S.[6], Kubota, M.[7], Kumar, B.P.[8], Kutsuwada, K.[7], Large, B.[9], Mathis, J.[1], McPhaden, M. [1], O'Neill, L.[10], Pinker, R. [11], Takahashi, K. [12], Tomita, H. [13], Mathis, J.[8], Weller, R.A.[3], Yu, L. [3], and Zhang, C.[2]

[1] NOAA Pacific Marine Environmental Laboratory, United States
[2] University of Miami, United States
[3] Woods Hole Oceanographic Institute, United States
[4] University of Connecticut, United States
[5] Michigan State University, United States
[6] National Environment Research Council, United Kingdom
[7] Tokai University, Japan
[8] Indian National Center for Ocean Information Services, India
[9] National Center for Atmospheric Research, United States
[10] Oregon State University, United States
[11] University of Maryland, United States
[12] Instituto Geofisico del Peru, Peru
[13] Japan Agency for Marine and Earth Science Technology, Japan

1. Introduction

1.1 Coupling between the Ocean and the Atmosphere in the Tropical Pacific

Coupling between the ocean and the atmosphere in the Tropical Pacific takes place on a broad range of timescales, in different dynamical regimes, and through different mechanisms. On the basin scale, according to the "Bjerknes Feedback", easterly Trade winds, blowing along the equator, result in a thermocline that is deep in the west and shallow in the east. Poleward Ekman divergence and upwelling, associated with the easterly winds, acting on the sloped thermocline then causes the sea surface temperature (SST) to be cooler in the east than in the west. The resulting zonal gradient in surface pressure, in equilibrium with the SST gradient, strengthens the zonal winds, which through upwelling, feedback to the SST zonal gradient, maintaining the "normal" or La Niña conditions. During El Niño, the feedback leads to weaker Trade winds, shallower thermocline in the west, and reduced SST zonal gradient. While the basic coupling mechanism is simple, the mechanisms that lead to the shifts in the feedback are not. Questions remain regarding interactions between the wind-forced thermocline variability and ocean mixed layer, and the effect of the resultant SST variations on the overlying atmosphere. The simplicity of these concepts also belies the range of El Niño Southern Oscillation (ENSO) events that have been observed in recent decades. For example, while the canonical El Niño has largest anomalous warming in the eastern equatorial Pacific, recent events referred to as "Midoki El Niño" have had anomalous warming in the central equatorial Pacific (Ashok et al., 2007; Takahashi et al., 2011). ENSO events have been more frequent in recent years and there is some evidence that extreme El Niño events may become more frequent in a warming world (Cai et al., 2014).

Atmospheric circulation in the tropics and teleconnections between the tropics and extratropics depend fundamentally upon the distribution of atmospheric deep convection (Gill, 1980; Wallace and Gutzler, 1981; Trenberth et al., 1998). It is thus important to understand how convection is organized and how it both affects and is affected by the underlying SST. Due to the nonlinear dependence of saturated specific humidity on temperature (i.e., the Clausius-Clapeyron effect), latent heat loss is amplified over warm water and enhanced latent heating can help destabilize the atmosphere and drive deep convection. Maximum SST creates a low surface pressure center and drives wind convergence. Deep convection thus tends to form over warm water, such as in the western Pacific warm pool, along the thermal equator in the Northern Hemisphere Intertropical Convergence Zone (ITCZ), and in the South Pacific Convergence Zone (SPCZ). Meanwhile, cloudiness associated with convection shades the ocean from solar radiation and convective gustiness enhances the latent and sensible heat fluxes, both of which lead to surface cooling. The intermittency of atmospheric convection helps maintain the warm sea surface in these mean convective regions.

On shorter (meso- to synoptic) timescales, fluctuations in surface wind stress, temperature, and humidity associated with atmospheric deep convective systems induces strong perturbations in air-sea fluxes, which, together with SST, determine how fast the atmospheric boundary layer would recover from being stabilized by convective cold pools and be ready for the next convective event. Erroneous representation of this recovery time in weather and climate models would inevitably introduce biases in their reproduction of precipitation and clouds over the western Pacific warm pool. The diurnal cycle in equatorial surface winds (e.g., Deser and Smith, 1998; Ueyama and Deser, 2008) appears to be driven by direct solar heating of the atmospheric water vapor and to be part of a deep tropospheric overturning cell (Takahashi, 2012), although the connection to the diurnal cycle in deep convection is unclear (Gray and Jacobson, 1977; Randall et al., 1991; Takahashi, 2012). Furthermore, a semi-diurnal cycle can also play a large role in the variability of cloud cover and precipitation. Simulations and forecast of the Madden-Julian Oscillation (MJO) can be improved when SST feedback to the atmosphere is correctly reproduced in models (Seo et al., 2009). The oceanic diurnal cycle plays a special role in air-sea interaction of the warm pool. In regions with low winds such as the western Pacific warm pool, daytime solar warming can lead stratification within the upper 5 meters of the water column (i.e., a “diurnal mixed layer”), so that the SST at 1 m can be significantly cooler than that at the air-sea interface. A shallow diurnal mixed layer can also trap wind-generated momentum, causing large vertical shears in the horizontal velocity. In the early evening, as the stratification weakens, shear instability can then form, causing enhanced turbulent mixing within the upper ocean. There are mixing parameterizations that account for this additional source of turbulence in global Ocean General Circulation Models (OGCMs) (Danabasoglu et al., 2006), but at best, verification has been sparse and indirect.

In the central equatorial Pacific, east of the warm pool boundary, atmospheric convection is normally absent except during the warm phase of the El Niño Southern Oscillation (ENSO) cycle and eastward penetration of extraordinarily strong MJO events. While equatorial zonal wind stress near the equator, through its effects on upwelling and mixing and on latent and sensible heat loss, plays an essential role in both interannual and intraseasonal variations, surface radiation has been shown to be another necessary ingredient in determining SST in the

ENSO cycle. The feedback of SST to the atmosphere is critical in this region to determine the fate of an ENSO or MJO event. Sharp meridional SST gradient exist in the central and eastern equatorial Pacific, between the “equatorial cold tongue” and the warm water beneath the ITCZ, the “thermal equator”, which extends across the entire northern tropical Pacific. In contrast, the SPCZ is found mainly in the western tropical Pacific. Coupled models often have an equatorial cold tongue that is too cold and a spurious double ITCZ. Both convergence zones are marked by active synoptic-scale atmospheric perturbations. SST modulation on the SPCZ is a crucial factor in models’ ability to reproduce realistic SPCZ or create spurious double ITCZ there.

In the eastern Pacific, atmospheric deep convection is normally confined to the ITCZ north of the equator, except during the peak phase of an ENSO warm event. In the SST front, between the equatorial cold tongue and the warm water of the thermal equator, tropical instability waves (TIW) thrive. The air-sea coupling associated with TIW take place through both modulation of the atmospheric boundary-layer (ABL) stability and barometric pressure gradients induced by the SST front (Chelton et al., 2001; Cronin et al. 2003): the barometric pressure effect results in stronger winds at the SST front; the destabilization of the ABL leads to vigorous vertical mixing that brings larger winds from aloft to the surface on the warm side of the front. This acceleration of the surface wind across the equatorial cold tongue SST front and convergence over the warm “thermal equator” is pivotal in determining the location of the ITCZ and double ITCZ (in boreal spring). Available evidence, however, is conflicting on whether the ascent in the ITCZ in the eastern Pacific is shallow (Zhang et al., 2004; Back and Bretherton, 2006) or deep (Schumacher et al., 2004). The ascending motion in the ITCZ helps form the upward branch of the Hadley cell in boreal summer, with its associated descending branches over the subtropical North and South Pacific. These descending motions are the essential ingredients for marine stratus clouds over the northeastern and southeastern Pacific, which are key components in the Earth’s radiation budget but poorly simulated in climate models. How these marine stratus clouds may vary in and feedback to a changing climate is a major uncertainty in ENSO simulations and climate projections. The air-sea coupling processes that determine the position, structure, and strength of the ITCZ must be better understood in order to improve coupled model representations of atmospheric ENSO feedbacks (e.g. Lloyd et al., 2009) and cloud feedback on seasonal-to-interannual and climate change time-scales (Lengaigne and Vecchi, 2010; Cai et al., 2014).

The large-scale mean and interannual convection patterns comprise systems of a variety of scales including mesoscale, diurnal, synoptic, intraseasonal and seasonal. How these different scales interact, and likewise how these coupled feedbacks and multiscale coupled processes will change in a warming world remain open questions. While the Tropical Pacific Observing System (TPOS) will not capture all of these processes in their full resolution, it must capture aspects of the multiscale coupled interactions that are critical to the evolving ENSO system.

As described in this white paper, information on surface fluxes and on parameters used in the surface flux computations within the atmospheric and oceanic boundary layers are needed to initialize, force, and nudge numerical models; to assess uncertainties in these numerical models and in satellite observations; and to better understand the coupled system and improve numerical model representations of this system. As such, it is critical that the observing array have coverage not only in regions where the coupled processes are most active for ENSO (i.e.

in the western Pacific and along the equator), but also in regions where biases and large uncertainties exist in satellite data and numerical model output (e.g. along the ITCZ and SPCZ latitudes).

1.2 Estimating fluxes of heat, moisture, momentum, and CO_2

The 2020 Tropical Pacific observing array will be integrated, with observing platforms that measure numerous variables. As described in this section, estimation of any turbulent air-sea flux, whether it be heat, moisture, momentum or gas, requires a common set of variables, including SST, wind, air temperature and humidity. It is therefore important to consider the larger goals and requirements for all air-sea flux observations. Locations of moored buoys, including those with net surface heat flux measuring capabilities, are shown in Figure 1.1.

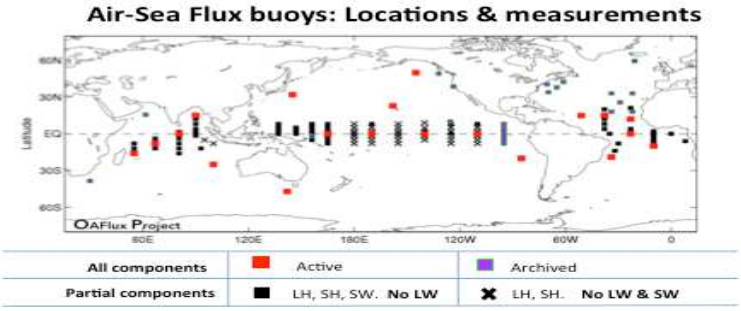

Figure 1.1 – Global distribution of flux and flux parameters.

Calculation of air-sea heat, moisture, momentum and gas exchanges are discussed at length elsewhere (e.g., McGillis et al., 2001; Fairall et al., 2003) and therefore will only be briefly discussed here. In particular, direct estimates of turbulent fluxes (e.g. wind stress, evaporation, latent and sensible heat, and CO_2 fluxes) require high frequency samples of the 3-component wind plus the appropriate scalar parameter, from which the covariance (turbulent flux) can be computed after removal, when necessary, of platform motion (e.g., Ancil et al., 1994; Edson et al., 1998). These measurements must be made within the surface layer directly above the air-sea interface, preferably above the wave-influenced flow but still within the layer where the turbulent fluxes are vertically uniform. By law of the wall arguments, the wind and parameter profiles vary logarithmically with height within this “constant flux layer”. Typically this layer extends from roughly 2 m to 50 m above the interface, with the variability largely a function of wind speed and stratification. Modern bulk algorithms, based upon this physics, estimate turbulent fluxes from two observations of state variables (at least wind, temperature and humidity) from different heights near the surface and within the “constant flux” portion of the atmospheric profile.

These measurements however are not sufficient to directly estimate the fluxes. Several aspects of the profiles must be parameterized and therefore introduce errors in the fluxes. In particular, the atmospheric stability can affect the shape of the profiles and must be parameterized based upon the measured quantities (primarily air-sea temperature difference). The atmospheric

stability can also affect the gustiness. The COARE bulk algorithm (Fairall et al., 1996a, 2003, 2011, Edson et al., 2013) computes a gustiness parameter assuming that the wind measurements are hourly vector averages. Cronin et al. (2006b) show that if the vector wind speed is based upon daily averages, such as is the case when using telemetered TAO data from the legacy ATLAS systems, the mean error associated with the scalar wind speed can increase to more than 1.5 m/s, causing an 8 W/m^2 bias in the latent heat flux in the ITCZ regions. Likewise, the roughness layer is generally parameterized in terms of wind speed, although some newer parameterizations also take into consideration surface wave characteristic (e.g. significant wave height and/or dominant wave period). The influence of other wave characteristics, such as steepness, age, breaking, white-capping, direction of propagation relative to the wind and the presence or absence of swell, is much less understood. Other complicating factors for flux calculations include rainfall, surfactants, and the relationship of the interface "skin" temperature to the measured bulk sea surface temperature. Measurements of these parameters under a full range of weather conditions are required to understand these effects on surface fluxes and for improving the flux parameterizations. Given this parameterization complexity, the TPOS should include flux observations from both bulk observations and direct measurements via turbulent covariance packages mounted on surface moorings (e.g., Ancil et al., 1994; Weller et al., 2012; Bigorre et al., 2013) and on research vessels maintaining the TPOS.

Table 1.1 - Observations required for evaluation of air-sea fluxes of momentum (TAU), heat (Q0), and moisture (Evaporation minus Precipitation); accuracy and standard deviation of a daily averaged measurement; and contribution of this error to the error in the air-sea fluxes. The signal-to-noise factor is the accuracy divided by the standard deviation and can be used to determine the sensitivity of the flux measurement to the flux parameter. The total measurement errors assume that these errors are independent and do not include errors associated with the bulk algorithm. Variables listed in bold font are flux variables; others are flux parameters.

		For daily averages			Contribution to		
	Flux	er	Std	Std/er	er(TAU)	er(Q0)	er(E-P)
Variable					Nt/m^2	W/m^2	mm/day
wind speed (m/s)	all	0.1	1.75	17.5	0.0027	2.1	0.053
SST (C)	all	0.1	1.45	14.5	0.0002	4.4	0.081
air temp. (C)	all	0.1	1.30	13.0	0.0002	3.6	0.075
rel. hum. (percent)	all	2.7	4.83	1.8	0.0002	11.9	0.32
SWR (W/m^2)	Q0	6	42.00	7.0	0	5.6	0
LWR (W/m^2)	Q0	4	13.75	3.4	0	3	0
sfc currents	all	0.05	0.25	5.0	0.0008	0.65	0.017

(m/s)							
BP (hPa)	FCO2	0.2	1.48	7.4	0	0	0
Rain (mm/day)	E-P	0.72	5.34	7.4	0	0	0.7
Total of meas. errors					0.0027	14.3	0.81
Meas. error for covariance fluxes					0.0008	8.2	0.7
Total meas. and sampling error for cov. fluxes					0.0021	9.2	0.7
					TAU	Q0	E, P, E-P
Mean (across equator)					0.039	125.6	2.0,1.9,0.12

Table 1.1 summarizes the accuracy of state variables measured from the Tropical Pacific mooring array as of 2005 (Colbo and Weller, 2009; Freitag et al., 1994), their signal-to-noise ratio, and their contribution to errors in the fluxes. These flux errors assume mean values averaged across the full equatorial Pacific. It should be noted that because of non-linearities (e.g., Clasius-Clapeyron), sensitivities to errors may be larger in the western Pacific than in the eastern Pacific. The standard suite of moored surface measurements (i.e., wind speed and direction, air temperature, relative humidity, and SST) are the most important state variables, being required for estimating all turbulent air-sea fluxes. In contrast, air-sea fluxes are relatively insensitive to barometric pressure variability and can be represented by its mean value. Likewise, because net longwave radiation has relatively small temporal variability in the tropics (Pinker et al., 2013), it is often parameterized in terms of other state variables (Fung et al., 1984; Gupta et al., 1992; Wang et al., 2000). These parameterizations however have an RMS error of ~12 W/m^2 (Cronin et al., 2006b) and thus will increase the error in the net surface heat flux above the target 10 W/m^2. It should also be noted that these variables can serve other purposes beside their role as state variables in flux calculations: Because of the geostrophic relationship between winds and pressure, barometric pressure, when assimilated into atmospheric models, can help produce more accurate representation of synoptic weather fields. Downwelling longwave radiation, in comparison to solar radiation and their clearsky values can provide important information about cloud properties. Directly measured downwelling longwave radiation are also important to evaluate various indirect techniques of estimating downwelling longwave radiation considering that none of those techniques have emerged as appropriate for different climate condition.

As shown in Table 1.1, due to the poor relative humidity sensor accuracy (Freitag et al., 1994), the 2005 TAO suite of sensors does not meet the target benchmark accuracy of ±10 W/m^2 for net surface heat flux when averaged over a day. With a more accurate humidity sensor this target could be met. New sensors are being evaluated for Ocean Climate Station moorings and PMEL RAMA and PIRATA moorings. Likewise, SST (i.e., skin temperature) error contributes substantially to the net surface heat flux errors. Much of this error is associated with the diurnal warm layer and cool skin that cause the bulk SST at 1 m to differ from the skin temperature (Clayson and Bogdanoff, 2013). Present corrections are based upon simple wind speed and/or 1-dimensional models that require full radiation and state variable estimates. With improvements in these models, the SST error might be reduced by as much as an order of magnitude. Rainfall is extremely hard to measure at sea, and its sampling errors are very large on 1-day time scales. The largest systematic error associated with this measurement is low catchment due to wind blowing the rain over the sensor rather than allowing precipitation to fall into the catchment. This however can be corrected to a certain extent (Serra et al., 2001), if wind measurements are collocated with the rain measurement, as is assumed in Table 1.1. With turbulent fluxes measured directly by high-frequency covariance methods, the target flux errors could be met. It should be noted that errors due to the bulk algorithm will contribute ±3.5 W/m^2 for a daily averaged Q_0 measurement and about 0.6 mole/m^2/yr to the CO_2 flux. These are not included in the Table 1.1.

1.3 Observing boundary layer processes

Air-sea fluxes influence the atmosphere and ocean most directly within the mixed layers immediately above and below the air-sea interface. The atmospheric boundary layer (ABL), in turn, is strongly connected to the troposphere through mixing and transport across the inversion layer. At present, routine *in situ* observations of the vertical structure of wind, temperature and humidity are made only on a few island stations, and infrequently from research vessels and research aircraft. From 1995-2002, upper-air soundings were launched from the vessel maintaining the 110W and 95W TAO lines in the eastern tropical Pacific. These data provide important information about the seasonal-interannual variations in the atmosphere (Zhang et al., 2004). These measurements, however, are too infrequent to effectively benefit operational weather forecast models. Island-based measurements using radar or radiometric atmospheric profilers (e.g. Ware et al., 2003), combined with planetary boundary layer soundings using tethered balloons (which could include turbulence measurements, i.e. Balsley et al., 2006) and surface meteorological stations would be an efficient way of providing continuous monitoring that would resolve the diurnal cycle of the lower atmosphere. The viability of using islands (Figure 1.2) as measurement stations was proven by the multiyear TOGA enhanced atmospheric network in the equatorial Pacific (McPhaden et al., 1998). Additionally, with engineering, repackaging, and testing, buoy technology may exist in 2020 that resolves ABL wind profiles and their variations down to the diurnal cycle. These measurements could be extremely useful for initializing operational models, validating climate models, calibrating satellites, observing flux parameters above the surface wave regime, and for studying boundary layer processes, particularly in areas of thin boundary layers or strong advection. Observing profiles above the roughness layer is of practical importance for small platforms that do not have a tower. Their measurements may be shielded by waves and not capture the open-ocean

surface meteorological conditions. It is recommended that atmospheric and oceanic boundary layer observations should routinely be made during the tropical Pacific mooring maintenance cruises. Furthermore, continuous atmospheric boundary layer profile and surface observations should be made at island and/or buoy sites.

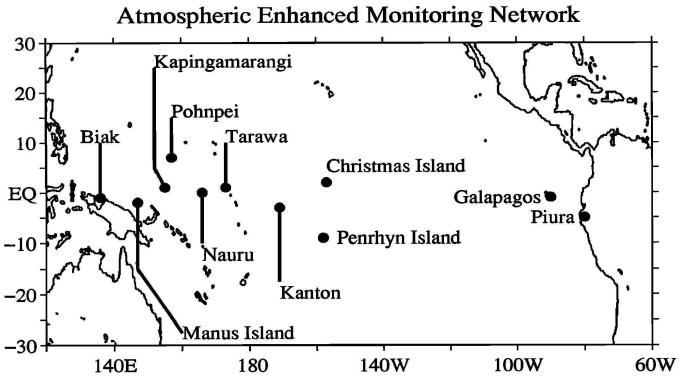

Figure 1.2 – Locations of wind profiler and radiosounding stations during TOGA (from McPhaden et al., 1998).

Within the ocean, temperature and salinity profiles have been measured by sensors attached to the surface mooring lines and by Argo floats. As discussed in the previous section, within the top 2 m, on days with light wind, a diurnal “warm layer” can form that can cause the “bulk” SST to differ substantially from the “skin” temperature felt by the atmosphere. High-resolution (e.g. 10 cm in vertical) Argo floats provide one of the few ways to directly measuring this layer. At nighttime, the homogenous “mixed layer” typically extends to ~20 m. It should be noted that while TRITON moorings and the equatorial TAO moorings resolve the mixed layer, many of the off-equatorial TAO moorings measure subsurface at intervals of 20 m and thus do not resolve the 0-25 m diurnal mixed layer. By their nature Argo floats are not at fixed location and are not co-located with air-sea flux measurements or state variables. Surface moorings in contrast, provide the surface and subsurface measurements at a fixed location with time resolution of order minutes. As discussed in the next section, depending upon the purpose of the measurement, these sampling capabilities can be important. Clearly though, at sites that measure fluxes, the mixed layer depth should be measured with similar temporal resolution. Because the diurnal warm layer depends fundamentally upon the absorption of solar warming within the water, which itself depends upon the biota in the water, the phytoplankton distribution can affect SST variability (Siegel et al., 1995, Murtugudde et al., 2002) and even impact ENSO (Jochum et al., 2010) and the large-scale climate system (Patara et al., 2012). Photosynthetically Active Radiation (PAR) and subsurface optical absorption should thus be measured at one or more biogeochemical flux stations in a region of light wind where there may be feedbacks between the diurnal warm layer and phytoplankton blooms. Pending technology development, observations of the direct and diffuse radiation components at this station would provide invaluable information for the extinction profile in water, for ocean heat budgets, and for cloud studies. Upward looking acoustic Doppler Current Profilers (ADCP) likewise are unable to observe currents above ~30m and thus miss current variability associated with the diurnal mixed layer. To observe currents within the mixed layer, generally current meters must be attached to the mooring line of a surface mooring. New autonomous buoy technology (e.g. wave

gliders) are being developed that may provide platforms for downward looking ADCP that could monitor the near-surface layer of direct wind forcing.

2. Air-sea flux observation requirements for satellite products and numerical models

2.1 Initializing, forcing, and nudging models

There are different modeling requirements for Tropical Pacific observations of air-sea fluxes (ASF) and flux parameters (FP). The major ASF dependencies are *flux type*: Upper Atmosphere, UA, (solar, down-welling longwave and precipitation), Turbulent (wind stress, sensible and latent heat, evaporation) and Ocean (upwelling longwave); *model configuration*: AGCM, OGCM and CGCM; and *simulation mode*: Prognostic; Predictive. For each combination, Table 1.2 indicates the primary purpose of the observations: Verification (V), Forcing (F) or Initialization (I). Model configurations are indicated by common examples; Prognostic AMIP (Atmosphere Model Intercomparison Project), CORE (Coordinated Ocean-ice Reference Experiments) and CMIP (Coupled Model Intercomparison Project) and Predictive NWP (Numerical Weather Prediction) including the (re)analysis. A major challenge of atmosphere models is to generate the UA-ASF from the UA-FP, such as clouds, stability and water vapor. The primary Ocean-FP is SST (both skin from remote sensing and bulk from surface buoy and drifters) and up-welling longwave flux is included here, because of its dependence on SST. Ocean surface current is secondary. Bulk formulae parameterize the turbulent fluxes in terms of the SST, and the Atmospheric Surface Layer (ASL)-FP (wind speed, air temperature and humidity). Additional observational requirements for modeling biogeochemical cycles include air and sea pCO_2 and upper ocean pH and O_2.

Table 1.2 – Primary purpose (verification, forcing, or initialization) for air sea flux (ASF) and flux parameter (FP) observations as functions or flux type (upper atmosphere, surface turbulent, oceanic, and atmospheric surface layer), model configuration and simulation mode (i.e., AGCM, OGCM, CGCM, prognostic or predictive).

	UA-ASF	Turb-ASF	Ocean-FP	UA-FP	ASL-FP
AGCM : AMIP	V	V	F	V	V
NWP/Reanalyses	V	V	F	I	I
OGCM : CORE	F	V	V		F
Ocean Prediction	F	V/F	I		F
CGCM : CMIP	V	V	V	V	V
Climate Prediction	I	I	I	I	I

The most common use of ASF and FP is verification of means and of variability from inter-annual to the seasonal cycle (Bates et al., 2012) and diurnal. Fidelity in solutions can be a consequence of compensating flux and model errors. AGCMs use observed SST as boundary condition, so there are requirements for SST to resolve down to the diurnal cycle and to spatially resolve Tropical Instability Waves.

OGCMs forced by air-sea fluxes have been found to drift far away from the SST used to compute the fluxes, but this method should be explored for ocean prediction where the data assimilation can control the drift. Alternatively, the CORE protocol (Griffies et al., 2009) computes fluxes using prognostic model SST with observed ASL-FP and UA-ASF with diurnal resolution. Tropical Pacific observations of these quantities were essential to reducing known global biases to acceptable levels (Large and Yeager, 2009) and will need to continue in case the biases are non-stationary.

The Group for High Resolution Sea Surface Temperature (GHRSST) Development and Implementation Plan (GDIP) (Donlon et al., 2009, 2010) provide numerous recommendations for a global in situ SST observing system that should be considered in the TPOS (see: https://www.ghrsst.org/files/download.php?m=documents&f=OO-ModernEraSST-v3.0.pdf). We highlight several recommendations here:

- GDIP recommends that the number of moored fiducial ("reference") sites with high quality instrumentation should be increased. Uncertainty estimates need to be delivered with all measurements and the depth of SST measurement reported with all measurements. Calibration stability must be assured and ideally demonstrated for all platforms.
- GDIP strongly recommends that all Argo floats are to be equipped with a capability to make high vertical resolution measurements of SST in the upper 10 m of the ocean surface and that shallow-water Argo floats be developed and deployed.
- GDIP recommends contemporaneous SST and wind stress in order to understand the context of the SST measurement (e.g. cool skin and thermal stratification), and to help blend the SST measurements from different measurements. Steps should be taken to secure high temporal resolution (ideally at an hourly resolution) wind fields over the global ocean for use in diurnal SST variability modeling.
- GDIP recommends that the SST community of producers and users establish and maintain: a. a programmeme of *in situ* measurements, both thermometers on buoys, ships and subsurface vehicles and radiometers on ships and platforms that can be used for validating the different products. For the sake of efficiency, it is desirable that this be a fully collaborative programmeme shared between all the agencies responsible for SST products. There is also a need to specify the requirements for new *in situ* data acquisition systems to support data integration, including wider coverage by shipbased radiometers, diurnally resolving moorings, Argo with additional sensors for near-surface sampling and the OceanSites approach.

Finally, initial conditions are paramount for atmosphere, ocean and coupled model predictions, and the assimilation of an observational data stream is an integral part of any system, regardless of the sophistication (from simple nudging to Ensemble Kalman filters). Fully coupled data assimilation where observations on one side of the air-sea interface influences the other and both sides use the same fluxes is the ultimate goal for climate prediction, so the associated research, development and operations require coincident observations of all the ASF and FP.

2.2 Assessing uncertainties in models

In order to understand where observations are most needed for assessing uncertainties in models, it is useful to review common biases. It should be noted however that without distributed high quality reference data, the presence of a bias may not be known (e.g. Figure 2.1).

Atmospheric reanalysis systems combine observations and models to provide global four-dimensional uniformly gridded datasets that are valuable for studying weather systems and climate variability. However, the quality of the reanalyzed air-sea fluxes is highly sensitive to the uncertainties in model parameterizations and to the temporal inhomogeneity of the observing system. For the reanalyzed surface heat fluxes (latent heat flux, sensible heat flux, longwave and shortwave radiation), major sources of uncertainties are attributable to the representation of near-surface physical processes, the choice of parameterization of subgrid-scale turbulent and convective processes, and the assimilation of observations from different platforms that causes spurious trends (Chen et al., 2008).

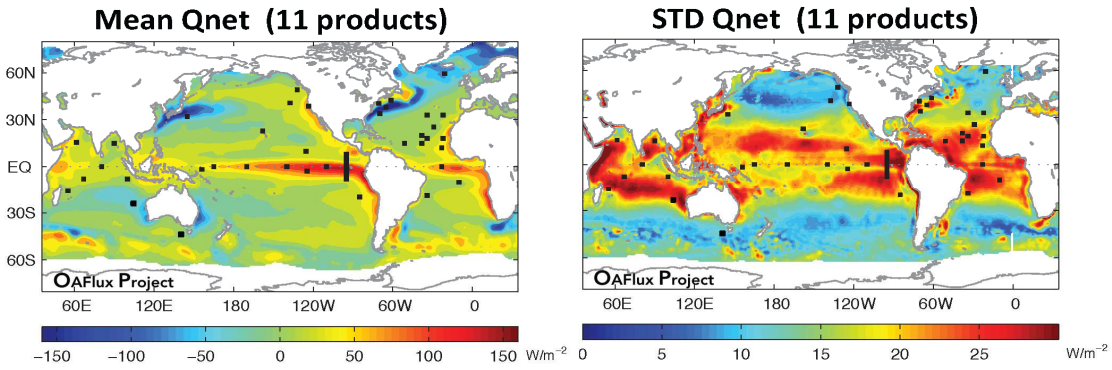

Figure 2.1 - Mean net surface heat flux from 11 products (left) and standard deviation of these 11 products (right). Products include: OAFlux, NOC2, ERAinterim, MERRA, CFSR, ERA40, NCEP1, NCEP2, CORE2, ISCCP, NASA/SRB, CERES. Squares indicate active and historical buoy reference sites.

The downward radiation fluxes at the surface are heavily modified by clouds, and the large uncertainties in the reanalysis cloud parameterizations lead to significant biases in the surface radiative fluxes (Allan et al., 2004). The bias in the incoming solar radiation is the dominant error source in the surface radiation budget over the tropical oceans (Song and Yu, 2013; Cronin et al., 2006b). Reanalyses (ERA40, NCEP/NCAR, and NCEP/DOE) tend to produce too much reflective cloud over the tropical oceans (i.e., negative bias in downward solar radiation), except for the stratocumulus regimes where model cloud cover is too low (Betts et al., 2006; Cronin et al., 2006a). The downward longwave radiation at the surface is dependent of the atmospheric structure and composition, as well as cloud base temperature. Differences in the reanalysis longwave radiation in the tropical oceans are also due to the differences in cloud cover and their vertical structure. However, in the tropical regions, which are saturated by water vapor, the water vapor has a strong impact on the downwelling longwave radiation as shown in Nussbaumer and Pinker (2011).

The reanalysis latent and sensible heat fluxes are affected primarily by the biases in near-surface air humidity and temperature (Yu et al., 2008), although the choice of the bulk flux

algorithm is also a factor (Smith et al., 2011). Air humidity in all reanalysis products is biased dry in the tropical oceans and hence, contributees to an overestimation of the reanalysis latent heat loss (evaporation) at the ocean surface (Jiang et al., 2005). Overall, the largest uncertainties in the reanalysis heat fluxes are due to the shortwave radiation and latent heat flux components, with the largest errors found off the equator (Figure 2.1).

Reanalysis wind stress show analogous large-scale features, however, differences are noted in the strengths of wind speed and wind stress curl and in the representation of small-scale features, such as the variability on frontal and eddy scales (Milliff et al., 2004; Collin et al., 2012). Differences are also observed in synoptic-scale variability of weather systems. Compared to QuikSCAT winds, reanalyses tend to have storms with larger horizontal extent that lack the depiction of the fine spatial details. The spatial resolution has been improved considerably in the latest reanalysis efforts and ERAinterim and CFSR have a more realistic representation of meso- and synoptic scale wind variability (Jin and Yu, 2013).

Over the tropical oceans, the precipitation in the reanalyses is much greater compared to satellite estimates from GPCP (Bosilovich et al., 2008). The bias in precipitation is consistent with the bias in evaporation. Reanalyses tend to produce excessive evaporation (latent heat loss). Since atmospheric water vapor cannot exceed the saturation limit, the excessive evaporation will lead to an excessive precipitation. Precipitation is an integral component of the water and energy cycles and is also largely related to model physical parameterizations. Newman et al. (2000) showed that there is a high internal consistency of precipitation, outgoing longwave radiation, and upper-level divergence within a reanalysis, but a low external consistency (i.e. the agreement between reanalyses), which suggests that the biases in evaporation and precipitation are dependent on the model physics.

While the coupling associated with ENSO is predominately an equatorial zonal process, for understanding the multiscale variability and uncertainties in the global energy balance it is important to monitor the flux parameters and all components of the net surface heat flux in the convective regimes of the western Pacific warm pool, the SPCZ, and ITCZ. Despite the importance of coupled processes in the tropical Pacific and the fact that the Tropical Pacific is larger than the tropical Indian and Atlantic Oceans combined, at present, there are as many active flux stations in the tropical Pacific as in the tropical Indian Ocean (Figure 1.1); and there are more flux stations in the tropical Atlantic than in either of the other basins. Finally, while both the RAMA and PIRATA arrays have full-flux buoys both on the equator and off, within the tropical Pacific Ocean, all components of the net surface heat flux are presently monitored at only 4 sites along the equatorial Pacific, and at the Stratus mooring (20S, 85W). It is recommended that all components be monitored at several sections that cross the SPCZ and ITCZ. In addition, it is recommended that reference stations be initiated in the Trade wind regime north of the ITCZ, similar to the other basins.

Because models that assimilate observations may not fully manifest the biases included in the physics of the model, it is useful to withhold some observations from assimilation. There are typically two ways this is done: withholding data from the Global Telecommunication System (GTS), or using a WMO number “84” to indicate that these data are reference data and should not be assimilated. We recommend the latter method be used, as these data, whether assimilated or not, can be useful to forecaster analyst interested in validation in real-time. This

method however relies upon the operational centers to sort through GTS data and ideally list which data are actually assimilated.

2.3 Common biases in satellite data

Satellite estimates of stress in the tropics are determined from scatterometer observations of equivalent neutral wind (U_{10EN}) relative to the surface current, which is the neutral 10m wind speed required to calculate the friction velocity (squareroot of the kinematic stress) using a neutral drag coefficient (Cardone, 1965; Ross et al., 1985; Cardone et al., 1996; Kara et al., 2008). Spatial oversampling allows estimates on 12.5 to 25 km scales. Scatterometers are wide swath instruments, allowing for calculations of area-averaged spatial derivatives over large areas. These derivatives are noisy unless the averaging scale is three or more times the grid spacing (Holbach and Bourassa, 2013). For rain-free conditions with wind speeds greater than 3 ms^{-1}, the random error in vector components is roughly 0.6 ms^{-1}, with an uncertainty in speed of less than 1 ms^{-1}.

There are several additional considerations. For wind speeds <3 ms^{-1} the surface is less homogeneous, making estimation of speed and direction more difficult. Also for these low wind speeds, retrievals tuned to friction velocity have proportionally large bias in stress due to squaring of random errors. And, while strong currents must always be taken into account to obtain an unbiased wind speed analysis from scatterometer observations, in regions such as the Tropical Pacific, where winds are weak and surface currents strong, this is particularly important (Yu and Jin, 2012). Fortunately, because flux models are dependent on the vertical shear in winds, accounting for currents is unnecessary if scatterometer winds are used in the bulk flux models. Rainfall also contributes to larger errors (Draper and Long, 2004; Weissman et al., 2012; and references therein); however, new retrievals that attempt to account for rain (Stiles et al., 2013) are a great improvement over traditional algorithms that were designed only for rain-free conditions. Lastly, the influences of waves on stress should be considered in the neutral drag coefficient used to convert U_{10EN} to stress (Bourassa, 2006; Edson et al., 2013). Most modern flux models are in general agreement regarding the dependence of the neutral drag coefficient on wind waves. The dependence on remotely forced swell, however, remains highly controversial (Donelan et al., 1997; Bourassa, 2006). The tropical Pacific Ocean has synoptically and seasonally varying swell, which could induce regional and temporally varying biases in surface wind stress.

The most recent release of QuikSCAT winds attempts to adjust for rain related errors, resulting in error characteristics similar to rain-free conditions where such adjustments are possible (Stiles et al., 2013). However, if the rain signal is too strong compared to the wind signal, the scatterometer data are flagged as seriously rain contaminated and generally excluded from further analysis. Not using these flagged data results in much better estimates of stress when compared with collocated data; however, it does bias space- and time-averages of wind stress curl and divergence fields (Milliff et al., 2004). Rain tends to be associated with cyclonic vorticity and convergence, therefore ignoring data associated with rain tends to result in averages and distributions that are biased anticyclonic and divergent.

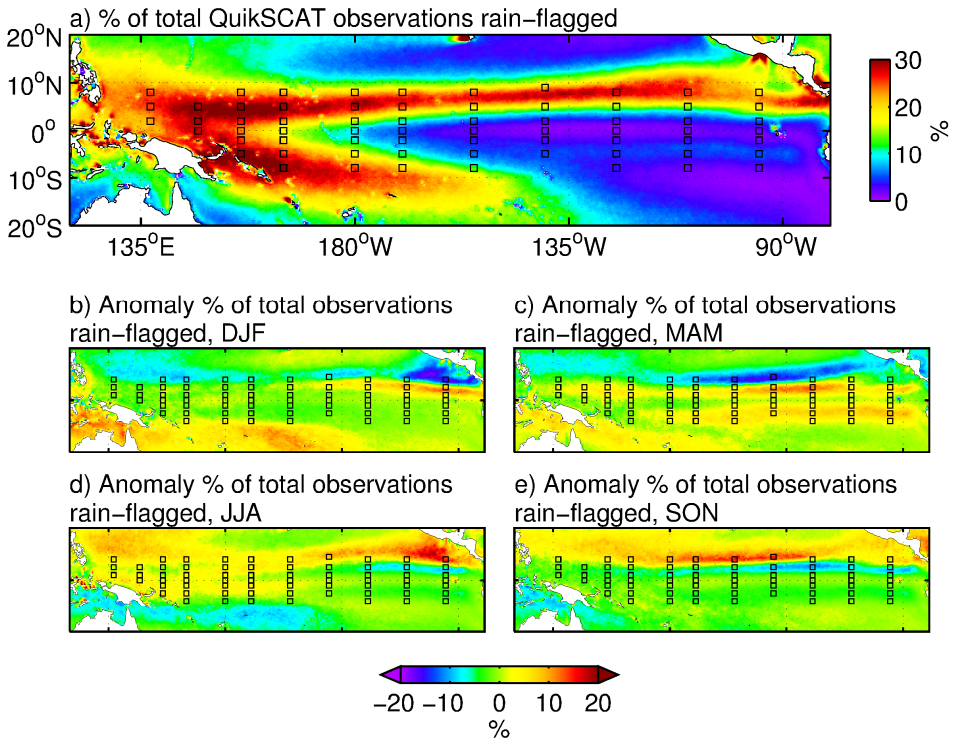

Figure 2.2 – (a) Map of the QuickSCAT rain-flag frequency over the 10-year period August-July 1999; (b-e) seasonal anomalies of the QuickSCAT rain-flag frequency relative to (a). Rain is determined from the QuickSCAT – only rain-flag and a collocted passive radiometer rain rate. The squares in each panel show the locations of the individual buoys in the TAO/TRITON array.

Although intermittent, rain limits the full utilization of QuikSCAT surface winds since rain degrades the ability of Ku-band scatterometers such as QuikSCAT to retrieve accurate vector winds over the ocean. The following examples are based on a product that does not attempt to correct for rain-related errors: they indicate how often rain occurs rather than how often it contributes to serious errors (which is harder to assess). If all observations flagged as coincident with rain are removed from an analysis, rain-induced sampling biases would be particularly acute in the western tropical Pacific and near the ITCZ and SPCZ, where 20-30% of all scatterometer wind measurements are rain contaminated (Figure 2.2).

During the 10 year period of August–July 2009, rain rarely occurred over the equatorial cold tongue and the southeast equatorial Pacific (<5% of the time). In contrast, the northern and western moorings (squares in Figure 2.2) are well-placed to measure winds in these rainy regions that are not measured accurately by satellite. Such locations will be very important for training wind retrieval algorithms to account for rain, and for determining when such corrections can be usefully done. Figures 2.2b-e show that rain frequency has strong seasonal variability over most of the tropical Pacific moorings.

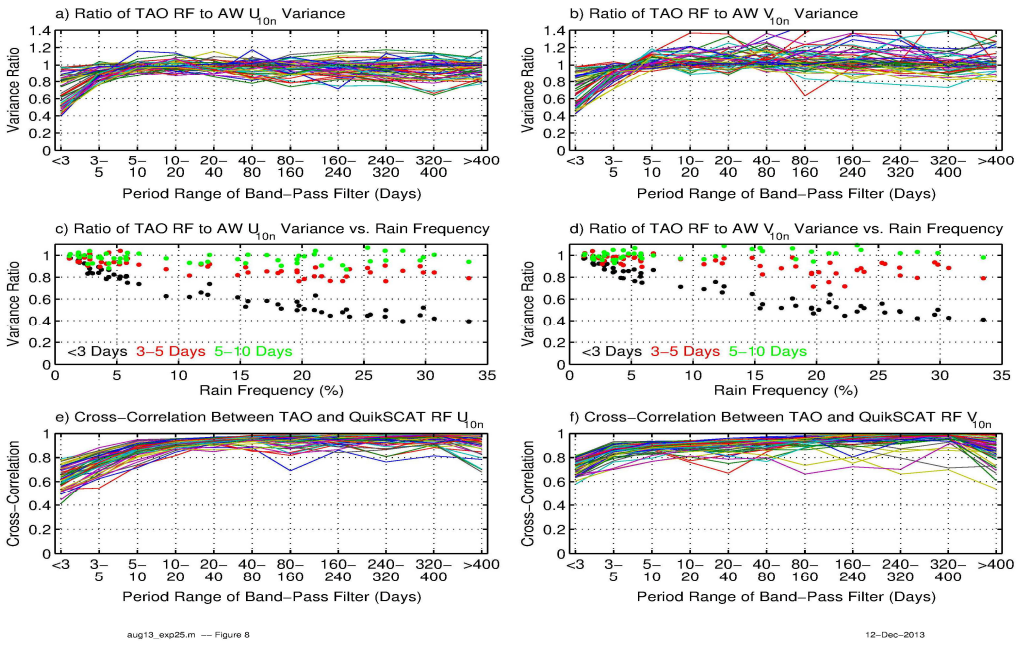

Figure 2.3 - Wind statistics computed over the 10-yr period August 1999-July 2009: (a-b) The ratio of temporal variance between rain-free (RF) and all-weather (AW) TAO equivalent neutral wind (ENW) components as a function of band-pass filtered time period. Each line corresponds to each of the buoys shown in Figure 4. (c-d) Ratio of TAO rain-free to all-weather wind variances as a function of rain-frequency for each buoy. Black points denote periods less than 3 days, red points are periods of 3-5 days, and green points are periods of 5-10 days. Each point represents an individual buoy. (e-f) Cross-correlation coefficients between the rain-free TAO and QuikSCAT ENW components as a function of band-pass filtered period. Each line corresponds to a different buoy. In all panels, only TAO winds collocated in time and space with QuikSCAT observations were used, and rain occurrence was determined from the QuikSCAT rain-flag. The RSS QuikSCAT dataset was used in these comparisons.

In light of the strong spatial and temporal rain variability, *in situ* TAO wind measurements, that provide all-weather sampling, are particularly valuable in the tropical Pacific. To demonstrate importance of all-weather sampling, TAO winds are used to compute the ratio of variances of rain-free and all-weather time series of zonal U_{10EN} and meridional V_{10EN} wind components at each buoy location shown in Figure 2.2. Figure 2.3a, b shows this variance ratio as a function of time-scale. For time-scales less than 5 days, the rain-free time series contain significantly less variance (due to exclusion of rain-flagged data) than the all-weather time-series, while longer than 5 days, the rain-free and all-weather variances are nearly equal. TAO wind measurements provide important information on temporal variability on time-scales less than 5 days that is degraded significantly in rain-free sampling, such as provided by most QuikSCAT products.

As Figures 2.3c,d shows, the variance reduction from rain-free sampling is strongly related to rain frequency for periods less than 3 days (black points); frequent rain strongly reduces measured wind variance. For rain frequencies greater than 20%, rain-free sampling captures only about half of the variance of the full all-weather time series. Even relatively modest occurrences of rain, 5% for example, reduces the measured wind variance to only about 80% of the all-weather wind variance. Rain still affects wind variability on time-scales of 3-5 days (red points), although less so; for periods greater than 5 days (green points), the variance ratios

approach unity for the whole range of rain frequencies encountered. The effect on time-scales less than 5 days is a consequence of the intermittent nature of precipitating weather disturbance in the tropics. Despite this analysis being based on a worst case assumption of no useful data during rain events, we are confident that qualitatively similar problems exist with the JPL v3 data set for which corrections were attempted.

Cross-correlations between rain-free TAO and QuikSCAT winds are shown in Figure 2.3e, f. These show that the winds from both platforms are highly correlated for time-scales greater than 5 days. For time-scales less than 3 days, the correlations are all below 0.8. Part of the drop-off in correlation is due to random instrument errors for each platform, but part is due to errors in the satellite rain-flag, which is known to misidentify rain-contaminated grid cells (e.g., Weissman et al., 2012). Thus for assessing uncertainties in satellite scatterometer wind stress, it is recommended to have in situ co-located wind speed and direction, surface currents, SST, air temperature, humidity, and rainfall observations in the convective regions of the western equatorial Pacific, ITCZ and SPCZ. It is also recommended that the future scatterometers (1) have smaller footprints to improve sampling and (2) have a capability of estimating rain rates (e.g., from a radiometer or from using two frequencies for scatterometry). Estimation of the turbulent fluxes over the oceans from satellites is a still-evolving field. Satellite-derived air-sea fluxes require retrievals of near-surface wind speed, temperature, and humidity, and SST, as well as any additional fields that are needed for the bulk flux parameterization (such as wave information). Issues associated with the wind fields have been noted above, as well as recommendations for improvements to in situ observations of SST. Recent advances have demonstrated improved capabilities of measuring the still-problematic near-surface specific humidity and temperature (Figure 2.4, from Roberts et al., 2010; see also Jackson and Wick, 2010; Bourassa et al., 2010; Clayson et al., 2014). Recent estimates of uncertainties of the near-surface temperature and humidity have indicated mean biases of less than 0.1 ^{o}C and 0.2 g kg^{-1}, respectively, are possible. However, there are still regime-based systematic differences between the products and the available observations. Figure 2.5 adapted from Prytherch et al. (2013) shows comparisons of several satellite-based products with the NOC dataset; clear regional biases which appear to be correlated with cloud and weather regimes are evident.

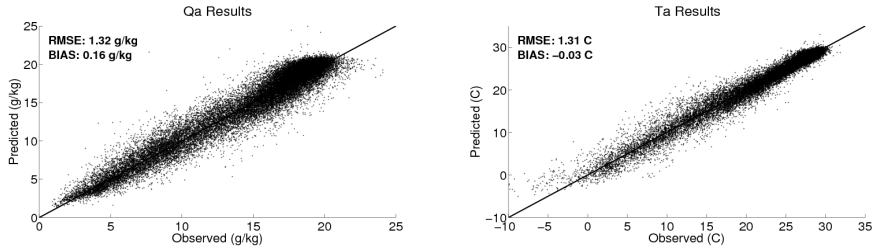

Figure 2.4 - Predicted (satellite-derived) vs. observed parameters for specific humidity (Qa), and air temperature (Ta). The predicted values are the output obtained directly from inversion of satellite brightness temperatures using the neural network as described in Roberts et al. (2010). Observations are from the SeaFlux in situ dataset.

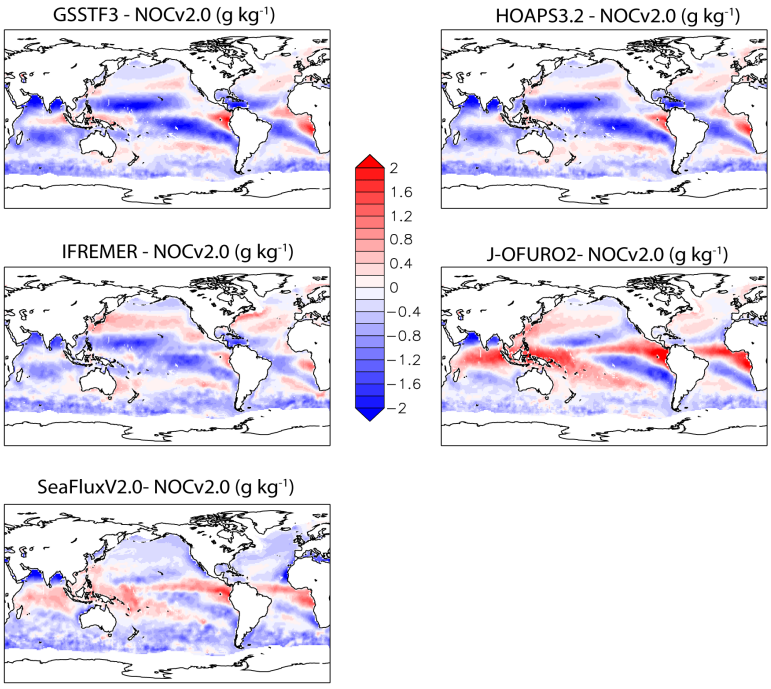

Figure 2.5 - Specific humidity satellite product difference (g kg^{-1}) from observations (satellite product - NOCv2.0, with no uncertainty limit applied), averaged over full period of satellite dataset (from Prytherch et al., 2013).

For the turbulent heat fluxes (and evaporation estimates) it is the difference between the near-surface and surface temperatures and humidities that affect the errors in the retrievals. As reported for one satellite dataset by Clayson et al. (2014), near-stable conditions have much reduced errors than those in highly stable or unstable conditions; extremes in air-sea stratification of humidity likewise have higher errors (Figure 2.6). Given the interest in understanding the distributions of the fluxes and input parameters (e.g. Gulev and Belyaev, 2012), and the importance of understanding the effects of extremes on our weather and climate system, these errors need to be reduced.

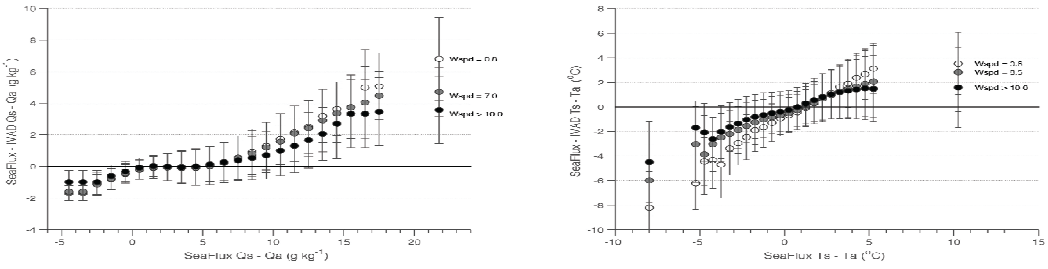

Figure 2.6 - Differences between retrieved satellite values of Qs – Qa and Ts – SST as compared to a matchup-dataset from IVAD, stratified by wind speed (adapted from Clayson et al., 2014).

As shown in Figure 2.7, mean air-sea differences in humidity leading to larger uncertainty are associated with the ITCZ and to a larger extent the SPCZ, while the cold tongue region has the highest mean uncertainty due to stable conditions. Thus to help assess uncertainties in satellite-

based retrievals of near surface temperature and humidity, it is recommended that humidity and temperature sensors be collocated with key wind speed and SST measurements in the tropical Pacific.

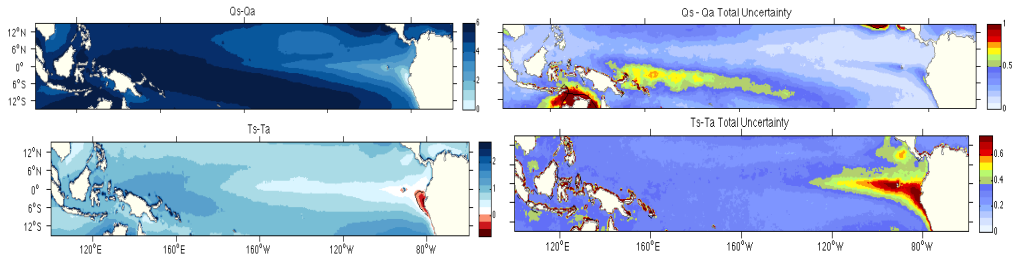

Figure 2.7 - Mean air-sea specific humidity difference and uncertainty (g kg^{-1}; top panels) and mean air-surface temperature (^{o}C; bottom panels) from the SeaFlux satellite-based product.

2.4 Air-sea interaction research for improving models

The primary purpose of the TPOS is to monitor developing ENSO conditions. In recent decades there have been dramatic changes in the location, timing, and frequency of the heat anomalies associated with ENSO. Long time series are required to study decadal variability and long-term changes in ENSO. It is essential that the existing long climate time series of air-sea flux and boundary layer observations continue to be made.

In recent years, there has been a shift in the location of the maximum equatorial heat anomaly associated with El Niño from the eastern Pacific to the central Pacific (Ashok et al., 2007). While some speculate that this is a new type of El Niño, a “Midoki” or pseudo El Niño, others speculate that non-linear dynamics can cause the spatial shift in the anomalies and thus these events are not independent (Takahashi et al., 2011). Clearly, four air-sea flux stations across the entire equatorial Pacific are insufficient to capture these non-linear dynamics. More unsettling however is the fact that these four stations may not have enough zonal resolution to observe the anomaly itself. It is thus recommended that all equatorial sites be enhanced to monitor the air-sea fluxes of heat, moisture and momentum, and the ocean boundary layer temperature, salinity, velocity, and thickness.

As discussed in Section 1.2, estimation of air-sea fluxes from flux parameters, whether observational or numerical, introduces error. Continued research is needed to improve the bulk algorithms used as stand-alone modules, and used within general circulation models. For this purpose, high quality direct observations of the fluxes and the flux parameters used to estimate the fluxes are needed. These have been traditionally made from research vessels and it is recommended that this should be done on the research vessels used to maintain the TPOS. New technology is emerging which allow direct flux estimates to be made from moored buoys as well (Weller et al., 2012; Bigorre et al., 2013). The advantage of the moored measurements is that a wider range of coupled processes are likely to be observed. For example, the surface mooring deployed in the Gulf Stream during the CLIMODE programme provided direct measurements of surface stress and buoyancy fluxes over a 15-month period, capturing the full seasonal cycle and atmospheric forcing for 18°C water formation events (Marshall et al., 2009). In addition, the extremely high-resolution geo-positioning information needed for these

observations can be used to quantify significant wave height and wave period characteristics. The influence of waves on the wind profile, on flux calculations, on gas exchange, and upper ocean turbulence are all subjects of active research that could be investigated through use of these direct flux sensors (Donelan et al., 1997, Bourassa, 2006; Edson et al., 2013). The disadvantages of these sensors are that they generally require more power, are technologically more complex (and thus more vulnerable to failure), and add expense.

While the covariance flux packages discussed above are used to measure heat and other property fluxes across the air-sea interface, other exciting new technology is making it possible to measure vertical turbulent heat fluxes within the water column. Referred to as Chi-pods, these small sensors can be mounted on the mooring line and deployed for over a year, providing long-term measurements of turbulent mixing (Moum et al., 2013). Mixing is fundamentally how warm surface water is transported downward in the presence of wind-generated Ekman upwelling. Better representation of ocean mixing is needed to improve the coupled ocean-atmosphere models used to forecast ENSO. It is recommended that a subset of the reference mooring sites, both on and off the equator, be enhanced with Chi-pods and covariance flux packages to provide direct observations of heat fluxes at the air-sea interface and within the water column. The covariance flux packages at the surface should also be used to measure wave height.

Observations that resolve important air-sea interaction processes and mechanism guide and inspire model development and are a cornerstone of efforts to improve numerical models used to forecast ENSO, the biogeochemical response and the ecosystems of the tropical Pacific. As discussed in section 1.1, important open research questions include understanding the role of high-frequency variability and multi-timescale variability: How the diurnal cycle affects MJO, or how MJO affects ENSO, for example, and likewise, how long-term climate change may affect MJO and ENSO. Such multiscale studies require measurements that are both high resolution (order minutes-hours) and long (years-decades). Fixed location data (e.g. mooring data) are ideal for such analyses and it is expected that TPOS mooring array will be the primary data set in many of these studies. To capture the spatial structure in these processes, data from floats, drifters, ships (including the ship servicing the TPOS mooring array) and other platforms within the TPOS must be used. These platforms may not observe all variables with the spatial and temporal resolution needed for the process in question. While not all process studies need to be as large as the TOGA-COARE or EPIC2001 climate experiments, these provide useful framework for how the TPOS ENSO observing array can be enhanced to study climate processes. It is recommended that limited duration, intensive observing arrays be embedded within the TPOS for process studies.

3. Recommendations for 2020 TPOS

For a summary of the air-sea flux and flux parameters deployed in the TPOS of 2005, see Appendix 1. Based upon the discussion within this White Paper, we make the following overall recommendation for the TPOS of 2020:

1. Long climate records should be continued.

2. The research vessel that is used to maintain the observing system should be treated as a platform within the observing system itself, making standard measurements along repeat tracks (e.g. ADCP, CTD, pCO_2, marine meteorology, atmospheric soundings, and other measurements). Emerging technology for making underway CTD measurements that would not impact the required seadays.
3. The TPOS array should integrate multi-disciplinary observations. Data should be freely provided for all users. The array should be designed to provide data needed to observe ENSO events through their full life cycle; to force, initialize, and nudge numerical models; to assess uncertainties in numerical models and satellite products; to calibrate remotely measured variables; to develop and test parameterizations needed for models and satellite products; and to better understand the climate system.
4. Interdisciplinary process studies should be built around the infrastructure of the TPOS.

Specific requirements and recommendations for air-sea flux and wind stress observations within the TPOS 2020 array are as follows. It should be noted that in many cases the present TPOS was designed to meet these requirements.

1. Long climate records from flux stations along the equator should be continued. In addition, wind stress, and all components of the net surface heat and moisture fluxes should be measured at all TPOS longitudes along the equator and at select longitudes off the equator in the convective regions of the western Pacific, SPZC and ITCZ. In the western Pacific, the TRITON buoys could become flux reference stations simply by adding a longwave radiation sensor. Along TAO meridionals such as 140°W, this would require additional shortwave and longwave radiation sensors, and a 10 m current meter. At least one meridional section that crosses the ITCZ should also sample the extratropical trade wind regime north of the ITCZ.
2. All variables, but particularly solar radiation, SST, air temperature, wind, and surface currents need to have their diurnal cycle resolved in near-realtime. Some method for extrapolating bulk SST to skin temperature needs to be used for calculating air-sea fluxes. GDIP recommendations (Donlon et al. 2009, 2010) should be considered for surface temperature observations of the TPOS.
3. All surface buoys should monitor winds, air temperature, relative humidity, and SST as these are state variables for every air-sea flux. Surface air temperature and humidity estimates from satellites also depend upon many assumptions and parameterizations, and thus have large structural errors that an in situ observing system might resolve. Some off-equatorial “standard” sites may be able to be replaced by small buoy platforms (e.g., mini-TRITON, “easy-to-deploy” buoys, wave gliders,…) that do not have a tower and either are less expensive or require less (or no) ship time. Sensors would be placed on a mast, but must be at least 2 m above the air-sea interface in the mean.
4. The 2020 TPOS array should have a better relative humidity sensor.
5. Atmospheric diurnal-cycle-resolving PBL profiling should be made continuously from islands in the equatorial Pacific.
6. Mixed layer depth should be resolved at all sites measuring air-sea fluxes and at other locations as well.

7. A subset of the flux stations should include observations of state variables and their covariance fluxes. Hopefully by 2020, the power requirements will be reduced sufficiently that these sensors could have a 1+ year endurance. These covariance flux sensors would additionally be able to monitor wave characteristics, and their influence on wind stress and fluxes. These sites could also carry Chi-pod sensors to monitor heat fluxes and mixing within the water column.
8. PAR and subsurface optical absorption should also be measured at one or more biogeochemical flux stations in a region of light wind where there may be feedbacks between the diurnal warm layer and phytoplankton blooms. Pending technology development, observations of the direct and diffuse radiation components at this station would provide invaluable information for the extinction profile in water, for ocean heat budgets, and cloud studies. Efforts should be made to have the TPOS radiation measurements meet the standards of the Baseline Surface Radiation (BSRN) protocols (Ohmura et al. 1998).
9. Although barometric pressure has little effect on the flux estimate, it can be an important surface observation to assimilate and to observe for understanding the physics of the boundary layer system. Because atmospheric tides cause large variability in barometric pressure, isolated sensors can be difficult to interpret. But these are filtered out when considering BP gradients (e.g. 2N minus equator). A single BP in the tropics will be difficult to interpret, but pairs may be quite interesting.

Appendix 1 – TPOS array of 2005

The present and past TPOS buoy array can be viewed through the TAO data display and delivery webpage: http://www.pmel.noaa.gov/tao/data_deliv/deliv.html.

By selecting “Availability” on this webpage, one can see the full time and space coverage of the selected variables. Figure A1 shows the 2005 configuration of TPOS for each flux parameter. Figure A1 summarizes the flux capabilities of the global buoy array.

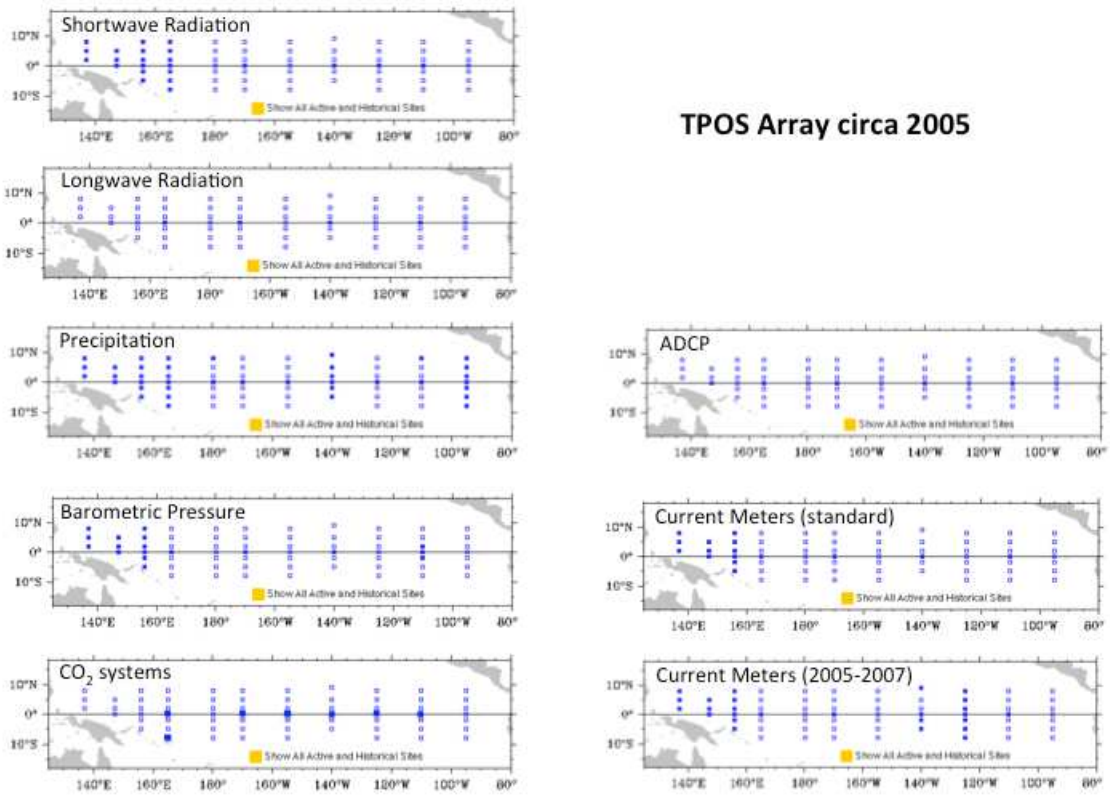

Figure A1 - Configuration of the 2005 TPOS for flux and flux parameters.

References

Anctil, F., Donelan, M.A., Drennan, W.M., and Graber, H.C. (1994): Eddy-Correlation Measurements of Air-Sea Fluxes from a Discus Buoy. J. Atmos. Oceanic Technol., 11, pp. 1144–1150.

Allan, R. P., Ringer, M.A., Pamment, J.A., and Slingo, A. (2004): Simulation of the Earth's radiation budget by the European Center for Medium Range Weather Forecasts 40-year Reanalysis (ERA40) J. Geophys. Res., 109, D18107, (doi: 10.1029/2004JD004816).

Ashok, K., Behera, S.K., Rao, S.A., *Weng*, H., and *Yamagata*, T. *(*2007*):* El Niño Modoki and its possible teleconnection*,* J. Geophys. Res*.,* 112*, C11007*, (doi: 10.1029/2006JC003798).

Balsley, B. B., Frehlich, R. G., Jensen, M. L., and Meillier, Y., (2006): High-Resolution In Situ Profiling through the Stable Boundary Layer: Examination of the SBL Top in Terms of Minimum Shear, Maximum Stratification, and Turbulence Decrease. J. Atmos. Sci., 63, pp. 1291–1307, (doi: 10.1175/JAS3671.1).

Betts, A. K., Zhao, M., Dirmeyer, P.A., and Beljaars, A.C.M. (2006): Comparison of ERA40 and NCEP/DOE near-surface data sets with other ISLSCP-II data sets, J. Geophys. Res., 111, D22S04, (doi:10.1029/2006JD007174).

Bigorre, S, Weller, R.A., Lord, J., Edson, J.B., and Ware, J.D. (2013): A surface mooring for air-sea interaction research in the Gulf Stream. Part 2: Analysis of the observations and their accuracies, J. Atmos. Oceanic Tech., 30, pp. 450–469.

Bosilovich, M. G., Chen, J., Robertson, F.R., and Adler, R.F. (2008): Evaluation of Global Precipitation in Reanalyses. J. Appl. Meteor. Climatol., 47, pp. 2279–2299. (doi: 10.1175/2008JAMC1921.1).

Bourassa, M. A. (2006): Satellite-based observations of surface turbulent stress during severe weather, Atmosphere - Ocean Interactions, Vol. 2., ed., W. Perrie, Southampton, UK, Wessex Institute of Technology Press, pp. 35 – 52.

Cai, W., and co-authors (2014): Increasing frequency of extreme El Niño events due to greenhouse warming. Nature Clim. Change, 4, pp. 111-116, (doi: 10.1038/nclimate2100).

Cardone, V.J. (1969): Specification of the wind distribution in the marine boundary layer for wave forecasting. Geophys. Sci. Lab. N.Y. Univ. Report TR-69-1 (NTIS AD 702-490).

Cardone, V.J., Jensen, R.E., Resio, D.T., Swail V.R., and Cox, A.T. (1996): Evaluation of contemporary ocean wave models in rare extreme events: the “Halloween Storm” of October, 1991 and the “Storm of the Century” of March 1993. Journal of Atmospheric and Oceanic Technology, 13, pp. 198–230.

Chelton, Dudley B., and Coauthors (2001): Observations of Coupling between Surface Wind Stress and Sea Surface Temperature in the Eastern Tropical Pacific. J. Climate, 14, pp. 1479–1498. (doi: 10.1175/1520-0442(2001)014<1479:OOCBSW>2.0.CO;2).

Chen, J., Del Genio, A.D., Carlson, B.E., and Bosilovich, M.G. (2008): The spatiotemporal structure of 20th-century climate variations in observations and reanalyses. Part I: Long-term trend. J. Climate, 21, pp. 2611–2633.

Clayson, C. A., and Bogdanoff, A.S. (2013): The Effect of Diurnal Sea Surface Temperature Warming on Climatological Air–Sea Fluxes. J. Climate, 26, pp. 2546–2556. (doi: 10.1175/JCLI-D-12-00062.1).

Clayson, C. A., Roberts, J.B., and Bogdanoff, A. (2014): SeaFlux Version 1: A new satellite-based ocean-atmosphere turbulent flux dataset. Int. J. Climatol., in revision.

Colbo, K., and Weller, R.A. (2009): Accuracy of the IMET Sensor Package in the Subtropics. J. Atmos. Oceanic Technol., 26, pp.1867–1890. (doi: http://dx.doi.org/10.1175/2009JTECHO667.1).

Collins, C., C. Reason, J.C., and Hermes, J.C. (2012): Scatterometer and reanalysis wind products over the western tropical Indian Ocean, J. Geophys. Res., 117, C03045, (doi:10.1029/2011JC007531).

Cronin, M. F., Bond, N. A., Fairall, C. W., and Weller, R. A. (2006a): Surface Cloud Forcing in the East Pacific Stratus Deck/Cold Tongue/ITCZ Complex. J. Climate, 19(3), pp. 392-409.

Cronin, M. F., Fairall, C.W., and McPhaden, M.J. (2006b): An assessment of buoy-derived and numerical weather prediction surface heat fluxes in the tropical Pacific, J. Geophys. Res., 111, C06038, (doi:10.1029/2005JC00332).

Cronin, M. F., Xie, S.P., and Hashizume, H. (2003): Barometric pressure variations associated with eastern Pacific tropical instability waves. J. Climate, 16, pp. 3050-3057.

Danabasoglu, G., Large, W.G., Tribbia, J.J., Gent, P.R., Briegleb, B.P., and McWilliams, J.C., (2006): Diurnal Coupling in the Tropical Oceans of CCSM3. J. Climate, 19, pp. 2347–2365. (doi: 10.1175/JCLI3739.1).

Deser, C., and Smith, C.A: (1998): Diurnal and semidiurnal variations of the surface wind field over the tropical Pacific Ocean, J. Clim., 11, pp. 1730–1748.

Donelan, M.A., Drennan, W.M., and Katsaros, K.B. (1997): The air-sea momentum flux in 2099.?conditions of wind sea and swell. J. Phys. Oceanogr., 27, pp. 2087

Donlon, C.J., and Coauthors (2010): Successes and challenges for the modern sea surface temperature observing system: The Group for High Resolution Sea Surface Temperature (GHRSST) Development and Implementation Plan (GDIP), Community whitepaper for OceanObs09, Venice, Italy, 21-25 September, 2009.

Donlon, C.J., and Coauthors (2009): Successes and challenges for the modern sea surface temperature observing system: The Group for High Resolution Sea Surface Temperature (GHRSST) Development and Implementation Plan (GDIP), available from: https://www.ghrsst.org/files/download.php?m=documents&f=OO-ModernEraSST-v3.0.pdf.

Draper, D. W., and Long, D.G. (2004): Evaluating the effect of rain on scatterometer measurements. J. Geophys. Res., 109, (doi:10.1029/2002JC001741).

Edson, James B., and Coauthors (2013): On the Exchange of Momentum over the Open Ocean. J. Phys. Oceanogr., 43, pp. 1589–1610. (doi: 10.1175/JPO-D-12-0173.1).

Edson, J.B., Hinton, A.A., Prada, K.E., Hare, J.E., and Fairall, C.W. (1998): Direct covariance flux estimates from mobile platforms at sea, J. Atmos. Oceanic Tech., 15, pp. 547-562.

Fairall, C. W., Bradley, E.F., Hare, J.E., Grachev, A.A., Edson, J.B. (2003): Bulk Parameterization of Air–Sea Fluxes: Updates and Verification for the COARE Algorithm. J. Climate, 16, pp. 571–591. (doi: 10.1175/1520-0442(2003)016<0571:BPOASF>2.0.CO;2).

Fairall, C. W., Bradley, E.F., Rogers, D.P., Edson, J.B., and Young, G.S. (1996a): Bulk parameterization of air-sea fluxes for Tropical Ocean-Global Atmosphere Coupled-Ocean Atmosphere Response Experiment, J. Geophys. Res., 101, pp. 3747–3764, (doi:10.1029/95JC03205).

Fairall, C. W., Bradley, E.F., Godfrey, J.S., Wick, G.A., Edson, J.B., and Young, G.S. (1996b): Cool-skin and warm-layer effects on sea surface temperature, J. Geophys. Res., 101(C1), pp. 1295–1308, (doi:10.1029/95JC03190).

Fairall, C. W., Yang, M., Bariteau, L., Edson, J.B., Helmig, D., McGillis, W., Pezoa, S., Hare, J.E., Huebert, B., and Blomquist, B. (2011): Implementation of the Coupled Ocean-Atmosphere Response

Experiment flux algorithm with CO_2, dimethyl sulfide, and O_3, J. Geophys. Res., 116, C00F09, (doi:10.1029/2010JC006884).

Freitag, H. P., Y. Feng, Y., Mangum, L.J., McPhaden, M.J., Neander, J., and Stratton, L.D. (1994): Calibration procedures and instrumental accuracy estimates of TAO temperature, relative humidity and radiation measurements. Tech. Memo. ERL PMEL-104 (PB95–174827), NOAA, Pacific Marine Environmental Laboratory, Seattle, WA, 32 pp.

Fung, I. Y., Harrison, D.E., and Lacis, A.A. (1984): On the variability of the net longwave radiation at the ocean surface, Rev. Geophys., 22, pp. 177–193.

Gill, Q. E. (1980): Some simple solutions for heat induced tropical circulations. Quart. J. Roy. Meteor. Soc., 106, pp. 447-462.

Gray, W. M., and Jacobson, R.W. (1977): Diurnal variation of deep cumulus convection, Mon. Weather Rev., 105, pp. 1171–1188.

Griffies, S.M., Biastoch, A., Boening, C., and Belyaev, K. (2012): Probability distribution characteristics for air-sea turbulent heat fluxes over the global ocean. J. Climate, 25, pp. 184-206.

Gupta, S. K., Darnell, W.L., and Wilber, A.C. (1992): A parameterization for longwave surface radiation from satellite data: Recent improvements, J. Appl. Meteorol., 31, pp. 1361–1367, (doi:10.1175/1520-0450).

Holbach, H. M., and Bourassa, M.A. (2013): The effects of gap–wind–induced vorticity, the monsoon trough, and the ITCZ on tropical cyclogenesis. Mon. Wea. Rev. (in press).

Jackson, D. L., and Wick, G.A. (2010): Near-Surface Air Temperature Retrieval Derived from AMSU-A and Sea Surface Temperature Observations. J. Atmos. Oceanic Technol., 27, pp. 1769–1776.

Jin, X., and Yu, L. (2013): Assessing high-resolution analysis of surface heat fluxes in the Gulf Stream region. J. Geophys. Res., 118, (doi: 10.1002/jgrc.20386).

Kara, A. B., Wallcraft, A.J., and Bourassa, M.A. (2008): Air-Sea Stability Effects on the 10m Winds Over the Global Ocean: Evaluations of Air-Sea Flux Algorithms. J. Geophys. Res., 113, C04009, (doi:10.1029/2007JC004324).

Large, W. G., and Yeager, S.G. (2009): The global climatology of an interannually varying air-sea flux data set. Climate Dynamics, 33, pp. 341-364 (doi: 10.1007/s00382-008-0441-3).

Lengaigne, M., and Vecchi, G.A. (2010): Contrasting the termination of moderate and extreme El Niño events in Coupled General Circulation Models. Climate Dynamics, (doi: 10.1007/s00382-009-0562-3).

Lloyd, J., Guilyardi, E., Weller, H., and Slingo, J. (2009): The role of atmosphere feedbacks during ENSO in the CMIP3 models. Atmos. Sci. Lett. 10 (3), pp. 170-176.

Marshall, J., Andersson, A., Bates, N., Dewar, W., Doney, S., Edson, J., Ferrari, R., Forget, G., Fratantoni, D., Gregg, M., Joyce, T., Kelly, K., Lozier, S., Lumpkin, R., Maze, G., Palter, J., Samelson, R., Silverthorne, K., Skyllingstad, E., Straneo, F., Talley, L., Thomas, L., Toole, J., and Weller, R. (2012): "The CLIMODE field campaign: Observing the cycle of convection and restratification over the Gulf Stream," Bull. Amer. Meteor. Soc., 90, pp. 1337-1350.

May, J., and Bourassa, M.A. (2011): Quantifying variance due to temporal and spatial difference between ship and satellite winds. J. Geophys. Res., 116, (doi:10.1029/2010JC006931).

McGillis, W. R., Edson, J.B., Hare, J.E., and Fairall, C.W. (2001): Direct covariance air-sea CO_2 fluxes, J. Geophys. Res., 106, pp. 16729-16745.

McPhaden, M. J., Busalacchi, A. J., Cheney, R., Donguy, J.-R., Gage, K. S., Halpern, D., Ji, M., Julian, P., Meyers, G., Mitchum, G. T., Niiler,P. P., Picaut, J., Reynolds, R. W., Smith, N., and Takeuchi, K. (1998): The Tropical Ocean-Global Atmosphere observing system: A decade of progress. J. Geophys. Res. 103, C7, pp. 14169–14240, (doi:10.1029/97JC02906).

Milliff, R. F., Morzel, J., Chelton, D.B., and Freilich, M.H. (2004): Wind stress curl and wind stress divergence biases from rain effects on QSCAT surface wind retrievals, J. Atmos. Oceanic Technol., 21, pp. 1216–1231.

Moum, J. N., Perlin, A., Nash, J.D., and McPhaden, M.J. (2013): Ocean mixing controls seasonal sea surface cooling in the equatorial Pacific cold tongue. Nature, 500, pp. 64-67.

Murtugudde, Raghu, Beauchamp, J., McClain, C.R., Lewis, M., Busalacchi, A.J. (2002): Effects of Penetrative Radiation on the Upper Tropical Ocean Circulation. J. Climate, 15, pp. 470–486. (doi: 10.1175/1520-0442(2002)015<0470:EOPROT>2.0.CO;2).

Newman, M., Sardeshmukh, P.D., and Bergman, J.W. (2000): An Assessment of the NCEP, NASA, and ECMWF Reanalyses over the Tropical West Pacific Warm Pool. Bull. Amer. Meteor. Soc., 81, pp. 41–48. (doi: 10.1175/1520-0477(2000)081<0041:AAOTNN>2.3.CO;2).

Ohmura, A., DeLuisi, J., Dutton, E., Heimo, A., Forgan, B., Pinker, R.T., Frohlich, C., Philipona, R., Konig-Langlo, G., Whitlock, C., McArthur, B., and Dehne, K. (1998): Baseline Surface Radiation Network (BSRN/WCRP), a new precision radiometry for climate research. Bull. Am. Met. Soc., 79, No. 10, pp. 2115-2137.

Patara, L., Vichi, M., Masina, S., Fogli, P.G., and Manzini, E. (2012): Global response to solar radiation absorbed by phytoplankton in a coupled climate model. Clim. Dyn., 39, pp. 1951-1968.

Pinker, R. T., Bentamy, A., Katsaros, K.B., Ma, Y., and Li, C. (2013): Estimates of net heat fluxes over the Atlantic Ocean. JGR-Oceans. Accepted, JGR-Oceans.

Prytherch, J., Kent, E.C., Fangohr, S., and Berry, D.I. (2013): A comparison of satellite-derived global marine surface specific humidity datasets. Int. J. Climatol., in revision.

Randall, D., Harshvardhan, A., and Dazlich, D.A. (1991): Diurnal variability of the hydrological cycle in a general circulation model, J. Atmos. Sci., 48, pp. 40–62.

Roberts, J. B., Clayson, C.A., Robertson, F.R., and Jackson, D. (2010): Predicting near-surface characteristics from SSM/I using neural networks with a first guess approach. J. Geophys. Res., 115, D19113, (doi: 10.1029/200d9JD013099).

Ross, D.B., Cardone, V.J., Overland, J., McPherson, M., Pierson, R.D., and Yu, T. (1985): Oceanic surface winds. Adv. Geophys., 27, pp. 101–138.

Seo, K.H., Wang, W., Gottschalck, J., Zhang, Q., Schemm, J.K.E., Higgins, W.R., and Kumar, A. (2009): Evaluation of MJO Forecast Skill from Several Statistical and Dynamical Forecast Models. J. Climate, 22, pp. 2372–2388.

Serra, Y.L., A'Hearn, P., Freitag, H.P., and McPhaden, M.J. (2001): ATLAS self-siphoning rain gauge error estimates. J. Atmos. Ocean. Technol., 18, pp. 1989-2002.

Siegel, D. A., Ohlmann, J.C., Washburn, L., Bidigare, R.R., Nosse, C.T., Fields, E., and Zhou, Y. (1995): Solar radiation, phytoplankton pigments and the radiant heating of the equatorial Pacific warm pool. J. Geophys. Res., 100(C3), pp. 4885–4891, (doi:10.1029/94JC03128).

Song, X., and Yu, L. (2013): How much net surface heat flux should go into the Western Pacific Warm Pool? J. Geophys. Res., 118, pp. 3569-3585, (doi: 10.1002/jgrc.20246).

Smith, S., Hughes, P., and Bourassa, M. (2011): A comparison of nine monthly air-sea flux products. Internat. J. Climatol., 31, pp. 1002-1027, (doi: 10.1002/joc.2225).

Stiles, B. W., Danielson, R.E., Poulsen, W.L., Brennan, M.J., Hristova-Veleva, S., Shen, T.P.J., and Fore, A.G. (2013): Optimized Tropical Cyclone Winds from QuikSCAT: A Neural Network Approach. TGARS, in press.

Takahashi, K., Montecinos, A., Goubanova, K., and Dewitte, B. (2011): ENSO regimes: Reinterpreting the canonical and Modoki El Niño, Geophys. Res. Lett., 38, L10704, (doi:10.1029/2011GL047364).

Takahashi, K. (2012): Thermotidal and land-heating forcing of the diurnal cycle of oceanic surface winds in the eastern tropical Pacific. Geophys. Res. Lett. 39, L04805, (doi:10.1029/2011GL050692).

Trenberth, K. E., Branstator, G.W., Karoly, D., Kumar, A., Lau, N.C., and Ropelewski, C. (1998): Progress during TOGA in understanding and modeling global teleconnections associated with tropical sea surface temperatures. J. Geophys. Res., 103 (special TOGA issue), pp. 14291-14324.

Ueyama, R., and Deser, C. (2008): A climatology of diurnal and semidiurnal surface wind variations over the tropical Pacific Ocean based on the tropical atmosphere ocean moored buoy array, J. Clim., 21, pp. 593–607.

Wallace, J.M., and Gutzler, D.S. (1981): Teleconnections in the Geopotential Height Field during the Northern Hemisphere Winter. Mon. Wea. Rev., 109, pp. 784–812.

Wang, J., Rossow, W.B., and Zhang, Y. (2000): Cloud vertical structure and its variations from a 20-yr global rawinsonde dataset. J. Climate, 13, pp. 3041–3056, (doi:10.1175/1520-0442).

Ware, R., Carpenter, R., Güldner, J., Liljegren, J., Nehrkorn, T., Solheim, F., and Vandenberghe, F. (2003): A multichannel radiometric profiler of temperature, humidity, and cloud liquid, Radio Science, (doi:10.1029/2002RS002856).

Weissman, D. E., Stiles, B.W., Hristova-Veleva, S.M., Long, D.G., Smith, D.K., Hilburn, K.A., and Jones, W.L. (2012): Challenges to satellite sensors of ocean winds: Addressing precipitation effects. J. Atmos. Oceanic Tech., 29, pp. 356-374

Weissman, D. E., Bourassa, M.A., and Tongue, J. (2002): Effects of rain rate and wind magnitude on SeaWinds scatterometer wind speed errors. J. Atmos. Ocean. Tech., 19, pp. 738-746.

Weller R. A., Bigorre, S. P., Lord, J., Ware, J.D., and Edson, J.B. (2012): A surface mooring for air-sea interaction research in the Gulf Stream. Part 1: Mooring design and instrumentation, J. Atmos. Ocean. Tech., 29, pp. 1363-1376.

Yu, L., Jin, X., and Weller, R. (2008): Multidecade global flux datasets from the Objectively Analyzed Air-sea Fluxes (OAFlux) project: Latent and sensible heat fluxes, ocean evaporation, and related surface meteorological variables. OAFlux Project Tech. Rep. OA-2008-01, 64 pp.

Zhang, C., McGauley, M., and Bond, N.A. (2004): Shallow Meridional Circulation in the Tropical Eastern Pacific. J. Climate, 17, pp. 133–139.

White Paper #12 – Emerging technology

Rudnick, D.L.[1], Meinig, C.[2], Ando, K.[3], Riser, S.[4], Send, U.[1], and Suga, T.[5]

[1] Scripps Institution of Oceanography, United States
[2] NOAA Pacific Marine Environmental Laboratory, United States
[3] Japan Agency for Marine Earth Science and Technology, Japan
[4] University of Washington, United States
[5] Tohoku University, Japan

1. Introduction

Modern observing systems benefit from the flexibility to adapt as technologies inevitably advance. Since the 1980's, when the TAO array was first conceived and deployed, ocean observing technology has certainly evolved and improved. If the tropical Pacific observing system were started from scratch today with no knowledge of TAO, it seems likely that it would look quite different, with a variety of observing technologies knit together to address the scientific requirements. This paper does not specify these requirements; rather we present a menu of observing technologies plausible for large-scale deployment by 2020. We consider both traditional observing platforms that continue to become more capable, and promising emerging technologies that have yet to be deployed in large numbers in the tropics. We hope that this compendium will provide the building blocks for the future tropical observing system.

Any comprehensive discussion of ocean observing must start with that most capable platform, the ship. Whether the ship is the most modern research vessel carrying scientists and state of the art lab equipment, a commercial ship of opportunity, or a chartered fishing boat from a small island, some method of getting equipment into the ocean is needed. Research vessels are unquestionably the bedrock upon which most scientific knowledge of the ocean is built. However, research vessels are expensive to operate and costs continue to rise. Most of the technological developments discussed below would reduce the use of research vessels, often through more robust instrumentation capable of longer deployment. There are also several technologies for which less expensive ships and boats are sufficient. While we acknowledge the need for ships, we also point out the clear trend toward a reduced dependence on large, dedicated vessels.

A common theme throughout the following discussion of observing technology is the potential for expansion of measured variables. The menu of observational platforms includes an even more extensive list of sensors already deployed successfully. This potential for expansion is central to the observing system of 2020, as in situ sensors for variables previously measurable only in a lab become increasingly practical to use autonomously at sea. The current tropical array of moorings offers a great example of these sorts of expanded measurements, with observations of the carbonate system, bio-optical properties, and acoustic sensing of fish among the valuable additions. An obvious requirement for the observing system of 2020 is that it be sustainable. None of the technologies can work on their own without substantial investment in their continued health. The sustenance of a comprehensive and evolving observing system is as much an organizational problem as it is a technical challenge. We offer no prescriptions for

addressing the organizational issues, but we are sure these issues must be raised, and we believe that more robust technology will help.

2. In situ observing technology

Our review of in situ observing technology is organized by platform. The discussion of each platform includes sections devoted to (1) a basic functional description of the technology, (2) an exposition of the sampling characteristics of the platform and the sensors carried, and (3) some words on typical operations. Included in the discussion of operations are comments on readiness level using the three categories of mature, pilot, and concept (Lindstrom et al., 2012).

2.1 Profiling Floats

Description

ALACE floats were developed in the 1980s as a part of WOCE, and within a decade the first CTD units were added to these instruments. The first Argo floats were deployed in 1999, and shortly after this the first CTD units from SeaBird Electronics (SBE) were tested on the floats. Argo has now been operational for well over a decade, with over 5000 floats deployed and over 3500 still active. The float technology has evolved since the early ALACE versions, and there are now at least 5 commercial versions of floats (instruments that include a buoyancy engine and a CTD) available. At present, all of these instruments still use various versions of the SBE 41 CTD that was first tested in 1999. The SBE 41 has proven to provide generally high stability and accuracy over many years in the water (Riser et al., 2008).

Argo floats typically profile from 0-2000 m and require 200-300 cm^3 of bladder inflation over this range. In recent years a newer instrument designed at Scripps and now commercially available through MRV Systems has returned to an updated variant on the rotary pump, with good results. This allows the float to be smaller and more efficient, resulting in potentially longer lifetimes after deployment. At the present time about 70% of the active floats in Argo originate from Teledyne/Webb Corporation, purchased either as fantail ready units or as components that are assembled and tested at a few research laboratories. The remaining 30% of the floats are composed of the original Scripps SOLO, the newer SIO/MRV SOLO-II, and the French Provor, with a few floats originating from other smaller vendors. All of these floats use the SBE CTD in various configurations.

Originally all floats in Argo used the Systems ARGOS for communications; beginning in 2003 the first Iridium prototype floats were deployed. In recent years the number of Iridium floats has increased greatly, and it is projected that by 2017 nearly all floats in the Argo array will communicate using Iridium. There are two types of Iridium communications used by these floats. The Teledyne/Webb floats use Iridium/RUDICS, a packet-switched version that requires floats to login to a land-based server to transmit their data. The SOLO-II floats use Iridium/SBD (Short Burst Data), a version that transmits data in a form analogous to a text message and is received as an email message. There are advantages and disadvantages to each of these methods. RUDICS requires a dedicated server and substantial processing software but allows nearly an unlimited amount of data to be transmitted during a single session. SBD is simpler

(and somewhat cheaper) but is more limited in the amount of data that can reasonably be transmitted in a single session.

At present, the Teledyne/Webb floats carry sufficient batteries to collect over 300 profiles from 0-2000 m, with data transmitted at 2 m intervals using Iridium; a number of these floats have lasted well over 7 years. The SOLO-II floats are as yet only a few years old, but their higher efficiency suggests that they should be able to last as long or even longer. The readiness of these profiling floats is considered mature.

Sensors and sampling

Given the reliability of the buoyancy engine on these floats, various groups have attempted to add additional capabilities and functionality to the instruments. Several versions of dissolved oxygen sensors have been added (SBE 43, Aanderaa 3830 and 4330, SBE 63), with varying results (Riser and Johnson, 2008). These sensors have proven to be reliable over times of several years in the sense that they continue to operate and provide useful data, but there are ongoing problems with calibration and drift that are being addressed. Additionally, several versions of dissolved nitrate sensors have been used successfully, including both ISUS and SUNA (Johnson et al., 2010). To date, these sensors have been built at MBARI and have not been generally available commercially; however, it is likely that a commercial version will be available from Satlantic, Inc. within a year or two. Additionally, MBARI has developed a Durafet-based pH sensor for deep-sea use that has been successfully deployed on several floats. Given the present interest in ocean acidification, it is likely that the use of these sensors will grow in the future. Efforts are now underway to find a suitable commercial vendor. Particulate backscatter and chlorophyll sensors (FLBB sensor, commercially available from Wet Labs, Inc.) have also been successfully added to floats (Boss et al., 2008). In addition, floats have carried hydrophones that can be used for low-frequency acoustic tracking (RAFOS) and also for higher-frequency studies that attempt to estimate wind-speed and rainfall rates acoustically (Riser et al., 2008). In the near future, it appears that a version of a pCO2 sensor will be marketed by Aanderaa, and it is likely that a prototype float carrying such a sensor will be deployed shortly after the sensor becomes available.

Other capabilities

Originally floats were deployed from research vessels while on station. By the 2002, it was possible to deploy floats from rapidly moving container ships, allowing important expansion in the geographical extent of the Argo array. Additionally, several hundred floats have been air-deployed by US Navy C130 aircraft, with good success. At this present time, this capability is not available to non-navy researchers (it was used by civilian scientists during the years 2003-2006), but there is hope that civilian air deployments might resume in the future. To allow the array to expand to higher latitudes, the capability of using floats under sea-ice has been developed and used extensively in the Antarctic (Wong and Riser, 2011). Using the present generation of floats in the Arctic, where the buoyancy requirements are more severe, is more problematic, but such deployments will be attempted in the near future.

Deep floats

There is considerable scientific interest in sampling the global ocean at much greater depth than is possible with present Argo-style profiling floats. To this end, several new prototype floats have been produced. In Japan, a 4000 m version of the Ninja float has been deployed, and in the US both Scripps and Teledyne/Webb have produced and tested versions of 6000 m floats. These testing efforts are ongoing, with the goal of having tested and reliable floats available by 2015. The Argo Steering Team has set a goal of eventually having such deep floats comprise as much as 1/3 of the Argo array, in order to examine the heat content of abyssal waters and the changes in properties of these waters over time.

Such deep floats will not be inexpensive, owing to their increased complexity in order to withstand extreme pressure cycling over many years. Additionally, increased CTD accuracy and precision will be required for such floats, given the considerably smaller temperature and salinity signals in abyssal waters. Issues such as a suitable sampling strategy for these deep floats, and additional sensors that might be carried, await the continued successful testing of these prototypes. The deep-floats have a readiness of pilot at this time.

2.2 Underwater gliders

Description

Autonomous underwater gliders developed over the last several years, and now operated routinely, offer the possibility of sustained fine resolution observations (Rudnick et al., 2004). In typical use gliders profile from the surface to 500-1000 m, taking 3-6 h to complete a cycle from the surface to depth and back. During the cycle the gliders travel 3-6 km in the horizontal for a speed of about 1 km/h. Deployments of 3-6 months are routine, during which time the gliders survey track extends well over 2000 km. During a few minutes on the surface, gliders obtain location by GPS and communicate through the Iridium satellite phone system. Gliders may be deployed and recovered from a wide range of platforms, including small boats and chartered fishing vessels.

Underwater gliders profile by changing buoyancy, and move horizontally through lift generated by wings. Missions of long durations are possible because gliders move slowly to limit the loss of energy to drag. Propeller-driven autonomous underwater vehicles (AUVs) might also be used to achieve similarly long missions if they were driven comparably slowly. Such long-range AUVs have been conceived and deployed, including hybrid vehicles that use both buoyancy and propeller. But it is fair to say that most propeller-driven AUVs are used for short-duration, high-speed missions, and do not have the record of sustained operations as do underwater gliders.

Sensors and sampling

Underwater gliders are profile generating machines, much like profiling floats, with the added capability of control over horizontal position. Sensors on gliders measure such physical variables as pressure, temperature, salinity, and velocity, biological variables relevant to the abundance of phytoplankton and zooplankton, and ecologically important chemical variables such as dissolved oxygen and nitrate. In sustained operation gliders are most often used to repeat a survey pattern, the simplest being a single repeated line. For example, three

approximately 500-km lines off California have been continuously occupied starting in 2006, constituting the longest running sustained glider network to date (Davis et al., 2008; Todd et al., 2011a; Todd et al., 2011b). In the first attempt at a sustained equatorial glider deployments two gliders were recently deployed from the Galapagos Islands, with the goal of making repeated sections along 93°W, between 2°N-2°S (Figure 2.1). One glider takes about 20 days to complete this line, so the two gliders provide a realization of this section on a roughly 10-day interval. To summarize, in an equatorial application, underwater gliders would provide 10-day resolution of a section between ±2°, with 150 profiles per section when profiling to 500 m.

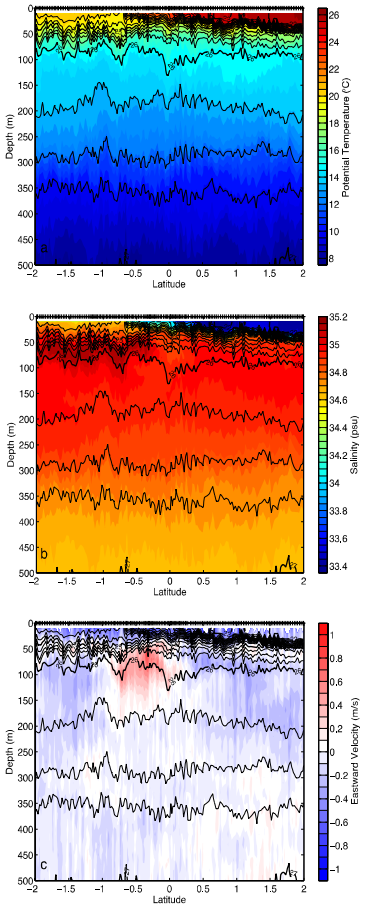

Figure 2.1 - Sections of (a) potential temperature, (b) salinity, and (c) eastward velocity at 93°W measured by two Spray underwater gliders equipped with CTDs and Doppler current profilers. Values for each variable are indicated by color shading, and potential density is contoured using black lines. Tick marks on upper axes of each panel indicate the locations of 170 profiles for an average spacing of 2.6 km. The section was occupied during 24 October – 6 November 2013. Note the equatorial front at the surface near 0.7°S, salty water from the south penetrating to 0.3°S between 25-26 kg m^{-3}, and the equatorial undercurrent near 80 m depth and 0.3°S.

Operations

Underwater glider operations involve a series of considerations with substantial effect on operations. Glider operations include refurbishment, shipping, deployment and recovery,

piloting, communication, and data acquisition, archiving and quality control. Glider operators in the US (Rudnick et al., 2012) are now doing routine sustained missions, with 3-4 glider deployments per year. Thus the readiness level of gliders can be considered mature. This sort of operation is practical from land exclusively using small boats for deployments and recoveries. A number of efficiencies may be achievable with a fully realized network of gliders. If glider missions can be lengthened the annual operating costs could be lowered. While it is fairly simple to add batteries to gliders, the ultimate limiting factor is likely biofouling. Capital costs could be dramatically lowered if the market for gliders were bigger, as is the market for profiling floats. In any case, with current operational constraints and costs it is practical to begin an equatorial glider network. Because gliders have not yet been used routinely in the equatorial Pacific, this particular appplication has a readiness level of pilot.

2.3 Emerging Surface Moorings

Description

Emerging surface mooring technology shows promise of integrating Surface Ocean and atmospheric measurements along with sub-surface profiles in real-time (Figure 2.2). The smaller, easier to deploy technology is not necessarily intended to replace all conventional moorings, such as those used as reference stations with heavy and redundant instrument loads. However, the low cost, ease of deployment high frequency sampling, long endurance, and potential for some vandal resistance will complement some observing needs and completely enable other fixed time series measurements. Significant size and weight reduction can be realized with an integrated, easy to deploy mooring. Up to 10 complete deep-ocean moorings can fit in a single 40 ft container. This type of mooring is commercially available for tsunami observations (Lawson et al., 2012) and the design has been proven in limited production quantities (<12) in high and low latitudes and in depths up to 5000 m. Small climate type buoys are now in the advanced R&D stage and have collected data in limited tropical deployments, see Figure 2.3.

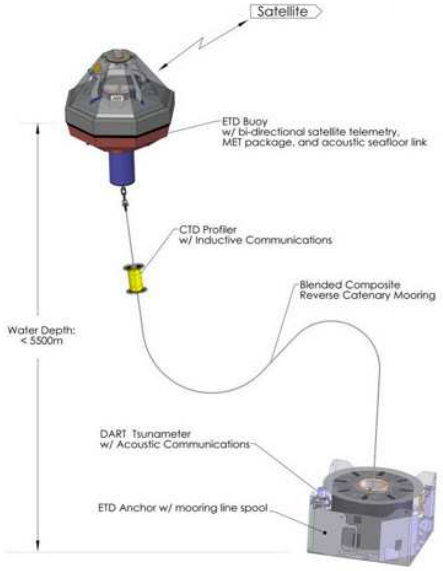

Figure 2.2 - Slack line PICO-PRAWLER mooring

Moored profilers that use wave energy from surface moorings to sample the water column are emerging and have made thousands of high resolution CTD profiles. Systems such as the Wirewalker (Pinkel et al., 2011), Brooke Ocean Technology Seahorse (Fowler et al., 1997) and the NOAA-PMEL PICO-PRAWLER (Milburn and Kessler, in prep) are potential candidates to fill a high-frequency/long endurance sampling niche. For example, a PMEL PRAWLER (Meinig, in prep.) has averaged ~25 profiles per day (over 6 months and up to 500 m depths) for a recent experiment at 20°N 38°W. The PRAWLER, Wirewalker and Seahorse use wave energy for locomotion and batteries control and inductive communications, and can accommodate a limited number of low-power sensors.

Sensors and sampling

Small surface buoys cannot host as many sensors as large traditional Ocean Climate Station type buoys. However, many small buoys are hosting meteorological and biogeochemical sensor payloads with sufficient power and real time communications. Profilers on surface moorings require a continuous length of wire to climb and make profiles. Although the surface wave action provides motive power, batteries are still required for sensor, processor and inductive communication.

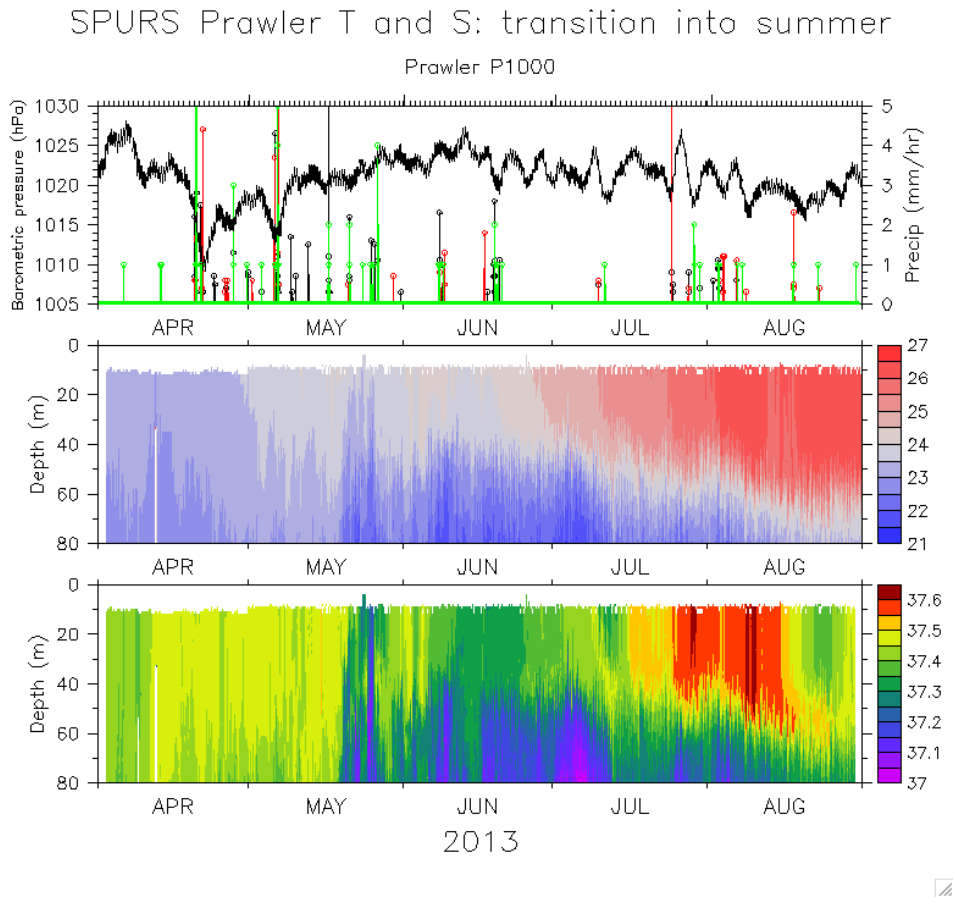

Figure 2.3 - The top panel includes rain rate from two SPURs PRAWLER moorings (black and red), and the WHOI mooring (green). Temperature and salinity shown from PRAWLER in bottom panel.

Operations

The comparison chart outlines the advantages and tradeoffs using small surface moorings.

Comparison Chart:

	Emerging Moorings	Conventional Moorings (CM)
Size	20 pre-packaged PICO units can fit into a single 40 ft. shipping container.	1-2 CMs fit into a 40 ft. container in ~15 pieces each (anchors, buoy, bridle, tower, wire rope, nylon line, barrels of chain, hardware, and tools).
Sea Transport	Can be sent aboard smaller vessels of opportunity, i.e. a fishing craft on its regular route. Able to deploy in higher sea states than CM.	Large research ships with specialized personnel and equipment.
Building & Assembly	Pre-built, factory assembled, and deployment-ready when shipped.	Deployments are sea state limited. Shipped in many parts and assembled on ship deck with skilled technicians in the field.
Manpower	Can be deployed by 1-3 people with basic seagoing skills. Buoy/mooring experience is unnecessary.	Requires 6-12 specialized crew and technicians.
Operational Life	Estimated 2-3 years.	1 year.
Vulnerability to Vandalism	Smaller surface expression that is harder to see and has less radar return. Nothing to climb on and no hardware to steal.	Vandalism is a major cause of failure for CMs.

A specialized organization and facilities are required to support sustained ocean climate observations. The stringent requirements on sensor accuracy and real-time quality control require constant vigilance. Functions include: specification, procurement, integration, calibrations, packaging, engineering, testing, quality control, advocacy and leadership for TPOS etc. Technology obsolescence, software development, sensor firmware upgrades and software maintenance need constant attention. These relatively new surface moorings have a readiness level of pilot.

2.4 Conventional Moorings: TRITON and m-TRITON system

TRITON

Description

The basic technology was developed in 1990's based on the ATLAS buoy taut-line mooring system. The biggest difference between ATLAS and TRITON is the concept for safety operation. The surface buoy was designed to persist under higher vandalized area with strong towing cases. The surface float is 2.4 tons in air, and has 7 tons of buoyancy. The wire cable is 18 mm diameter down to 750 m, and Nylon is 24 mm diameter down to the sea bottom. The scope is 0.9, which is similar to ATLAS. The TRITON is equipped with mid-depth buoyancy to aid recovery sensors in case the surface buoy is lost.

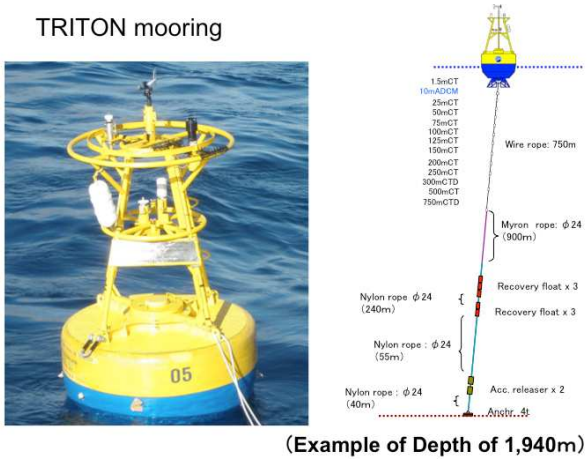

Figure 2.4 - A TRITON mooring.

Sensor and sampling

The ocean sensors are SBE37IM for underwater temperature and salinity measurements, and Teledyne current meter for 10 m velocity. In addition to the commercial CTD sensors, a JAMSTEC original CTD sensor has been developed and tested, including a calibration system adhering to Japanese national standards (Ando et al., 2005). The meteorological sensors are packages of JAMSTEC original signal processing system with commercial sensors from R.M. Young and other manufacturers. The sampling strategies are the same as ATLAS and the depth of ocean sensors are the same as TAO in the western Pacific.

Argos-2 is used for the data telemetry system, which collects the 1 hour data in near real time. The data return rate in real time and delayed modes are continuously higher than 80% in the last 13 years, except for the sites near the coasts of New Guinea and Sumatra.

The main cause of reduced data return is vandalism. Various countermeasures have been used over the years, but it is impossible to protect from vandalism perfectly. Even in such severe conditions, the countermeasures worked to some degree, and the data return rate from TRITON buoy system was higher than m-TRITON and ATLAS. Following is a list of vandalism countermeasures for the TRITON buoy system.

- Pentagon type bolts and nuts
- Stainless steel tower
- Hidden satellite transmitter to send position for backup
- Flat type transmitter to send data
- Double steeled wire rope down to 750 meters
- Underwater sensor protectors from long-line
- Iron-mask met tower for the heavily vandalized region
- Meteorological sensor and tower painted to look old and vandalized

Operations

TRITON moorings are a highly mature technology. A goal is to lengthen mooring deployments from the current 1 year to 1.5 year, to at least 2 years in future. The main challenges are vandalism and biofouling to sensors. For vandalism, towing by fishing boats is the main issue, so we are testing double steeled wire rope. Biofouling problems are not well solved yet, and it is just confirming stage about the quality of data from 1.5 year mooring.

m-TRITON

Description

Unlike the TRITON buoy system, m-TRITON is designed to be deployed by smaller vessel of 2000 tons. The system is not taut line but slack line type (Ueki et al., 2010). By using slack line, the weight of the surface buoy is 1/3 as much as TRITON. Below the surface buoy, buoyant line is used below nylon line to keep the mooring S-shaped below sea surface.

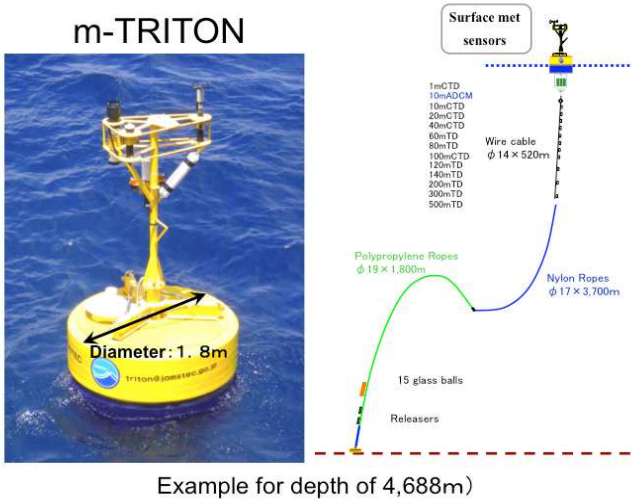

Figure 2.5 - An m-TRITON mooring.

Sensors and sampling

The sensors for m-TRITON are the same as for TRITON. The data telemetry system for m-TRITON is Argos-3, which allows two-way communication with higher data transmission, as

often as every 10 minutes. The data return rate is lower than TRITON as the mooring system is small. Again vandalism is the main cause of reduced data return. The prevention of vandalism is particularly important in the eastern Indian Ocean, where vandalism occurs more often than in the western Pacific Ocean. Countermeasures are almost same as TRITON.

Operations

m-TRITON moorings are a mature technology. A goal is the same as that of TRITON, but it would be more difficult to lengthen mooring deployments from the current 1 year to 1.5 year, to at least 2 years in future. The main challenges are vandalism and biofouling to sensors. For vandalism, towing by fishing boats is the main issue, so we are also testing double armored wire rope. Biofouling problems are not well solved yet.

2.5 Subsurface moorings with acoustic links

Description

Subsurface moorings with acoustic telemetry links are candidates for adding capability to the sustained tropical observing system. They are fully submerged and thus not subject to vandalism, and also exhibit reduced impact of biofouling compared to platforms permanently or frequently at the surface. Experience has shown that they can be deployed such that the uppermost sensors are within about 30 m of the surface (Send et al., 2011), providing good vertical coverage except right at the surface. Deployment durations of 2-3 years are routine, and the design and cost is relatively cheap since the subsurface environment is not very demanding. In addition to telemetering data acoustically, other methods to recover data from subsurface moorings exist, including data capsules that get released to the surface at fixed intervals, and loose small tethered telemetry floats with very low profiles at the surface.

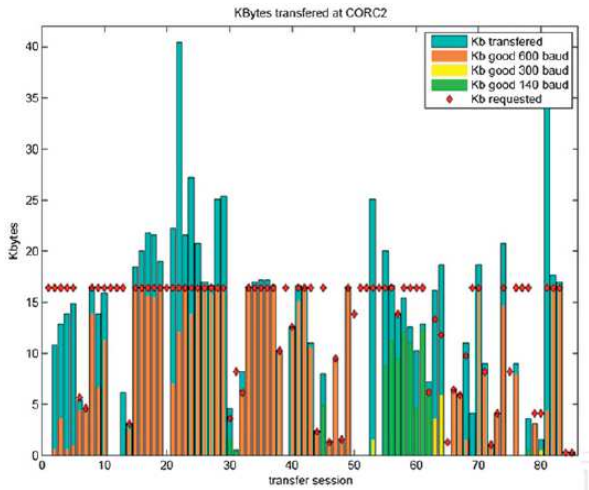

Figure 2.6 - Diagram summarizing the data transfer success from a 160-day Spray glider mission, for the CORC2 mooring in the California Current; each bar represents one dive. The red diamonds show the number of kbytes requested/sought during the dive. The overall height of the bar shows the number of kbytes received, and green/yellow/brown show the amount of good data received (color coded by baud rate).

Technical developments from the NOAA CORC project have resulted in the now routine capability to use commercially available acoustic modems, and inductive communication *within* the mooring, to telemeter all sensor data to gliders or ships which pass by the mooring (Send et al., 2013a). This works well over horizontal ranges of 2-5 km, with the modem in the mooring at a depth between 1500 m and 4000 m. A typical data transfer session by a glider requests 16 kB of data, and a typical data transfer success rate is 75% (Figure 2.6). A standard modem has sufficient battery power to transmit 2-3 Mb of data during a deployment, which is sufficient for most discrete sensors and ADCP current profilers using standard sampling/ensemble intervals of 30 minutes to 2 hours. Projects where this is being used routinely at present are the California Current NOAA CORC (Figure 2.7) and the NSF OOI (http://oceanobservatories.org/infra- structure/ooi-station-map/station-papa/).

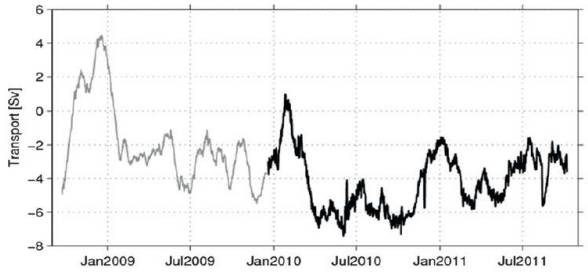

Figure 2.7 - Geostrophic transport (relative to 3500 dbar) of the California Current component over deep water, derived from microCat data on two CORC moorings. The black line shows transports entirely derived from data downloaded acoustically with gliders.

Two brands of gliders are now available with this capability, the SIO Spray glider and the Teledyne Webb Slocum glider (Rudnick et al., 2004). While the transducer takes up some payload space and weight in the glider, the additional task of retrieving mooring data does not seriously impact the power budget since the glider modem mainly listens which consumes less energy than the mooring modem requires. As such, in a tropical array, gliders traversing a meridional section as suggested in the glider description above, could pass by subsurface moorings on each transect and retrieve/telemeter the mooring data. In those areas which are too remote for glider deployments from land/islands and where gliders need to be deployed/recovered with ships, glider endurance can be enhanced by profiling less often, loitering at depth for periods of one or several days. The longest mission achieved in this way is 375 days.

Sensors and sampling

A minimum suite of physical sensors for the subsurface moorings probably is a set of high-precision temperature/conductivity instruments, clamped onto the wire and communicating inductively, in order to observe stratification changes and to calculate dynamic height relative to e.g. 1500 m depth (for zonal pressure gradients). This usually requires 10-15 instruments from the top of the mooring down to 1500 m (Kanzow et al., 2006). In addition, an upward-looking ADCP can cover the layer from near the surface to depths of 150m or 500m, depending on resolution and proximity of bins near the surface required.

Subsurface moorings are able to carry virtually any set of biogeochemical autonomous sensors, including large, heavy, or power-hungry instruments. These can be incorporated into the

uppermost floatation if measurements near the surface are of interest, or they can be distributed along the mooring wire, either clamped-on or integrated into larger load-cages (Ohman et al., 2013). Typical sensors on such moorings would measure dissolved oxygen, pH, nutrients, chlorophyll fluorescence, optical backscatter/absorption, or down welling irradiance (measuring this at several levels allows determination of column-integrated chlorophyll). Passive and active acoustic instruments for sensing of marine organisms or mammals can also be accommodated, as well as water samplers, wet-chemistry analyzers, or genomic instruments. Most of these data can be telemetered inductively and acoustically.

Operations

For estimating manpower effort and ship time needs, two sample cases are considered – one where a total of 3 moorings are operated by an agency or institution, and one where 10 moorings are operated, both with a 2-year service interval.

Purchasing, assembly, maintenance, and testing of mooring components in the lab requires approximately 9 person-months of technical staff (shared between one engineer and one mooring technician), for approximately 3 moorings, or 12 person-months for 10 moorings. The work related to cruise preparation, shipping, execution, demobilization, is estimated to require the same person-months again. This means that a team of 2 FTEs can service and deploy 10 subsurface moorings each year (1.5 FTE for 3 moorings). If data retrieval, processing, dealing with telemetry issues, basic quality-control, and dissemination is added, that requires another FTE for 10 moorings continuously (or 0.75 FTE for 3 moorings continuously). Since the moorings only need to be deployed every 2 years, the average FTE effort would be 2 FTE for 10 moorings, or 1.5 FTE for 3 moorings (in terms of expertise, 3 people are desirable, but they can do other things 1/3 to 1/2 of the year). A medium-size research vessel is required for deployment and recovery of these moorings, the requirements of the ship are modest since no single component is very large or heavy (with the exception of maybe the anchors, which can be slid/tipped into the water without need of lifting them). Two cruise participants are needed who are trained in the handling of this type of equipment, while another 2-3 people are required to assist in handling gear and lines on deck.

For ship time needs, we could make the most conservative assumption that a cruise is executed every 2 years for nothing other than servicing 3 or 10 subsurface moorings. For this scenario, we estimate 3 weeks of transit and 1.5 days station time per mooring, every 2 years. Then the ship days (including transit) needed are 4.25 days/mooring/yr for 3 moorings, and 1.8 days/mooring/yr for 10 moorings. Since in general the ship time will be shared, the assumption can be made that half the ship costs are assigned to the subsurface mooring work. In that case the annual ship time need per mooring is 1.5-2 days, depending on the number of subsurface moorings operated. The technologies employed for this approach are mature, and are being routinely used in a number on ongoing ocean observing programmes.

2.6 Moored profilers

Description

Moorings can carry vehicles that profile vertically with a diverse sensor suite. Currently existing types of moored profilers are wire-crawlers, wire-ratcheting systems, and underwater winches.

Wire crawlers are the most widely used moored profiler, with the MMP sold commercially by McLane Research Labs. It is only deployed on subsurface moorings (a surface buoy causes too much vertical wire excursion), and uses a motor/wheel mechanism to roll up and down the mooring wire. It can cover the entire water column, but experience has shown that failure risk increases when the top of the mooring and profiling range is closer than about 150m from the surface. The total profiling distance with full batteries is about 800,000 meters. Versions are now available which can communicate inductively through the mooring wire, so the data could be assembled in a deep mooring controller and telemetered acoustically from there. The advantage is that no surface mooring is needed (no vandalism, less fouling, longer endurance), but the method does not provide observations near the surface.

A different technology uses the vertical excursion of the wire underneath a surface buoy in the presence of surface wave activity, in order to ratchet a buoyant platform down the mooring wire. Once it reaches a pre-determined lower profile depth, it stops, and then can rise up the wire using its buoyancy. This uses no battery power for the profiling itself. Available models are the Seahorse profiler and the WireWalker. They also communicate inductively, here with the surface buoy, which allows telemetry to shore. These systems require a surface buoy, which may be perceived as a drawback given problems with vandalism and endurance of some tropical surface moorings.

Moored winched profilers use mechanical winching of a wire in order to profile from the upper end of the static subsurface mooring to typically the surface. When the platform breaks the surface, it can establish communication to shore. At first sight this is an elegant approach, since the mooring itself avoids the surface, making it more robust and long-endurance, reducing fouling and vandalism, and reducing the fish-attracting “reef effect”. However, building and operating a reliable underwater cable spooling mechanism is demanding. In the model by WET Labs (AMP/”Thetis”) the winch and the sensors are both located inside the profiling body, which raises itself to the surface and then winches itself down again against its buoyancy. It has a maximum working depth of 100 m, can carry out 180 profiles (to 100 m). The Ocean Profiler by NiGK has the winch stationary at depths up to 250 m, and the sensor float is raised to the surface/pulled down again. The maximum profiling depth is 250 m and it can perform 250 profiles to 100 m. The buoyancy and sensor payload of both models is limited, which may pose problems when operating in stronger currents.

Another winched approach is the “SeaCycler” developed by BIO/Halifax and being commercialized by Rolls Royce Canada (Send et al., 2013b). In this system, the winch remains at depth, and in fact winches itself down as the sensor platform is raised to the surface. The buoyancies of the two bodies are balanced such that potential energy is exactly conserved during profiling, meaning that (other than friction and motor inefficiencies) no energy is required for the profiling itself. This allows large buoyancy for the sensor platform (over 75 kg), enabling operation also in larger currents. Typical lower parking depth is 150-250 m (depending on expected currents), number of profiles is 400 or 800 depending on battery (alkaline or lithium) . A drawback is a much larger size (and cost) of the system, which in its current version is designed to withstand pressures up to 1000 dbar (which can result from mooring blow-over by strong currents).

Sensors and sampling

All profilers usually carry a diverse suite of sensors in their current applications, measuring for example temperature/salinity, currents, oxygen, chlorophyll fluorescence, and other optical quantities. The SeaCycler is designed for larger, heavier, or more power-hungry sensors, which can include CO_2, nutrients, acoustic backscatter systems, or wet-chemistry systems.

Operations

The most common type of wire crawler must be considered mature due its wide-spread use, but many users report that highly specialized expertise and great care is required to make them function reliably, so maybe it is less than “operational” or “sustained”. The wire-ratcheting profilers are in an advanced pilot phase, possibly bordering on mature. All winched profilers are still in the early demonstration or pilot phases, and extensive field experience with long deployments in diverse environmental conditions is still lacking. The overall less-than-mature development stages of the moored profilers also imply that more specialized staff and more effort is needed to successfully operate these systems in a sustained mode. By 2020 however, some of these system should be operational.

2.7 Unmanned surface vehicle (USV)

Description

Unmanned surface vehicles are rapidly evolving and offer the possibility of sustained fine resolution surface and subsurface observations. Only USVs with the potential of long ranges and high endurances will be discussed.

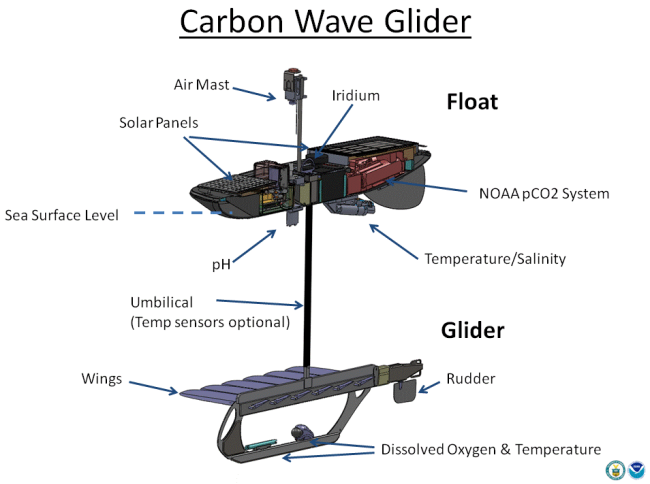

Figure 2.8 - Schematic of a NOAA Carbon Wave Glider.

USVs such as the Liquid Robotics Wave Glider (Hine et al., 2009), that use wave power for propulsion and solar power for electrical power, have crossed the entire Pacific and the first generation SV2 fleet has logged over 400,000 NM. A limiting factor for MET measurements is the small mast and low height to the water. A larger SV3 vehicle with significantly larger payload, slightly higher mast and additional power is now commercially available as well.

Speed is wave and current dependent, but has averaged around 1 kt in several missions over 30 days in duration (Meinig et al., 2012). Numerous scientific, military and national security missions with a broad array of sensors (including carbon, see Figure 2.8) have been completed in high and low latitudes.

Wind powered USVs (Sailbuoy, Saildrone, Ocean Aero, Harbor Wing, Robotboat) are also rapidly developing, but less mature and have only been deployed with limited sensors. This class of USVs is typically 2-4 m long with a 4-5 m mast. Speed is wind and current dependent, on a recent deployment of the Saildrone from San Francisco-Hawaii-Palmyra, the vessel averaged 3-4 kts over >100 days (Saildrone.com). Deployments of 3-6 months are now possible with very limited proven scientific payloads.

Figure 2.9 - Wind Powered Saildrone.

Sensors and sampling

The unique advantage of USVs is that they have persistent surface presence and use wave, wind and currents for propulsion and can navigate thru waypoints in high and low latitudes. Solar cells and batteries provide payload power and the space available is larger than profiling floats and underwater gliders, but smaller than surface moorings.

Operations

USV operations involve a series of considerations with substantial effect on piloting and costs. Wave gliders require a small boat to recover and deploy from the near shore. Some present USVs have been successfully deployed and recovered from a dock, requiring only a small harbor tender. USV operations include refurbishment, shipping, deployment and recovery, piloting, communication, and data acquisition. This sort of operation is practical from land using exclusively small boats for deployments and recoveries for several classes of vehicles. A number of efficiencies may be achievable with a fully realized network of USVs, underwater gliders and buoys since the personnel and physical infrastructure to deploy and maintain them is similar. In any case, given the large distances that USVs have already proven themselves, the technology should be strongly considered for inclusion into the R&D portfolio for tropical measurements with a readiness level of pilot.

2.8 Dual-Use Subsea Telecommunication Cables

Description

For the first time, serious considerations are being given to add sensors to commercial subsea telecommunications cables. Over the past three years, the International Telecommunication Union (ITU), the Intergovernmental Oceanographic Commission of the United Nations Educational, Scientific and Cultural Organization (UNESCO/IOC), and the World Meteorological Organization (WMO) have organized three workshops to bring the science, engineering, business and law communities together. Focus has been on disaster mitigation (tsunami, sea level rise, earthquakes) and moving towards a demonstration project. Three publications are available (http://www.itu.int/en/ITU-T/climatechange/task-force-sc/Pages/default.aspx)

Sensors and sampling

The initial sensors being explored for inclusion on future cables include 1) high resolution pressure, 2) seafloor temperature and 3) seismic instrumentation. Subsea cables have a proven life of > 20 years and provide wide bandwidth and power to seafloor sensors.

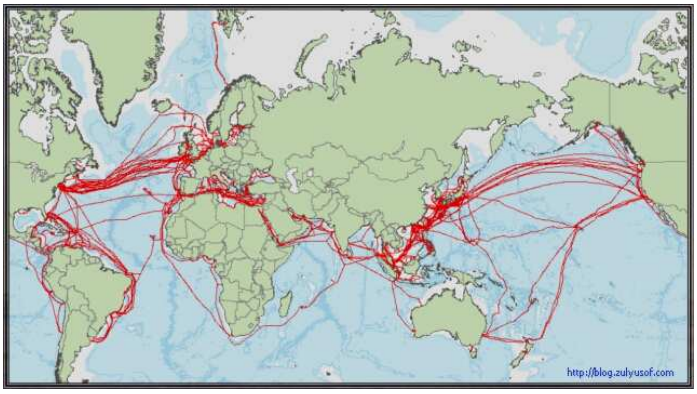

Figure 2.10 – Overview of subsea cables.

Operations

A large trans-Pacific cable is a substantial undertaking with significant unknowns. As such, the readiness level is considered concept.

2.9 Surface drifters

Description

Floating objects were likely used to make the earliest observations of ocean currents, hundreds of years ago. Over the last few decades, the Global Drifter Programmeme (GDP) has pioneered the global observation of surface current, with an average of 1250 drifters in the water over the last ten years (Maximenko et al., 2013). A GDP drifter uses a holey-sock drogue at 15-m depth tethered to a surface float that communicates via satellite. Most current GDP drifters use the Argos satellite system, but a growing number are moving to Iridium communication and GPS navigation. The GDP is a firmly established component of the global ocean observing system,

and the combination of drifter velocities with satellite sea surface height has produced definitive maps of global mean geostrophic surface currents.

Sensors and sampling

The standard sensor suite on a GDP drifter includes temperature and atmospheric pressure in addition to the estimates of velocity from displacement. With standard Argos communication, these observations are transferred to shore several times per day. A large variety of sensors have been deployed on drifting platforms, including acoustic Doppler profilers, conductivity sensors, meteorological instrumentation, and wave sensors. The surface waves themselves provide the energy for drifting profilers, such as the Wirewalker (Pinkel et al., 2011).

Operations

GDP drifters are deployed from ships of opportunity, from research to commercial container vessels. The drifters are relatively easy to deploy by minimally trained personnel. Operational costs include the price of the drifters, shipping, and communication. More capable drifting profiling platforms may require a dedicated research ship for deployment and recovery. The GDP drifters are very mature observing platforms.

3. Discussion

The tropical Pacific observing system of 2020 will be some combination of the technologies discussed above. Deciding on the balance between these different approaches is a challenging problem that depends intimately on the scientific requirements. Until these scientific requirements are determined, presumably as an outcome of the TPOS planning process, any attempt at scoping out an observing system is probably a futile task. However, as an exercise of the tradeoffs involved, we think it is worthwhile to discuss how the technologies might be combined to achieve resolution in space and time, and to realize operational efficiencies.

One conception of a tropical observing system would start with enhanced Argo float density in a band around the equator. With standard Argo float density of one float every 3° square, there are about 50 floats in the equatorial band ±1.5°. Doubling this density would require an additional 50 floats, which might be deployed from either volunteer ships or a relatively inexpensive dedicated vessel. An open question is how long the increased observational density would last considering dispersion of floats off the equator. Finer resolution in space and time, atmospheric reference observations, and more intensive chemical/biological sampling can be achieved using moorings, underwater gliders, and USVs, perhaps a few of each deployed at a finite set of different longitudes. While such an array would require dedicated ship time because of the distances to be covered, the servicing of several platforms of different types is an operational efficiency. Savings might also be realized to the extent that some of the mobile platforms can be deployed near land or from less expensive vessels. The implementation of the observing system requires careful analysis far beyond this brief discussion, but the creative process of going through the possibilities will be valuable in and of itself.

Transitioning an observing system to new technology is a challenging task. An aspect of this challenge is to preserve the integrity of long time series during the transition. The guidelines provided by the 10 GCOS monitoring principles are helpful. For example, running new and

established technology in parallel for some time is essential. In the end, it takes a certain measure of daring to move on from methods that are tried and true. As long as this boldness is tempered by the resolve needed to sustain observations, the emerging technologies summarized above will likely lead to an improved tropical Pacific observing system.

References

Ando, K., Matsumoto, T., Nagahama, T., Ueki, I., Takatsuki, Y., and Kuroda, Y. (2005): Drift characteristics of a moored conductivity-temperature-depth sensor and correction of salinity data. Journal of Atmospheric and Oceanic Technology, 22, pp. 282-291, (doi:10.1175/Jtech1704.1).

Boss, E., Swift, D., Taylor, L., Brickley, P., Zaneveld, R., Riser, S., Perry, M.J., and Strutton, P.G. (2008): Observations of pigment and particle distributions in the western North Atlantic from an autonomous float and ocean color satellite. Limnology and Oceanography, 53, pp. 2112-2122, (doi:10.4319/Lo.2008.53.5_Part_2.2112).

Davis, R. E., Ohman, M.D., Rudnick, D.L., Sherman, J.T., and Hodges, B. (2008): Glider surveillance of physics and biology in the southern California Current system. Limnology and Oceanography, 53, pp. 2151-2168.

Fowler, G. A., Hamilton, J.M., Beanlands, B.D., Belliveau, D.J., and Furlong, A.R. (1997): A wave powered profiler for long term monitoring. Oceans '97 Mts/Ieee Conference Proceedings, Vols 1 and 2, pp. 225-228.

Hine, R., Willcox, S., Hine, G., and Richardson, T. (2009): The Wave Glider: A Wave-Powered Autonomous Marine Vehicle. Oceans 2009, Vols 1-3, pp. 1300-1305.

Johnson, K. S., Riser, S.C., and Karl, D.M. (2010): Nitrate supply from deep to near-surface waters of the North Pacific subtropical gyre. Nature, 465, pp. 1062-1065, (doi:10.1038/Nature09170).

Kanzow, T., Send, U., Zenk, W., Chave, A.D., and Rhein, M. (2006): Monitoring the integrated deep meridional flow in the tropical North Atlantic: Long-term performance of a geostrophic array. Deep-Sea Research Part I-Oceanographic Research Papers, 53, pp. 528-546, (doi:10.1016/J.Dsr.2005.12.007).

Lawson, R. A., Graham, D., Stalin, S., Meinig, C., Tagawa, D., Lawrence-Slavas, N., Hibbins, R., and Ingham, B. (2012): Next Generation Easy-to-Deploy (ETD) Tsunami Assessment Buoy. Oceans, 2012 - Yeosu.

Lindstrom, E., Gunn, J., Fischer, A., McCurdy, A., and Glover, L.K. (2012): A Framework for Ocean Observing. UNESCO 2012, IOC/INF-1284, doi: 10.5270/OceanObs09-FOO.

Maximenko, N. A., Lumpkin, R., and Centurioni, L. (2013): Ocean Surface Circulation. Ocean Circulation and Climate, G. Siedler, S. M. Griffies, J. Gould, and J. A. Church, Eds., Academic Press, pp. 283-304.

Meinig, C., Steele, M., and Wood, K. (2012): Taking the Temperature Of the Arctic With UMVs. Sea Technology, 53, 23 pp.

Ohman, M. D., Rudnick, D.L., Chekalyuk, A., Davis, R.E., Feely, R.A., Kahru, M., Kim, H.J., Landry, M.R., Martz, T.R., Sabine, C.L., and Send, U. (2013): Autonomous ocean measurements in the California Current Ecosystem. Oceanography, 26, pp. 18-25, (doi:10.5670/oceanog.2013.41).

Pinkel, R., Goldin, M.A., Smith, J.A., Sun, O.M., Aja, A.A., Bui, M.N., and Hughen, T. (2011): The Wirewalker: A Vertically Profiling Instrument Carrier Powered by Ocean Waves. Journal of Atmospheric and Oceanic Technology, 28, pp. 426-435, (doi:10.1175/2010jtecho805.1).

Riser, S. C., and Johnson, K.S. (2008): Net production of oxygen in the subtropical ocean. Nature, 451, pp. 323-U5, (doi:10.1038/Nature06441).

Riser, S. C., Nystuen, J., and A. Rogers, A. (2008): Monsoon effects in the Bay of Bengal inferred from profiling float-based measurements of wind speed and rainfall. Limnology and Oceanography, 53, pp. 2080-2093, (doi:10.4319/Lo.2008.53.5_Part_2.2080).

Rudnick, D. L., Davis, R.E., Eriksen, C.C., Fratantoni, D.M., and Perry, M.J. (2004): Underwater gliders for ocean research. Marine Technology Society Journal, 38, pp. 73-84.

Rudnick, D. L., Baltes, R., Crowley, M., Schofield, O., Lee, C.M., and Lembke, C. (2012): A national glider network for sustained observation of the coastal ocean. Oceans 2012, (doi:10.1109/OCEANS.2012.6404956).

Send, U., Lankhorst, M., and Kanzow, T. (2011): Observation of decadal change in the Atlantic meridional overturning circulation using 10 years of continuous transport data. Geophysical Research Letters, 38, (doi:10.1029/2011gl049801).

Send, U., Regier, L., and Jones, B. (2013a): Use of Underwater Gliders for Acoustic Data Retrieval from Subsurface Oceanographic Instrumentation and Bidirectional Communication in the Deep Ocean. Journal of Atmospheric and Oceanic Technology, 30, pp. 984-998, (doi:10.1175/Jtech-D-11-00169.1).

Send, U., G. Fowler, G. Siddall, B. Beanlands, M. Pittman, C. Waldmann, J. Karstensen, and R. Lampitt, 2013b: SeaCycler: A Moored Open-Ocean Profiling System for the Upper Ocean in Extended Self-Contained Deployments. Journal of Atmospheric and Oceanic Technology, 30, pp. 1555-1565, (doi: 10.1175/Jtech-D-11-00168.1).

Todd, R. E., Rudnick, D.L., Davis, R.E., and Ohman, M.D. (2011a): Underwater gliders reveal rapid arrival of El Niño effects off California's coast. Geophysical Research Letters, 38, L03609, (doi:10.1029/2010GL046376).

Todd, R. E., Rudnick, D.L., Mazloff, M.R., Davis, R.E., and Cornuelle, B.D. (2011b): Poleward flows in the southern California Current System: Glider observations and numerical simulation. Journal of Geophysical Research, 116, C02026, (doi:10.1029/2010JC006536).

Ueki, I., Fujii, N., Masumoto, Y., and Mizuno, K. (2010): Data Evaluation for a Newly Developed Slack-Line Mooring Buoy Deployed in the Eastern Indian Ocean. Journal of Atmospheric and Oceanic Technology, 27, pp. 1195-1214, (doi:10.1175/2010jtecho735.1).

Wong, A. P. S. and Riser, S.C. (2011): Profiling Float Observations of the Upper Ocean under Sea Ice off the Wilkes Land Coast of Antarctica. Journal of Physical Oceanography, 41, pp. 1102-1115, (doi:10.1175/2011jpo4516.1).

White Paper #13 – Data and information delivery: communication, assembly and uptake*

Smith, N.R.[1], and Hankin, S.[2]

[1] Retired Scientist, Melbourne, Australia
[2] NOAA Pacific Marine Environmental Laboratory, United States

* This white paper has not undergone the extensive community consultation of other white papers for this Review. Instead, it draws on material previously published as community papers, particularly for OceanObs09, and on relevant data and information findings from the other draft white papers. It also draws on input from Sylvie Pouliquen, Ken Casey, Scott Woodruff, Jim Cumming and Steve Worley, among others.

1. Introduction and history

This paper is principally addressing the 8th Term of Reference for the Tropical Pacific Observing System (TPOS) 2020 Workshop and Review:

Evaluate requirements for delivery of data, and derived products and information, in real time and delayed mode (e.g. availability, quality, latency, integration/interoperability); evaluate the existing data systems for fitness for purpose.

The view has been taken that recent community consultation, findings and recommendations on this topic remain largely relevant and appropriate for TPOS and that as a result further extensive review and evaluation was not warranted. As important as data and information management and delivery may be, it was also reasoned that the current systems did not contribute a major risk to the operation and impact of the TPOS now, or its evolution toward 2020. The TPOS 2020 Workshop will determine whether these judgments were sound.

The paper will largely focus on high-level aspects and general requirements rather than those for specific facilities such as TAO/TRITON or Argo which are largely covered elsewhere, and will be more in the context of the global systems than focused on TPOS.

Just as the Tropical Oceans-Global Atmosphere Experiment and OceanObs ’99 introduced paradigm shifts in our approach to data and information systems and exchange, this paper will argue that it is timely to consider yet another major change in our approach, with greater consolidation and integration of information management across the component parts of the Observing System, recognizing the data process and information systems as a service, both for the TPOS facilities/networks and for the ultimate users (scientists, operational agencies, policy and decision makers).

The tropical Pacific Ocean has long been a focus for innovation in ocean observation and science, from the early deployment of XBTs and monitoring of sea level, through to the major network and model development undertaken in TOGA (e.g., the initial TAO array; the first coupled model predictions of El Nino; the first free and open exchange of data in real-time) and WOCE (the development of floats and Argo; high-resolution models of the global ocean; innovations in scientific quality control, assembly and management of data).

McPhaden et al. (1998) provide background on the TOGA observing system and the importance of providing real-time, quality measurement; both were lacking for the 1982-83 event and

precipitated a major rethink in the approach. TAO introduced a new paradigm and systematic approach for ocean data and information delivery, a system that still underpins the current TAO/TRITON array. McPhaden et al. (2010) and TPOS WP1 highlighted the legacy of TOGA and the data and information systems established for the tropical Pacific, concluding they remain strong, particularly through the TRITON-TAO array and its pioneering role in open data exchange, real-time provision of subsurface data, and innovation in the assembly and serving of data and gridded data sets.

The community papers prepared for OceanObs ’09 cover much of the background and evaluation needed for TPOS 2020 (e.g., Pouliquen et al., 2010; Blanc et al. 2010; Hankin et al., 2010; de la Beaujardière et al., 2010; Beegle-Krause et al., 2010; Snowden et al., 2010). It is clear from those papers that data and information management has evolved and matured significantly since OceanObs ’99 and that the community of practice has also grown. In later sections we draw on these papers for conclusions and findings and, as appropriate place their recommendations into the current context.

The paper first examines some of the implications drawn from drafts of other papers contributing to the TPOS 2020 Workshop and Review. Next we draw out relevant findings and conclusions from previous community papers, and document implications for TPOS. The fourth section provides an evaluation and findings against the Terms of Reference, while the last section focuses on conclusions and recommendations.

2. Findings from other white papers

While at the time of writing a number of white papers remain in draft or outline form, a number of themes are already clear. The Global Ocean Observing System Framework for Ocean Observations provides the overarching context for TPOS 2020, and this is true for data and information management as much as it is for the observations process. At the most fundamental level the Framework consists of (a) scientific requirements, (b) the observation process, and (c) a data and products/output layer which we will term the data process. Part (a) influences priorities for (b) and (c); the solutions available for (c) influence choices in (a) and (b), and so on. Just as there are essential ocean variables, there are essential information system elements, and the feasibility and impact (utility) of possible information system contributions guide assessments of readiness and priorities for investment.

The Framework background document does address data and products but is less explicit around the definition of the data process or the way ‘readiness’ is assessed. Given the fact that TPOS will likely remain at the head of innovation, it may be timely to highlight essential ocean information system functions and promote assessments and metrics for these functions just as we do for ECVs.

The second theme running through many of the papers is the demand from science/research for efficient access to even more data; TPOS WP3, WP4 and WP5, among other papers highlight the need for even more detailed and comprehensive data in order to understand processes that are limiting advances in climate prediction and data assimilation. In the words of TPOS WP3 “We believe that this progress will come from observing, diagnosing, understanding and teaching models to simulate the physical processes that underlie ocean-atmosphere coupling,

and that this will have further benefits to much other science." Similar sentiments are expressed in several other papers.

The take home message here is that the scientific requirements will continue to be a key driver of information systems, not just for managing data and information from the sustained observation networks, but also from the several underway/planned and *ad hoc* process experiments that are targeting the tropical Pacific Ocean. In an ideal world, the information system would be designed to accommodate information services to such initiatives, but we are some distance from that at present. TAO/TRITON and Argo track the use of their data in scientific publications but we lack more general metrics to measure impact. Figure 2.1 provides an example of metrics maintained by IMOS for impact within the research community.

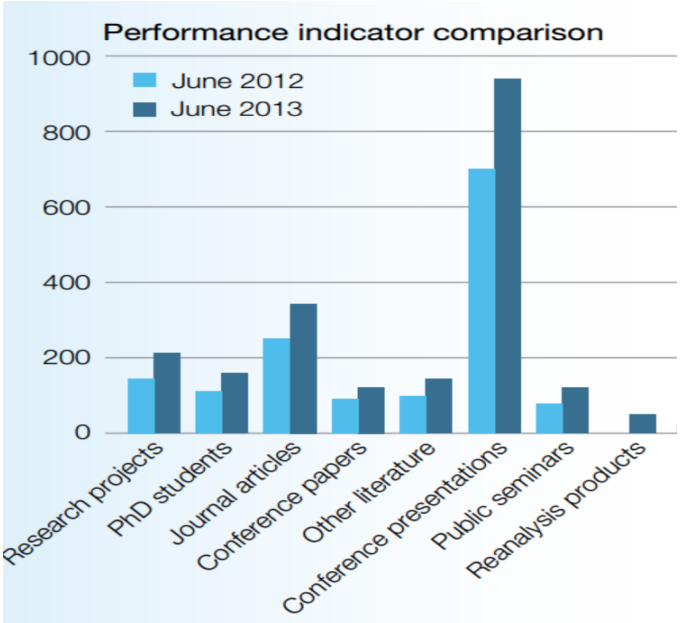

Figure 2.1 – Some metrics from 2012-13 from the Australian Integrated Marine Observing System (IMOS, 2013).

Another common theme was around the impact of modern information systems on the uptake of ocean data, products and information (see TPOS WP2 and TPOS WP8a, b in particular). This aligns directly with the concepts espoused in the Framework. We perhaps forget just how much change has occurred in the way the community accesses information, including in areas like the Pacific Islands, and that the notion "we want it all, and we want it now" is impacting information systems at a fundamental level.

TPOS WP3, WP9, WP10 and WP11 among other papers highlighted the importance of being able to bring diverse data to bear in both research and operational environments. The uses included validation of models, quality control, cross-calibration (satellites, Argo salinity), design and derivation of flux ECVs. In meteorology, Numerical Weather Prediction (NWP) systems play a dominant role in this area, however for TPOS we are still mainly operating at the lower levels of the data hierarchy (e.g., Level 2; see TPOS WP3 and TPOS WP11). Such requirements remain a challenge for our information systems. The effectiveness of both automated and subjective scientific quality control is directly dependent on our ability to place/view the data in

the context of related data streams and scientific knowledge; information systems are a key enabler. In this context it is also evident that information systems provide services to the observation process.

TPOS WP10 discusses data and information managements systems relevant to TPOS. The paper notes, among other things, that for “the global broad-scale in situ networks, data and information systems have developed around the individual networks” and that “if the primary utility of the high-resolution data is for regional observations including multiple data types, then consideration is needed for joint distribution of all datasets needed for a particular boundary current or other high-resolution phenomenon”. Our interpretation of these findings is that consideration should now be given to taking the data and information process up a level where it is feasible and practical to do so, a theme we will pick up later.

Finally, a number of papers highlighted data and information services that were needed but not provided, usually because of lack of resources. For example, in TPOS WP10, they note that there has been “no funding for Shipboard ADCP data processing within TAO since the 1990s” and that the onus often falls to individuals. Other papers note the challenges for managing underway SSS and SST data, and in Section 3 we note the difficulties in managing delayed-mode ocean-atmosphere data. At the edges of the core networks of TPOS support for data and information management is often thin or absent, in part because there is not the necessary scale of activity to justify investment. This does invite consideration of the concept of a (data and) information service, with an architecture capable of embracing *ad hoc*, experimental or small scale activities. If TPOS was to embrace the concept of an integrated approach to data and information management, built from the existing distributed network-based systems, then the data process would be seen as both a set of information systems and a suite of information services, to users within and beyond the TPOS.

3. Findings from previous community papers

TAO/TRITON and Argo have been exemplars for the development and implementation of effective and efficient data and information management systems. Pouliquen et al. (2010) describe the Argo data system (Figure 3.1 below) and highlight its ability to deliver to multiple requirements: fast data for real-time and near-real-time applications; delayed-mode data with higher levels of scientific quality control for climate applications and reanalysis; and data streams for general *ad hoc* scientific use. The use of selected hydrographic data to improve the quality of the larger Argo datasets exemplifies the power of the whole compared with individual datasets. Guinehot et al. (2009) provides yet another example of the whole system being used to add value to individual elements; TPOS WP9 provides other examples for satellite data. The key message here is that the data processing phase can and does add value to the observations process (observations of the ECVs) and vice versa.

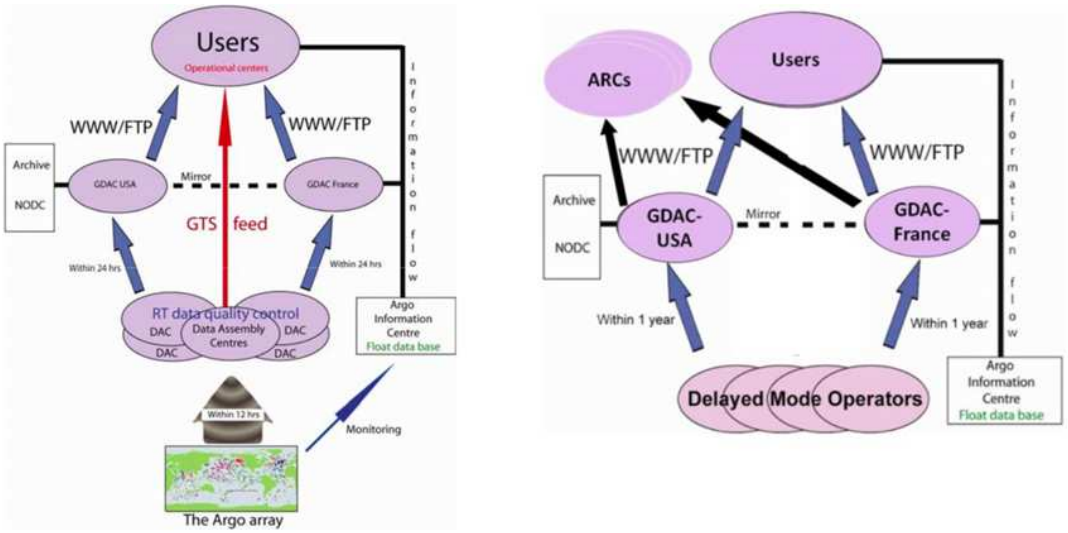

Figure 3.1 – (right) Panel showing the flow of real-time data from the network to users; (left) showing the value-add of delayed mode processing (after Pouliquen et al., 2010).

Blanc et al. (2010) discuss the contributions of GODAE to harmonising the production and exchange of various outputs and the development of essential and generic functionality to allow users access to products.

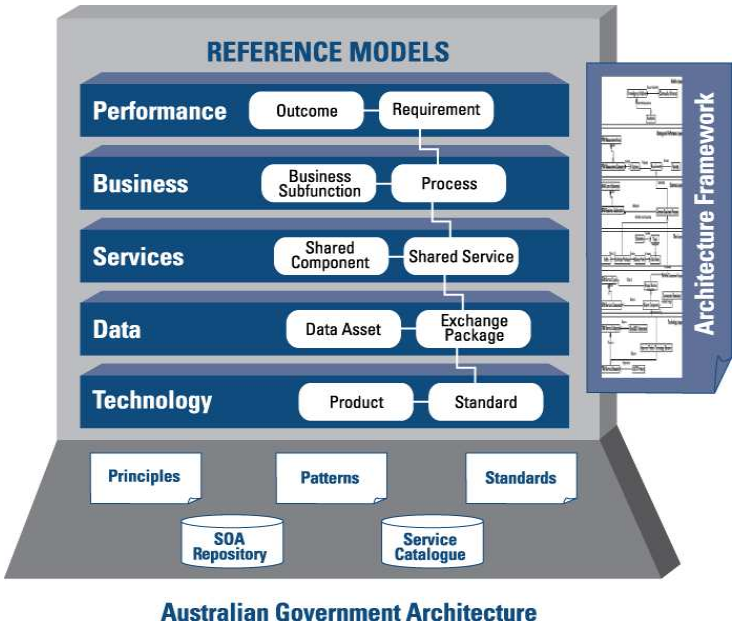

Figure 3.2 - Australian Government architecture model.

Hankin et al. (2010) pursue the discussion in the context of standards and exchange protocols. What both papers highlight is the importance of agreeing on a system architecture that serves of geospatial data and products. Agencies are often encouraged to adopt enterprise architecture approaches to ICT planning and development (Figure 3.2 shows the Australian Government model; you will note significant similarities to the architecture approach for ocean information

management).

Blanc et al. (2010) note the importance of joining up the global community and perhaps it is timely, in the context of an integrated approach to data management across not just TPOS but the whole of GOOS, to agree on an architecture for that (data and information processing) system. The importance of a community of practice is implicit in the discussions of both Hankin et al. (2010) and Blanc et al. (2010), among other papers. As the latter notes progress "is dependent upon the [the ability of the] community to work together, to maintain a network of experts and to agree upon common approaches … concrete implementation is done through large integrated projects or programmemes". TOGA and WOCE both fostered communities of practice and with consideration of TPOS 2020 it is timely to be more explicit about the role of a community of practice, to ensure an efficient approach to the essential ocean data management functions.

Belbeoch et al. (2010), and de la Beaujardière et al. (2010) refer to the scope of activities now being undertaken and the former highlights the value of a consolidated central information capability (JCOMMOPS) serving a broad range of users. De la Beaujardière notes "we have come to expect instantly available data and information" and as previously highlighted, the 'we want it all, and we want it now' culture is inevitably changing the architecture of our approach, with greater emphasis on the 'now'. De la Beaujardière et al. (2010) also pursue a theme around standards and recommend "existing open-standard approaches be used in preference to purpose-built or proprietary technologies", but emphasize the need for any standards to be purposeful and feasible (practical) (a pragmatic and sceptical approach; Hankin et al., 2010). We wish the community to move away from a culture where the investment is focused on IT innovation and focus more on using what we already have.

These same papers, as well as other white papers in this review, note that we have matured to the point where customised approaches for individual networks perhaps should be phased out in favor of more generic approaches (including for metadata), using industry-wide standards wherever practical and useful (the thinking behind Figure 3 is similar). Hankin et al conclude "We believe that a higher level of thoughtful awareness by the scientists, programme managers and technology experts of the vital role of standards and the merits of alternative standards processes can help us as a community to reach our interoperability goals faster." It would be timely for TPOS 2020 to make similar findings/recommendations.

De la Beaujardière et al. (2010) make reference to levels of maturity and the need to inform the user community about these levels. Such 'levels of maturity' are often used in areas such as project management and ICT implementation and such an idea is worthy of deeper exploration here. JCOMM, GODAE-OceanView and Argo, among others do provide a level of oversight and review of their data and information capabilities but there is an opportunity to take this to a new level in keeping with the risks associated with weaknesses/failures of the system. One such idea is a more formal approach to data publishing whereby there are agreed (formalised mechanisms) such as DOIs, perhaps even licences to publish certain data streams. The idea is not so much top down imposition of criteria but ensuring that the maturity levels are recognised and respected. Consideration of the handling of delayed-mode surface data has raised a number of issues (K. Casey, S. Worley, S. Woodruff, personal; communication). The

International Comprehensive Ocean-Atmosphere Data Set (ICOADS) is usually regarded as the definitive holding of ocean-atmosphere data. For the Global Tropical Moored Buoy Array (GTMBA) ICOADS usually relies on real-time transmissions over the GTS; this has worked reasonably well though the ability to produce high-quality data sets is constrained by the limitation on metadata transmission.

Delayed-mode data management and archiving is rather more problematic, partly due to the PMEL-NDBC transition; PMEL were good stewards of the data in the past. It is also partly because the governance around delayed mode GTMBA data is less well defined compared with real-time transmissions. The split of responsibilities within the US – NCDC, NDBC (previously PMEL), NODC, and then ICOADS probably does not help. NODC has been working with NDBC to improve the ocean data feed to the NODC archive. While the historical collection is not as clean and homogeneous as they would desire, data from January 2011 onward are now in excellent, interoperable netCDF formats. While not all data are coming in via this new modernized feed yet, NODC is confident the groundwork is now in place to enable the full and comprehensive datasets from NDBC to be archived at NODC with good metadata. The new data are already available to users by all of NODC's modern web services (not just ftp and http, but also via the THREDDS Data Server/OPeNDAP).

There are issues of substance with respect to the (historical) management and archive of GTMBA data, of which TPOS is a major subset:

- a high degree of format, resolution, and availability fragmentation.
- the ideal of a single dataset in a single format, of uniform quality is some way off.

There may be value in an effort to harmonise the metadata and data quality. There is at least potential in having someone look into this in more detail, to see the degree to which the above mentioned fragmentation has harmed the high quality delayed-mode data set.

4. Findings relative to the Terms of Reference

It is clear the TPOS and its predecessor forms have sponsored many of the more significant achievements in data and information management (ToR 1); the TAO/TRITON system is one such case (Figure 4.1), but the we should also acknowledge the significant achievements in the way data and products are now made accessible and usable, as highlighted in TPOS WP2 and TPOS WP8a, b (ToR 2).

Terms of Reference 3 and 4 are couched in terms of ECVs but, as noted in Section 2, we should consider essential data and information management capability in parallel since the ECVs cannot achieve the desired impact without such capability. A similar remark applies to Terms of Reference 5 and 6, particularly as we are now considering feasibility and impact (readiness) within the envelope of available resources. Are the information services in place to accommodate extensions and/or innovations?

Modern ICT systems and their broad availability generally mean that logistics for information systems and services are becoming more readily available, not scarcer. Telecommunication still limits the exchange of some data (see TPOS WP10, WP6 and WP7, WP11) and metadata;

arguable this remains the biggest risk to an effective and efficient TPOS in 2020 from an information perspective.

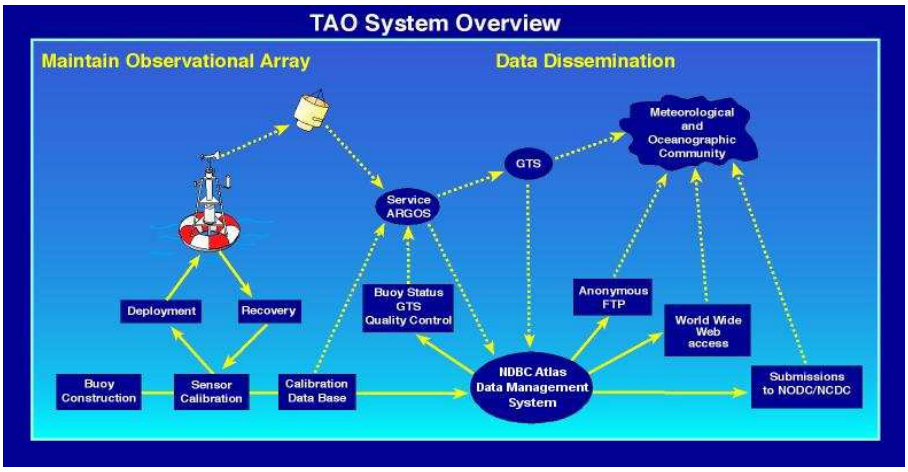

Figure 4.1 – The TAO system, including the data and information system.

Term of Reference 8 has been the main focus of this paper and we have relied heavily on more general evaluations performed for OceanObs '09 as well as a preliminary assessment of implications from other papers. Our main findings were:

1) It would appear timely to further elaborate the GOOS Framework to include explicit recognition of a data process, sitting alongside and working with the observations process. Figure 5 provides one depiction of such a separation, in this particular case to provide a clear separation of concerns in terms of governance for Australian Bureau of Meteorology observations and data. Arguable this is not the key issue here but such a concept also aids clarity in terms of implementation and encourages an integrated approach to information systems rather than a network-by-network approach. We should be testing and evaluating potential elements of the data process in the same way we use ECVs for the observations process.

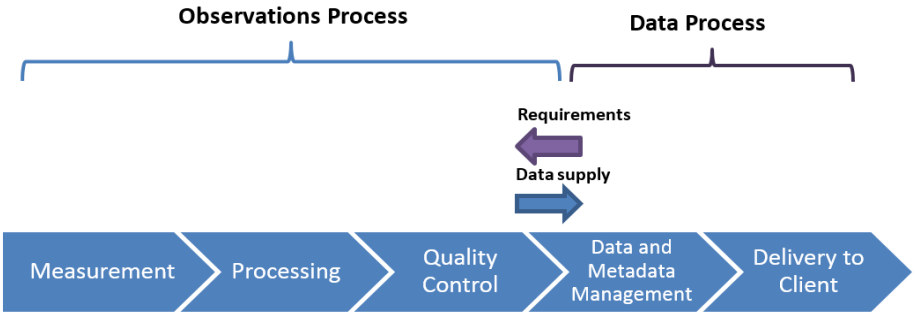

Figure 4.2 - One depiction of the separation of the data process from the observation process (Bureau of Meteorology, personal communication).

2) A second conceptual change would be to recommend greater attention to the architecture of the data process, to guide and promote effective implementation. A (GOOS) enterprise architecture approach would allow better articulation of the dependencies and risks

and allow greater advantage to be taken of frameworks being developed elsewhere (see for example Figure 4.2). This architecture should take account of the 'want it now' culture that characterises the new generation of users.

3) The first two findings should underpin a renewed drive toward integration and a culture of information systems and services, serving both the players internal to TPOS but also the external user community. Such an approach for TPOS might serve as a pilot for greater integration across the observing system as a whole (of course, working with and within JCOMM, IODE and the WMO Information Systems). In this way, we should avoid over investment in new IT solutions in favor of greater utilisation of already established systems and services.

4) From (3), it follows that we should focus on greater use of standards and protocols that have already been established rather than creating new ones. We should be testing all standards for their readiness (fitness for purpose) just as we would any proposed solution for ECVs.

5) The OceanObs '09 papers strongly emphasized the positive impact of what we have termed here a 'Community of Practice' for observing system information systems and services. TOGA and WOCE promoted such concepts and TPOS can provide leadership by promoting and supporting such communities; it is important that such communities are able to work within an agreed Framework and have agreed positions on approaches such as outlined in (1) – (4) above.

6) The requirements of research and science continue to be a high priority, perhaps higher than we might have anticipated at the last Review of the tropical observing system in 2001. Progress has been significant but models and data assimilation have yet to mature to the point where they add significant value in the data process (c.f. to the situation for NWP). The information systems therefore must continue to give priority to needs aligned with inquiry and investigation, often from small teams or individuals within universities. The value add from such engagement has been significant for both TAO/TRITON and Argo.

7) Operational requirements (by which we mean regular, routine needs, either from operational agencies or from policy/decisions makers) are now better known and better characterised. Data and products are required for levels 1 through 4 (see TPOS WP4 discussion), for immediate applications (real-time and behind real-time) and for reanalysis and climate assessments and monitoring. Ease of access and use remains a key characteristic (TPOS WP4 and WP5) as does the need for high quality for climate change monitoring and detection.

8) For all users, we need better metrics on the way the information systems and services are being used (Figure 1 provided one example). Taking a line from improved knowledge of the architecture, we should be following uptake and use of services in all their forms. The Framework notes (in the context of the change in societal use of ocean information) that "We cannot manage what we do not measure"; this is also true of information management.

9) The importance of data and information services for improving the quality of outputs from the TPOS has been highlighted numerous times. Quality assurance and control happens within the observations process (at the point of measurement, in processing and in producing level 2

datasets; see Figure 5) but also within the data process as different data streams are brought to bear. TPOS 2020 might consider building on this strength with a clearer articulation within the enterprise architecture and in the service offerings.

10) There are issues of substance with respect to the (historical) management and archive of GTMBA data, of which TPOS is a major subset. TPOS WP11 explains in some detail the challenges of producing high-quality surface wind and flux datasets. It may be timely to get more precise guidance on the integrity and quality of data and metadata holdings for TPOS ocean-atmosphere data.

11) Finally, we noted levels of maturity vary across the information systems and services and that it may be timely to consider ways to formalise/capture this in the data process.

5. Conclusions

The tropical Pacific Ocean has hosted some of most innovative ocean data and information management initiatives over the last 30 years, beginning with sea level monitoring and TOGA and WOCE, and continuing through initiatives such as TAO/TRITON and Argo. The community is justifiably proud of these achievements.

The assessment and analysis of this paper does not point to any major risks for TPOS 2020 from the approach to information systems but it has identified a number of areas that may need improvement. Contemplation of the evolution of TPOS through to 2020 provides opportunities to consolidate and rationalise our overall approach, including through further integration and adoption of a community approach to the data and information process; there is no longer a strong case for platform specific approaches, and potentially much to be gained from joining up existing efforts. Some believe such a transformation and paradigm change is realisable prior to 2020.

For all users, there is strength in supporting an information system that delivers services through multiple channels, and with different offerings in terms of integration and quality. Acquire once and serve in multiple ways. Enabling improvements in quality, most of which are only possible with off-line scientific interventions, is an important function of the system. Further harmonisation of metadata management, versioning and publishing is possible.

The record of the data and information management community for TPOS is strong but can be improved, in terms of efficiency, robustness and effectiveness. TPOS 2020 provides a perfect opportunity to do this. In the event a major project around is supported, an underlying principle should be that around 10% of the total effort should be directed towards data and information management. This is particularly important for emerging and prototype technologies that will provide the basis for a future TPOS.

References

de la Beaujardière, J, Beegle-Krause, C. J., Bermudez, L., Hankin, S., Hazard, L., Howlett, E., Le, S., Proctor, R., Signell, R.P., Snowden, D., and Thomas, J. (2010): “Ocean and coastal data management”, in Proceedings of the "OceanObs’09: Sustained Ocean Observations and Information for Society" Conference (Annex), Venice, Italy, 21-25 September 2009, Hall, J., Harrison D.E. and Stammer, D., Eds., ESA Publication WPP-306.

Beegle-Krause, C.J., Allen, A., Bub, F.L., Howlett, E., Glenn, S., Kohut, J., Schofield, O., Terrill,E., Thomas, J., Tomlinson, M.C., and Tintoré, J. (2010): “Observations as Assets in Decision Support”, in Proceedings of the "OceanObs’09 - Sustained Ocean Observations and Information for Society" Conference (Annex), Venice, Italy, 21-25 September 2009, Hall, J., Harrison D.E. and Stammer, D., Eds., ESA Publication WPP-306.

Belbeoch M. & Co-authors (2010): "The JCOMM in situ Observing Platform Support Center: A decade of progress and remaining challenges", in Proceedings of the "OceanObs’09: Sustained Ocean Observations and Information for Society" Conference (Vol. 2), Venice, Italy, 21-25 September 2009, Hall, J., Harrison D.E. and Stammer, D., Eds., ESA Publication WPP-306.

Blanc, F., Baralle, V., Blower, J.D., Bronner, E., Cornillon, P., de La Beaujardiere, J., Donlon, C., Gemmel, A., Hankin, S.C., Keeley, R., Lauret, O., Loubrieu, T., Petiteville, I., Pouliquen, S., Price, M., Pugh, T., and Srinavasan, A. (2010): “Evolution in data and product management for serving operational oceanography, a GODAE feedback”, in Proceedings of the "OceanObs’09: Sustained Ocean Observations and Information for Society" Conference (Annex), Venice, Italy, 21-25 September 2009, Hall, J., Harrison D.E. and Stammer, D., Eds., ESA Publication WPP-306, 2010.

Guinehut S., Coatanoan, C., Dhomps, A.L., Le Traon, P.Y., and Larnicol, G. (2009): "On the use of satellite altimeter data in Argo quality control". J. Atmos. Oceanic Technol. 26: pp. 395-402.

McPhaden, M. J., et al. (1998): The tropical ocean global atmosphere observing system: A decade of progress, Journal of Geophysical Research – Oceans, 103(C7), pp. 14169-14240, (doi:10.1029/97jc02906).

Integrated Marine Observing System (IMOS), (2013): “Annual Highlights Document 2012-13”, available from http://imos.org.au/, edited by T.Moltmann et al, 2013.

McPhaden, M. J., Ando, K., Bourlès, B., Freitag, H.P., Lumpkin, R., Masumoto, Y., Murty, V.S.N., Nobre, P., Ravichandran, M., Vialard, J., Vousden, D., and Yu, W. (2010): “The Global Tropical Moored Buoy Array”, in Proceedings of the "OceanObs’09: Sustained Ocean Observations and Information for Society" Conference (Annex), Venice, Italy, 21-25 September 2009, Hall, J., Harrison D.E. and Stammer, D., Eds., ESA Publication WPP-306, 2010.

Pouliquen, S., Schmid, C., Wong, A., Guinehut, S., and Belbeoch, M. (2010): “Argo Data Management”, in Proceedings of the "OceanObs’09: Sustained Ocean Observations and Information for Society" Conference (Annex), Venice, Italy, 21-25 September 2009, Hall, J., Harrison D.E. and Stammer, D., Eds., ESA Publication WPP-306, 2010.

Snowden, D., Belbeoch, M., Burnett, B., Carval, T., Graybeal, J., Habermann, T., Snaith, H., Viola, H., and Woodruff, S. (2010): “Metadata Management in Global Distributed Ocean Observing Networks”, in Proceedings of the "OceanObs’09: Sustained Ocean Observations and Information for Society" Conference (Annex), Venice, Italy, 21-25 September 2009, Hall, J., Harrison D.E. and Stammer, D., Eds., ESA Publication WPP-306, 2010.

White Paper #14 – Logistical considerations and ship resources

Legler, D.[1], Ando, K.[2], Thurston, S.[1], Belbeoch, M.[3], Stroker, K.[3], Kramp, M.[3], McArthur, S.[1], and Clark, C.[1]

[1] National Oceanic and Atmospheric Administration, United States
[2] Japan Agency for Marine Earth Science and Technology, Japan
[3] JCOMM In situ Observing Platform Support Center, France

1. Introduction

The availability of data, information, and products for the in situ Tropical Pacific Observing System is strongly dependent on two dominant factors: resources in support for the observing system and ship resources necessary for deployments, servicing, and routine observing of the ocean and its overlying boundary layer. This whitepaper will describe resources and logistical (e.g. ship resource) needs for in situ ocean observing in the Tropical Pacific, how well the current needs are met, and explore the possibilities for increased resources and coordination/ governance to address logistical and ship resource needs of the future.

2. Service needs/strategies for TAO/TRITON-class buoys

What are the current cost and ship-time requirements for TAO and TRITON-class buoys? How have these changed historically? What are the cost-drivers and/or limiting logistical factors (e.g. ship time availability/scheduling, piracy, ship-speed, crew scientific expertise, etc) that are the most challenging to overcome to reduce costs and still meet the requirements?

The TAO/TRITON array is a network of deep ocean moorings at 67 sites (55 TAO buoys maintained by the US and 12 TRITON buoys maintained by the Japanese) in the tropical Pacific. Regular maintenance of the array is required to maintain continued integrity of the data. Historically, NOAA's strategy was to visit US buoy every 6-8 months for maintenance and replace each buoy every 12-16 months. The NOAA ship *Ka'imimoana* (KA) was dedicated to providing ship time, approximately 280 days per year, to service the US TAO buoys to meet these requirements and provide additional support for other requirements (see next section). The data return rate for the US TAO buoys has been excellent (80% or better) before mid-2012. Constrained ship resources from NOAA continues to be a key challenge to servicing the TAO array, deploying additional elements of TPOS, and supporting research endeavors in the Tropical Pacific.

This requirement of 280 days for US servicing in order to maintain the historical performance measure could change if NOAA chose to lengthen the service intervals, used a faster ship, and/or used a different mix of ships and routing to reduce transit time.

Beyond technological improvements such as sensor and battery life, non-technical issues such as buoy vandalism shape the requirements for ship servicing. Vandalism is common in areas of commercial fishing and is well-documented (http://www.gc.noaa.gov/gcil_buoys.html) (Figure 2.1). NDBC recently initiated a programme to monitor and identify (through use of on-buoy cameras) ship traffic near and adjacent to select TAO buoys. It is too early to assess the potential success of such efforts, but testing solutions to widespread limiting factors such as

vandalism could help reduce servicing requirements.

Because of the retirement of the KA, in 2012 and 2013 NOAA expanded its use of chartered commercial vessels to fulfill TAO servicing needs. However such ships have somewhat more limited capabilities and opportunities for deployments of other observing instruments, research field work, and hydrographic casts throughout the tropical Pacific.

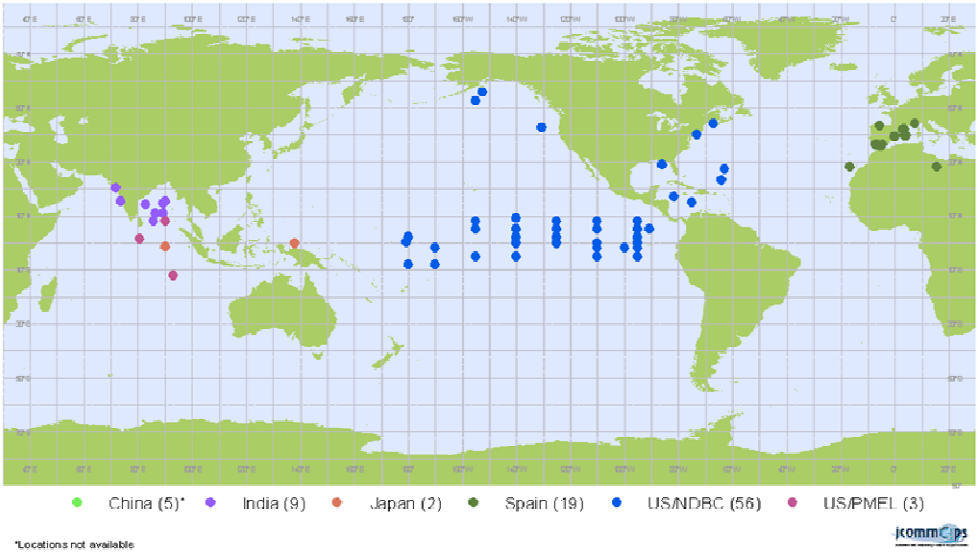

Figure 2.1 – 2012-2013 Vandalism events as reported by DBCP member countries.

JAMSTEC has relied on the R/V Mirai for 60-100 days per year (the ship-cost was from 2400K to 4000K US$ per year) to service the array of TRITON buoys. The maintenance and ship time cost has decreased due to the technological buoy improvements and developments by JAMSTEC engineers. The current ship time requirement has been effectively reduced to one half of the original cost. Looking ahead, JAMSTEC has decided to allocate ship-time for the western Pacific TRITON based on an annual research proposal. Because of increased requirements from Japanese science communities including geology, seismology, along with total budget cuts to JAMSTEC from our government, the sea days provided to R/V Mirai was decreased originally from 280 days per year to 190 days at present, with less in the future. Consequently, JAMSTEC decided to increase mooring servicing interval from one-year to 18 months for all TRITON and m-TRITON buoys, and to stop measurements along 130E, will relay one site to Indonesia, and will stop two sites at 5°N 147°E and 8°N 156°E.

3. Service needs/strategies for other in situ elements (e.g. Argo, drifters, hydrography, etc) of the TPOS

What are the current cost and ship-time requirements for other (not TAO) in situ elements of the TPOS? What are the cost-drivers and/or limiting logistical factors (e.g. deployment scheduling, EEZ issues, crew scientific expertise, etc) that are the most challenging to overcome to reduce costs and still meet the requirements?

3.1 Global Drifter Programme (GDP)

Aside from the TAO servicing cruises, drifter deployments in the Tropical Pacific are few and far between. Of course, there are one-off opportunities from the US Coast Guard and/or Navy while transiting through these regions, but because few shipping lines transect the central equatorial Pacific; the options here are extremely limited. The GDP has a very limited budget and historically has had drifters deployed on a volunteer basis. Thus a reduction of servicing cruises for TAO buoys, without alternate deployment opportunities, will result in reduced surface drifters in the Tropical Pacific.

3.2 Argo

The vessel requirements for Argo floats and gliders are quite different than those for moorings, repeat hydrography and other conventional oceanography. Argo floats deployments in the tropical Pacific have piggy-backed on the TAO/TRITON servicing cruises. Additional deployments have been achieved through other research vessel deployments, dedicated cruises such as the 28-m research vessel, R/V Kaharoa (over 1200 floats deployed since 2004, including in the tropical Pacific), and of sailing vessels such as the Lady Amber. Dedicated deployment cruises for floats are not often considered ship charters (typically we send no one on board) but as contracts for the deployment of floats. The bottom line is the cost per float deployment runs about $5K per float using a vessel the size of Kaharoa and perhaps $3K per float for smaller vessels. In recent years, with the use of smaller sailing vessels (coordinated through JCOMMOPS), such as the Lady Amber, the cost has been reduced to approximately half. The Lady Amber is available for chartering deployments and this can be arranged through the ship coordinator at JCOMMOPS. International partners such as Australia and New Zealand have been willing to share such costs with the U.S., and there is growing international interest.

3.3 SOT-SOOP (e.g. XBT)

Whilst a number of SOOP-XBT lines which transit the tropical Pacific are declared active (Figure 3.1), the yearly map of 2013 (Figure 3.2) shows that only a few lines are regularly occupied.

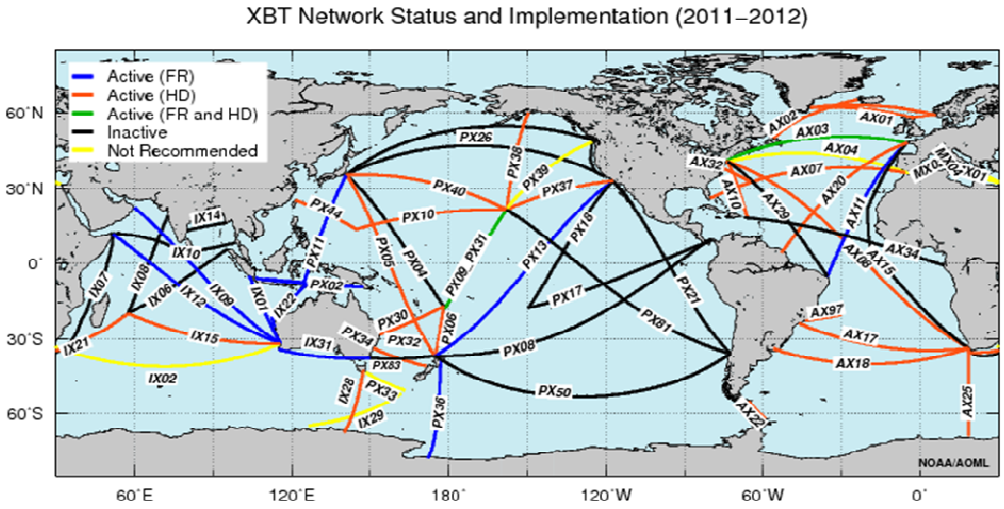

Figure 3.1 – XBT Network Status and Implementation (2011-2012).

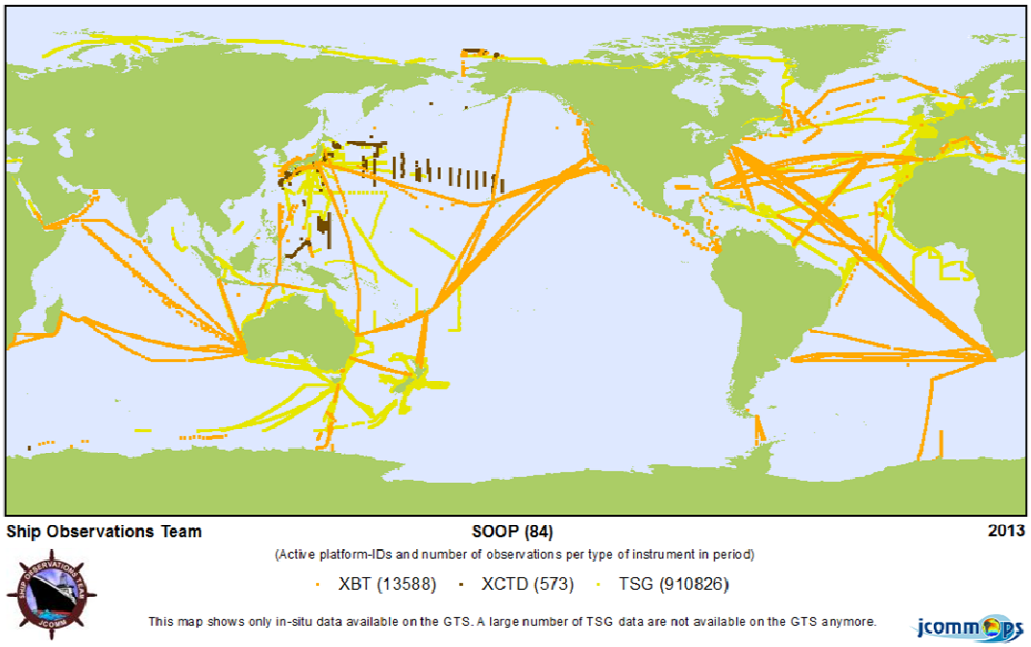

Figure 3.2 – XBT Network Status in 2013.

3.4 SOT-VOS

Even on a yearly basis, the number of Voluntary Observing Ships in the tropical Pacific is poor compared to other ocean basins, and there are almost no VOSClim ships that provide high-quality data.

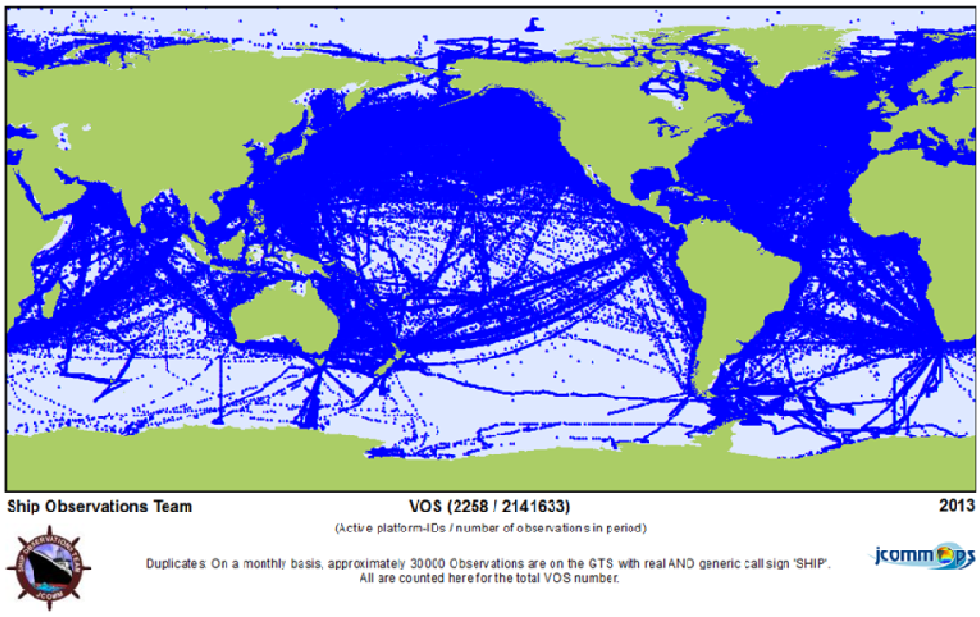

Figure 3.3 – Global overview map of VOS routes.

3.5 GO-SHIP

The global repeat hydrography programme has one line in the tropical Pacific in East-West

direction that is occupied by Japan every six years on its westerly part (P04W). A numbers of other active North-South lines are planned in the TPOS area (Figure 3.4).

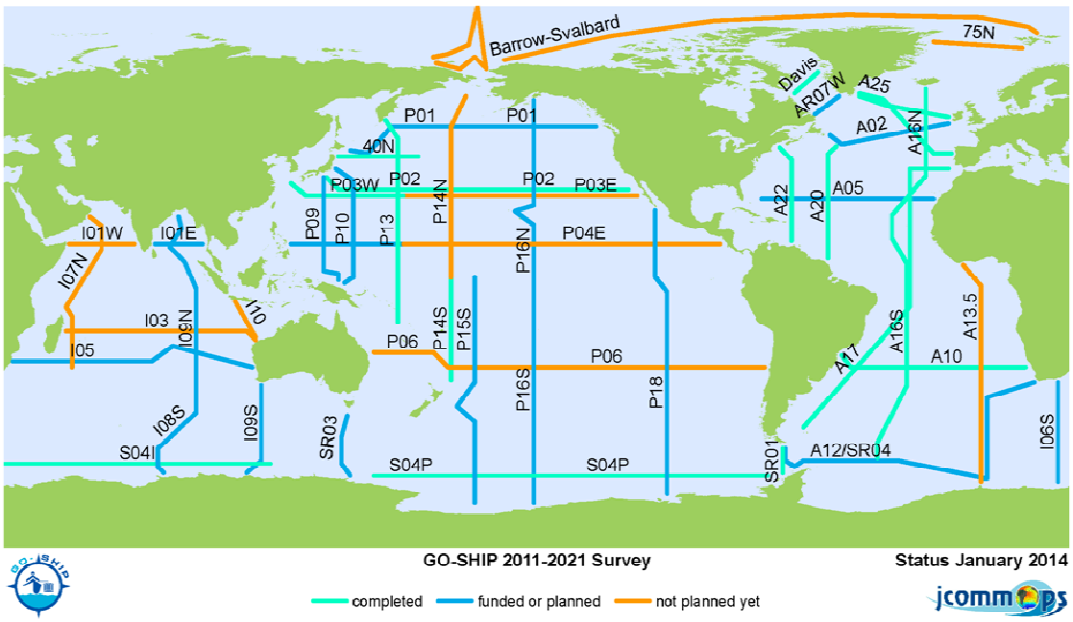

Figure 3.4 – Planned N-S lines in the TPOS area.

3.6 Underway pCO_2

Underway pCO_2 measurements are recorded by a number of ships (some are research vessels; others are "VOS" ships (not clear if these VOS ships are also part of the JCOMM VOS programme).

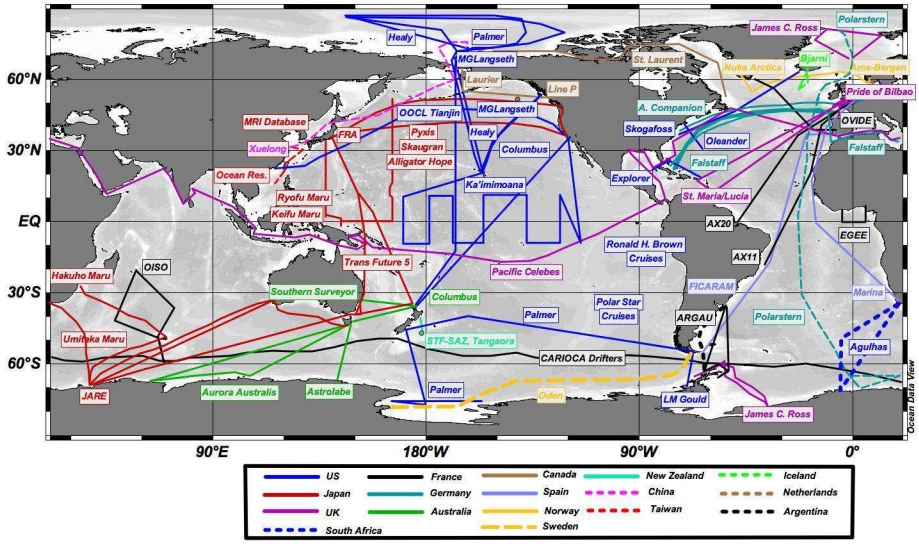

Figure 3.6 – VOS ship routes recording pCO_2 measurements.

4. Observing system performance, monitoring tools/diagnostics (current and future)

What monitoring tools/diagnostics are current being used to monitor the state of the TPOS? What improvements and/or new tools would help?

The global ocean observing arrays are monitored at JCOMMOPS with the DBCP Technical Coordinator responsible for the moored and drifting buoys, the Argo Technical Coordinator (TC) responsible for the Argo float status, and the Ship Logistics coordinator responsible for vessel availability and SOT coordination in the region. The DBCP TC works with programme operators to receive updates on the status of the TAO, RAMA and PIRATA arrays as well as monitors the data available via the GTS. In the case of the PIRATA and RAMA buoys, maintenance updates are received via direct emails on a weekly basis from NOAA/PMEL. Monthly updates are received from the NOAA/NDBC for the TAO array on percentage of data reported, but there is currently no automated or reported mechanism on maintenance for the TAO array. The DBCP TC monitors closely the GTS distribution and creates monthly maps on availability of data. At present, the tools and statistics are created by the DBCP TC, however in the future; these tools will be available to all programme managers and operators on a more dynamic basis as JCOMMOPS improves its website.

The coordination of ship schedules and maintenance is necessary and needs to be improved. JCOMMOPS will work with programmes to prepare and maintain an updated database with ships that can perform the necessary replacements, installations, and maintenance of TAO/TRITON moorings. This will require communication and updates from the operators of all networks on future plans and a goal is to have an online system where the operators can enter this information and it is tracked by JCOMMOPS. At that point, all of this valuable information could be viewed by any interested member of the community.

Monitoring of observational density by variable is possible through use of GTS feeds and some such tools are available via JCOMMOPS and OSMC, but there are known issues of completeness and timeliness associated with relying on a single GTS access node. Moreover, data not reported via GTS are not represented in such tools.

5. TPOS Performance/Data Return

Describe the data return rate of the TAO array and other TPOS elements. Are there regions where the return rate suggests that some observing strategies are better than others? From a logistics and resources point of view, what metrics are needed?

Overall, the metrics for TPOS performance have been pursued by each observing component (TAO, TRITON, Argo, drifters, satellites, etc). Such an approach fails to consider like measurements (e.g. subsurface temperatures/salinities from TAO, TRITON, XBT, hydrography, and Argo) for addressing key requirements. Moreover, for some components (e.g. TAO), the metrics for performance have focused on data return by the entire system. While this has driven good data return performance for many years, it fails to capture any connection to impacts on research and/or models, as well as any desired outcomes such as research findings and better forecasts. Recent efforts by OOPC and others (see http://www.globalchange.gov/what-we-do/assessment/indicators-system) to develop and expand current ocean indicators, along with an appropriate suite of products, should also be considered. In summary, Suitable metrics on

observing performance and downstream information and capabilities need to be developed and promoted.

The data return rate in the TRITON project has been one important indicator, and the ship-time dedicated to TRITON has been determined one or two years in advance. So, we could decide how many buoys we will service in advance for keeping high data return rate at least from buoys we will maintain in future, and it gave us time to decide how we maintain (and recently stop) our array.

Returns of data in regions near coastal area (e.g. north of New Guinea) has generally lower data return rate, but demonstrations of gliders in some coastal regions (e.g. Solomon Sea) have been working well. Would glider measurements be appropriate near coastal region?

6. Assessment of current and future resources (ships and maintenance) in the Tropical Pacific

Considering all of the above requirements for ship time and servicing resources for sustaining a TPOS, what resources have been made available to support the TPOS? How has this changed in time? In times of constrained resources, how are decisions made on servicing priorities (how should this process be improved)? What additional ship resources could be solicited to address needed requirements? What are the pros and cons of commercial chartering? What are the prospects for engagement of additional international sponsors of TPOS and what should be done to enlist such support? What types of arrangements (e.g. multi-lateral agreements, resource forums, etc) are likely to be beneficial towards sustaining the TPOS of the future?

The past two decades of sustained observing in the tropical Pacific has catalyzed new research and supported the growth of operational ocean, weather, and climate forecasting enterprises. However, the financial underpinnings of some of these observing systems are somewhat fragile and subject to change without warning.

Many countries have been supporting components of TPOS. Such support is often dependent on national priorities, availability of funding, and even on the success of independent research proposals evaluated amongst many others for limited research funds. Additionally, support for the TPOS has historically been provided through both operational (e.g. for US-TAO) and research enterprises (Japan-JAMSTEC) and for many of the other in situ ocean observing components that needs to be factored into future development and support considerations.

6.1 Ship resources

An inventory of available ships capable of contributing towards the TPOS and those ships capable of servicing deep moorings is currently being prepared through the Ship Coordinator at JCOMMOPS. However, this is beyond the scope of this paper and will be available in 2014. Chartering ships from the private sector has also been used (e.g. by the US for TAO and Argo) and can be coordinated through JCOMMOPS.

JCOMMOPS works on worldwide integrated ship coordination. Across the different programmes, information are gathered on operational needs on the one side (deployments, retrievals and maintenance of different instrument types) and matched with opportunities on the other side (merging research cruise information from different sources, volunteer and charter

vessels).

Different ship types and corresponding operation complexity (professional, advanced, basic) must be distinguished, and are all coordinated by JCOMMOPS:

- Research vessels establishing campaigns in, or transiting the tropical Pacific, offering in particular free of charge deployment opportunities with qualified staff, and dedicated equipment for professional operations
- Research or survey vessels chartered for TPOS operations. JCOMMOPS cooperates with a global ship operator and can provide cross-programme solutions for all needs and instrument types and numbers. The available fleet also comprises innovative and economic multi-purpose vessels for substantial missions, and approved sailing survey ships such as Lady Amber for advanced operations - at lowest daily rates.
- Commercial ships, in particular vessels recruited by JCOMM's Ship Observations Team for the VOS and SOOP programmes, offering basic, but free operations: Gathering of underway data (S,T,C, meteo), XBT/XCTD launches and deployment opportunities whilst transiting the target zone, but often from deck heights of 10 meters and more, and at speeds of up to 20 knots.
- Sailing ships, in particular fleets organized in rallies (without competition) or races, allowing for facilitated logistics and training (clear schedules) and basic operations (deployments, retrievals, meteo data) of smaller number of instruments, but at safe deployment speed and close to the sea level, and with additional potential in education and communication dimensions. A pilot project has been carried out successfully in November 2013 in the tropical Atlantic (JCOMMOPS/NOAA-AOML) and first operations are now planned in the tropical Pacific in 2015.

The ship coordinator position was established to gather, compile and distribute information on available ship time, or to search for solutions for specific queries. Forms are available at JCOMMOPS to transmit your needs in standardized structure. OceanSITES recently provided detailed information on ship requirements per instrument type, which can now be matched with specifications of available ships. The aim is to provide this for all programmes, included in the JCOMMOPS database for access amongst all interested parties.

6.2 Expanding and Coordinating International Support

Increased international support (particularly for ship resourcing) of TPOS is likely to be possible in the coming decade, and should be encouraged through appropriate mechanisms (e.g. joint research projects, partnerships, bilateral agreements, etc). With increased sponsorship possibilities and the need to better strategize how best to sustain and evolve the TPOS, some consideration of coordination (governance if you will) is necessary. There are a few successful models already in place for other basin-scale ocean observing that may provide guidance for a successful TPOS.

The Indian Ocean Observing System (IndOOS) Resource Forum (IRF) has been set up to facilitate the allocation and alignment of resources in the Indian Ocean to achieve a sustained, basin-wide ocean observing system. IRF activities include the following:

- Review the requirements for the implementation of IndOOS as established by the

Indian Ocean (climate) Panel (IOP) and the Scientific Steering Committee for Sustained Indian Ocean Biogeochemical and Ecological Research (SIBER);

- Facilitate and coordinate resources that may be applied to the system, especially ship time for the Research Moored Array for African-Asian-Australian Monsoon Analysis and Prediction (RAMA); and
- Encourage scientific and technological initiatives, in the participating countries, to meet the objectives of IndOOS.

Similarly, for the Pilot Research Moored Array in the Tropical Atlantic (PIRATA), a Resources Board has been established to implement the array based on the following criteria:

- Identification of infrastructure needed for implementation (ship time, laboratory, technical support, etc.),
- Implementation must occur on a not to interfere basis with the backbone,
- Schedule of implementation,
- Funding requirements/cost justification,
- Identification/source of funding.

Both the IRF and PIRATA Resources Board share common traits of 1) encouraging stakeholders to routinely discuss in appropriate venues system requirements, operational considerations, system advances, and resourcing needs/gaps; 2) encouraging cross-dialogue amongst those operating the systems, product and knowledge developers, end-users, and those sponsoring the observing arrays to improve system sustainability and encourage progress towards a range of goals.

A similar approach to governance and coordination should be considered for TPOS. Discussions on the potential to form a TPOS Resources forum will be carried out after the TPOS Workshop. The TRF could meet to monitor and critique the rationale for implementation of the TPOS Plan, as it is articulated by TPOS‐2020, with input from the Ocean Observations Panel for Climate, the CLIVAR Pacific Science Panel, Pacific Island GOOS, DBCP TAO Implementation Panel (TIP) and other relevant expert‐bodies. Based on its deliberations, the TRF will work to facilitate and coordinate the provision of the resources required for TPOS evolution, implementation, and maintenance by member institutions, similar to the IRF for the Indian Ocean and the PIRATA Resources Board for the Atlantic. The TRF activity will promote contributions from institutions in the participating countries, with a view toward fully implementing the TPOS Plan by 2020 and sustaining TPOS thereafter. Such an approach wis also recommended at the POGO (Partnership of Observation for Global Ocean) 15th meeting, held in Hobart Australia hosted by CSIRO and IMAS.

7. Recommendations

1) Logistical requirements (e.g. deployments and servicing by ships) will continue to be a potentially limiting factor in the development of TPOS for the coming decade.
2) A new suite of useful products, indicators, and access tools should be developed to better take advantage of an “integrated” TPOS that depends less on specific

observational platforms and focuses instead on integration across TPOS, e.g. against variable-based requirements

3) Tools to monitor the state of the integrated TPOS are needed to identify gaps and document the evolution of the system
4) More effort is required to identify deployment and servicing needs, and coordinate potential opportunities (e.g. ships, cruises) to address them. The JCOMMOPS ship coordination will be helpful here, and the community should provide JCOMMOPS with all related information (needs and opportunities).
5) US research engagement in support of TPOS (and in particular TAO) needs to be strengthened to encourage and strengthen ties to international research partners, to advance research and technology development, and observing system development.
6) Increased international support (particularly for ship resourcing) of TPOS is likely to be key and will be possible in the coming decade, and should be encouraged through appropriate mechanisms (e.g. joint research projects, partnerships, bilateral agreements, etc).
7) The formation of a TPOS Resource Forum should be considered to encourage multi-partner coordination of observing system support to address key observing requirements and evolution of the TPOS.
8) Increased communication, dialogue, and interaction between research and operational USERS (supporters of TPOS) are needed to insure requirements are updated, observations are fully utilized, and feedback on value/impact/assessment of observations by the forecasting communities is considered. Engagement with the Resource Forum would insure gaps, needs, and progress towards strategic goals are discussed and addressed.
9) Partnerships leading to an improved TPOS should be predicated on mutual interests of all partners for advancing research and/or operational forecasting capabilities.
10) International partnerships in support of TPOS should include coordination and sharing of observing technologies. Technical exchanges between the US and Japan have not been occurring for some time. As TPOS moves forward, such exchanges across all the tropical mooring buoy arrays (TAO, TRITON, RAMA, and PIRATA) need to be an integral activity amongst all partners.